Principles of Proton-coupled Electron Transfer Mediator Design

Thesis by

Enric Healey Adillon

In Partial Fulfillment of the Requirements for

the degree of

Doctor of Philosophy

CALIFORNIA INSTITUTE OF TECHNOLOGY

Pasadena, California

2026

(Defended April 30, 2026)

© 2026

Enric Healey Adillon
ORCID: 0000-0001-8695-0637

ACKNOWLEDGEMENTS

First of all, thanks to all my friends and family for their unwavering support. While California has felt like a world away from New Jersey, these are the people who remind me of my roots and keep me true to myself. Thanks Mom and Dad, Louise, Miquel and Grace, and of course our newest family member, Theodore.

The greatest discovery of my PhD has been the love I have for my dear partner, Ute. You make me a better person. You are the source of my strength. Ich liebe dich sehr, und ich freue mich auf unsere Zukunft zusammen. Danke, auch, an deine Eltern, Walter und Claudia, die mich herzlich in eurer Familie und in Deutschland willkommen geheißen haben.

I would like to thank Jonas for his guidance. Through my time here, I have honed the skill that I came to learn, asking (and answering) good scientific questions. This skill is the heart of a good lab, and it is the crux of Jonas' leadership of this group. The search for good questions can be frustrating at times, but in doing so, I have learned to be patient, to think carefully, to be thorough, because through that arduous process, good questions are born. In some ways, this is as much a curse as a blessing, as I now take the same critical lens to the work of others as I do my own. But that is what makes for a strong community, people who are unafraid to question each other in search for the truth. This is the culture of the Peters group that Jonas has curated through the years. Thank you, Jonas, for allowing me to be a part of it. I will carry that spirit with me wherever I go.

I would like to thank my committee members, Theo, Hosea, and Harry for their guidance. It is profound how impactful our brief discussions can be. I remember in my third-year meeting, I presented some thermochemistry and reactivity on the carborane project. Theo suggested that a stepwise ET-PT mechanism might be operative. Hosea asked about why *ortho*-carborane, specifically with phenyl groups, had unique redox properties. These questions became central to the investigation that followed. I am thankful for their attention to detail, and especially that they made the most of our time together.

Harry is my inspiration. We first met at a Beckman Symposium in Irvine in 2018. He gave the opening remarks which amounted to a stand-up routine comprised of bits about Arnold Beckman. Following advice from Jeff Byers, I invited Harry to Boston College for a symposium, where we spent the day together and got to know one another. The opportunity to spend more time with Harry helped sway me to come to Caltech. Through many visits to the BI, Harry has been a source of counsel, giving

advice on scientific and personal matters, and of course, he has been a great storyteller. Speaking with Harry is like traveling through time. He told me about the time he met Niels Bohr in Copenhagen, about his early days at Columbia with his French lecture demo assistant with a ridiculous name, Jaquez or Gusteau or something, about many years and happenings at Caltech. For someone of his stature, he's so easy to talk to. He listens and makes you feel important. For all our discussions, and I hope more to come, thank you Harry.

To all my colleagues in the Peters group, thank you for keeping up high spirits in a really challenging environment. First, I want to thank Sasha. Based off a first impression, I thought of Sasha as what I expected to encounter at Caltech, someone who is smart, well-read, passionate. But what I came to understand is that Sasha loves the game for the game. He embodies the spirit of basic science, the will to understand regardless of how jagged, messy, windy the road may be to reach that understanding. The more I have gotten to know Sasha, the more I appreciate his love for the Avant Garde. Be it a cool structure in Dalton or rediscovering *Donnie Brasco*, he cuts through the flashiness to the core of what makes something beautiful. Sasha, it has been a pleasure to work with you, and I am excited to see where your career takes you. Madeline, you have charted a path in the lab completely your own which really speaks to your fearless and determined personality. It has been amazing to see you grow into the confident researcher you have become. I will miss our nights out dancing. Thank you to my box mates, Joe, Mengdi, John, and David, for putting up with my paranoia. Christian, thanks for many helpful discussions and for never shying away from a disagreement if it meant getting it right. Emily, thanks for keeping up the high standards of the lab. Sungchan, thanks for jumping on the mediator project with us and carrying on the torch in the search for mediators. I am glad to see you are making headway in new directions. Stefan, thanks for bringing rigor and kindness… and for bringing donuts in on the holidays. Paul Oyala, our unofficial staff scientist, thanks for making the EPR facility easy to use and being an all-around fun guy. I am leaving the group in good hands knowing that Catherine, Alex, Seungju, and Drew will be at the helm. It has been a pleasure to see all of you grow into ever more mature and capable chemists. It was a pleasure to work for a summer with Matthew Ong, *the carborane kid*, who helped with the synthesis discussed in Chapter 3. I would like to extend a special note of gratitude to Lucie, a mentor early in my time in the group who I will once again have as my colleague and mentor at Terraform Industries.

I hoped to make some good friends in grad school, but I feel lucky to say I have made some great friends. Samir and Skylar, you have been there for me every step of the way, balancing empathy with a fun-loving attitude that has nurtured my tired spirit. If we made it through this, I am sure we can make it through anything. To the others in my COVID trauma bonded cohort—Helena, Nathan,

Katie—and to all the golfers on Schlinger 3, thanks for making grad school more fun than it had to be.

I would like to thank Jeff Byers. I joined his lab at Boston College in the fall of my freshman year, pretty much as soon as I could. I wanted to see if I liked research. He helped me fall in love with research. Jeff's passion for chemistry was even strong enough to convince the group to put up with his sadistic 7-11 pm chalk talk group meetings on Monday nights, and that's if they were on time. Jeff made a point to have monthly one-on-one meetings with me. He would occasionally help me set up things in the lab, like my first distillation. I got to know Jeff personally on our drives together to the annual summer camping trip which took place in the biggest pick-up truck that they had at the Enterprise rental car that year. No one else from the group was brave enough to drive with him, maybe because he made us navigate with print-out Mapquest instructions like it was 2005. Missing all the turns would let us spend lots of time together. I came to admire Jeff as an advisor and as a person, and he played an important role in my decision to go to Caltech. I just wish that he could have seen what I did here.

I want to also thank Frank Tsung for his mentorship. He, too, cared for his students dearly, myself included. The last time I saw Frank was during my last week at BC in March of 2020. A few of the chemistry majors roamed Merkert with a bottle of tequila in search of faculty who would share a drink with us to send us off. Frank was the only one we found, and even though it was silly, it meant a lot to me.

It takes a village, and that village was all the grad students in the Byers lab: Michael, Alex, Chet, Matt, Miao, Tom, Zee, Kayla, Eric, Connor, and Adam, and technically not a grad student, also Crystal. Thank you all for taking the time to show me how to work on a Schlenk line and in a glovebox, how to analyze NMR spectra, how to set up and work up reactions, and thank you for your friendship. To my fellow undergrads, Nancy, Gretchen, Jason, Alex, other Alex, it was a joy to grow with all of you. The Byers lab was a warm and welcoming lab environment because of the people that occupied it, and that's why I chose to spend so much time there.

I would also like to thank all the staff that keep Caltech a well-oiled machine: Dave Vandervelde, Mike Takase, Mona Shahgholi, and Leslie Corado. Ich möchte mich auch bei Andreas Aebi für seine Geduld mit meine deutscher Grammatik bedanken. Ich habe es genossen, mit Ihnen Schweizer und Deutscher Literature zu lesen.

ABSTRACT

This thesis explores a series of structurally related reagents for formal H-atom transfer reactions. The work builds upon a previous discovery that an aniline-appended cobaltocene complex, upon protonation and reduction, is capable of concerted proton-electron transfer which enables its use as an electrochemical mediator for a variety of unsaturated small molecule reduction reactions. Given its potent reactivity and simple design, the aniline-appended cobaltocene complex is a wonderful platform for structure-function studies, and accordingly, three distinct structure-function relationships are investigated.

Chapters 2 and 3 examine the reductive component by substituting cobaltocene for a main group reductant of a similar potential, diaryl-*o*-carborane. The *o*-carborane can be reduced and protonated to generate an N–H bond with a weak effective bond dissociation free energy of 31 kcal/mol. Crystal structures of the diaryl-*o*-carborane radical anions are disclosed. The reactivity of the singly reduced, protonated form of the diaryl-*o*-carborane towards substrates and towards proton reduction is discussed. Then, the synthesis, thermochemistry, and reactivity of a family of *o*-carborane PCET reagents is described. Cyclic voltammetry using acetophenone reduction as an indicator of concerted proton-electron transfer suggests that the thermochemical perturbations do not categorically change the reactivity.

The second section examines the bridging group that separates the redox and acid/base moieties. Across the series of four complexes, the PCET driving force remains relatively constant while the thermodynamic coupling is varied substantially. Kinetic measurements of PCET reduction reveal that the reaction proceeds by a rate-limiting CPET step in all cases, the rate of which is modestly varied across the series. In particular, the *o*-phenylene-bridged complex has the fastest PCET rate despite the least driving force, which is attributed to a stabilizing orbital interaction between cobaltocene and the substrate.

In Chapter 5, the synthesis of phosphonium-appended cobaltocene is disclosed as well as its PCET thermochemistry and reactivity with acetophenone. Despite substantially less driving force for PCET than its nitrogen congener, the phosphonium-cobaltocene complex is more reactive.

PUBLISHED CONTENT AND CONTRIBUTIONS

1. Adillon, E. H.; Peters, J. C. A Carborane-derived Proton-coupled Electron Transfer Reagent. *J. Am. Chem. Soc.* **2024**, 146, 30204–30211. DOI: 10.1021/jacs.4c09007

E. H. A. conceptualized the project, performed the experiments, and wrote the manuscript.

TABLE OF CONTENTS

Acknowledgements iii
Abstract vii
Published Content and Contributions viii
Table of Contents ix
Abbreviations and Symbols xi

Chapter 1: Introduction 1
1.1 Opening Remarks 1
1.2 Background on Proton-coupled Electron Transfer 2
1.3 Electrocatalytic Proton-coupled Electron Transfer Mediators 6
1.4 Proton-coupled Electron Transfer Mediator Design 10
1.5 Chapter Overview 12
1.6 References 14

Chapter 2: A Carborane-derived Proton-coupled Electron Transfer Reagent 16
2.1 Introduction 17
2.2 Results and Discussion 19
2.3 Conclusion 25
2.4 References 26

Chapter 3: Independent Modulation of Proton and Electron Transfer Driving Forces in a Family of Carborane-derived H-atom Donors 33
3.1 Introduction 34
3.2 Results and Discussion 37
3.3 Conclusion 45
3.4 References 46

Chapter 4: Repositioning Proton and Electron Donors in a Series of Proton-coupled Electron Transfer Mediators 48
4.1 Introduction 49
4.2 Results and Discussion 51
4.3 Conclusion 59
4.4 References 60

Chapter 5: A Phosphonium-derived Proton-coupled Electron Transfer Reagent 67
5.1 Introduction 68
5.2 Results and Discussion 70
5.3 Conclusion 75
5.4 References 76

Appendix A: Supplemental Information for Chapter 2 78

Appendix B: Supplemental Information for Chapter 3 165

Appendix C: Supplemental Information for Chapter 4 230

Appendix D: Supplemental Information for Chapter 5 351

Appendix E: Miscellaneous X-ray Diffraction Structures 381

ABBREVIATIONS AND SYMBOLS

Ar^F. 3,5-bis(trifluoromethyl)phenyl
BDD. Boron Doped Diamond
BDFE. Bond Dissociation Free Energy
Cb. *o*-Carborane
CO_2R. Carbon Dioxide Reduction
Cp. Cyclopentadienyl
CPC. Controlled Potential Coulometry
CPET. Concerted proton-electron transfer
CV. Cyclic Voltammetry (or Voltammogram)
°C. Degrees Celsius
Et. Ethyl
Δ*G*. Gibbs Free Energy
Δ*G*‡. Transition State Free Energy
DBU. 1,8-Diazabicyclo[5.4.0]undec-7-ene
DFT. Density Functional Theory
DME. 1,2-dimethoxyethane
DPV. Differential Pulse Voltammetry (or Voltammogram) ***E***. Potential
***E*$_{1/2}$**. Half-Wave Potential
Eq. Equation
equiv. Equivalent
ET. Electron Transfer
F. Faraday's Constant
Fc. Ferrocene
FE. Faradaic Efficiency
GC. Gas Chromatography *or* Glassy Carbon
h. Hours
H_{AB}. Electronic Coupling
HAT. Hydrogen Atom Transfer
HER. Hydrogen Evolution Reaction
K. Kelvin
KIE. Kinetic Isotope Effect
k_{obs}. Observed Rate Constant
kcal. Kilocalorie
LFER. Linear Free Energy Relationship
LSV. Linear Sweep Voltammetry (or Voltammogram)
λ. Wavelength (or Reorganization Energy)
M. Molar
Me. Methyl
mL. Milliliters
MLCT. Metal-to-Ligand Charge Transfer
MS. Mass Spectrometry
μB. Bohr magneton

^{n}Bu. n-butyl
nm. Nanometers
N_2R. Nitrogen reduction
PCET. Proton-coupled electron transfer
Ph. Phenyl
pK_a. Acid Dissociation Constant
PT. Proton Transfer
R. Gas Constant
RT. Room Temperature
s. Seconds
S. Electron Spin
SI. Supporting Information
SOMO. Singly Occupied Molecular Orbital
T. Temperature
TS. Transition State
THF. Tetrahydrofuran
TON. Turnover Number
UV-Vis. Ultraviolet-visible
V. Volt
XRD. X-ray Diffraction

Chapter 1

INTRODUCTION

1.1 Opening Remarks

Electron transfer reactions appear remarkably simple, at first glance. They are a unique class of reactions in that the rate can be determined from first principles with knowledge of a few parameters—mainly the free energy change and the reorganization energy—as described by Marcus theory.[1] They do not involve the transfer of any atoms. Since nuclear motion is slow on the electron transfer timescale, the motion of atoms in the transition state can be ignored, according to the Born-Oppenheimer approximation.[2]

Yet the mechanisms of electron transfer reactions remain some of nature's most fiercely guarded secrets. For example, the nitrogenase enzyme converts dinitrogen in our atmosphere into ammonia, a bioavailable form which organisms use in the synthesis of amino acids.[3] For each N_2 substrate, nitrogenase performs eight electron transfers and eight proton transfers to yield two equivalents of ammonia and one equivalent of dihydrogen. The mechanistic details of this reaction in the nitrogenase cofactor—the site of N_2 binding, the structure of intermediates, the cleavage of the N-N bond—remain up for debate. Other proteins responsible for biological redox reactions whose mechanisms remain elusive include the oxygen-evolving complex in photosystem II, cytochrome P450, and nitrate reductases.[4–6] These enzymes, along with those in the Calvin cycle,[7] perform electron and proton transfer reactions to interconvert molecules between their atmospheric, oxidized forms (N_2, CO_2, O_2) and bioavailable, reduced forms (NH_3, carbohydrates, H_2O). Proton-coupled electron transfer reactions, catalyzed by a few families of enzymes, are responsible for the conversion of matter between our atmosphere and our biosphere, which are the largest scale chemical reactions on Earth. This thesis examines proton-coupled electron transfer reactions using structure-function studies of molecular models, ultimately to provide context for enzymatic proton-coupled electron transfer mechanisms.

1.2 Background on Proton-coupled Electron Transfer

Proton-coupled electron transfer (PCET) is an electron transfer reaction which occurs along the coordinate of a proton transfer reaction. It is ubiquitous in biological redox processes such as nitrogen fixation, cellular respiration, and photosynthesis,[5,6,8,9] and is increasingly exploited in catalytic methods for chemical synthesis.[10] A few reductive PCET reactions of present interest are shown in **Scheme 1.1**, including dinitrogen reduction to ammonia (N_2R), carbon dioxide reduction to ethylene (CO_2R), and organic small molecule hydrogenation (H_2ation). To kinetically drive these reactions, strong acids and reductants are needed, which can react in the absence of substrate to undergo the hydrogen evolution reaction (HER). The dual mandate of reductive PCET reactions is to maximize the substrate reduction rate while minimizing the HER rate.

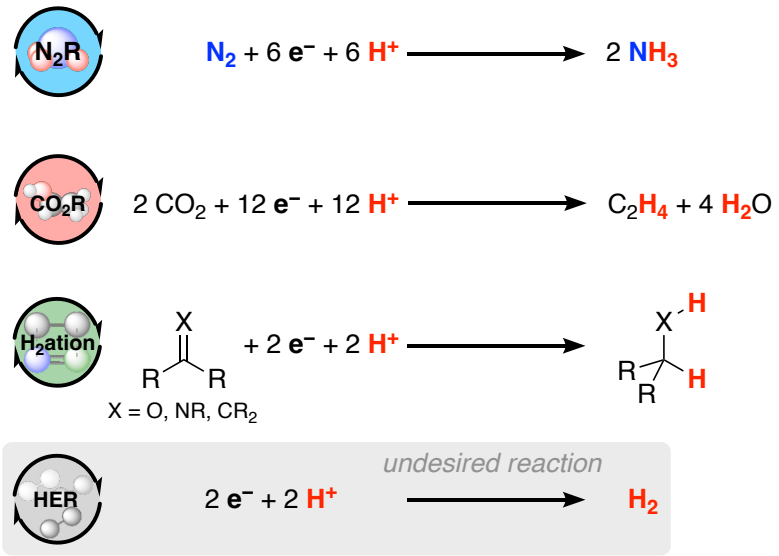

Scheme 1.1 Reductive PCET reactions, including nitrogen reduction, CO_2 reduction, organic small molecule reduction, and hydrogen evolution.

PCET reactions can be formally decomposed into electron transfer (ET) and proton transfer (PT) steps. When these occur in a single elementary step without intermediates, the process is termed concerted proton–electron transfer (CPET) (**Scheme 1.2**).[2,11] By correlating proton and electron motion, CPET pathways can provide a kinetic advantage that avoids high-

energy charged intermediates. Accordingly, H-atom donors that operate through CPET trajectories can enable substrate reduction under milder conditions than stepwise ET–PT or PT–ET pathways, which often require strong acids or reductants to promote the rate-limiting charge transfer step. Thus, CPET is a kinetic strategy to outcompete the hydrogen evolution reaction, but despite its advantages, predicting *a priori* whether a given reagent will react through a concerted or stepwise pathway remains nontrivial.[12]

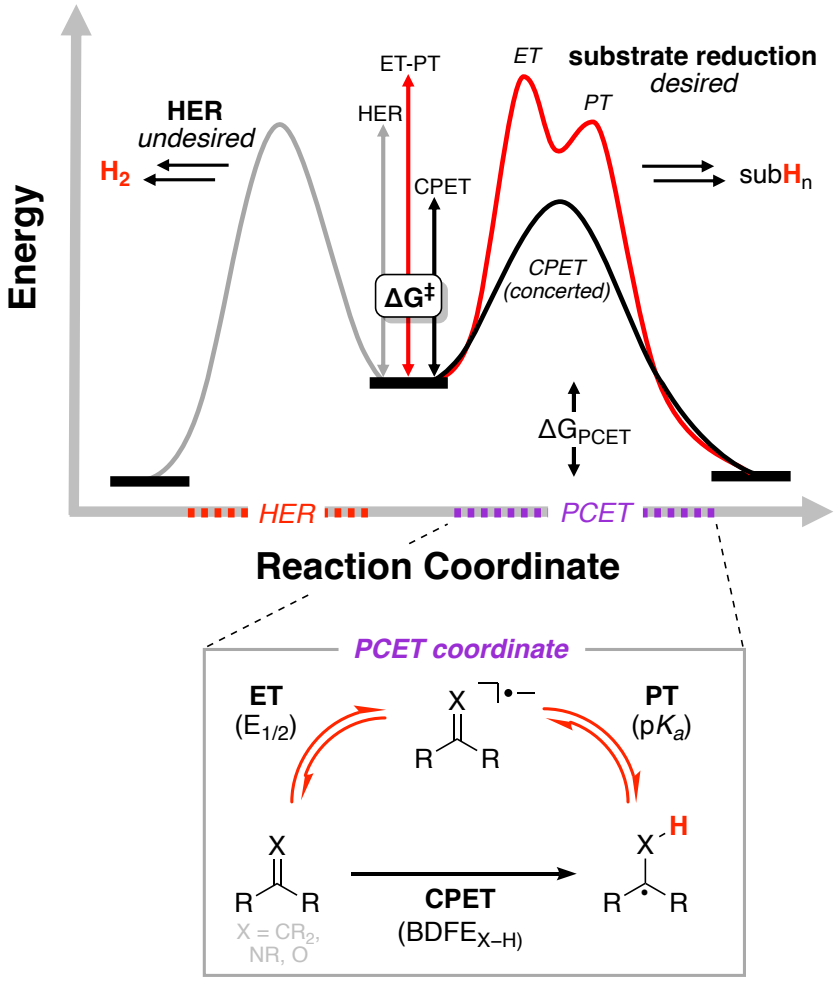

Scheme 1.2 (top) Reaction coordinate diagram for PCET (right) via concerted (black line) or ET–PT (red line) paths as well as HER (left, gray line). (bottom) Pathways for PCET to an unsaturated substrate.

The thermodynamics of PCET are described by the free energy changes for ET and PT, quantified by the half-wave potential ($E_{1/2}$) and acid dissociation constant (pK_a), respectively (**Scheme 1.3**). Together, these experimental observables define the effective bond dissociation free energy ($BDFE_{X–H}$) via the Bordwell equation, which is widely used to rationalize H-atom transfer reactivity (**Scheme 1.3**, where C_g is a solvent-dependent constant).[13] Knowing the $BDFE_{X–H}$ of the breaking and forming bonds ($BDFE_{X–H}$ and $BDFE_{sub–H}$, respectively) allows for the reaction free energy (ΔG_{PCET}) to be determined. In turn, ΔG_{PCET} can be used to identify reasonable ET and PT donors (i.e., sufficiently strong acids and reductants) for a target substrate $BDFE_{X–H}$.

A useful formalism for describing ET and PT equilibria is the square scheme as shown in **Scheme 1.3**. The PT equilibria are shown along the two horizontals while the ET equilibria are shown along the two verticals. The diagonal line from bottom left to top right relates two compounds differing formally by an H-atom and describes the $BDFE_{X–H}$. This type of diagram is essentially a graphical depiction of the Bordwell equation. A useful metric which

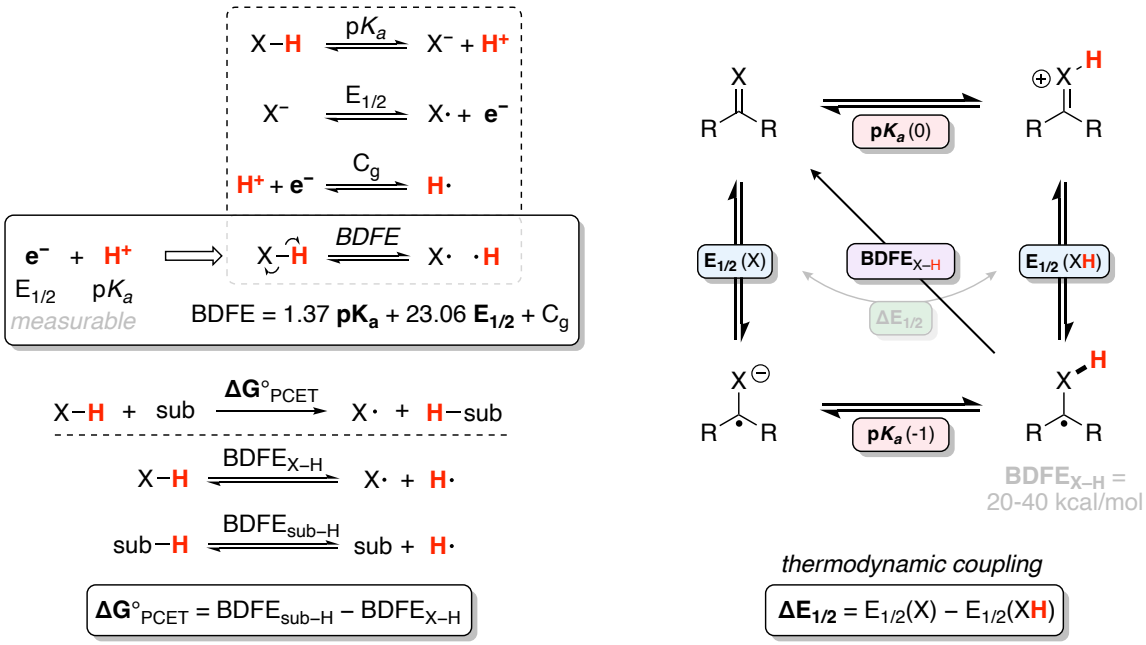

Scheme 1.3 Overview of PCET thermodynamics for PCET to a generic substrate with PT and ET equilibria, the Bordwell equation, the reaction driving force, and the square scheme.

is apparent from the square is the thermodynamic coupling, described as the shift in the redox potential in response to a change in protonation state.[11] This potential shift is equal in free energy to the shift in pK_a upon a change in redox state.

In PCET reactions, the reaction driving force has been widely shown to correlate linearly with the reaction rate, and ΔG_{PCET} is often observed to be the leading-order determinant of the PCET rate. To show how the rate and driving force of a PCET reaction are related using first principles, it is helpful to first consider only the electron transfer component of a PCET reaction. Doing so, one arrives at Marcus theory which quantifies the relationship between the barrier for an electron transfer and driving force:

$$k_{ET} = \frac{|H_{AB}|^2}{\hbar}\sqrt{\frac{\pi}{\lambda k_B T}}\,exp\left(-\frac{(\Delta G°_{ET} + \lambda)^2}{4\lambda k_B T}\right)$$

where k_{ET} is the electron transfer rate, H_{AB} is the electronic coupling, λ is the reorganization energy, $\Delta G°_{ET}$ is the driving force, T is temperature, $\hbar$ is the reduced Planck constant, and k_B is the Boltzmann constant.[14]

Including the proton, (non-adiabatic) PCET is constructed as a perturbation on Marcus theory that adds the proton's effects on driving force, reorganization energy, and coupling terms:

$$k_{PCET} = \sum_{\boldsymbol{u}} \boldsymbol{P_u} \sum_{\boldsymbol{v}} \frac{|H_{AB}|^2 |\boldsymbol{S_{uv}}|^2}{\hbar}\sqrt{\frac{\pi}{\lambda k_B T}}\,exp\left(-\frac{(\Delta \boldsymbol{G}°_{\boldsymbol{PCET}} + \lambda)^2}{4\lambda k_B T}\right)$$

where u and v refer to the vibrational states of the PCET donor and acceptors, P_u is the Boltzmann distribution of the reactant vibrational states, and S_{uv} is the Franck-Condon overlap of the proton vibrational wavefunctions in the reactant and product states.[2] This resembles the equation for Marcus theory, albeit with a few important differences. Foremost, the driving force term, $\Delta G°_{PCET}$, includes the free energy of PT, which can be a substantial perturbation, as electron transfer reactions which are uphill can be made much more favorable by coupling with PT. Similarly, the reorganization energy and the coupling terms in the pre-factor now consider both ET and PT components. The vibronic coupling term has

a steeper distance dependence than the purely electronic coupling term, requiring short proton donor-acceptor distances.

These equations can be implemented both quantitatively to understand mechanism and qualitatively to rationalize behavior. For instance, plotting rate against driving force for PCET, ET, or PT has been shown to be a helpful tool to distinguish the different mechanistic pathways.[2] In a more qualitative sense, this theoretical framework helps connect structural features to rate-contributing terms to aid one's chemical intuition.

1.3 Electrocatalytic Proton-coupled Electron Transfer Mediators

Interest has grown in using renewable electricity as an energy input in chemical synthesis.[15,16] Electrical to chemical energy conversion can be effected by applying a variable potential at a working electrode to induce an ET step in a desired chemical reaction, while a counter reaction, the source or drain of electrons, occurs at another electrode. Current which passes in response to an applied potential can be used to measure the reaction kinetics, ET equilibria, stability of reactive intermediates, and reaction progress.[17] Such electroanalytical methods, like cyclic voltammetry and differential pulse voltammetry, are indispensable tools in the study of ET reactions.

Molecules can mediate ET between an electrode surface and species in the bulk, improving mass transport and avoiding fouling reactions at the electrode surface.[18,19] More importantly, coupling ET and PT reactions can increase the rate of ET, meaning that electrochemical PCET mediators which react via CPET can improve the intrinsic rate for electrolytic reactions and lower the required applied potential.

The strategic application of PCET mediators has led to the discovery of new electrochemical reactions.[12] These mediators facilitate indirect electrochemical processes, where ET at the electrode generates the reactive redox state of the mediator. A few illustrative mediators are shown in **Scheme 1.4**. In the depicted form, the mediator performs the key CPET step such as dihydrogen oxidation to protons,[20] alcohol oxidation to aldehyde,[21] C-H oxidation to allyl

radical,[22] or ketone reduction to ketyl radical.[23] The forming radical can be quenched by further ET or PT, or it can be used in downstream bond-forming reactions.

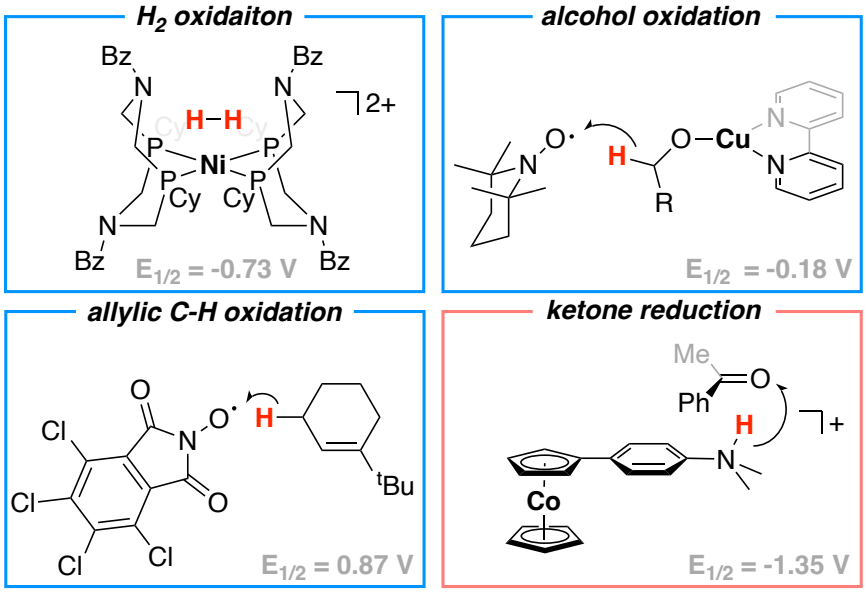

Scheme 1.4 PCET mediators that have been demonstrated as electrocatalysts accompanied by their redox potentials. (*top left*) Amine-appended bis(diphosphine)nickel complex for H_2 oxidation. (*top right*) Aminoxyl radical which abstracts an H-atom from primary alkoxides bound to (2,2'-bipyridine)Cu. (*bottom left*) Phthalimide N-oxyl radical which abstracts an H-atom from allylic C-H bonds. (*bottom right*) Aniline-appended cobaltocene that transfers an H-atom to a variety of unsaturated substrates including acetophenone.

To understand why PCET mediation in electrocatalysis provides a selectivity advantage over direct electrolysis or ET mediation, we can examine one of these PCET mediators, the anilinium-appended cobaltocene shown in the bottom right of Scheme **1.4**, using voltammetry. As mentioned, this compound has been shown to mediate acetophenone reduction. The direct reduction of acetophenone occurs at approximately −2 V (all potentials reported in V vs. ferrocene/ferrocenium redox couple),[24] so in principle, controlled potential coulometry at this potential should produce ketyl anions. However, acid is needed to trap the ketyl anion, which introduces HER as a competing reaction; the acid background is shown as the dashed red trace.[25] HER appears to have an onset potential anodic to the acetophenone

reduction, so HER would be expected to be the dominant reaction at the potential of the substrate. Cobaltocenium might act as an ET mediator since it is a strong reductant and since its potential sits anodic of the HER onset. However, the reduction of acetophenone by cobaltocene is still uphill by roughly 1 V and thus is slow. Attempts at using cobaltocenium as an ET mediator for acetophenone reduction were ineffective.[23]

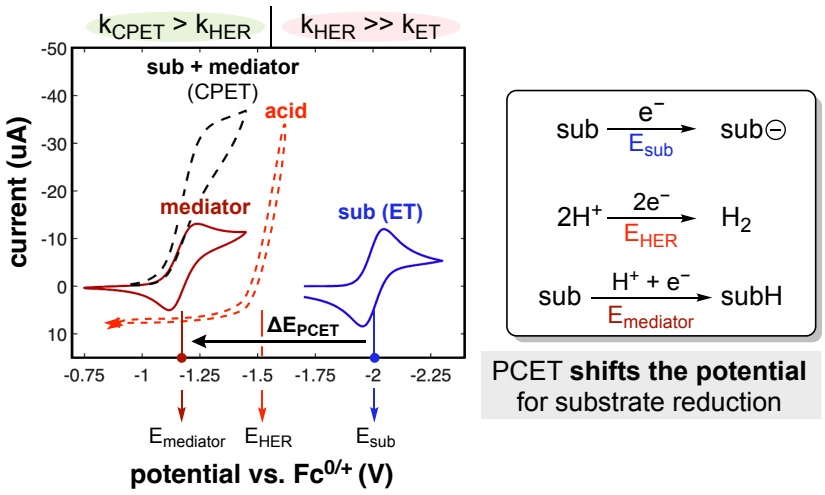

Scheme 1.5 Representative cyclic voltammograms for reductive PCET. The reaction can proceed by direct reduction (purple) or reduction via a PCET mediator (black trace), highlighting that the shift in potential (ΔE_{PCET}) allows the electrolysis to occur at the mediator's potential (E_{med}) where HER is not the kinetically dominant reaction.

Synthetic integration of cobaltocenium and a Brønsted acid, anilinium, enables acetophenone reduction to ketyl at the potential of the cobaltocenium, a shift nearly one volt anodic of the acetophenone potential. At the cobaltocene potential, background HER is attenuated, and substrate reduction is the dominant reaction. The role of an electrochemical PCET mediator is to shift the applied potential required for a redox reaction by changing the nature of the rate-determining chemical step from charge transfer to CPET, as captured by the difference in potential (ΔE_{PCET}) from direct substrate reduction (E_{sub}) to PCET mediation (E_{med}).

The ability of the cobaltocene PCET mediator to shift the electrolysis potential is not specific to acetophenone. Such an effect has also been demonstrated in the reduction of the electron-

deficient C=C bond of fumarates, forming C-H bonds at a potential which is 0.5 V anodic of the substrate redox potential.[26]

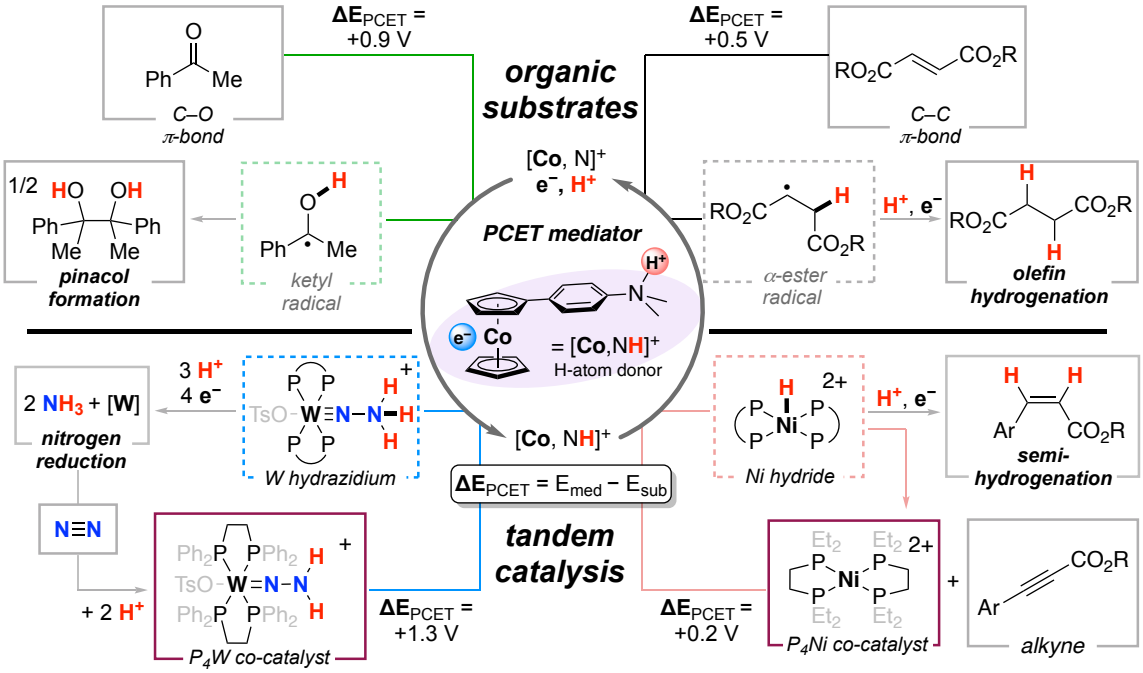

Scheme 1.6 Substrate scope for electrocatalytic PCET mediated by aniline-appended cobaltocene, including acetophenone reduction to pinacol, fumarate reduction to succinate, catalytic N_2 reduction to ammonia, and alkyne hydrogenation to alkene.

Transition metal complexes are also viable substrates with this approach, accomplishing complex tandem transformations. A tandem N_2 reduction reaction was realized using the cobaltocene mediator to perform a key CPET step to a bis(diphosphine)tungsten(hydrazido) complex, forming a hydrazinium which undergoes spontaneous N-N bond cleavage to yield ammonia and tungsten nitride which is also reduced to ammonia.[27] The direct electrolysis of the hydrazido is nearly 1.3 V cathodic of the PCET mediator potential, demonstrating PCET mediation as an especially potent strategy for nitrogen reduction. Another example of tandem catalysis is the hydrogenation of alkynes by Ni-hydride, where the PCET step allows the key Ni-H intermediate to be formed at a 0.2 V milder potential than what is required by direct

electrolysis of the nickel complex.[28] While this seems to be a small change in potential, it avoids reduction of Ni(II) complexes to Ni(0) which are especially prone to HER, improving selectivity of the electrolysis for the desired hydrogenation. Performing the electrolysis at more cathodic potentials leads to a drop in Faradaic efficiency for the hydrogenation product.

These remain some of the only examples of reductive PCET mediation, despite efforts from other groups to achieve the same reactivity on other platforms.[29–33] Through a careful analysis of the aniline-appended cobaltocene, it may be possible to identify the features that make it a uniquely potent platform for PCET mediation, and in doing so offer guidance to others interested in developing novel platforms that expand the field of reductive PCET mediation.

1.4 Proton-coupled Electron Transfer Mediator Design

Electrochemical PCET mediators are an enabling discovery for the development of reductive electrolysis reactions. In response, there has been growing interest in recent years to develop new, and ideally, more reactive and selective PCET mediators.[29–36] To do so, one must identify the building blocks of a PCET mediator and understand how they control its properties:

1) The **redox** unit responsible for *electron transfer*

2) The **acid/base** unit responsible for *proton transfer*

3) The **bridge** unit *connecting* the redox and acid/base units

These units are demarcated on the aniline-appended cobaltocene mediator in **Scheme 1.7**.

Each unit determines a thermodynamic property of the PCET mediator.[11] The redox and acid/base units set the ET and PT driving forces, respectively. The bridging component determines the thermodynamic coupling, but it can also perturb the ET and PT driving forces in such a way that the BDFE remains roughly constant. Though thermodynamic in nature, these properties will affect the PCET rate and potentially the mechanism.[37]

Each unit also influences kinetic properties, but because these properties are not routinely measured and can be challenging to determine, it is presently unclear how much these are changing and to what extent they affect reactivity. The assignment of kinetic terms to each subunit is based on an intuition for structure-function relationships. The redox subunit contributes to the reorganization energy and electronic coupling. The acid/base subunit sets the vibronic coupling. The bridging unit can influence the electronic coupling.

Several of these properties are inherent to the PCET mediator, like the driving force terms and reorganization energy. They are independent of the substrate, but the overall driving force and reorganization energy of a PCET reaction will depend on both that of the mediator and the substrate.[38] The coupling terms, H_{AB} and S_{uv}, will likely depend on the substrate, although it is possible that some mediators tend to have stronger coupling than others across multiple classes of substrates.

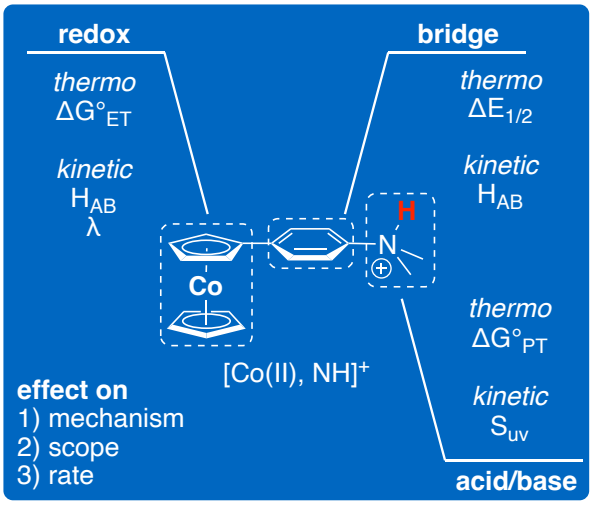

Scheme 1.7 Blueprint for the construction of a PCET mediator, delineating how each subunit may perturb thermodynamic and kinetic properties of the compound.

1.5 Chapter Overview

The mission of this thesis is to strengthen the intuition for PCET mediator design through structural perturbations, thermodynamic analysis, and kinetic studies so that combinations of redox, bridge, and acid/base subunits can be more intentionally chosen. Each of the chapters can be mapped onto the PCET mediator blueprint as shown in Scheme 1.8. Chapters 2-3 explore substituting the cobaltocene redox unit with a main group reductant, the *ortho*-carborane radical anion. Chapter 4 describes the perturbation of the bridging group between a cobaltocene reductant and anilinium acid. Chapter 5 investigates substituting the anilinium acid with phosphonium. Together, these chapters explore a broad structural chemical space on a unified PCET mediator platform.

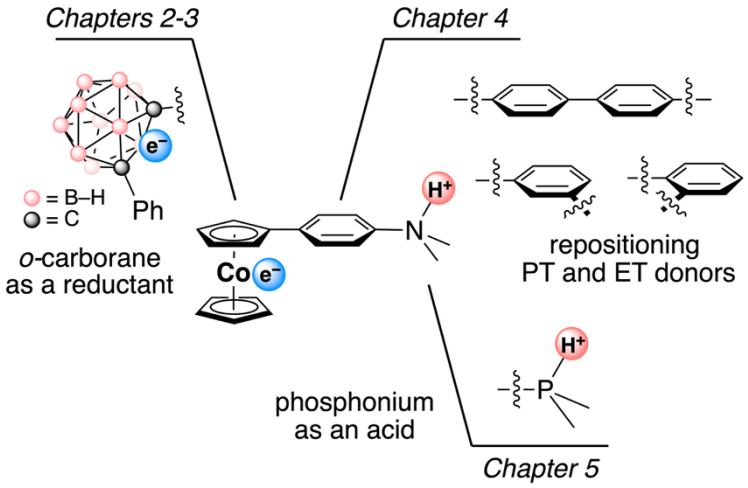

Scheme 1.8 Chapter overview.

1.6 References

1 Marcus, R. A.; Sutin, N. Electron Transfers in Chemistry and Biology. *Biochim. Biophys. Acta BBA - Rev. Bioenerg.* **1985**, *811* (3), 265–322. DOI: 10.1016/0304-4173(85)90014-X.

2 Tyburski, R.; Liu, T.; Glover, S. D.; Hammarström, L. Proton-Coupled Electron Transfer Guidelines, Fair and Square. *J. Am. Chem. Soc.* **2021**, *143* (2), 560–576. DOI: 10.1021/jacs.0c09106.

3 Seefeldt, L. C.; Yang, Z. Y.; Lukoyanov, D. A.; Harris, D. F.; Dean, D. R.; Raugei, S.; Hoffman, B. M. Reduction of Substrates by Nitrogenases. *Chem. Rev.* **2020**, *120* (12), 5082–5106. DOI: 10.1021/acs.chemrev.9b00556.

4 Kisker, C.; Schindelin, H.; Rees, D. C. MOLYBDENUM-COFACTOR–CONTAINING ENZYMES: Structure and Mechanism. *Annu. Rev. Biochem.* **1997**, *66* (Volume 66, 1997), 233–267. DOI: 10.1146/annurev.biochem.66.1.233.

5 Tommos, C.; Babcock, G. T. Proton and Hydrogen Currents in Photosynthetic Water Oxidation. *Biochim. Biophys. Acta BBA - Bioenerg.* **2000**, *1458* (1), 199–219. DOI: 10.1016/S0005-2728(00)00069-4.

6 Kaila, V. R. I.; Verkhovsky, M. I.; Wikström, M. Proton-Coupled Electron Transfer in Cytochrome Oxidase. *Chem. Rev.* **2010**, *110* (12), 7062–7081. DOI: 10.1021/cr1002003.

7 Shively, J. M.; Keulen, G. van; Meijer, W. G. SOMETHING FROM ALMOST NOTHING: Carbon Dioxide Fixation in Chemoautotrophs. *Annu. Rev. Microbiol.* **1998**, *52* (Volume 52, 1998), 191–230. DOI: 10.1146/annurev.micro.52.1.191.

8 Dempsey, J. L.; Winkler, J. R.; Gray, H. B. Proton-Coupled Electron Flow in Protein Redox Machines. *Chem. Rev.* **2010**, *110* (12), 7024–7039. DOI: 10.1021/cr100182b.

9 Hoffman, B. M.; Lukoyanov, D.; Yang, Z.-Y.; Dean, D. R.; Seefeldt, L. C. Mechanism of Nitrogen Fixation by Nitrogenase: The Next Stage. *Chem. Rev.* **2014**, *114* (8), 4041–4062. DOI: 10.1021/cr400641x.

10 Murray, P. R. D.; Cox, J. H.; Chiappini, N. D.; Roos, C. B.; McLoughlin, E. A.; Hejna, B. G.; Nguyen, S. T.; Ripberger, H. H.; Ganley, J. M.; Tsui, E.; Shin, N. Y.; Koronkiewicz, B.; Qiu, G.; Knowles, R. R. Photochemical and Electrochemical Applications of Proton-Coupled Electron Transfer in Organic Synthesis. *Chem. Rev.* **2022**, *122* (2), 2017–2291. DOI: 10.1021/acs.chemrev.1c00374.

11 Agarwal, R. G.; Coste, S. C.; Groff, B. D.; Heuer, A. M.; Noh, H.; Parada, G. A.; Wise, C. F.; Nichols, E. M.; Warren, J. J.; Mayer, J. M. Free Energies of Proton-Coupled Electron Transfer Reagents and Their Applications. *Chem. Rev.* **2022**, *122* (1), 1–49. DOI: 10.1021/acs.chemrev.1c00521.

12 Peters, J. C. Advancing Electrocatalytic Nitrogen Fixation: Insights from Molecular Systems. *Faraday Discuss.* **2023**, *243* (0), 450–472. DOI: 10.1039/D3FD00017F.

13 Bordwell, F. G.; Cheng, J. Pei.; Harrelson, J. A. Homolytic Bond Dissociation Energies in Solution from Equilibrium Acidity and Electrochemical Data. *J. Am. Chem. Soc.* **1988**, *110* (4), 1229–1231. DOI: 10.1021/ja00212a035.

14 Marcus, R. A.; Sutin, N. Electron Transfers in Chemistry and Biology. *BBA Rev. Bioenerg.* **1985**, *811* (3), 265–322. DOI: 10.1016/0304-4173(85)90014-X.

15 Oliver, Z. J.; Abrams, D. J.; Cardinale, L.; Chen, C.-J.; Beutner, G. L.; Caille, S.; Cohen, B.; Deng, L.; Diwan, M.; Frederick, M. O.; Harper, K.; Hawkins, J. M.; Lehnherr, D.; Lucky, C.; Meyer, A.; Noh, S.; Nunez, D.; Quasdorf, K.; Teli, J.; Stahl, S. S.; Schreier, M. Scaling Organic Electrosynthesis: The Crucial Interplay between Mechanism and Mass Transport. *ACS Cent. Sci.* **2025**, *11* (4), 528–538. DOI: 10.1021/acscentsci.4c01733.

16 Lehnherr, D.; Chen, L. Overview of Recent Scale-Ups in Organic Electrosynthesis (2000–2023). *Org. Process Res. Dev.* **2024**, *28* (2), 338–366. DOI: 10.1021/acs.oprd.3c00340.

17 Rafiee, M.; Abrams, D. J.; Cardinale, L.; Goss, Z.; Romero-Arenas, A.; Stahl, S. S. Cyclic Voltammetry and Chronoamperometry: Mechanistic Tools for Organic Electrosynthesis. *Chem. Soc. Rev.* **2024**, *53* (2), 566–585. DOI: 10.1039/D2CS00706A.

18 Yan, M.; Kawamata, Y.; Baran, P. S. Synthetic Organic Electrochemical Methods Since 2000: On the Verge of a Renaissance. *Chem. Rev.* **2017**, *117* (21), 13230–13319. DOI: 10.1021/acs.chemrev.7b00397.

19 Malapit, C. A.; Prater, M. B.; Cabrera-Pardo, J. R.; Li, M.; Pham, T. D.; McFadden, T. P.; Blank, S.; Minteer, S. D. Advances on the Merger of Electrochemistry and Transition Metal Catalysis for Organic Synthesis. *Chem. Rev.* **2022**, *122* (3), 3180–3218. DOI: 10.1021/acs.chemrev.1c00614.

20 Rakowski Dubois, M.; Dubois, D. L. Development of Molecular Electrocatalysts for CO2 Reduction and H2 Production/Oxidation. *Acc. Chem. Res.* **2009**, *42* (12), 1974–1982. DOI: 10.1021/ar900110c.

21 Badalyan, A.; Stahl, S. S. Cooperative Electrocatalytic Alcohol Oxidation with Electron-Proton-Transfer Mediators. *Nature* **2016**, *535* (7612), 406–410. DOI: 10.1038/nature18008.

22 Horn, E. J.; Rosen, B. R.; Chen, Y.; Tang, J.; Chen, K.; Eastgate, M. D.; Baran, P. S. Scalable and Sustainable Electrochemical Allylic C–H Oxidation. *Nature* **2016**, *533* (7601), 77–81. DOI: 10.1038/nature17431.

23 Chalkley, M. J.; Garrido-Barros, P.; Peters, J. C. A Molecular Mediator for Reductive Concerted Proton-Electron Transfers via Electrocatalysis. *Science* **2020**, *369* (6505), 850–854. DOI: 10.1126/science.abc1607.

24 Zhang, J.; Zhang, L.; Xie, W.; Chen, M.; Zhang, C.; Qin, Y.; Zhao, J.; Wang, F.; Liu, Z.-Q. Electrochemical Allylation of Aldehydes and Ketones with Allylic Alcohols. *Green Chem.* **2024**, *26* (12), 7002–7006. DOI: 10.1039/D4GC01838A.

25 McCarthy, B. D.; Martin, D. J.; Rountree, E. S.; Ullman, A. C.; Dempsey, J. L. Electrochemical Reduction of Brønsted Acids by Glassy Carbon in Acetonitrile—Implications for Electrocatalytic Hydrogen Evolution. *Inorg. Chem.* **2014**, *53* (16), 8350–8361. DOI: 10.1021/ic500770k.

26 Derosa, J.; Garrido-Barros, P.; Peters, J. C. Electrocatalytic Reduction of C–C π-Bonds via a Cobaltocene-Derived Concerted Proton–Electron Transfer Mediator: Fumarate Hydrogenation as a Model Study. *J. Am. Chem. Soc.* **2021**, *143* (25), 9303–9307. DOI: 10.1021/jacs.1c03335.

27 Garrido-Barros, P.; Derosa, J.; Chalkley, M. J.; Peters, J. C. Tandem Electrocatalytic N2 Fixation via Proton-Coupled Electron Transfer. *Nature* **2022**, *609* (7925), 71–76. DOI: 10.1038/s41586-022-05011-6.

28 Derosa, J.; Garrido-Barros, P.; Li, M.; Peters, J. C. Use of a PCET Mediator Enables a Ni-HER Electrocatalyst to Act as a Hydride Delivery Agent. *J. Am. Chem. Soc.* **2022**, *144* (43), 20118–20125. DOI: 10.1021/jacs.2c09786.

29 Mukherjee, J.; Ostermann, N.; Pecak, J.; Otte, M.; Podewitz, M.; Siewert, I. Mechanistic Studies of the Proton-Coupled Electron Transfer Reactivity of a Cobalt Complex with a Proton-Responsive PNP Pincer-Type Ligand. *Inorg. Chem.* **2025**, *64* (28), 14466–14474. DOI: 10.1021/acs.inorgchem.5c01792.

30 Dey, S.; Masero, F.; Brack, E.; Fontecave, M.; Mougel, V. Electrocatalytic Metal Hydride Generation Using CPET Mediators. *Nature* **2022**, *607* (7919), 499–506. DOI: 10.1038/s41586-022-04874-z.

31 Won, C.; Kwon, S.; Kim, D.; Baek, Y. Orchestrating the Semiquinone Stability for Catalytic Proton-Coupled Electron Transfer. *J. Am. Chem. Soc.* **2026**, *148* (8), 8761–8771. DOI: 10.1021/jacs.5c21171.

32 Mitsumoto, T.; Nakamura, T.; Tanaka, H.; Yoshizawa, K.; Nishibayashi, Y. Cooperative Ammonia Formation Catalyzed by Molybdenum and Samarium Complexes. *Angew. Chem. Int. Ed.* **2025**, *64* (32), e202507061. DOI: 10.1002/anie.202507061.

33 Kuriyama, S.; Zhang, Y.; Tanaka, H.; Konomi, A.; Egi, A.; Yoshizawa, K.; Nishibayashi, Y. Synthesis and Reactivity of Iron-Oxocyclohexadienyl Complexes toward Proton-Coupled Electron Transfer. *Organometallics* **2024**, *43* (21), 2736–2746. DOI: 10.1021/acs.organomet.4c00286.

34 Otsuka, H.; Arashiba, K.; Nakamura, T.; Tanaka, H.; Yoshizawa, K.; Nishibayashi, Y. Synthesis of Cobaltocenes Bearing 4-(2,6-Dimethylpyridin-1-Ium-4-Yl)Phenyl Moiety and Their Stoichiometric and Catalytic Reactivity toward Ammonia Formation. *Organometallics* **2026**. DOI: 10.1021/acs.organomet.5c00492.

35 Jiang, N.; Darù, A.; Kunstelj, Š.; Vitillo, J. G.; Czaikowski, M. E.; Filatov, A. S.; Wuttig, A.; Gagliardi, L.; Anderson, J. S. Catalytic, Spectroscopic, and Theoretical Studies of Fe4S4-Based Coordination Polymers as Heterogenous Coupled Proton–Electron Transfer Mediators for Electrocatalysis. *J. Am. Chem. Soc.* **2024**, *146* (17), 12243–12252. DOI: 10.1021/jacs.4c03726.

36 Galvin, C. M.; Marron, D. P.; Dressel, J. M.; Waymouth, R. M. Coordination-Induced Bond Weakening and Electrocatalytic Proton-Coupled Electron Transfer of a Ruthenium Verdazyl Complex. *Inorg. Chem.* **2024**, *63* (2), 954–960. DOI: 10.1021/acs.inorgchem.3c02775.

37 Tyburski, R.; Hammarström, L. Strategies for Switching the Mechanism of Proton-Coupled Electron Transfer Reactions Illustrated by Mechanistic Zone Diagrams. *Chem. Sci.* **2022**, *13* (1), 290–301. DOI: 10.1039/d1sc05230f.

38 Mayer, J. M. Simple Marcus-Theory-Type Model for Hydrogen-Atom Transfer/Proton-Coupled Electron Transfer. *J. Phys. Chem. Lett.* **2011**, *2* (12), 1481–1489. DOI: 10.1021/jz200021y.

Chapter 2

A Carborane-derived Proton-coupled Electron Transfer Reagent

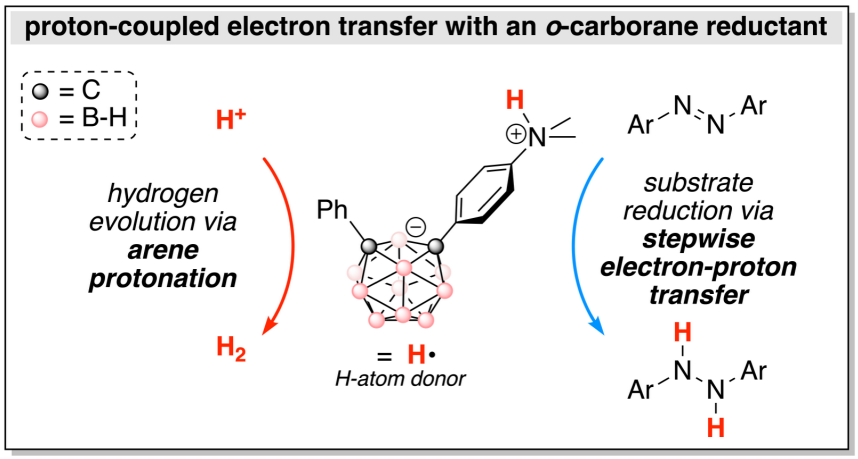

Adapted from:

Adillon, E. H.; Peters, J. C.

J. Am. Chem. Soc. **2024**, 147, 30204-30211

DOI: 10.1021/jacs4c09007

2.1 Introduction

Proton-coupled electron transfer (PCET) reagents can facilitate challenging substrate reductions via pathways that are efficient compared with stepwise ET-PT pathways.[1] Such reagents have been demonstrated to be useful tools for selective hydrogen atom delivery (or abstraction) with organic and inorganic substrates.[2]

Systems that mediate reductive PCET transformations have largely utilized the well-behaved redox properties of transition metal and lanthanide complexes **(Scheme 2.1A)**.[3,4,5,6,7] To access PCET reactivity, the reduced form of these systems (e.g., Co(II) or Sm(II)) can be coupled to a Brønsted acid via covalent linkage, coordination, or substrate pre-organization to form a reactive net hydrogen atom equivalent that can be delivered to substrates. Redox potential and acid pK_a govern the effective X−H bond dissociation free energy (BDFE$_{X–H}$, X = C, N, O) as in **Eq 1**,[8] allowing H-atom reactivity to be measured and tuned via the individual proton and electron transfer equilibria (pK_a and E°, respectively, where C_g is a solvent-dependent constant).

$$\textbf{(Eq 1)}\ \mathrm{BDFE_{eff}} = 23.06\ \mathbf{E°} + 1.37\ \mathbf{p}\boldsymbol{K}_\mathbf{a} + C_g$$

While weakening the BDFE$_{X–H}$ can promote net H-atom transfer reactivity, it can in turn predispose a reagent towards the hydrogen evolution reaction (HER); the latter is thermodynamically favorable when the BDFE$_{X–H}$ is less than half that of the dihydrogen bond (BDFE$_{H–H}$ = 104 kcal/mol).[3] Strategies for mitigating HER are central to reductive PCET reagent design.[4,9]

One strategy for promoting PCET reactions in a fashion compatible with electrocatalysis involves covalent tethering of a Brønsted acid to a reductant, as illustrated in **Scheme 2.1B**.[10] Our lab has shown that attaching an anilinium fragment to cobaltocene (left) yields Cp**Co**Cp^{NH+} (right), a complex with a weak BDFE$_{N–H}$. This species operates as an electrocatalytic PCET (*e*PCET) mediator under controlled potential electrolysis conditions, effecting ketone and olefin reductions,[11] ketyl-olefin cyclizations,[12] and with transition metal co-catalysts, alkyne semi-hydrogenation[13] and nitrogen reduction to ammonia.[14] The turnover-limiting PCET step can be concerted, as evidenced by zero order acid concentration dependence on the catalytic rate but still a substantial primary kinetic isotope effect (KIE).

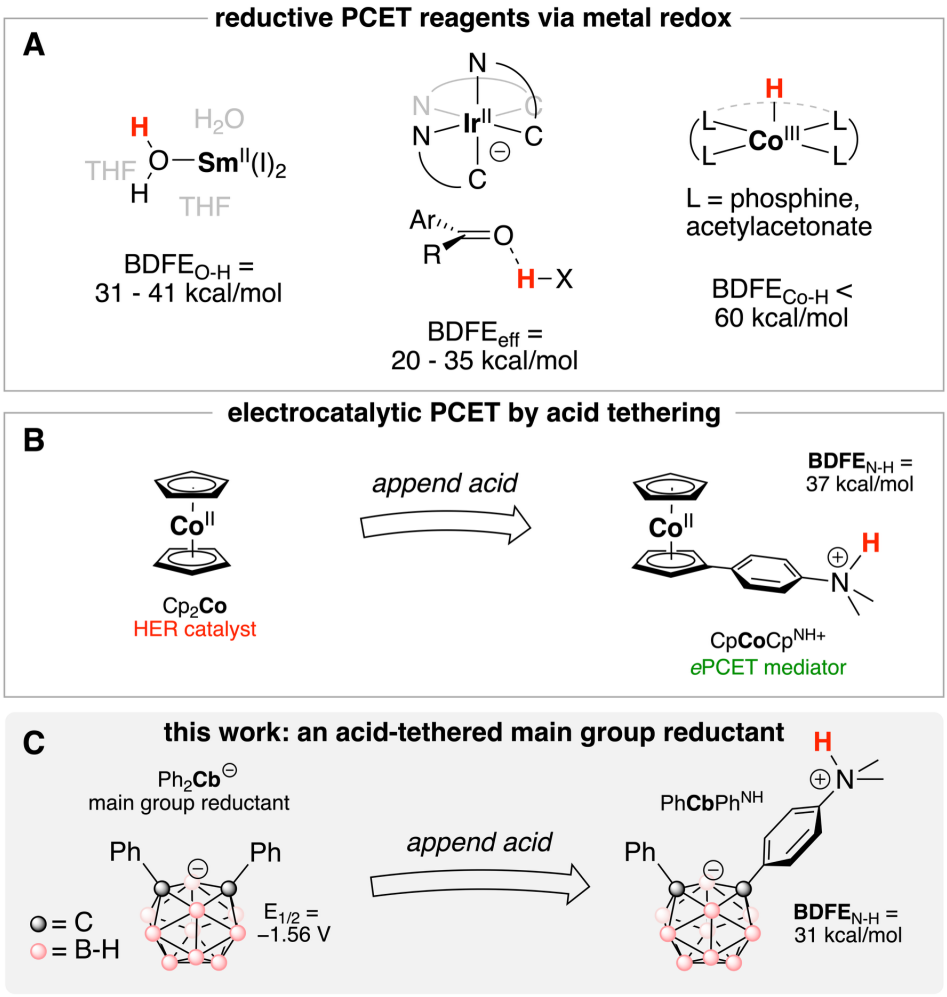

Scheme 2.1 (A) Widely Adopted PCET Reagents Derived from Metal Reductants; (B) An Aniline-Appended Cobaltocene *e*PCET Mediator; (C) Exploring the Reactivity of a Main-Group Reductant with An Appended Brønsted-Acid

Given the observed PCET reactivity of aniline-modified cobaltocene, we sought to explore an alternative system wherein the cobaltocene redox relay is replaced by another redox subunit, focusing herein on a main group cluster. We selected the *o*-carborane platform for its synthetic malleability and its compatibility with strongly reducing anionic states.[15,16] In particular, *o*-carboranes—icosahedral clusters comprised of ten boron atoms and two adjacent carbon atoms—are reported to have two one-electron redox features between −1 V and −3 V (all potentials reported in acetonitrile referenced to the ferrocene/ferrocenium couple).[17] Whereas the potentials of *o*-carboranes can be modulated by over 2 V by changing the carbon substituents, the use of reduced

carboranes as stoichiometric reductants (whether in ET or PCET steps) has not to our knowledge been previously explored.

2.2 Results and Discussion

Structure of Reduced Carboranes. As an entry point for reductive carborane chemistry, we first determined the structures of diaryl-*o*-carboranes following one- and two-electron reduction. Samples of the anionic and dianionic compounds were generated according to prior reports by reducing diphenyl-*o*-carborane (Ph_2**Cb**) with potassium metal; one equivalent yields the radical anion (Ph_2**Cb**$^{-}$) and excess affords the closed-shell dianion (Ph_2**Cb**$^{2-}$).[18] The radical nature of [Ph_2**Cb**]K is supported by Evans method and a CW-EPR spectrum featuring a broad resonance with no resolvable hyperfine interactions centered at g = 2.026 (**Figure A36**). [Ph_2**Cb**]K_2 has diagnostic ^{1}H, ^{11}B, and ^{13}C NMR signals consistent with the formation of a closed-shell species (**Figure A2-A4**).

The mono- and dianions were characterized by single crystal XRD as their respective K(18-crown-6) salts (crown = c hereafter). The structure of [Ph_2**Cb**]K(18-c-6) is shown in **Figure 2.1** (top) with the neutral Ph_2**Cb** for reference and counterions omitted for clarity.[19] Comparing these two structures, the largest change is a lengthening of the C−C bond between the two adjacent carbon atoms of the icosahedron core (which lengthens from 1.733 Å to 2.374 Å). In addition, the C−C bond length between the core carbon atoms and the aryl *ipso*-atoms shortens considerably (1.504 Å to 1.470 Å).[20] The lengthening of C−C bond is consistent with previous theoretical studies and related structures.[15,21,22,23,24,25,26,27]

The structural parameters suggest that the SOMO is chiefly comprised of the tangential p-orbitals of the two adjacent carbon atoms of the cluster (**Figure 2.1**, bottom). The cluster carbon atoms engage in a σ* interaction leading to the observed breaking of the C−C bond upon reduction to the radical anion. Because the carbon p-orbitals are aligned with the aryl π* orbitals, they form a partial π bond that distributes negative charge away from the *o*-carborane core. For the dianionic Ph_2**Cb**$^{2-}$, the structure follows the Wade's rules prediction of a *nido*-icosahedron (**Figure A52**).[28]

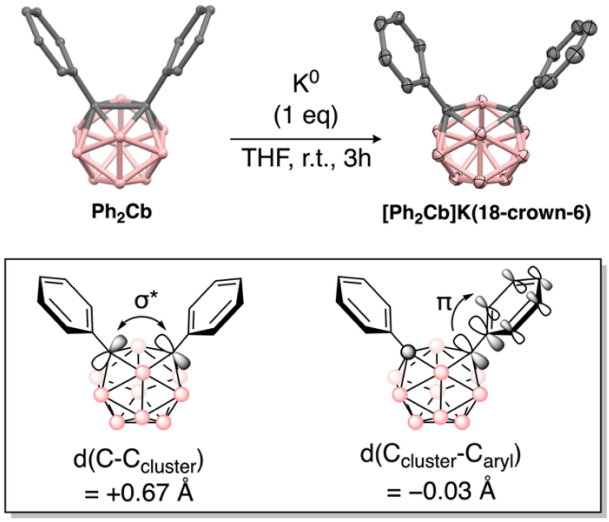

Figure 2.1 X-ray Crystal Structures of **Ph_2Cb** and **[Ph_2Cb]K(18-crown-6)** with a cartoon of the SOMO highlighting its σ* and π bonding character.

Thermochemistry of PhCbPh^{NH}. Through incorporation of a Brønsted base on the aryl substituents, we envisaged forming a compound which could be reduced at the carborane core and protonated at the base to yield a net H-atom donor. 1-(4-N,N-dimethylaniline)-2-phenyl-*o*-carborane (Ph**Cb**Ph^{N}) is a previously reported carborane which contains an appended base and was readily prepared.[15] Chemical reduction of Ph**Cb**Ph^{N} with one equivalent of potassium metal and two equivalents of benzo-15-c-5 yielded the radical anion as red needles. XRD analysis provides a structure featuring an icosahedron core structure similar to Ph_2**Cb**$^{-}$ (**Figure 2.2A**).

UV-vis spectroscopy was used to study the protonation of [Ph**Cb**Ph^{N}]$^{-}$ to furnish Ph**Cb**Ph^{NH}. [Ph**Cb**Ph^{N}]K(b-15-c-5)$_2$ (blue trace) in THF solution cooled to −80 °C was protonated by addition of up to one equivalent of 4-cyanoanilinium triflate ([$^{4\text{-CN}}$PhNH$_3$]OTf), forming a new species assigned as Ph**Cb**Ph^{NH} (**Figure 2.2B**). Addition of triazabicyclodecene (TBD) as base produces a spectrum consistent with Ph**Cb**Ph^{N-}, suggesting that the protonation is reversible (**Figure 2.2B, *inset***). Addition of the same acid to Ph_2**Cb**$^{-}$ does not yield any new features, suggesting that incorporation of the aniline moiety allows for reversible protonation of the carborane species (**Figure A68**).

Next, we set out to determine the effective BDFE$_{N-H}$ of Ph**Cb**Ph^{NH} by measuring the PT and ET equilibria depicted along the edges of the square scheme in **Figure 2.2A**. Ph**Cb**Ph^{N} was analyzed by

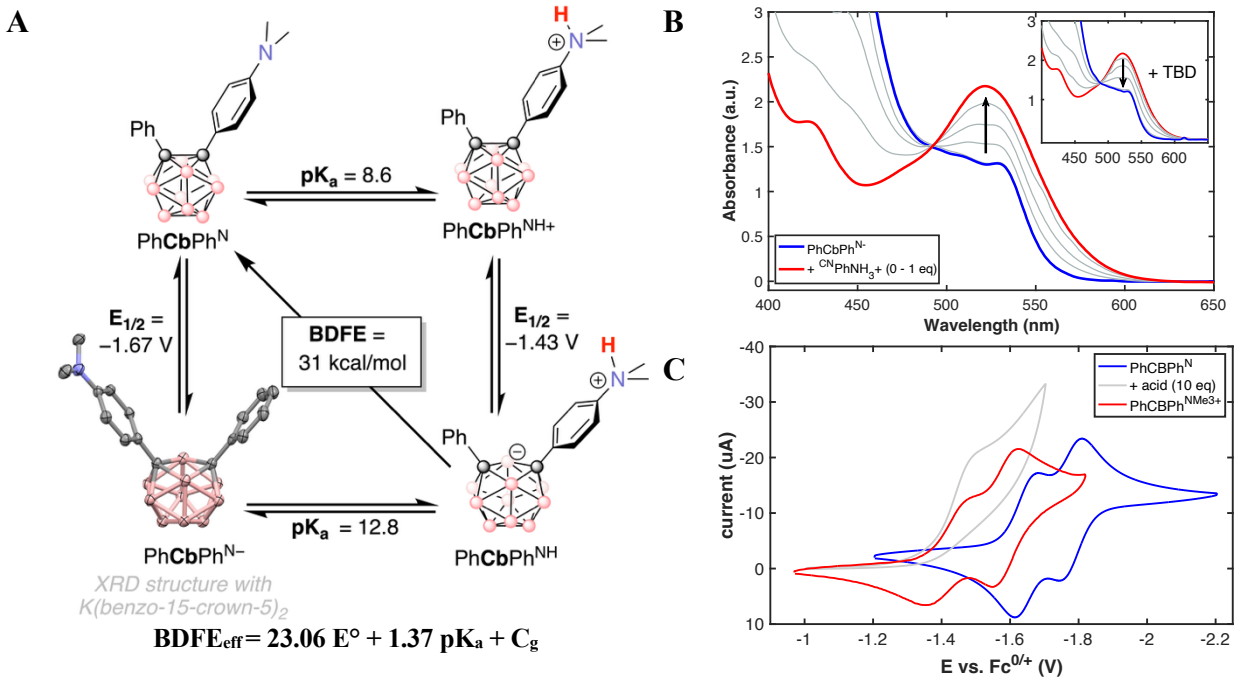

Figure 2.2 (A) square scheme of Ph**Cb**Ph^{NH} with the X-ray crystal structure of [Ph**Cb**Ph^{N}]K(b-15-c-5)$_2$ (bottom left). **(B)** UV-vis spectra of [Ph**Cb**Ph^{N}]K(b-15-c-5)$_2$ (1 mM) in THF at −80 °C with [$^{4\text{-CN}}$PhNH$_3$]OTf titrant (0-1 eq in 0.2 eq increments) and (*inset*) TBD titrant (0-1 eq in 0.2 eq increments). **(C)** Cyclic voltammograms of Ph**Cb**Ph^{N} (1 mM, *blue*) with [$^{4\text{ CN}}$PhNH$_3$]OTf (10 mM, *gray*) and [Ph**Cb**Ph^{NMe3}]OTf (1mM, *red*) in acetonitrile with ^{n}Bu$_4$PF$_6$ (200 mM) supporting electrolyte. The scans are swept cathodic, then anodic at 100 mV/s.

cyclic voltammetry to determine its reduction potential and the shift in potential upon protonation (**Figure 2.2C**). First, the voltammogram of Ph**Cb**Ph^{N} (blue trace) shows two reversible features at −1.67 V and −1.80 V corresponding to the formation of the radical anionic and dianionic carboranes. Upon addition of acid to generate Ph**Cb**Ph^{NH}, we observe an anodically-shifted irreversible multi-electron wave (gray trace), suggesting that formation of Ph**Cb**Ph^{NH} is coupled to a fast chemical step. To estimate the reduction potential of [Ph**Cb**Ph^{NH}]$^{+/0}$, the N-methylated analog 1-(4-N,N,N-trimethylanilinium)-2-phenyl-*o*-carborane triflate ([Ph**Cb**Ph^{NMe3}]OTf) was prepared and isolated by addition of methyl triflate to Ph**Cb**Ph^{N}. Its voltammogram (red trace) contains two reversible features at −1.43 V and −1.59 V which are anodically shifted relative to Ph**Cb**Ph^{N}. Since the onset

of the cathodic waves corresponding to reduction of [Ph**C**b**B**Ph^{NMe3}]$^{+/0}$ and [Ph**C**b**B**Ph^{NH}]$^{+/0}$ overlay, we deduce that the [Ph**C**b**B**Ph^{NMe3}]$^{+/0}$ $E_{1/2}$ is a good approximation of the [Ph**C**b**B**Ph^{NH}]$^{+/0}$ $E_{1/2}$.

The pK_a of Ph**C**b**B**Ph^{NH+} was determined by titration with 2-chloroanilinium triflate in CD_3CN and quantification of the equilibrium constant by ^{1}H NMR spectroscopy (see **S8**). The pK_a was measured to be 8.6—much lower than N,N-dimethylaniline (pK_a = 11.5)—demonstrating the strong electron-withdrawing nature of neutral *o*-carborane.[29]

With the [Ph**C**b**B**Ph^{NH}]$^{+/0}$ $E_{1/2}$ and the Ph**C**b**B**Ph^{NH+} pK_a in hand, the Ph**C**b**B**Ph^{NH} $BDFE_{N–H}$ can be estimated to be 31 kcal/mol. This is a very low $BDFE_{N–H}$, especially for a non-metal compound. To our knowledge, only one non-metal compound, the nicotinamide radical cation, has a weaker experimentally measured value for a condensed phase element-hydrogen BDFE ($BDFE_{C–H}$ = 26 kcal/mol).[3,30,31] Akin to the nicotinamide radical cation, the *o*-carborane's driving force for H-atom loss can be linked to restoring aromaticity upon oxidation by reforming the icosahedral core and breaking $C_{cluster}$−C_{aryl} π-bond. Relatedly, restoring aromaticity has been invoked by our laboratory to rationalize the very weak C−H bond of ring-protonated cobaltocenes.[32]

Reactivity of PhC**b**B**Ph^{NH}.** The weak $BDFE_{N–H}$ of Ph**C**b**B**Ph^{NH} indicates that it should serve as a potent H-atom donor but may also be disposed to HER. To probe its reactivity, we first studied its stability in solution in the absence of a substrate. Ph**C**b**B**Ph^{NH} was generated in THF at −40 °C by protonation of [Ph**C**b**B**Ph^{N}]K(b-15-c-5)$_2$ with [Ph$_3$PH]OTf. Its concentration was monitored by UV-Vis spectroscopy (**Figure A71**). The behavior of its absorbance at 550 nm reflects first-order decay with $t_{1/2}$ = 7.9 min which we ascribe to HER (*vide infra*).

Next, we studied the reactivity of Ph**C**b**B**Ph^{NH} towards model organic substrates. To do so, Ph**C**b**B**Ph^{NH} was pre-formed by mixing [Ph**C**b**B**Ph^{N}]K(b-15-c-5)$_2$ and [Ph$_3$PH]OTf in THF solution at −40 °C, followed by substrate addition. We chose the substrates acetophenone and diphenylfumarate as they had been previously shown to react with Cp**C**o**B**Cp^{NH+}, in addition to azoarenes which may also be reduced via PCET pathways.[33,34,35] The results are summarized in **Scheme 2.2**. In each case, the only observed boron-containing product by ^{11}B NMR spectroscopy is Ph**C**b**B**Ph^{N}, as expected if Ph**C**b**B**Ph^{NH} serves as a net H-atom donor (**Figure A13**).

Scheme 2.2 Reduction of model organic substrates by Ph**Cb**Ph^{NH} plotted as a function of their calculated reduction potential

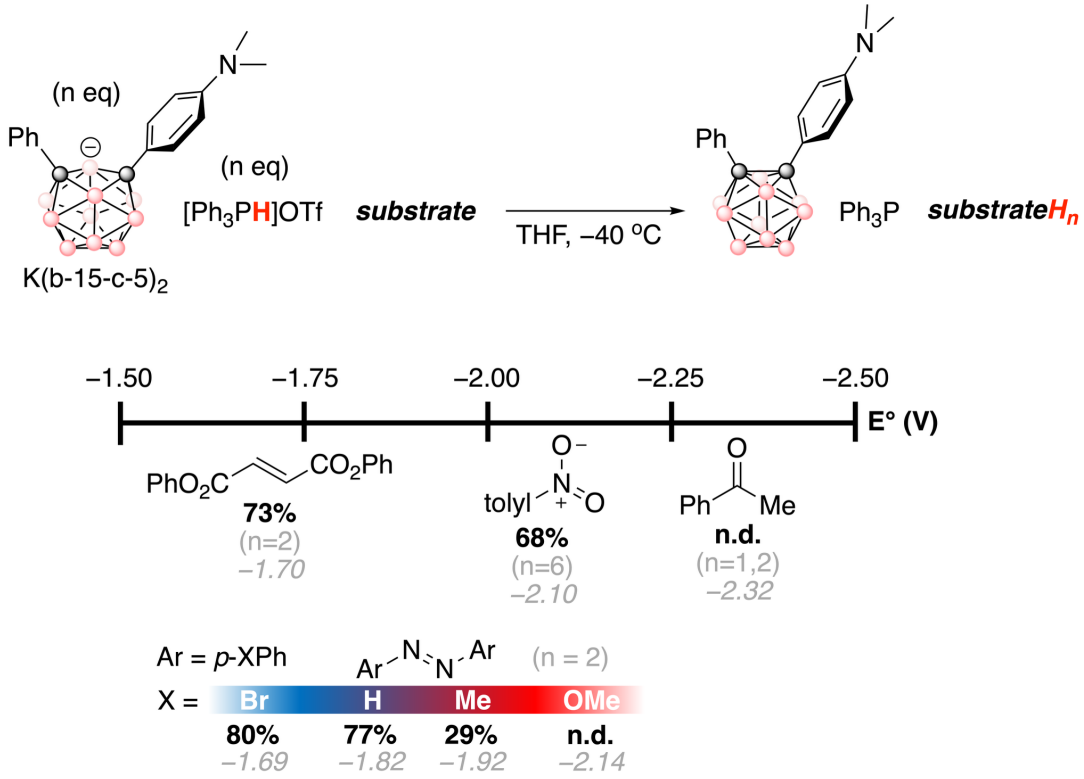

Diphenylfumarate, nitrotoluene, and azobenzene were reduced in good yield, suggesting that the transfer of reducing equivalents from Ph**Cb**Ph^{NH} to these substrates can outcompete HER. However, for acetophenone and electron-rich azoarenes (Ar = *p*-tolyl, *p*-MeOPh), little to none of the reduced products were formed despite the substantial driving force for the first net H-atom transfer. We note that similar substrate classes have been assessed for reactions with bismuth- and phosphorus-derived reductants.[36,37]

To probe the mechanism through which reduction by Ph**Cb**Ph^{NH} operates, we performed a competition experiment between azobenzene and *para*-substituted azoarenes, extracting the relative rates from starting material conversion to generate linear free-energy relationships (**Figure 2.3**). Should azoarene reduction by Ph**Cb**Ph^{NH} be occurring through a CPET step rather than ET-PT steps, we would expect that the relative rate (k_X/k_H) should be fairly insensitive to substitution on the azoarenes. Previous Hammett analyses of reactions occurring through CPET steps returned shallow

slopes, implying that a decrease in ET-driving force is compensated by an increase in PT-driving force.[10,11,38,39]

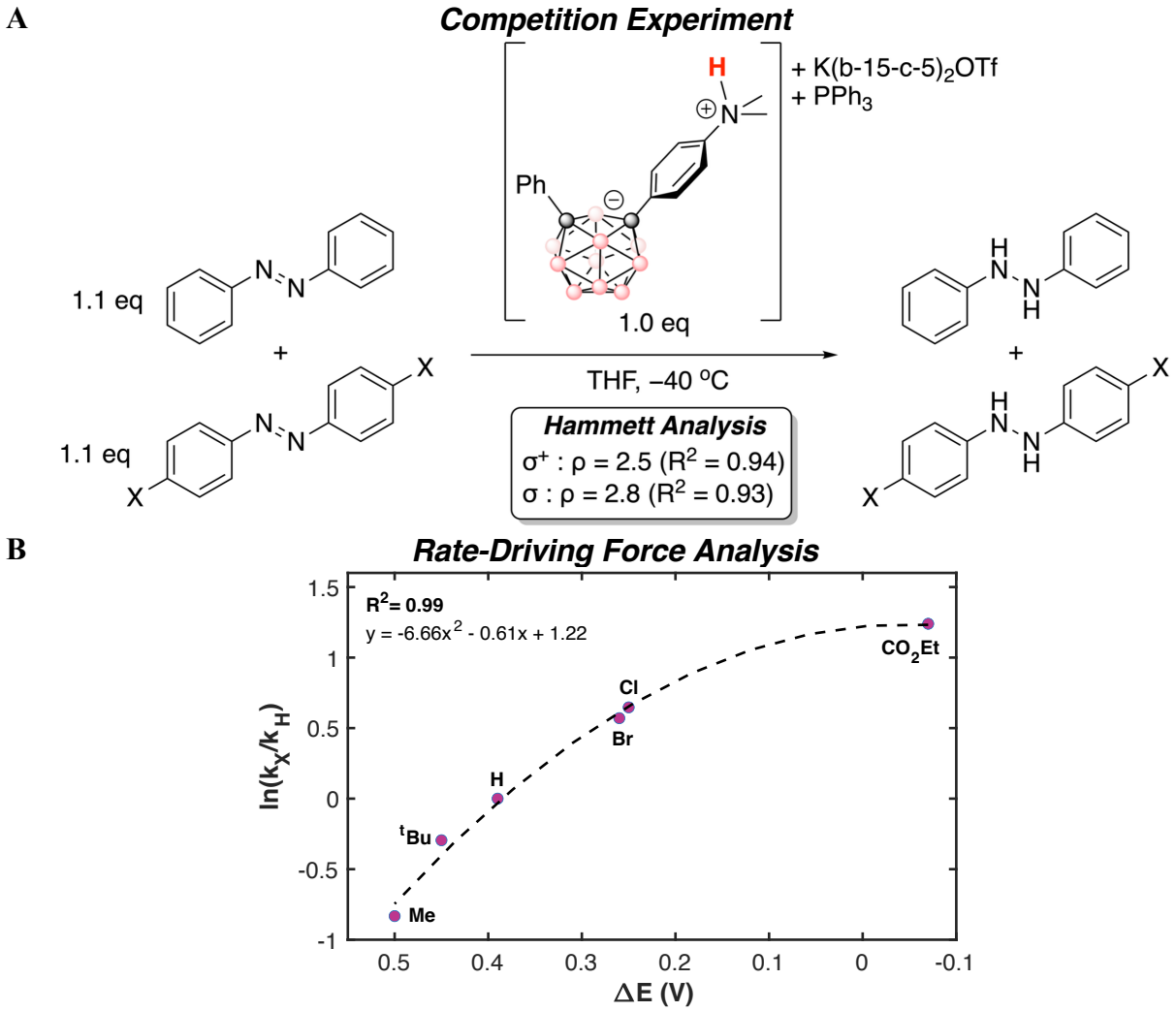

Figure 2.3 (A) Azoarene reduction competition experiment using Ph**Cb**Ph^{NH} as the reductant. **(B)** Rate-driving force analysis for an ET step.

Plotting the relative rates against the substituent Hammett parameter, a large positive slope ($\rho = 2.5$ or 2.8 for σ^+ and σ, respectively) is observed (**Figure A61-A62**). For general comparison, in this case ρ is substantially larger than that observed for reductive CPET from Cp**Co**Cp^{NH+} to acetophenone ($\rho = -0.55$) or fumarate ($\rho = 0.44$) as substrates.[40] These analyses support a rate-limiting step involving a substantial negative charge accumulation on the substrate in the transition state relative to the ground state.

To further disentangle whether azoarene reduction occurs through a rate-limiting ET or CPET step, we plotted the relative rates against the driving force for ET and net H-atom transfer. The relative rates plotted against the driving force (Marcus plots) for ET (ΔE) or CPET (ΔG_{CPET}) yield excellent ($R^2 = 0.99$) and moderate ($R^2 = 0.70$) correlations, respectively (**Figure 2.3B**, **A66**).[41,42] These plots demonstrate that the reduction potential, not the BDFE, most accurately trends with the observed rates. Also considering that the Hammett analysis yields a large and positive slope, we deduce that these data support azoarene reduction by Ph**C**b**C**Ph^{NH} proceeding by a rate-limiting ET step rather than a CPET step.

The stepwise ET-PT reactivity of Ph**C**b**C**Ph^{NH} contrasts the apparent CPET-type reactivity of Cp**C**o**C**Cp^{NH+} studied on different classes of substrates (e.g., acetophenones, fumarates, as well as N_2 and phenylmethylpropriolate via tandem catalysis).[10–14] This difference is noted despite shared thermochemical properties (they have the same pK_a (8.6, *in MeCN*) and similar shifts in potential upon protonation (ΔE = +240 mV vs. +140 mV, respectively); the carborane system is nevertheless moderately more reducing ($E_{1/2}$ = −1.43 V vs. −1.21 V, respectively). The absence of observed CPET-type reactivity for Ph**C**b**C**Ph^{NH} may be due to the large degree of structural reorganization that can be anticipated between Ph**C**b**C**Ph^{NH} and Ph**C**b**C**Ph^{N} (*vide supra*). Previous theoretical studies on CPET reactivity point to reorganization energy and vibronic coupling as factors that can gate CPET.[43]

Ph_2Cb^- Hydrogen Evolution Reaction. For a better understanding of the competing HER from reduced diaryl-*o*-carboranes, we sought to understand the mechanism through which H_2 is formed. Combining [Ph_2**C**b]K(18-c-6) with [Ph_3PH]OTf yields Ph_2**C**b (only observed boron-containing product by ^{11}B NMR) and H_2 (measured at 78% yield). We considered two plausible pathways through which Ph_2Cb^- could combine with acid to form H_2 (**Scheme 2.3A**). First, Ph_2Cb^- could be protonated, generating a neutral intermediate that could then be rapidly reduced and protonated to generate hydrogen (PT/ET/PT). This mechanism is analogous to the proposed HER mechanism for cobaltocenes.[32,44] Secondly, we considered that a disproportionation reaction could generate Ph_2Cb^{2-} which could then be twice protonated to yield hydrogen (ET/PT/PT). In either case, we deduced that the first PT must be rate limiting since no intermediates are observed upon addition of acid to a THF solution of [Ph_2**C**b]K(18-c-6) at −40 °C by UV-vis spectroscopy (**Figure A68**).

Scheme 2.3 (A) Plausible HER mechanisms for Ph_2Cb^- with relevant measured and computed thermochemical parameters of intermediates. **(B)** Regioselectivity of the rate-determining PT step for Ph_2Cb^- and Cp^*_2Co.

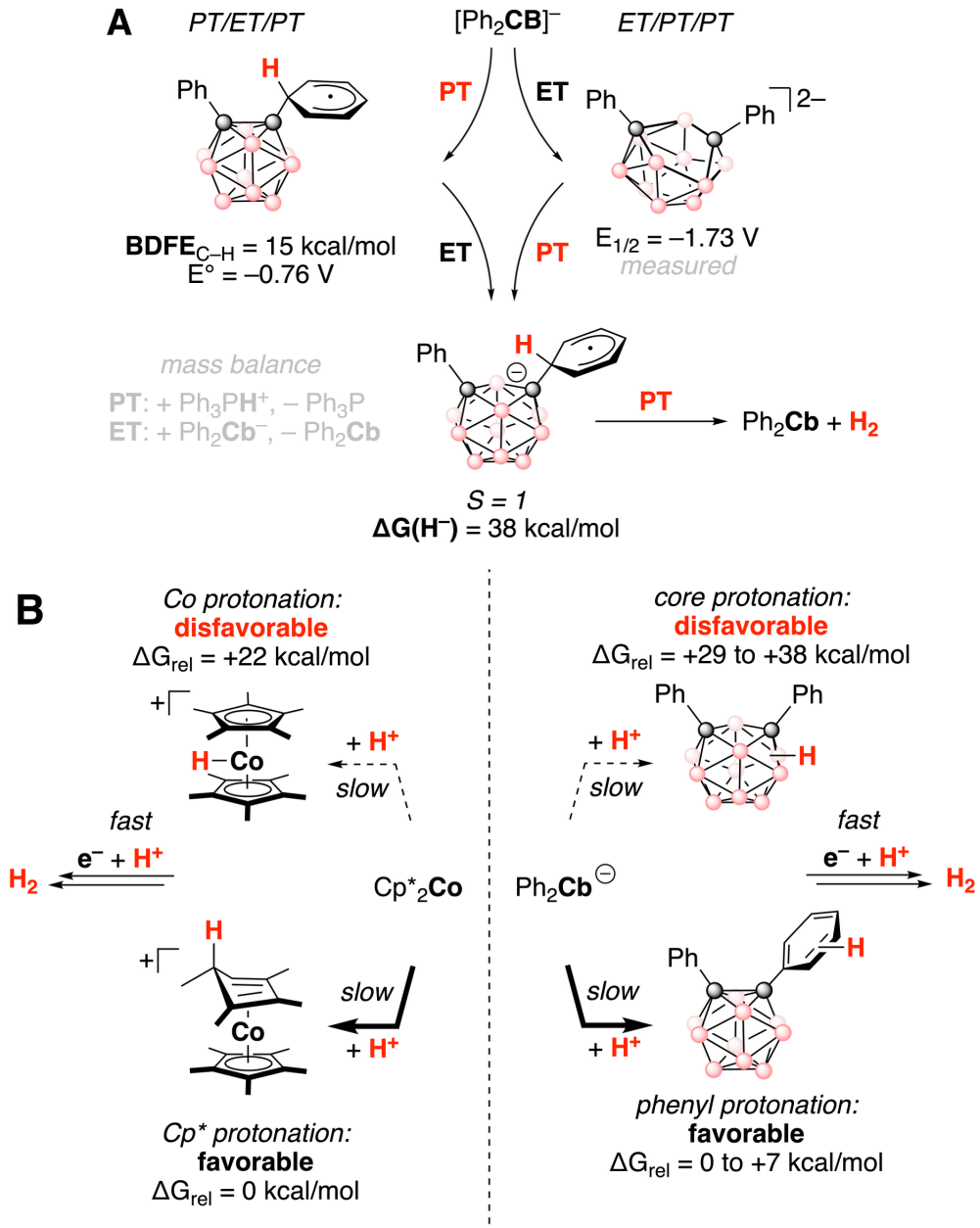

A distinguishing feature of these two HER mechanisms is the carborane order in the rate law, where a PT-limited mechanism would have a first-order carborane dependence while a disproportionation mechanism would have a second-order carborane dependence. The decay of [Ph_2Cb^-] in the presence of excess acid fits first-order kinetics, suggesting that HER is first-order in carborane and

that the disproportionation pathway is (if operative) a minor contributor (**Figure A68**). We note that at low conversion—and thus high [Ph_2**Cb**$^-$]—the fit to the data deviates from ideal first order, providing circumstantial evidence that another pathway, perhaps a disproportionation pathway, may be rate contributing at early time points.

Using [Ph_3PD]OTf as the acid, a kinetic isotope effect of 2.0 is observed, consistent with a rate-limiting protonation step (**Figure A69-A70**).

Notably, when Ph**Cb**Ph^{N-} is used as the reductant, the rate of HER decreases threefold compared to Ph_2**Cb**$^-$, reflecting the lower driving force of Ph**Cb**Ph^{NH} for HER.[10]

Next, we set out to determine the site-selectivity of the rate-limiting PT step through an isotopic labeling experiment using the deuterated acid [Ph_3PD]OTf as a reporter of the protonation site. ^{11}B NMR analysis demonstrates clean formation of Ph_2**Cb** (**Figure A34**). In the ^{2}H NMR spectrum, no signals could be detected in the aromatic or carborane *B–H* regions (**Figure A35**). These data suggest that the carborane is not protonated on sites where we expect deuterium incorporation, namely the *ortho*-, *meta*-, and *para*-phenyl positions. Rather, PT presumably occurs at sites where deuterium is cleaved in a later step, either at the *ipso*-phenyl position, or possibly on the icosahedral core. These latter two cases are not easily distinguished by isotopic labeling of the acid.

To better identify the likely protonation site, we turned to density functional theory to assess which sites are thermodynamically plausible. We determined the relative energies of four cage-protonated and six phenyl-protonated isomers whose energies and structures can be found in the supporting information (**Figure A82**). For all isomers considered, protonation of the phenyl groups is much more favorable; with *p-H*-Ph_2**Cb** as a reference (ΔG_{rel} = 0), the phenyl protonated isomers vary modestly (ΔG_{rel} = 0 to 7 kcal/mol) and all feature a carborane core which has reverted to an ideal icosahedron. In contrast, cage protonation isomers are much higher in energy (ΔG_{rel} = +29 to +38 kcal/mol) featuring distorted icosahedra, suggesting that cage protonation is unlikely.

Although the most stable computed isomer is protonated at the *para*-position, this scenario is inconsistent with the ^{2}H NMR data. Instead, the *ipso*-protonated isomer is higher in energy (ΔG_{rel} = +7 kcal/mol) but also consistent with the ^{2}H NMR data, suggesting that *ipso*-phenyl may be the kinetic protonation site. If true, this would not be surprising considering that the structural data show

that the carborane core dissipates charge directly to the *ipso* carbon through a π-bonding interaction, rendering it modestly basic. More broadly, irreversible proton transfer with kinetic control, rather than thermodynamic control, has been established in other systems that invoke a relatively higher energy tautomer as an intermediate.[45] Regardless, the calculated isomer energies make a compelling case that the driving force for Ph_2**Cb**$^-$ protonation stems from restoring the carborane aromaticity despite breaking aromaticity of the phenyl groups.

We calculated thermochemical parameters of downstream intermediates to understand the feasibility of the latter steps of the PT/ET/PT HER mechanism (**Scheme 2.3A**). Once Ph_2**Cb**$^-$ is protonated, its reduction potential shifts by +0.80 V, a similar potential shift to decamethylcobaltocene (Cp^*_2**Co**) protonation at the cyclopentadienyl ligand. The follow-up ET step from another equivalent of Ph_2**Cb**$^-$ is thus exergonic, forming a hydridic C−H bond. The calculated C−H hydricity is 38 kcal/mol, akin to that of aluminum hydride.[46] The final PT generates H_2 and Ph_2**Cb**, the observed products.

The HER mechanism most consistent with our experimental and computational data, PT/ET/PT, mirrors that of the proposed HER mechanism of Cp^*_2**Co** (**Scheme 2.3**). In both cases, rate-limiting protonation of an aromatic group anodically shifts the potential and generates an intermediate with a weak C−H bond. The magnitude of the anodic potential shift is less for Ph_2**Cb** (+0.80 V) than Cp^*_2**Co** (+1.29 V), suggesting weaker coupling in Ph_2**Cb**$^-$. Notably, Ph_2**Cb** and Cp^*_2**Co** have different structures and yet appear to generate hydrogen by a similar mechanism. The aromatic groups used in each case to stabilize their reducing states appear to open a pathway for HER. In both cases, appending a Brønsted base (an aniline group) mitigates HER, although less so for Ph**Cb**Ph^{NH} than Cp**Co**Cp^{NH+}.

2.3 Conclusion

Herein, we have introduced the synthesis and study of Ph**Cb**Ph^{NH}, a diaryl-*o*-carborane radical anion with an appended Brønsted acid that acts as a net H-atom donor for fumarate, azoarene, and nitrotoluene reductions. The study hence provides a new view of carboranes as candidates for mediating PT/ET transformations. Through crystallographic analysis of one- and two-electron reduced diaryl-*o*-carboranes, we better understand their interesting redox properties. The Ph**Cb**Ph^{NH}

reagent has one of the weakest measured element-hydrogen bonds of non-metal compounds. Mechanistic study of azoarene reduction points toward a rate-limiting ET step. These data highlight a key consideration in the design of new CPET reagents: the mechanism of net H-atom transfer may depend on both thermodynamic parameters (ΔG_{ET}, ΔG_{PT}, electrostatic/electronic coupling) as well as kinetic parameters (reorganization energy, vibronic coupling), which are not easily predicted. The proposed PT/ET/PT mechanism for HER herein implicates the aromatic groups as the site of protonation, suggesting that the anionic icosahedral core is robust to strong acid. Continued studies of compounds with unusually weak net element-H bonds will inform improved understanding of H-atom transfer reactivity towards more selective, lower overpotential systems for catalytic reductions.

2.4 References

[1] Tyburski, R.; Liu, T.; Glover, S. D.; Hammarström, L. Proton-Coupled Electron Transfer Guidelines, Fair and Square. *J. Am. Chem. Soc.* **2021**, *143* (2), 560–576, DOI: 10.1021/jacs.0c09106

[2] Murray, P. R. D.; Cox, J. H.; Chiappini, N. D.; Roos, C. B.; McLoughlin, E. A.; Hejna, B. G.; Nguyen, S. T.; Ripberger, H. H.; Ganley, J. M.; Tsui, E.; Shin, N. Y.; Koronkiewicz, B.; Qiu, G.; Knowles, R. R. Photochemical and Electrochemical Applications of Proton-Coupled Electron Transfer in Organic Synthesis. *Chem. Rev.* **2022**, *122* (2), 2017–2291, DOI: 10.1021/acs.chemrev.1c00374

[3] Agarwal, R. G.; Coste, S. C.; Groff, B. D.; Heuer, A. M.; Noh, H.; Parada, G. A.; Wise, C. F.; Nichols, E. M.; Warren, J. J.; Mayer, J. M. Free Energies of Proton-Coupled Electron Transfer Reagents and Their Applications. *Chem. Rev.*, **2022**, *122* (1), 1–49. DOI: 10.1021/acs.chemrev.1C00521

[4] Boyd, E. A.; Peters, J. C. Sm(II)-Mediated Proton-Coupled Electron Transfer: Quantifying Very Weak N–H and O–H Homolytic Bond Strengths and Factors Controlling Them. *J. Am. Chem. Soc.* **2022**, *144*, 21337-21346. DOI: 10.1021/jacs.2c09580

[5] Gnaim, S.; Bauer, A.; Zhang, H. J.; Chen, L.; Gannett, C.; Malapit, C. A.; Hill, D. E.; Vogt, D.; Tang, T.; Daley, R. A.; Hao, W.; Zeng, R.; Quertenmont, M.; Beck, W. D.; Kandahari, E.; Vantourout, J. C.; Echeverria, P. G.; Abruna, H. D.; Blackmond, D. G.; Baran, P. S. Cobalt-electrocatalytic HAT for Functionalization of Unsaturated C–C bonds. *Nature* **2022**, *605* (7911), 687–695. DOI: 10.1038/s41586-022-04595-3

[6] van der Puyl, V.; Shenvi, R. A. Manganese-, Iron-, and Cobalt-Catalyzed Radical Alkene Hydrofunctionalization. In *Base-Metal Catalysis 2*; Science of Synthesis, Vol. 3; Georg Thieme Verlag KG, **2023**; pp. 623–701. DOI: 10.1055/sos-SD-239-00183

[7] Isayama, S.; Mukaiyama, T. Novel Method for the Preparation of Triethylsilyl Peroxides from Olefins by the Reaction with Molecular Oxygen and Triethylsilane Catalyzed by Bis(1,3-diketonato)cobalt(II). *Chem. Lett.* **1989**, *18*(4), 573–576. DOI: 10.1246/cl.1989.573

[8] Bordwell, F. G.; Cheng, J. P.; Harrelson, J. A. Homolytic Bond Dissociation Energies in Solution from Equilibrium Acidity and Electrochemical Data. *J. Am. Chem. Soc.* **1988**, *110* (4), 1229–1231. DOI: 10.1021/ja00212a035

[9] Peters, J. C. Advancing Electrocatalytic Nitrogen Fixation: Insights from Molecular Systems. *Farad. Disc.* **2023**, *243*(0), 450–472. DOI: 10.1039/d3fd00017f

[10] Chalkley, M. J.; Garrido-Barros, P.; Peters, J. C. A Molecular Mediator for Reductive Concerted Proton-Electron Transfers via Electrocatalysis. *Science* **2020**, *369* (6505), 850–854. DOI: 10.1126/science.abc1607

[11] Derosa, J.; Garrido-Barros, P.; Peters, J. C. Electrocatalytic Reduction of C–C π-Bonds via a Cobaltocene-Derived Concerted Proton–Electron Transfer Mediator: Fumarate Hydrogenation as a Model Study. *J. Am. Chem. Soc.* **2021**, *143* (25), 9303–9307. DOI: 10.1021/jacs.1C03335

[12] Derosa, J.; Garrido-Barros, P.; Peters, J. C. Electrocatalytic Ketyl-Olefin Cyclization at a Favorable Applied Bias Enabled by a Concerted Proton-Electron Transfer Mediator. *Inorg. Chem.* **2022**, *61* (17), 6672–6678. DOI: 10.1021/acs.inorgchem.2c00839

[13] Derosa, J.; Garrido-Barros, P.; Li, M.; Peters, J. C. Use of a PCET Mediator Enables a Ni-HER Electrocatalyst to Act as a Hydride Delivery Agent. *J. Am. Chem. Soc.* **2022**, *144* (43), 20118–20125. DOI: 10.1021/jacs.2c09786

[14] Garrido-Barros, P.; Derosa, J.; Chalkley, M. J.; Peters, J. C. Tandem Electrocatalytic N_2 Fixation via Proton-Coupled Electron Transfer. *Nature* **2022**, *609* (7925), 71–76. DOI: 10.1038/s41586-022-05011-6

[15] Fox, M. A.; Nervi, C.; Crivello, A.; Batsanov, A. S.; Howard, J. A. K.; Wade, K.; Low, P. J. Structural, Spectroscopic, Electrochemical and Computational Studies of C,C′-diaryl-ortho-carboranes, 1-(4-XC_6H_4)-2-Ph-1,2-$C_2B_{10}H_{10}$ (X = H, F, OMe, NMe_2, NH_2, OH and O^-). *J. Solid State Electrochem.* **2009**, *13* (10), 1483–1495. DOI: 10.1007/s10008-008-0686-0

[16] Morris, J. H.; Gysling, H. J.; Reed, D. Electrochemistry of Boron Compounds. *Chem. Rev.*, **1985**, *85* (1), 51–76. DOI: 10.1021/cr00065a003

[17] Núñez, R.; Tarrés, M.; Ferrer-Ugalde, A.; de Biani, F. F.; Teixidor, F. Electrochemistry and Photoluminescence of Icosahedral Carboranes, Boranes, Metallacarboranes, and Their Derivatives. *Chem. Rev.* **2016**, *116* (23), 14307–14378. DOI: 10.1021/acs.chemrev.6b00198

[18] Bilevich, K. A.; Zakharkin, L. I.; Okhlobystin, O. Y. Anion Radicals of the Barene Series. *Izv. Akad. Nauk, Ser. Khim.* **1965**, *10*, 1914.

[19] Lewis, Z. G.; Welch, A. J. Structure of 1,2-diphenylcarbaborane, 1,2-Ph_2-1,2-closo-$C_2B_{10}H_{10}$. *Acta Cryst.* **1993**, C*49*(4), 705–710. DOI: 10.1107/s0108270192012125

[20] These changes in bond lengths are more substantial than those in the B−B bonds of the icosahedron core which modestly lengthen (1.76 Å to 1.80 Å, *averaged*).

[21] Kahlert, J.; Stammler, H.; Neumann, B.; Harder, R. A.; Weber, L.; Fox, M. A. Crystal Structures of the Carborane Dianions [1,4-$(PhCB_{10}H_{10}C)_2C_6H_4$]$^{2-}$ and [1,4-$(PhCB_{10}H_{10}C)_2C_6F_4$]$^{2-}$ and the Stabilizing Role of the *para* -Phenylene Unit on 2*n* + 3 Skeletal Electron Clusters. *Angew. Chem. Int. Ed.* **2014**, *53*(14), 3702–3705. DOI: 10.1002/anie.201310718

[22] Yao, S.; Kostenko, A.; Xiong, Y.; Lorent, C.; Ruzicka, A.; Driess, M. Changing the Reactivity of Zero- and Mono-Valent Germanium with a Redox Non-Innocent Bis(silylenyl)carborane Ligand. *Angew. Chem. Int. Ed.* **2021**, *60*(27), 14864–14868. DOI: 10.1002/anie.202103769

[23] Krebs, J.; Haehnel, M.; Krummenacher, I.; Friedrich, A.; Braunschweig, H.; Finze, M.; Ji, L.; Marder, T. B. Synthesis and Structure of an *o*-Carboranyl-Substituted Three-Coordinate Borane Radical Anion. *Chem. Eur. J.* **2021**, *27*(31), 8159–8167. DOI: 10.1002/chem.202100938

[24] Boyd, L. A.; Clegg, W.; Copley, R. C. B.; Davidson, M. G.; Fox, M. A.; Hibbert, T. G.; Howard, J. A. K.; Mackinnon, A.; Peace, R. J.; Wade, K. Exo-π-bonding to an Ortho-carborane Hypercarbon Atom: Systematic Icosahedral Cage Distortions Reflected in the Structures of the Fluoro-, Hydroxy- and Amino-carboranes, 1-X-2-Ph-1,2-$C_2B_{10}H_{10}$ (X = F, OH or NH_2) and Related Anions. *Dalton Trans.* **2004**, *17*, 2786–2799. DOI: 10.1039/b406422d

[25] Oliva, J. M.; Allan, N. L.; Schleyer, P. V. R.; Viñas, C.; Teixidor, F. Strikingly Long C···C Distances in 1,2-Disubstituted Ortho-Carboranes and their Dianions. *J. Am. Chem. Soc.* **2005**, *127*(39), 13538–13547. DOI: 10.1021/ja052091b

[26] Fox, M. A.; Nervi, C.; Crivello, A.; Low, P. J. Carborane Radical Anions: Spectroscopic and Electronic Properties of a Carborane Radical Anion with a 2n + 3 Skeletal Electron Count. *Chem. Comm.* **2007**, *23*, 2372–2374.

DOI: 10.1039/b700110j

[27] Wu, L.; Zhang, X.; Moos, M.; Krummenacher, I.; Dietz, M.; Jayaraman, A.; Bertermann, R.; Ye, Q.; Finze, M.; Wenzel, M.; Mitric, R.; Lambert, C.; Braunschweig, H.; Ji, L. Full Electron Delocalization across the Cluster in 1,12-bisBMes$_2$-*p*-Carborane Radical Anion. *J. Am. Chem. Soc.* **2024**, X,YY-YY DOI: 10.1021/jacs.4c03873

[28] Wade, K. The Structural Significance of the Number of Skeletal Bonding Electron-Pairs in Carboranes, the Higher Boranes and Borane Anions, and Various Transition-Metal Carbonyl Cluster Compounds. *J. Chem. Soc. D.* **1971**, *15*, 792–793. DOI: 10.1039/C29710000792

[29] Tshepelevitsh, S.; Kütt, A.; Lõkov, M.; Kaljurand, I.; Saame, J.; Heering, A.; Plieger, P. G.; Vianello, R.; Leito, I. On the Basicity of Organic Bases in Different Media. *Eur J. Org. Chem.* **2019**, 6735–6748 DOI: 10.1002/ejoc.201900956

[30] Carlson, B. W.; Miller, L. L.; Neta, P.; Grodkowski, J. Oxidation of NADH Involving Rate-Limiting One-Electron Transfer. *J. Am. Chem. Soc.*, **1984**, *106* (23), 7233–7239. DOI: 10.1021/ja00335a062

[31] Zhu, X. Q.; Li, H. R.; Li, Q.; Ai, T.; Lu, J. Y.; Yang, Y.; Cheng, J. P. Determination of the C4-H Bond Dissociation Energies of NADH Models and Their Radical Cations in Acetonitrile. *Chem. Eur. J.* **2003**, *9* (4), 871–880. DOI: 10.1002/chem.200390108

[32] Chalkley, M. J.; Oyala, P. H.; Peters, J. C. Cp* Noninnocence Leads to a Remarkably Weak C–H Bond via Metallocene Protonation. *J. Am. Chem. Soc.* **2019**, *141*, 4721-4729 DOI: 10.1021/jacs.9b00193

[33] Savéant, J. M.; Tard, C. Proton-Coupled Electron Transfer in Azobenzene/Hydrazobenzene Couples with Pendant Acid-Base Functions. Hydrogen-Bonding and Structural Effects. *J. Am. Chem. Soc.* **2014**, *136* (25), 8907–8910. DOI: 10.1021/ja504484a

[34] Cattaneo, M.; Ryken, S. A.; Mayer, J. M. Outer-Sphere $2e^-/2H^+$ Transfer Reactions of Ruthenium(II)-Amine and Ruthenium(IV)-Amido Complexes. *Angew. Chem. Int. Ed.* **2017**, *56* (13), 3675–3678. DOI: 10.1002/anie.201612642

[35] Schild, D. J.; Drover, M. W.; Oyala, P. H.; Peters, J. C. Generating Potent C-H PCET Donors: Ligand-Induced Fe-to-Ring Proton Migration from a Cp*Fe^{III}-H Complex Demonstrates a Promising Strategy. *J. Am. Chem. Soc.* **2020**, *142* (44), 18963–18970. DOI: 10.1021/jacs.0c09363

[36] Wang, F.; Planas, O.; Cornella, J. Bi(I)-Catalyzed Transfer-Hydrogenation with Ammonia-Borane. *J. Am. Chem. Soc.* **2019**,*141* (10), 4235–4240. DOI: 10.1021/jacs.9b00594

[37] Dunn, N. L.; Ha, M.; Radosevich, A. T. Main Group Redox Catalysis: Reversible P^{III}/P^{V} Redox Cycling at a Phosphorus Platform. *J. Am. Chem. Soc.* **2012**, *134* (28), 11330–11333. DOI: 10.1021/ja302963p

[38] McManus, C.; Mondal, P.; Lovisari, M.; Twamley, B.; McDonald, A. R. Carboxamidate Ligand Noninnocence in Proton Coupled Electron Transfer. *Inorg. Chem.* **2019**, *58* (7), 4515–4523. DOI: 10.1021/acs.inorgchem.9b00055

[39] Lanksy, D. E.; Goldberg, D. P. Hydrogen Atom Abstraction by a High-Valent Manganese(V)−Oxo Corrolazine. *Inorg. Chem.* **2006**, *45* (13), 5119-5125. DOI: 10.1021/ic060491

[40] The Hammett slope encodes the charge accumulation in the transition state *relative* to the ground state, so an alternative explanation for the observed large slope could be that the transition state is charge neutral while the ground state has significant positive charge. This would be the case for strong hydrogen-bonding in the ground state. To test this scenario, azobenzene was monitored by UV-vis spectroscopy in THF at -40 °C as 4-methoxy-N,N-dimethylanilinium triflate (pK_a match for Ph**Cb**Ph^{NH}) was added (**Figure A51**). The azobenzene absorbance was unaffected as acid was titrated in, suggesting limiting hydrogen bonding and that it is not a plausible explanation for the observed Hammett slope.

[41] Marcus, R. A.; Sutin, N. Electron Transfers in Chemistry and Biology. *BBA* **1985**, *811*(3), 265–322. DOI: 10.1016/0304-4173(85)90014-X

[42] Gray, H. B.; Winkler, J. R. Electron Transfer in Proteins. *Annu. Rev. Biochem.* **1996**, *65*, 537–561. DOI: 10.1146/annurev.bi.65.070196.002541

[43] Tyburski, R.; Hammarström, L. Strategies for Switching the Mechanism of Proton-coupled Electron Transfer Reactions Illustrated by Mechanistic Zone Diagrams. *Chem. Sci.* **2020**, *13*(1), 290–301. DOI: 10.1039/d1sc05230f

[44] Koelle, U.; Infelta, P. P.; Grätzel, M. Kinetics and Mechanism of the Reduction of Protons to Hydrogen by Cobaltocene. *Inorg. Chem.* **1988**, *27* (5), 879–883. DOI: 10.1021/ic00278a026

[45] D'Angelo, J. Ketone Enolates: Regiospecific Preparation and Synthetic Uses. *Tetrahedron* **1976**, *32* (24), 2979–2990. DOI: 10.1016/0040-4020(76)80156-1

[46] Heiden, Z. M.; Lathem, A. P. Establishing the Hydride Donor Abilities of Main Group Hydrides. *Organomet.* **2015**, *34* (10), 1818–1827. DOI: 10.1021/om5011512

Chapter 3

Independent Modulation of Proton and Electron Transfer Driving Forces in a Family of Carborane-derived H-atom Donors

3.1 Introduction

Proton-coupled electron transfer (PCET) reactions are a foundational method for molecular oxidation state control.[1,2] PCET reactions pair the transfer of two charge-carrying particles, the proton and electron, to alleviate charge accumulation, allowing for electron transfer (ET) at relatively mild potentials. This is especially important within biological energy conversion processes, where a substrate must be selectively activated in the presence of potentially reactive residues.[3] The principles of biological PCET have been strategically incorporated into organic synthesis for functional group redox or generation of reactive organic radicals.[4]

The driving force of PCET reactions is among the leading-order determinants of its kinetics. The half wave potential ($E_{1/2}$) and acid dissociation constant (pK_a) can be readily measured to determine the ET and proton transfer (PT) driving forces, respectively. In sequence, the $E_{1/2}$ and pK_a determine the effective bond dissociation free energy (BDFE), a descriptor of the free energy of proton and electron–*or H-atom*–transfer (HAT).[5] Small changes in ET, PT, and HAT driving force correlate with changes in rate according to established linear (or *quadratic* for ET) rate-driving force relationships.[6,7] Large changes in ET, PT, and HAT driving forces can result in crossover between PCET mechanisms.[8,9] Knowing the driving forces for ET, PT, and HAT is essential to propose a reasonable PCET reaction mechanism.

A desirable feature of a reagent or catalyst for PCET is the ability to finely control the proton and electron transfer driving forces. The prospect of thermodynamic modulation of ET and PT driving force is to control mechanism, namely to steer a PCET reaction toward the concerted proton-electron transfer (CPET) pathway in which the proton and electron are transferred in a single elementary step in contrast to stepwise charge-transfer (e.g. ET/PT) steps.[7] CPET paths are desirable because they are often kinetically preferable to stepwise paths, and changing the relative PT or ET driving force has been shown in some systems to shift the PCET mechanism between rate-limiting CPET and charge transfer steps.[8,9] Control over driving force can also lower the overpotential for the reaction to improve selectivity.[10] Optimizing a desired PCET reaction outcome would benefit from screening these driving forces to achieve a favorable mechanism, rate, and selectivity.

Independent tuning of the PT, ET, and HAT driving forces, however, is only possible in systems in which the proton donor and electron donor are sufficiently insulated from one another.[11] For example, the bimetallic complex shown in **Scheme 3.1A** features a manganese complex with an imido ligand and an adjacent crown moiety capable of binding several non-redox active ions.[12] These secondary ions make the imido more acidic but less reducing, leaving the BDFE largely unchanged. In contrast, the ruthenium complex shown in **Scheme 3.1B** can access a broad range of pK_a, $E_{1/2}$, and BDFE values owing to the distinct functional handles for controlling ET and PT driving force.[13,14] The substituents on the acylacetonato ligands are more coupled to the reductant than the acid, meaning they control the redox potential. Similarly, the substituents on the imidazole control the pK_a with minimal effect on the $E_{1/2}$. Combining the orthogonal pK_a and $E_{1/2}$ control allows for control over the BDFE. As a result, the Mayer lab has been able to study both PCET rate-driving force effects and polar effects, where PCET driving force is constant but the contributions from ΔG°(ET) and ΔG°(PT) vary.

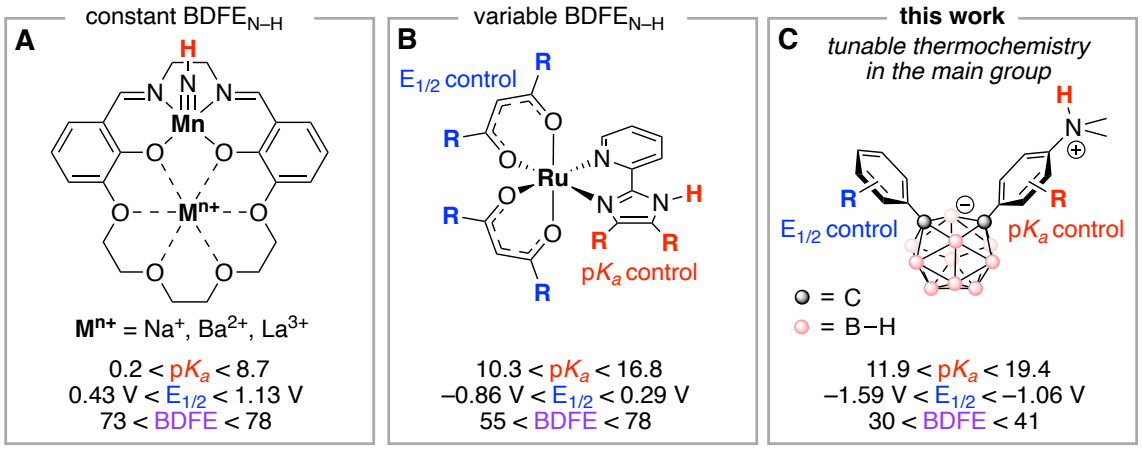

Scheme 3.1 (A) A manganese imido within a salen-crown framework bound to various non-redox active cations. (B) A ruthenium-imidazole complex with separate functional handles for changing redox potential and pK_a. (C) A carborane-based PCET reagent whose two aromatic groups function as orthogonal handles for controlling PCET driving forces.

The thermochemistry of transition metal platforms can be controlled through ligands which tune the driving force, but it is less obvious how main group platforms could be similarly controlled and thus have been comparatively less explored.[15] In biology, however, transition metals co-factors are not required for PCET, like in classes of flavin-depended enzymes such as glucose or monoamine oxidases.[16–18] These enzymes are thought to control the thermochemistry of the flavin to promote one- or two-electron PCET processes, though the precise structural origin of thermodynamic modulation remains unclear. Reproducing such reactivity on a purely main group platform could serve as a synthetic reference point to understand how residues might modulate the reactivity of flavin-dependent enzymes.

One such synthetic main group platform that has been recently reported as a PCET reagent is the acid-appended *ortho*-carborane (abbreviated as Ph**Cb**Ph$^{\mathbf{NH}}$) depicted in **Scheme 3.1C**.[19] It stores a net-hydrogen atom—a reducing electron within the *o*-carborane and an acidic proton on the anilinium fragment—with a remarkably low $BDFE_{N–H}$ of 31 kcal/mol, making it a unique example of a main group species capable of reversible electron and proton transfer. Ph**Cb**Ph$^{\mathbf{NH}}$ has been shown to reduce a variety of small molecules including fumarate, azobenzene, and nitrotoluene.

The PCET scope of Ph**Cb**Ph$^{\mathbf{NH}}$ suggests that the reaction proceeds by a charge transfer (ET-PT) mechanism and consequently is limited by the redox potential of the substrate rather than the BDFE. For example, while PCET from Ph**Cb**Ph$^{\mathbf{NH}}$ to acetophenone to form the ketyl radical is exergonic, ET to form the ketyl anion is substantially uphill, so the reaction does not occur. The proposed ET-PT mechanism is further supported by mechanistic studies of azoarene reduction. This reactivity contrasts that of the analogous cobaltocene-based PCET mediator which reduces acetophenone by a CPET mechanism.[20]

The origin of the diverging reactivity is presently unknown and could arise from thermodynamic effects (PT, ET, or HAT driving force) and/or kinetic effects (reorganization energy or vibronic coupling).[21] With the goal of mechanistic crossover into CPET, the driving forces on the carborane platform ($\Delta G°_{PT}$ and $\Delta G°_{ET}$) could be tuned by synthetic modification. If doing so leads to concerted reactivity, it could enable *o*-carboranes as viable PCET electrocatalysts. The ET and PT driving forces could be separately controlled using

the two aromatic groups bound to *o*-carborane's carbon atoms, where the acid-containing aryl group would control the pK_a while the other aryl group would control $E_{1/2}$.

Another motivation for controlling the thermochemical properties of Ph**C**_**b**_Ph$^{\mathbf{NH}}$ is to reduce its propensity for HER, which is in part due to its low $BDFE_{N–H}$. As a result, the H-atom form of the reagent can only be generated at low temperature. For example, cyclic voltammograms (CVs) of Ph**C**_**b**_Ph^{N} in the presence of acid feature an irreversible wave at the potential of the *o*-carborane reduction even at high scan rates, demonstrating the instability of Ph**C**_**b**_Ph$^{\mathbf{NH}}$ in solution at room temperature.[19] Thermodynamic modulation of the *o*-carborane could increase the $BDFE_{N–H}$ to improve the stability of its H-atom form towards HER, either by increasing the pK_a or the redox potential.

Towards optimizing the PCET reactivity of the *o*-carborane platform, this study describes the preparation of a library of *o*-carboranes that have been thermochemically characterized and electrochemically canvassed for CPET reactivity. The two aryl groups are shown to have orthogonal influence on the pK_a and $E_{1/2}$, and as a result, allow for the effective BDFE to be varied by 10 kcal/mol. The changes in thermochemistry allow for more stable *o*-carborane H-atom carriers to be generated, but they do not appear to react via CPET with unsaturated substrates. These data provide a holistic description of *o*-carborane as a redox subunit in the context of PCET mediators.

3.2 Results and Discussion

Synthesis and Structure

The library of *o*-carborane compounds was prepared by a sequence depicted in **Scheme 3.2A**. The desired diarylalkyne was synthesized through a Sonogashira coupling between an aryl halide and an arylalkyne fragment. The resulting diarylalkyne was heated with decaborane, a commercially available B_{10} synthon, to produce the targeted *o*-carborane in good yield.

The selected aryl groups are categorized by their anticipated effect on the thermochemistry of the *o*-carborane in **Scheme 3.2B**. The three aromatics on the left do not contain the acid and are expected to control the ET driving force; inversely, the acid-containing groups on

the right are expected to control the driving force for PT. Because the two aromatic groups are separated by the *o*-carborane core, they should be thermochemically insulated from one another. The series of *o*-carboranes is depicted in **Scheme 3.2C**.

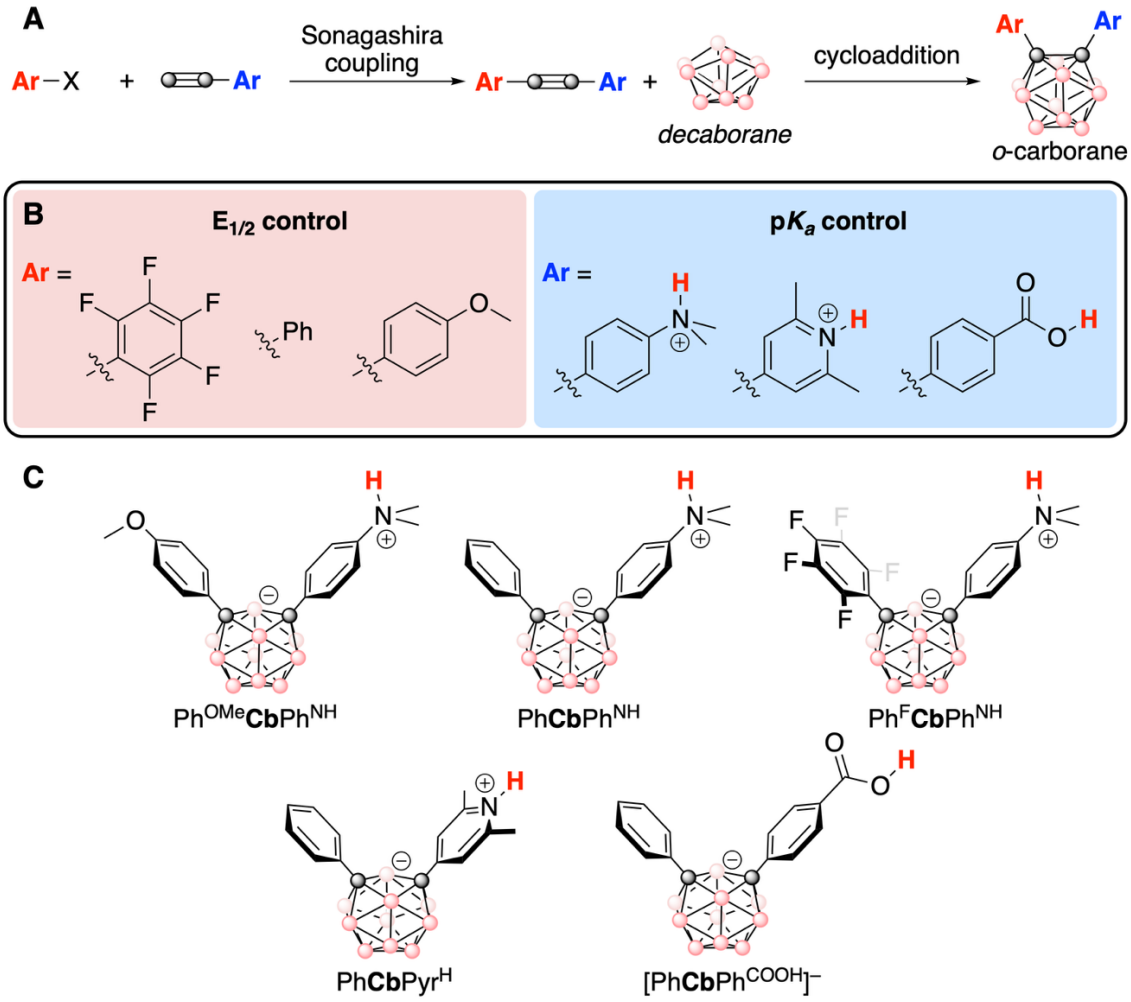

Scheme 3.2 (A) Synthetic route for generating a thermochemically-diverse library of *o*-carborane PCET donors. (B) Functionalized arenes incorporated into the carborane library, highlighting their intended thermochemical role. (C) Representations of the *o*-carborane library in their reactive reduced, protonated state.

Single-crystal X-ray diffraction of the neutral *o*-carboranes reveals an ideal icosahedral structure that suggests that the flanking aromatic groups do not substantially influence the core (**Figure B21-B23**). Structural analysis of the singly reduced *o*-carborane radicals was performed by density functional theory (DFT) calculations, which were previously shown to

reproduce the *o*-carborane radical anion structure with high fidelity.[19] Optimized geometries of the reduced *o*-carboranes are shown in **Figure B33-B37**. They are qualitatively similar, featuring a substantially lengthened *o*-carborane cage C–C bond and shortened C–C bonds between the *o*-carborane and the aryl groups. Functionality on the aryl groups does not appear to alter the structure of the *o*-carboranes in the neutral or reduced states.

Thermochemistry

The relevant thermochemical observables, $E_{1/2}$ and pK_a, were measured by CV and ^{1}H NMR spectroscopy, respectively, and the values are reported in **Table 3.1**. The series Ph^{F}**Cb**Ph^{NH}, Ph**Cb**Ph^{NH}, and Ph^{OMe}**Cb**Ph^{NH} all contain the same N,N-dimethylanilinium group but differ in their second aromatic. The pK_a varies in the range 8.4-8.8, translating to a change in the $BDFE_{N–H}$ by 0.5 kcal/mol. The redox potential, however, varies by 430 mV, translating to a modulation of the BDFE by nearly 10 kcal/mol.

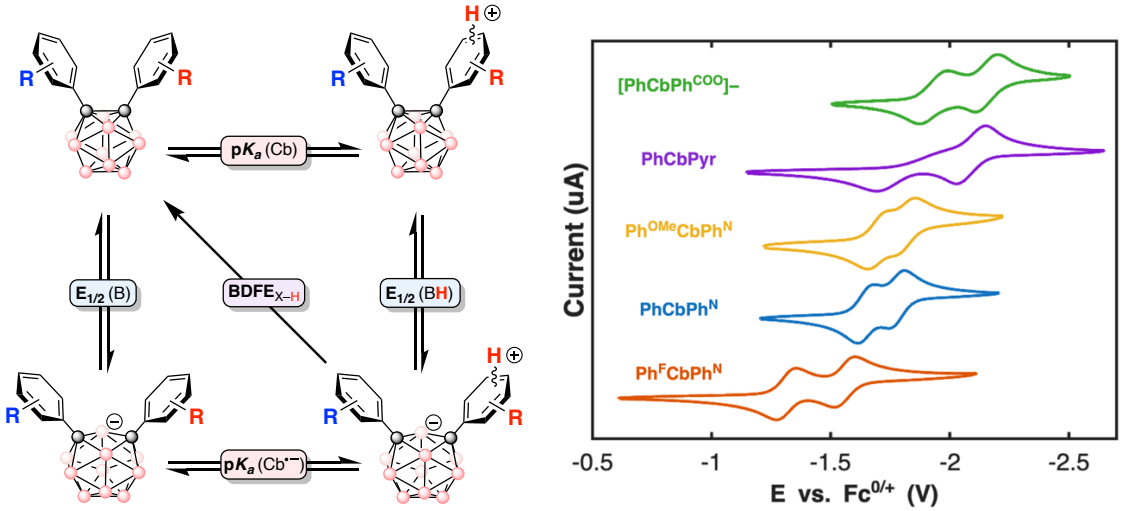

Figure 3.1 (left) Square scheme of the *o*-carborane system. (right) CVs of the *o*-carboranes (1mM) in their free-base form in acetonitrile with ^{n}Bu$_4$PF$_6$ (200 mM) supporting electrolyte. The scans are swept cathodic, then anodic at 100 mV/s

Table 3.1 PCET Thermochemistry of the *o*-carborane library in acetonitrile solvent

carborane	$E_{1/2}$(N) (V vs $Fc^{0/+}$)	$E_{1/2}$(NH) (V vs $Fc^{0/+}$)	pK_a(Cb)	pK_a($Cb^{\bullet-}$)	$BDFE_{X–H}$ (kcal/mol)	$\Delta E_{1/2}$ (mV)
Ph**Cb**Ph^{NH}	−1.67	−1.43	8.6	12.6	31.4	240
Ph^{F}**Cb**Ph^{NH}	−1.27	−1.06	8.4	11.9	39.6	210
Ph^{OMe}**Cb**Ph^{NH}	−1.70	−1.46	8.8	12.8	30.9	240
[Ph**Cb**Ph^{COOH}]$^{-}$	−1.69	−1.59	18.5	19.4	41.3	100
Ph**Cb**Pyr^{H}	−1.58	−1.28	11.2	16.2	38.4	300

Similarly, the series Ph**Cb**Ph^{NH}, Ph**Cb**Pyr^{H}, and [Ph**Cb**Ph^{COOH}]$^{-}$ differ in their acid groups but have phenyl as the second aromatic group. Here, the pK_a varies by nearly 10, from 8.6 in the anilinium-appended *o*-carborane to 18.5 in the benzoic acid-appended *o*-carborane. These acidic aryl groups also modestly affect the redox potential, which varies by 120 mV. The overall range of BDFE spans 9.9 kcal/mol, demonstrating the orthogonal control of ET and PT driving forces on this platform.

Reactivity

The reactivity of the *o*-carborane family was screened electrochemically using CV, in which application of a sufficiently reducing potential generated the reactive oxidation state of the *o*-carborane, the radical anion, in the presence of acid and substrate. The current response was used as a read-out of the reactivity, where a multi-electron catalytic wave would indicate possible PCET mediation in comparison to the current of the one-electron redox wave of the *o*-carborane alone or the background wave of the acid and substrate without the *o*-carborane.

First, the CVs of Ph^{OMe}**Cb**Ph^{N} are very similar to those of Ph**Cb**Ph^{N}, where the [Ph^{OMe}**Cb**Ph^{NH}]$^{0/-}$ feature appears irreversible, and Ph^{OMe}**Cb**Ph^{N} is slightly more reducing (**Figure B32**).

The CVs of Ph^{F}**Cb**$Ph^{N\mathbf{H}}$ were collected to explore its reactivity. Thermochemical measurements demonstrate that it has a much higher $BDFE_{N–H}$ compared to Ph**Cb**$Ph^{N\mathbf{H}}$, suggesting that it may be more stable to HER and could be generated as a long-lived intermediate. The CVs of Ph^{F}**Cb**$Ph^{N\mathbf{H}}$ have two fully reversible one-electron waves (*blue*

trace), as shown in **Figure 3.2**. Upon the addition of acid, these features shift anodically (*red trace*), where current is observed in the anodic return sweep. The [Ph^{F}**Cb**Ph^{NH}]$^{+/0}$ appears to be quasi-reversible even at modest scan rates, as opposed to the fully irreversible [Ph**Cb**Ph^{NH}]$^{+/0}$ feature observed previously. Addition of acetophenone (*gray trace*) resulted in a marginal increase in the current and little change in the reversibility of the feature, indicating minimal reactivity with acetophenone.

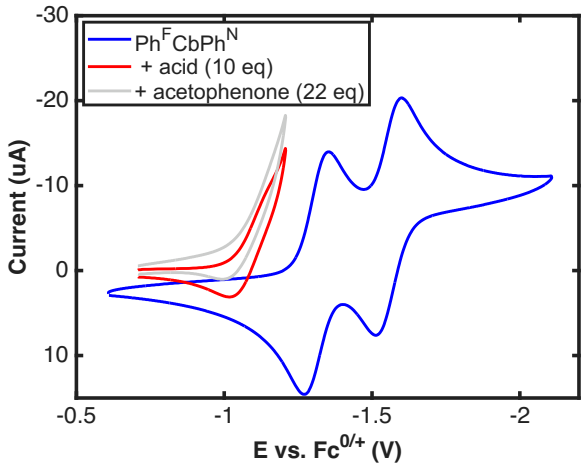

Figure 3.2 CVs of Ph^{F}**Cb**Ph^{NH} (1mM, *blue*) with [$^{4\text{-CN}}$PhNH$_3$]OTf (10 mM, *red*) and acetophenone (22 mM, *gray*) in acetonitrile with ^{n}Bu$_4$PF$_6$ (200 mM) supporting electrolyte. The scans are swept cathodic, then anodic at 100 mV/s

The CVs of Ph**Cb**Pyr are shown in **Figure 3.3**. As with Ph^{F}**Cb**Ph^{NH}, this *o*-carborane has a modestly higher BDFE$_{N–H}$ of 38.4 owing to the weaker base fragment, 2,6-dimethylpyridinium, compared to the N,N-dimethylanilinium fragment in Ph**Cb**Ph^{NH}. The CVs of Ph**Cb**Pyr (*blue trace*) alone feature two reversible one-electron waves, albeit the peak-to-peak spacing on the first wave is large, indicating slow electron transfer kinetics. Upon addition of acid (*red trace*), a large anodic shift of +300 mV is observed to yield a reversible feature at −1.28 V. Like Ph^{F}**Cb**Ph^{NH}, the attenuation of the BDFE$_{N–H}$ has led to a more stable H-atom form of the *o*-carborane, although in this case, the attenuation is related to the acidity rather than the redox potential. Addition of acetophenone (*gray trace*) minimally affects the profile of the feature, with a small increase in current and no change in the reversibility of the feature. Based on these CVs, Ph**Cb**Pyr^{H} does not appear to react with acetophenone.

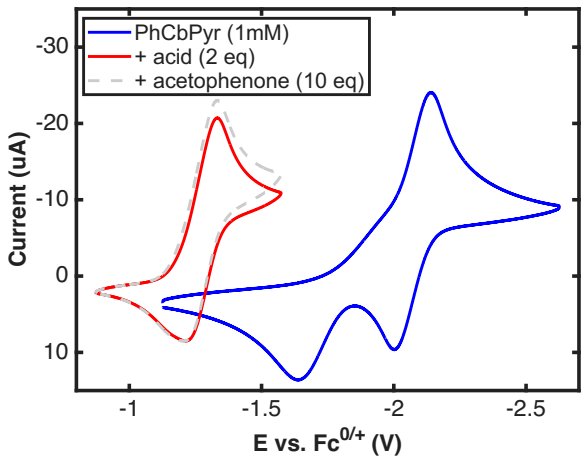

Figure 3.3 CVs of Ph**Cb**Pyr (1mM, *blue*) with [PhNH$_3$]OTf (2 mM, *red*) and acetophenone (10 mM, *gray*) in acetonitrile with ^{n}Bu$_4$PF$_6$ (200 mM) supporting electrolyte. The scans are swept cathodic, then anodic at 100 mV/s.

These two sets of CVs demonstrate that the H-atom form of the *o*-carborane PCET platform can be stabilized through control of the redox potential or the pK_a, yielding long-lived H-atom forms that can be readily observed by CV. However, the longer lifetimes do not necessarily translate to new reactivity. Using reactivity with acetophenone as an indicator of CPET, these two *o*-carborane platforms do not appear to react, and like Ph**Cb**Ph$^{\mathbf{NH}}$, may still be limited to stepwise ET-PT pathways that offer limited kinetic advantage for mediated electrolysis over direct electrolysis.

The [Ph**Cb**Ph^{COOH}]$^-$ has a few qualitative differences that distinguish it from other entries in the series that could lead to changes in behavior. It has the least driving force for PCET, with a BDFE$_{O–H}$ of 41.3 kcal/mol. It contains oxygen, rather than nitrogen, in the carboxylate Brønsted base. In its H-atom form, it carries a negative charge, while the other entries are neutral in their H-atom state. The CVs of [Ph**Cb**Ph^{COOH}]$^-$ are shown in **Figure 3.4**.

The CV of [^{n}Bu$_4$][Ph**Cb**Ph^{COO}] (*blue trace*) has two reversible features which shift anodically upon the addition of acid (*red trace*). Surprisingly, the [Ph**Cb**Ph$^{\mathbf{COOH}}$]$^{1-/2-}$ feature appears to be reversible, suggesting a possible role for this *o*-carborane as a hydride transfer mediator rather than an H-atom transfer mediator. Addition of acetophenone does not affect the reversibility and leads to a small change in the current, indicating little if any reactivity.

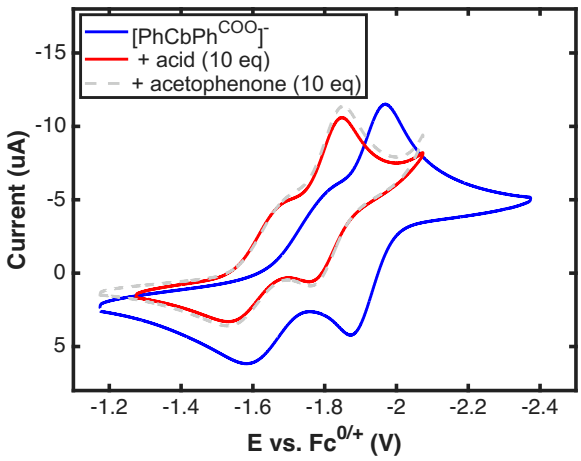

Figure 3.4 CVs of [^{n}Bu$_4$][Ph**Cb**Ph^{COO}] (1mM, *blue*) with chloroacetic acid (10 mM, *red*) and acetophenone (10 mM, *gray*) in acetonitrile with ^{n}Bu$_4$PF$_6$ (200 mM) supporting electrolyte. The scans are swept cathodic, then anodic at 100 mV/s.

[Ph**Cb**Ph$^{COO\mathbf{H}}$]$^{2-}$ could potentially act as a hydride transfer mediator. The thermodynamic hydricity of [Ph**Cb**Ph$^{COO\mathbf{H}}$]$^{2-}$ is 26.8 kcal/mol, on par with the hydricity of potent transition metal hydrides such as bis(diphosphine)Rh(H).[22] To explore its hydride transfer reactivity, substrates with unsaturated C=N bonds were selected, such as phenyl-(1-phenylethylidene)amine, lepidine, and phenanthridine. These were combined with the *o*-carborane and chloroacetic acid, and the CVs are shown in **Figure 3.5**. The *o*-carborane in the presence of the substrates features a large, irreversible wave, indicative of catalytic substrate reduction. However, comparison with the background current, that of the substrate and acid in the absence of *o*-carborane, shows that much of the observed current may be attributable to the direct electrolysis of the substrate in the absence of the mediator. These data seem to indicate that hydride transfer mediation does not substantially outcompete the direct reduction of substrates at the electrode.

Overall, these reactivity data suggest that this candidate mediator platform provides little advantage over direct electrolysis. This is consistent with our previous understanding that Ph**Cb**Ph^{NH} reacts via charge transfer (ET-PT) pathways rather than CPET steps. These data broaden our understanding of *o*-carborane PCET reactivity into a wider thermochemical space, throughout which the stepwise charge transfer pathway appears to be operative. In effect, its PCET scope is limited compared to structurally analogous mediators containing cobaltocene as the redox subunit, which react via rate-limiting CPET.[20]

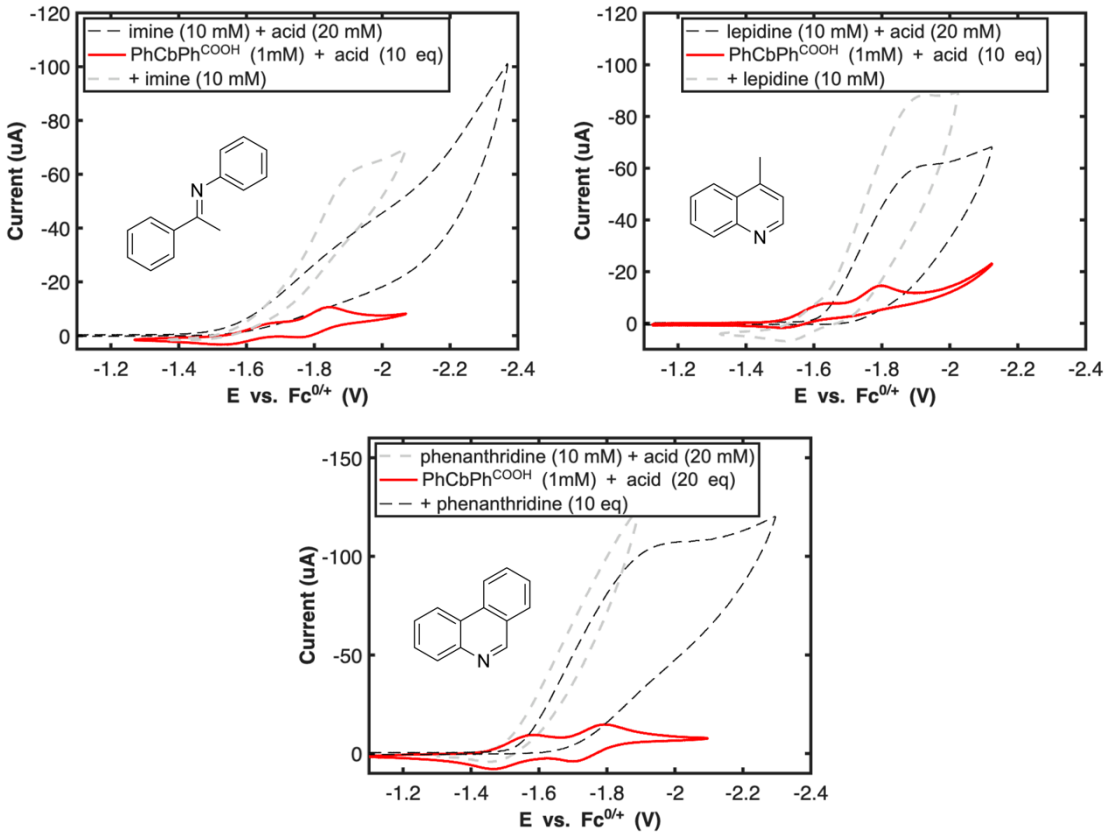

Figure 3.5 CVs of Ph**Cb**Ph^{COOH} (1 mM) with chloroacetic acid (20 mM, *red trace*) and substrate (10 mM, *gray trace*) compared to the background substrate reduction (black trace) in 1,2-dimethoxyethane with $^{n}Bu_4PF_6$ (200 mM) supporting electrolyte. The scans are swept cathodic, then anodic at 100 mV/s.

These data suggest that the stepwise reactivity of the *o*-carborane mediator arises from kinetic effects rather than thermodynamic effects. Based on the change in the *o*-carborane core structure upon one-electron reduction (**Figure B33-B37**), the substantial lengthening of the C–C bond, it seems reasonable to suggest that diaryl-*o*-carboranes have a larger ET reorganization energy than cobaltocenes, whose structural reorganization upon ET is smaller due to the non-bonding nature of the SOMO.[23] Theoretical models of PCET suggest that changes in reorganization energy could lead to changes in mechanism (i.e. the relative CPET and ET barrier heights).[21] Here, the CPET barrier appears to be higher than the ET barrier, according to the reactivity observed by CV.

3.3 Conclusion

A family of diaryl-*o*-carboranes with appended Brønsted bases was synthesized, in which the composition of the two aryl groups was varied. The driving forces for ET and PT could be independently modified, permitting the driving force for PCET to be controlled as well. Increasing the effective BDFE of the *o*-carborane platform allowed for the reactive reduced and protonated form to be generated as a long-lived species at room temperature, according to observations by CV. The reactivity of the *o*-carboranes was explored using CV, indicating limited H-atom or hydride transfer to substrates containing C=O and C=N bonds.

This study provides a comprehensive overview of the synthesis, thermochemistry, and reactivity of *o*-carboranes in the context of PCET. Like the Ph**C**_**b**_Ph$^{\mathbf{NH}}$ platform studied previously, these new entries in the *o*-carborane PCET library do not appear to react via CPET steps, which are responsible for the potential shift and rate enhancement of PCET mediators. Rather, the *o*-carborane platform has the inherent property of reacting via charge transfer (ET-PT) steps. These data support the interpretation that the charge transfer nature of *o*-carborane arises from kinetic, rather than thermodynamic, properties. The reorganization energy seems to be a likely explanation for these reactivity differences, especially given the structural homogeneity of the *o*-carborane library. Since the *o*-carborane core structure is conserved across the series, the reorganization energies are likely similar, and the stepwise ET-PT mechanism remains operative. In the search for main group platforms that react via CPET pathways, efforts may be guided by this study toward other main group candidates that preserve the desirable features of the *o*-carborane platform, like its multiple stable oxidation states and reversible single electron transfer, but without the large structural rearrangement upon ET. Doing so may identify platforms whose PCET thermochemistry and mechanism are modular.

3.4 References

1 Murray, P. R. D.; Cox, J. H.; Chiappini, N. D.; Roos, C. B.; McLoughlin, E. A.; Hejna, B. G.; Nguyen, S. T.; Ripberger, H. H.; Ganley, J. M.; Tsui, E.; Shin, N. Y.; Koronkiewicz, B.; Qiu, G.; Knowles, R. R. Photochemical and Electrochemical Applications of Proton-Coupled Electron Transfer in Organic Synthesis. *Chem. Rev.* **2022**, *122* (2), 2017–2291. DOI: 10.1021/acs.chemrev.1c00374.

2 Tyburski, R.; Liu, T.; Glover, S. D.; Hammarström, L. Proton-Coupled Electron Transfer Guidelines, Fair and Square. *J. Am. Chem. Soc.* **2021**, *143* (2), 560–576. DOI: 10.1021/jacs.0c09106.

3 Gray, H. B.; Winkler, J. R. Living with Oxygen. *Acc. Chem. Res.* **2018**, *51* (8), 1850–1857. DOI: 10.1021/acs.accounts.8b00245.

4 Gentry, E. C.; Knowles, R. R. Synthetic Applications of Proton-Coupled Electron Transfer. *Acc. Chem. Res.* **2016**, *49* (8), 1546–1556. DOI: 10.1021/acs.accounts.6b00272.

5 Bordwell, F. G.; Cheng, J. Pei.; Harrelson, J. A. Homolytic Bond Dissociation Energies in Solution from Equilibrium Acidity and Electrochemical Data. *J. Am. Chem. Soc.* **1988**, *110* (4), 1229–1231. DOI: 10.1021/ja00212a035.

6 Marcus, R. A.; Sutin, N. Electron Transfers in Chemistry and Biology. *BBA Rev. Bioenerg.* **1985**, *811* (3), 265–322. DOI: 10.1016/0304-4173(85)90014-X.

7 Tyburski, R.; Liu, T.; Glover, S. D.; Hammarström, L. Proton-Coupled Electron Transfer Guidelines, Fair and Square. *J. Am. Chem. Soc.* **2021**, *143* (2), 560–576. DOI: 10.1021/jacs.0c09106.

8 Mondal, S.; Myers, P.; Doss, E. N.; Zhang, W.; Zhang, S. Mechanistic Continuum from Stepwise to Concerted Proton-Coupled Electron Transfer Pathways at a Synthetic Tricopper Cluster. *J. Am. Chem. Soc.* **2026**, *148* (13), 14170–14176. DOI: 10.1021/jacs.6c00324.

9 Cooney, S. E.; Duggan, S. G.; Walls, M. R. A.; Gibson, N. J.; Mayer, J. M.; Miro, P.; Matson, E. M. Engineering Mechanisms of Proton-Coupled Electron Transfer to a Titanium-Substituted Polyoxovanadate–Alkoxide. *Chem. Sci.* **2025**, *16* (6), 2886–2897. DOI: 10.1039/D4SC06468B.

10 Chalkley, M. J.; Peters, J. C. Relating N–H Bond Strengths to the Overpotential for Catalytic Nitrogen Fixation. *Eur. J. Inorg. Chem.* **2020**, *2020* (15–16), 1353–1357. DOI: 10.1002/ejic.202000232.

11 Warren, J. J.; Tronic, T. A.; Mayer, J. M. Thermochemistry of Proton-Coupled Electron Transfer Reagents and Its Implications. *Chem. Rev.* **2010**, *110* (12), 6961–7001. DOI: 10.1021/CR100085K.

12 Léonard, N. G.; Chantarojsiri, T.; Ziller, J. W.; Yang, J. Y. Cationic Effects on the Net Hydrogen Atom Bond Dissociation Free Energy of High-Valent Manganese Imido Complexes. *J. Am. Chem. Soc.* **2022**, *144* (4), 1503–1508. DOI: 10.1021/jacs.1c09583.

13 Groff, B. D.; Cattaneo, M.; Rinaolo, K. C.; Mercado, B. Q.; Mayer, J. M. Disentangling Driving Force Effects, Polar Effects, e–/H+ Imbalance, and Other Influences on H-Atom Transfer Reactions. *J. Am. Chem. Soc.* **2025**, *147* (6), 4766–4777. DOI: 10.1021/jacs.4c10596.

14 Groff, B. D.; Cattaneo, M.; Coste, S. C.; Pressley, C. A.; Mercado, B. Q.; Mayer, J. M. Independent Tuning of the pKa or the E1/2 in a Family of Ruthenium Pyridine–Imidazole

Complexes. *Inorg. Chem.* **2023**, *62* (26), 10031–10038. DOI: 10.1021/acs.inorgchem.3c01241.

15 Agarwal, R. G.; Coste, S. C.; Groff, B. D.; Heuer, A. M.; Noh, H.; Parada, G. A.; Wise, C. F.; Nichols, E. M.; Warren, J. J.; Mayer, J. M. Free Energies of Proton-Coupled Electron Transfer Reagents and Their Applications. *Chem. Rev.* **2022**, *122* (1), 1–49. DOI: 10.1021/acs.chemrev.1c00521.

16 Fitzpatrick, P. F. Oxidation of Amines by Flavoproteins. *Arch. Biochem. Biophys.* **2010**, *493* (1), 13–25. DOI: 10.1016/j.abb.2009.07.019.

17 Roth, J. P.; Klinman, J. P. Catalysis of Electron Transfer during Activation of O2 by the Flavoprotein Glucose Oxidase. *Proc. Natl. Acad. Sci.* **2003**, *100* (1), 62–67. DOI: 10.1073/pnas.252644599.

18 Fitzpatrick, P. F. Substrate Dehydrogenation by Flavoproteins. *Acc. Chem. Res.* **2001**, *34* (4), 299–307. DOI: 10.1021/ar0000511.

19 Adillon, E. H.; Peters, J. C. A Carborane-Derived Proton-Coupled Electron Transfer Reagent. *J. Am. Chem. Soc.* **2024**, *18*, 8–8. DOI: 10.1021/JACS.4C09007.

20 Chalkley, M. J.; Garrido-Barros, P.; Peters, J. C. A Molecular Mediator for Reductive Concerted Proton-Electron Transfers via Electrocatalysis. *Science* **2020**, *369* (6505), 850–854. DOI: 10.1126/science.abc1607.

21 Tyburski, R.; Hammarström, L. Strategies for Switching the Mechanism of Proton-Coupled Electron Transfer Reactions Illustrated by Mechanistic Zone Diagrams. *Chem. Sci.* **2022**, *13* (1), 290–301. DOI: 10.1039/d1sc05230f.

22 Wiedner, E. S.; Chambers, M. B.; Pitman, C. L.; Bullock, R. M.; Miller, A. J. M.; Appel, A. M. Thermodynamic Hydricity of Transition Metal Hydrides. *Chem. Rev.* **2016**, *116* (15), 8655–8692. DOI: 10.1021/acs.chemrev.6b00168.

23 Lauher, J. W.; Hoffmann, R. Structure and Chemistry of Bis(Cyclopentadienyl)-MLn Complexes. *J. Am. Chem. Soc.* **1976**, *98* (7), 1729–1742. DOI: 10.1021/ja00423a017.

Chapter 4

Repositioning Proton and Electron Donors in a Family of Proton-coupled Electron Transfer Mediators

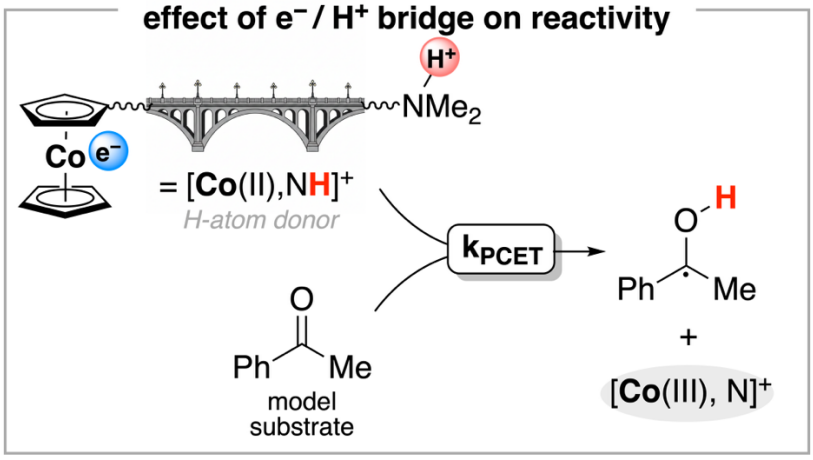

4.1 Introduction

Proton-coupled electron transfer (PCET) is ubiquitous in biological redox processes such as nitrogen fixation, cellular respiration, and photosynthesis,[1,2,3,4] and is increasingly exploited in catalytic methods for chemical synthesis.[5] In recent years, molecular catalysts for PCET (herein referred to as PCET mediators) have emerged as effective tools for the electrolytic reduction of N_2, CO_2, and unsaturated organic small molecules. Such mediators, upon protonation and reduction, act as well-defined H-atom equivalents which can be more reactive and selective than direct electrolysis in acidic media, as shown in **Scheme 4.1a**. In this way, mediated electrolysis can lower the overpotential and improve the Faradaic efficiency of reductive protonation reactions.

One such PCET mediator is an aniline-appended cobaltocene (**Scheme 4.1a**) devised by our group, which effects substrate reduction via concerted proton-electron transfer (CPET) to generate O–H, N–H, C–H (and metal-hydride) radical intermediates under mild conditions.[6,7,8,9,10,11] In this system, a reduced and protonated Co(II) state is the key reactive intermediate, with a weak $BDFE_{eff}$ of 37 kcal/mol. Following PCET, protonation and electrochemical reduction of the resulting Co(III) species turns over the catalytic cycle.

While interest in electrocatalytic PCET mediators is growing,[12] reductive PCET mediators in particular remain few in number. Representative examples of PCET mediators are depicted in **Scheme 4.1b**. Mayer and coworkers have studied ruthenium-imidazole complexes as tunable PCET platforms, which have been used as electrocatalysts by Waymouth and coworkers for a PCET-driven oxidation reaction, propanol oxidation to acetone.[13,14] Nishibayashi and coworkers are exploring iron and cobalt sandwich compounds as stoichiometric PCET reagents as well as a samarium system featuring a protic arm that may act as a PCET mediator.[15,16] A reduced and protonated Cp*Fe-phenol system shows potency for reducing acetophenone, anthracene, and a molybdenum nitride.[17] Other examples include phenol-appended cobalt and nickel pincer complexes from the Siewert group, and a titanium semiquinone complex from the Baek group; both have been used as stoichiometric PCET donors.[18,19,20] These are just a few relevant instances among others.[21,22,23,24]

With respect to PCET mediator design, a reasonable first choice of proton and electron donors for a target PCET reaction can be made on thermodynamic grounds using known redox potentials,

acidities, and bond energies. These thermodynamic terms set the driving force for PCET (either H-atom addition or abstraction), which influences PCET rate via a well-established linear free energy relationship. Yet it is not obvious how the connection of the electron and proton transfer subunits

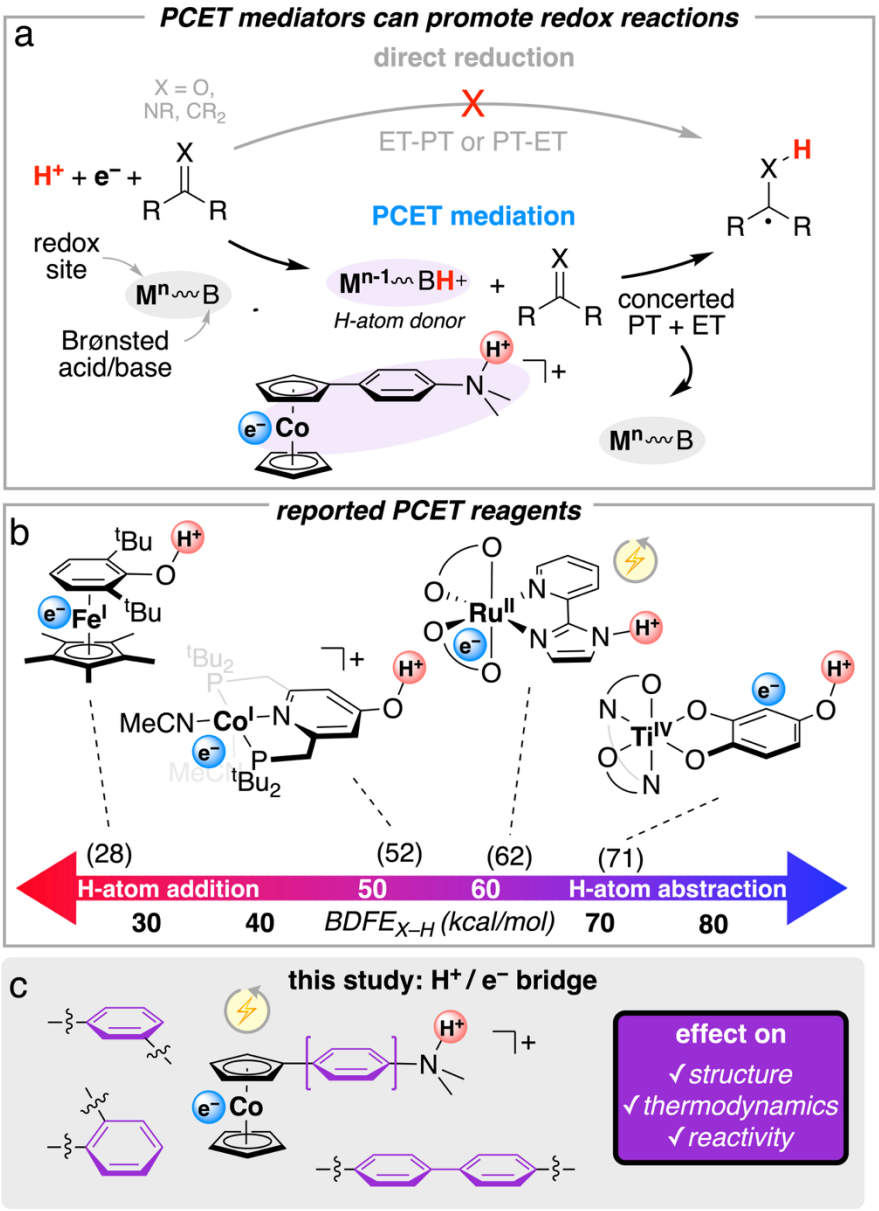

Scheme 4.1 (a) Reduction of an unsaturated substrate by using a PCET mediator. (b) A sample of reported PCET catalysts and reagents containing sites for proton and electron transfer. (c) Exploration of the effects of the bridging groups on the properties of cobaltocene- and anilinium-derived PCET electrocatalysts.

will affect the PCET mechanism or its rate. Treating bridge position as a PCET design variable, and obtaining benchmark kinetic data on its effect, serves the growing interest in PCET mediators—especially if kinetic activity can be improved at decreased thermodynamic overpotential.

To address this gap, we have synthesized and examined a series of cobaltocene-derived PCET mediators based on our original design (**Scheme 4.1a**), herein differing solely in the covalent bridge (**Scheme 4.1c**). Importantly, this series maintains the same electron and proton-bearing fragments and thereby controls for the anticipated influence of driving force. This allows the intrinsic effect of the bridging group to be isolated. Through determination of the crystal structures, measurements of ET and PT equilibria, PCET kinetics, isotope effects, Hammett parameters, and computational analysis, we quantify the bridging group's influence on the mechanism and rate of PCET. We find that the PCET rate is relatively insensitive to changes in the bridge but also identify a surprising electronic rationale for how a specific bridge can augment metallocene PCET reactivity: the geometry of the acid can direct donor-acceptor orbital interactions reminiscent of a pericyclic reaction with the substrate, promoting electron transfer. As a result, an *ortho*-substituted analog, which features the least driving force for the model PCET reaction, reacts most rapidly in contrast to the expected rate-driving force relationship. This finding points toward secondary-sphere design, inclusive of the linker, as a means to control activity and perhaps selectivity in mediated PCET.

4.2 Results and Discussion

Synthesis

Our series of phenylene-bridged mediators (discussed herein as [**Co**(II/III)$^{\text{bridge}}$, N/N**H**]$^{0/+/2+}$) was prepared in two steps by a variation of our previously reported route to the *p*-phenylene isomer (**Scheme 4.2a**).[6] Aryllithium addition to $[Cp_2Co][PF_6]$ followed by abstraction of the ring endo-hydride from Cp(η^4-CpH-PhNMe$_2$)Co(I) with the tritylium reagent $[Ph_3C][BAr^F{}_4]$ (Ar^F = 3,5-bis(trifluoromethyl)phenyl) afforded [**Co**(III)$^{o,m,p\text{-Ph}}$, N]$BAr^F{}_4$ salts.[25,26,27,28] As necessary, Co(II) forms of the mediators were prepared by thermolysis of the corresponding Co(I) diene complexes or by reduction of Co(III) with sodium amalgam (see the Supporting Information for details).

A parallel mediator synthesis was devised which places the harshest and least chemoselective steps — Cp-aryl bond formation and cobalt oxidation — ahead of coupling to the Brønsted acid. As shown

in the route in **Scheme 4.2b**, replacement of the lithioaniline synthons with *p*-lithiobromobenzene or the complex magnesiate $Mg(PhBr)_3LiBu$ yielded Cp(η^4-CpH-PhBr)Co(I), an air-stable Co(I) diene with an *exo* aryl bromide. Hydride abstraction afforded the cobaltocenium salt [CpCo(III)Cp^{Br}]$BAr^F{}_4$, a highly activated electrophilic substrate for Pd cross-coupling chemistry under aqueous Suzuki-Miyaura conditions.[29] The use of a $BAr^F{}_4^-$ counterion makes purification straightforward via silica gel chromatography. A key advantage of this new cross-coupling methodology is that it enables late-stage diversification of cobaltocenes with functional groups intrinsically incompatible with organolithium addition to $[Cp_2Co]^+$ and oxidation of Co(I).[30]

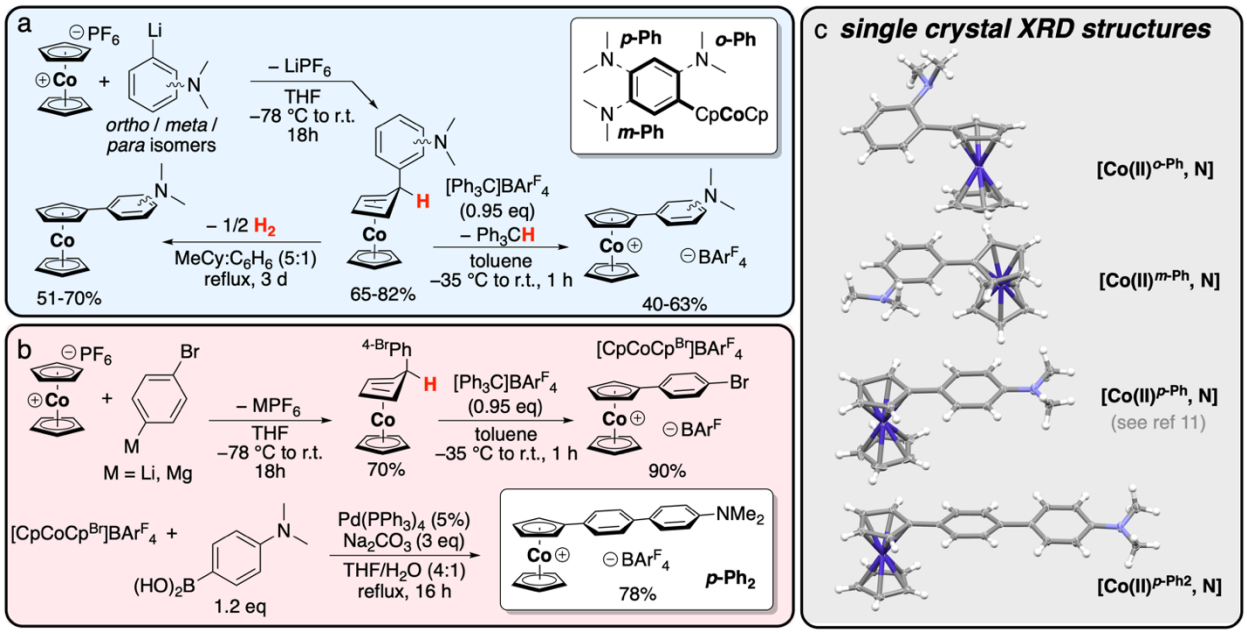

Scheme 4.2. Synthetic routes for the preparation of (a) [**Co**$^{o-Ph}$, N], [**Co**$^{m-Ph}$, N], and [**Co**$^{p-Ph}$, N] and (b) [**Co**(III)$^{p-Ph2}$, N]$BAr^F{}_4$. (c) X-ray crystal structures listed from top to bottom: [**Co**(II)$^{o-Ph}$, N], [**Co**(II)$^{m-Ph}$, N], [**Co**(II)$^{p-Ph}$, N],[6] and [**Co**(II)$^{p-Ph2}$, N].

In addition to the newly reported *o*-$PhNMe_2$, *m*-$PhNMe_2$ and *p*-PhBr substituted Co(I) dienes, each metallocene complex has been structurally authenticated by single-crystal X-ray diffraction in the neutral (Co^{II}, shown in **Scheme 4.2c**) and cationic (Co^{III}, see S4) states. The aryl substituents do not significantly perturb the structure of the cobaltocene fragment. C(Cp)–C(Ph) torsional strain is evident in [**Co**$^{o-Ph}$, N], while the biphenylene moiety in [**Co**(II)$^{p-Ph2}$, N] exhibits slight torsion about the C(Ph)–C(Ph) bond.

Thermochemistry

Relevant thermochemistry of the cobaltocene series was obtained by measurements of the proton and electron transfer equilibria, as illustrated in **Figure 4.1a**. Accordingly, the pK_a of each [**Co**(III), N**H**]$^{2+}$ was measured by titration with anilinium acids and quantification of the relevant species' concentrations by ^{1}H NMR spectroscopy (see S6). The half-wave potentials were measured by cyclic voltammetry in both the aniline ($E_{1/2}$(N)) and anilinium ($E_{1/2}$(NH)) protonation states, providing the necessary data to determine the $BDFE_{N–H}$ and the thermodynamic coupling values ($\Delta E_{1/2}$).

The thermochemical profiles are summarized in **Table 4.1** and depicted graphically in **Figure 4.1b-c**. There are small variations in pK_a and $E_{1/2}$ across the series, but the spread in the BDFEs is very small (36.5 to 37.2 kcal/mol with an estimated error of ±0.4 kcal/mol). Variation in pK_a is compensated for by a proportional change in $E_{1/2}$ (and vice versa). The exception is [**Co**(II)$^{o\text{-Ph}}$, N**H**]$^+$, with a $BDFE_{N–H}$ (38.8 kcal/mol) that is modestly higher, possibly due to electrostatic or steric interactions unique to *ortho* substitution. In the absence of a covalent linker, the formal $BDFE_{N–H}$ of a combination of cobaltocene ($E_{1/2}$ = −1.33 V) and N,N-dimethylanilinium (pK_a = 11.47) is estimated as 38 kcal/mol.[31,32]

While the substitution pattern of the linker has little influence on $BDFE_{N–H}$, it has a significant effect on the thermodynamic (acid–reductant) coupling, which has been inferred to bias systems toward concerted PCET.[33] We measure thermodynamic coupling electrochemically as the shift in $E_{1/2}$ upon changing protonation state.[34] For example, the thermodynamic coupling for [**Co**(III)$^{o–\text{Ph}}$, N]$^+$ is shown in **Figure 4.1d** as the shift in $E_{1/2}$ from [**Co**(III)$^{o–\text{Ph}}$, N]$^+$ (blue trace) to [**Co**(III)$^{o–\text{Ph}}$, N**H**]$^{2+}$ (black trace) upon addition of acid, approximately +210 mV. An alternative reporter of acid–reductant coupling can be gleaned spectroscopically as a shift in the visible metal-to-ligand charge transfer (MLCT) band upon protonation. This spectroscopic coupling is illustrated using [**Co**(II)$^{o–\text{Ph}}$, N] whose UV-vis spectrum (blue trace) is depicted in **Figure 4.1e**. Upon addition of acid to form [**Co**(II)$^{o–\text{Ph}}$,N**H**]$^+$ (black trace), the feature at 526 nm shifts to 546 nm. For comparison to the thermodynamic coupling, the spectroscopic coupling is reported in **Table 4.1**. It reflects the sensitivity of the (Co^{II}/Cp)→(Ar π^*) MLCT to protonation state.

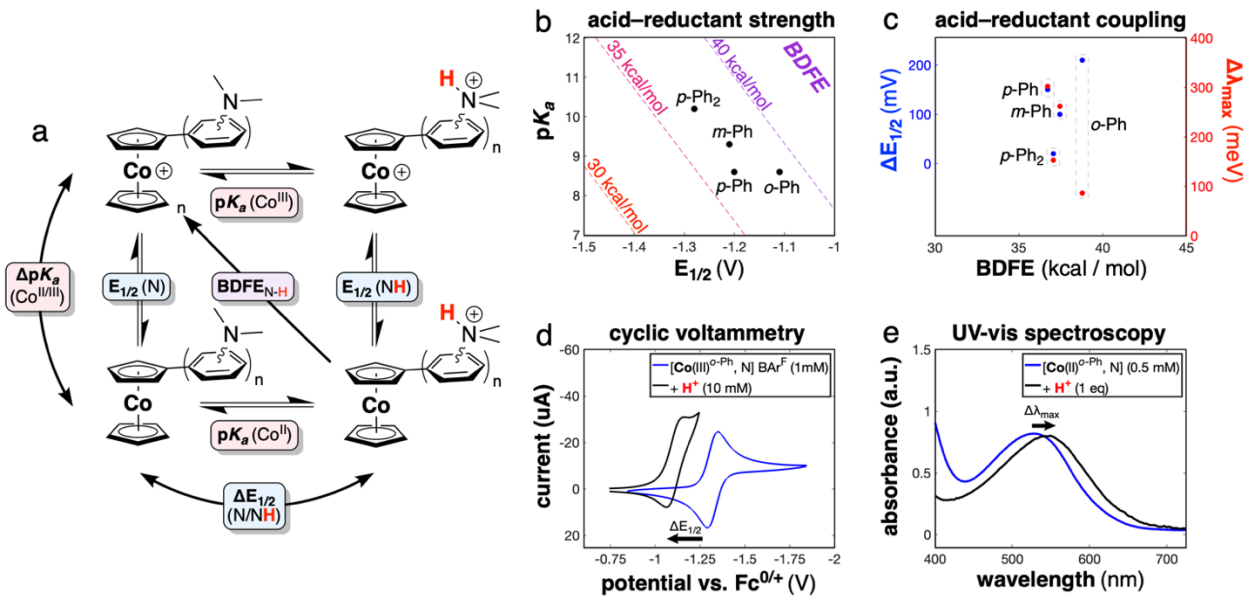

Figure 4.1. (a) Square scheme of [**Co**(II), N**H**]$^{+}$ with coupling highlighted around the outside of the square. (b) pK_a(Co^{III})-E$_{1/2}$(NH) plot of the set of mediators bracketed by diagonal lines of constant BDFE. (c) Electrochemical (blue, left) and spectroscopic (red, right) measurements plotted as a function of BDFE$_{N–H}$, demonstrating that coupling and driving force in this series are essentially independent. (d) Cyclic voltammograms of [**Co**(III), N]$^{+}$ (blue trace) and [**Co**(III), N**H**]$^{2+}$ with 10 mM [$^{4\text{-CN}}$PhNH$_3$][OTf] (black trace) which exemplify how coupling is measured electrochemically. (e) UV-vis spectra of [**Co**(II)$^{o\text{-Ph}}$, N] and [**Co**(II)$^{o\text{-Ph}}$, N**H**]BAr$^{F}_4$ which exemplify how coupling is measured spectroscopically.

Table 4.1 Thermochemistry of Aniline-appended Cobaltocene Complexes

bridge	E$_{1/2}$ (N) (V vs. Fc$^{0/+}$)	E$_{1/2}$ (NH) (V vs. Fc$^{0/+}$)	pK_a (Co^{III})	pK_a (Co^{II})	BDFE[a] (kcal/mol)	ΔE$_{1/2}$ (N/NH) (mV)	Δλ$_{max}$ (N/NH) (meV)
o-Ph	−1.32	−1.11	8.6	12.1	38.8	210	87
m-Ph	−1.31	−1.22	9.3	10.8	37.2	90	261
p-Ph	−1.35	−1.21	8.6	11.0	36.5	140	302
p-Ph$_2$	−1.30	−1.28	10.2	10.5	37.1	20	153

[a]The relative error in the bond dissociation free energy measurement is estimated to be ± 0.4 kcal/mol.

For three of the complexes in the series, the thermodynamic and spectroscopic coupling are linearly correlated, reflected by an overlay of the red and blue data points in **Figure 4.1c**. However, [Co^{o-Ph}, N] is a clear outlier, with the strongest thermodynamic coupling and weakest spectroscopic coupling. The divergent coupling behavior in [Co^{o-Ph}, N] likely arises from a combination of electrostatics and structural strain. *Ortho* substitution leads to particularly close contact between the two formal charge centers (Co and N) and thus a large observed thermodynamic coupling. The *ortho*-disposed groups also induce torsion along the C(Cp)−C(Ph) bond axis, disrupting conjugation between the two π systems and destabilizing the phenyl-centered acceptor orbital in the MLCT transition (Figure S103).

Kinetics

To compare the PCET reactivity of this cobaltocene series, we chose the reduction of acetophenone as a convenient model reaction that proceeds via a ketyl radical intermediate to a pinacol coupling product (**Figure 4.2a**). We electrolyzed the cobaltocenium complexes at −1.30 V vs. $Fc^{0/+}$ in the presence of excess acetophenone and tosic acid, confirming that each yield electrocatalytic quantities of pinacol (Table S8). For kinetic analysis using UV-vis spectroscopy, the reactive form of the cobaltocene complexes, [**Co**(II), N**H**]BAr^F_4, was generated *in situ* by protonation of [**Co**(II), N] with one equivalent of [**H**$(Et_2O)_2$]BAr^F_4 (**Figure 4.2b**). Then, acetophenone addition (**Figure 4.2b**, black trace) led to formation of the [**Co**(III), N]$^+$ complexes, and the resulting kinetic trace was fit to an exponential decay to extract a first-order rate constant (k_{obs}, **Figure 4.2c**). Plotting k_{obs} as a function of substrate concentration (**Figure 4.2d**) allowed us to extract k_{PCET}, the second-order rate constant (**Figure 4.2e**). For each complex, we measured k_{PCET} using [**D**$(Et_2O)_2$]BAr^F_4 to determine the H/D kinetic isotope effect (KIE). We also measured k_{PCET} for a series of *p*-substituted acetophenones to determine the Hammett slope (ρ) as a measure of charge-transfer character in the PCET transition state (**Figure 4.2e**).

With this thermodynamic and kinetic dataset, we can probe the mechanism for acetophenone reduction by each complex. First, we consider the ET-PT pathway, but we find it is inconsistent with the observed primary KIEs (1.5–2.1) and can be further ruled out by a thermodynamic exclusionary argument, as the free energy for ET from cobaltocene to acetophenone ($\Delta G°_{ET}$ = 19–23 kcal/mol) is greater than the kinetically inferred barrier height ($\Delta G^‡$ = 16–17 kcal/mol). Next, we consider the PT-ET pathway, which cannot be ruled out on thermodynamic grounds (e.g. $\Delta G_{PT,calc}$ = 14–16

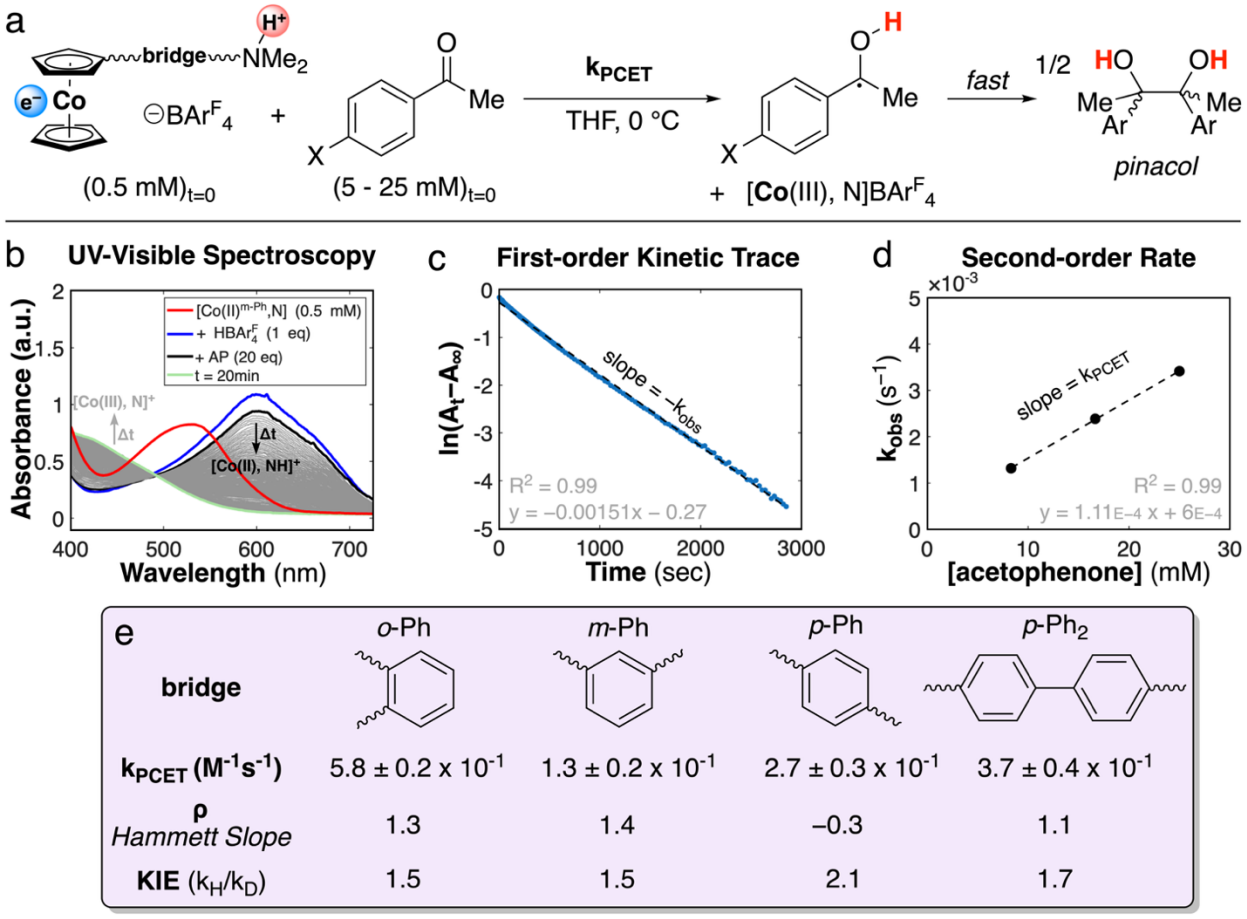

Figure 4.2. (a) Strategy for determination of the PCET rate constant. (b) UV-vis spectra of [**Co**(II)$^{m\text{-Ph}}$, N] (red trace) and [**Co**(II)$^{m\text{-Ph}}$, N**H**]BAr$^{F}_4$ (blue trace) which decays upon addition of acetophenone (black trace) to yield [**Co**(III)$^{m\text{-Ph}}$, N]BAr$^{F}_4$ (green trace). (c) Kinetic trace (absorbance vs. time) fit to an exponential decay, characteristic of first-order kinetics in which the slope of the fit line yields the observed first-order rate constant. (d) Plot of the first-order rate constants (k_{obs}) against substrate concentration, yielding the second-order rate constant (k_{PCET}) as the slope of the fit line. (e) PCET rate, Hammett slope, and kinetic isotope effect reported for each bridging group.

kcal/mol). However, we observe negative slopes for the PT rate–driving force relationships with the *p*-substituted acetophenones (i.e. $\Delta G_{PT,calc}$ vs. $\Delta G^{\ddagger}$), which is inconsistent with a rate-limiting PT step. We conclude CPET is the mechanism consistent with the observed data, as was previously concluded for the [**Co**(II)$^{p\text{-Ph}}$, N**H**]$^{+}$ mediator.[6]

These data demonstrate that the concerted mechanism is conserved across all the bridges. This implies that despite substantial variations in the thermodynamic coupling and the individual PT and ET driving forces available at [**Co**(II), N**H**]$^+$, the mode of PCET reactivity is here invariant to the position of the electron and proton donors. In contrast, we have previously shown that modifying the redox subunit from cobaltocene to *o*-carborane switches the mechanism of the PCET reaction from CPET to ET-PT, pre-empting the carborane's viability as an electrochemical PCET mediator.[35]

Interestingly, **Figure 4.2e** shows a positive and moderately steep Hammett slope (ρ) for [**Co**(II)$^{o\text{-Ph}}$, N**H**]$^+$, [**Co**(II)$^{m\text{-Ph}}$, N**H**]$^+$, and [**Co**(II)$^{p\text{-Ph2}}$, N**H**]$^+$ (ρ = 1.4, 1.3, 1.1), whereas the slope is negative and shallow for [**Co**(II)$^{p\text{-Ph}}$, N**H**]$^+$ (ρ = −0.3). The variation in ρ shows that the bridge modulates the charge-transfer nature of the PCET transition state. ρ does not correlate with PCET rate in this system, suggesting that ET–PT asynchronicity here is not a strong predictor of reactivity. This finding contrasts examples of oxidative PCET where basic asynchronous (PT-led) mechanisms predominate.[34,36,37,38]

The distinctive ρ value for PCET from [**Co**(II)$^{p\text{-Ph}}$, N**H**]$^+$ can be rationalized via Bernasconi's principle of nonperfect synchronization (PNS).[39] Here, the *para*-phenylene bridge is particularly suited to stabilize the [**Co**(III), N]$^+$ product state by delocalizing the N lone pair into the π-accepting Cp**Co**(III)Cp-Ar moiety. This is evident in the crystal structure of [**Co**(III)$^{p\text{-Ph}}$, N]OTf, which features a trigonal planar N-center (Σ ∠CNC = 360˚).**Error! Bookmark not defined.** By comparison, the N-centers are more pyramidal in the *para*-biphenylene, *meta*- and *ortho*-phenylene bridged [**Co**(III), N]$^+$ complexes (Σ ∠CNC = 357˚, 356˚, and 341˚, respectively). Maximizing the quinoidal resonance contribution requires N to rehybridize from a pyramidal to a fully planar geometry, which lags the fast proton motion. The result is an imbalanced transition state characterized by advanced proton transfer and negative ρ (positive charge buildup on the ketone).[40,41,42] A quinoidal resonance form is unavailable to the *meta* bridge, and extended π-orbital overlap in the *para*-biphenylene is frustrated by the biphenyl torsion. The *ortho* analog is sterically blocked from aligning the N lone pair with the Ar π orbitals. As it remains substantially pyramidal in the [**Co**(III), N]$^+$ product, the *ortho* compound undergoes the least rehybridization of the 4 mediators.

We plotted k_{PCET} against the available thermodynamic, structural, and kinetic parameters to determine which factors most affect PCET reactivity. Surprisingly, we found poor correlations between rate and component driving forces (pK_a and $E_{1/2}$), thermodynamic coupling ($\Delta E_{1/2}$), and

Co–N distance (Figure S86–S90). Plotting rate against the spectroscopic coupling ($\Delta\lambda_{max}$), we find a modest correlation ($R^2 = 0.61$) in which stronger coupling tracks with slower rate. One explanation for this behavior is that $\Delta\lambda_{max}$ crudely correlates with the PCET reorganization energy. However, equilibrium exchange measurements of the PCET reorganization energy in such reactive systems are complicated by spontaneous hydrogen evolution, so establishing a direct rather than inferred relationship between reorganization energy and $\Delta\lambda_{max}$ is challenging.

Plotting rate against driving force (the difference in experimental $BDFE_{N–H}$ and calculated ketyl $BDFE_{O–H}$) does not show the rate–driving force relationship expected of CPET reactions with structurally similar reactants (**Figure 4.3a**). In the low driving force regime, we expect the slope of the fit line (α) from the plot of $\Delta G^{‡}_{PCET}$ vs. $\Delta G°_{PCET}$ to be approximately 0.5. Rather, three complexes with the same $BDFE_{N–H}$ (within error) measurably differ in their PCET rates, while [**Co**(II)$^{o\text{-Ph}}$, N**H**]$^+$ has the least driving force and yet the fastest rate. Consequently, non-driving force parameters such as vibrational overlap, electronic coupling, and reorganization energy are likely the dominant rate-controlling factors for PCET in the series, which is uncommon. Examples of structural studies that intentionally seek to isolate these variables are instructive, but few in number.

Evidently, the rate-contributing factors for PCET across this series of bridges are not captured by ground state (thermochemical and structural) descriptors of the mediator in the absence of substrate. We employed theoretical models of the transition state (TS) for PCET to acetophenone, using density functional theory (DFT) calculations in ORCA 6 with a def2-TZVPP basis, the TPSSh hybrid functional, and implicit SMD(THF) solvation.[43,44] The computed barrier heights ($\Delta G^{‡}_{calc}$ = 13–18 kcal/mol) varied more than the experimental barriers ($\Delta G^{‡}$ = 16–17 kcal/mol), meaning that even at a reasonable level of theory, the precision of the DFT energies does not quantitatively resolve the fine differences in rates. Nevertheless, the transition state geometries offer qualitative insights. For each mediator, we identified transition states in which hydrogen bonding directs acetophenone over the phenylene linker (Figure S98–S101). With the meta-, para-, and bi-phenylene bridges, this is the lowest TS barrier. For [**Co**(II)$^{o\text{-Ph}}$, N**H**]$^+$, however, we identified a TS geometry where hydrogen bonding directs acetophenone over the Cp-face of cobaltocene (**Figure 4.3b**). The *o*-phenylene bridge is uniquely able to pre-organize the substrate over the Cp ring due to its proximity to Co, while Cp-stacking is geometrically inaccessible in the other complexes. The resulting $O–C_{Cp}$ distance in the transition state is 2.8 Å, shorter than the computed $O–C_{Cp}$ distance in a tight Co^{III}-

succinyl ion-pair implicated as an intermediate in the two-electron PCET reduction of fumarate by [**Co**(II)$^{p\text{-Ph}}$, N**H**]$^{+}$.[6]

Inspecting the computed transition state SOMO reveals that the carbonyl lies across the face of the Cp ring such that the empty C–O π* orbital overlaps with the half-filled Co–Cp π* orbital. Such an orbital interaction is isolobal with the Diels-Alder transition state (**Figure 4.3c)**, contributing to the unexpected transition state stabilization by the *o*-phenylene bridge.[45] More generally, this could help explain cobaltocene's apparent ability as an ET mediator, lowering the overpotential for reduction of substrates that are recognizable dienophiles.[46,47] Dienophile activation by Brønsted acids is well-known; hydrogen bonding from [**Co**(II), N**H**]$^{+}$ both directs and electronically activates the key orbital interaction.[48]

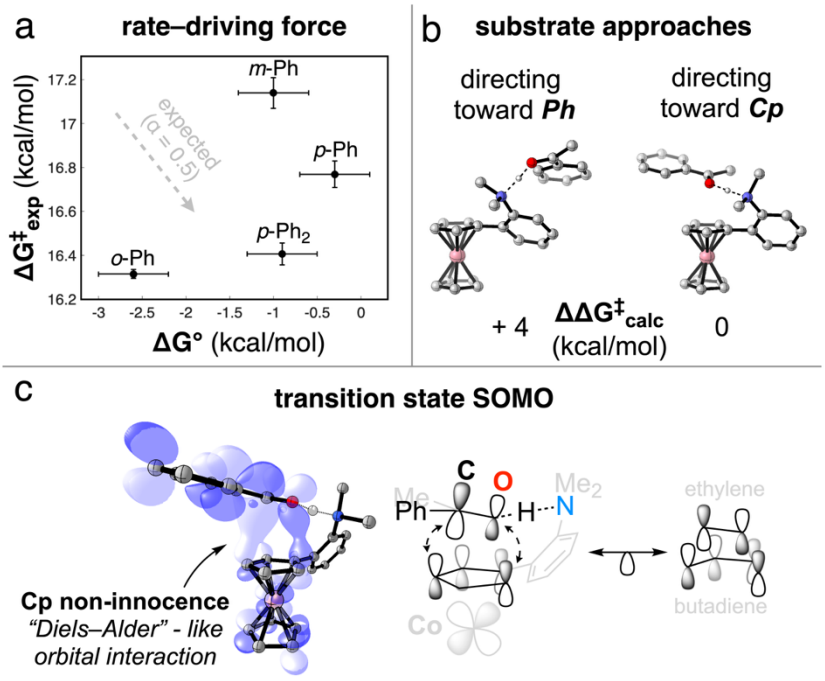

Figure 4.3. (a) Rate–driving force relationship for acetophenone reduction by [**Co**(II), N**H**]$^{+}$. (b) Computed transition state geometries for PCET from [**Co**(II)$^{o\text{-Ph}}$, N**H**]$^{+}$ to acetophenone in which the acid directs the substrate toward the Ph group (left) or the Cp group (right). (c) Transition state SOMO, highlighting the orbital interaction of the Cp group with the carbonyl.

Driving force asynchronicity has been a productive recent focal point for the PCET community, especially because polar effects are shown to influence rate without changing the overall driving

force.[34] Here, we offer an orthogonal design consideration, independent of driving force and polarity, that may improve PCET reactivity. Since the PT distance is short, the acid can be considered as a directing group to orient the electron donor and acceptor. We suggest that the bridge as a directing group may also be a productive focal point for PCET mediator design.

4.3 Conclusion

To close, we have interrogated how the connection between a Brønsted acid and reductant influences PCET reactivity in a cobaltocene-derived mediator system. We synthesized a series of anilinium-appended cobaltocene complexes that vary only in the identity of the covalent bridging group. Within this set of PCET reductants, thermodynamic measurements establish that the bridge significantly affects acid–reductant coupling while preserving similar H-atom transfer driving force. Kinetic measurements establish that the anilinium-appended cobaltocenes all reduce acetophenone via a rate-limiting CPET step, the rate of which is modestly perturbed and contradicts the anticipated rate–driving force relationship. The bridging group exerts its unexpected influence on rate by pre-organizing substrates in geometries that differ in their intrinsic barriers, demonstrating the modulation of PCET kinetics at nearly constant driving force.

4.4 References

[1] Tommos, C.; Babcock, G. T. Proton and Hydrogen Currents in Photosynthetic Water Oxidation. *Biochimica et Biophysica Acta (BBA) - Bioenergetics* **2000**, *1458* (1), 199–219. DOI: 10.1016/s0005-2728(00)00069-4.

[2] Dempsey, J. L.; Winkler, J. R.; Gray, H. B. Proton-Coupled Electron Flow in Protein Redox Machines. *Chem. Rev.* **2010**, *110* (12), 7024–7039. DOI: 10.1021/cr100182b.

[3] Hoffman, B. M.; Lukoyanov, D.; Yang, Z.-Y.; Dean, D. R.; Seefeldt, L. C. Mechanism of Nitrogen Fixation by Nitrogenase: The Next Stage. *Chem. Rev.* **2014**, *114* (8), 4041–4062. DOI: 10.1021/cr400641x.

[4] Kaila, V. R. I.; Verkhovsky, M. I.; Wikström, M. Proton-Coupled Electron Transfer in Cytochrome Oxidase. *Chem. Rev.* **2010**, *110* (12), 7062–7081. DOI: 10.1021/cr1002003.

[5] Murray, P. R. D.; Cox, J. H.; Chiappini, N. D.; Roos, C. B.; McLoughlin, E. A.; Hejna, B. G.; Nguyen, S. T.; Ripberger, H. H.; Ganley, J. M.; Tsui, E.; Shin, N. Y.; Koronkiewicz, B.; Qiu, G.; Knowles, R. R. Photochemical and Electrochemical Applications of Proton-Coupled Electron Transfer in Organic Synthesis. *Chem. Rev.* **2022**, *122* (2), 2017–2291. DOI: 10.1021/acs.chemrev.1c00374.

[6] Chalkley, M. J.; Garrido-Barros, P.; Peters, J. C. A Molecular Mediator for Reductive Concerted Proton-Electron Transfers via Electrocatalysis. *Science* **2020**, *369* (6505), 850–854. DOI: 10.1126/science.abc1607

[7] Derosa, J.; Garrido-Barros, P.; Peters, J. C. Electrocatalytic Reduction of C–C π-Bonds via a Cobaltocene-Derived Concerted Proton–Electron Transfer Mediator: Fumarate Hydrogenation as a Model Study. *J. Am. Chem. Soc.* **2021**, *143* (25), 9303–9307. DOI: 10.1021/jacs.1c03335.

[8] Garrido-Barros, P.; Derosa, J.; Chalkley, M. J.; Peters, J. C. Tandem Electrocatalytic N2 Fixation via Proton-Coupled Electron Transfer. *Nature* **2022**, *609* (7925), 71–76. DOI: 10.1038/s41586-022-05011-6.

[9] Derosa, J.; Garrido-Barros, P.; Li, M.; Peters, J. C. Use of a PCET Mediator Enables a Ni-HER Electrocatalyst to Act as a Hydride Delivery Agent. *J. Am. Chem. Soc.* **2022**, *144* (43), 20118–20125. DOI: 10.1021/jacs.2c09786.

[10] Li, M.; Peters, J. C. Electrochemical Nickel-Catalyzed Asymmetric Hydrogenation of C═C Bonds Facilitated by a Proton-Coupled Electron Transfer Mediator. *ACS Catal.* **2025**, *15* (16), 13720–13726. DOI: 10.1021/acscatal.5c04130.

[11] Ovian, J. M.; Derosa, J.; Li, M.; Peters, J. C. Tunable Multisite Proton-Coupled Electron Transfer Mediators: Distinct Pathways for Substrate Reduction Versus Competing Hydrogen Evolution *J. Am. Chem. Soc.* **2026**, *148* (2), 2609-2616. DOI: 10.1021/jacs.5c18522.

[12] Badalyan, A.; Stahl, S. S. Cooperative Electrocatalytic Alcohol Oxidation with Electron-Proton-Transfer Mediators. *Nature* **2016**, *535* (7612), 406–410. DOI: 10.1038/nature18008.

[13] McLoughlin, E. A.; Armstrong, K. C.; Waymouth, R. M. Electrochemically Regenerable Hydrogen Atom Acceptors: Mediators in Electrocatalytic Alcohol Oxidation Reactions. *ACS Catal.* **2020**, *10* (19), 11654–11662. DOI: 10.1021/acscatal.0c03240.

[14] Wu, A.; Masland, J.; Swartz, R. D.; Kaminsky, W.; Mayer, J. M. Synthesis and Characterization of Ruthenium Bis(β-Diketonato) Pyridine-Imidazole Complexes for Hydrogen Atom Transfer. *Inorg. Chem.* **2007**, *46* (26), 11190–11201. DOI: 10.1021/ic7015726.

[15] Otsuka, H.; Arashiba, K.; Nakamura, T.; Tanaka, H.; Yoshizawa, K.; Nishibayashi, Y. Synthesis of Cobaltocenes Bearing 4-(2,6-Dimethylpyridin-1-Ium-4-Yl)Phenyl Moiety and Their Stoichiometric and Catalytic Reactivity toward Ammonia Formation. *Organometallics* **2026**. DOI: 10.1021/acs.organomet.5c00492.

[16] Mitsumoto, T.; Nakamura, T.; Tanaka, H.; Yoshizawa, K.; Nishibayashi, Y. Cooperative Ammonia Formation Catalyzed by Molybdenum and Samarium Complexes. *Angew. Chem. Int. Ed.* **2025**, *64* (32), e202507061. DOI: 10.1002/anie.202507061.

[17] Kuriyama, S.; Zhang, Y.; Tanaka, H.; Konomi, A.; Egi, A.; Yoshizawa, K.; Nishibayashi, Y. Synthesis and Reactivity of Iron-Oxocyclohexadienyl Complexes toward Proton-Coupled Electron Transfer. *Organometallics* **2024**, *43* (21), 2736–2746. DOI: 10.1021/acs.organomet.4c00286.

[18] Mukherjee, J.; Ostermann, N.; Aniban, X.; Safianova, I.; Rotthowe, N.; Mata, R.; Siewert, I. A Nickel Complex with a Proton-Responsive PNP Pincer-Type Ligand as a Proton-Coupled Electron

Transfer Reagent. *Organometallics* **2023**, *42* (22), 3258–3265 DOI: 10.1021/acs.organomet.3c00378.

[19] Mukherjee, J.; Ostermann, N.; Pecak, J.; Otte, M.; Podewitz, M.; Siewert, I. Mechanistic Studies of the Proton-Coupled Electron Transfer Reactivity of a Cobalt Complex with a Proton-Responsive PNP Pincer-Type Ligand. *Inorg. Chem.* **2025**, *64* (28), 14466–14474. DOI: 10.1021/acs.inorgchem.5c01792.

[20] Won, C.; Kwon, S.; Kim, D.; Baek, Y. Orchestrating the Semiquinone Stability for Catalytic Proton-Coupled Electron Transfer. *J. Am. Chem. Soc.* **2026**, *148* (8), 8761–8771. DOI: 10.1021/jacs.5c21171.

[21] Dey, S.; Masero, F.; Brack, E.; Fontecave, M.; Mougel, V. Electrocatalytic Metal Hydride Generation Using CPET Mediators. *Nature* **2022**, *607* (7919), 499–506. DOI: 10.1038/s41586-022-04874-z.

[22] Proe, K. R.; Schreiber, E.; Matson, E. M. Proton-Coupled Electron Transfer at the Surface of Polyoxovanadate-Alkoxide Clusters. *Acc. Chem. Res.* **2023**, *56* (12), 1602–1612. DOI: 10.1021/acs.accounts.3c00166.

[23] Amtawong, J.; Montgomery, C. L.; Bein, G. P.; Raithel, A. L.; Hamann, T. W.; Chen, C.-H.; Dempsey, J. L. Mechanism-Guided Kinetic Analysis of Electrocatalytic Proton Reduction Mediated by a Cobalt Catalyst Bearing a Pendant Basic Site. *J. Am. Chem. Soc.* **2024**, *146* (6), 3742–3754. DOI: 10.1021/jacs.3c10408.

[24] Fisher, K. J.; Kelly, H. R.; Cody, C. C.; Decavoli, C.; Mercado, B. Q.; Troiano, J. L.; Crabtree, R. H.; Batista, V. S.; Brudvig, G. W. Metal-Dependent Asynchronicity of Concerted Proton–Electron Transfer to a High-Valent Copper(III) Complex and Its Nickel(III) Analogue. *Inorg. Chem.* **2025**, *64* (28), 14552–14565. DOI: 10.1021/acs.inorgchem.5c02005.

[25] Fischer, E. O.; Herberich, G. E. Über Aromatenkomplexe von Metallen, XLIV. Über die Reaktivität des Di-cyclopentadienyl-kobalt(III)-Kations. *Chemische Berichte* **1961**, *94* (6), 1517–1523. DOI: 10.1002/cber.19610940615.

[26] El Murr, N. Endo-Hydride Abstraction from Exo-Substituted Cyclopentadienecyclopentadienylcobalt; Synthesis of Monosubstituted Cobalticinium Salts. *J. Organomet. Chem.* **1981**, *208* (1), C9–C11. DOI: 10.1016/s0022-328x(00)89185-8.

[27] Vanicek, S.; Kopacka, H.; Wurst, K.; Müller, T.; Schottenberger, H.; Bildstein, B. Chemoselective, Practical Synthesis of Cobaltocenium Carboxylic Acid Hexafluorophosphate. *Organometallics* **2014**, *33* (5), 1152–1156 DOI: 10.1021/om401120h.

[28] Bahr, S. R.; Boudjouk, P. Trityl Tetrakis[3,5-Bis(Trifluoromethyl)Phenyl]Borate: A New Hydride Abstraction Reagent. *J. Org. Chem.* **1992**, *57* (20), 5545–5547. DOI: 10.1021/jo00046a048.

[29] Imrie, C.; Loubser, C.; Engelbrecht, P.; McCleland, C. W. The Use of a Modified Suzuki Reaction for the Synthesis of Monoarylferrocenes. *J. Chem. Soc., Perkin Trans. 1* **1999**, 17, 2513–2523. DOI: 10.1039/a903058a.

[30] Börgel, J.; Ritter, T. Late-Stage Functionalization. *Chem* **2020**, *6* (8), 1877–1887. DOI: 10.1016/j.chempr.2020.07.007.

[31] Kütt, A.; Tshepelevitsh, S.; Saame, J.; Lõkov, M.; Kaljurand, I.; Selberg, S.; Leito, I. Strengths of Acids in Acetonitrile. *Eur. J. Org. Chem.* **2021**, *2021* (9), 1407–1419. DOI: 10.1002/ejoc.202001649.

[32] Connelly, N. G.; Geiger, W. E. Chemical Redox Agents for Organometallic Chemistry. *Chem. Rev.* **1996**, *96* (2), 877–910. DOI: 10.1021/cr940053x.

[33] Warren, J. J.; Tronic, T. A.; Mayer, J. M. Thermochemistry of Proton-Coupled Electron Transfer Reagents and Its Implications. *Chem. Rev.* **2010**, *110* (12), 6961–7001. DOI: 10.1021/cr100085k.

[34] Groff, B. D.; Cattaneo, M.; Rinaolo, K. C.; Mercado, B. Q.; Mayer, J. M. Disentangling Driving Force Effects, Polar Effects, e–/H+ Imbalance, and Other Influences on H-Atom Transfer Reactions. *J. Am. Chem. Soc.* **2025**, *147* (6), 4766–4777. DOI: 10.1021/jacs.4c10596.

[35] Adillon, E. H.; Peters, J. C. A Carborane-Derived Proton-Coupled Electron Transfer Reagent. *J. Am. Chem. Soc.* **2024**, *146* (44), 30204–30211. DOI: 10.1021/jacs.4c09007.

[36] Fisher, K. J.; Kelly, H. R.; Cody, C. C.; Decavoli, C.; Mercado, B. Q.; Troiano, J. L.; Crabtree, R. H.; Batista, V. S.; Brudvig, G. W. Metal-Dependent Asynchronicity of Concerted Proton–Electron Transfer to a High-Valent Copper(III) Complex and Its Nickel(III) Analogue. *Inorg. Chem.* **2025**, *64* (28), 14552–14565. DOI: 10.1021/acs.inorgchem.5c02005.

[37] Zhao, N.; Goetz, M. K.; Schneider, J. E.; Anderson, J. S. Testing the Limits of Imbalanced CPET Reactivity: Mechanistic Crossover in H-Atom Abstraction by Co(III)–Oxo Complexes. *J. Am. Chem. Soc.* **2023**, *145* (10), 5664–5673. DOI: 10.1021/jacs.2c10553.

[38] Kotani, H.; Shimomura, H.; Ikeda, K.; Ishizuka, T.; Shiota, Y.; Yoshizawa, K.; Kojima, T. Mechanistic Insight into Concerted Proton–Electron Transfer of a Ru(IV)-Oxo Complex: A Possible Oxidative Asynchronicity. *J. Am. Chem. Soc.* **2020**, *142* (40), 16982–16989. DOI: 10.1021/jacs.0c05738.

[39] Bernasconi, C. F. The Principle of Nonperfect Synchronization: More than a Qualitative Concept? *Acc. Chem. Res.* **1992**, *25* (1), 9–16. DOI: 10.1021/ar00013a002.

[40] Qiu, G.; Knowles, R. R. Rate–Driving Force Relationships in the Multisite Proton-Coupled Electron Transfer Activation of Ketones. *J. Am. Chem. Soc.* **2019**, *141* (6), 2721–2730. DOI: 10.1021/jacs.8b13451.

[41] Groff, B. D.; Koronkiewicz, B.; Mayer, J. M. Polar Effects in Hydrogen Atom Transfer Reactions from a Proton-Coupled Electron Transfer (PCET) Perspective: Abstractions from Toluenes. *J. Org. Chem.* **2023**, *88* (23), 16259–16269. DOI: 10.1021/acs.joc.3c01748.

[42] Darcy, J. W.; Kolmar, S. S.; Mayer, J. M. Transition State Asymmetry in C–H Bond Cleavage by Proton-Coupled Electron Transfer. *J. Am. Chem. Soc.* **2019**, *141* (27), 10777–10787. DOI: 10.1021/jacs.9b04303.

[43] Neese, F. Software update: The ORCA program system—Version 6.0 *WIREs Computational Molecular Science* **2025**, *15* (2), e70019: DOI: 10.1002/wcms.70019.

[44] Bannerjee, S.;Peters, J. C.First-Principles Insights into Proton-Coupled Electron Transfer versus Hydrogen Evolution Reaction Selectivity from a Base-Appended Cobaltocene Mediator *manuscript submitted for publication* **2026**

[45] Fringuelli, F.; Taticchi, A. *The Diels-Alder Reaction: Selected Practical Methods*; John Wiley & Sons, **2002**.

[46] Xuan, Z.; Gerhardt, E.; Parnitzke, B.; Derosa, J. Electroreductive Iron Catalysis Enabled by a Redox Mediator: Alkyne Semi-Hydrogenation as a Model System. *ACS Catal.* **2025**, *15* (16), 13904–13909. DOI: 10.1021/acscatal.5c03611.

[47] Zhu, J.; Stahl, S. S. Use of Electron-Transfer Mediators to Access Higher Electrochemical Current Densities in Ni-Catalyzed Cross-Electrophile Coupling. *J. Am. Chem. Soc.* **2025**, *147* (40), 36053–36058. DOI: 10.1021/jacs.5c10599.

[48] Rueping, M.; Kuenkel, A.; Atodiresei, I. Chiral Brønsted Acids in Enantioselective Carbonyl Activations–Activation Modes and Applications. *Chem. Soc. Rev.* **2011**, *40* (9), 4539–4549. DOI: 10.1039/c1cs15087a

Chapter 5

A Phosphonium-derived Proton-coupled Electron Transfer Mediator

5.1 Introduction

Proton-coupled electron transfer (PCET) reactions promote redox at mild potentials by circumventing charge transfer steps.[1] In the context of electrocatalysis, PCET has been borne out as a powerful strategy for the discovery of new catalysts and conditions for electrolytic small molecule reduction reactions.[2] Through coupling with proton transfer, the rate of electron transfer can be enhanced at milder potentials, enabling the reduction of substrates which otherwise require harsh conditions. PCET can help to minimize the necessary applied potential and reagent acidity needed for reductive protonation.

Our group's interests lie in reductive PCET reactions, where a species containing a weak element–hydrogen bond can readily transfer an H-atom to a substrate. For example, the anilinium-appended cobaltocene complex (**Scheme 5.1A**, X = N) has been shown to react via CPET with a variety of organic substrates including acetophenone, fumarate as well as transition metal substrates like nickel(II) phosphine complexes and transition metal–dinitrogen complexes.[3–6] Structure-activity relationships of this platform have been investigated through substitution of the reductant moiety, which changes the mechanism, or the bridging linker, which modulates the rate.[7,8] A challenge of reductive PCET is the competing hydrogen evolution reaction (HER), in which protons and electrons combine in the absence of a substrate to generate H_2, making the imperative of these reactions optimizing PCET while surpressing HER.

Herein, we present a structure-activity study of the Brønsted acid, where we substitute the anilinium unit with phosphonium and observe its effects on PCET thermochemistry and reactivity. We anticipate two primary features to distinguish the nitrogen and phosphorus analogs. First, we considered that phosphorus is less electronegative than nitrogen (2.19 vs. 3.04) which should result in a less polarized X–H bond.[9] This is illustrated quantitatively in **Scheme 5.1B** as electrostatic potential maps computed using ORCA, where the nitrogen leads to a more polarized acid fragment than phosphorus.[10] In effect, the phosphonium acid should be a weaker hydrogen bond donor but should also be more polarizable. Secondly, the phosphine and aniline geometries should differ, where the phosphine will contain a stereochemically-active lone pair and the aniline will be planar with a lone pair in conjugation with the adjacent aromatic group (**Scheme 5.1C**).[11]

To establish a relationship between the properties of the Brønsted acid and PCET reactivity, we prepared a phosphorus-analog of the aniline-appended cobaltocene mediator, determined its structure, measured its PT and ET thermochemistry, and studied its PCET reactivity with a model substrate reaction. In doing so, we present a unique study of the PCET properties of Brønsted acid congeners.

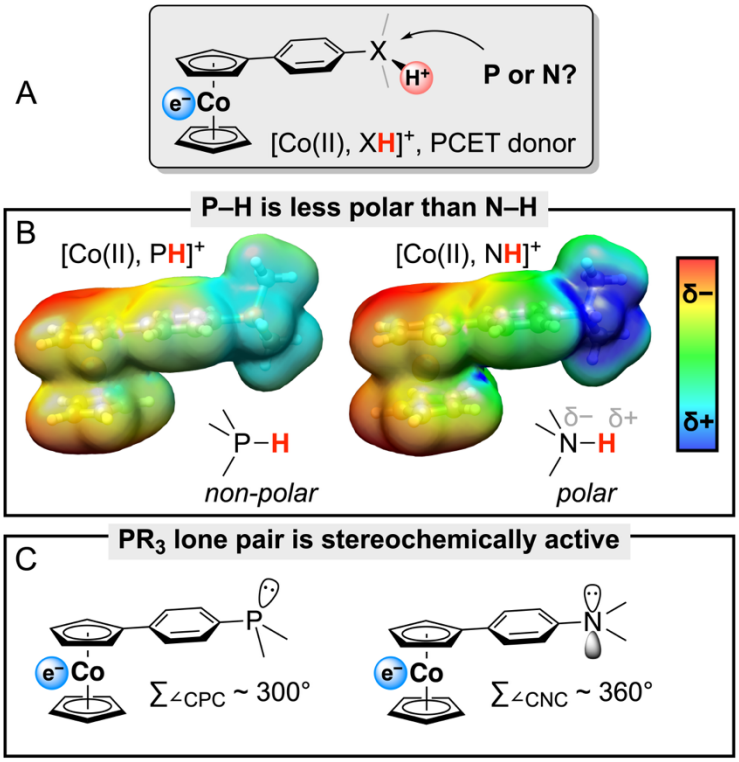

Scheme 5.1 (A) A cobaltocene complex containing an appended Brønsted-basic nitrogen or phosphorus atom. (B) Calculated electrostatic potential maps with phosphonium (left) or anilinium (right). (C) Geometric differences between P- or N-derived bases appended to cobaltocene.

5.2 Results and Discussion

Synthesis.

The phosphine-appended cobaltocene complex was prepared according to **Scheme 5.2**. First, 1,4-dibromobenzene was converted to (4-bromophenyl)dimethylphosphine by a known two-step sequence.[12,13] Then, lithium-halogen exchange with the aryl bromide afforded the corresponding aryl lithium nucleophile *in situ* which was added to cobaltocenium to yield the desired (η^4-CpHPh^P)**Co**Cp complex. The phosphine was protected with borane, allowing the Co(I) complex to be thermolyzed to yield Co(II). Oxidation of the Co(II) was accomplished using ferrocenium triflate, yielding the borane-protected cobaltocenium complex. The borane was subsequently removed upon heating in THF with a highly nucleophilic amine, 1,4-diazabicyclooctane (or DABCO), and protonation of the phosphine with diphenylammonium triflate allowed for its isolation as a dication.

Diffraction quality crystals could be grown by cooling a benzene solution of [Cp**Co**Cp^P]BAr$^F{}_4$. The X-ray diffraction structure reveals that the geometry of the phosphorus center is pyramidal, as expected for a phosphine, where the sum of the C–P–C bond angles about phosphorus is 301°. In contrast, the structure of the nitrogen analog features a trigonal planar nitrogen center. The cobaltocene fragments of the two structures are qualitatively similar.

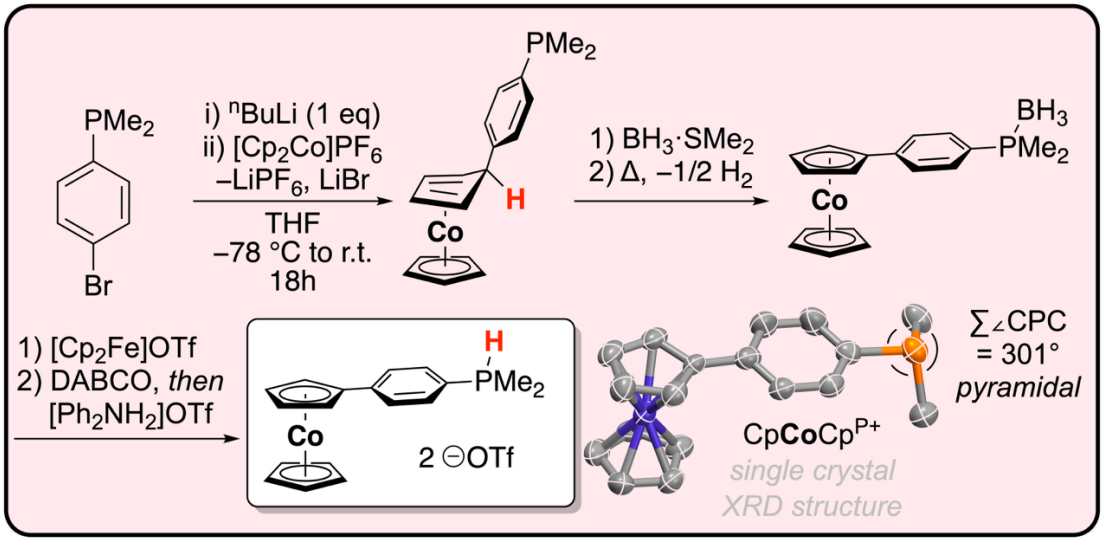

Scheme 5.2 Synthetic route for the preparation of [Cp**Co**Cp^{PH}](OTf)$_2$

Thermochemistry

The relevant thermochemical descriptors were measured and are summarized in **Figure 5.1A**. The acid dissociation constant was measured using ^{1}H NMR spectroscopy by titrating 3-chloropyridine (pK_{aH} = 9.6) into a solution of [Cp**Co**Cp^{PH}](OTf)$_2$ in acetonitrile-d$_3$ and quantifying the resulting acid and base concentrations (see D6). The phosphonium pK_a was determined to be 10.9 ± 0.1, modestly more acidic than dimethylphenylphosphonium (pK_a = 12.6). The half-wave potentials ($E_{1/2}$) were measured by cyclic voltammetry (CV) as shown in **Figure 5.1B**. A reversible feature at −1.27 V was observed, corresponding to Co(III/II) redox. Upon addition of 4-cyanoanilinium acid (pK_a = 7.0), this redox couple becomes quasi-reversible and shifts anodically to −1.18 V, indicating protonation of the phosphine. The $E_{1/2}$ shift ($\Delta E_{1/2}$ = 90 mV) is modestly smaller than that of the N-analog ($\Delta E_{1/2}$ = 140 mV).[5]

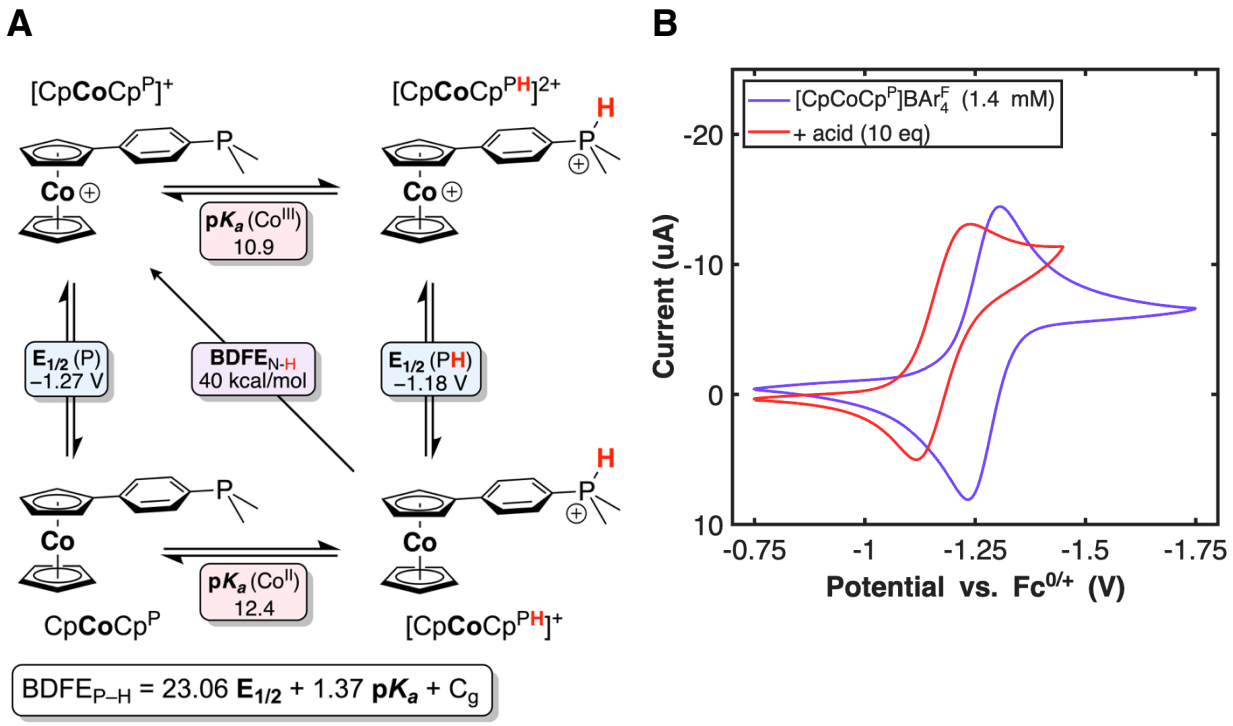

Figure 5.1 (left) Square scheme for Cp**Co**Cp^{PH+}. (right) CVs of [Cp**Co**Cp^{P}]BAr$^{F}_4$ (1.4 mM, *blue*) with [$^{4\text{-CN}}$PhNH$_3$]OTf (14 mM, *red*) in acetonitrile with ^{n}Bu$_4$NPF$_6$ (200 mM) supporting electrolyte. The scans are swept cathodic, then anodic at 100 mV/s.

Table 5.1: PCET thermochemistry of phosphine- and aniline-appended cobaltocene complexes

congener	$E_{1/2}$ (N) (V vs. $Fc^{0/+}$)	$E_{1/2}$ (NH) (V vs. $Fc^{0/+}$)	pK_a (Co^{III})	pK_a (Co^{II})	BDFE[a] (kcal/mol)	$\Delta E_{1/2}$ (N/NH) (mV)
N[a]	−1.35	−1.21	8.6	11.0	36.5	140
P	−1.27	−1.18	10.9	12.4	40.3	90

[a] Values reported in reference 5.

The effective P–H bond dissociation free energy ($BDFE_{P–H}$) can be determined by summing the PT and ET equilibrium constants with a solvent-dependent constant (C_g), according to the Bordwell equation in **Figure 5.1A**.[14] From this equation, the $BDFE_{P–H}$ is determined to be 40.3 kcal/mol. This $BDFE_{P–H}$ is modestly higher than the $BDFE_{N–H}$ in the nitrogen analog, primarily because the phosphonium fragment is a weaker acid than the anilinium fragment in the cobaltocenium complexes (pK_a = 10.9 *vs.* 8.6).

Reactivity

According to the thermochemistry measurements, Cp**Co**Cp^{PH+} contains a weak P–H bond that may serve as a potent H-atom donor to unsaturated substrates. To probe the PCET reactivity of Cp**Co**Cp^{PH+}, we opted to use acetophenone reduction to ketyl as a model reaction (**Figure 5.2A**). Previous work has shown that the PCET rate can be directly determined using CV by modeling the reaction as an E_rC_i mechanism.[3–6,15] Specifically, the PCET rate constant can be extracted from the ratio of the peak currents of the Co(III/II) wave in the presence and absence of substrate, according to Eq 1:

$$\text{(Eq 1.)}\ \left(\frac{i_c}{i_p}\right)^2 = \left(\frac{1}{0.446}\right)^2 \left(\frac{RT}{Fv}\right) k_{PCET} C^0_{sub}$$

where i_c is the catalytic plateau current, i_p is the peak cathodic current in the absence of substrate, k_{PCET} is the PCET rate constant, C^0_{sub} is the concentration of the substrate, T is temperature, v is the scan rate, R is the universal gas constant, and F is the Faraday constant. Plotting $\left(\frac{i_c}{i_p}\right)^2$ as a function of substrate concentration yields the PCET rate constant as the slope. Under controlled

potential electrolysis conditions, the ketyl radical formed upon PCET to acetophenone rapidly dimerizes to form the pinacol as the observed product of electrolysis.

The voltammograms of [Cp**Co**Cp^{PH}](OTf)$_2$ with tosic acid and increasing concentrations of acetophenone are shown in **Figure 5.2B**. Addition of acetophenone led to formation of an irreversible, multi-electron wave, consistent with mediated electrocatalysis. As the acetophenone concentration was increased, the plateau current also increases. An equivalent set of CVs with the nitrogen analog, Cp**Co**Cp^{NH+}, were collected for comparison (**Figure D25**).

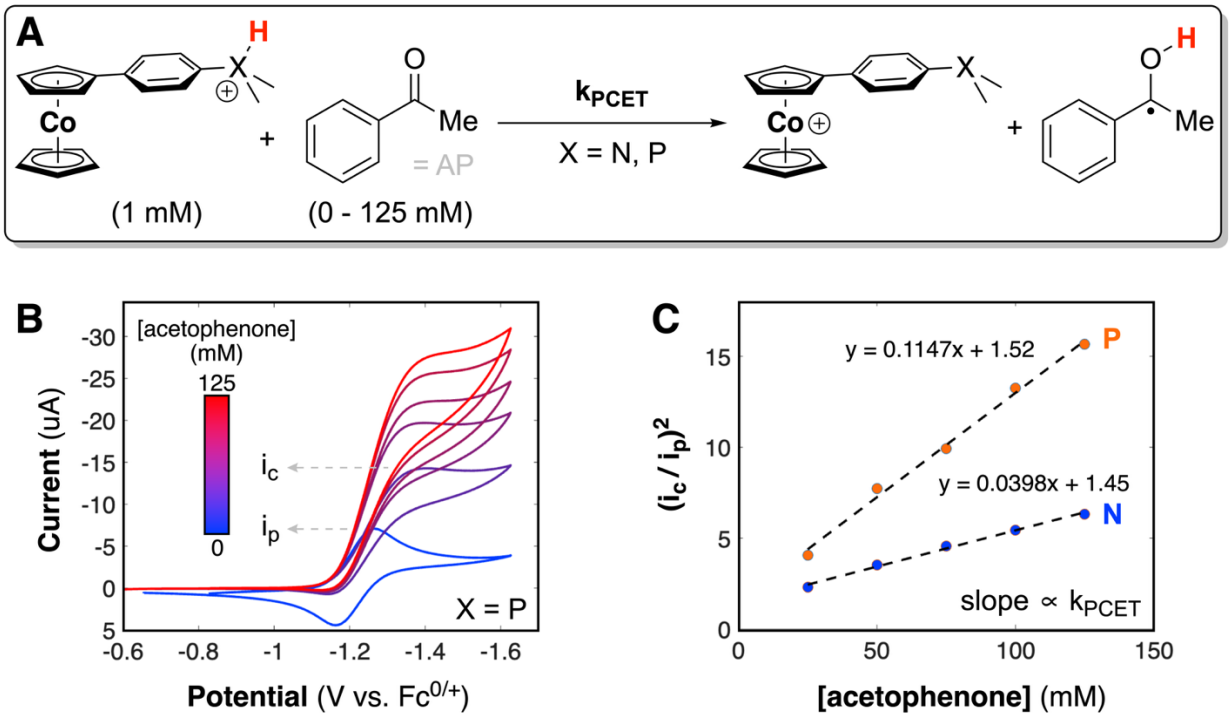

Figure 5.2 (top) Schematic for PCET from [CpCoCp^{XH}]$^+$ (X = N, P) to acetophenone. (left) CVs [Cp**Co**Cp^{PH}](OTf)$_2$ (1 mM) with tosic acid (20 mM, *blue*) and increasing concentrations of acetophenone (0-125 mM) in DME with ^{n}Bu$_4$NPF$_6$ (100 mM) supporting electrolyte. The scans are swept cathodic, then anodic at 100 mV/s. (right) Scatter plots of $(i_c/i_p)^2$ vs. acetophenone concentration for the phosphorus (*orange*) and nitrogen (*blue*) congeners of [CpCoCp^{XH}]$^+$, where the slope of the fit line is proportional to the PCET rate constant.

For the two congeners, the squares of current ratios were plotted as a function of acetophenone concentration, where the slope of $(i_c/i_p)^2$ vs. acetophenone is proportional to k_{PCET} (**Figure 5.2C**). For

Cp**Co**Cp^{PH+}, k_{PCET} was determined to be 89 $M^{-1}s^{-1}$ while measurements of Cp**Co**Cp^{NH+} under identical conditions determined k_{PCET} to be 31 $M^{-1}s^{-1}$.

The PCET rate for the phosphonium-appended cobaltocene is a factor of three faster than the anilinium-appended cobaltocene. This modest difference in rate is surprising considering the difference in driving force. Because the $BDFE_{P–H}$ (= 40.3 kcal/mol) is approximately 4 kcal/mol higher than the $BDFE_{N–H}$ (= 36.5 kcal/mol) of the nitrogen congener, it is reasonable to expect that the PCET rate to a given substrate would be considerably slower based on a rate–driving force relationship expected for structurally related compounds.[16] From the difference in driving force alone, one would expect the rate to decrease by approximately a factor of 25.[17]

One argument for the difference in rates is a difference in reorganization energy which describes the extent of structural change in response to a change in oxidation and protonation state (**Scheme 5.2**). Both the ET and PT can contribute to reorganization energy. The two congeners contain the same ET fragment, cobaltocene, whose reorganization energy is not likely to differ significantly. However, the PT fragments are quite different, as manifest through their C-X-C bond angles (X = N, P). In their protonated forms, the nitrogen and phosphorus-derived acids are both tetrahedral, where the C-X-C and C-X-H bond angles are approximately 109.5° (Figure D27-D28). In the free-base form of

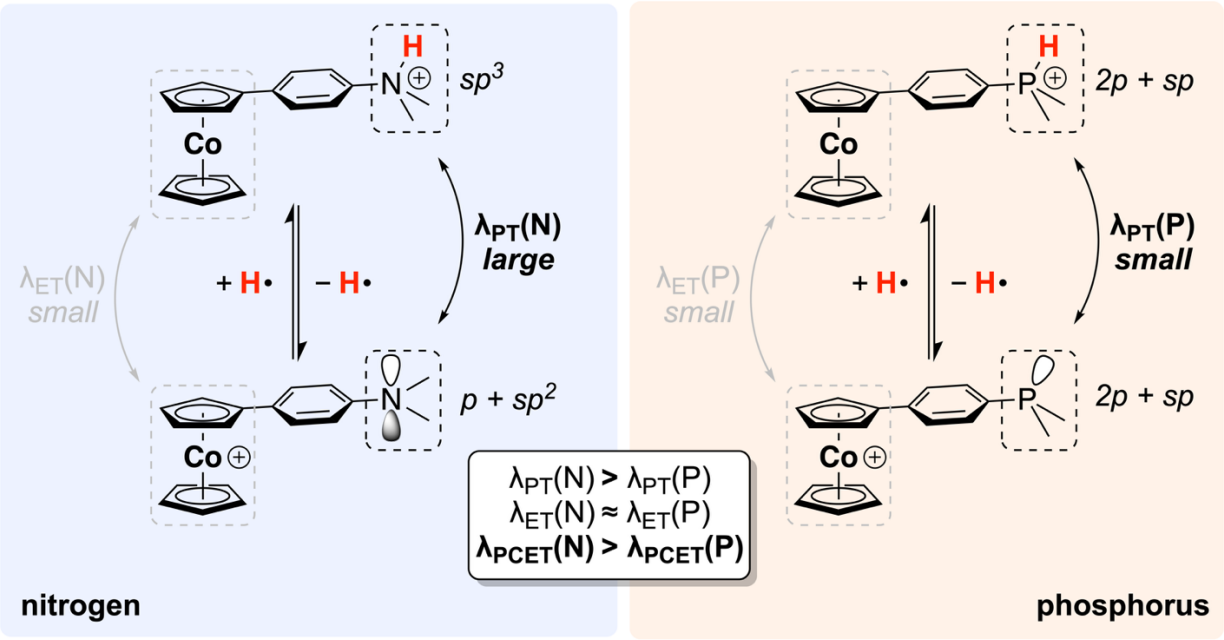

Scheme 5.3 Illustration of differences in reorganization energy between the nitrogen (left) and phosphorus (right) analogs of Cp**Co**Cp^{XH+}.

the nitrogen congener, the geometry about nitrogen is trigonal planar, with C-N-C bond angles approximately equal to 120°. In the phosphorus congener, the geometry about phosphorus is between trigonal pyramidal and T-shaped, with C-P-C bond angles approximately equal to 100°.

The aniline is planar about nitrogen in part due to the overlap between its lone pair and the adjacent aromatic group. This conjugation is manifest as a more reducing Co(III/II) couple compared to the phosphine, whose lone pair has poor overlap with the aromatic system ($E_{1/2}$(N) = −1.35 V vs. $E_{1/2}$(P) = −1.27 V). The reorganization associated with a change in conjugation, or equivalently hybridization, is evoked to explain the slow PT kinetics of α-C–H bonds in carbonyls to form enolates, as well as the slow H-atom transfer kinetics of C–H PCET reactions.[18–21] Here, it seems reasonable to propose that PT with aniline, which is isolobal to PT in enolates, involves conjugation of the nitrogen lone pair with the aromatic group. Consequently, the aniline base has a higher reorganization energy compared to the phosphine base which is not in conjugation with the aromatic system.

5.3 Conclusion

Here, we describe the synthesis of a phosphorus congener of anilinium-appended cobaltocene, a known PCET electrocatalyst. The structure of the phosphorus platform is determined as well as its PCET thermochemistry and reactivity. Despite having substantially less driving force for PCET to acetophenone, the Cp**Co**Cp$^{\mathbf{PH}+}$ reacts three-times faster than Cp**Co**Cp$^{\mathbf{NH}+}$. The inverse rate-driving force relationship between the congeners likely arises from a difference in reorganization energy, where the geometric and electronic properties of the phosphine render it kinetically more acidic despite being thermodynamically more basic. Measuring the reorganization energy would further support this viewpoint, and efforts to do so using the PCET self-exchange rate are ongoing.

This study builds upon an ongoing line of inquiry into the role of reorganization energy in reductive PCET reactions. A previous study described a main group congener of the anilinium-appended cobaltocene complex in which the cobaltocene fragment is substituted for C,C'-diaryl-*o*-carborane, a redox-active main group reductant with a similar redox potential to cobaltocene.[7] In contrast to its transition metal analog, the carborane-derived PCET donor did not react with acetophenone, in part due to the substantial ET structural reorganization of the *o*-carborane fragment apparent from X-ray

diffraction structures. By substituting the redox subunit, the reorganization energy increased, and the reactivity was attenuated. Here, we find that by substituting the acid/base subunit of the anilinium-appended cobaltocene with phosphonium, the reactivity is enhanced, in part due to reorganization energy. These studies make a compelling case for reorganization as an intuitive design parameter as it can be inferred as structural changes across oxidation and protonation states. By minimizing the structural differences across the various oxidation and protonation states, one should in principle maximize the inherent PCET rate.

5.4 References

1 Agarwal, R. G.; Coste, S. C.; Groff, B. D.; Heuer, A. M.; Noh, H.; Parada, G. A.; Wise, C. F.; Nichols, E. M.; Warren, J. J.; Mayer, J. M. Free Energies of Proton-Coupled Electron Transfer Reagents and Their Applications. *Chem. Rev.* **2022**, *122* (1), 1–49. DOI: 10.1021/acs.chemrev.1c00521.

2 Peters, J. C. Advancing Electrocatalytic Nitrogen Fixation: Insights from Molecular Systems. *Faraday Discuss.* **2023**, *243* (0), 450–472. DOI: 10.1039/D3FD00017F.

3 Derosa, J.; Garrido-Barros, P.; Peters, J. C. Electrocatalytic Reduction of C–C π-Bonds via a Cobaltocene-Derived Concerted Proton–Electron Transfer Mediator: Fumarate Hydrogenation as a Model Study. *J. Am. Chem. Soc.* **2021**, *143* (25), 9303–9307. DOI: 10.1021/jacs.1c03335.

4 Garrido-Barros, P.; Derosa, J.; Chalkley, M. J.; Peters, J. C. Tandem Electrocatalytic N2 Fixation via Proton-Coupled Electron Transfer. *Nature* **2022**, *609* (7925), 71–76. DOI: 10.1038/s41586-022-05011-6.

5 Chalkley, M. J.; Garrido-Barros, P.; Peters, J. C. A Molecular Mediator for Reductive Concerted Proton-Electron Transfers via Electrocatalysis. *Science* **2020**, *369* (6505), 850–854. DOI: 10.1126/science.abc1607.

6 Derosa, J.; Garrido-Barros, P.; Li, M.; Peters, J. C. Use of a PCET Mediator Enables a Ni-HER Electrocatalyst to Act as a Hydride Delivery Agent. *J. Am. Chem. Soc.* **2022**, *144* (43), 20118–20125. DOI: 10.1021/jacs.2c09786.

7 Adillon, E. H.; Peters, J. C. A Carborane-Derived Proton-Coupled Electron Transfer Reagent. *J. Am. Chem. Soc.* **2024**, *18*, 8–8. DOI: 10.1021/JACS.4C09007.

8 See Chapter 4: “Repositioning Proton and Electron Donors in a Family of Proton-Coupled Electron Transfer Mediators.”

9 Pauling, L. The Nature of the Chemical Bond. IV. The Energy of Single Bonds and the Relative Electronegativity of Atoms. *J. Am. Chem. Soc.* **1932**, *54* (9), 3570–3582. DOI: 10.1021/ja01348a011.

10 Neese, F. Software Update: The ORCA Program System—Version 6.0. *WIREs Comput. Mol. Sci.* **2025**, *15* (2), e70019. DOI: 10.1002/wcms.70019.

11 Albright, T. A.; Burdett, J. K.; Whangbo, M.-H. Molecular Orbitals of Small Building Blocks. In *Orbital Interactions in Chemistry*; John Wiley and Sons, Inc, 2013; pp 179–203. DOI: 10.1002/9781118558409.ch9.

12 Davies, W. C.; Walters, W. P. The Constitution of Some Additive Compounds of Tertiary Phosphines. *J. Chem. Soc.* **1935**, No. 0, 1786–1792. DOI: 10.1039/JR9350001786.

13 Kirst, C.; Tietze, J.; Ebeling, M.; Horndasch, L.; Karaghiosoff, K. The Formation of P–C Bonds Utilizing Organozinc Reagents for the Synthesis of Aryl- and Heteroaryl-Dichlorophosphines. *J. Org. Chem.* **2021**, *86* (23), 17337–17343. DOI: 10.1021/acs.joc.1c01560.
14 Bordwell, F. G.; Cheng, J. Pei.; Harrelson, J. A. Homolytic Bond Dissociation Energies in Solution from Equilibrium Acidity and Electrochemical Data. *J. Am. Chem. Soc.* **1988**, *110* (4), 1229–1231. DOI: 10.1021/ja00212a035.
15 Rountree, E. S.; McCarthy, B. D.; Eisenhart, T. T.; Dempsey, J. L. Evaluation of Homogeneous Electrocatalysts by Cyclic Voltammetry. *Inorg. Chem.* **2014**, *53* (19), 9983–10002. DOI: 10.1021/ic500658x.
16 Tyburski, R.; Liu, T.; Glover, S. D.; Hammarström, L. Proton-Coupled Electron Transfer Guidelines, Fair and Square. *J. Am. Chem. Soc.* **2021**, *143* (2), 560–576. DOI: 10.1021/jacs.0c09106.
17 According to the expected Brønsted relationship for a PCET reaction in the low driving force regime (i.e. $\Delta G^\circ << \lambda$), the change in the barrier is approximately half the change in driving force. Considering the 3.8 kcal/mol decrease in ΔG°, this translates to a decrease in the barrier height ($\Delta\Delta G^\ddagger$) of 1.9 kcal/mol. Plugging this $\Delta\Delta G^\ddagger$ into the Eyring equation for relative rates ($k_2/k_1 = \exp(\Delta\Delta G^\ddagger/RT)$ yields a ratio of the rate constants of 24.7 at room temperature.
18 Richard, J. P.; Williams, G.; O'Donoghu, A. C.; Amyes, T. L. Formation and Stability of Enolates of Acetamide and Acetate Anion: An Eigen Plot for Proton Transfer at α-Carbonyl Carbon. *J. Am. Chem. Soc.* **2002**, *124* (12), 2957–2968. DOI: 10.1021/ja0125321.
19 Bernasconi, C. F.; Wenzel, P. J. Is There a Transition-State Imbalance for Proton Transfers in the Gas Phase? Ab Initio Study of the Carbon-to-Carbon Proton Transfer from Acetaldehyde to Its Enolate Ion. *J. Am. Chem. Soc.* **1994**, *116* (12), 5405–5413. DOI: 10.1021/ja00091a052.
20 Mayer, J. M. Understanding Hydrogen Atom Transfer: From Bond Strengths to Marcus Theory. *Acc. Chem. Res.* **2011**, *44* (1), 36–46. DOI: 10.1021/ar100093z.
21 Henderson, R. A. Protonation of Unsaturated Hydrocarbon Ligands: Regioselectivity, Stereoselectivity, and Product Specificity. *Angew. Chem. Int. Ed. Engl.* **1996**, *35* (9), 946–967. DOI: 10.1002/anie.199609461.

A p p e n d i x A

Supplementary Information for Chapter 2

Adapted from:

Adillon, E. H.; Peters, J. C.

J. Am. Chem. Soc. **2024**, 147, 30204-30211

DOI: 10.1021/jacs4c09007

A.1 General Procedures

General Considerations

All manipulations were carried out using standard Schlenk or glovebox techniques under an N_2 atmosphere unless stated otherwise. Solvents were degassed by thoroughly sparging with N_2 gas and dried by passage through an activated alumina column in the solvent purification system by SG Water, USA LLC. All solvents were stored over activated 3 Å sieves prior to use. THF, 2-MeTHF, and diethyl ether were dried over NaK alloy and passed over activated alumina prior to use and were checked with a standard solution of sodium benzophenone ketyl in tetrahydrofuran to test for the presence of oxygen and moisture. All reagents were purchased from commercial vendors and used without further purification unless otherwise stated. Decaborane bis(acetonitrile), diphenyl-o-carborane,[1] N,N-dimethyl-4-(phenylethynylaniline),[2] 1-(4-N,N-dimethylaniline)-2-phenyl-o-carborane,[3] 1,2-di-p-tolyldiazene,[4] 1,2-bis-(4-bromo)diazene,[4] 1,2-bis-(4-chloro)diazene,[44] 1,2-bis-(4-methoxy)diazene,[4] diethyl 4,4'-(diazene-1,2-diyl)-dibenzoate,[4] diphenylfumarate,[5] 4-cyanoanilinium triflate,[6] and 2-chloroanilinium triflate,[6] and triphenylphosphonium triflate[7] were prepared by reported methods. $^{n}Bu_4NPF_6$ was recrystallized from hot EtOH three times and dried under vacuum at 100 °C overnight. High resolution mass spectra (HRMS) were obtained from the Caltech Mass Spectral Facility using JEOL JMS-T2000GC AccuTOF™ GC-Alpha High Resolution Mass Spectrometer in field desorption (FD+) mode.

NMR Spectroscopy

NMR spectroscopy was performed using Varian and Bruker 400 MHz NMR spectrometers fitted with broadband auto-tune probes. Deuterated solvents were purchased from Cambridge Isotope Laboratories, Inc.. Acetonitrile-d_3 was degassed by three freeze-pump-thaw cycles, dried over activated 3 Å sieves, and passed over activated alumina. ^{1}H and ^{13}C chemical shifts are reported in ppm relative to tetramethylsilane using residual solvent resonances as internal standards. ^{11}B chemical shifts are reported in ppm relative to boron trifluoride etherate using absolute referencing to a ^{1}H NMR spectrum collected concurrently. ^{19}F chemical shifts are reported in ppm relative to trichlorofluoromethane using absolute referencing to a ^{13}C NMR spectrum collected concurrently.

Products Quantification

GC-FID analyses were performed using an Agilent 6890N Gas Chromatograph. Substrate reductions were pumped down to remove solvent and redissolved in either chloroform-d_1 (600 uL) for NMR analysis or ethyl acetate (2 mL) for GC-FID analysis. For quantitative NMR analyses, dibromomethane (5 mmol, 1 eq) was added as an internal standard. For GC-FID analysis, a dodecane solution in ethyl acetate (50 uL, 200 mM) was added as an internal standard, and analyte response factors were measured via calibration curves with known analyte concentrations. GC-TCD analysis was performed in the Caltech Environmental Analysis Center using a Hewlett Packard 5890 Series II Gas Chromatograph. A calibration curve was generated by direct injection

of known quantities of hydrogen gas. Aliquot of the headspace (100 uL) were analyzed in triplicate and reported as an average.

CW EPR Spectroscopy

77 K X-Band EPR spectra were collected on a Bruker EMX spectrometer. Solutions were prepared as frozen glasses in NaK alloy dried 2-MeTHF filtered over activated alumina. Spectra were simulated using the Easy Spin simulation toolbox (release 5.2.35).[8]

UV-vis Spectroscopy

Spectra were collected using a Cary 60 instrument with Cary WinUV software. Time-course spectra were collected with the Scanning Kinetics application of the Cary WinUV software. 1-cm path quartz cells were pre-cooled in a Unisoku cryostat prior to analysis. All spectra were background corrected at the temperature at which spectra were collected.

X-ray Crystallography

X-ray diffraction (XRD) studies were carried out at the Beckman Institute Crystallography Facility on a Bruker Kappa Apex II diffractometer (Cu Kα radiation, λ = 1.5406 Å). All crystals were mounted on a glass fiber loop under Paratone N oil. Structures were solved using SHELXS or SHELXT and refined against F2 on all data by full-matrix least squares with SHELXL.[9] All of the solutions were performed in the Olex2 program.[10] Hydrogen atoms were placed in calculated positions. Non-hydrogen atoms were refined anisotropically.

Electrochemistry

Electrochemical measurements were carried out in an N_2-filled glovebox in a 20 mL scintillation vial fitted with a septum cap containing punched-out holes for insertion of electrodes. A CH Instruments 600B electrochemical analyzer was used for data collection. For all experiments, a boron-doped diamond disk electrode was used as the working electrode; a freshly polished glassy carbon disk electrode was used as the counter electrode; a silver wire immersed in a solution of silver triflate (5 mM) and $^{n}Bu_4NPF_6$ (200 mM) separated from the working solution by a Vycor frit was used as pseudoreference electrode. $E_{1/2}$ values for reversible waves were determined as the half potential between the peak oxidative and reductive potentials. Solution resistance was measured, and a correction of 85% of the uncompensated resistance was applied. All reported potentials are referenced to the ferrocene/ferrocenium couple, measured at the end of each experiment. Electrochemistry solvents were passed over a pipet filter of activated alumina immediately before use.

DFT Calculations

All calculations were performed using the ORCA 5.0.3 program using the B3LYP functional with the def2-SVP basis set.[11,12] In cases where crystal structures were available, those coordinates were used as the input. Geometry optimization calculations were performed using the SMD solvation

model with acetonitrile.[13] Single-point vibrational frequency calculations were performed to ensure that stationary points were absent of any imaginary frequencies and thus were local minima on the potential energy surface. Bond dissociation free energies (BDFEs) were calculated by an established method using the calculated free energy of the H atom.[12] Reduction potentials were determined by a semi-empirical method using the calculated exchange reactions relative to an experimental reduction potential. In the case of carboranes, the potential was calculated as an exchange reaction with the 1,2-diphenyl-o-carborane anion using its measure potential as a reference ($E_{1/2}$ = -1.56 V vs. $Fc^{0/+}$). In the case of diazenes, the potential was calculated as an exchange reaction with the azobenzene anion was using its reported potential as a reference ($E_{1/2}$ = -1.82 V vs. $Fc^{0/+}$). Hydricities were calculated using the BDFE and reduction potential methods to yield a net hydride transfer free energy.

A.2 Synthetic Procedures

[Diphenyl-*o*-carborane]K(18-crown-6) (1)

Potassium metal [33 mg, 0.85 mmol] was smeared onto the interior wall of a 20 mL scintillation vial. Diphenyl-*o*-carborane [300 mg, 1.0 mmol] was dissolved in 15 mL of THF and added to the potassium, quickly forming a red solution. The reaction was stirred until all potassium was consumed, approximately three hours. A solution of 18-crown-6 [264 mg, 1.0 mmol] in THF [~2 mL] was added dropwise. The solution was filtered through celite, and the solvent was removed under vacuum. The resulting red solid was washed with pentane [3 x 5 mL] and dried under vacuum, yielding 398 mg (79%) of a red solid. The solid was recrystallized by vapor diffusion of pentane into a concentrated THF solution. μ_{eff} (CD_3CN, Evans method, 298 K): 1.68 μ_B.

[Diphenyl-*o*-carborane][K(18-crown-6)]$_2$ (2)

Potassium metal [12 mg, 0.30 mmol] was smeared onto the interior wall of a 20 mL scintillation vial. Diphenyl-*o*-carborane [35 mg, 0.12 mmol] was dissolved in 5 mL of THF and added to the potassium, quickly forming a red solution which later became light yellow. The reaction was stirred until all potassium was consumed, approximately three hours. The solution was filtered through celite, and a solution of 18-crown-6 [63 mg] in THF [~2 mL] was added dropwise, yielding a yellow precipitate. The solvent was removed under vacuum. The resulting yellow powder was washed with pentane [3 x 3 mL] and dried under vacuum, yielding 91 mg (84%) of a pale-yellow powder. Diffraction quality crystals were grown by layering Et_2O/MeCN and cooling at -35 °C. ^{1}H NMR (CD_3CN, 400 MHz, 298 K) δ 7.19 (d, *J* = 7.5 Hz, 1H), 6.87 (t, *J* = 7.5 Hz, 1H), 6.60 (t, *J* = 7.2 Hz, 1H), 0-3.2 (bm, 10H). ^{11}B{^{1}H} NMR (CD_3CN, 128 MHz, 298 K) δ: 7.81 (bs, 2B), -8.52 (bs, 2B), -17.68 (bs, 4B), -27.28 (bs, 2B). ^{13}C{^{1}H} (CD_3CN, 128 MHz, 298 K) δ: 157.66, 127.28, 127.12, 120.01, 70.84.

[1-(4-N,N-dimethylaniline)-2-phenyl-*o*-carborane]K(benzo-15-crown-5)$_2$ (3)

Potassium metal [110 mg, 2.8 mmol] was smeared onto the interior wall of a 20 mL scintillation vial. 1-(4-N,N-dimethylaniline)-2-phenyl-o-carborane [1.00 g, 2.95 mmol] was dissolved in 20 mL of THF and added to the potassium, quickly changing from a colorless to red solution. The reaction was stirred until all potassium was consumed, approximately three hours. The solution was filtered through celite, and the solvent was reduced under vacuum to 10 mL. Benzo-15-crown-5 [1.52 g, 2.80 mmol] was added, forming a red precipitate. The remaining solvent was removed, washed with pentane [3 x 3 mL] and recrystallized by THF/pentane vapor diffusion, yielding 2.33 g (91%) of a red microcrystalline solid. X-Ray quality crystals were grown by acetonitrile/ether vapor diffusion, yielding red needles. μ_{eff} (CD_3CN, Evans method, 298 K): 1.78 μ_B.

[1-(4-N,N,N-trimethylanilinium)-2-phenyl-*o*-carborane]OTf (4)

Carborane **3** [250 mg, 0.74 mmol] was dissolved in diethyl ether [15 mL] in a 20 mL scintillation vial and cooled in the cold well chilled by a dry ice-acetone bath. Methyl triflate [139 uL, 0.89 mmol] was added, and shortly after, the vial was removed from the cold well and stirred for 18 hours, during which time a white precipitate formed. The white solid was filtered over a celite frit, washed with diethyl ether [5 x 3 mL], and then dissolved in THF [5 mL]. The solvent of the THF filtrate was removed under vacuum, resulting in 260 mg (70%) of a white solid. ^{1}H NMR (CD_3CN, 400 MHz, 298 K) δ: 7.74 (d, J = 9.3 Hz, 2H), 7.57 (d, J = 9.3 Hz, 2H), 7.53 (d, J = 7.4 Hz, 2H), 7.33 (t, J = 7.4 Hz, 1H), 7.23 (dd, 8.3, 7.4 Hz, 2H), 3.40 (s, 9H), 3.37 (bs, 2H), 2.40 (bs, 6H), 2.33 (bs, 2H). ^{11}B{^{1}H} NMR (CD_3CN, 128 MHz, 298 K) δ: -3.55 (bs, 2B), -11.23 (m, 8B). ^{13}C{^{1}H} (CD_3CN, 100 MHz, 298 K) δ: 149.04, 133.72, 133.56, 131.81, 131.66, 130.65, 129.64, 86.79, 84.01, 57.80. ^{19}F (CD_3CN, 376 MHz, 298 K) δ: -79.4 (s, 3F). HRMS: (FD+) calculated for $C_{17}H_{28}B_{10}N$ [M^+]: 354.32278, found: 354.32284.

1-(4-N,N,N-trimethylanilinium)-2-phenyl-*o*-carborane (5)

Carborane **4** [47 mg, 0.09 mmol] was dissolved in THF [5 mL] in a 20 mL scintillation vial and cooled to -78 °C in the cold well. A freshly prepared solution of sodium napthalanide [0.09 mmol] was added dropwise to the carborane solution, forming a dark pink solution. The solution was pumped down under vacuum, and the solid was washed with pentane [3 x 1 mL]. The solid was redissolved in THF, filtered, layered with diethyl ether, and placed in the freezer overnight, forming 15 mg (47%) of a fine pink powder. μ_{eff} (CD_3CN, Evans method, 298 K): 1.60 μ_B.

General procedure for substrate reduction by carborane and acid

A solution of carborane in THF [2 mL, 5 mM, 2.0 eq] was added to a scintillation vial with a stir bar and cooled in the cold well chilled by a dry ice-acetonitrile bath [−40 °C]. A pre-cooled solution of acid in THF [100 uL, 100 mM, 2.0 eq] was added, and shortly thereafter, a pre-cooled solution of substrate in THF [100 uL, 50 mM, 1.0 eq] was added. The reaction was allowed to stir for one hour. The volatiles were removed on the rotovap, and the remaining material was dissolved in $CDCl_3$ [600 uL] containing 8.33 mM CH_2Br_2 (5 umol, 1.0 eq) and analyzed by ^{1}H NMR.

A.3 NMR Spectra

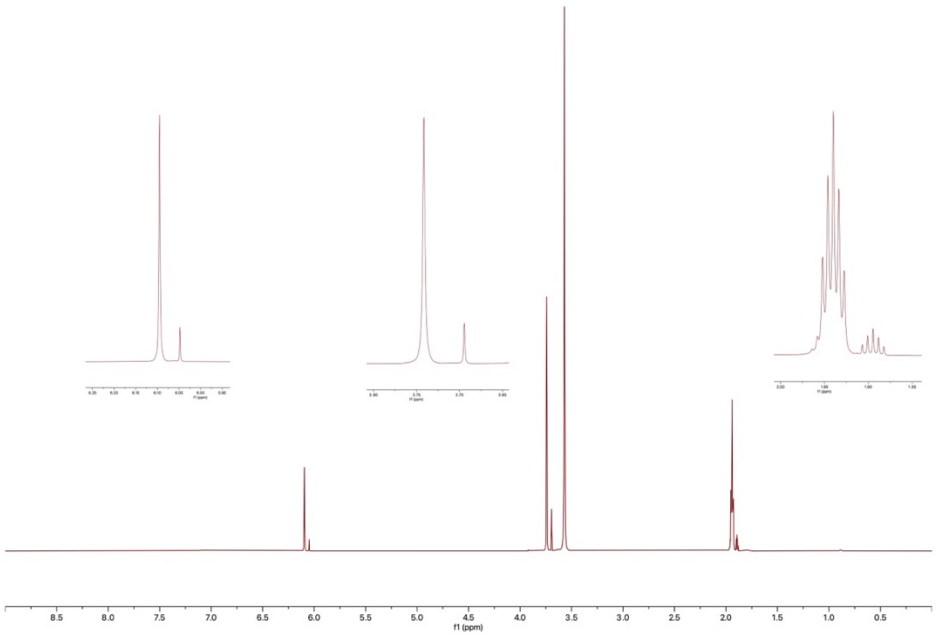

Figure A1. ^{1}H NMR spectrum of **[Ph$_2$Cb]K(18-crown-6)** in CD_3CN (400 MHz). Trimethoxybenzene was added for the Evan's method measurement. [Ph$_2$Cb]K(18-crown-6) = 11.8 mM, $\Delta\nu$ = 18.6 Hz, ν = 400.15 MHz, μ_{eff} = 1.68 μ_B

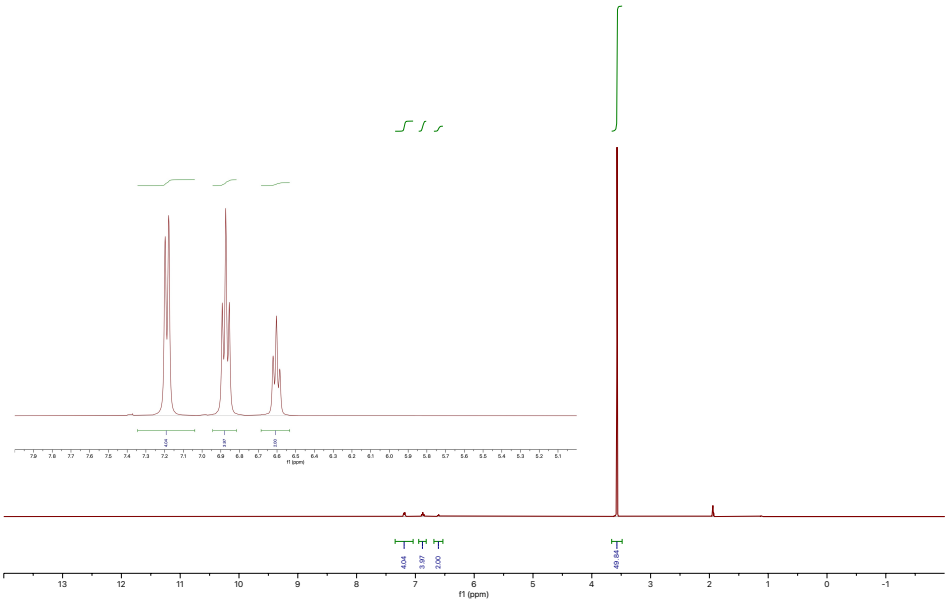

Figure A2. ^{1}H NMR spectrum of **[Ph$_2$Cb][K(18-crown-6)]$_2$** in CD_3CN (400 MHz)

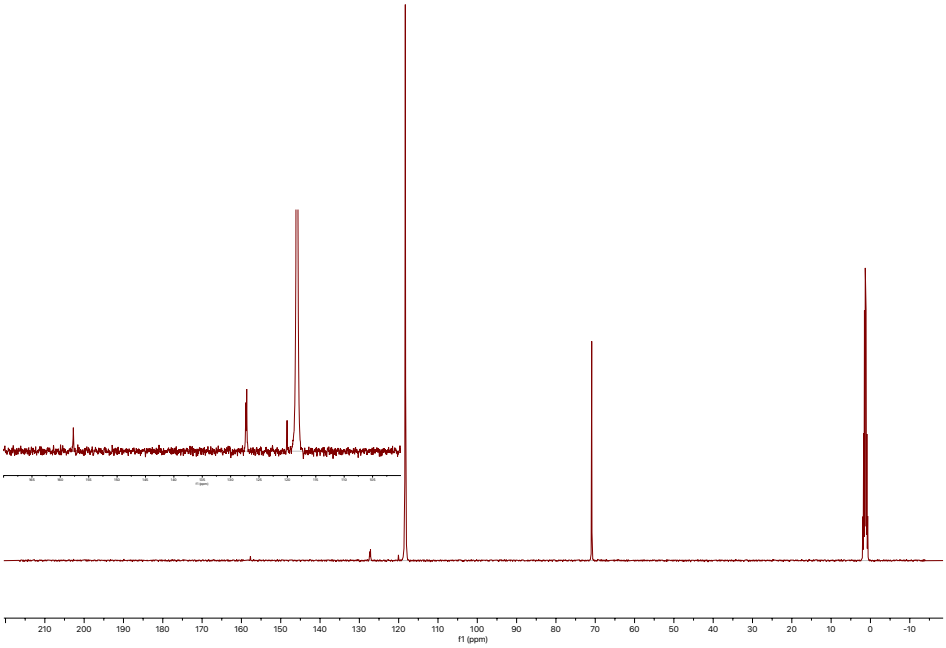

Figure A3. ^{13}C NMR spectrum of **[Ph$_2$Cb][K(18-crown-6)]$_2$** in CD_3CN (100 MHz)

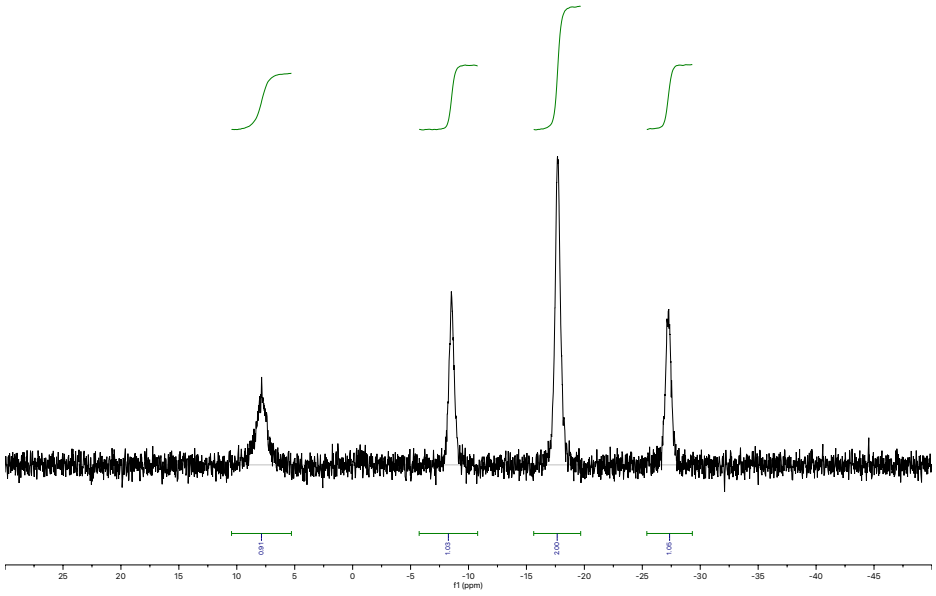

Figure A4. ^{11}B NMR spectrum of **[Ph$_2$Cb][K(18-crown-6)]$_2$** in CD_3CN (128 MHz)

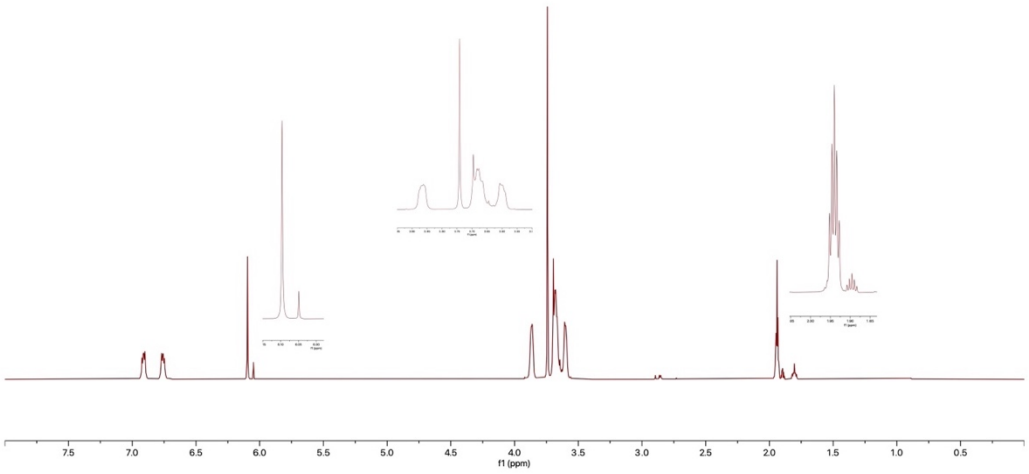

Figure A5. $^{1}H\{^{11}B\}$ NMR spectrum of **[PhCbPh^{N}]K(benzo-15-crown-5)$_2$** in CD_3CN (400 MHz). Trimethoxybenzene was added for the Evan's method measurement. [PhCbPh^{N}] = 11.4 mM, $\Delta\nu$ = 18.2 Hz, ν = 400.15 MHz, μ_{eff} = 1.78 μ_B

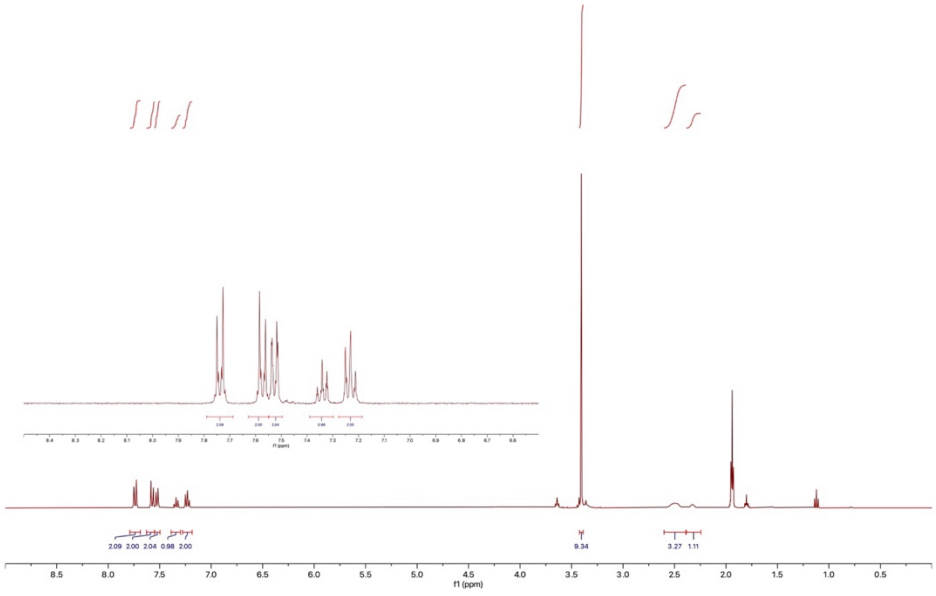

Figure A6. $^{1}H\{^{11}B\}$ NMR spectrum of **[PhCbPh^{NMe3}]OTf** in CD_3CN (400 MHz).

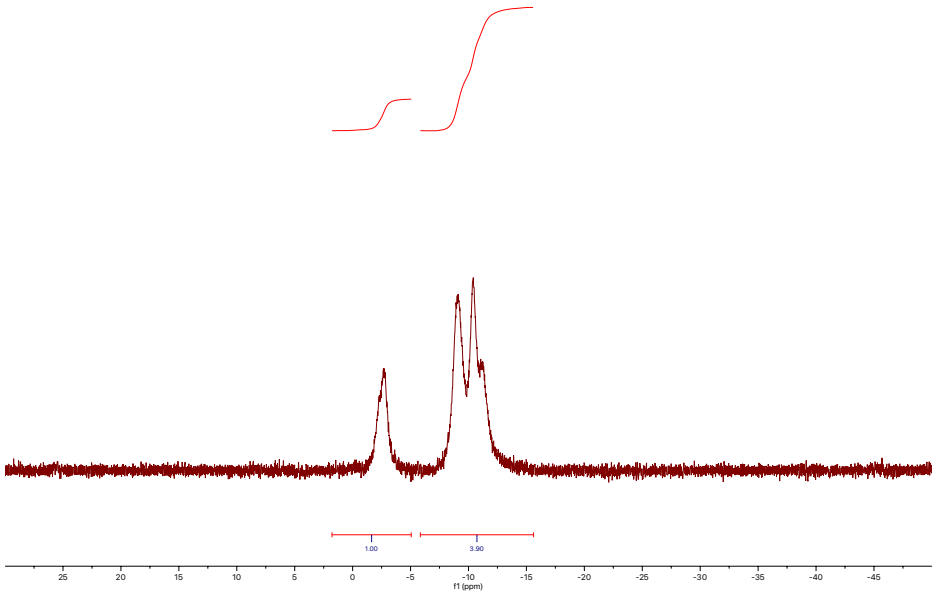

Figure A7. $^{11}B\{^{1}H\}$ NMR spectrum of **[PhCbPh^{NMe3}]OTf** in CD_3CN (400 MHz).

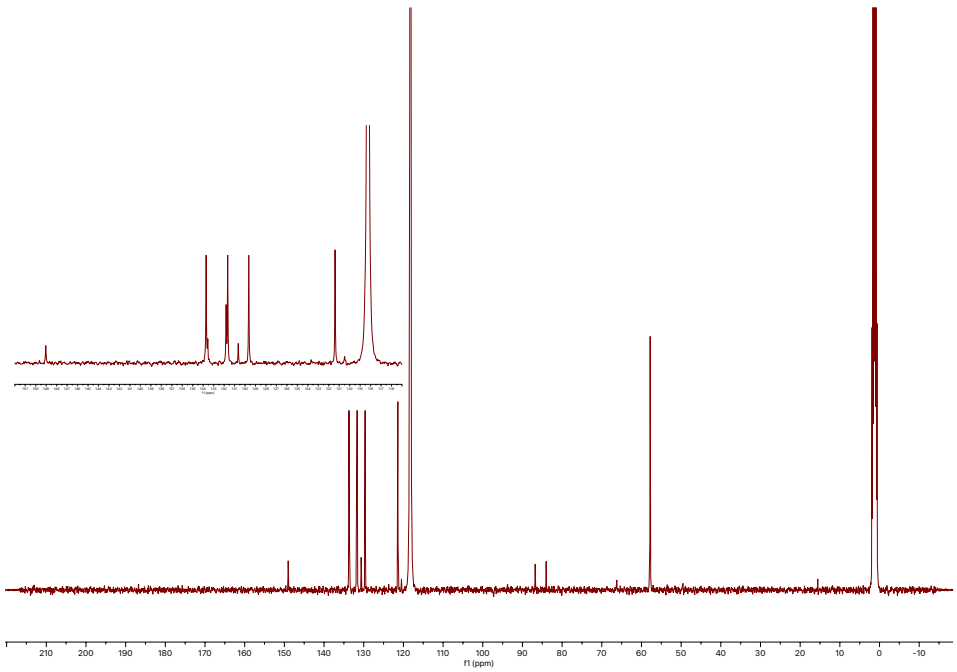

Figure A8. $^{13}C\{^{1}H\}$ NMR spectrum of **[PhCbPh^{NMe3}]OTf** in CD_3CN (100 MHz).

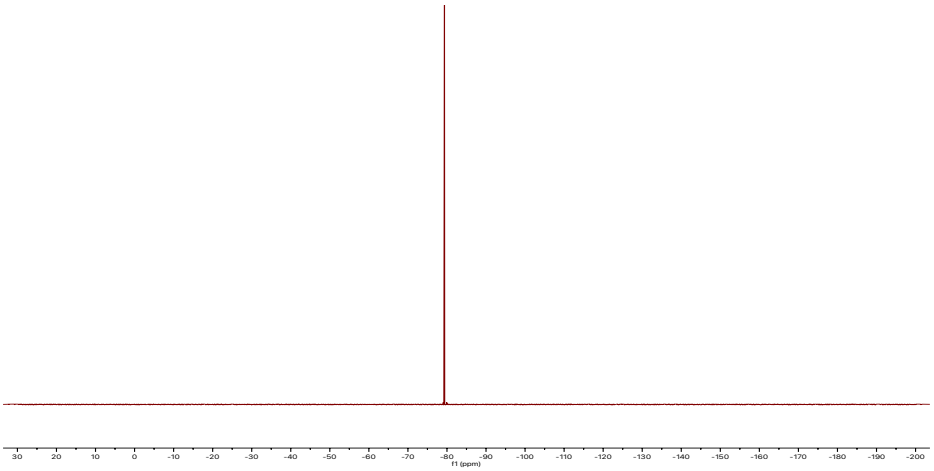

Figure A9. ^{19}F NMR spectrum of **[PhCbPh^{NMe3}]OTf** in CD_3CN (400 MHz).

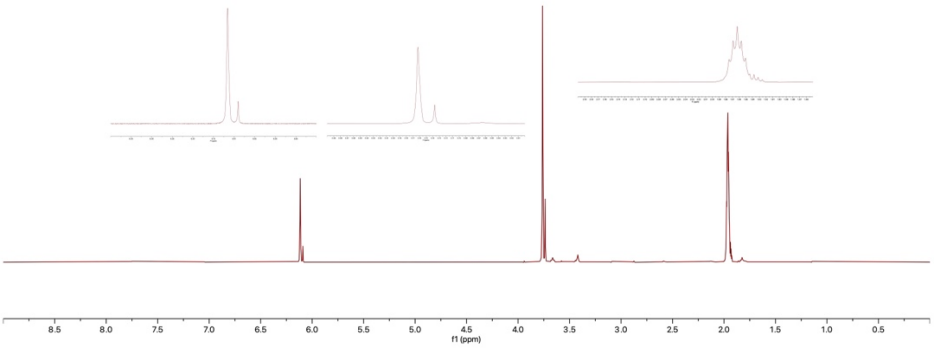

Figure A10. $^{1}H\{^{11}B\}$ NMR spectrum of **PhCbPh^{NMe3}** in CD_3CN (400 MHz). Trimethoxybenzene was added for the Evan's method measurement. [**PhCbPh^{NMe3}**] = 2.2 mM, $\Delta\nu$ = 10.2 Hz, ν = 400.15 MHz, μ_{eff} = 1.60 μ_B

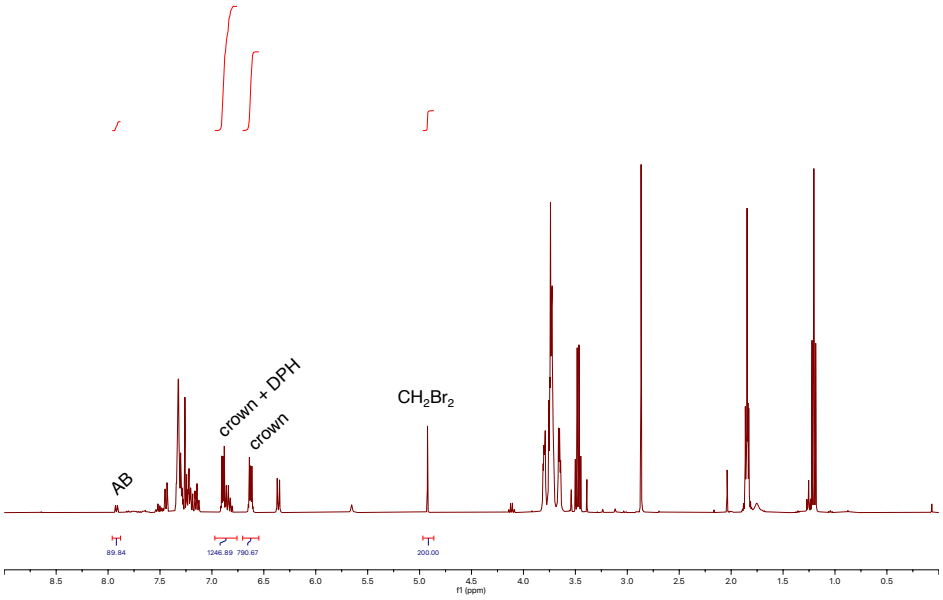

Figure A11. ^{1}H NMR spectrum of the products of azobenzene (AB, 5 umol) reduction to 1,2-diphenylhydrazine (DPH) using [PhCbPh^N]K(benzo-15-crown-5)$_2$ and [Ph_3PH]OTf in THF with 5 umol CH_2Br_2 as an internal standard in $CDCl_3$ (400 MHz).

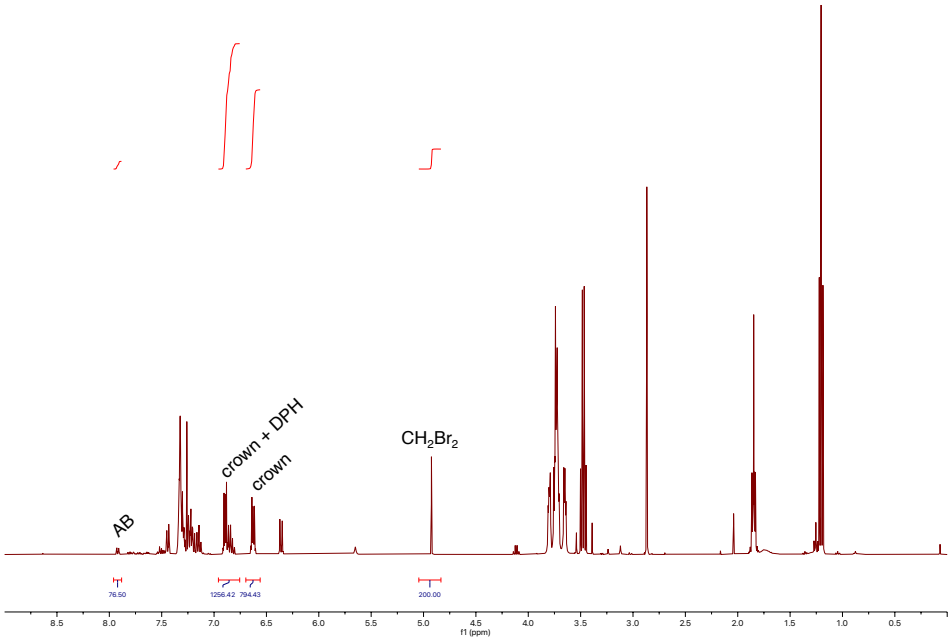

Figure A12. ^{1}H NMR spectrum of the products of azobenzene (AB, 5 umol) reduction to 1,2-diphenylhydrazine (DPH) using [PhCbPh^{N}]K(benzo-15-crown-5)$_2$ and [Ph$_3$PH]OTf in THF with 5 umol CH_2Br_2 as an internal standard in $CDCl_3$ (400 MHz).

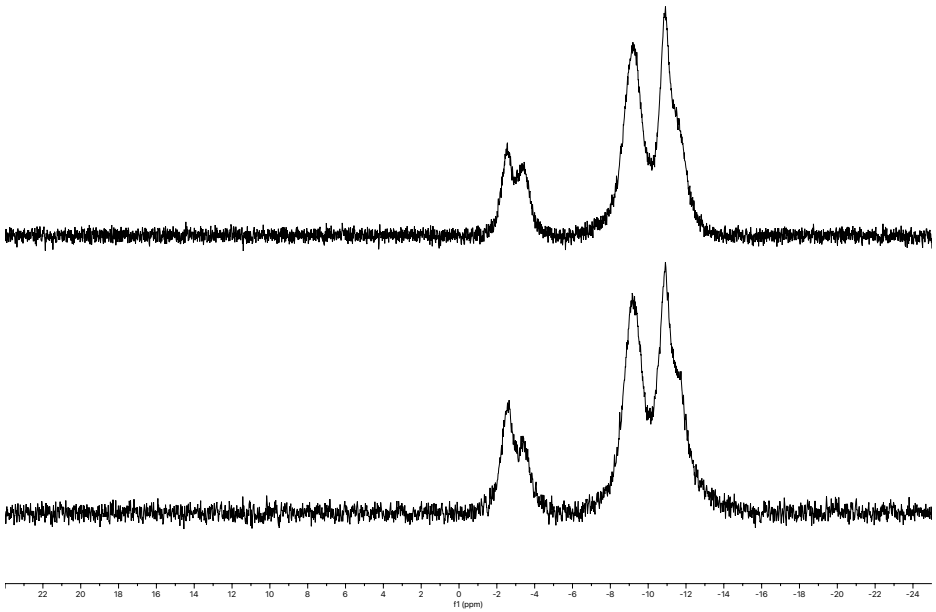

Figure A13. (Top) $^{11}B\{1H\}$ NMR spectrum of **PhCbPh^{N}** and (bottom) $^{11}B\{1H\}$ NMR spectrum of the products of azobenzene (AB, 5 umol) reduction to 1,2-diphenylhydrazine (DPH) using [PhCbPh^{N}]K(benzo-15-crown-5)$_2$ and [Ph$_3$PH]OTf in THF, both in $CDCl_3$ (400 MHz)

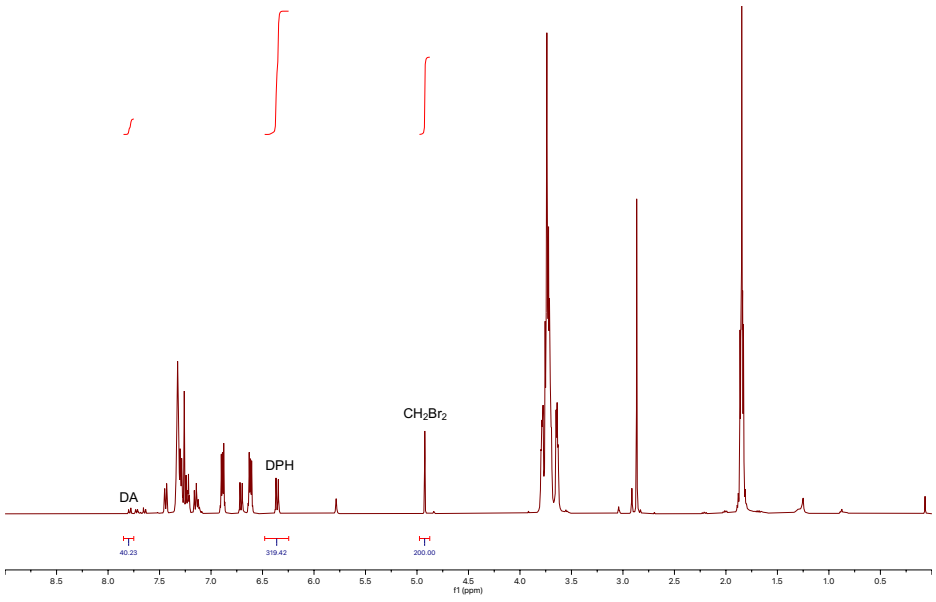

Figure A14. ^{1}H NMR spectrum of the products of 1,2-bis-(4-bromophenyl)diazene (DA, 5 umol) reduction to 1,2-bis(4-bromophenyl)hydrazine (DPH) using [PhCbPh^{N}]K(benzo-15-crown-5)$_2$ and [Ph$_3$PH]OTf in THF with 5 umol CH_2Br_2 as an internal standard in $CDCl_3$ (400 MHz).

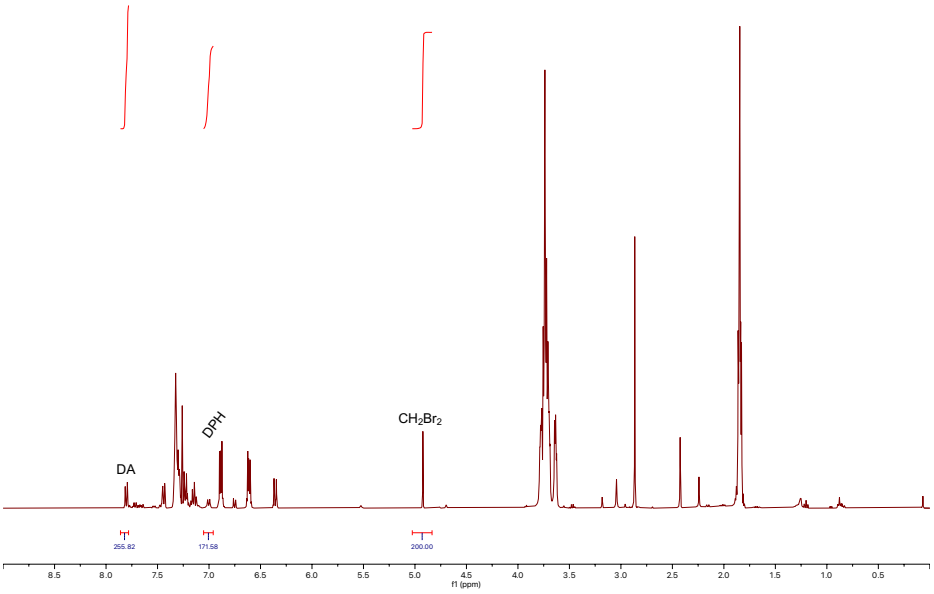

Figure A15. ^{1}H NMR spectrum of the products of 1,2-di-p-tolyldiazene (DA, 5 umol) reduction to 1,2-di-p-tolylhydrazine (DPH) using [PhCbPh^{N}]K(benzo-15-crown-5)$_2$ and [Ph$_3$PH]OTf in THF with 5 umol CH_2Br_2 as an internal standard in $CDCl_3$ (400 MHz).

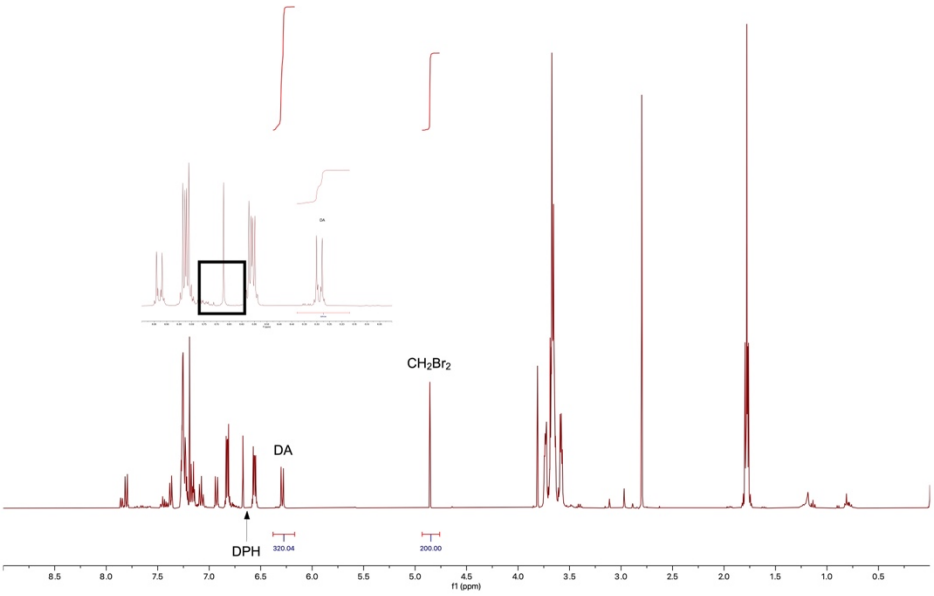

Figure A16. ^{1}H NMR spectrum of the products of 1,2-bis-(4-methoxyphenyl)diazene (DA, 5 umol) reduction to 1,2-bis(4-methoxyphenyl)hydrazine (DPH) using [PhCbPh^{N}]K(benzo-15-crown-5)$_2$ and [Ph$_3$PH]OTf in THF with 5 umol CH_2Br_2 as an internal standard in $CDCl_3$ (400 MHz). Note that peaks of the hydrazine product at 6.75 and 6.66 ppm (marked with arrow) are not observed.

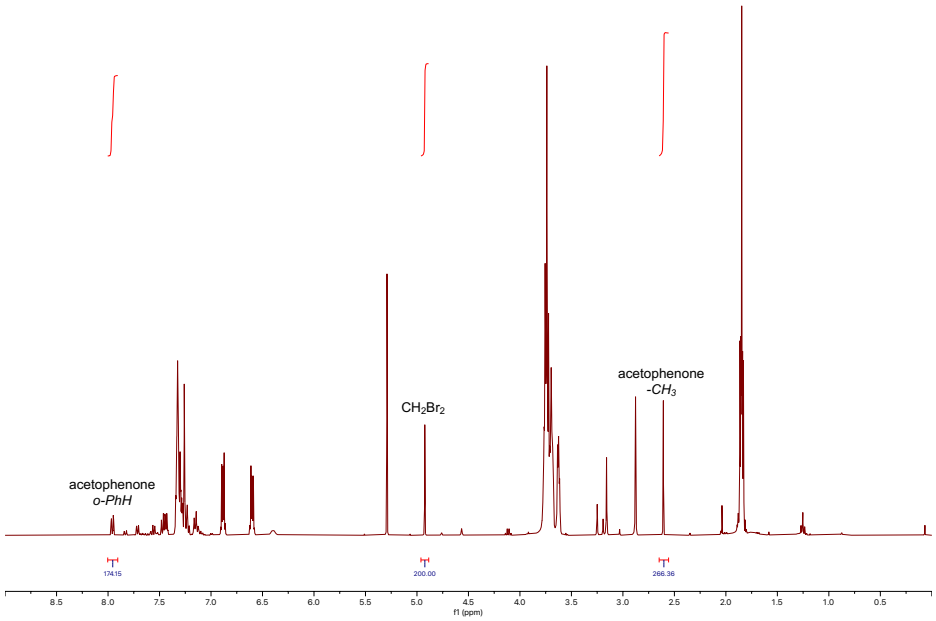

Figure A17. ^{1}H NMR spectrum of the products of acetophenone (5 umol) reduction using [PhCbPh^{N}]K(benzo-15-crown-5) and [Ph$_3$PH]OTf in THF with 5 umol CH_2Br_2 as an internal standard in $CDCl_3$ (400 MHz).

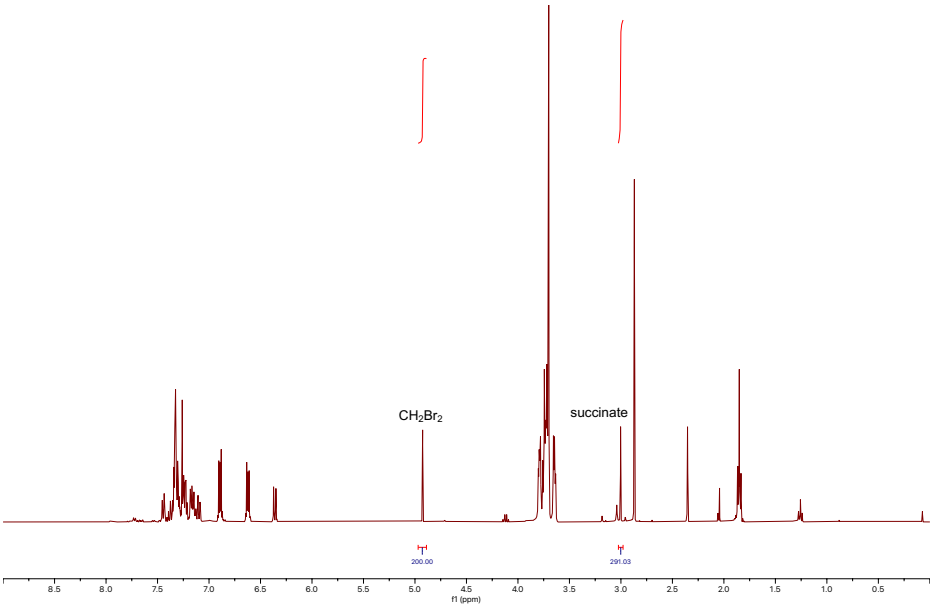

Figure A18. ^{1}H NMR spectrum of the products of diphenyl fumarate (5 umol) reduction to diphenylsuccinate using [PhCbPh^{N}]K(benzo-15-crown-5) and [Ph$_3$PH]OTf in THF with 5 umol CH_2Br_2 as an internal standard in $CDCl_3$ (400 MHz).

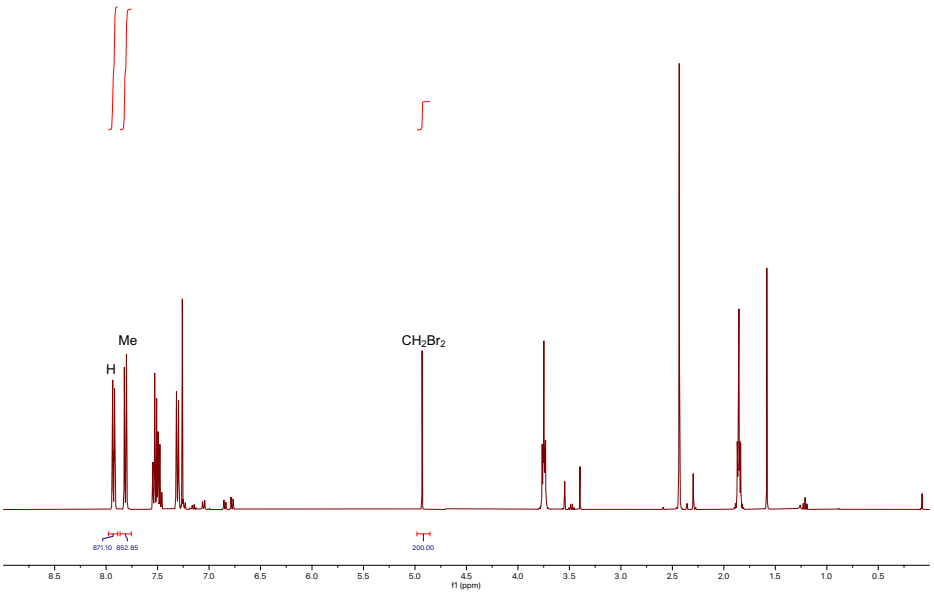

Figure A19. ^{1}H NMR spectrum of a 200 uL aliquot of the substrate solution for the competition experiment (H vs. Me), approximately 11 umol each, after concentration *in vacuo* with 5 umol CH_2Br_2 as an internal standard in $CDCl_3$ (400 MHz).

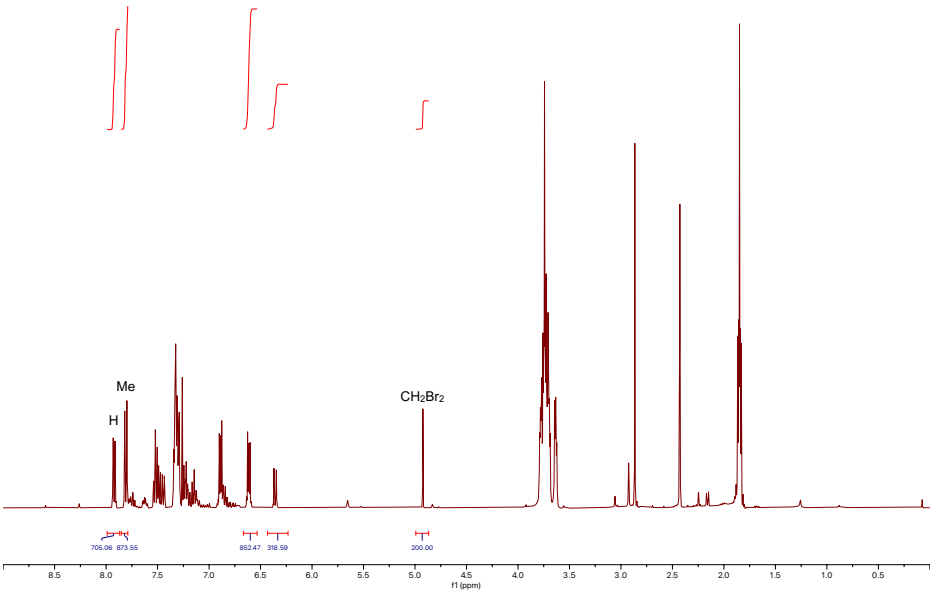

Figure A20. ^{1}H NMR spectrum of the products of the azoarene competition experiment (H vs. Me, run A) with substrates (11 umol) using [PhCbPh^{N}]K(benzo-15-crown-5) and [Ph$_3$PH]OTf in THF with 5 umol CH_2Br_2 as an internal standard in $CDCl_3$ (400 MHz).

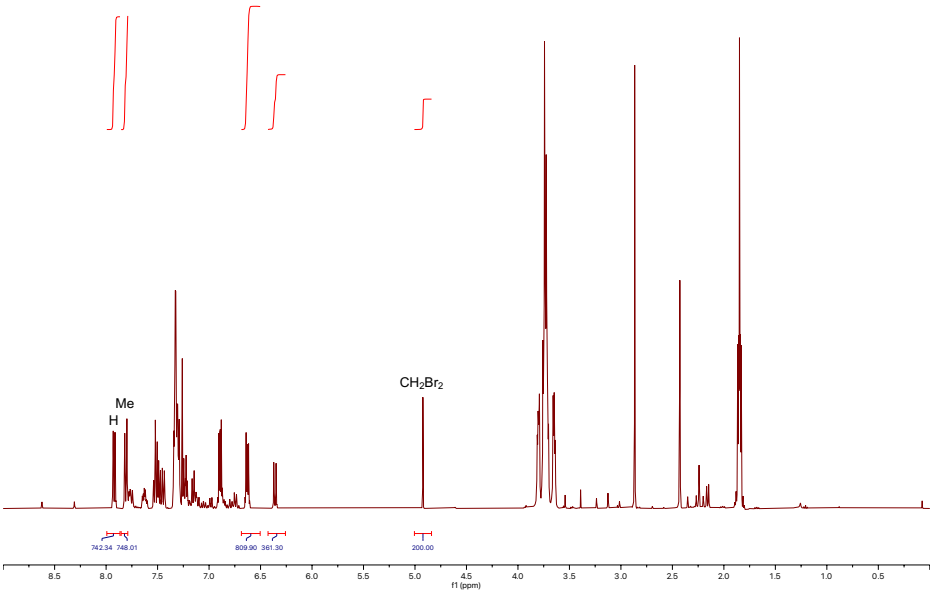

Figure A21. ^{1}H NMR spectrum of the products of the azoarene competition experiment (H vs. Me, run B) with substrates (11 umol) using [PhCbPh^{N}]K(benzo-15-crown-5) and [Ph$_3$PH]OTf in THF with 5 umol CH_2Br_2 as an internal standard in $CDCl_3$ (400 MHz).

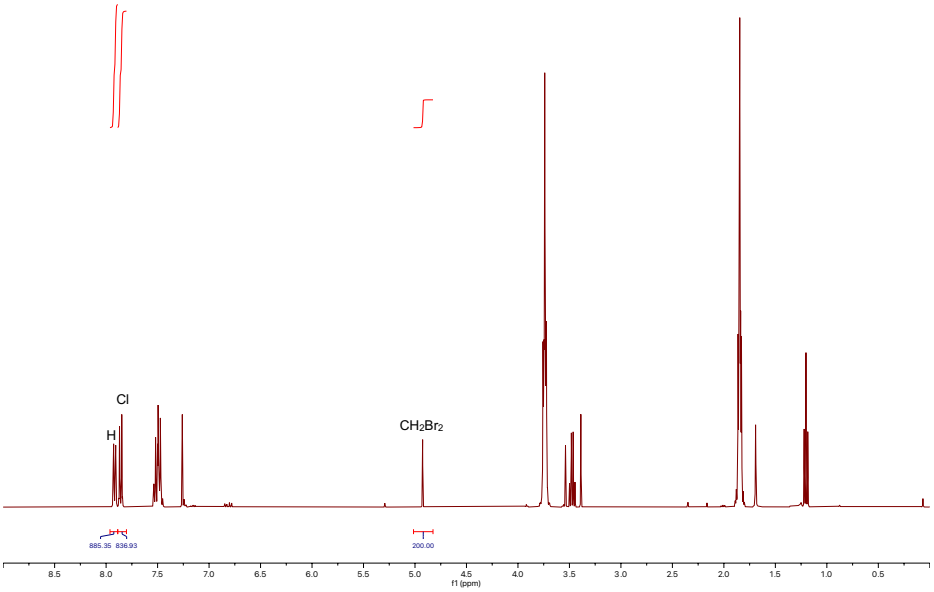

Figure A22. ^{1}H NMR spectrum of a 200 uL aliquot of the substrate solution for the competition experiment (H vs. Cl), approximately 11 umol each, after concentration *in vacuo* with 5 umol CH_2Br_2 as an internal standard in $CDCl_3$ (400 MHz).

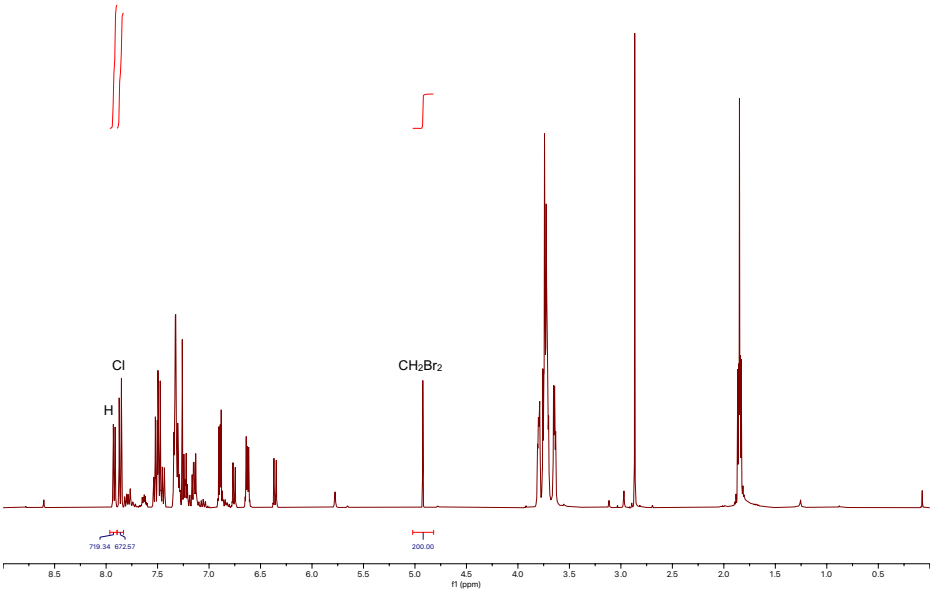

Figure A23. ^{1}H NMR spectrum of the products of the azoarene competition experiment (H vs. Cl, run A) with substrates (11 umol) using [PhCbPh^{N}]K(benzo-15-crown-5) and [Ph_3PH]OTf in THF with 5 umol CH_2Br_2 as an internal standard in $CDCl_3$ (400 MHz).

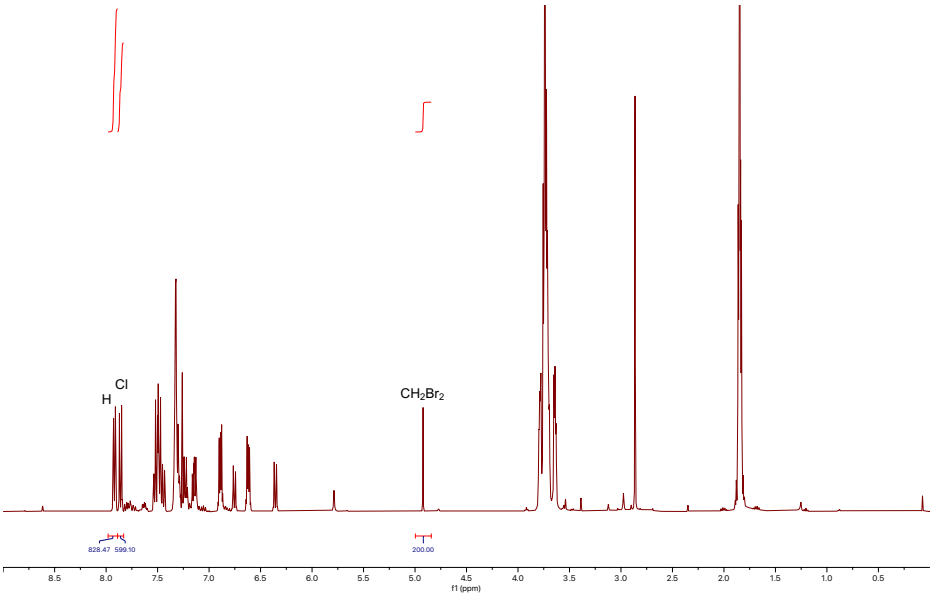

Figure A24. ^{1}H NMR spectrum of the products of the azoarene competition experiment (H vs. Cl, run B) with substrates (11 umol) using [PhCbPh^{N}]K(benzo-15-crown-5) and [Ph_3PH]OTf in THF with 5 umol CH_2Br_2 as an internal standard in $CDCl_3$ (400 MHz).

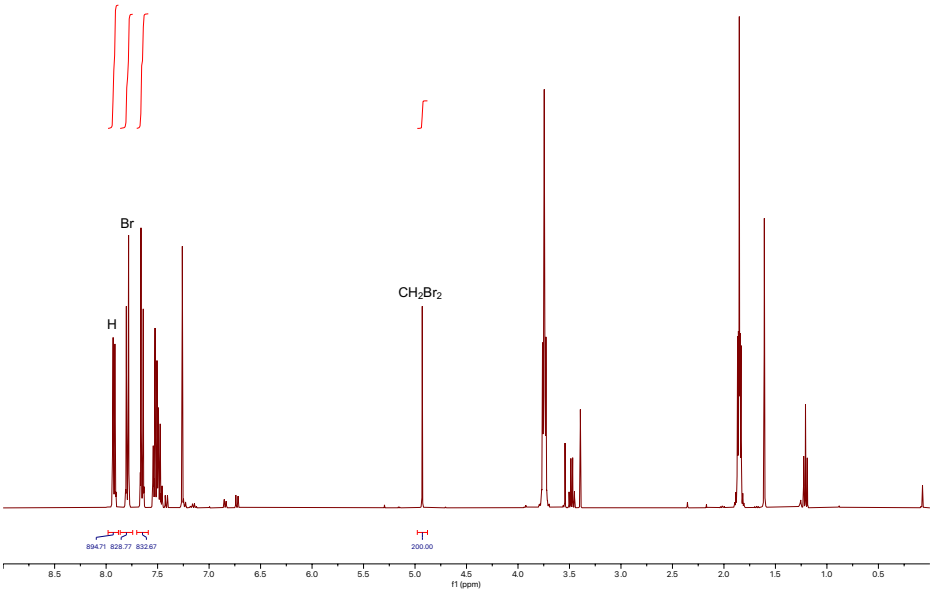

Figure A25. ^{1}H NMR spectrum of a 200 uL aliquot of the substrate solution for the competition experiment (H vs. Br), approximately 11 umol each, after concentration *in vacuo* with 5 umol CH_2Br_2 as an internal standard in $CDCl_3$ (400 MHz).

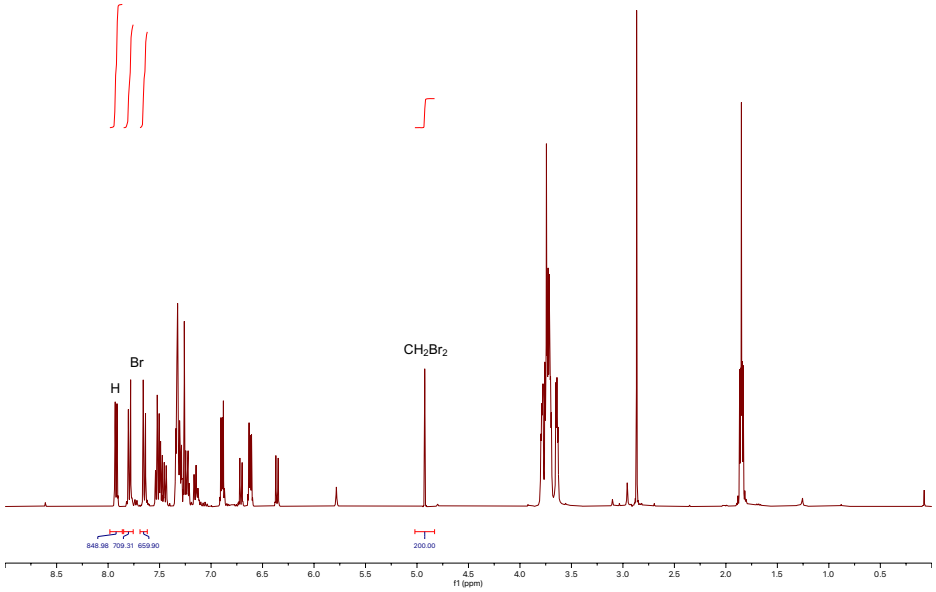

Figure A26. ^{1}H NMR spectrum of the products of the azoarene competition experiment (H vs. Br, run A) with substrates (11 umol) using [PhCbPh^{N}]K(benzo-15-crown-5) and [Ph_3PH]OTf in THF with 5 umol CH_2Br_2 as an internal standard in $CDCl_3$ (400 MHz).

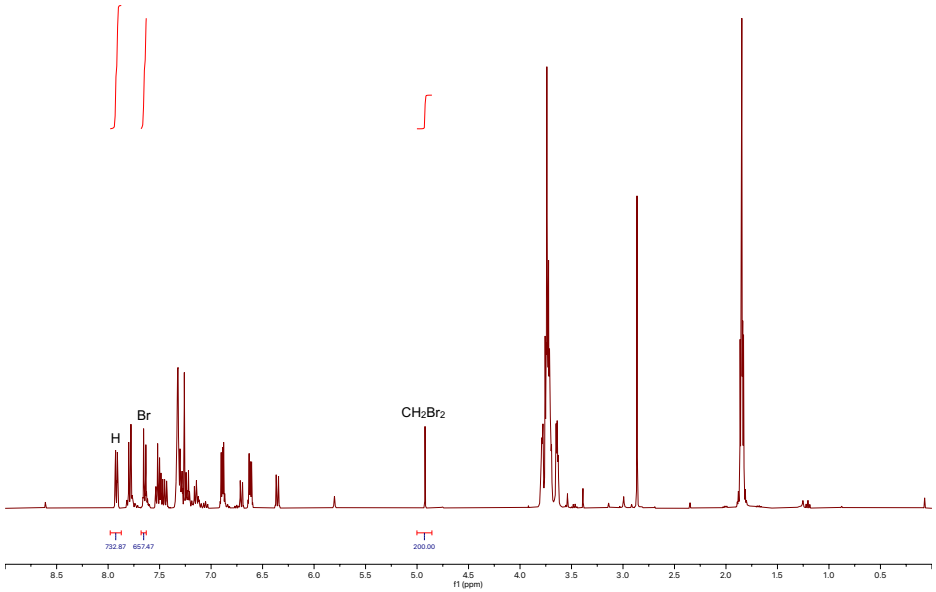

Figure A27. ^{1}H NMR spectrum of the products of the azoarene competition experiment (H vs. Br, run B) with substrates (11 umol) using [PhCbPh^{N}]K(benzo-15-crown-5) and [Ph_3PH]OTf in THF with 5 umol CH_2Br_2 as an internal standard in $CDCl_3$ (400 MHz).

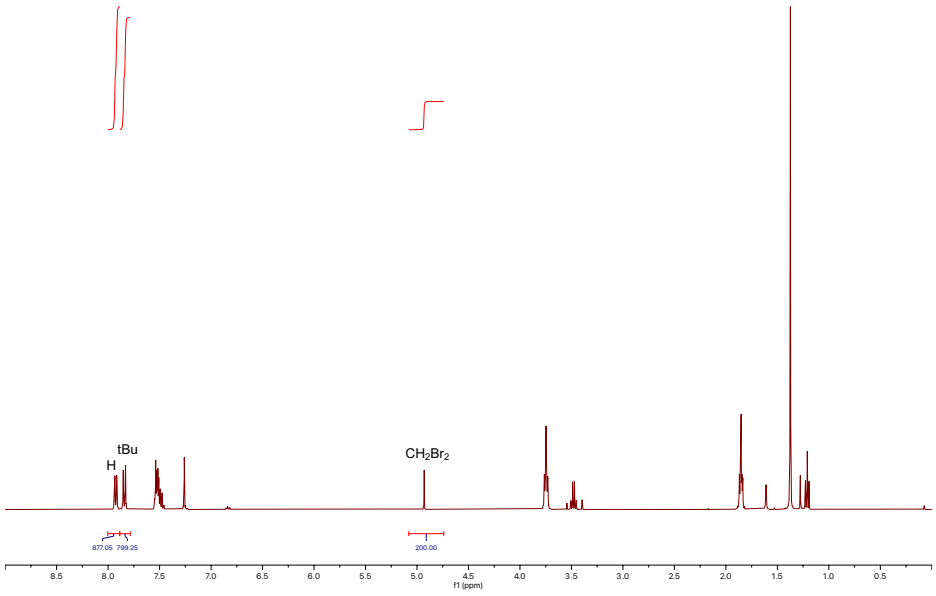

Figure A28. ^{1}H NMR spectrum of a 200 uL aliquot of the substrate solution for the competition experiment (H vs. ^{t}Bu), approximately 11 umol each, after concentration *in vacuo* with 5 umol CH_2Br_2 as an internal standard in $CDCl_3$ (400 MHz).

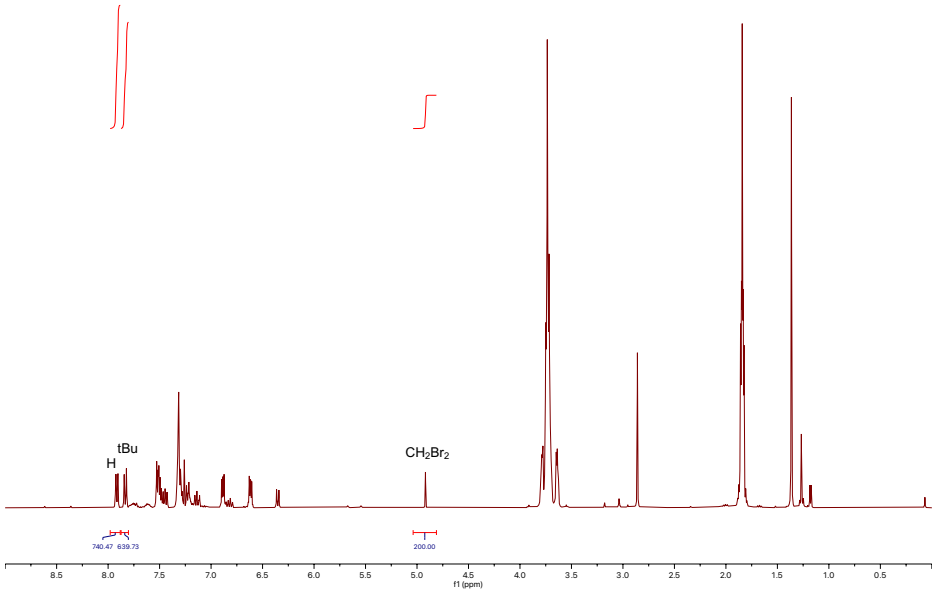

Figure A29. ^{1}H NMR spectrum of the products of the azoarene competition experiment (H vs. ^{t}Bu, run A) with substrates (11 umol) using [PhCbPh^{N}]K(benzo-15-crown-5) and [Ph_3PH]OTf in THF with 5 umol CH_2Br_2 as an internal standard in $CDCl_3$ (400 MHz).

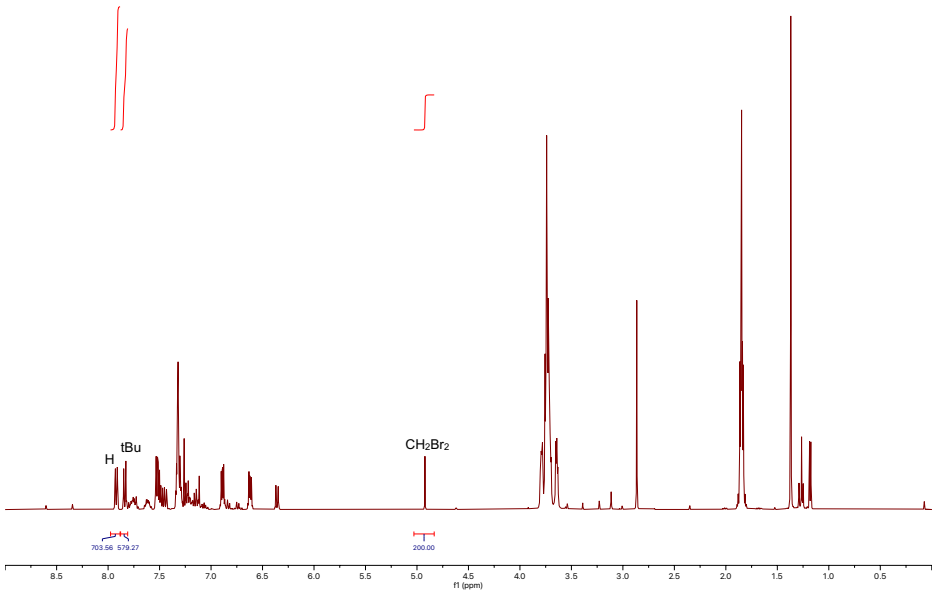

Figure A30. ^{1}H NMR spectrum of the products of the azoarene competition experiment (H vs.^{t}Bu, run B) with substrates (11 umol) using [PhCbPh^{N}]K(benzo-15-crown-5) and [Ph$_3$PH]OTf in THF with 5 umol CH_2Br_2 as an internal standard in $CDCl_3$ (400 MHz).

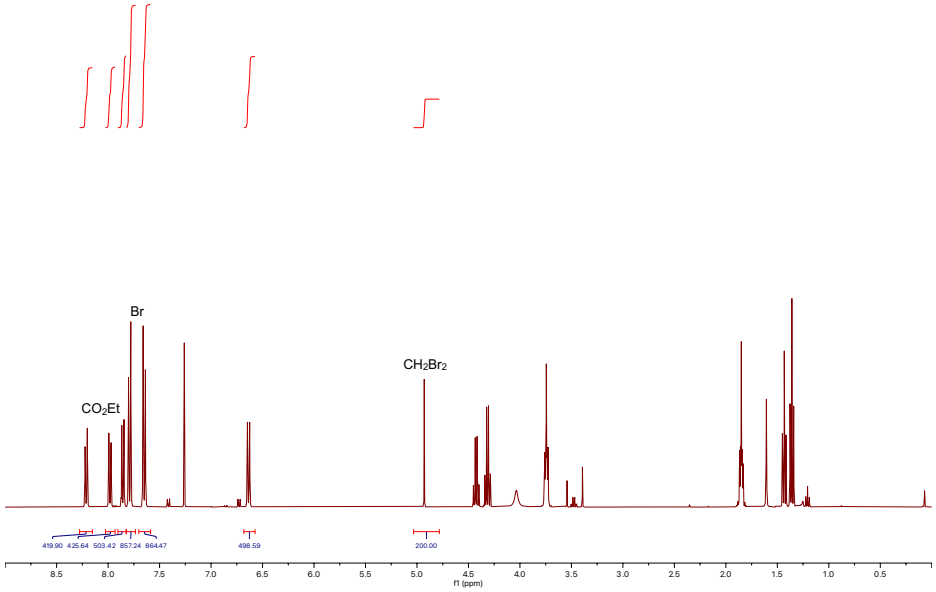

Figure A31. ^{1}H NMR spectrum of a 200 uL aliquot of the substrate solution for the competition experiment (Br vs. CO_2Et), approximately 11 umol each, after concentration *in vacuo* with 5 umol CH_2Br_2 as an internal standard in $CDCl_3$ (400 MHz).

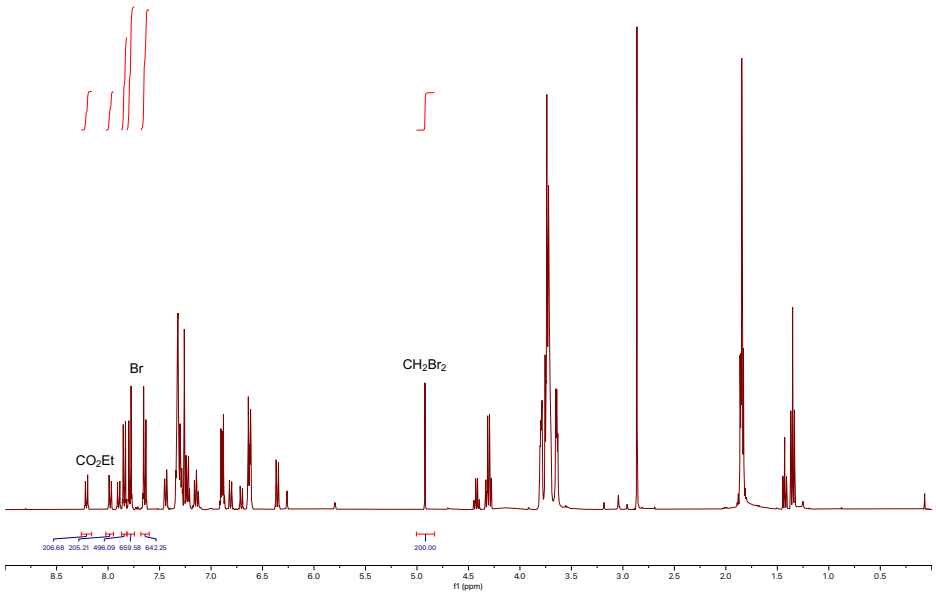

Figure A32. ^{1}H NMR spectrum of the products of the azoarene competition experiment (Br vs. CO_2Et, run A) with substrates (11 umol) using [PhCbPh^{N}]K(benzo-15-crown-5) and [Ph_3PH]OTf in THF with 5 umol CH_2Br_2 as an internal standard in $CDCl_3$ (400 MHz).

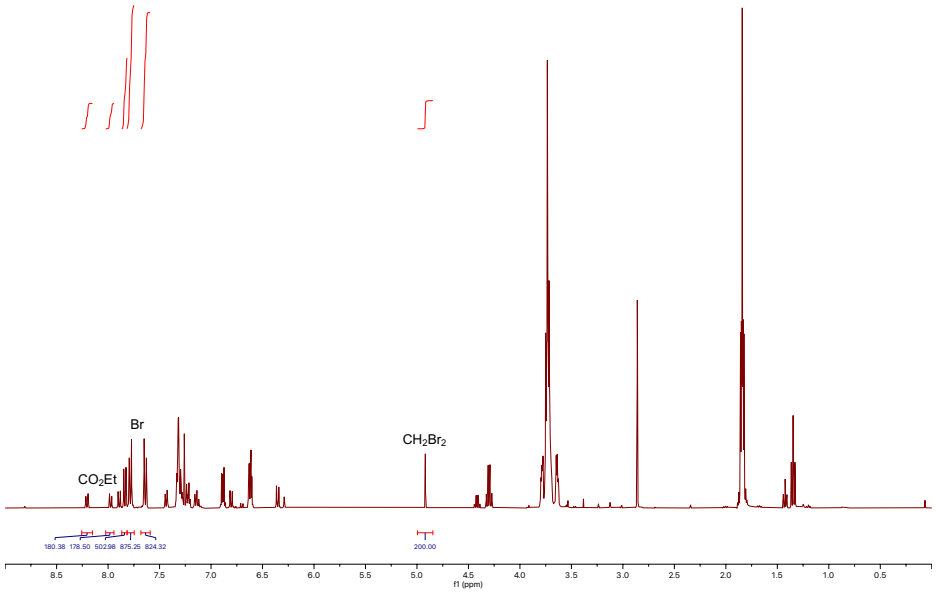

Figure A33. ^{1}H NMR spectrum of the products azoarene competition experiment (Br vs. CO_2Et, run B) with substrates (11 umol) using [PhCbPh^{N}]K(benzo-15-crown-5) and [Ph_3PH]OTf in THF with 5 umol CH_2Br_2 as an internal standard in $CDCl_3$ (400 MHz).

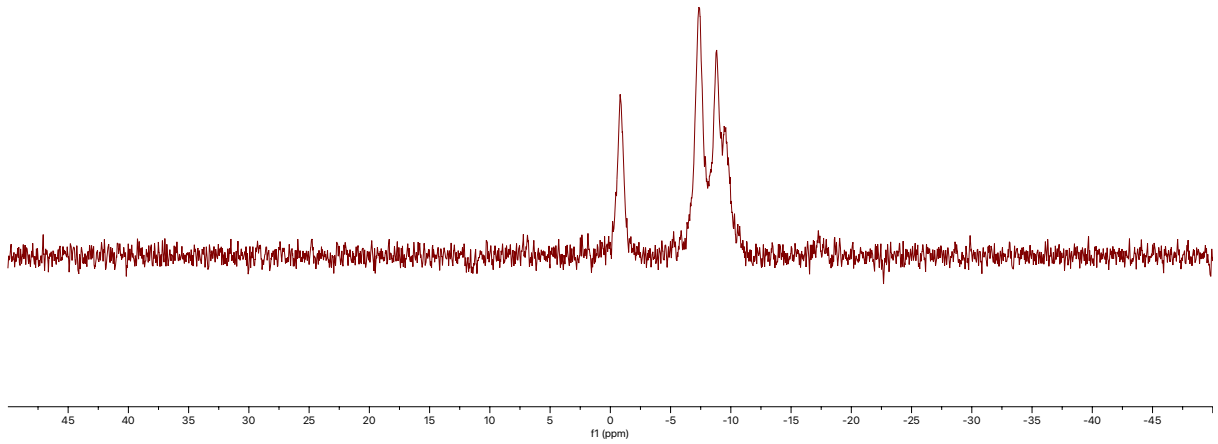

Figure A34. $^{11}B\{^{1}H\}$ NMR spectrum of the products of hydrogen evolution with $[Ph_2Cb]K$(18-crown-6) [1 mM, 0.6 umol] and $[Ph_3PD]OTf$ [1 mM, 0.6 umol] in THF-H_8 (400 MHz).

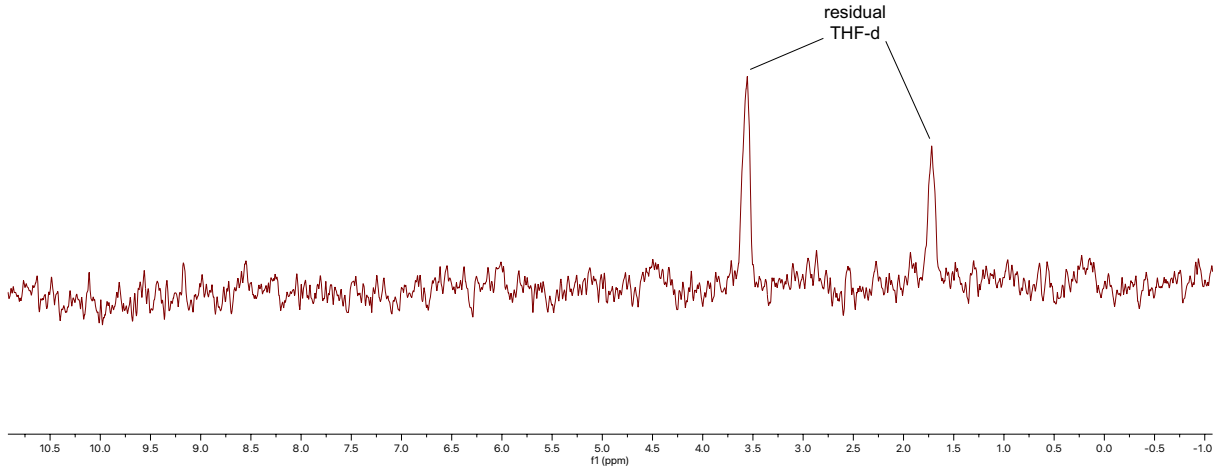

Figure A35. ^{2}H NMR spectrum of the products of hydrogen evolution with $[Ph_2Cb]K$(18-crown-6) [1 mM, 0.6 umol] and $[Ph_3P\mathbf{D}]OTf$ [1 mM, 0.6 umol] in THF-H_8 (400 MHz).

A.4 EPR Spectra

Note on sample preparation: A sample of $PhCbPh^{NH}$ was prepared by cooling a solution of $[PhCbPh^{N}]K(crown)_2$ in 2-MeTHF to -40 °C in the nitrogen glovebox and adding 2 eq. of $[Ph_3PH]OTf$ as a 2-MeTHF solution. The solution immediately changed color from red to pink, indicating protonation, and the solution was transferred to a pre-cooled quartz EPR tube, removed from the glovebox, and frozen in liquid nitrogen to form a glass.

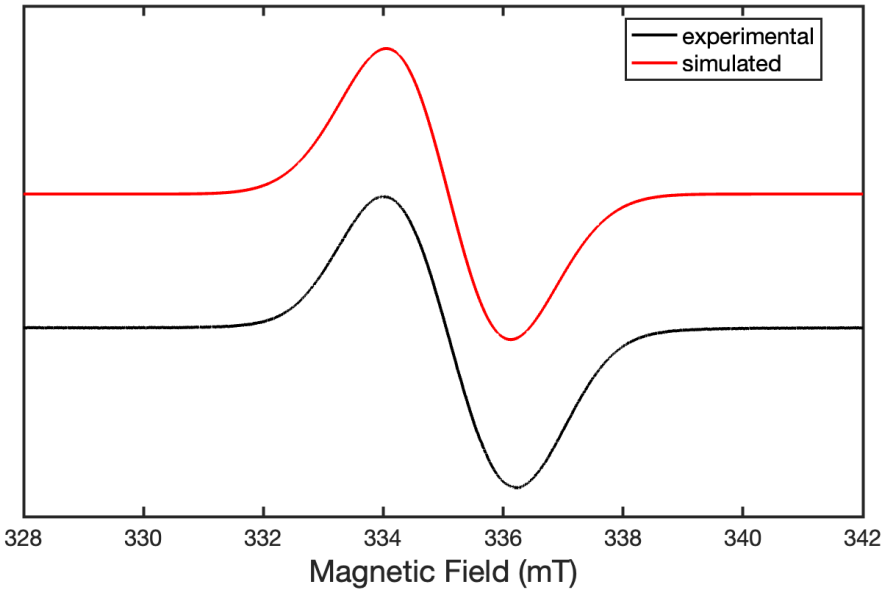

Figure A36. X-Band CW EPR spectrum of **$[Ph_2Cb]K(18\text{-}c\text{-}6)$** in 2-MeTHF. Acquisition parameters: S = 1/2; g = 2.026; H strain = 59 MHz. MW Frequency = 9.40 GHz; temperature = 77 K; MW power = 2.18 mW; modulation amplitude = 1.0 G

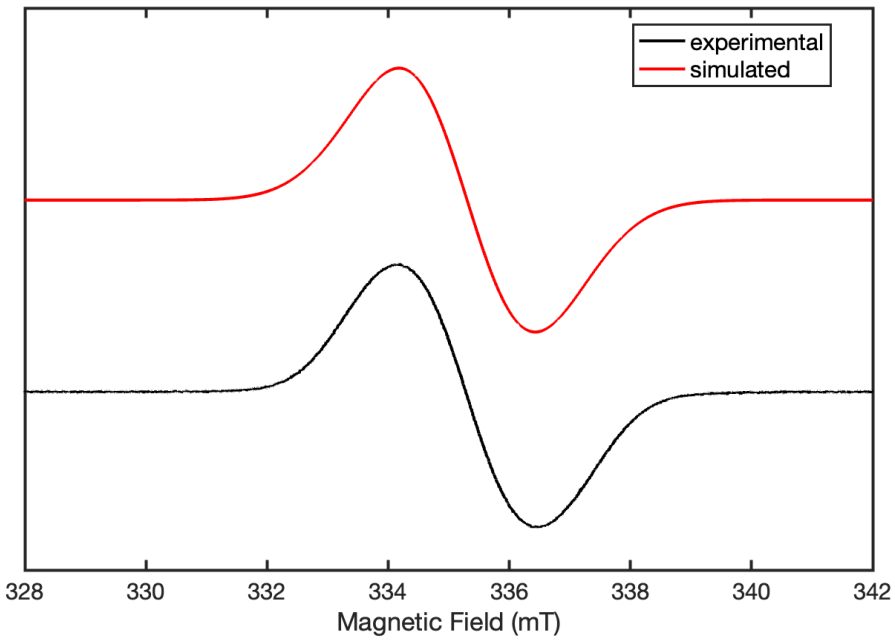

Figure A37. X-Band CW EPR spectrum of **[PhCbPh^{N}]K(b-15-c-5)$_2$** in 2-MeTHF. Simulation parameters: S = 1/2,; g = 2.024; H Strain = 71 MHz. Acquisition parameters: MW Frequency = 9.40 GHz; temperature = 77 K; MW power = 140 uW; modulation amplitude = 0.5 G

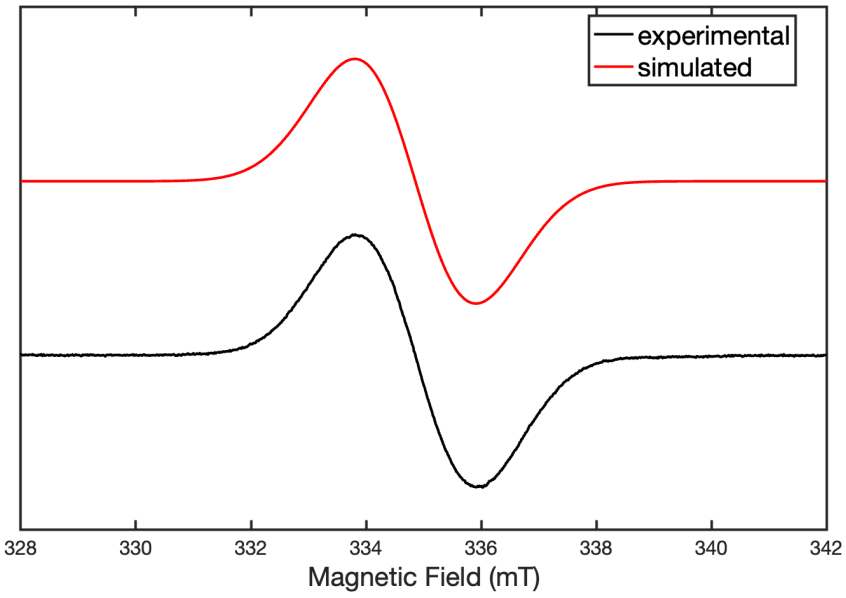

Figure A38. X-Band CW EPR spectrum of **PhCbPh^{NH}** in 2-MeTHF. Simulation parameters: S = 1/2, g = 2.027; H Strain = 66 MHz. Acquisition parameters: MW Frequency = 9.39 GHz; temperature = 77 K; MW power = 219 uW; modulation amplitude = 1.0 G

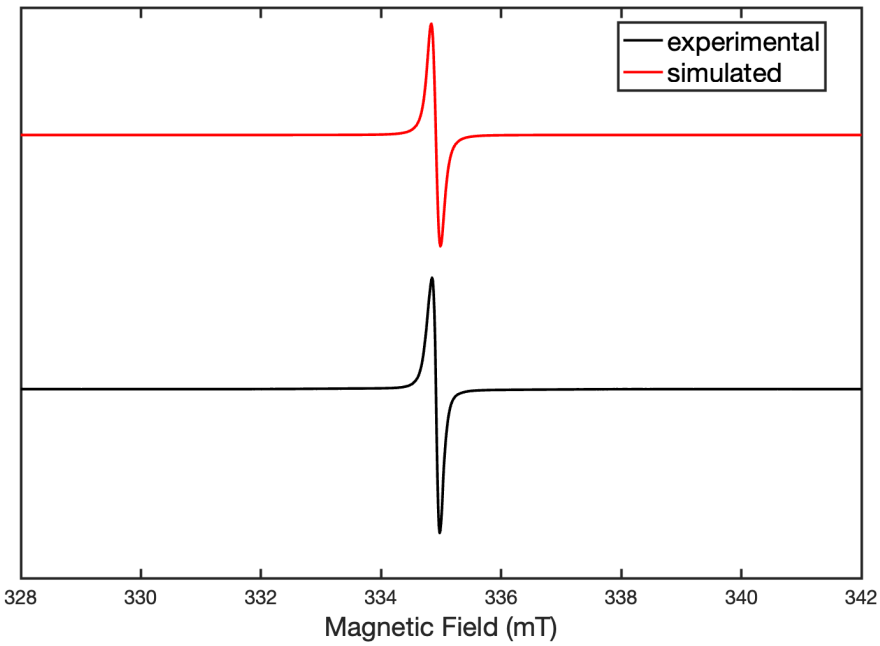

Figure A39. X-Band CW EPR spectrum of **PhCbPh^{NMe3}** in 2-MeTHF. Simulation parameters: S = 1/2, g = 2.027; H Strain = 3 MHz. Acquisition parameters: MW Frequency = 9.39 GHz; temperature = 77 K; MW power = 2.18 uW; modulation amplitude = 1.0 G

A.5 UV-Vis Spectra

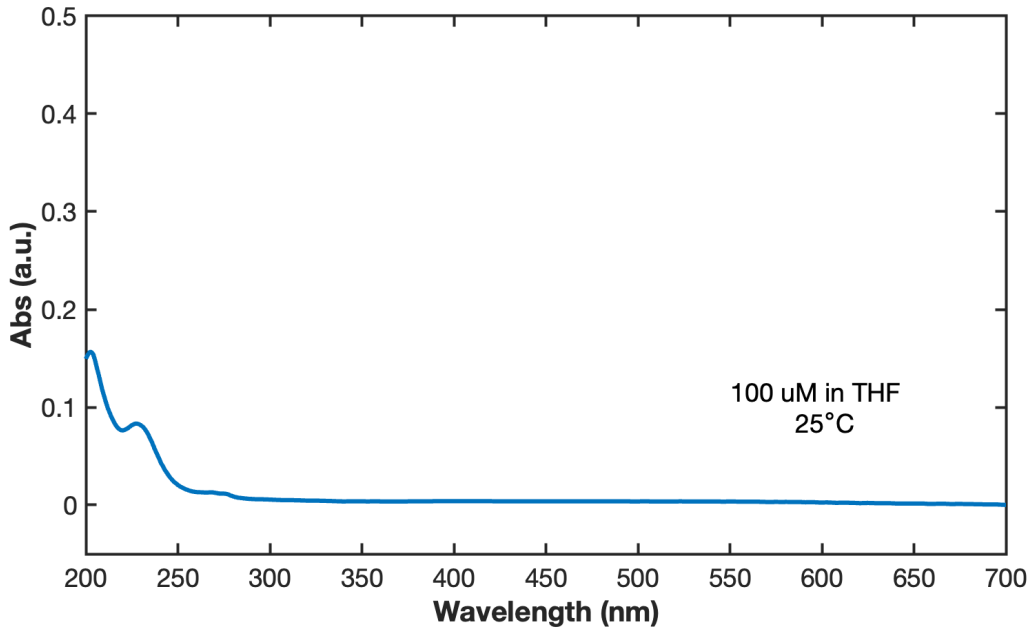

Figure A40. UV-vis Absorbance Spectrum of 100 uM **Ph_2Cb** in THF at 25°C

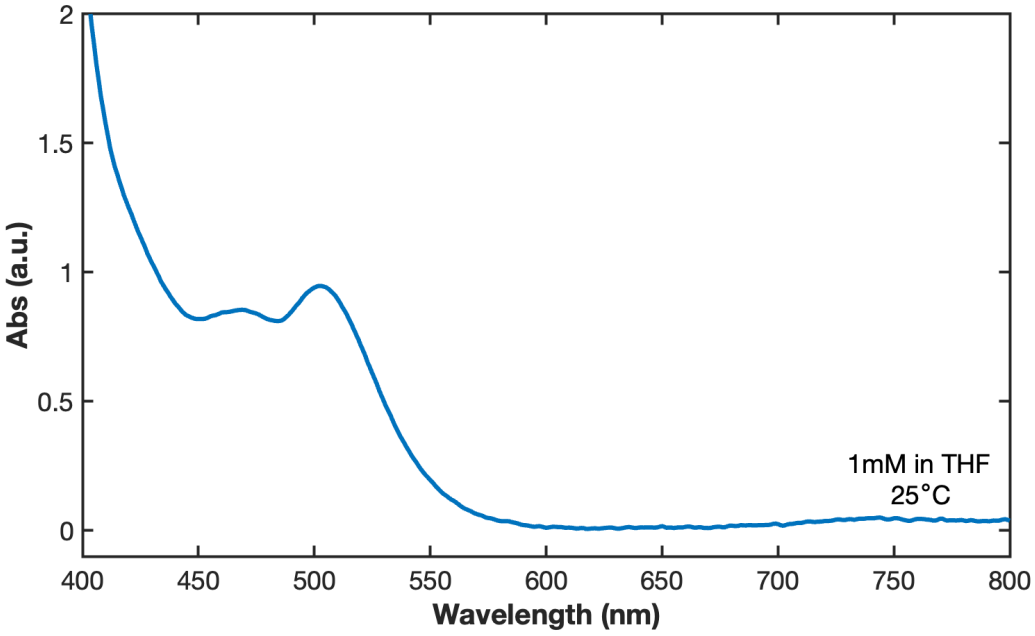

Figure A41. UV-vis Absorbance Spectrum of 1 mM **[Ph_2Cb]K(18-c-6)** in THF at 25°C

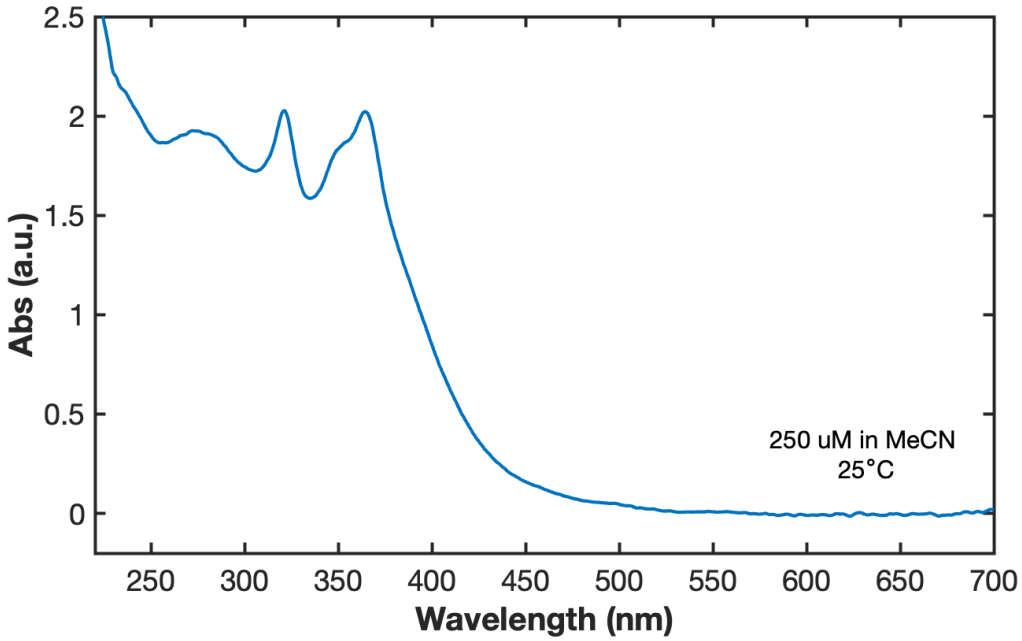

Figure A42. UV-vis Absorbance Spectrum of 250 uM **[Ph$_2$Cb][K(18-c-6)]$_2$** in MeCN at 25°C

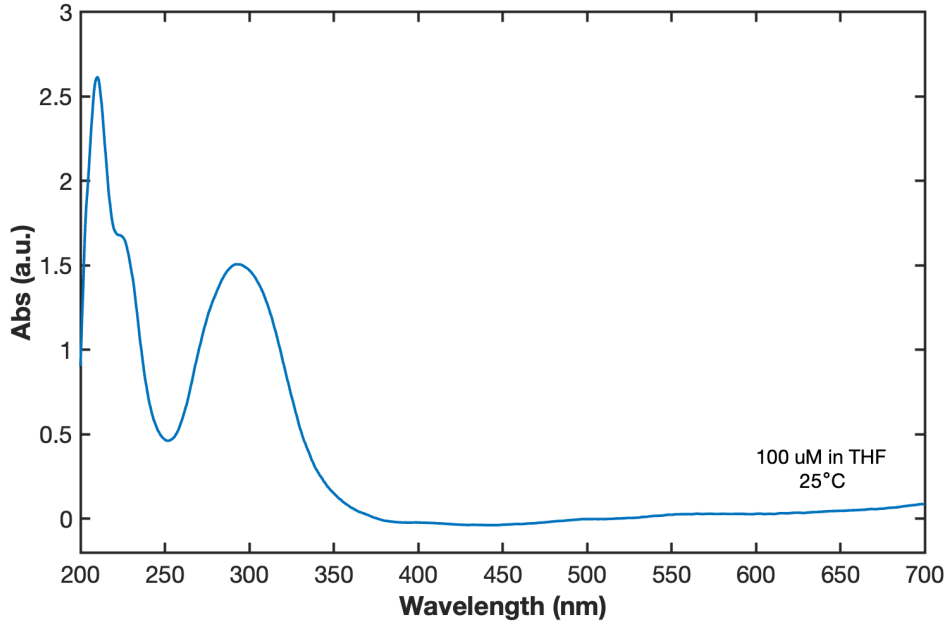

Figure A43. UV-vis Absorbance Spectrum of 100 uM **PhCbPh^N** in THF at 25°C

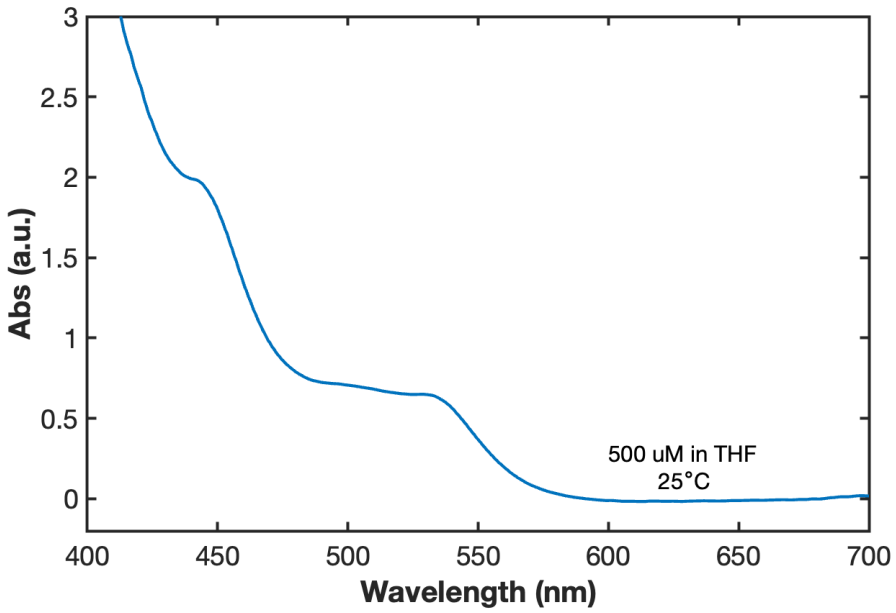

Figure A44. UV-vis Absorbance Spectrum of 500 uM **[PhCbPh^{N}]K(b-15-c-5)$_2$** in THF at 25°C

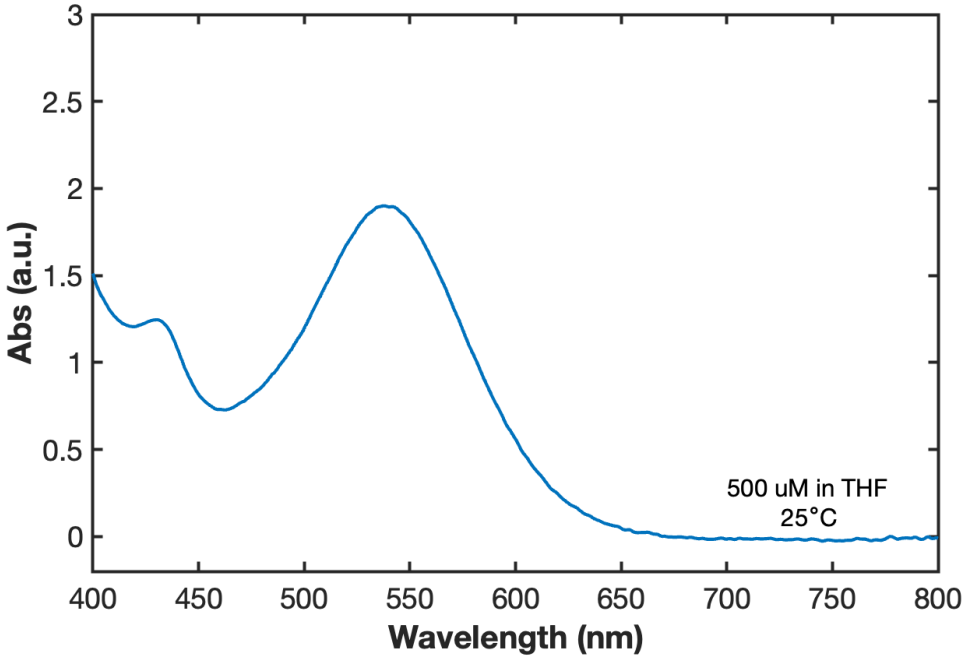

Figure A45. UV-vis Absorbance Spectrum of 500 uM **PhCbPh^{NMe3}** in THF at 25°C

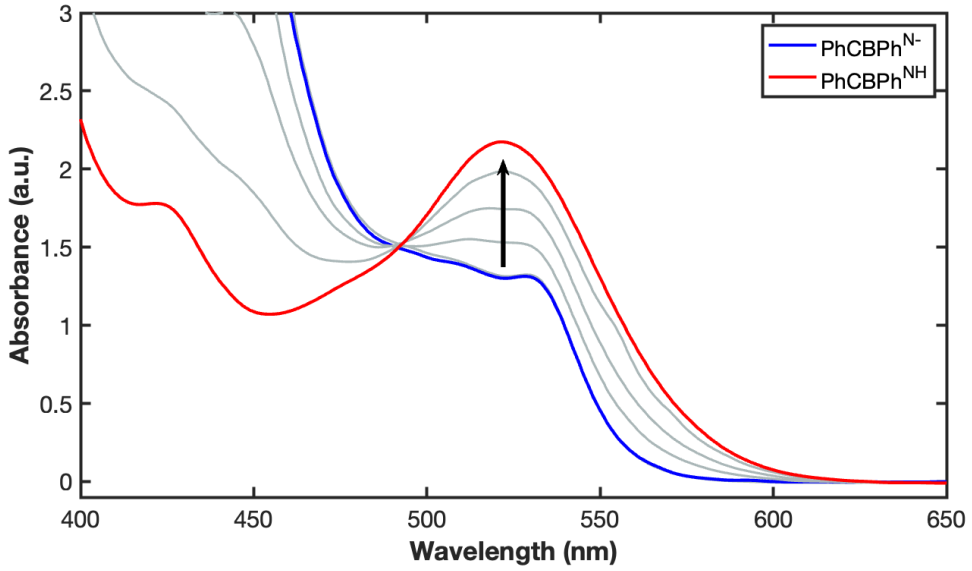

Figure A46. Acid Titration: [$^{4\text{-CN}}$PhNH$_3$]OTf (0 - 1.0 eq in 0.2 eq increments) added to **[PhCbPh^{N}]K(b-15-c-5)$_2$** (1 mM) and monitored by UV-vis Spectroscopy in THF at -80 °C

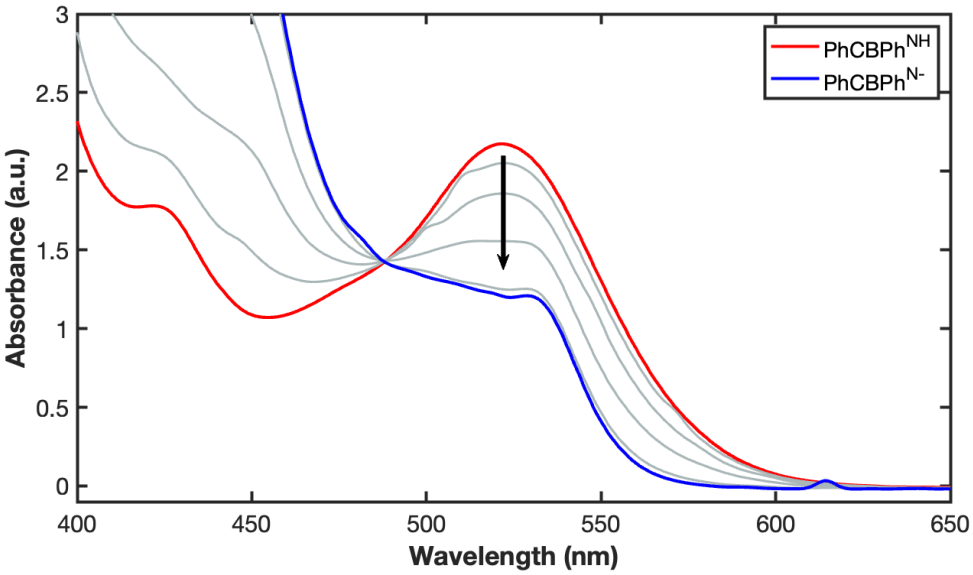

Figure A47. Base Titration: Triazabicyclodecene (0 – 1.0 eq in 0.2 eq increments) added to in **[PhCbPh^{N}]K(b-15-c-5)$_2$** (1 mM) and [$^{4\text{-CN}}$PhNH$_3$]OTf (1 mM) monitored by UV-vis spectroscopy in THF at -80 °C

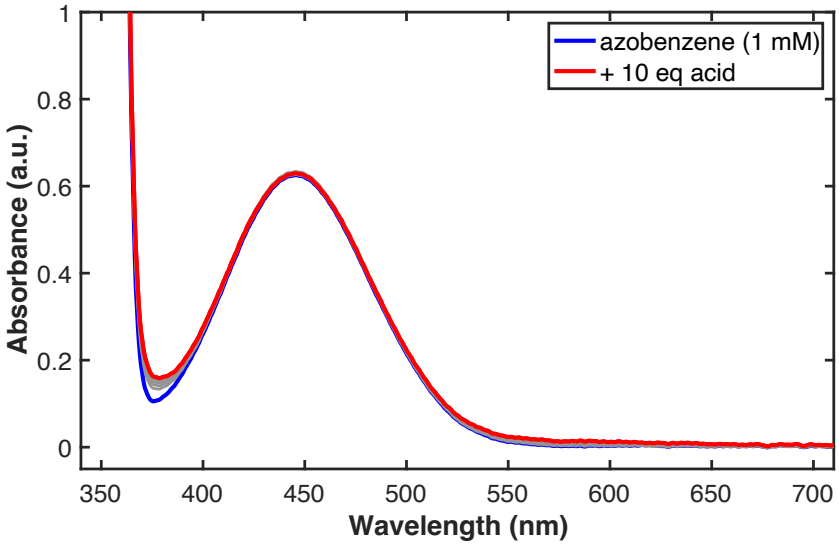

Figure A48. Titration of [$^{4\text{-MeO}}$PhNMe$_2$H]OTf (pK_a = 12.7 in MeCN) (0 – 10 eq in 2 eq increments) added to azobenzene (*blue*, 1 mM) in THF at -80 °C monitored by UV-vis spectroscopy

A.6 X-ray Crystallography

CCDC 2367450-2367452 contains the supplementary crystallographic data for this paper. These data can be obtained free of charge from the Cambridge Crystallographic Data Centre via http://www.ccdc.cam.ac.uk/data_request/cif

[Ph_2Cb][K(18-crown-6)]	**[Ph_2Cb][K(18-crown-6)]$_2$**	**[PhCbPh^N][K(benzo-15-crown-5)]**
	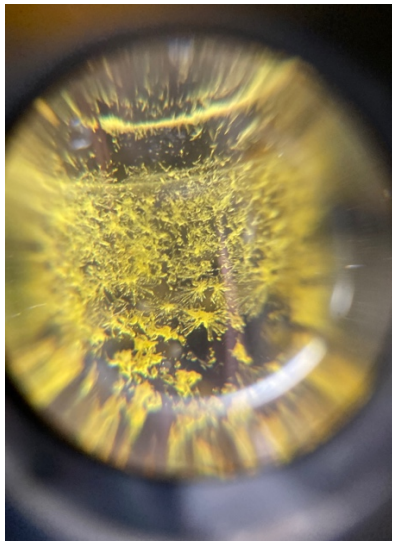	
red needles	yellow stars	red needles

Figure A49. Images and descriptions of diffraction quality crystals used for structure determination.

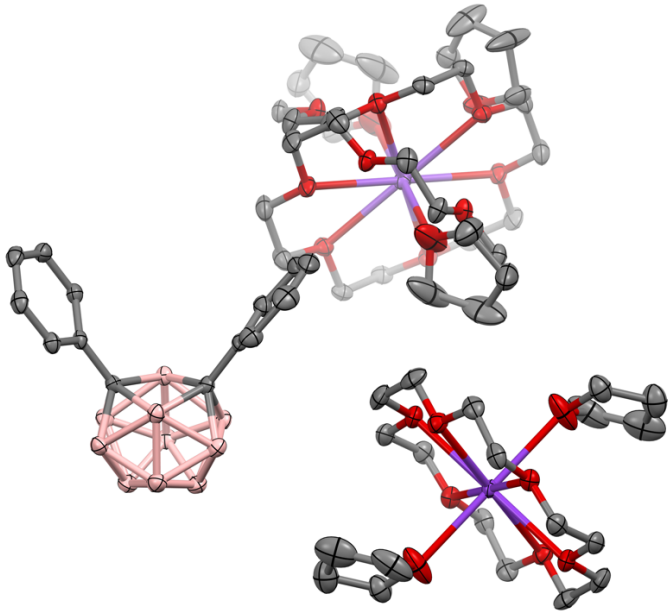

Figure A50. X-Ray Diffraction structure of $[Ph_2Cb][K(18\text{-crown-6})(THF)_2]$ with thermal ellipsoids set at 50%. The structure contains both positional disorder of the $K(18\text{-crown-6})(THF)_2$ moiety and rotation disorder of crown/THF_2 about the K center in one of the two cation positions in the structure.

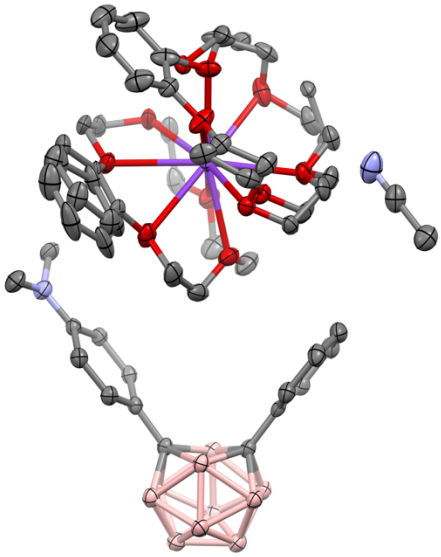

Figure A51. X-Ray Diffraction structure of $[PhCbPh^N][K(benzo\text{-}15\text{-}crown\text{-}5)_2]$ with thermal ellipsoids set at 50%. The structure contains rotational disorder of the benzo-15-crown-5 moiety.

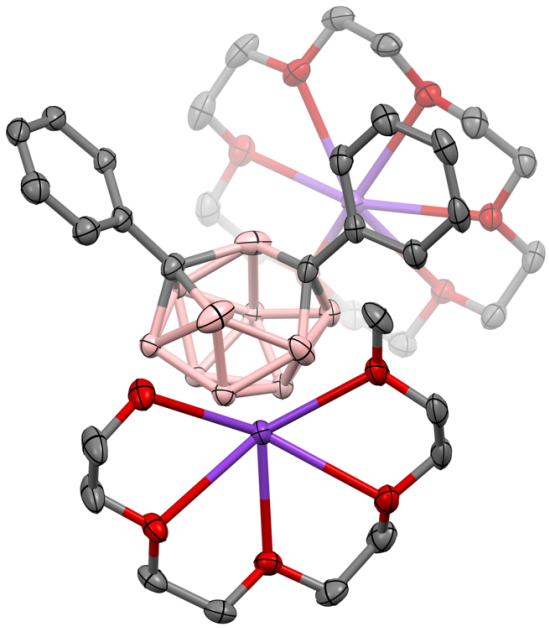

Figure A52. X-Ray Diffraction structure of $[Ph_2Cb][K(18\text{-crown-6})]_2$ with thermal ellipsoids set at 50%. A portion of the 18-crown-6 moiety is omitted for clarity.

	Ph_2CB	$[PhCBPh^N]^-$	$[Ph_2CB]^-$	$[Ph_2CB]^{2-}$
	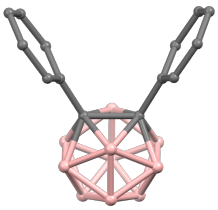	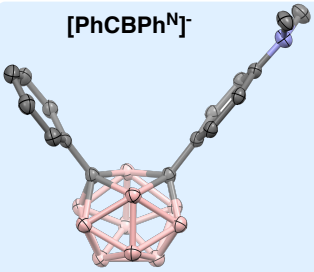	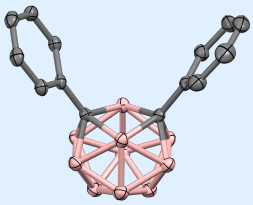	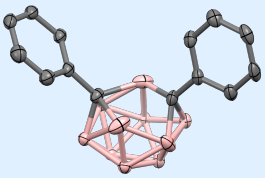
$E_{1/2}$ (V vs. $Fc^{0/+}$)	-	-1.67	-1.56	-1.67
C-$C_{cluster}$ (Å)	1.733	2.400	2.374	2.689
$C_{cluster}$-C_{aryl} (Å)	1.504	1.469	1.470	1.470
B-$B_{cluster}$ (Å)	1.76 (0.01)	1.80 (0.04)	1.80 (0.04)	1.82 (0.08)

Figure A53. Comparison of potentials and structural features of the series of reduced diaryl-carboranes.

Table S1. Crystallographic data for complexes 1crown, 2crown, 3crown

Compound	**[Ph$_2$Cb]K**	**[Ph$_2$Cb]K$_2$**	**[PhCbPh^N]K**
Empirical formula	$C_{34}H_{60}B_{10}KO_8$	$C_{19}H_{34}B_5KO_6$	$C_{46}H_{68}B_{10}N_2O_{10}K$
Formula weight	495.72	451.61	956.22
Temperature (K)	100.0	100.0	100.0
Crystal system	Orthorhombic	Triclinic	Triclinic
Space group	Pbca	P-1	P-1
a (Å)	18.3349(6)	10.8113(5)	12.4562(12)
b (Å)	19.8101(5)	15.9554(8)	13.1790(11)
c (Å)	22.8927(6)	16.6524(8)	16.5016(13)
α (°)	90	91.396(3)	102.107(6)
β (°)	90	103.147(3)	105.716(5)
γ (°)	90	109.352(3)	90.513(6)
Volume (Å^3)	8315.0(4)	2623.6(2)	2543.4(4)
Z	12	4	2
ρ_{calc} [g/cm^3]	1.188	1.143	1.249
μ (mm^{-1})	0.172	2.007	1.376
F (000)	3174.0	960.0	1014.0
Radiation	MoKα (λ = 0.71073)	CuKα(λ = 1.54178)	CuKα(λ = 1.54178)
Reflections collected	58560	56484	64893
Unique reflections	9534	11295	10407
Data/restraints /parameters	9534/9/615	11295/9/592	10407/9/800
R(int)	0.0354	0.0949	0.0623
R_1 (I > 2 σ(I))	0.0440	0.0454	0.0494
wR_2	0.1115	0.1169	0.1244
GOOF	1.021	1.035	1.041

A.7 Electrochemistry

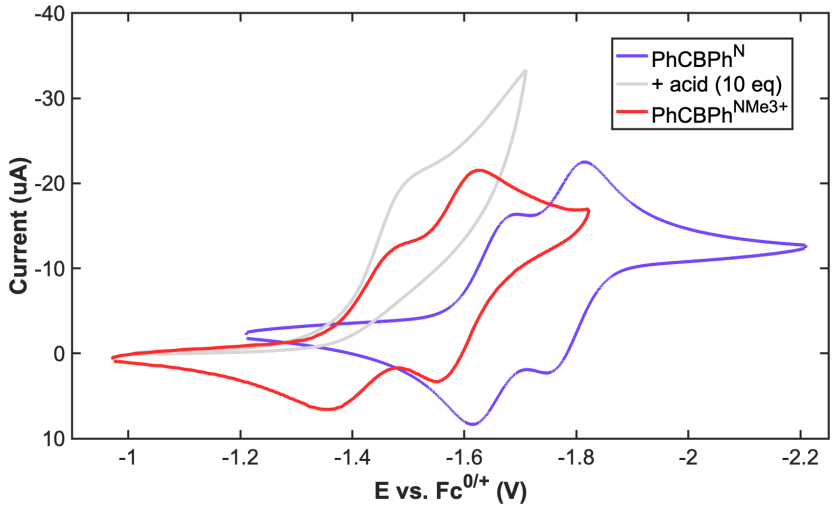

Figure A54. Cyclic voltammogram of **PhCbPh^{N}** (1 mM, *blue*) with 4-cyanoanilinium triflate (10 mM, *grey*) and **[PhCbPh^{NMe3}]OTf** (1mM, *red*) in MeCN with $^{n}Bu_4NPF_6$ (200 mM) supporting electrolyte. The scans are swept cathodic, then anodic at 100 mV/s.

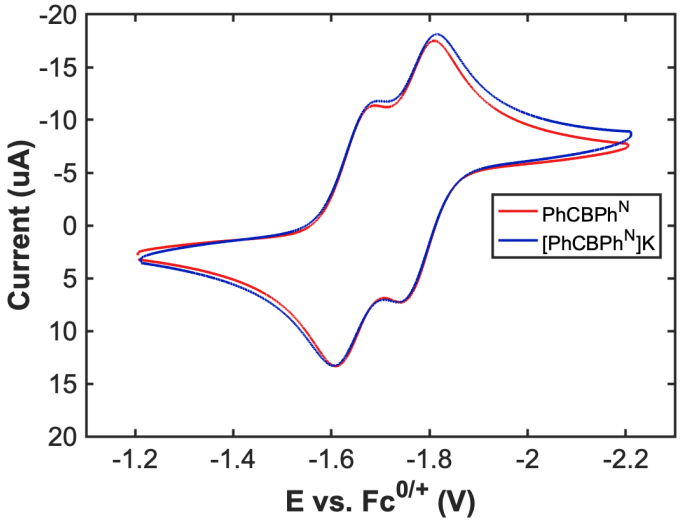

Figure A55. Cyclic voltammogram of **[PhCbPh^{N}]K** (1 mM, *blue*) and **PhCbPh^{N}** (1mM, *red*) in MeCN with $^{n}Bu_4NPF_6$ (200 mM) supporting electrolyte. The scans are swept cathodic, then anodic at 100 mV/s.

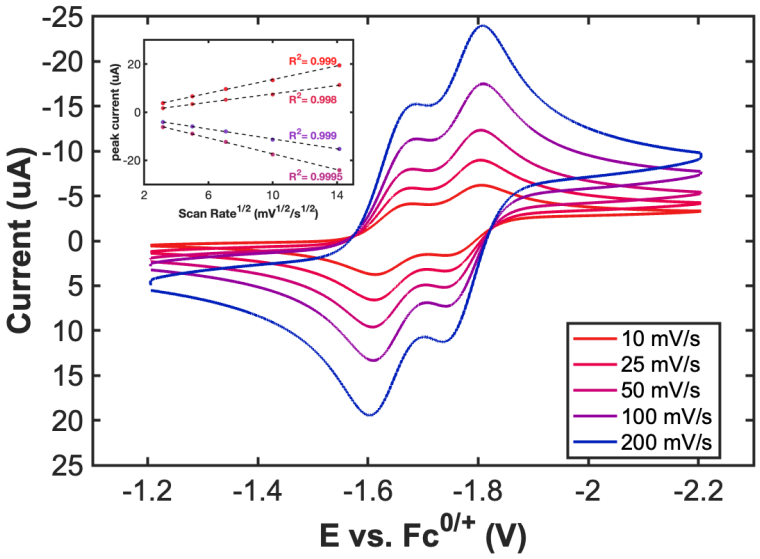

Figure A56. Cyclic voltammograms of **PhCbPh^{N}** (1 mM) at various scan rates in MeCN with $^{n}Bu_4NPF_6$ (200 mM) supporting electrolyte. The scans are swept cathodic, then anodic at the scan rate indicated in the legend. *Inset*: peak cathodic and peak anodic currents plotted as a function of the square of the scan rate.

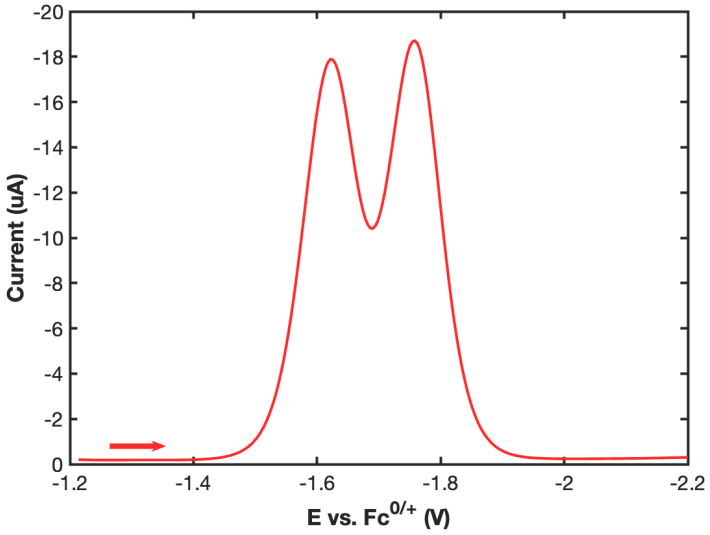

Figure A57. Differential pulse voltammogram of **PhCbPh^{N}** (1 mM) in MeCN with $^{n}Bu_4NPF_6$ (200 mM) supporting electrolyte with following parameters: increment potential = 4 mV, amplitude potential = 50 mV, pulse width = 50 ms, sample width = 16.7 ms, pulse period = 0.5 s.

A.8 pK_a Determination

The pK_a of compound **2** was determined using a method used in previous studies from our group.[14] In brief, ^{1}H NMR spectroscopy is used to measure the equilibrium depicted in Figure A39 at several different concentrations of base. The chemical shifts of the PhCbPh^N and $^{2\text{-Cl}}$PhNH$_2$ can be used to determine their concentration as well as their conjugate acid concentrations using the following equation:

$$[PhCbPh^{NH+}] = \frac{\delta_{obs} - \delta_{PhCbPh^N}}{\delta_{PhCbPh^{NH+}} - \delta_{PhCbPh^N}}$$

$$[PhCbPh^N] = [PhCbPh^N]_{tot} - [PhCbPh^{NH+}]$$

Similarly for $^{2\text{-Cl}}$PhNH$_3^+$ / $^{2\text{-Cl}}$PhNH$_2$:

$$[^{2-Cl}PhNH_3^+] = \frac{\delta_{obs} - \delta_{^{2-Cl}PhNH_2}}{\delta_{^{2-Cl}PhNH_3^+} - \delta_{^{2-Cl}PhNH_2}}$$

$$[^{2-Cl}PhNH_2] = [^{2-Cl}PhNH_2]_{tot} - [^{2-Cl}PhNH_3^+]$$

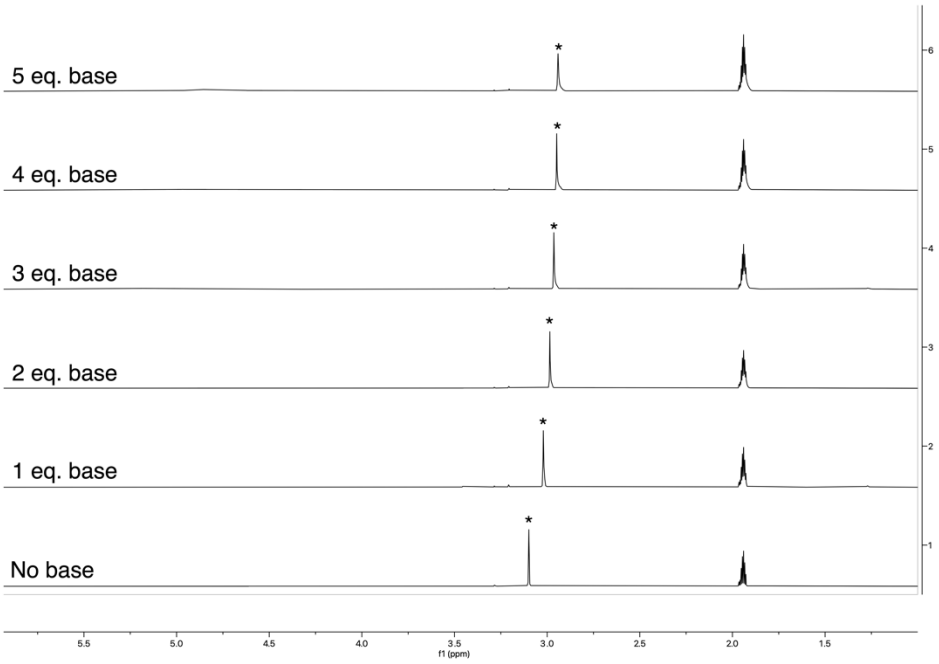

Figure A58. ^{1}H NMR Spectra of [PhCbPh^{NH}]OTf with 0-5 equivalents of $^{2\text{-Cl}}$PhNH$_2$ added, focused on the starred (*) methyl-shift of the dimethylaniline fragment as a reporter of the PhCbPh^{NH+} concentration.

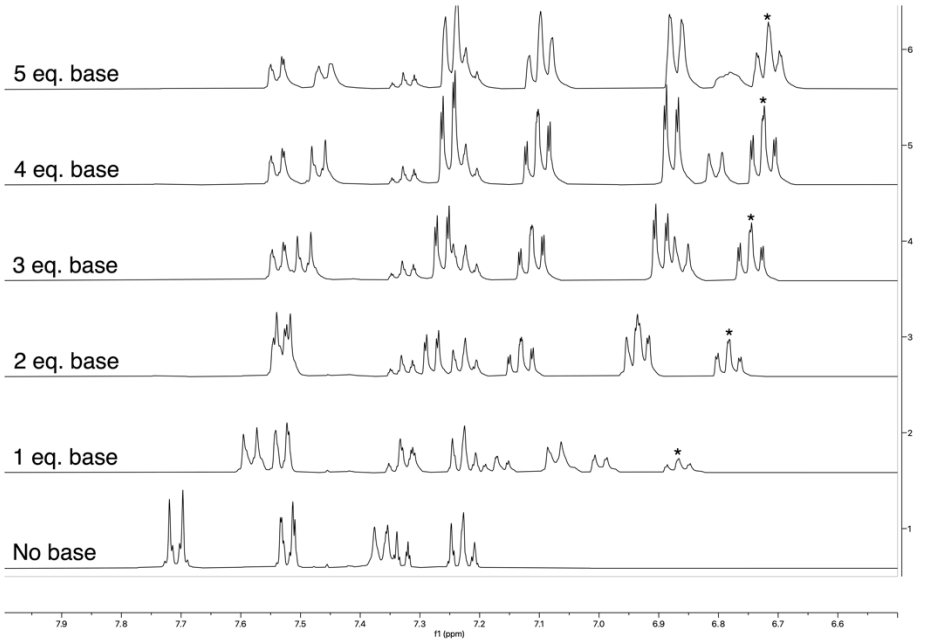

Figure A59. ^{1}H NMR Spectra of [PhCbPh^{NH}]OTf with 0-5 equivalents of $^{2\text{-Cl}}$PhNH$_2$ added. The starred (*) $^{2\text{-Cl}}$PhNH$_2$ *ortho*-H peak is used as a reporter of the $^{2\text{-Cl}}$PhNH$_2$ concentration.

From these concentrations, the K_{eq} can be determined:

$$K_{eq} = \frac{[PhCbPh^{N}][^{2-Cl}PhNH_3^{+}]}{[PhCbPh^{NH+}][^{2-Cl}PhNH_2]}$$

Table A2. Reporter peak shifts from the ^{1}H NMR base titration and the resulting K_{eq}

Eq. base added	PhCbPh^{N} methyl shift (ppm)	$^{2\text{-Cl}}$PhNH$_2$ *ortho*-H shift (ppm)	[PhCbPh^{N}]	[PhCbPh^{NH+}]	[$^{2\text{-Cl}}$PhNH$_2$]	[$^{2\text{-Cl}}$PhNH$_3^{+}$]	K_{eq}
0	3.140	7.740	0	1.00	0	0	-
1	3.021	6.867	0.412	0.588	0.792	0.208	0.184
2	2.985	6.783	0.536	0.463	1.734	0.264	0.176
3	2.964	6.746	0.609	0.391	2.704	0.295	0.170
4	2.945	6.724	0.675	0.325	3.685	0.314	0.177
5	2.941	6.716	0.689	0.311	4.643	0.357	0.170

As summarized in the above table, the resulting equilibrium constant K_{eq} is determined to be 0.176. From this K_{eq} value and the known pK_a of $^{2\text{-Cl}}$PhNH$_3^{+}$ in MeCN, the pK_a of PhCbPh^{NH+} can be determined.

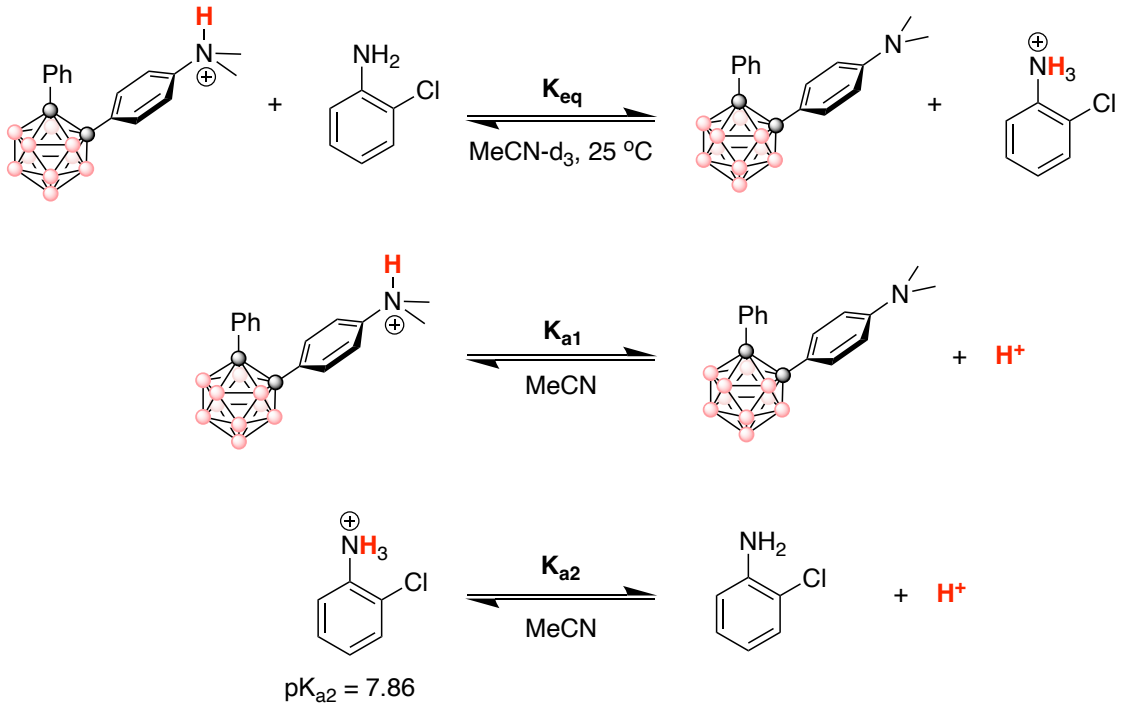

Figure A60. Relevant equilibria for the determination of the PhCbPh^{NH+} pK_a

$$K_{a2} = \frac{K_{eq}}{K_{a2}}$$

$$pK_{a1} = -\log\{K_{eq} - K_{a2}\} = pK_{a2} - log(K_{eq})$$

$$pK_{a1} = 8.6$$

A.9 Kinetic Analysis of Azoarene Reduction

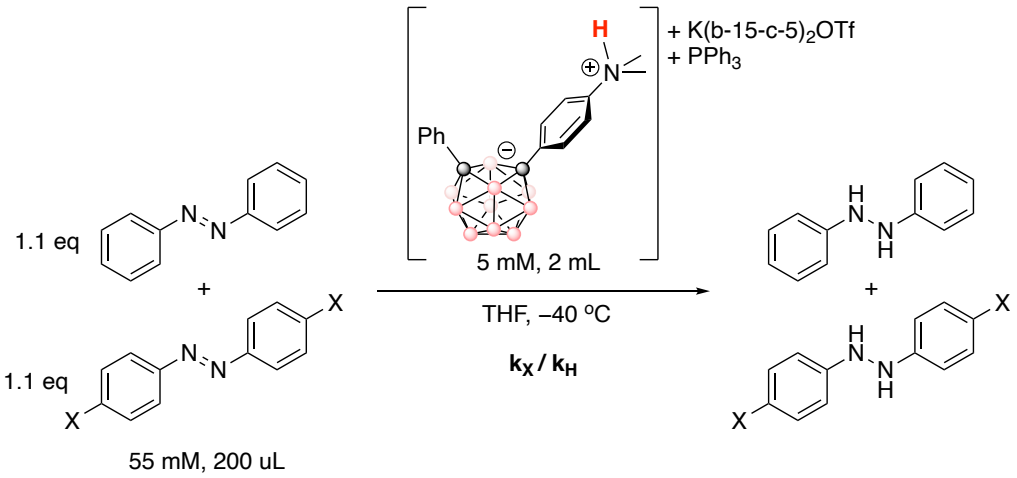

To determine the relative rates of the reduction of azobenzene and *para*-substituted azoarenes by Ph**C**b**P**h^{NH}, the consumption of two competing azoarenes was quantified by ^{1}H NMR spectroscopy.[15] Samples of the mixed substrate solution were prepared by adding a solution of azobenzene in THF [55 mM] to a weighed quantity of azoarene to generate a solution of approximately 55 mM of each substrate. The exact amounts of each substrate in the mixed azoarene solutions were determined by sampling a 200 uL aliquot of the solution, drying under vacuum, and analyzing by quantitative ^{1}H NMR in 600 uL of $CDCl_3$ with 8.33 mM (5 umol) CH_2Br_2 as an internal reference, the same method used for quantifying the products of the reactions. The reduction reactions were performed in duplicate by preparing a solution of [Ph**C**b**P**h^{N}]K(b-15-c-5)$_2$ in THF [2 mL, 5 mM, 10 umol] and adding to it a solution of [Ph_3PH]OTf [100 mM, 100 uL, 10 umol] to generate 10 umol of Ph**C**b**P**h^{NH} *in situ*. Then, the mixed substrate solution was added, and the reaction was allowed to stir for one hour. The reaction products were analyzed by quantitative ^{1}H NMR spectroscopy, and the integrals of the mixed substrate solutions and reaction products are summarized in Table S3 (with the integral of the standard set to 200). In the case of the ester substrate (X = CO_2Et), 1,2-bis(4-bromophenyl)diazene (X = Br) was competed to determine k_{CO2Et}/k_{Br} which was then multiplied with the measured ratio k_{Br}/k_H to yield k_{CO2Et}/k_H.

Linear free-energy relationships were generated using the known Hammett parameters (σ, σ$^+$, and σ$^-$)[16] for the *para*-substituted phenyl groups as well as calculated thermochemical parameters $BDFE_{N\text{-}H}$ and $E°_{calc}$ (see S12 for details). Plotting the log of the relative rates ($k_{rel} = k_X/k_H$) against these free-energy parameters yields Hammett plots and rate-driving force relationships depicted below with the slope, intercept, and coefficient of determination (R^2) indicated on or below the plot.

Table A3: ^{1}H NMR Integrals, Conversion, and Relative Rates for Azoarene Competition

X	$I(X)_{t=0}$	$I(H)_{t=0}$	$I(X)_{t=f}$	$I(H)_{t=0}$	%conv(X)	%conv(H)	k_{rel}	$\ln(k_{rel})$
Me	852.85	871.1	810.78	723.7	7.4	16.9	0.43	-0.83
^{t}Bu	799.25	877.05	659.87	671.645	17.4	23.4	0.74	-0.29
Br	829.74	894.71	658.685	790.925	20.6	11.6	1.78	0.58
Cl	836.93	885.35	635.835	773.955	24.0	12.6	1.91	0.65
CO_2Et	923.78	860.86	692.23	750.35	25.0	12.8 (Br)	3.47	1.24

Table A4: Experimental and Calculated Free-Energy Descriptors of Azoarene Substrates

X	σ	σ^{+}	σ^{-}	$BDFE_{calc}$ (kcal/mol)	$E°_{calc}$ (V vs. $Fc^{0/+}$)
H	0	0	0	53.3	-1.82*
Me	-0.17	-0.31	-0.17	51.8	-1.93
^{t}Bu	0.23	0.11	0.19	54.4	-1.68
Br	0.23	0.15	0.25	53.1	-1.69
Cl	-0.2	-0.26	-0.13	53.7	-1.88
CO_2Et	0.45	0.48	0.64	58.0	-1.36

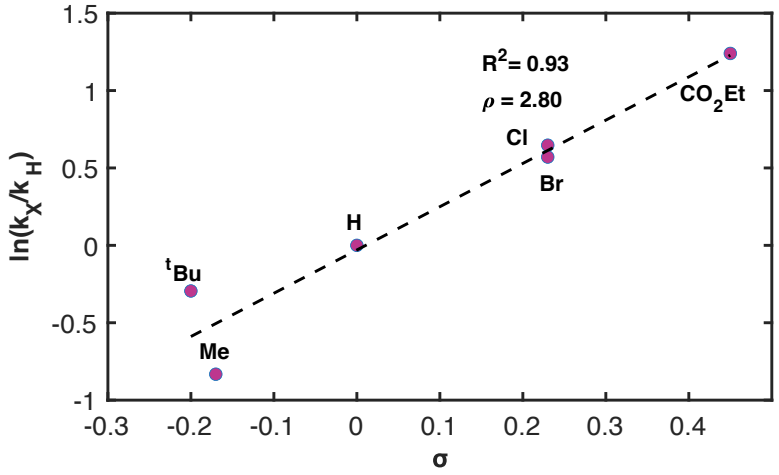

Figure A61. Hammett Plot for the rate azoarene reduction relative to azobenzene reduction as a function of σ for the given substituent. slope = 2.80, intercept = 0.03

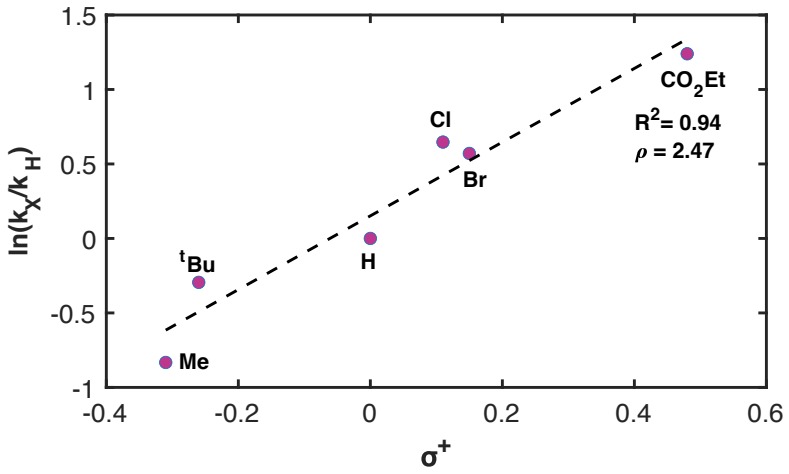

Figure A62. Hammett plot for the rate azoarene reduction relative to azobenzene reduction as a function of σ^+ for the given substituent. slope = 2.47, intercept = 0.15

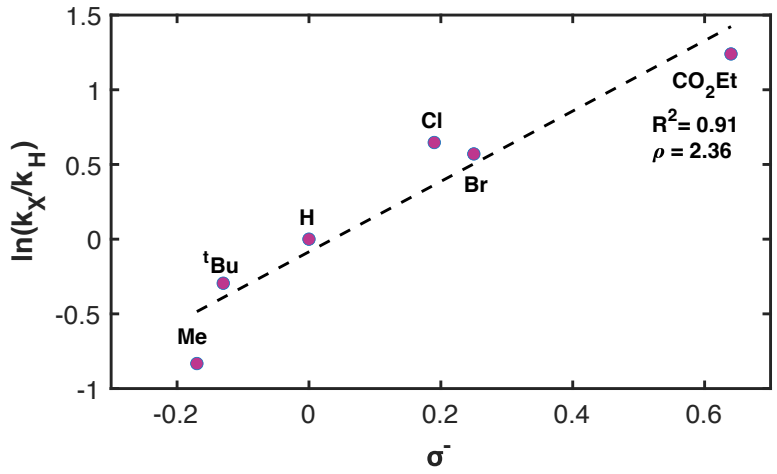

Figure A63. Hammett plot for the rate azoarene reduction relative to azobenzene reduction as a function of σ^- for the given substituent. slope = 2.36, intercept = -0.08

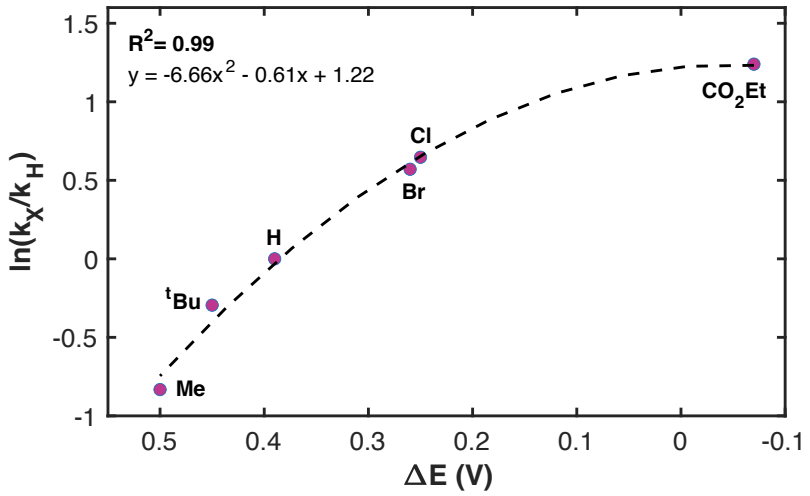

Figure A64. Rate-driving force relationship for the rate of azoarene reduction relative to azobenzene reduction as a function of the calculated reduction potential of the substrate fit with a quadratic function.

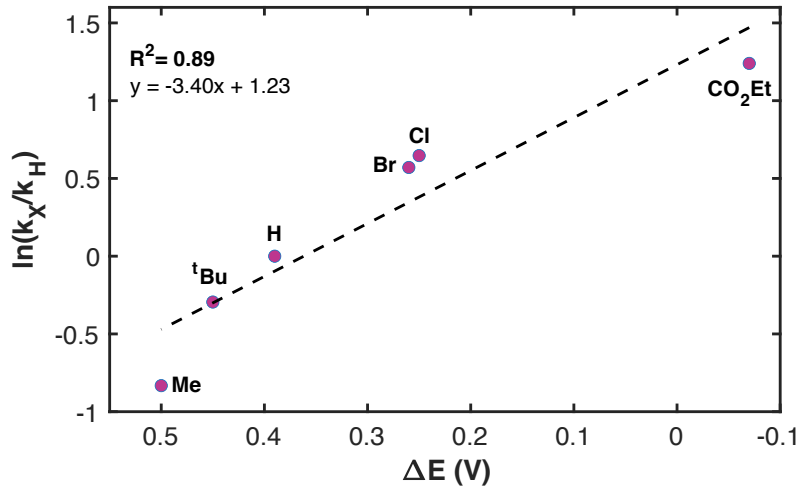

Figure A65. Rate-driving force relationship for the rate of azoarene reduction relative to azobenzene reduction as a function of the calculated reduction potential of the substrate fit with a linear function.

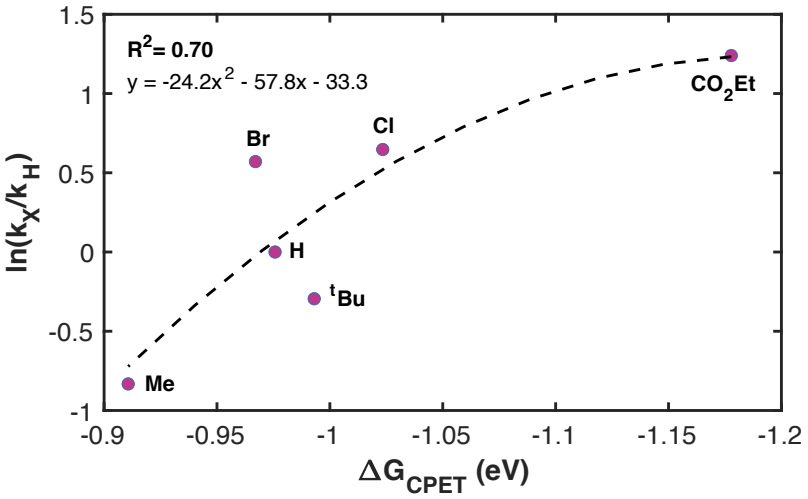

Figure A66. Rate-driving force relationship for the rate of azoarene reduction relative to azobenzene reduction as a function of the calculated $BDFE_{N\text{-}H}$ of the substrate fit with a quadratic function.

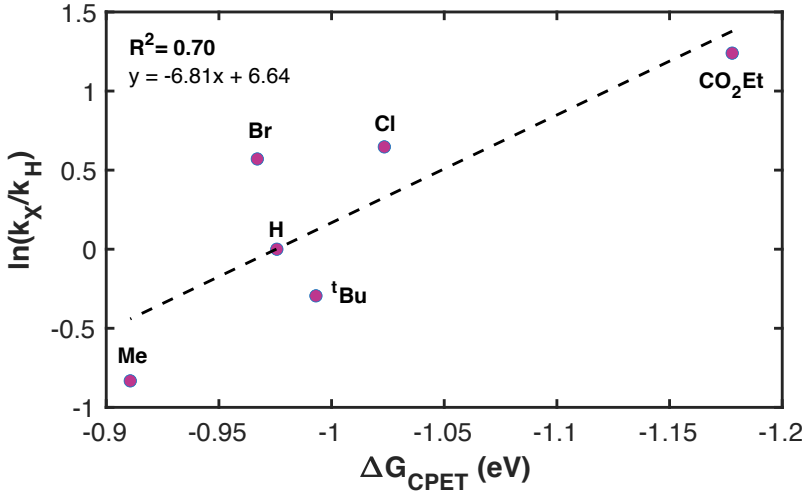

Figure A67. Rate-driving force relationship for the rate of azoarene reduction relative to azobenzene reduction as a function of the square of the calculated $BDFE_{N\text{-}H}$ of the substrate fit with a linear function.

A.10 Kinetic Analysis of Hydrogen Evolution

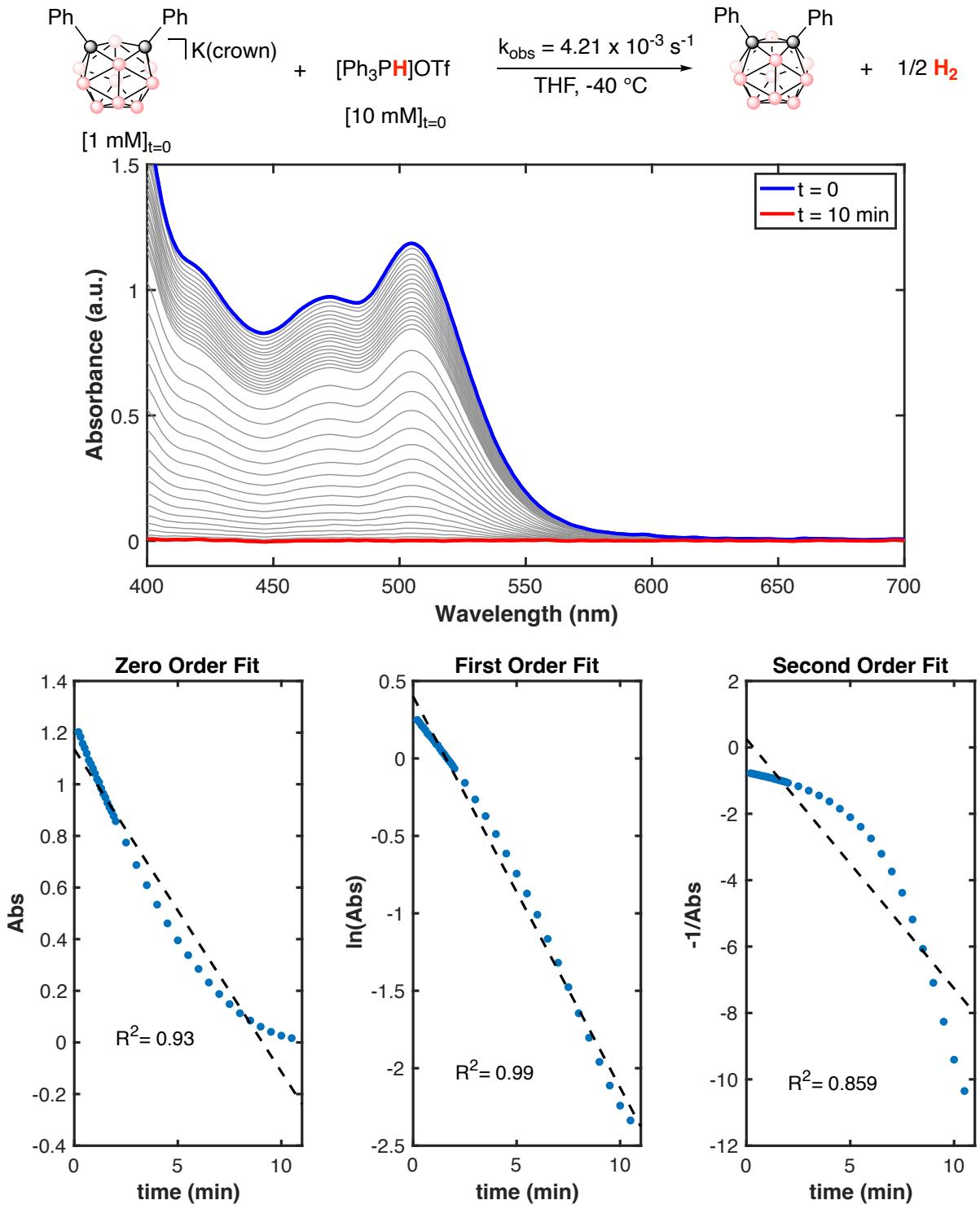

Figure A68. Hydrogen evolution reaction kinetics monitored by the decay of the absorbance of $[Ph_2Cb]K(18\text{-crown-6})$ (1 mM at t = 0) at 505 nm in THF at -40 °C.

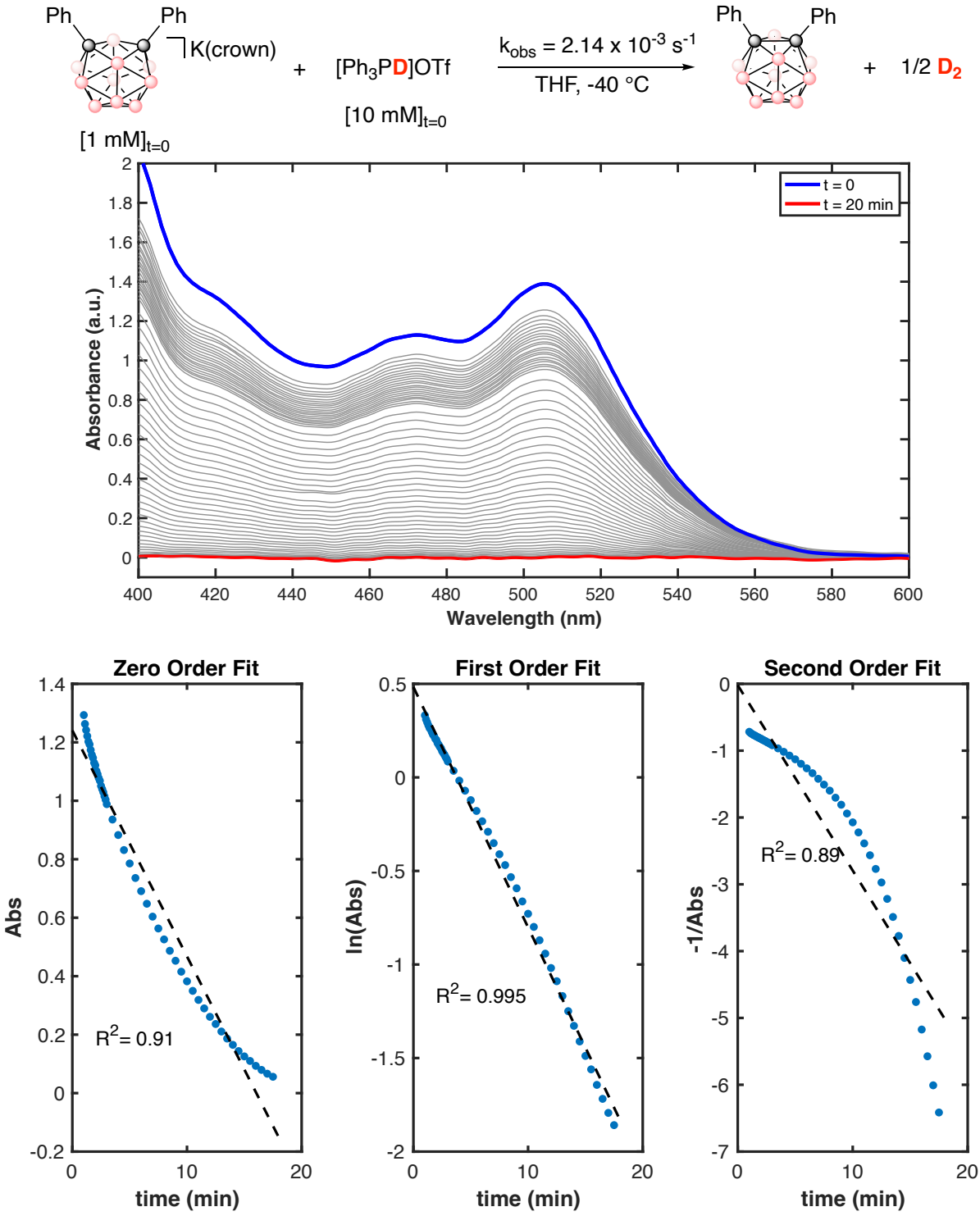

Figure A69. Hydrogen evolution reaction kinetics monitored by the decay of the absorbance of [Ph_2Cb]K(18-crown-6) (1 mM at t = 0) at 505 nm in THF at -40 °C.

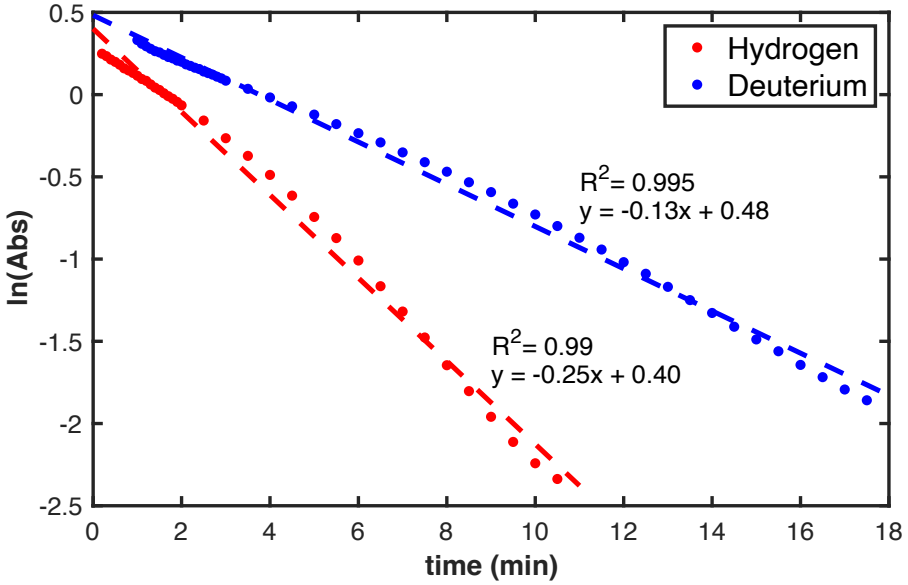

Figure A70. Kinetic isotope effect for the hydrogen evolution reaction from $[Ph_2Cb]K$(18-crown-6) with $[Ph_3PH]OTf$ and $[Ph_3PD]OTf$ in THF at -40 °C.

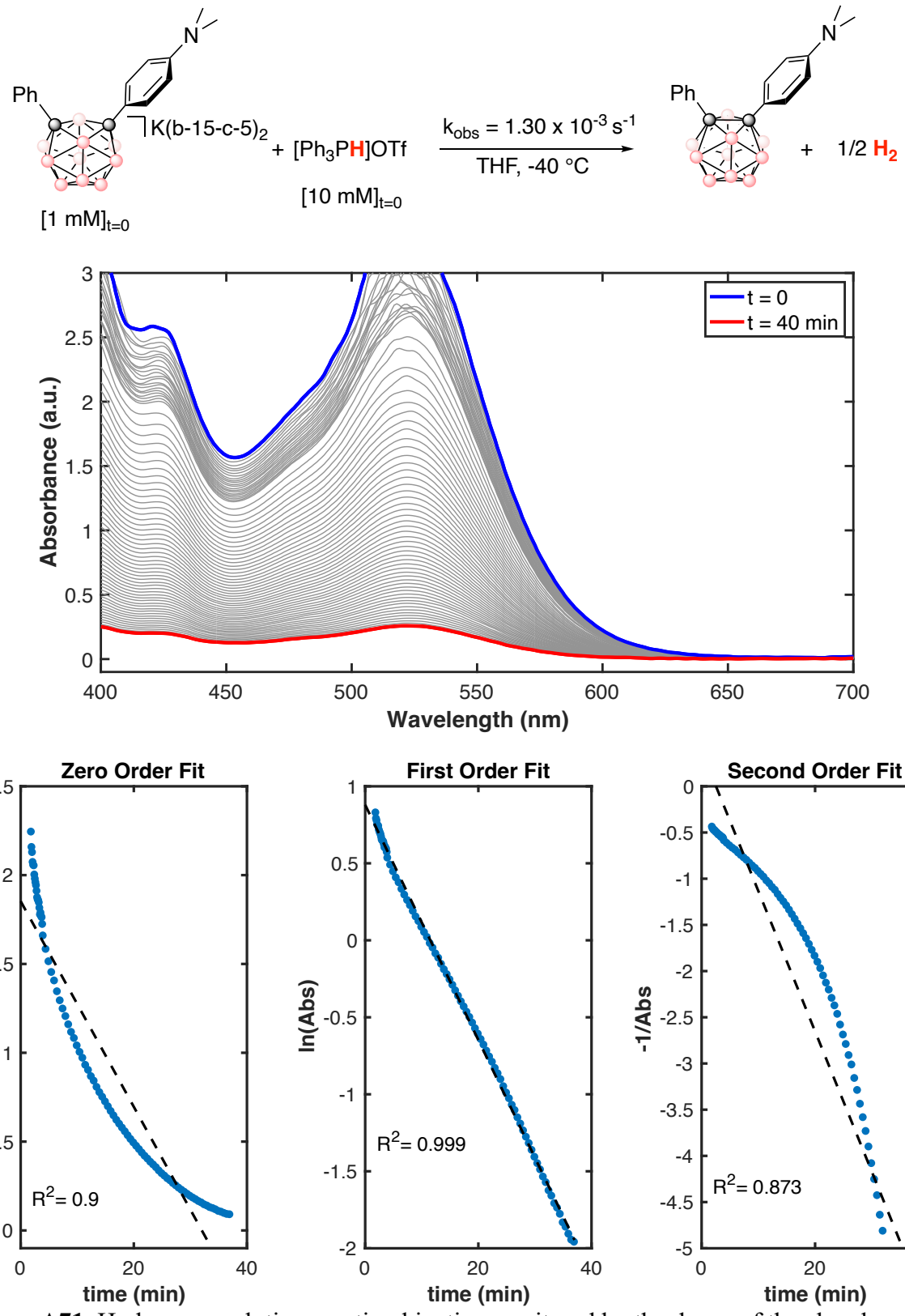

Figure A71. Hydrogen evolution reaction kinetics monitored by the decay of the absorbance of [PhCbPh^{N}]K(benzo-15-crown-5)$_2$ (1 mM at t = 0) at 550 nm in THF at -40 °C.

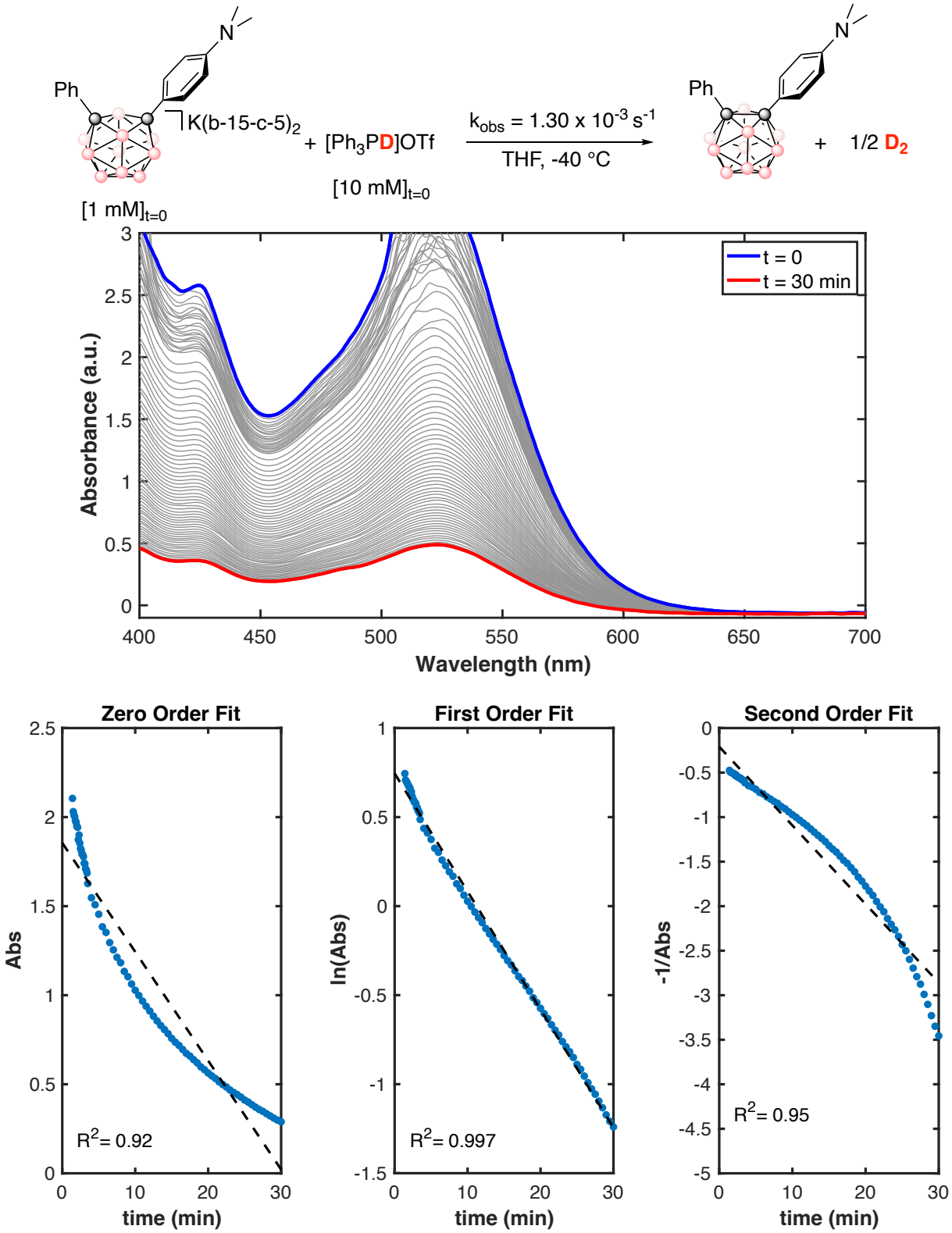

Figure A72. Hydrogen evolution reaction kinetics monitored by the decay of the absorbance of [PhCbPh^{N}]K(bezno-15-crown-5)$_2$ at 550 nm in THF at -40 °C.

A.11 Gas Chromatography: Calibration Curves and Chromatograms

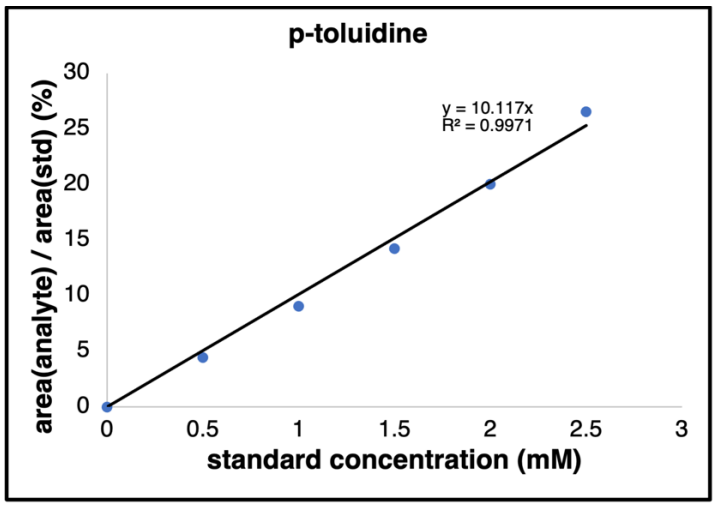

Figure A73. Calibration curve for the quantification of p-toluidine by GC-FID, where the analyte peak area at a given concentration is reported as a percentage of the dodecane internal standard peak area.

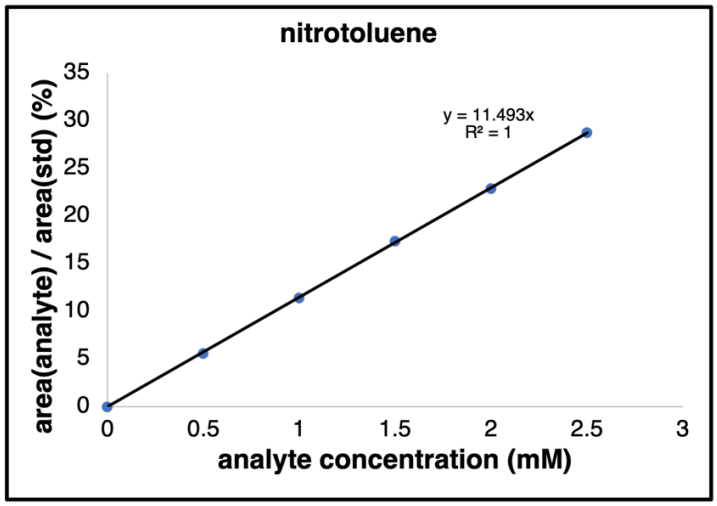

Figure A74. Calibration curve for the quantification of nitrotoluene by GC-FID, where the analyte peak area at a given concentration is reported as a percentage of the dodecane internal standard peak area.

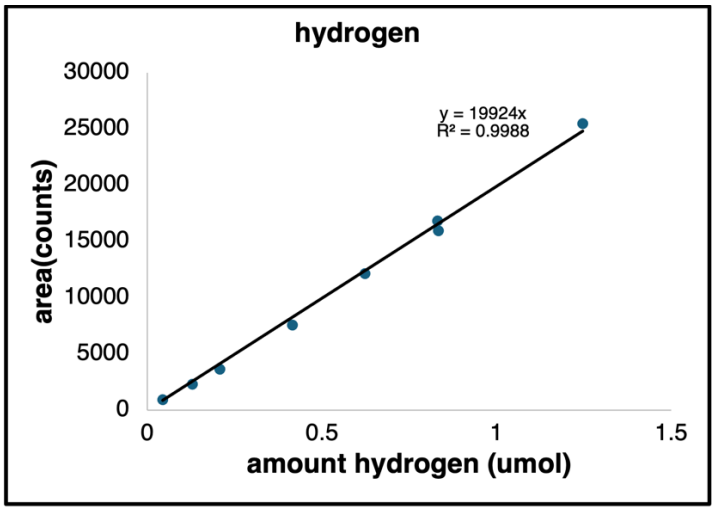

Figure A75. Calibration curve for the quantification of hydrogen by GC-TCD

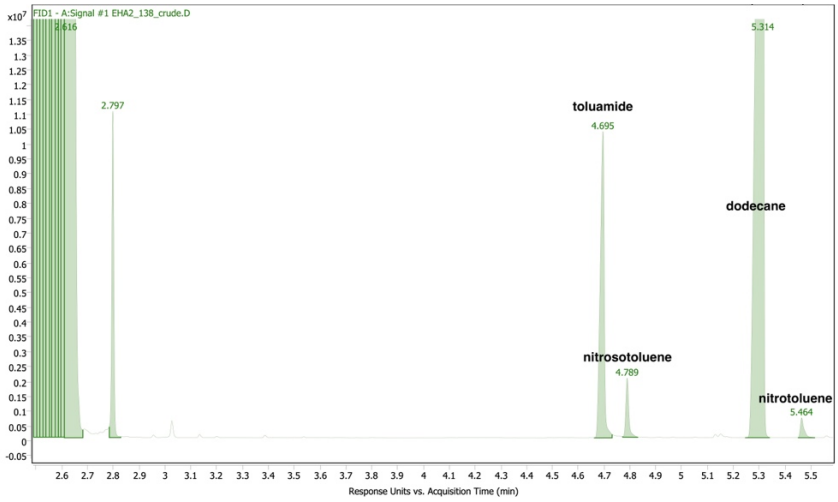

Figure A76. GC-FID trace of the crude nitrotoluene reduction reaction products in ethyl acetate solution with dodecane as an internal standard. Yields: *p*-nitrotoluene (4%), *p*-toluidine (67%)

A.12 Computational Details

Table A6. Calculated Thermochemical Descriptors

Compound	Calculated free energy (Hartrees)	BDFE (kcal/mol)	Reduction Potential (V vs. $Fc^{0/+}$)	Hydricity (kcal/mol)
Ph_2Cb	-792.7806611	-	-	-
Ph_2Cb^-	-792.9006186	-	-	-
$PhCbPh^N$	-926.5039312	-	-	-
$PhCbPh^{NH}$	-927.0612502	33.6	-	-
para-H-Ph_2Cb	-793.3192069	21.7	-	-
meta-H-Ph_2Cb	-793.3142728	18.6	-	-
ortho-H-Ph_2Cb	-793.318031	21.0	-	-
endo-ipso-H-Ph_2Cb	-793.3084601	15.0	-0.76	-
exo-ipso-H-Ph_2Cb	-793.3044896	12.5	-	-
endo-ipso-H-Ph_2Cb^- (S=0)	-793.3990036	-3.6	-	24.0
endo-ipso-H-Ph_2Cb^- (S=1)	-793.4242396	10.8	-	38.4
endo-C-H-Ph_2Cb	-793.2728472	-7.5	-	
exo-C-H-Ph_2Cb	-793.258491	-16.5	-	-
B1-H-Ph_2Cb	-793.2645844	-12.7	-	-
B11-H-Ph_2Cb	-793.2719479	-8.0	-	-
nitrotoluene	-475.3696293	-	-	-
H-nitrotoluene	-475.93984149	41.5	-	-
nitrotoluene *anion*	-475.4648668	-	-2.10	-
azobenzene	-571.8547541	-	-	-
H-azobenzene	-572.4437546	53.5	-	-
azobenzene *anion*	-571.960384	-	-1.82*	-
1,2-bis(4-chloro phenyl)diazene	-1490.687031	-	-	-
H-1,2-bis(4-chloro phenyl)diazene	-1491.277789	54.4	-	-
1,2-bis(4-chloro phenyl)diazene *anion*	-1490.797812	-	-1.68	-
1,2-bis(4-bromo phenyl)diazene	-5718.146775	-	-	-
H-1,2-bis(4-bromo phenyl)diazene	-5718.735487	53.1	-	-
1,2-bis(4-bromo phenyl)diazene *anion*	-5718.257337	-	-1.69	-
1,2-bis(4-methyl phenyl)diazene	-650.3266433	-	-	-
H-1,2-bis(4-methyl phenyl)diazene	-650.9131778	51.8	-	-
1,2-bis(4-methyl phenyl)diazene *anion*	-650.4279083	-	-1.94	-

1,2-bis(4-tert-butyl phenyl)diazene	-885.6933796	-	-	-
H-1,2-bis(4-tert-butyl phenyl)diazene	-886.2829305	53.7	-	-
1,2-bis(4-tert-butyl phenyl)diazene *anion*	-885.7967298	-	-1.88	-
1,2-bis(4-ethylester phenyl)diazene	-1105.454583	-	-	-
H-1,2-bis(4-ethylester phenyl)diazene	-1106.050992	58.0	-	-
1,2-bis(4-ethyl ester phenyl)diazene *anion*	-1105.577086	-	-1.36	-
1,2-bis(4-methoxy phenyl)diazene	-800.5608713	-	-	-
H-1,2-bis(4-methoxy phenyl)diazene	-801.1435463	49.3	-	-
H-1,2-bis(4-methoxy phenyl)diazene *anion*	-800.6546193	-	-2.14	-

*Experimentally measure value[17]

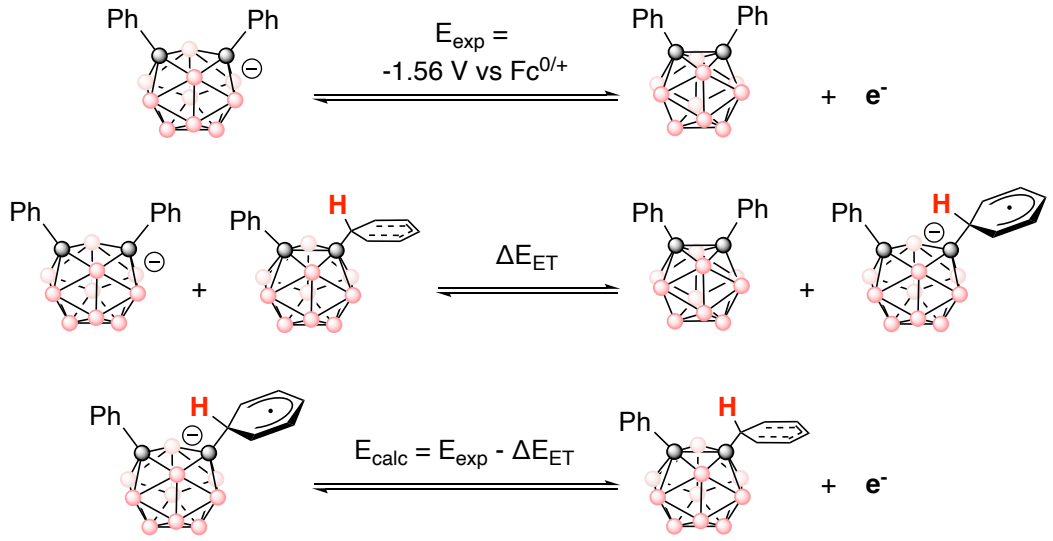

Figure A77. Hess cycle for the semi-empirical calculation of the *endo-ipso-H*-Ph_2Cb potential

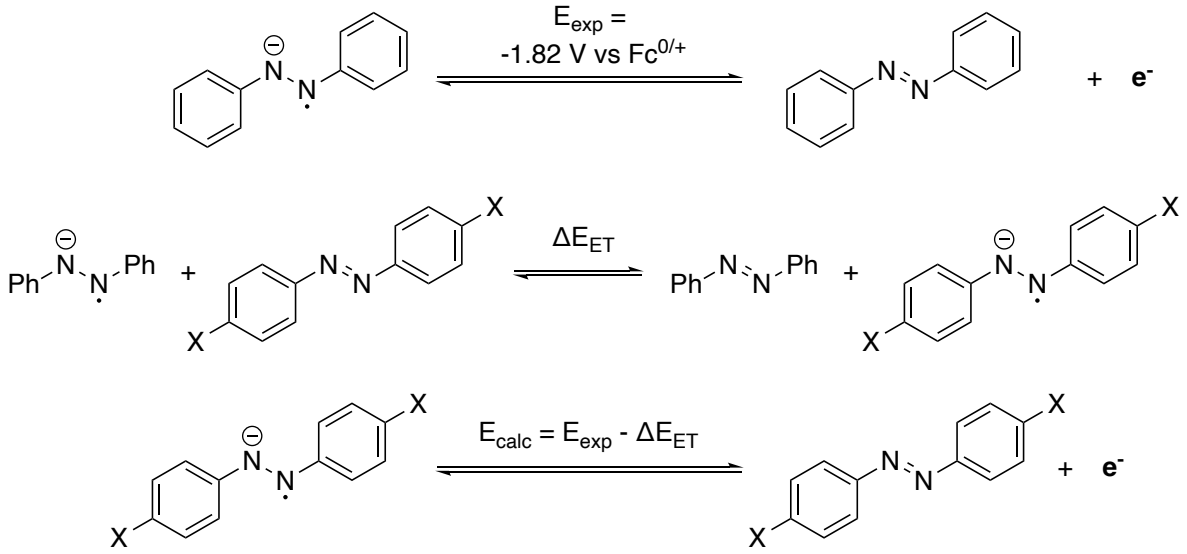

Figure A78. Hess cycle for the semi-empirical calculation of 1,2-bis(diaryl)diazene potentials

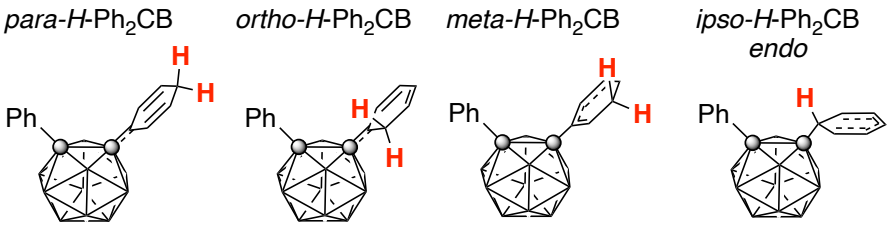

	para-*H*-Ph_2CB	*ortho*-*H*-Ph_2CB	*meta*-*H*-Ph_2CB	*ipso*-*H*-Ph_2CB *endo*
$BDFE_{calc}$ (kcal/mol)	21.7	21.0	18.6	15.0
relative energy (kcal/mol)	0	+0.7	+ 3.1	+6.7

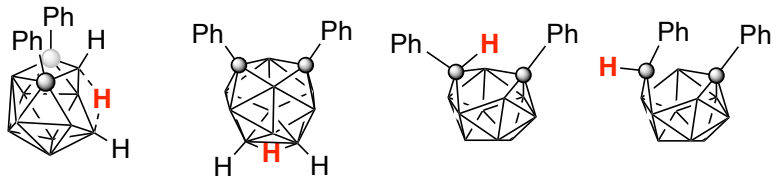

	B1-*H*-Ph_2CB	*B11*-*H*-Ph_2CB	*C*-*H*-Ph_2CB *endo*	*C*-*H*-Ph_2CB *exo*
$BDFE_{calc}$ (kcal/mol)	-12.7	-8.0	-7.5	-16.5
relative energy (kcal/mol)	+34.4	+29.7	+29.2	+38.2

Figure A79. Calculated relative energies and BDFEs of isomers of the *H*-Ph_2Cb radical (blue spheres representing B-H units are omitted for clarity).

Sample Input Files and Optimized Coordinates

DFT METHODS AND MINIMUM GEOMETRY COORDINATES (5.0.1)

The Cartesian coordinates resulting from geometry optimization using ORCA are attached below for the specified species of interest. A sample input file is included here for reference and convenience:

###start input file###

```
! B3LYP def2-SVP Opt NumFreq SlowConv

!CPCM
%cpcm smd true
     SMDsolvent "ACETONITRILE"
end

%pal
nprocs 16
end

%maxcore 1000

%scf
maxiter 1000
end

* xyz #charge #spin state
#insert coordinates here#
*
```

C A R B O R A N E S # # # # # # #

1,2-diphenyl-o-carborane (S = 0)

```
C   -0.88974237315336    -0.00136626508585     1.34320694646059
C    0.86388737949462    -0.00119755754079     1.36000350127141
B   -0.00829407849884    -1.41570384640265     0.89783514013018
H   -0.01523561441838    -2.35609725822157     1.62046844668948
B   -1.44346985829506    -0.88771933336349    -0.00815000256180
H   -2.45782514581959    -1.50575237392558     0.12734997764277
B   -1.44378023287703     0.88758373784829    -0.00659525349035
H   -2.45865925579619     1.50453966095847     0.12947175673097
B   -0.00895132837773     1.41459917626369     0.90090976475148
H   -0.01550931445626     2.35062416599139     1.62997618069540
B    1.44359278070256    -0.88743816760854     0.01910774277466
H    2.45517173616635    -1.50542181742149     0.17435886891712
B    0.00836033966154    -1.44294882608420    -0.87244831280658
H    0.01401065455403    -2.49113240348059    -1.45732467082097
 B   -0.87625503698378     0.00147932190607    -1.44311894479025
 H   -1.52218859974120     0.00236074290662    -2.45604654746074
 B    0.00779453945473     1.44529328593716    -0.86926651892272
 H    0.01327166601923     2.49446203788049    -1.45237725026119
 B    1.44301194608438     0.88774156889445     0.02073276211332
 H    2.45453333102503     1.50563776068521     0.17575907864417
 B    0.90316709129171     0.00175636893048    -1.42622809170190
 H    1.56805860121053     0.00301323713181    -2.42682526094011
```

C	-1.64869903835265	-0.00110249085573	2.64822313919680
C	-2.01669511928912	-1.21003930586312	3.26648332784495
H	-1.74038775325402	-2.16453862895850	2.81841437919576
C	-2.74907015073272	-1.20651898276021	4.45636720273030
H	-3.02391881809178	-2.15755149468993	4.91995800133988
C	-3.12989626940518	0.00179708437323	5.04771154893256
H	-3.70274258070282	0.00289348771057	5.97893548579809
C	-2.77840267161926	1.20862000254996	4.43541560310767
H	-3.07628270181915	2.16059571702405	4.88252751580597
C	-2.04600116137431	1.20908200904009	3.24565178330617
H	-1.79206053698116	2.16202159994022	2.78114416507573
C	1.59674610819719	0.00224882388380	2.68000023062236
C	1.93483634388260	-1.20386820027472	3.32035360924323
H	1.65445848205182	-2.16008166144326	2.87858713877588
C	2.64284060574011	-1.19552167530504	4.52496394720848
H	2.89484137369631	-2.14443280611678	5.00558787554367
C	3.02877028324126	0.01459406905365	5.10922363036410
H	3.58264441467177	0.01930287501062	6.05184724866237
C	2.70713744300739	1.21843716362652	4.47504269858058
H	3.00951208855194	2.17168851459042	4.91638552083589
C	1.99897468167973	1.21415433251184	3.27075868134575
H	1.76799034865478	2.16473063575298	2.78962029241885

1,2-diphenyl-o-carborane anion (S = 1/2)

C	-2.03735110187910	0.00179967136150	2.51601504880379
C	2.45990623022929	-1.20593116611362	3.11640357452715
H	2.15601454396285	-2.15959229097907	2.67966413226677
C	2.04277919005018	0.00223591715131	2.51256309012731
C	2.46541056954689	1.21241785697359	3.10849792318579
H	2.16580621532667	2.16457454419364	2.66555593927762
C	3.26467520463921	1.21280388796651	4.25372431923279
H	3.57677425664139	2.16546342991212	4.69177277398937
C	-1.20182561483484	0.00167221218196	1.29581620746557
C	1.20510885269628	0.00028210682385	1.29384266908667
C	3.25926140114501	-1.20243672506173	4.26158307944032
H	3.56710418453700	-2.15362229345893	4.70580810974019
C	-2.45847034268565	-1.20731310114038	3.11518311558692
H	-2.15940678122542	-2.16026811159733	2.67359368087771
C	-2.45375626031624	1.21104575012110	3.11819996051534
H	-2.15101758399279	2.16392450320867	2.67895910041142
C	3.66645206731946	0.00616254754946	4.84007792780268
H	4.29102266638479	0.00768233411905	5.73769541274884
C	-3.25551446501501	-1.20564018218674	4.26196417782646
H	-3.56645578999902	-2.15751324240471	4.70254024498881
C	-3.25089113487988	1.20961165424641	4.26492790208032
H	-3.55820163052186	2.16159362032769	4.70781392894128
C	-3.65654722646243	0.00204837223430	4.84666352981163
H	-4.27937058604988	0.00213757236547	5.74549553197781
B	0.00237359917291	-1.21018625114587	1.01902079576667
H	0.00193884938750	-2.16838310504837	1.74197962473048
B	1.50156420264554	-0.89712023078239	-0.04125763968148
H	2.48298803660346	-1.59398957319221	-0.03123312893427
B	-1.50052865032222	0.89700744933403	-0.04018247926205
H	-2.48193722464516	1.59388714253663	-0.02959770986557
B	-1.49894218488082	-0.89756578811764	-0.03750705677478

H	-2.47936415739670	-1.59579944086214	-0.02550012401991
B	1.49998182119034	0.89745247952793	-0.04134881495419
H	2.48044085188210	1.59567152994957	-0.03210499200419
B	0.00048464577136	-1.43468887049759	-0.80415775887946
H	-0.00050395363330	-2.49524863624748	-1.38050167201393
B	-0.88284670279715	-0.00151457587616	-1.44600626431572
H	-1.49630463556865	-0.00285226860131	-2.48601146596912
B	0.00042882221555	1.21173339457516	1.01714426196625
H	0.00202681816870	2.17099252761882	1.73868784004439
B	0.88159312476701	-0.00075008680432	-1.44744779510051
H	1.49337612517757	-0.00102454233522	-2.48844057530641
B	-0.00070747738570	1.43338868827884	-0.80637856223984
H	-0.00064789296919	2.49306017289557	-1.38435567789898

1,2-diphenyl-o-carborane dianion (S = 0)

C	-2.22212767683743	0.00198698155966	2.50581929792781
C	2.70236402198562	-1.20231751449875	3.07719962733213
H	2.36596374215207	-2.15800902138645	2.66697639639507
C	2.22758756000608	0.00196493781298	2.50201208924278
C	2.70456774123502	1.20754538200351	3.07262067930008
H	2.36988448949093	2.16228654890984	2.65880827551866
C	3.59572812914065	1.20882430088682	4.14914664955860
H	3.94070378018911	2.16338545985935	4.55951298962892
C	-1.27782874510696	0.00142173018832	1.36855065634874
C	1.28129174473490	0.00063015375393	1.36641598002840
C	3.59353825306492	-1.20112185246444	4.15371055749964
H	3.93678029828762	-2.15473887706331	4.56770982498222
C	-2.69727672517951	-1.20257766254546	3.08008802764565
H	-2.36273083581923	-2.15805562610151	2.66786451165925
C	-2.69663661570453	1.20728862578037	3.07910234179340
H	-2.36163018875508	2.16224164866192	2.66602836947197
C	4.04955508809203	0.00448500783361	4.70258432017318
H	4.74755431387253	0.00544347831281	5.54461731617659
C	-3.58640093974482	-1.20193190501819	4.15829895122494
H	-3.92996048274975	-2.15575925251155	4.57155078183686
C	-3.58576754015419	1.20802059294066	4.15728966497460
H	-3.92885116293581	2.16237378762633	4.56972212976919
C	-4.03996090229928	0.00338867272315	4.70981341979292
H	-4.73635304691371	0.00392273090102	5.55317626146782
B	0.00201379760663	-1.09016371578799	1.19421002402261
H	0.00225557421278	-2.05409056754436	1.92846266018539
B	1.53700909201719	-0.88638099835618	0.00672866558104
H	2.53214592274088	-1.57548334163408	-0.04136934609173
B	-1.53587288334675	0.88642448215213	0.00799637604426
H	-2.53109499413331	1.57544099421715	-0.03947726708018
B	-1.53409352189992	-0.88763361204370	0.01017209157541
H	-2.52819449978059	-1.57838908689339	-0.03526188444291
B	1.53524098561470	0.88767359615960	0.00630281202556
H	2.52923989182459	1.57838071203085	-0.04179382866730
B	0.00083487208991	-1.43487645191299	-0.67091542624330
H	0.00028288273751	-2.50503515086853	-1.24594183829453
B	-0.88771298418980	-0.00142157330902	-1.36094383098986
H	-1.45627246786937	-0.00255906138403	-2.43414326134296
B	0.00114632664628	1.09198538877028	1.19260245000046
H	0.00210839538588	2.05691704238495	1.92553880896739

B	0.88658864214542	-0.00050801596927	-1.36243154393273
H	1.45333641355398	-0.00091568095818	-2.43659461901157
B	-0.00081972889289	1.43392260812891	-0.67298725134351
H	-0.00121513451427	2.50322298765324	-1.24961072471102

1-(4-dimethylaniline)-2-phenyl-o-carborane (S = 0)

C	-0.88109807513760	-0.00535815436165	1.36878223903351
C	0.90870765104199	0.01887923758000	1.37831533598866
B	0.02905970370025	-1.39727196855879	0.92706612070838
H	0.04248221097018	-2.34104886781351	1.64652212659567
B	-1.42414154156739	-0.89747759773797	0.02533567101157
H	-2.42691323956827	-1.53422294789814	0.16408285532908
B	-1.44609975938240	0.87689697023979	0.02888572032361
H	-2.46485256487975	1.48747814086722	0.16724765363084
B	-0.00602064493877	1.41238674805366	0.93233406991820
H	-0.02184411564257	2.35249353309947	1.65682400860542
B	1.46677016237442	-0.85839866846717	0.02728898102237
H	2.48580592497334	-1.46962339958406	0.16139394898701
B	0.03014952679441	-1.43268203611233	-0.84712919718776
H	0.04444799278255	-2.48106302423700	-1.43229665328063
B	-0.87904455920201	0.00022786027588	-1.41325458362262
H	-1.53279866355070	-0.00590198770089	-2.42148102823382
B	-0.00672916059000	1.45410373307742	-0.84203372457295
H	-0.02092053664484	2.50444598353815	-1.42367998296881
B	1.44442061137812	0.91555253857954	0.02968492273602
H	2.44749488173318	1.55194371200716	0.16789728525097
B	0.89858660966479	0.02308270105910	-1.41273329275960
H	1.55297980253893	0.03288304262509	-2.42062923097661
C	-1.62579135676362	-0.00970467969090	2.68003964671392
C	-1.93794564486596	-1.21724339382873	3.33108868603754
H	-1.62748913701025	-2.17005278546536	2.90223605617145
C	-2.65749605569977	-1.21511513192114	4.52891897568895
H	-2.88889877484644	-2.16525530225941	5.01748423911369
C	-3.08088438290882	-0.00966866402866	5.09672022896375
H	-3.64363420498956	-0.00976781790396	6.03410444739182
C	-2.78451591639771	1.19561404832456	4.45282998282676
H	-3.11555242132034	2.14514407006618	4.88152345855462
C	-2.06465254957108	1.19712854814037	3.25560577687349
H	-1.85235099042715	2.14838414229272	2.76709559561445
C	1.64294503624707	0.02076149977493	2.68181753512690
C	2.07499622810128	-1.17912610734476	3.28197987238819
H	1.85859272451415	-2.13709444180356	2.80680728174547
C	2.78833357723948	-1.18972067463936	4.47404814764169
H	3.09463905888094	-2.15131268061992	4.88451231070858
C	3.11650140950368	0.01935750432804	5.14977473236699
N	3.80972936335283	0.01849249893515	6.33024141924877
C	2.69183932008754	1.22971430972363	4.53267982639361
H	2.92321228020585	2.19164319559747	4.98890818787283
C	1.98059613753619	1.22073587905152	3.33917641983728
H	1.69020316096195	2.18039337567281	2.90938344754302
C	4.13115049583972	1.27256464528224	6.99145347575445
C	4.24828897779617	-1.23546872754199	6.92076158140671
H	4.93121916355866	-1.79125719500813	6.25289473955887
H	3.39836538608587	-1.89989630343783	7.15979794927995
H	4.78561635874716	-1.02728341646067	7.85438493840189

H	3.22354910525570	1.84933061384537	7.24468759773501
H	4.77587032295220	1.91827031281634	6.36759219897600
H	4.66742796308639	1.06203655057206	7.92508882852469

1-(4-dimethylaniline)-2-phenyl-o-carborane anion (S = 1/2)

N	7.54255865320178	6.90332912054107	11.81923642517229
C	7.74436957756651	4.93038316978508	13.25028357835893
H	7.59408405193889	5.52721414133132	14.14998367077429
C	5.18594731574281	-0.12159994620610	12.33467173679451
C	8.12841652452774	3.32377161334628	11.01147491758394
H	8.27743215122364	2.71458929077606	10.11675768596309
C	7.73230345393817	5.54715619401560	11.96905741978583
C	7.92670942668333	4.69145511894451	10.85008691090336
H	7.92376291769928	5.09883457124946	9.83898783070024
C	8.14926700086424	2.70856227971369	12.28311121144795
C	6.62923478663549	-0.41093862726692	12.47798905888005
C	8.38127173228741	1.26097311114943	12.44613312829199
C	7.94795929152018	3.56090970686604	13.39170223384951
H	7.95229018224469	3.14045212330125	14.40015459428963
C	4.56088623148201	-0.11828339214471	11.06656041619163
H	5.15275568984801	-0.32937281283050	10.17339557948532
C	4.37751905611337	0.15138130065474	13.46198819462729
H	4.82512327074179	0.15234444657487	14.45805592016657
C	3.01296373113246	0.41658348765605	13.32636839956247
H	2.41420421546774	0.62385432416920	14.21823810599144
C	7.45840113686513	7.48477350808199	10.49177509593014
H	8.37779618134695	7.30713041461050	9.90537677160658
H	7.32339834892904	8.57041014970289	10.57956250502910
H	6.60871404681426	7.08203942166160	9.90792920400861
C	3.19584516730250	0.14616730201570	10.93394215814094
H	2.74085163717209	0.13935120297909	9.93903683533342
C	2.41131974123221	0.41808594206086	12.06170951025957
H	1.34315898712204	0.62708875341814	11.95632614711275
C	7.28741118480467	7.73699505645143	12.97960914585756
H	6.34740473626324	7.46599762913652	13.49810241120517
H	7.20779681823026	8.78470600825018	12.66253923506036
H	8.10480889538907	7.67266754980315	13.71978628763161
B	7.78379085681799	0.10597897780965	11.30388819587980
H	7.36324186263216	0.52695063570048	10.26098938018064
B	9.43195259451017	0.59042207666345	13.50365084814961
H	10.08370249411028	1.33941112219859	14.18407577282183
B	9.57542696238131	0.40997437786145	11.72385574403279
H	10.33921073838100	1.01704073682084	11.01841756006090
B	7.59298060249369	0.34596321260699	13.68939527965899
H	7.02183571233515	0.96154103141739	14.54778858522416
B	7.25984600789970	-1.48501650847236	13.53969124886243
H	6.48854257334258	-2.08730875735329	14.24053111290738
B	9.05308714584581	-1.22658893334958	11.30742914556119
H	9.53247068022294	-1.74582625022080	10.32889066380466
B	8.82635522963610	-0.93938451006580	14.15157663725555
H	9.14125217211904	-1.24637391687036	15.27573587031676
B	10.01824420423136	-0.93542447712562	12.80100320613544
H	11.17437302133280	-1.26145541120606	12.92691878575737
B	7.40128573194150	-1.66234138234573	11.76127557643104
H	6.74311507121778	-2.40589880745617	11.08081663112292

B	8.74188226422170	-2.15300514945388	12.82196817980887
H	9.01714793199557	-3.32063522695771	12.96157225003095

1-(4-dimethylanilinium)-2-phenyl-o-carboranyl radical (S = 1/2)

C	1.98811108370008	-0.19345940114119	2.59701658588970
C	-2.38488871334321	1.42007351109392	3.06817628555875
H	-1.98352282236354	2.33022619292213	2.61761918872057
C	-2.06994071662239	0.16358534233518	2.50318460614487
C	-2.61676572502953	-0.98667160121262	3.11572842646341
H	-2.39879826932218	-1.97346465227897	2.70198971592834
C	-3.43850680796478	-0.88387391415965	4.24010387671325
H	-3.84900261699770	-1.79190974773561	4.69133261378462
C	1.18209028421986	-0.16423027958740	1.36208877059324
C	-1.21207836663180	0.05691778520744	1.30315682962290
C	-3.20729616012307	1.51972984694928	4.19246751464235
H	-3.43527678097025	2.50631671322379	4.60638595159784
C	2.57745528234781	0.98510192695886	3.11159766490366
H	2.42866117609969	1.93502472050426	2.59566896816686
C	2.21219360689046	-1.39682941869589	3.30154447176152
H	1.77645094177799	-2.32894873420180	2.93879241209712
C	-3.73878649967382	0.36937247420144	4.78807161900777
H	-4.38148465983550	0.44853733465959	5.66916094859554
C	3.35872280670526	0.96669150796836	4.26483128706017
H	3.80788989946834	1.89264126323557	4.63046302754857
C	2.98848241954340	-1.42459532115769	4.45966047128355
H	3.15102072223680	-2.36844238907408	4.98786234587629
C	3.55906242890508	-0.24316098567668	4.93425408285063
N	4.39543368972386	-0.29714066557213	6.15315626892062
B	0.09983898976200	1.14677832034167	1.02276516875192
H	0.17545468637358	2.11756005238557	1.72368425767969
B	-1.39640811511496	0.93731532398043	-0.06206088152892
H	-2.31070773945045	1.71831196728650	-0.09615778157035
B	1.43032674187848	-1.12248878802066	0.05912639100150
H	2.34376493327088	-1.90323549788224	0.11750936935356
B	1.58878710074786	0.66612981030739	0.01395007962136
H	2.62702201259946	1.27303827199257	0.03027692235616
B	-1.55552451169104	-0.85159170767691	-0.01041432665267
H	-2.59278827452593	-1.46056305691963	-0.00631876288191
B	0.16314451118117	1.31346308936479	-0.80583815550090
H	0.27316464977873	2.35103760431545	-1.41103906378564
B	0.92600387346396	-0.21161980443548	-1.38492072192421
H	1.56193483506464	-0.29459305038830	-2.40708755125061
B	-0.11402987520625	-1.26843355687044	1.08877453912882
H	-0.22015140024448	-2.20032264255883	1.83605398035272
B	-0.82959597953504	-0.05533727710706	-1.42755117857498
H	-1.41924550209750	-0.03212845124315	-2.48012958219658
B	-0.09441073223132	-1.54297752043566	-0.72827013367118
H	-0.18043826738450	-2.61461845340755	-1.27522678617967
C	3.85931529224762	0.53601657153472	7.28130984754726
C	5.84395248316615	-0.00518988920764	5.88321609322177
H	3.92145227745107	1.59503470874986	7.00427972314901
H	4.47364585808501	0.34041643202866	8.16935598941289
H	2.81803497987785	0.24433875351313	7.46346118861019
H	6.19316348990097	-0.68296018065133	5.09493566994839
H	6.40527174378455	-0.17391442371117	6.81121997760263

H	5.94175031422383	1.03958900560140	5.56474655096172
H	4.35980702888271	-1.27272924765218	6.48040368828566

para-phenylprotonated diphenyl-o-carboranyl radical (S = 1/2)

C	-1.65110471957180	0.00247879759044	2.55116924385165
C	2.08002404333048	-1.22732709199432	3.13738058263144
C	1.68389356452906	0.00185785776113	2.51249004985414
C	2.07772464426424	1.23177792239661	3.13735127533011
C	2.78176861377400	1.25105852297403	4.30741772066461
C	-0.92362081471102	0.00099521386840	1.23526116062252
C	0.93925905550306	0.00102225835513	1.22920597297540
C	2.78411953249993	-1.24528916247202	4.30742836632667
C	-2.01832947479020	-1.20671463565495	3.17137100301032
H	-1.76015993465955	-2.16083167271701	2.71128439891737
C	-2.02150882108779	1.21321451198215	3.16647942714457
H	-1.76576320774003	2.16613171784911	2.70255405147863
C	3.18430731722661	0.00326524931877	5.02315682031707
C	-2.72515607841504	-1.20324951236940	4.37624378134039
H	-3.00029028332180	-2.15405593448634	4.84020677337052
C	-2.72834787700550	1.21280711397971	4.37132967492098
H	-3.00596998223914	2.16476277807443	4.83143464361783
C	-3.08000118692688	0.00554768937851	4.98325491384253
H	-3.63236270400748	0.00673567971719	5.92679771151941
B	0.00002662663611	-1.38845607528425	0.80556970089821
H	0.00435161168278	-2.33380885902709	1.52413547979027
B	1.44178561103076	-0.89001438819781	-0.12089557546901
H	2.44861966990538	-1.52481614791253	-0.00216156063731
B	-1.45839360184494	0.88828508727103	-0.09907870827040
H	-2.46182007271898	1.52435597713933	0.03901142235756
B	-1.45855479975744	-0.88849195508571	-0.09768800850690
H	-2.46206377170786	-1.52416851616469	0.04165858987310
B	1.44194393446165	0.88968130506947	-0.12253360150837
H	2.44887817238510	1.52451446669377	-0.00476174731300
B	-0.01418768254369	-1.44368883750122	-0.97337944611886
H	-0.01928603029984	-2.49380071059771	-1.55565666159811
B	-0.90765038344452	-0.00129754421532	-1.54233472637782
H	-1.56658938974038	-0.00209159314576	-2.54722479516030
B	0.00030076443176	1.38976216256013	0.80318448988874
H	0.00426597548910	2.33630680069844	1.52018109981835
B	0.86740835061134	-0.00140095207291	-1.55591602579905
H	1.51168143518897	-0.00235710206363	-2.57035394637301
B	-0.01404288530897	1.44195439331472	-0.97585847194302
H	-0.01923681099160	2.49108546997542	-1.55989847491673
H	1.82095492323900	-2.17507622351317	2.66312686163803
H	3.07210959191736	-2.20410484576437	4.74915303503360
H	2.76682670531994	0.00287211526360	6.05545526808488
H	4.28043531893868	0.00430181483452	5.21129232827198
H	1.81691217216993	2.17903078652249	2.66307271229782
H	3.06796287829919	2.21041606765166	4.74913319030311

meta-phenylprotonated diphenyl-o-carboranyl radical (S = 1/2)

C	-1.59857290726368	0.02786326045913	2.56019722009369
C	2.09882452396566	-1.22084222769136	3.09209202011444
H	1.89979665628118	-2.16180505215036	2.58176887615587

C	1.63910152283433	0.01749178159571	2.54183845568895
C	1.92159470205060	1.20030808823569	3.18458274410376
H	1.59629298961656	2.15196327866263	2.76303183956382
C	2.69096616337745	1.25995599706093	4.46818146771335
H	3.56774381680720	1.93451865498284	4.34500259771185
C	-0.86104353708317	0.01077712250144	1.24240923333156
C	0.88331240087130	0.01295744364367	1.23013825286450
C	2.83654765931017	-1.23062996178728	4.30556987404202
H	3.17468443296814	-2.19322782520562	4.70102424691117
C	-1.98628638074522	-1.17406868289598	3.17990365840074
H	-1.74294496772109	-2.13326107255722	2.72258379492505
C	-1.95266750250061	1.24484230820161	3.17061908647499
H	-1.68375375695726	2.19342519918959	2.70585693578550
C	3.12882292179968	-0.07637579439575	4.98125089516304
H	3.69688815159748	-0.10830427385760	5.91578389777243
C	-2.69613363330502	-1.15770773059387	4.38328118243770
H	-2.98706844643183	-2.10368360045304	4.84741909291329
C	-2.66258950047825	1.25727980596739	4.37411066176874
H	-2.92714418444511	2.21447480890293	4.83098434278416
C	-3.03400376697704	0.05704748412762	4.98747547762234
H	-3.58912839861267	0.06837654042527	5.92931204683150
B	0.00687690948287	-1.41169861871339	0.80111829137884
H	0.01388236225138	-2.34013366425660	1.53988106243205
B	1.44385996923217	-0.89245431274574	-0.10686921422396
H	2.45725694348106	-1.50995031769946	0.03641174794561
B	-1.44227400624895	0.88042009939015	-0.11107790641830
H	-2.45383377614407	1.50055686553889	0.03528717829587
B	-1.44253670173364	-0.89481175648651	-0.08779551449859
H	-2.45408690665247	-1.51088499162675	0.07431415599117
B	1.44429002227413	0.88237379564491	-0.13206872506739
H	2.45817665932822	1.50234848525098	-0.00270449250358
B	-0.00511524875845	-1.46209154545023	-0.96886744053565
H	-0.00770485667862	-2.51846591172447	-1.53892681317545
B	-0.89952156492968	-0.02668835716781	-1.54471204428945
H	-1.56328084498838	-0.04026147920483	-2.54603633442765
B	0.00745915550975	1.42282678665256	0.76184849461723
H	0.00871877776145	2.37640778595293	1.46637046064243
B	0.88014861142703	-0.02561028468455	-1.55722073066283
H	1.52933594730742	-0.04038818171430	-2.56804910974183
B	-0.00610716669100	1.42474733238289	-1.00880138467142
H	-0.01173834830831	2.46575517588468	-1.60647303304461
H	2.08978510411930	1.79354754240825	5.23845345078293

ortho-phenylprotonated diphenyl-o-carboranyl radical (S = 1/2)

C	-1.63056236592710	0.03296604264415	2.55281358362103
C	2.15776114445865	-1.24071835929701	3.04478942217837
C	1.64259804838608	-0.05642071525706	2.54597791040777
C	1.86926498590468	1.24003681800320	3.28663291549111
C	2.70577588607860	1.10829070944953	4.52187195454132
C	-0.88676847028782	0.00203283537531	1.24118297928732
C	0.90795163388285	-0.03456161159238	1.24716606878286
C	2.91830164784353	-1.28827275169688	4.23179666169018
C	-1.92148790400176	-1.15132341805544	3.25365232202634
H	-1.59329875481250	-2.11535102310566	2.86544212331433
C	-2.09227233404448	1.25542974993661	3.07650548827851

H	-1.89520239207301	2.18903840694579	2.54879289114366
C	3.18767314175395	-0.09283414851207	4.95821018268310
C	-2.64369729449644	-1.11134106291157	4.44970812465955
H	-2.85864015334705	-2.04401442267990	4.97782354226389
C	-2.81545173850927	1.29132408672029	4.27079520808242
H	-3.16570930615200	2.25167576284608	4.65806269635307
C	-3.09098175779296	0.10867342940820	4.96477140175963
H	-3.65639099370208	0.13788398667263	5.90009190712383
B	-0.02170268835906	-1.42197607813547	0.80283799371070
H	-0.03202904109177	-2.36160781119074	1.52836864198121
B	1.43197478264264	-0.93501333382825	-0.10318225790125
H	2.43166949632739	-1.57744454881565	0.02473768474607
B	-1.42001217639695	0.89780080526591	-0.09977819880639
H	-2.41736339145586	1.54307864461679	0.03455721744767
B	-1.45878473730619	-0.87740202568755	-0.09941066364742
H	-2.48257691303141	-1.47879580927573	0.04442204599760
B	1.47085298381249	0.84043041157924	-0.10671123686649
H	2.49373811430777	1.44563953161583	0.02844109529500
B	-0.02547895382535	-1.46338047611780	-0.97115613453895
H	-0.04731231149434	-2.51323187339300	-1.55333824682679
B	-0.88535589319985	-0.00125790752283	-1.54080511429245
H	-1.54057944232352	0.01208018256349	-2.54791091792910
B	0.03946946344985	1.38798662956591	0.79801538903696
H	0.05809179462348	2.32928908657845	1.52076146918734
B	0.89158780445633	-0.03940567705985	-1.54325662529197
H	1.54509242950766	-0.05608336970636	-2.55152000342118
B	0.03602840734431	1.42358278116523	-0.97669564622263
H	0.05464499916407	2.47153889947315	-1.56231712822057
H	0.89738628519993	1.70289009889313	3.55913720712787
H	2.32016649086774	1.99547504868493	2.60887131638417
H	2.91364939900560	2.02603600788038	5.08013942630745
H	3.78944550962626	-0.14355982478986	5.87034032341124
H	1.98971133134840	-2.17395729755609	2.50416118900284
H	3.30746083963849	-2.24622972969711	4.58358760364067

ipso-phenylprotonated diphenyl-o-carboranyl radical (S = 1/2)

C	-1.94809117371899	0.01146105067696	2.47101681981236
C	2.02479720373970	-1.20445695922126	3.33103486051213
H	1.53322763305248	-2.16396824759204	3.16006021165573
C	1.25947503776786	0.04579228647767	2.96854458427925
C	2.03219177062905	1.30468535255343	3.28180650619873
H	1.54582483644285	2.25972254348479	3.07404111612714
C	3.27979548150884	1.28086521974574	3.84751029000805
H	3.78075274703644	2.22861944004902	4.06783833693692
C	-1.01489783738090	0.00142528920776	1.28156986967625
C	0.70817643923278	0.01868591911033	1.50338778062475
C	3.27251169433593	-1.16621557099181	3.89556742786777
H	3.76786935970120	-2.10771607113134	4.15241471823056
C	-2.41228460220883	-1.19438118119257	3.02833430718460
H	-2.07336976177866	-2.15088912114233	2.63025807723272
C	-2.42423073749440	1.22537278486737	3.00002684953902
H	-2.09487494970938	2.17563378994516	2.57959532104179
C	3.93506784671144	0.06097897448477	4.16112046894927
H	4.93229574638334	0.06669338161403	4.60678172963182
C	-3.32035350790276	-1.18434528300260	4.08987879515450

H	-3.66894655667670	-2.13280211375529	4.50669721622926
C	-3.33213071373282	1.23116525493191	4.06179096265294
H	-3.69000629267513	2.18562414419571	4.45644629929727
C	-3.78277543125146	0.02742564741810	4.61213961572976
H	-4.49469232376001	0.03358180366783	5.44189525970258
B	-0.08184825162307	-1.41401411770208	0.97031524574315
H	-0.15868475018790	-2.33472147422752	1.71699380281172
B	1.45628265567965	-0.87873452676462	0.25764903194942
H	2.44680914230506	-1.48764413341937	0.53252946887371
B	-1.41875718227262	0.86513135082701	-0.13669384403675
H	-2.44988804751703	1.47014368773274	-0.13203606988992
B	-1.40376081856277	-0.91247567281234	-0.10911756369426
H	-2.42502835030063	-1.53357820281119	-0.08661889596179
B	1.44132108096286	0.89024681213380	0.22976987506339
H	2.42171939884070	1.52314363927384	0.48556641568858
B	0.14165779326359	-1.46659161130039	-0.78718904180801
H	0.22401955081541	-2.52254522838080	-1.35238367392743
B	-0.68048481324664	-0.03879386777470	-1.48167246149094
H	-1.20357106077583	-0.05952896780525	-2.56306348213695
B	-0.10508711154822	1.42151480024790	0.92664908723995
H	-0.19435224900513	2.36275807920992	1.64609875199051
B	1.08298695479064	-0.02044534019990	-1.25536300402833
H	1.86143396535547	-0.02801307406739	-2.17063229156922
B	0.11727350122540	1.42360264944383	-0.83223731435070
H	0.18311521037301	2.46295070111233	-1.42945013745898
H	0.33736176317619	0.06115790588281	3.58936355671761

ipso-phenylprotonated diphenyl-o-carboranyl anion singlet (S = 0)

C	2.31529733472089	-0.96081105350134	1.94928323572016
C	-1.73314888635935	0.94359179836767	3.43858648377483
H	-1.26482451712448	1.88120896109093	3.13183038125260
C	-1.70062642174220	-0.17032397646168	2.56654389960206
C	-2.32405062746699	-1.36235008941458	3.00678731437269
H	-2.32191060932623	-2.24131580451129	2.35860742302712
C	-2.95093205739328	-1.43344526502444	4.25211088281622
H	-3.42784834447277	-2.36798428586268	4.56200977588345
C	1.34686874398073	-0.57213817735905	0.88177422545514
C	-1.03654453816002	-0.09828286586061	1.25312041749232
C	-2.36051760283280	0.86848713655542	4.68394929757227
H	-2.37082153437191	1.74763189662164	5.33494565553723
C	3.35530880583755	0.03177804106265	2.38950954418943
H	3.16739664311022	1.09226755778693	2.20943088667565
C	2.80329298308963	-2.38144768986278	2.01211040814379
H	2.19522377646820	-3.15867135502437	1.54451480876333
C	-2.97242775299622	-0.32001456629239	5.10194422736164
H	-3.46084303764428	-0.37804648431914	6.07848331498896
C	4.44811905543916	-0.36654112713854	3.12439869745524
H	5.13582786968851	0.39563535902663	3.50576871477766
C	3.91001411935283	-2.71751808763102	2.75726094797695
H	4.18132257846171	-3.77395737652908	2.85530459436066
C	4.73364287043366	-1.73376780072809	3.35590957342937
H	5.61232367086961	-2.02544902867687	3.93570017559481
B	0.38737785292074	0.84643299672830	1.01095539978122
H	0.68962475046724	1.62193885170293	1.87819020090371
B	-1.24797520821668	1.06676337497777	0.13901849081353

H	-2.03795560559861	1.94144431091818	0.38381550861519
B	1.27872676958212	-1.24894449831039	-0.59358491288036
H	2.07960955669724	-2.12181984476915	-0.82011341572726
B	1.66837058656279	0.48236228648616	-0.31155221111486
H	2.77374198657470	0.96460295028524	-0.31822179204029
B	-1.63614879781768	-0.67128652987886	-0.14441092711836
H	-2.73436607818180	-1.16339081310980	-0.12187767791491
B	0.24646193631369	1.42896208802238	-0.74558651980142
H	0.39296195464093	2.56153071925176	-1.13588331884489
B	0.71059394571343	-0.00292369348259	-1.73135363722150
H	1.19568308447136	0.06829454289129	-2.83498326593326
B	-0.12082268266956	-1.42947295302849	0.64081933066904
H	-0.23259491426179	-2.48154860487189	1.21188376596191
B	-0.99559170325606	0.33613016771924	-1.46816107423751
H	-1.70752630963475	0.64482005869807	-2.39352612774690
B	-0.37348423073411	-1.33670982862323	-1.19598056503457
H	-0.68312844658562	-2.25070221455667	-1.92064591692650
H	1.61797904745021	-0.94080519736421	2.84047712257431

ipso-phenylprotonated diphenyl-o-carboranyl anion triplet (S = 1)

C	2.18005378205036	-1.00063109044753	2.26114896387020
C	-1.85705655953820	0.99919062070306	3.41259214787109
H	-1.36076890158821	1.92373908106802	3.10987763334274
C	-1.77732154255472	-0.14033207934968	2.57784708932789
C	-2.44134176777031	-1.31380705809884	3.00711921439277
H	-2.40556666186116	-2.21063531391081	2.38491859088291
C	-3.14574653713612	-1.34510456116171	4.21220592515925
H	-3.65063355309203	-2.26671983458461	4.51656065347404
C	1.31058171886019	-0.60732516958315	1.04522327041003
C	-1.03776845778947	-0.10489701979183	1.30315657390358
C	-2.56214808942621	0.96371009507520	4.61727936397885
H	-2.60659295255004	1.86114760347345	5.24134436311790
C	3.24449609337413	0.01612597639393	2.59394983560030
H	2.93190391461036	1.06045578113217	2.67368621006523
C	2.73631544730943	-2.40108128741828	2.17381327354154
H	2.03543237482574	-3.20409387485762	1.93159248148238
C	-3.20997708731404	-0.20839254135469	5.02826032368263
H	-3.75986051242078	-0.23533144129860	5.97299888823037
C	4.55180239137178	-0.32646692112035	2.82316774589444
H	5.27413125819922	0.45684814386032	3.07509007310319
C	4.05510914882498	-2.69088240733056	2.41003457006644
H	4.39582544963623	-3.72922758861881	2.34241650369178
C	4.99303362192096	-1.67494597248269	2.73994710053929
H	6.04050058569338	-1.92697651142243	2.92203953737684
B	0.41085356445200	0.83771697049353	1.09222677912981
H	0.67936474695006	1.63182204919096	1.95345577002461
B	-1.18417309298281	1.04334298688491	0.15445117563929
H	-1.97851245692196	1.92525700319347	0.35480769664341
B	1.34762876003779	-1.30601616228435	-0.43231939216211
H	2.14458384361015	-2.18556960577351	-0.62631486271804
B	1.74140611083546	0.40891244876535	-0.15949707654881
H	2.84811471986642	0.87956454107645	-0.14016153721101
B	-1.57977060622065	-0.69448401620824	-0.11668395121773
H	-2.68589505834501	-1.16876366684731	-0.12932682533486
B	0.34481714701364	1.37359234803126	-0.67114456473137

H	0.53404026007282	2.49489467394672	-1.07652557161274
B	0.84334528081689	-0.07958807053568	-1.61293444521879
H	1.36020546026408	-0.02661473512758	-2.70304160857374
B	-0.11745706581423	-1.47395790902911	0.72828697113437
H	-0.27538546345737	-2.51614357925358	1.30668441063830
B	-0.87344830058763	0.28447688791235	-1.42703804440170
H	-1.54045976413586	0.58715922731125	-2.38736967360255
B	-0.28892059048218	-1.38857382649995	-1.10546257647502
H	-0.57059630066999	-2.31048484075770	-1.83197162408577
H	1.45753565806289	-0.99669546736316	3.11277196067872

endo-C(cage)protonated diphenyl-o-carboranyl radical (S = 1/2)

C	4.74108938983903	5.16412155394540	8.78283529120397
C	1.81140628650257	2.61047420966205	5.13917540472209
H	1.45686908581866	3.64377326047925	5.14058682495186
C	3.17445987147731	2.33680968193256	5.34610180783681
C	3.61270864433975	1.00202033887688	5.36333252472946
H	4.66560994319319	0.77630210357329	5.54611198794789
C	2.70713529935653	-0.03959708549895	5.13975745063434
H	3.06315328859284	-1.07344562828781	5.14328340994304
C	5.16672133370751	5.18086476180840	7.37530196700101
C	4.16032343752727	3.45810510072474	5.63471656341658
C	0.90969796399497	1.56576850968189	4.91917547982153
H	-0.14633533645646	1.79202371802140	4.74807580910064
C	3.58135448588196	5.86448553662342	9.20532620439900
H	2.97722891773231	6.40257330561416	8.47389002833091
C	5.50322526162618	4.47848051116844	9.76450511327484
H	6.39821361380677	3.92933016622384	9.46823575744575
C	1.35422832601700	0.23806204939946	4.91557376557590
H	0.64685573964875	-0.57770054545869	4.74345521232618
C	3.21131004576025	5.88530826247621	10.54582378640838
H	2.31782293724453	6.43499419826608	10.85254130580085
C	5.13092815839978	4.50770161054244	11.10443366740771
H	5.73581488246091	3.98079298577177	11.84663014870179
C	3.98186995879064	5.20717997753304	11.50242702301998
H	3.68700489854820	5.22325467435406	12.55496527592049
B	3.89160811165830	5.31732275598498	6.06750149661793
H	2.77493631746023	5.55318490041996	6.41635236181286
B	4.27845146853349	4.59101461603987	4.45570780673652
H	3.50331865924363	4.37868769468635	3.56792422710797
B	6.69728910523565	5.58478615317533	6.86339491747094
H	7.49814347500524	5.90120849987423	7.69678776223807
B	5.21754919004605	6.54736665745072	6.47478159239692
H	4.93639314806838	7.57635103112284	7.02145911501441
B	5.67462290273623	3.48539205127947	4.94477893273808
H	5.98898789031398	2.47807937491048	4.37241768946992
B	4.77531889355912	6.24370273506943	4.79243308167271
H	4.26473643460049	7.11945298357610	4.14656424591226
B	6.49486692219157	6.28161620261811	5.23371904352902
H	7.23239028996677	7.18211908991053	4.92928057334128
B	6.11385181625737	3.89178937849769	6.74226857195759
H	6.37875957084880	2.96520395704646	7.44553833495576
B	5.94385584007238	5.06907626292499	4.09094767839902
H	6.31686914504924	5.10514204061454	2.94757812476753
B	7.02302230189037	4.57341522681379	5.42953656758740

H	8.13563278605725	4.18753250388301	5.18577622031538
H	4.12649534639479	3.48080451466761	6.73709169203716

exo-C(cage)protonated diphenyl-o-carboranyl radical (S = 1/2)

C	-2.95903501107263	0.08213176037363	1.10547881983231
C	0.03086367937588	-1.18724198997436	4.05637401227792
H	0.56581347579583	-1.99781566664212	3.55995323476133
C	-0.14962685110560	0.04559780125166	3.39871695318070
C	-0.81499437034628	1.09076645685978	4.07212508081336
H	-0.93802889579885	2.05997477102044	3.58765941750820
C	-1.32109911200103	0.88980455846548	5.35724235117328
H	-1.84599499178746	1.70556437459354	5.86125739356807
C	-1.58506127969994	-0.00499703372522	0.54754680372838
C	0.44535117055714	0.27402675147382	2.02125264536521
C	-0.47490146014149	-1.37743046341751	5.34323175123319
H	-0.33550573093535	-2.34255610944740	5.83748155940713
C	-3.67883638740863	-1.08735390159191	1.44278852435761
H	-3.21309607606958	-2.06598196021356	1.31546613713304
C	-3.59970156598854	1.33016749899310	1.28393840935795
H	-3.07570312253446	2.25133158550748	1.02494017313305
C	-1.15587540615326	-0.34351159230662	5.99775169898507
H	-1.55156231249975	-0.49763035768554	7.00510552941251
C	-4.98224126783733	-1.01106609262161	1.93219747287053
H	-5.51977547323749	-1.92952242932416	2.18263904010870
C	-4.90155554412380	1.40292980359120	1.77816744228431
H	-5.37690694933408	2.37918801105454	1.90552252518279
C	-5.59973899851947	0.23386746275267	2.10644351674833
H	-6.61977997043434	0.29276665462324	2.49552435249590
B	-0.64004885554862	-1.33529422367104	0.83907904411385
H	-1.02621947478054	-2.17578161562888	1.59143179725440
B	1.18679978865356	-0.87598434969635	1.06767569152928
H	1.98778749777755	-1.58500842982270	1.61432719390261
B	-1.10979266690550	0.87218810910234	-0.74552942659279
H	-1.90753574868919	1.59727436354769	-1.26915670142948
B	-1.18262171943322	-0.91578380705972	-0.80319834353881
H	-2.04526123180893	-1.53630293079971	-1.35726370721004
B	1.41991261024389	0.96172932388188	0.85280876992295
H	2.31914441103154	1.68461061382821	1.20225098862823
B	0.47790054008786	-1.48738797465456	-0.47409002937456
H	0.86197045894273	-2.56281171801829	-0.85184046918280
B	0.18969761235605	-0.07653153960611	-1.56847973054003
B	-0.43260332343882	1.28468336686634	0.91907260961752
H	-0.85185153007401	2.30343986529419	1.38369397319142
B	1.61297327723229	-0.11246184229453	-0.53401869991648
B	0.57538338739195	1.37958534421674	-0.63102129649289
H	0.92609835077428	2.40248656446040	-1.15480897154833
H	1.30679884891290	0.88196756015433	2.49492867277111
H	0.29034160447529	-0.10995780432488	-2.76621240369393
H	2.71184761509956	-0.20216270338593	-1.01438135933028

B1-protonated diphenyl-o-carboranyl radical (S = 1/2)

C	4.60351441027996	5.05881104252186	8.72662779268616
C	1.91164423271424	2.73352976542211	5.25078844231399
H	1.52720109859419	3.73816419584912	5.06131546722950

C	3.29433284725775	2.53719726547744	5.43808207426619
C	3.75393052755909	1.22634015561043	5.67107978781971
H	4.82010871439600	1.04593672194310	5.81772866181280
C	2.86327522122247	0.15257330782936	5.71217810976388
H	3.24382983046785	-0.85628463924593	5.89230146816746
C	5.01829544616152	5.16388652697303	7.29643269470464
C	4.24590198289478	3.68491815513103	5.36578052622954
C	1.02245454900119	1.65900504166045	5.28974900090561
H	-0.04538429916770	1.83552332848733	5.13623973157653
C	3.50569861076962	5.79671022557561	9.21272360283193
H	2.94681175088274	6.44618674118210	8.53535803514595
C	5.30659595695174	4.23958995035353	9.63082124759188
H	6.16224337660113	3.65943204019759	9.28131953706463
C	1.49357265502225	0.36248822571254	5.52279376745011
H	0.79718079553733	-0.47938014677465	5.55569940957710
C	3.12799006608019	5.72190027703301	10.55365328252599
H	2.27657172961149	6.30836440060736	10.90888196768749
C	4.92566983632107	4.16287622029426	10.97154432355486
H	5.48701727451548	3.52076743484676	11.65536848125142
C	3.83458154518277	4.90184142603453	11.43988274900321
H	3.53690683844226	4.84056926303791	12.48982548470864
B	3.86316387807256	5.06374626894101	6.14834427692571
H	3.74729035221143	6.21883464767549	5.31618199218984
B	4.36816770466515	4.67454387434403	4.07599355653117
H	3.53715976476131	4.62205365234266	3.21703908665655
B	6.59101213506872	5.30843951848382	6.84634919272045
H	7.40656662353729	5.38139728526526	7.71924965251210
B	5.36333832858236	6.57764814632207	6.56229891677846
H	5.09947788885956	7.60610622144781	7.11348131062546
B	5.68605876931870	3.57790745867523	4.58594088080105
H	5.92894181671082	2.55122615286185	4.02103430812461
B	4.88411578770043	6.41931016743372	4.70382036924402
H	4.53729286017814	7.39446674783871	4.09522936629822
B	6.55339982927944	6.27607253138046	5.34169635420035
H	7.33236821569397	7.15592430659574	5.10052559299584
B	5.68758429309729	3.75983962757881	6.41953829366690
H	5.88428932819903	2.78615130371145	7.08391279433759
B	6.00589568540915	5.22724960883191	3.97347636416675
H	6.44296901478526	5.45385231616873	2.87952295373763
B	6.96540294219748	4.52341214265005	5.32399803082205
H	8.09336923448201	4.15309381396272	5.15529285123215
H	2.72072054988979	5.25552728172797	6.46042820956285

B11-protonated diphenyl-o-carboranyl radical (S = 1/2)

C	2.12719743086528	-0.00459890670963	2.44756130414884
C	-2.46084397072920	1.16865534978494	3.12105795199441
H	-2.16728166971370	2.12777907320178	2.68961555002551
C	-2.03720517472339	-0.03302254890097	2.51427511176634
C	-2.43909424216150	-1.25342553123013	3.09859199173886
H	-2.12856822470156	-2.19887681627333	2.64906108640667
C	-3.23701958693823	-1.26909545882288	4.24403971597485
H	-3.53844429073385	-2.22679203348538	4.67730183109058
C	1.25371902079007	-0.00019141907180	1.25000965308862
C	-1.20260873504189	-0.01530799675246	1.28918064523716
C	-3.25752654097799	1.14847487822509	4.26780992170291

H	-3.57496041546913	2.09232506263526	4.71960227495027
C	2.55715931158904	1.20382413750019	3.03611535207549
H	2.23691878433820	2.15793479109501	2.61262881460841
C	2.56275589869916	-1.21851230423707	3.02120121495782
H	2.24749607434895	-2.16866112432826	2.58510232271297
C	-3.64946701180220	-0.06924656613657	4.83632265604641
H	-4.27239165816491	-0.08340484156708	5.73472069927535
C	3.39400056606338	1.19649540545417	4.15401678300530
H	3.71595582630920	2.14535866466012	4.59189098643202
C	3.40080232690484	-1.22132037004116	4.13763242040067
H	3.72844404550409	-2.17402865049806	4.56274136338946
C	3.82012838776554	-0.01480984575682	4.71142110902910
H	4.47464884787233	-0.01886459931915	5.58717820032588
B	0.01094181883291	1.20636106202917	1.01495550070465
H	0.01698144877864	2.15427507825083	1.74352387370872
B	-1.50296179313275	0.90884025161339	0.00300085344825
H	-2.48482386018716	1.59366060229766	-0.02030746645533
B	1.53241467940038	-0.87625203861470	-0.10002630937586
H	2.51026416622725	-1.56744530056728	-0.13127902080710
B	1.49637805496151	0.93128236911002	-0.04220792334283
H	2.46558245449172	1.63224927666768	-0.09557697428345
B	-1.50952253355072	-0.89911519597581	-0.04934848563712
H	-2.47600512976455	-1.60678983649804	-0.04755278013782
B	-0.01939221847060	1.45043430918331	-0.82031403517245
H	-0.03489444192796	2.50711854405875	-1.38941501470653
B	0.93114898867873	0.07647419533079	-1.49307102115284
H	1.53161965695808	0.10514512466573	-2.52997361740270
B	0.03051607912890	-1.14793225799408	1.04687482213963
H	0.04667630445000	-2.14052109258045	1.71277480329107
B	-0.96901509381188	0.06128577891747	-1.46321148463922
H	-1.60183313817954	0.08023667992527	-2.48085081906624
B	0.00445096413454	-1.49434545721644	-0.78397236837490
H	0.00258959047208	-2.55800771911649	-1.33583408252816
H	-0.02058620238211	-0.83197174291259	-2.02270471359375

A Z O A R E N E S # # # # # # #

azobenzene (S = 0)

N	-4.66413111415400	2.98965967910612	-0.06526628303248
N	-3.62415882360860	2.29020176648313	-0.06280818857948
C	-2.39859014630831	2.99678700931185	-0.06338921434394
C	-5.88969982675366	2.28307443700060	-0.06464924913413
C	-7.05041502688090	3.07650684737389	-0.06784103087048
C	-8.31241142496695	2.47762485137312	-0.06759027989260
C	-8.42144669410285	1.08275285652287	-0.06410551109177
C	-7.26413566266272	0.28741233062329	-0.06087705379041
C	-6.00225842823165	0.87742519706077	-0.06112158699319
C	-2.28603196539576	4.40243731621343	-0.06646762468537
C	-1.02415485107563	4.99245050586774	-0.06670263878469
C	0.13315661993184	4.19710901867754	-0.06391175827351
C	0.02412185608214	2.80223594425388	-0.06086240124779
C	-1.23787446553011	2.20335369443058	-0.06060678746106
H	-6.93803749947049	4.16358526339089	-0.07051400629269
H	-5.09533037871579	0.27089227152957	-0.05861729703999
H	-7.35316759111661	-0.80261046057136	-0.05815323180021

H	-9.21138222127920	3.09960255244804	-0.07011275789273
H	-9.40756349412140	0.61039846567118	-0.06388541107321
H	-3.19296056444468	5.00897081515743	-0.06862203296457
H	0.92309307675051	2.18025756822227	-0.05867514441529
H	-1.35025138784940	1.11627449039179	-0.05825388795280
H	-0.93512344900284	6.08247420387485	-0.06906783933091
H	1.11927346290711	4.66946337558650	-0.06411878305669

azobenzene anion (S = 1/2)

N	-4.68961750090961	3.01637204934164	-0.06547824715268
N	-3.59867353286352	2.26349128209292	-0.06277753963246
C	-2.41148368107242	2.95504493766699	-0.06332886620551
C	-5.87680705595291	2.32481773372506	-0.06481290346756
C	-7.08238174596619	3.08570819031171	-0.06785001980556
C	-8.33170500582206	2.47249530966057	-0.06749127938044
C	-8.44317796141002	1.06995536814784	-0.06401348479538
C	-7.26760405119648	0.30110707488404	-0.06097012487085
C	-6.01002781409434	0.90251305604216	-0.06129771619744
C	-2.27826150595671	4.37735026624738	-0.06650542380691
C	-1.02068473726472	4.97875524126736	-0.06671894564105
C	0.15488856667466	4.20990528516424	-0.06388673350085
C	0.04341429939535	2.80736465833115	-0.06074249158973
C	-1.20590948258738	2.19415283023265	-0.06049647029067
H	-6.99364772688448	4.17666474366732	-0.07051078912443
H	-5.10088556827035	0.29996221648899	-0.05888513981365
H	-7.33774102064577	-0.79236337372509	-0.05828299069863
H	-9.23532044029009	3.09090267367010	-0.06992256786375
H	-9.42482897227699	0.58832131978878	-0.06373135655891
H	-3.18740315363609	4.97990274069713	-0.06873586646294
H	0.94702926244459	2.18895592682656	-0.05848068526421
H	-1.29464427392911	1.10319575128850	-0.05808805755872
H	-0.95054695306656	6.07222629638928	-0.06913949727736
H	1.13654005558124	4.69153842179271	-0.06407280304032

1,2-diphenylhydrazinyl radical (S = 1/2)

N	-4.66733592955977	2.93850754320977	-0.05318826596358
N	-3.52627159569143	2.27130798219162	-0.05729067707371
C	-2.35430814139423	2.98589118121088	-0.05629941816050
C	-5.90294091471658	2.29631457148091	-0.05412885148594
C	-7.07307954761274	3.08432024283724	-0.04818962560420
C	-8.32606663700077	2.47224779762486	-0.04879644085308
C	-8.43732631270326	1.07487360214103	-0.05532848574667
C	-7.27283747659780	0.29572559437533	-0.06126405479621
C	-6.01006118953482	0.89074358961108	-0.06078549391314
C	-2.22469111482620	4.40408442781738	-0.05245858264469
C	-0.96180411516397	4.99566280309554	-0.05194038259449
C	0.20317467416867	4.21558914469181	-0.05515166886272
C	0.09069328445830	2.81524088849342	-0.05904228450148
C	-1.16069066841042	2.21036099581201	-0.05963089807121
H	-6.98776693744799	4.17516655393293	-0.04304351997363
H	-5.10379232263109	0.28500894305200	-0.06547110177498
H	-7.34665761037883	-0.79569921176654	-0.06636729913672
H	-9.22549765696464	3.09433407005713	-0.04408013328275
H	-9.42110063390952	0.59866999616985	-0.05574983557560

H	-3.10109644842365	5.05624984568724	-0.05011435290062
H	0.99084534848346	2.19391892185131	-0.06163707856789
H	-1.25872924334542	1.12168309458702	-0.06262201539259
H	-0.88536069059876	6.08701500754620	-0.04905298605697
H	1.18662220461752	4.69261493643193	-0.05470982744339
H	-4.69008032481602	3.96087747785805	-0.04820671962324

1,2-bis(4-bromophenyl)diazene (S = 0)

N	-4.74568626412429	2.91381356988099	0.07475213329920
N	-3.71628251967843	2.19878477694688	0.03510355910694
C	-2.48530532136438	2.88819288347537	-0.01386521030297
C	-5.97666618859993	2.22438261924063	0.12339553795969
C	-7.12802896631818	3.02887596188474	0.16581519309511
C	-8.39835389587897	2.45324028017403	0.21406699118848
C	-8.50767795864472	1.05932837306600	0.21977891542199
C	-7.37059417385760	0.23772725257977	0.17891166864679
C	-6.10822373928396	0.82079391670796	0.13084226717615
C	-2.35384199196941	4.29176505463561	-0.02515121639241
C	-1.09145381427588	4.87478743039977	-0.07331838668364
C	0.04574292390173	4.05316178934851	-0.11036358327894
C	-0.06348809388080	2.65926331276563	-0.10090569774250
C	-1.33383563703492	2.08367169338423	-0.05275395971221
H	-7.01074359623883	4.11513802996915	0.15973633879742
H	-5.21299123557369	0.19822134733123	0.09845344595666
H	-7.47224172193587	-0.84955384513336	0.18420534515826
H	-9.28755689442067	3.08563597095749	0.24626201424871
Br	-10.23714769550831	0.25269485010374	0.28277489265691
H	-3.24915553169863	4.91437071163651	0.00420982945524
H	0.82580197742637	2.02684823339764	-0.13018847766493
H	-1.45105743263732	0.99742216832160	-0.04389762981361
H	-0.98988083003196	5.96205497955623	-0.08170705565524
Br	1.77522860162869	4.85974863936962	-0.17351691492109

1,2-bis(4-bromophenyl)diazene anion (S = 1/2)

N	-4.77004351776549	2.94032875118516	0.07745379936852
N	-3.69188286267396	2.17240864079777	0.03562954814210
C	-2.49845517030237	2.84690393033581	-0.01257471829716
C	-5.96350430489394	2.26576145869295	0.12393708609778
C	-7.15854447125813	3.04033248769546	0.16776085326229
C	-8.41710850323243	2.45054611318884	0.21434477025754
C	-8.52500822270198	1.05018572400163	0.21932093080543
C	-7.37331354989569	0.25159946175189	0.17840426227313
C	-6.11462798114450	0.84562143617253	0.13183370642685
C	-2.34736634572914	4.26701427467066	-0.02552253070063
C	-1.08868123019331	4.86090339331933	-0.07383850492170
C	0.06305369772272	4.06221942017056	-0.11155747108889
C	-0.04480804539366	2.66188142578285	-0.10166458802543
C	-1.30336945560557	2.07222962914013	-0.05341918827172
H	-7.06308705475444	4.13021629914047	0.16331772366561
H	-5.21671701010729	0.22777810205132	0.09996138217479
H	-7.46124462982397	-0.83822548898050	0.18244243328963
H	-9.31319555464415	3.07502240192497	0.24676633921565
Br	-10.25755842888574	0.22589742857835	0.28138860999356
H	-3.24527406654286	4.88500343751640	0.00360724962079

H	0.85130429775968	2.03731809808384	-0.13162625291468
H	-1.39879830564200	0.98236559971110	-0.04523520636363
H	-1.00079445897386	5.95070873734488	-0.08187892541815
Br	1.79558517468211	4.88634923772359	-0.17621130859167

1,2-bis(4-bromophenyl)diazenyl radical (S = 1/2)

N	-4.66968795440780	2.94910849014719	-0.05336197468930
N	-3.53201806593483	2.27758483833848	-0.05736020839195
C	-2.35823899432685	2.98276345813568	-0.05631036971615
C	-5.90373365757698	2.30887485889320	-0.05421022113069
C	-7.07500274668417	3.09389816921789	-0.04848297859690
C	-8.33003586324509	2.48892840947645	-0.04893740644082
C	-8.42289710299142	1.09171483265424	-0.05516474581907
C	-7.26880849466003	0.30032806860727	-0.06093016057643
C	-6.01167622216367	0.90386581180338	-0.06050760311252
C	-2.21607760173898	4.39983091444411	-0.05218691076437
C	-0.95410488312689	4.98938312737501	-0.05163015861055
C	0.19426475959340	4.18743940742869	-0.05514738148561
C	0.08872611399763	2.78757281977053	-0.05932481298305
C	-1.16925041620013	2.20048825275231	-0.05989768700653
H	-6.99707873152891	4.18494132614253	-0.04357805069952
H	-5.10845956098682	0.29393297339771	-0.06502875293315
H	-7.34291023659222	-0.78926112051544	-0.06579989474924
H	-9.22902797562315	3.10864576345020	-0.04440185586199
Br	-10.14442779256508	0.25597861084965	-0.05590010030494
H	-3.08375246388109	5.06300603487243	-0.04957778904938
H	0.98340330928315	2.16140597479766	-0.06210740355735
H	-1.26850589412929	1.11227231924791	-0.06310514126464
H	-0.86818969397964	6.07821875975368	-0.04850796261700
Br	1.92013997140093	5.00808974447084	-0.05427084699500
H	-4.69100980193204	3.97177815448837	-0.04865958264385

1,2-bis(4-methylphenyl)diazene (S = 0)

N	-4.74878823018482	2.91385055857110	0.07680557064360
N	-3.71528425456587	2.20250504417476	0.03633548858577
C	-2.48505862967423	2.89323060156771	-0.01330990054770
C	-5.97883459126454	2.22346563731659	0.12372738457782
C	-7.13314407618912	3.02177414459969	0.17710170591319
C	-8.39938729427601	2.43497149098585	0.22549702460594
C	-8.54876268488839	1.03861610506416	0.22101425387672
C	-7.38071178279412	0.24570786292044	0.16692037220096
C	-6.11553001073566	0.81859490675120	0.11920769606460
C	-2.34839899026519	4.29515271893097	-0.03672538278032
C	-1.08012498221370	4.86822676768794	-0.08514145840766
C	0.08578489218566	4.07628345732779	-0.11161844533571
C	-0.06419241181138	2.67714960709257	-0.08891424574645
C	-1.32828175024804	2.09265915888973	-0.04116046009137
H	-7.01628319335826	4.10854324225504	0.17992886883315
H	-5.21992107990698	0.19669850547626	0.07754702903462
H	-7.47683563209588	-0.84460779114933	0.16236528037480
H	-9.28751397828032	3.07189483504046	0.26720316486601
C	-9.90782313914994	0.39143069046856	0.27142794582550
H	-3.24347873269281	4.91887714817789	-0.01707790286889
H	0.82470927921094	2.03959356038350	-0.10918838742871

H	-1.44643331629898	1.00612043592697	-0.02360573517360
H	-0.98452182379015	5.95807670671886	-0.10311297960167
C	1.45538081847126	4.70155789694882	-0.16261526431515
H	-10.71308409121110	1.13999592432653	0.31163352681573
H	-10.00431961358978	-0.26328476633510	1.15473711075314
H	-10.07742795160840	-0.24662729170515	-0.61308575215326
H	1.39974599639194	5.80017788389928	-0.17893812166498
H	2.00980440881230	4.37371260447985	-1.05877381752884
H	2.06188684602162	4.40307235320705	0.70983543067274

1,2-bis(4-methylphenyl)diazene anion (S = 1/2)

N	-4.77175762442940	2.94240820586075	0.09129463930758
N	-3.69083427686488	2.17452309545245	0.04791411716516
C	-2.49587237297177	2.85071451096758	-0.00644082872234
C	-5.96764832659113	2.26680760544149	0.13317154289301
C	-7.16478385969760	3.03462322385208	0.18802645430730
C	-8.42019083051659	2.43267230434441	0.23004799224748
C	-8.57034007969634	1.03040413524204	0.21980580253363
C	-7.38766173371145	0.26259217363442	0.16665637952780
C	-6.12465019622609	0.84696772579926	0.12490339785495
C	-2.33700175161891	4.26776758246072	-0.03825723968774
C	-1.06960972895172	4.84923995723561	-0.09062161779274
C	0.10918558495207	4.08017392010937	-0.11614385319948
C	-0.04351884721166	2.67494922065379	-0.08798369839547
C	-1.29786878791890	2.07859751612254	-0.03562885907653
H	-7.07011466600464	4.12523701372449	0.19599835624644
H	-5.22660507954812	0.22914277223833	0.08369699826032
H	-7.46639486649232	-0.83122764661779	0.15729752718898
H	-9.31386515063405	3.06513846659884	0.27173074610792
C	-9.92862813901951	0.37238242514081	0.26218454505544
H	-3.23289094534285	4.88976438941157	-0.02077158128372
H	0.84930822816109	2.03966507888025	-0.10754248577618
H	-1.39621386533529	0.98841624654120	-0.01401109215835
H	-0.98870649687724	5.94240543891204	-0.11259931623393
C	1.47717291488368	4.71599626473858	-0.17030181128072
H	-10.73705921297046	1.11935250239230	0.30536415303979
H	-10.04065906233271	-0.28799414059606	1.14115020327955
H	-10.10920588901704	-0.25919941038300	-0.62656526506349
H	1.40977451601977	5.81534736277725	-0.18695143065898
H	2.04230256986314	4.40506416921350	-1.06772165605781
H	2.09750797610096	4.43548788985113	0.70031788037212

1,2-bis(4-methylphenyl)diazenyl radical (S = 1/2)

N	-4.66424988588758	2.93634060365752	-0.05318621314628
N	-3.52437785854299	2.26429584546615	-0.05722483383102
C	-2.35141948870992	2.97570472172329	-0.05623084837555
C	-5.90207027993414	2.29837947192430	-0.05415951310310
C	-7.07292263689058	3.08550956680796	-0.04833324420392
C	-8.32564879236513	2.47773199309856	-0.04893078964194
C	-8.46593224905439	1.07568359378784	-0.05532268506719
C	-7.28877310758335	0.30826096712736	-0.06116691760263
C	-6.02181228068569	0.89624854411690	-0.06073519050346
C	-2.21383296275741	4.39369645247106	-0.05228811692763
C	-0.95202726460298	4.98155053617760	-0.05183173739899

C	0.23124490932213	4.21548848880901	-0.05518095260062
C	0.09474056432009	2.81279485786498	-0.05910947308962
C	-1.15624567729154	2.20630216290323	-0.05964572743498
H	-6.98873031228321	4.17664398295764	-0.04325845632053
H	-5.12196251367580	0.28080195573910	-0.06541272548201
H	-7.36232545059441	-0.78373343931658	-0.06622916585212
H	-9.22033335427991	3.10823082985589	-0.04427410017301
C	-9.83103241245675	0.43305824391446	-0.05576655963579
H	-3.08689311827058	5.05065367382148	-0.04980033885457
H	0.99223105118712	2.18661718126176	-0.06180906568888
H	-1.24828764564562	1.11694765884572	-0.06269757530781
H	-0.87938337407498	6.07405069240477	-0.04885518728590
C	1.58405176947218	4.88106631360150	-0.05465078469029
H	-4.68235757550139	3.95846244138770	-0.04829434530587
H	-9.75884494183887	-0.66528742506195	-0.06105934088153
H	-10.42103314828203	0.73587999824561	-0.93841437043636
H	-10.41767413179712	0.72753942148581	0.83193301770448
H	2.39835029220433	4.14056143995976	-0.05757027234408
H	1.71705911928504	5.52557975066949	0.83200159416141
H	1.71526275721554	5.53061947429210	-0.93788608068021

1,2-bis(4-methoxyphenyl)diazene (S = 0)

N	-4.74488494238050	2.94718356460173	0.07232261672564
N	-3.70841533979047	2.23484342885290	0.03092514175491
C	-2.48042202440568	2.91955591031019	-0.01852595926620
C	-5.97125325107576	2.26115899846753	0.12251224519079
C	-7.12896902967423	3.05586723544449	0.16300295399120
C	-8.40212167717123	2.48580679476140	0.21283046347491
C	-8.53253949850138	1.08530291535649	0.22305760719807
C	-7.37100900063333	0.27807414143905	0.18399893705583
C	-6.11244841653583	0.85336001926059	0.13460446063390
C	-2.33545136085399	4.32112459565956	-0.02961113589453
C	-1.07395976115373	4.90807904027852	-0.07687643343809
C	0.08078766531983	4.09717548551563	-0.11435515016980
C	-0.05770467208072	2.69418138006791	-0.10568740878106
C	-1.32027758770302	2.11874850091069	-0.05849714839248
H	-7.01266307707527	4.14273447160213	0.15410497246986
H	-5.21822409582123	0.22885780398501	0.10461107636304
H	-7.49315405377452	-0.80812981373073	0.19349381770181
H	-9.27970398452003	3.13213710776479	0.24309152024306
O	-9.70772652047467	0.42724583157393	0.26840394156530
H	-3.22932176337858	4.94641576596548	-0.00037117304215
H	0.84383762428682	2.07778895532734	-0.13588030589797
H	-1.43693058117510	1.03196230257613	-0.05053028643627
H	-0.98982436694160	5.99553974152990	-0.08427220967801
O	1.34106300778735	4.57296803116747	-0.15891985969187
C	-10.92383818030549	1.16186187627921	0.30610994099724
C	1.56489626642353	5.97658314507080	-0.16395577624711
H	-11.73279454695619	0.41927935356628	0.33591992210345
H	-11.04542965541492	1.79089386310291	-0.59238411291178
H	-10.98608750959282	1.79790758791521	1.20585479681682
H	2.65409107616064	6.11545879395870	-0.19744681563814
H	1.16933478865595	6.45391119747744	0.74903310903049
H	1.11405446875621	6.45676197394127	-1.04946374783084

1,2-bis(4-methoxyphenyl)diazene anion (S = 1/2)

N	-4.76453250698690	2.97948896722442	0.05457492129149
N	-3.68508833713948	2.20569264514943	0.01184280035517
C	-2.48729010904566	2.87959091323647	-0.03357833386423
C	-5.96217081277737	2.30611894323007	0.11432466278301
C	-7.15970429364240	3.07093577824634	0.14230328545102
C	-8.42451923030533	2.48275694336884	0.20032761976377
C	-8.55007967605130	1.08055469620918	0.23427149036961
C	-7.37872233185746	0.29833199661741	0.21096170636613
C	-6.11957810858043	0.88591013541320	0.15362081356007
C	-2.32215865027214	4.29429842471699	-0.03177799044011
C	-1.05628646451791	4.88972956066115	-0.07436029045246
C	0.10420135745889	4.09944074375110	-0.12211941711358
C	-0.03442278000699	2.69414067480261	-0.12799371935871
C	-1.29036205294501	2.10559540613335	-0.08500291642001
H	-7.06685937249440	4.16133077524582	0.11546131910090
H	-5.22207320349018	0.26635043684429	0.13781349985775
H	-7.48409694769096	-0.79102576459209	0.23954590357303
H	-9.30798939594482	3.12377287334465	0.21859010557322
O	-9.73722895239454	0.40384644302388	0.28950565300672
H	-3.21641492181550	4.91758479852549	0.00575511488193
H	0.87102239944422	2.08129709722922	-0.16624411761931
H	-1.38892826023098	1.01538727345450	-0.08853442293438
H	-0.98479042455799	5.97967962768926	-0.06930487190669
O	1.38166725336426	4.58525845944184	-0.16417849545976
C	-10.94159901673192	1.14007078677670	0.31141076574038
C	1.57902159674872	5.98288609508301	-0.14458967168563
H	-11.76051257877633	0.40705165105185	0.35184955517895
H	-11.06713502431193	1.75962953117975	-0.59587864094555
H	-11.01226068499896	1.79678130928236	1.19836798161563
H	2.66543075891127	6.15071358463845	-0.17867317114340
H	1.17878343641761	6.44639278886202	0.77631511548349
H	1.11758733522197	6.48104640415837	-1.01750625460843

1,2-bis(4-methoxyphenyl)diazenyl radical (S = 1/2)

N	-4.67206782634584	2.95146305271526	-0.05279364341125
N	-3.53002889009381	2.27863638450336	-0.05656401049572
C	-2.35917217407952	2.99239560393475	-0.05583778730552
C	-5.90996035933106	2.31168035949031	-0.05382874244363
C	-7.08436816860616	3.09591437389917	-0.04756983159477
C	-8.33553879459456	2.49247609446333	-0.04822226375176
C	-8.45814699621520	1.08848439502175	-0.05515888628636
C	-7.29189000720853	0.30538360748530	-0.06150436680114
C	-6.03096516026277	0.91131021721553	-0.06090612183055
C	-2.22320276575421	4.41238588224295	-0.05271339126411
C	-0.96828534065823	5.00712129877607	-0.05253888826593
C	0.20845025650407	4.23086174004807	-0.05539053053791
C	0.09693277985621	2.82587055370265	-0.05845289400026
C	-1.16039712581087	2.23009764644962	-0.05868591926911
H	-7.00540843194609	4.18730458450906	-0.04207750067218
H	-5.13033838378458	0.29695577195277	-0.06595326355016
H	-7.35077800140299	-0.78391252520350	-0.06700063420411
H	-9.24463429610428	3.09900817971427	-0.04329954721671
O	-9.72247196158061	0.59318007430304	-0.05514821590850

H	-3.09618231430897	5.06923354098789	-0.05067058659482
H	0.98577239628790	2.19346115234203	-0.06068415851277
H	-1.24832387369054	1.14042375748841	-0.06108530922887
H	-0.87289930837455	6.09627510804864	-0.05026964418607
O	1.37984856113464	4.91239696761357	-0.05502845741081
H	-4.69127103083325	3.97294644798635	-0.04779172410853
C	2.60250565701444	4.19433282924527	-0.05773643915941
H	3.40497572241000	4.94517415241891	-0.05689111241772
H	2.70517493623366	3.56339522503764	-0.95822342885010
H	2.70687360278493	3.55954749333430	0.83984545291791
C	-9.91347970441621	-0.81046364808281	-0.06203261867880
H	-10.99962938079105	-0.97871238774560	-0.06045875409274
H	-9.47773429693499	-1.28912895663345	0.83324101375330
H	-9.48177931909693	-1.27975897726494	-0.96419779462090

1,2-bis(4-chlorophenyl)diazene (S = 0)

C	-4.66382212849056	1.98429382461061	0.02316065421164
C	-4.62803310235135	0.58656537860852	0.00369361621890
C	-3.45962322323439	2.68833839824905	0.02644823779304
C	-2.22991408791393	2.00771542095759	0.01051131379786
C	-2.21558915152770	0.59795840803145	-0.00901210398911
C	-3.41104434841782	-0.11248378370325	-0.01241626886103
Cl	-6.12919039801674	-0.31420154349376	-0.00092563706800
N	-1.07600168078161	2.82025226742141	0.01577483298532
N	0.02288156804243	2.21582729193302	0.00130290778629
C	1.17679394486844	3.02836410394485	0.00656910117578
C	1.16246824659804	4.43812294984541	0.02596310980772
C	2.35792366856573	5.14856469476328	0.02939660459279
C	3.57491326872207	4.44951333253593	0.01344731700395
C	3.61070293090921	3.05178329725704	-0.00590259813985
C	2.40650386540512	2.34773919573653	-0.00922664053989
Cl	5.07607095442495	5.35027934469093	0.01811528430960
H	-5.61917495308054	2.51219297460505	0.03562048013471
H	-3.45417058405051	3.78081394609105	0.04149041244429
H	-1.25949137902108	0.07282892443354	-0.02139035477067
H	-3.40846797821601	-1.20428943875869	-0.02746758844830
H	0.20636988955501	4.96325414398636	0.03821747279683
H	2.35534642072611	6.24037171859596	0.04434564062556
H	4.56605654265850	2.52388272200660	-0.01824426045516
H	2.40105171462666	1.25526242765150	-0.02418153341228

1,2-bis(4-chlorophenyl)diazene anion (S = 1/2)

C	-4.68148488754603	1.97978733178246	0.02320282446671
C	-4.64244566429179	0.57612116182356	0.00357655012655
C	-3.49060373660567	2.69748957916504	0.02674903171685
C	-2.22093442816664	2.05135333157312	0.01120050933739
C	-2.22269461226991	0.62346361730777	-0.00856798865836
C	-3.41348958305225	-0.09822564473620	-0.01210167106669
Cl	-6.14813119045815	-0.34271517233858	-0.00141522414231
N	-1.10218014635258	2.84525890290314	0.01616038153905
N	0.04906104367727	2.19081929915997	0.00096861246958
C	1.16781495957643	2.98472542817723	0.00591977449575
C	1.16957423647970	4.41261540711116	0.02566514894492
C	2.36036900234858	5.13430512126643	0.02918583102598

C	3.58932529329246	4.45995840383035	0.01351835674733
C	3.62836528372774	3.05629189774374	-0.00608228088086
C	2.43748439890923	2.33858922475133	-0.00961624803646
Cl	5.09501039648274	5.37879550236093	0.01848963906412
H	-5.64229719999314	2.50023856904848	0.03548005240357
H	-3.50798095136910	3.79125195555853	0.04175591390503
H	-1.26354443216658	0.10468466733399	-0.02093795870264
H	-3.39523962971806	-1.19137046359949	-0.02712975344496
H	0.21042394605366	4.93139429547763	0.03802622165098
H	2.34211868744841	6.22745018677893	0.04419517051875
H	4.58917785172240	2.53584084675332	-0.01834940846326
H	2.45486136227129	1.24482655076715	-0.02460348501703

1,2-bis(4-chlorophenyl)diazenyl radical (S = 1/2)

C	-4.71496659824399	1.96198296442188	0.02989181161310
C	-4.66701467448813	0.56298099179702	0.00365291645210
C	-3.52712054767789	2.68958028637421	0.03367891927533
C	-2.28317189091032	2.02682426193895	0.01127842571962
C	-2.24964710648738	0.61814046703568	-0.01516647169975
C	-3.43943373515870	-0.10842779915466	-0.01875536797844
Cl	-6.16230841814093	-0.35860844941651	-0.00135162501615
N	-1.11764177121836	2.78579430412428	0.01609088372930
N	0.07795145681755	2.22332532403789	0.00134578177745
C	1.18198019257726	3.03251369789038	0.00616457498619
C	1.19271619675650	4.45624688163571	0.01873550580893
C	2.39476388703936	5.15924143945943	0.02273836911113
C	3.61183210985233	4.46626723926459	0.01427367580665
C	3.63618526338280	3.06272602726464	0.00106387352863
C	2.43801465996258	2.36254956903659	-0.00306221298875
Cl	5.11973831296454	5.36196595775437	0.01997326544951
H	-5.67575574017360	2.48041986924993	0.04750636054969
H	-3.55888551991888	3.78252473488744	0.05435957194787
H	-1.28868270876196	0.10410667503789	-0.03272201556017
H	-3.41218763099097	-1.19994670171289	-0.03906671617212
H	0.26718190976486	5.03572662127097	0.02431391243105
H	2.38845411266371	6.25132793411266	0.03211307746755
H	4.58930550508222	2.52977615996961	-0.00588893965854
H	2.43805895478327	1.26986958164148	-0.01315529176594
H	-1.23651621947586	3.80145196207845	0.03732771518576

diethyl 4,4'-(diazene-1,2-diiyl)-dibenzoate (S = 0)

C	-4.66463010466346	1.90937341651627	-0.02496951350395
C	-4.64141881360705	0.50584382625109	-0.00456243685044
C	-3.47159660629880	2.62835652830099	-0.02282051274869
C	-2.23885711118067	1.95251844933121	-0.00004531288667
C	-2.21219970684978	0.54309296558170	0.02073027548765
C	-3.40503500425800	-0.17038458907527	0.01831051865550
C	-5.94903690570278	-0.22329552171672	-0.00783434323894
N	-1.08896646341449	2.77461280458271	-0.00011026290072
N	0.01223269483325	2.17619937905028	0.02031605423576
C	1.16212325989116	2.99829313411279	0.02025963331584
C	1.13546666576977	4.40771969609304	-0.00044622939227
C	2.32830295627188	5.12119571733127	0.00197535155050
C	3.56468650024869	4.44496466641093	0.02478270381622

C	3.58789702198656	3.04143417996891	0.04512281425833
C	2.39486267700446	2.32245267120182	0.04297372717863
C	4.87230563581959	5.17410166114380	0.02805916248430
H	-5.62641097337064	2.42556417488443	-0.04261211272843
H	-3.46954549779439	3.72069050779191	-0.03865190432896
H	-1.25144910717626	0.02718334812586	0.03855750579615
H	-3.38716106977896	-1.26104177509867	0.03433235050608
H	0.17471607293441	4.92363134304190	-0.01821786142594
H	2.31043000265561	6.21185377918241	-0.01398879544222
H	4.54967777477907	2.52524164605533	0.06271861254876
H	2.39281078155284	1.23011802270057	0.05875774228835
O	5.95408337010078	4.62337651262409	0.04423023345291
O	4.72012620412820	6.50320810976116	0.01114137874735
O	-7.03081458722726	0.32742577077689	-0.02413544279705
O	-5.79685361972310	-1.55240250063073	0.00900168302263
C	5.91765746729636	7.31121190744610	0.01300205315096
C	5.50441215989143	8.76549780935977	-0.00726334767075
H	6.52460480355409	7.04497019065719	-0.86745800781197
H	6.50818298966113	7.06503826957127	0.91032860745627
H	4.91828954163182	9.00087319298466	-0.91012937312958
H	6.40344911601068	9.40226427559375	-0.00617732986928
H	4.90177889158436	9.02113767916797	0.87906724173889
C	-6.99438141673874	-2.36041119145124	0.00701092372935
C	-6.58113135860176	-3.81469677345610	0.02720507208622
H	-7.58485026442899	-2.11418056425899	-0.89033734906158
H	-7.60138655595982	-2.09423057136692	0.88744958952198
H	-5.97843658321095	-4.07027329934383	-0.85910192487331
H	-7.48016558178671	-4.45146690462364	0.02601398078559
H	-5.99506925583349	-4.05013194457999	0.93009484484649

diethyl 4,4'-(diazene-1,2-diiyl)-dibenzoate anion (S = 1/2)

C	-4.67757672322655	1.92018272430006	-0.02601516187965
C	-4.66239182290702	0.50472244553711	-0.00341821137851
C	-3.49843481230372	2.64489654367532	-0.02459914117170
C	-2.22716212451555	1.99767253621273	-0.00033063364497
C	-2.22196675159494	0.56827609938253	0.02300059308754
C	-3.40750866878029	-0.14920832138215	0.02099870848111
C	-5.94729165927399	-0.22212606251802	-0.00667628396931
N	-1.11447427702854	2.79516227242502	-0.00115714188060
N	0.03774531978914	2.15564435256271	0.02124937354023
C	1.15043358141101	2.95313392723611	0.02042119302863
C	1.14523869823332	4.38253039950008	-0.00291164913907
C	2.33078088232343	5.10001436485697	-0.00091362086021
C	3.58566400482209	4.44608312971163	0.02349974455022
C	3.60084828034776	3.03062299883433	0.04610084921470
C	2.42170607950635	2.30590960883813	0.04468895012713
C	4.87056387400529	5.17293158397698	0.02675042799552
H	-5.64221854581243	2.43337434539889	-0.04495212686867
H	-3.51308294848619	3.73847447904298	-0.04228301819594
H	-1.26006451731434	0.05506367355909	0.04242990101928
H	-3.37759003850423	-1.24097125481535	0.03885209805291
H	0.18333666217053	4.89574300960880	-0.02233930518582
H	2.30086261354448	6.19177719597495	-0.01876821231464
H	4.56548983711099	2.51743080091263	0.06503660826262
H	2.43635349123155	1.21233169938062	0.06237494007322

O	5.96991682515378	4.64459951161189	0.04295220002476
O	4.71733538954835	6.51529024781847	0.00980921061790
O	-7.04664493756794	0.30620653380311	-0.02284508464245
O	-5.79406383008544	-1.56448460384800	0.01029928524634
C	5.91223726231423	7.31433436822637	0.01208566728124
C	5.50645030977999	8.77214254874932	-0.00496475343856
H	6.52338824188334	7.05338272147698	-0.86807131113414
H	6.50865325323981	7.07011299822131	0.90702052855631
H	4.91894138619544	9.01149047656187	-0.90615505995874
H	6.40663023071259	9.40762775401798	-0.00351320082860
H	4.90427969497238	9.02821512463457	0.88183713471150
C	-6.98896602172155	-2.36352810172927	0.00806524138529
C	-6.58317958203580	-3.82133580984922	0.02517500052398
H	-7.58538737332728	-2.11934478989020	-0.88687661669576
H	-7.60011171666343	-2.10253872064693	0.88821457776129
H	-5.98101511695897	-4.07744678135126	-0.86161998518231
H	-7.48335985141672	-4.45682062344070	0.02375674970780
H	-5.99566459877094	-4.06064540657847	0.92637153512013

diethyl 4,4'-(diazenyl-1,2-diiyl)-dibenzoate radical (S = 1/2)

C	-4.71866565004864	1.89985659133684	-0.03280287843097
C	-4.68683530591172	0.49233170025218	-0.00650456714504
C	-3.54302636972711	2.63861647206349	-0.03172173195086
C	-2.29548846366677	1.97822320176751	-0.00365190075600
C	-2.25213470497313	0.56822585757735	0.02309527193578
C	-3.43790328942782	-0.15781285810348	0.02126509457066
C	-5.97786398399859	-0.24837870240702	-0.00920051921867
N	-1.13755821100192	2.74330870877815	-0.00337456613884
N	0.06048512643757	2.19370260426594	0.01762160733740
C	1.15846151148137	3.00667138130981	0.01763633967927
C	1.16033368595654	4.43196581288630	0.00213083409019
C	2.35835572605663	5.13401181348007	0.00461797253177
C	3.59735767727191	4.46150080090191	0.02214538820298
C	3.60456311536310	3.05013399857045	0.03753415137525
C	2.41735270987341	2.33877037015161	0.03561298444458
C	4.89938311024798	5.18059902465732	0.02539837109547
H	-5.68509146810926	2.40777057009289	-0.05457078266955
H	-3.57517002195246	3.73145234176549	-0.05272756380913
H	-1.28701218248734	0.06250505665857	0.04507839367777
H	-3.39829724869700	-1.24803067046723	0.04196529885406
H	0.23009086984754	5.00364130653125	-0.01087743911744
H	2.33989680586591	6.22497296401085	-0.00706826210191
H	4.56295146727582	2.52670942116183	0.05123206240910
H	2.41777486921821	1.24623605133724	0.04762425423844
O	5.98393269428442	4.63037689343685	0.03726454808350
O	4.75562211225428	6.51580617416088	0.01322906976507
O	-7.07133019024227	0.28297366968560	-0.02900263129288
O	-5.81162221437972	-1.58048274113499	0.01200071520627
C	5.95755045039357	7.31241062550953	0.01523775438423
C	5.55707735914822	8.77083473298652	0.00143828752812
H	6.56257417491552	7.04682265219756	-0.86710719787148
H	6.55054699249190	7.06034521813637	0.90964410324789
H	4.97033842522622	9.01463598032489	-0.89889524073258
H	6.46103022124076	9.40071502405764	0.00279043684812
H	4.95821324359875	9.02820719479856	0.88993133284344

C	-6.99972180554892	-2.39771717632106	0.01022420827679
C	-6.57383171566373	-3.84879625897330	0.03428156705077
H	-7.59335283299315	-2.16117602123286	-0.88797453366466
H	-7.61259004301040	-2.13735956216178	0.88868347919474
H	-5.96708196332744	-4.10076888223594	-0.85039949813797
H	-7.46648490649883	-4.49458233071052	0.03336283255837
H	-5.98626754347995	-4.07675548496608	0.93821976194909
H	-1.26428223330346	3.75897647386280	-0.02372680834110

1,2-bis(4-tert-butylphenyl)diazene (S = 0)

C	-4.61353071829179	1.90895513843966	0.00329089478903
C	-4.62584293860663	0.50350363191008	-0.00656260646643
C	-3.41247529983052	2.62353367797801	0.00565337180374
C	-2.17979824653056	1.95420998664060	-0.00185941680219
C	-2.17282565986785	0.54380130178886	-0.01171242013111
C	-3.37323949763811	-0.15569114997331	-0.01382133201453
C	-5.92555537869001	-0.32238895003793	-0.00964502977282
C	-7.18235084133526	0.56559725618567	-0.00245456585817
H	-7.23286512852760	1.20521440231307	0.89339738807102
H	-8.08281740209323	-0.06958488454251	-0.00538940598533
H	-7.23481396120140	1.21635988126533	-0.89012930436244
C	-5.95867844164906	-1.22490569172813	1.24634583189782
C	-5.96247780727754	-1.20948396610701	-1.27650865074464
H	-5.93507657734391	-0.62305102144783	2.16992058685097
H	-5.10677995201668	-1.92218963505148	1.27468185762905
H	-6.88262464873861	-1.82707829088012	1.25869880609586
H	-5.94244984038020	-0.59628051202439	-2.19268090704669
H	-6.88607724943071	-1.81207927148552	-1.29308830458082
H	-5.11016937842857	-1.90567909636188	-1.31626879621957
N	-1.02711165418941	2.76836159763707	0.00116014171783
N	0.07472611922849	2.16662869153556	-0.00618476267479
C	1.22741180221968	2.98077915550519	-0.00311461494477
C	1.22044083895930	4.39118754786540	0.00678745691826
C	2.42085501815624	5.09067911445589	0.00895141026087
C	3.67345810102891	4.43148495232697	0.00165586104502
C	3.66114519447794	3.02603410737285	-0.00830105406233
C	2.46008923595172	2.31145596989239	-0.01068341729117
C	4.97317033157819	5.25737782736423	0.00474437287999
C	6.22996559703797	4.36939400075975	-0.00272543958920
C	5.01022358190683	6.14426380212839	1.27175225759499
C	5.00616138007911	6.16010232574334	-1.25109950453469
H	6.28252745522788	3.71848435126131	0.88483616245820
H	7.13043151578614	5.00457700224572	0.00021558289912
H	6.28038174573954	3.72992500092173	-0.89868825756487
H	4.98247902500156	5.55840005145576	-2.17477161982411
H	5.93009806470829	6.76228987333454	-1.26344032532338
H	4.15424958203741	6.85737891236888	-1.27923660873890
H	4.99027336093577	5.53090861031280	2.18782449019332
H	4.15792908814271	6.84046372486084	1.31170830134385
H	5.93383301516954	6.74684318724887	1.28834620936916
H	-5.54883291138896	2.46921382371814	0.00921617888609
H	-3.41271963677519	3.71663505618897	0.01332241880045
H	-1.21828747711903	0.01513704976918	-0.01761840134848
H	-3.33751289869511	-1.24790939778938	-0.02144540580887
H	0.26590375779650	4.91985321313025	0.01270202605252

H	2.38512882611979	6.18289726763197	0.01660814814824
H	4.59644698769333	2.46577516177958	-0.01428242927747
H	2.46033392106313	1.21835521209261	-0.01842717473768

1,2-bis(4-tert-butylphenyl)diazene anion (S = 1/2)

C	-4.63529037769399	1.91463570633729	0.00608998175088
C	-4.64955847373694	0.50288375865558	-0.00701944275809
C	-3.44533012358704	2.64040477442886	0.00902119341901
C	-2.17438646449386	2.00393659951476	-0.00090568458607
C	-2.18811966482999	0.57672743285307	-0.01403195247852
C	-3.38599961571084	-0.13192104692776	-0.01655153468038
C	-5.94398297292791	-0.33453332429966	-0.00996584168218
C	-7.20703682986400	0.54580711044380	-0.00442269348348
H	-7.26081202065079	1.18720097987801	0.89024287715031
H	-8.10690523901162	-0.09122489805034	-0.00762855137392
H	-7.26123624775477	1.19707527402165	-0.89192795138295
C	-5.98211432132171	-1.23907288746888	1.24452236688774
C	-5.98500128636134	-1.22668087108000	-1.27321414123444
H	-5.96822672425284	-0.63723592116909	2.16870700900830
H	-5.12193010695180	-1.92652092069895	1.27873932484563
H	-6.89895321536737	-1.85364841468329	1.25589865281486
H	-5.97317775710159	-0.61577430699577	-2.19145891474307
H	-6.90193336462253	-1.84100218322700	-1.28846004179953
H	-5.12505353689227	-1.91387173162513	-1.31615257728111
N	-1.05241269442904	2.79644659421720	0.00257549142550
N	0.10003685673744	2.13852472963310	-0.00735020826570
C	1.22200941162315	2.93103809167137	-0.00391041168427
C	1.23573653319864	4.35824839016503	0.00908615429979
C	2.43361277577007	5.06690255183889	0.01155865348414
C	3.69717444126629	4.43210327414766	0.00210329640392
C	3.68291336146930	3.02034997734039	-0.01086757284814
C	2.49295639266943	2.29457452290355	-0.01375378490666
C	4.99159440180447	5.26952747248336	0.00499497082290
C	6.25465302896737	4.38919402575357	-0.00048786890010
C	5.03260252885127	6.16176035753629	1.26818272925957
C	5.02972647747855	6.17398284095901	-1.24955484572898
H	6.30886861451694	3.73799676095435	0.88706837842713
H	7.15451733186001	5.02623219895577	0.00265807407814
H	6.30842084726521	3.74772933608814	-0.89510313979686
H	5.01585400082982	5.57208065827698	-2.17369720486234
H	5.94655923672040	6.78856653266454	-1.26096353208679
H	4.16953528045809	6.86141884794014	-1.28382601874489
H	5.02076799236714	5.55091755592364	2.18646971687776
H	4.17265550786087	6.84895616601862	1.31106504970803
H	5.94953528578865	6.77608169081889	1.28339735825858
H	-5.57432128614354	2.47191952238131	0.01405217773759
H	-3.46690340914691	3.73500788656220	0.01905006904337
H	-1.23187485639160	0.05133281248806	-0.02203165827637
H	-3.33562438547064	-1.22570773047492	-0.02638038399191
H	0.27948927971922	4.88363921274054	0.01701723183545
H	2.38323215236006	6.16068990621767	0.02128587039132
H	4.62194722637595	2.46307007261296	-0.01876017434637
H	2.51453600875658	1.19997061127451	-0.02368049600681

1,2-bis(4-tert-butylphenyl)diazenyl radical (S = 1/2)

C	-4.66372750837849	1.87591235727472	0.01434075620312
C	-4.67037748146858	0.46884192823692	-0.00412851657095
C	-3.47495009108499	2.60847174981649	0.01757309243866
C	-2.23220131031822	1.95049949309889	0.00219315083268
C	-2.21289493938077	0.54165233541361	-0.01651775278613
C	-3.41152264096404	-0.16850154652827	-0.01912008002185
C	-5.96409470076257	-0.36911495363744	-0.00744901384541
C	-7.22689117207923	0.51075469372186	0.00478676202412
H	-7.27974363397020	1.14745248747717	0.90273011549458
H	-8.12466860465812	-0.12856844498233	0.00091047801056
H	-7.28416194622424	1.16485005288862	-0.88030691177148
C	-5.99244659454026	-1.27664362441304	1.24460895467353
C	-6.00144913424939	-1.25369855149085	-1.27562703280712
H	-5.97360753162210	-0.67800465330237	2.17055660618878
H	-5.13358643632867	-1.96585645474295	1.27105521325308
H	-6.91023947648502	-1.88877254190168	1.25674628433254
H	-5.98996812355382	-0.63820089575938	-2.19058621939030
H	-6.91898017585168	-1.86609006031224	-1.29194139151921
H	-5.14244434042148	-1.94165291165646	-1.32107633920616
N	-1.06225602155705	2.70528650939440	0.00580977922667
N	0.13502001311791	2.14114630681867	-0.00561319104825
C	1.23750766580979	2.95631768060601	-0.00167393037615
C	1.24765316199122	4.37947793233792	0.00988039470051
C	2.45071998554892	5.07883635413472	0.01279680331355
C	3.70687867883790	4.43299612452685	0.00481513497761
C	3.69057499620320	3.02246563955879	-0.00708070079818
C	2.49878837242176	2.30474222582571	-0.01034198154346
C	5.00439424757243	5.26283356263625	0.00884029392307
C	6.26233488139754	4.37597538399120	0.00138131826221
C	5.04326978338278	6.15030049402031	1.27530672063010
C	5.04010304615277	6.16745188457988	-1.24548961901155
H	6.31445897482553	3.72401821787952	0.88831888373946
H	7.16340634853966	5.01060502679181	0.00516996411322
H	6.31321519204297	3.73662431458696	-0.89475340252322
H	5.01967694481581	5.56680509866515	-2.17005896684657
H	5.96173534606723	6.77374077628222	-1.25674142919454
H	4.18558381855589	6.86181119261258	-1.27506577036643
H	5.02594809903158	5.53702345466396	2.19161851264848
H	4.18834719842998	6.84351508287898	1.31681151360712
H	5.96455191351840	6.75698022504350	1.29213363885240
H	-5.60228831401073	2.43156308718476	0.02659585463756
H	-3.50691964163643	3.70208293275033	0.03216584488034
H	-1.25576456862521	0.01955059904819	-0.02884086245567
H	-3.35704182017969	-1.26028994640022	-0.03345156845566
H	0.31954271206668	4.95595796917237	0.01597313098610
H	2.40565428466172	6.17115080479932	0.02152698057136
H	4.62641883135346	2.46190020393530	-0.01389765347030
H	2.51090580569675	1.21150219182116	-0.01948878032316
H	-1.17660409369089	3.72112821065206	0.02103493181036

########OTHER#SUBSTRATES########

nitrotoluene (S = 0)

C	-3.92586919266104	-1.01221386988813	-0.00997304133545

C	-3.94172558000371	0.39420158728632	-0.00917365811899
C	-2.75908732975343	1.13168162945226	0.04847047633811
C	-1.54276347580593	0.44781727526658	0.10602027192575
C	-1.48751052812104	-0.95021169519492	0.10701976825551
C	-2.67922739303000	-1.66733395615161	0.04914782922208
N	-0.29207750176105	1.21452635195780	0.16749531131780
O	0.76295951380390	0.59478949476899	0.21646449009688
O	-0.36376553767762	2.43683436584452	0.16710941530015
H	-0.52356213770304	-1.45708082467474	0.15273523573314
H	-4.89769532811050	0.92257036384035	-0.05452467015868
H	-2.77234024324780	2.22160420842860	0.04920611538499
C	-5.20154851542776	-1.80855416120479	-0.07153952797892
H	-2.64468371655676	-2.76035945048195	0.04953993089199
H	-6.08588580578094	-1.15652252119372	-0.11862155964473
H	-5.30064590654986	-2.46182788543045	0.81212451082567
H	-5.21134132161340	-2.46892091262512	-0.95533089805529

nitrotoluene anion (S = 1/2)

C	-3.93409945447031	-1.02118980911928	-0.01070167173385
C	-3.93530057871979	0.39014417033840	-0.00847186152764
C	-2.75837093234745	1.13272202484071	0.04904718078363
C	-1.50127773671760	0.47258170726442	0.10804634405522
C	-1.48259741399522	-0.94982435438747	0.10578278526293
C	-2.67391004594894	-1.66322974723078	0.04825594610735
N	-0.31238832788021	1.20299773207164	0.16706501025184
O	0.80538281660761	0.57750288196334	0.21790322522890
O	-0.36776898684974	2.48357693913231	0.16912386474395
H	-0.51542794815787	-1.45093618738186	0.15119204358672
H	-4.89313373250353	0.92067388510137	-0.05395525783655
H	-2.76836734997797	2.22266289827562	0.05027661579305
C	-5.21367574800068	-1.81967580727044	-0.07167214914316
H	-2.63499554152175	-2.75873433858189	0.04827180005959
H	-6.09585349338738	-1.16190894195136	-0.12426906074980
H	-5.33954577638463	-2.47024100643831	0.81337024406112
H	-5.24543974974450	-2.48612204662642	-0.95309505894328

nitrotoluene-OH radical (S = 1/2)

C	-3.76294883884656	-0.85358939345528	-0.01036077355782
C	-3.75570497710362	0.55244579379771	-0.01921031128498
C	-2.56910884990444	1.28447057745083	0.03110564024900
C	-1.34128944790210	0.59716949631580	0.09245164298223
C	-1.31928586136594	-0.81427744184951	0.10287854643179
C	-2.51849471872098	-1.51513142125405	0.05198993151273
N	-0.12443869763752	1.27812226238401	0.14396221447120
O	1.01069415532910	0.76670622071251	0.19710543781829
O	-0.22081456406295	2.66811875078833	0.13239440117787
H	-0.36144924995043	-1.33329136716282	0.15092351746095
H	-4.70524173363697	1.09347190915207	-0.06712811226655
H	-2.58958358855585	2.37370056227197	0.02300697194267
C	-5.04892130728240	-1.63757355506642	-0.06505067782821
H	-2.49169408404787	-2.60902669877294	0.06045128089597
H	-5.92512726684008	-0.97378210836165	-0.11499061709300
H	-5.16252276925066	-2.28412518300628	0.82245036244565
H	-5.07580434030685	-2.30309632730935	-0.94528401899134

H 0.71710614008614 2.94409792336506 0.16834456363354

A.13 References

[1] Brown, D. A.; Colquhoun, H. M.; Daniels, J. A.; MacBride, J. A. H.; Stephenson, I. R.; Wade, K. Polymers and Ceramics Based on Icosahedral Carboranes: Model Studies of the Formation and Hydrolytic Stability of Aryl Ether, Ketone, Amide and Borane Linkages between Carborane Units. *J. Mater. Chem.* **1992**, *2*, 793–804.

[2] Tanaka, K.; Shigematsu, Y.; Sukekawa, M.; Hoshino, Y.; Honda, K. Regioselective One-Pot Synthesis of 2,3-Diaryl-2H-1-Benzopyrans via Brønsted Acid-Catalyzed [4+2] Cycloaddition of Salicylaldehydes with Diarylacetylenes. *Tetrahedron Lett.* **2016**, *57*, 5914–5918.

[3] Fox, M. A.; Nervi, C.; Crivello, A.; Batsanov, A. S.; Howard, J. A. K.; Wade, K.; Low, P. J. Structural, Spectroscopic, Electrochemical and Computational Studies of C,C′-diaryl-ortho-carboranes, 1-(4-XC_6H_4)-2-Ph-1,2-$C_2B_{10}H_{10}$ (X = H, F, OMe, NMe_2, NH_2, OH and O^-). *J. Solid State Electrochem.* **2009**, *13*, 1483–1495.

[4] Zhang, C.; Jiao, N. Copper-Catalyzed Aerobic Oxidative Dehydrogenative Coupling of Anilines Leading to Aromatic Azo Compounds using Dioxygen as an Oxidant. *Angew. Chem. Int. Ed.* **2010**, *49*, 6174–6177.

[5] Derosa, J.; Garrido-Barros, P.; Peters, J. C. Electrocatalytic Reduction of C–C π-Bonds via a Cobaltocene-Derived Concerted Proton–Electron Transfer Mediator: Fumarate Hydrogenation as a Model Study. *J. Am. Chem. Soc.* **2021**, *143* (25), 9303–9307. DOI: 10.1021/jacs.1C03335

[6] Chalkley, M. J.; Castillo, T. J.; Matson, B. D.; Peters, J. C. Fe-Mediated Nitrogen Fixation with a Metallocene Mediator: Exploring pKa Effects and Demonstrating Electrocatalysis. *J. Am. Chem. Soc.* **2018**, *140*, 6122–6129.

[7] Fong, T. P.; Forde, C. E.; Lough, A. J.; Morris, R. H.; Rigo, P.; Rocchini, E.; Stephan, T. Synthesis of the Acidic Dihydrogen Complexes trans-$[M(H_2)(CN)L_2]^+$ and trans-$[M(H_2)(CNH)L_2]^{2+}$ where M = Fe, Ru, Os and L = dppm, dppe, dppp, depe, and Dihydrogen Substitution by the Trifluoromethanesulfonate Anion to Give trans-$[Ru(OTf)(CN)L_2]$ or trans-$[Ru(OTf)(CNH)L_2]$OTf. *J. Chem. Soc., Dalton Trans.* **1999**, *24*, 4475–4486. DOI: 10.1039/a906717e

[8] Stoll, S.; Schweiger, A. EasySpin, a Comprehensive Software Package for Spectra Simulation and Analysis in EPR. *J. Magn. Reson.* **2006**, *178*, 42-55.

[9] Sheldrick, G. M. A short history of SHELX. *Acta Cryst. A*, **2008**, *64*, 112–122.

[10] Dolomanov, O. V.; Bourhis, L. J.; Gildea, R. J.; Howard, J. A. K.; Puschmann, H. OLEX2: A Complete Structure Solution, Refinement and Analysis Program. *J. Appl. Crystallogr.* **2009**, *42*, 339.

[11] Neese, F.; Wennmohs, F.; Becker, U.; Riplinger, C. The ORCA Quantum Chemistry Program Package. *J. Chem. Phys.* **2020**, *152*, 224108.

[12] Neese, F. Software update: The ORCA program system—Version 5.0. *WIREs Comput. Mol. Sci*. **2022**, 12:e1606.

[13] Marenich, A. V.; Cramer, C. J.; Truhlar. D. G. Universal Solvation Model Based on Solute Electron Density and on a Continuum Model of the Solvent Defined by the Bulk Dielectric Constant and Atomic Surface Tensions. *J. Phys. Chem. B* **2009**, *113*, 6378–6396.

[14] Chalkley, M. J.; Garrido-Barros, P.; Peters, J. C. A Molecular Mediator for Reductive Concerted Proton-electron Transfers via Electrocatalysis. *Science* **2020**, *369*, 850–854.

[15] Sharma, H. A.; Mennie, K. M.; Kwan, E. E.; Jacobsen, E. N. Enantioselective Aryl-Iodide-Catalyzed Wagner-Meerwein Rearrangements. *J. Am. Chem. Soc.* **2020**, *142*(37), 16090–16096. DOI: 10.1021/jacs.0c08150

[16] Hansch, C.; Leo, A.; Taft, R. W. A Survey of Hammett Substituent Constants and Resonance and Field Parameters. *Chem. Rev.* **1991**, *91*(2), 165–195. DOI: 10.1021/cr00002a004

[17] Goulet-Hanssens, A.; Utecht, M.; Mutruc, D.; Titov, E.; Schwarz, J.; Grubert, L.; Bléger, D.; Saalfrank, P.; Hecht, S. Electrocatalytic Z → E Isomerization of Azobenzenes. *J. Am. Chem. Soc.* **2017**, *139*(1), 335–341. DOI: 10.1021/jacs.6b10822

Appendix B

Supplementary Information for Chapter 3

B1. EXPERIMENTAL DETAILS

General Considerations

All manipulations were performed under inert N_2 atmosphere using standard Schlenk or glovebox techniques unless otherwise specified. Solvents were dried and degassed using a solvent purification system (SG Water, USA LLC) with activated alumina drying columns after sparging with N_2 gas. Solvents in the glovebox were stored over 3 or 4 Å molecular sieves. THF and diethyl ether were further dried over NaK alloy and filtered over activated alumina prior to use, and the dryness was verified by sodium benzophenone (ketyl) radical solution as a colorimetric indicator. Reagents were purchased from commercial vendors and used without additional purification unless indicated. Decaborane bis(acetonitrile), N,N-dimethyl-4-(phenylethynylaniline), and 1-(4-N,N- dimethylaniline)-2-phenyl-o-carborane were prepared according to the literature.

NMR Spectroscopy

NMR spectra were collected using Varian and Bruker 400 MHz NMR spectrometers with broadband auto-tune probes. Deuterated solvents were purchased from Cambridge Isotope Laboratories, Inc.. Acetonitrile-d_3 was degassed by three freeze-pump-thaw cycles, dried over activated 3 Å sieves, and passed over activated alumina. ^{1}H and ^{13}C chemical shifts are reported in ppm relative to tetramethylsilane using residual solvent resonances as internal standards. ^{11}B chemical shifts are reported in ppm relative to boron trifluoride etherate using absolute referencing to a ^{1}H NMR spectrum collected concurrently. ^{19}F chemical shifts are reported in ppm relative to trichlorofluoromethane using absolute referencing to a ^{13}C NMR spectrum collected concurrently.

X-ray Crystallography

X-ray diffraction (XRD) studies were carried out at the Beckman Institute Crystallography Facility on a Bruker Kappa Apex II diffractometer (Cu Kα radiation, λ = 1.5406 Å). All crystals were mounted on a glass fiber loop under Paratone N oil. Structures were solved using SHELXS or SHELXT and refined against F2 on all data by full-matrix least squares with SHELXL.[1] All structure solutions were performed in the Olex2 program.[2] Hydrogen atoms were placed in calculated positions. Non-hydrogen atoms were refined anisotropically.

Electrochemistry

Electrochemical measurements were carried out in an N_2 glovebox in a 20 mL scintillation vial fitted with a septum cap. A CH Instruments 600B electrochemical analyzer was used for data collection. A boron-doped diamond disk electrode was used as the working electrode; a freshly polished glassy carbon disk electrode was used as the counter electrode; a silver wire immersed in a solution of silver triflate (5 mM) and $^{n}Bu_4PF_6$ (200 mM) separated from the working solution by a Vycor frit was used as pseudoreference electrode. $E_{1/2}$ values for reversible waves were determined as the half potential between the peak oxidative and reductive potentials. Solution resistance was measured, and a correction of 85% of the uncompensated resistance was applied. All reported potentials are referenced to the ferrocene/ferrocenium couple, measured at the end of

each experiment. Electrochemistry solvents were passed over a pipet filter of activated alumina immediately before use.

Calculations

All calculations were performed using density functional theory (DFT) implemented in the ORCA 6.0.1 program.[3,4] The B3LYP functional was used with the def2-SVP basis set[5] with the SMD solvation model using acetonitrile.[6] When available, coordinates from X-ray diffraction structures were used as an input. Geometry optimizations were performed along with frequency calculations to ensure that optimized structures were free of imaginary frequencies. Bond dissociation free energies (BDFEs) were calculated by an established method using the calculated free energy of the H atom.

B2. SYNTHETIC PROCEDURES

1-(4-methyl-carboxyphenyl)-2-phenyl-*o*-carborane

On the nitrogen Schlenk line, decaborane bis(acetonitrile) [172 mg] and methyl-4-(phenylethynyl)benzoate [300 mg] were to a 100 mL Schlenk flask. Dry toluene [10 mL] was added, forming a pale yellow solution. The solution was heated in an oil bath [110 °C] for 24 hours. The flask was cooled, and the toluene was removed under vacuum. Methanol [10 mL] was added to the solution and stirred for 14 hours. The solvent was removed under vacuum, leaving behind a 463 mg of a yellow-orange solid. The solid was extracted with boiling hexanes and filtered, and the resulting filtrate was pumped down on the rotovap, leaving 238 mg of a crystalline pale-yellow powder (54%).

$^{1}H\{^{11}B\}$ NMR (400 MHz, $CDCl_3$) δ 7.79 (d, J = 8.6 Hz, 1H), 7.50 (d, J = 8.6 Hz, 1H), 7.42 (d, J = 7.6 Hz, 1H), 7.24 (d, J = 7.3 Hz, 2H), 7.14 (d, J = 7.6 Hz, 1H), 3.86 (s, 1H), 3.27 (s, 1H), 2.54 (s, 2H), 2.37 (s, 1H). ^{11}B NMR (128 MHz, $CDCl_3$) δ -2.30 (bs, 2H), -6.37 – -14.70 (m, 8H).

1-(4-carboxyphenyl)-2-phenyl-*o*-carborane

In a 100-mL Schlenk flask, 1-(4-methyl-carboxyphenyl)-2-phenyl-o-carborane [417 mg] was combined with aluminum powder [37 mg], iodine [236 mg], and acetonitrile [40 ml], forming a red solution. The solution was heated in an oil bath to reflux [80 °C] for 18 hours, forming a pale-yellow solution. The flask was cooled to room temperature and quenched with 2M HCl, forming a white precipitate. The solid was extracted with diethyl ether [3 x 15 mL], and the combined organic fractions were dried over sodium sulfate and concentrated *in vacuo*, leaving behind 324 mg (81%) of a yellow powder. Diffraction quality crystals were grown by hot filtration in toluene, and then cooling in the freezer.

$^{1}H\{^{11}B\}$ (400 MHz, $CDCl_3$) δ 7.87 – 7.80 (m, 1H), 7.55 – 7.50 (m, 1H), 7.45 – 7.39 (m, 1H), 7.28 – 7.20 (m, 3H), 7.15 (dd, J = 8.5, 7.0 Hz, 1H), 3.27 (s, 1H), 2.54 (s, 3H), 2.38 (s, 1H). ^{11}B NMR (128 MHz, $CDCl_3$) δ -2.30 (bs, 2H), -7.01 – -13.76 (m, 8H).

2,6-dimethyl-4-(phenylethynyl)pyridine

In the nitrogen glovebox, 4-bromo-2,6-dimethylpyridine [500 mg], $Pd(PPh_3)_4$ [155 mg], and copper iodide [51 mg] were added to a 50 mL Schlenk flask with a stir bar, forming a yellow solution. The flask was removed from the box and connected to the nitrogen Schlenk line. Diisopropylamine [1.1 mL] and phenylacetylene [0.44 mL] were added, forming a pale yellow-green solution. The reaction was stirred for 24 hours in an oil bath [40 °C], during which time it became brown. The reaction was monitored by ^{1}H NMR spectroscopy and ESI-MS. The solvent was removed, leaving behind a brown solid. The solid was purified by silica column chromatography (25% ethyl acetate/hexanes, pdt R_f = 0.30), yielding 442 mg (80%) of a light yellow solid.

^{1}H NMR (400 MHz, $CDCl_3$) δ 7.57 – 7.50 (m, 1H), 7.42 – 7.31 (m, 2H), 7.08 (s, 1H), 2.53 (s, 3H). ^{13}C NMR (101 MHz, $CDCl_3$) δ 157.99, 131.98, 131.85, 129.13, 128.60, 122.51, 122.20, 92.91, 87.35, 24.54.

1-(2,6-dimethyl-4-pyridinyl)-2-phenyl-*o*-carborane

In the nitrogen glovebox, decaborane bis(acetonitrile) [200 mg] and 2,6-dimethyl-4-(phenylethynyl)pyridine [205 mg] were added to a 50 mL Schlenk tube. Toluene [20 mL] was added, forming a pale-yellow suspension. The solution was heated in an oil bath [110 °C] for 24 hours, forming a bright red solution which became yellow overnight (with some red solids/oils on the sides of the flask). The flask was cooled, and methanol [20 mL] was added. The reaction stirred for an additional 18 hours. The volatiles were removed under vacuum, leaving behind a tan solid. The solid was extracted with boiling hexanes and filtered. The resulting pale green filtrate was pumped down on the rotovap, leaving 150 mg of a pale yellow oil which was purified by silica chromatography (50% Hex/EtOAc, pdt R_f = 0.48), yielding 79 mg of a white powder.

$^1H\{^{11}B\}$ NMR (400 MHz, $CDCl_3$) δ 7.43 (d, J = 7.5 Hz, 2H), 7.26 (t, *J* = 7.8 Hz, 2H), 7.19 (d, *J* = 8.0 Hz, 2H), 6.91 (s, 2H), 3.19 (s, 2H), 2.57 (s, 2H), 2.51 (s, 6H), 2.38 (s, 6H). ^{11}B NMR (128 MHz, $CDCl_3$) δ -1.89, -2.52, -5.79 – -13.90 (m).

***N*,*N*-dimethyl-4-((pentafluorophenyl)ethynyl)aniline**

In a 100 mL Schlenk flask in the nitrogen glovebox, $Pd(PPh_3)_4$ [27 mg] and CuI [36 mg] were added to the flask with a stir bar. Benzene [20 mL] was added, forming a cloudy yellow solution. The flask was sealed, removed from the box, and connected to the Schlenk line. 1,8-diazabicyclo[5.4.0]undec-7-ene [2.8 mL] was added, forming a clear yellow solution. Degassed water [0.06 mL] was added. Trimethyl(pentafluorophenylethynyl)silane [1.00 g] and iodoaniline [779 mg] were added to the flask, forming a dark yellow (brown) solution. Shortly after, a precipitate began to form. The reaction was heated overnight in an oil bath [60 °C]. The reaction was cooled to room temperature. Diethyl ether was added [50 mL], and the organic layer was washed with water [50 mL], adjusted to pH 7 with HCl, and washed with brine. The combined organic layers were pumped down, leaving 1.2 g of orange crude solid which purified over a silica plug (10% EtOAc/Hexanes), yielding 217 mg (18 %) of an orange solid. NOTE: The ^1H NMR spectrum contains two distinct rotamers (in a ratio of approximately 1 to 0.85), resulting in apparent splitting of the methyl peak and one of the aromatic peaks. The rotamers are likely the parallel and perpendicular configurations of the aryl groups.

^1H NMR (400 MHz, $CDCl_3$) δ 7.51 – 7.41 (m, 1H), 6.57 (dd, *J* = 67.0, 8.9 Hz, 1H), 2.97 (d, *J* = 39.8 Hz, 3H). ^{19}F NMR (376 MHz, $CDCl_3$) δ -129.88, -147.84 (tt, *J* = 22.3, 7.1 Hz), -159.80 – -160.04 (m).

1-*(N*,*N*-dimethylaniline)-2-(pentafluorophenyl)-*o*-carborane

In the nitrogen glovebox in a Schlenk tube, decaborane bis(acetonitrile) [140 mg] and N,N-dimethyl-4-((pentafluorophenyl)ethynyl)aniline [216 mg] were added. Toluene [10 mL] was added. The flask was removed from the glovebox, and the solution was heated in an oil bath [110 °C] for 24 hours during which time a pale-yellow solution formed. Methanol [15 mL] was added to the solution, and the reaction stirred at room temperature for 14 hours. The volatiles were removed under vacuum, leaving behind a red solid. The solid was extracted with boiling hexanes and filtered, and the resulting yellow filtrate was concentrated *in vacuo*, yielding 110 mg of an

orange solid (37%). Diffraction quality crystals were grown by cooling a concentrated hexanes solution.

$^{1}H\{^{11}B\}$ NMR (400 MHz, $CDCl_3$) δ 7.38 (d, *J* = 9.1 Hz, 2H), 6.46 (d, *J* = 9.1 Hz, 2H), 3.44 (bs, 2H), 2.94 (s, 6H), 2.68 (bs, 2H), 2.45 (bs, 2H), 2.39 (bs, 4H). $^{11}B\{^{1}H\}$ NMR (128 MHz) δ -1.74, -6.83, -12.10. ^{19}F NMR (376 MHz, $CDCl_3$) δ -129.88, -147.84 (tt, *J* = 22.3, 7.1 Hz), -159.80 – -160.04 (m).

1-*(N,N*-dimethylaniline)-2-(4-methoxyphenyl)-*o*-carborane

In the nitrogen glovebox in a Schlenk tube, decaborane bis(acetonitrile) [81 mg] and N,N-dimethyl-4-((4-methoxyphenyl)ethynyl)aniline [100 mg] were added. Toluene [15 mL] was added. The flask was removed from the glovebox, and the solution was heated in an oil bath [110 °C] for 24 hours. Methanol [15 mL] was added to the solution, forming an orange solution, and the reaction stirred at room temperature overnight. The volatiles were removed under vacuum, leaving behind a yellow-brown solid. The solid was extracted with boiling hexanes and filtered over celite, and the resulting yellow filtrate was concentrated *in vacuo*, yielding 70 mg of a pale-yellow crystalline powder (51%). Diffraction quality crystals were grown from cooling a concentrated hexanes solution.

$^{1}H\{^{11}B\}$ NMR (400 MHz, $CDCl_3$) δ 7.36 (d, *J* = 8.9 Hz, 2H), 7.25 (d, *J* = 9.9 Hz, 2H), 6.64 (d, *J* = 8.9 Hz, 2H), 6.38 (d, *J* = 9.0 Hz, 2H), 3.72 (s, 3H), 3.16 (bs, 2H), 2.89 (s, 6H), 2.47 (bs, 4H), 2.24 (bs, 2H). $^{11}B\{^{1}H\}$ NMR (128 MHz, $CDCl_3$) δ -3.19, -9.23, -11.13. $^{13}C\{^{1}H\}$ (101 MHz, $CDCl_3$) δ 160.77, 151.09, 132.28, 131.81, 123.73, 118.16, 113.53, 111.05, 87.93, 86.42, 55.39, 40.08.

B3. NMR SPECTRA

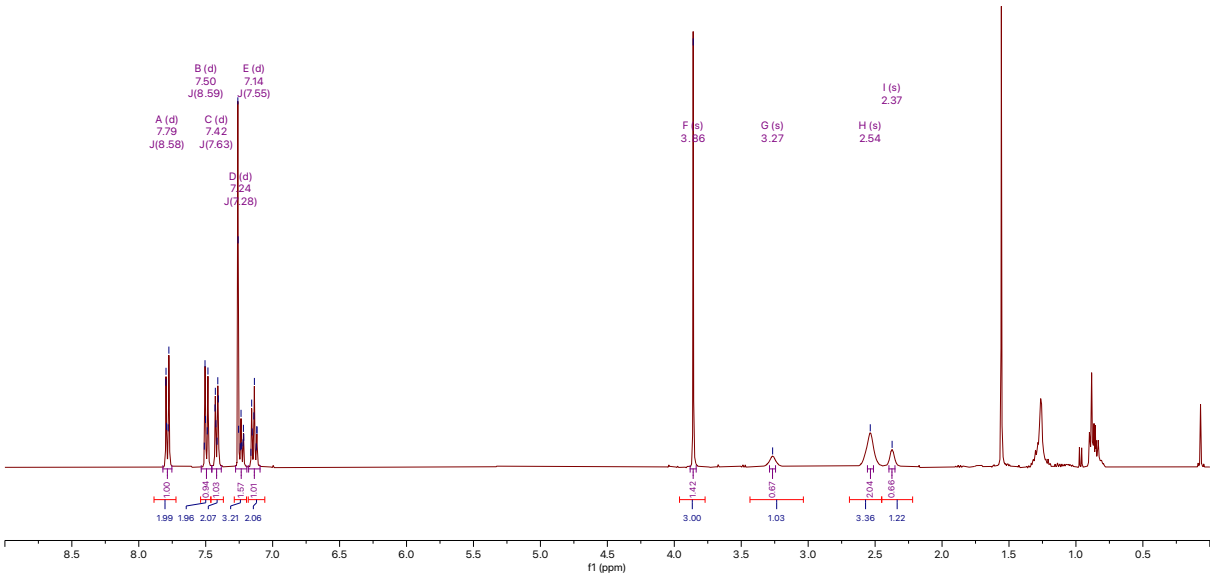

Figure B1. ^{1}H NMR spectrum of **1-(4-methyl-carboxyphenyl)-2-phenyl-*o*-carborane** in $CDCl_3$ (400 MHz)

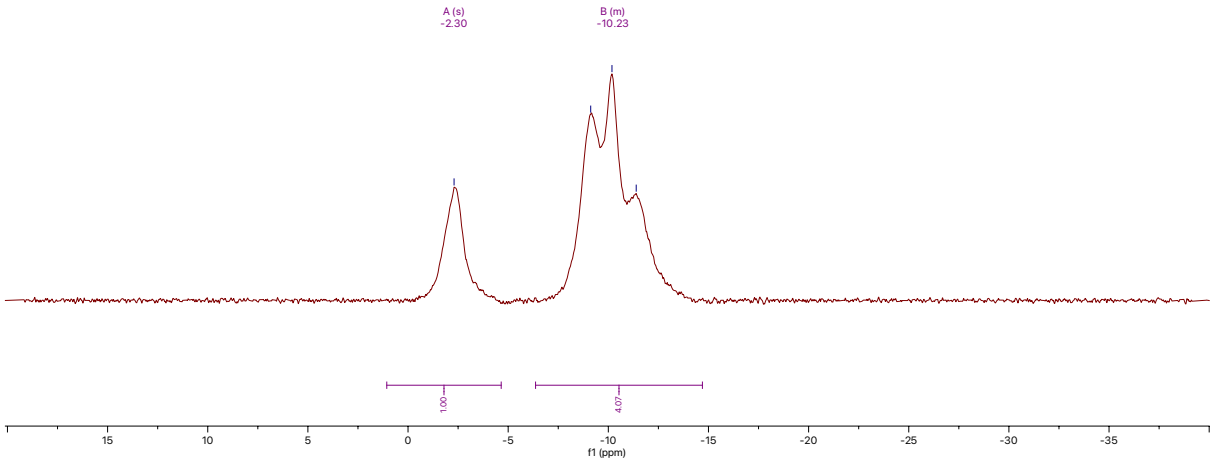

Figure B2. ^{11}B NMR spectrum of **1-(4-methyl-carboxyphenyl)-2-phenyl-*o*-carborane** in $CDCl_3$ (128 MHz)

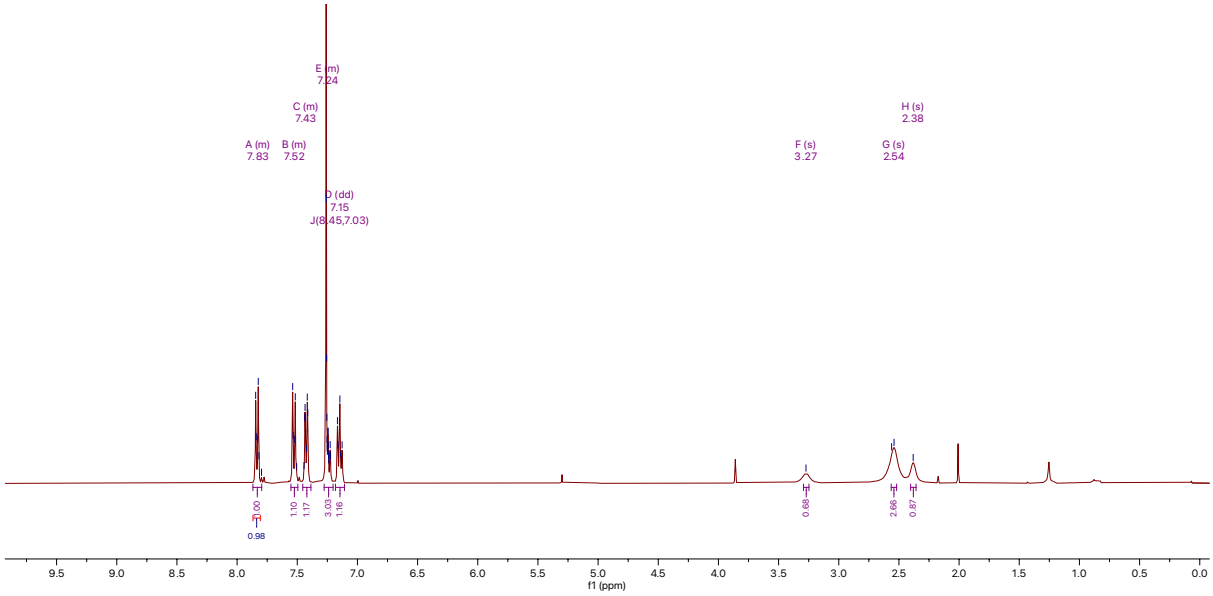

Figure B3. ^{1}H NMR spectrum of **1-(4-carboxyphenyl)-2-phenyl-*o*-carborane** in $CDCl_3$ (400 MHz)

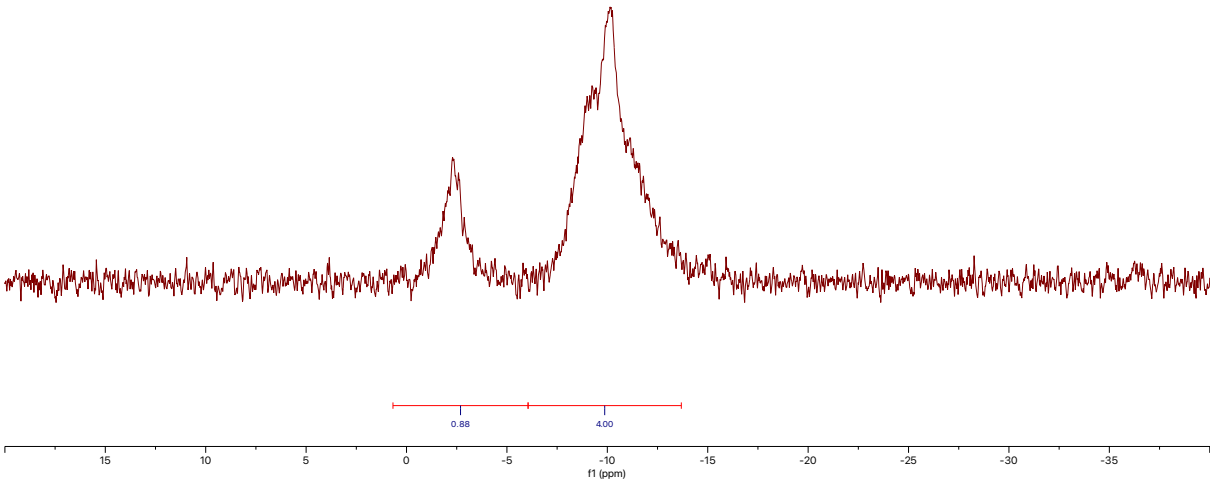

Figure B4. ^{11}B NMR spectrum of **1-(4-carboxyphenyl)-2-phenyl-*o*-carborane** in $CDCl_3$ (128 MHz)

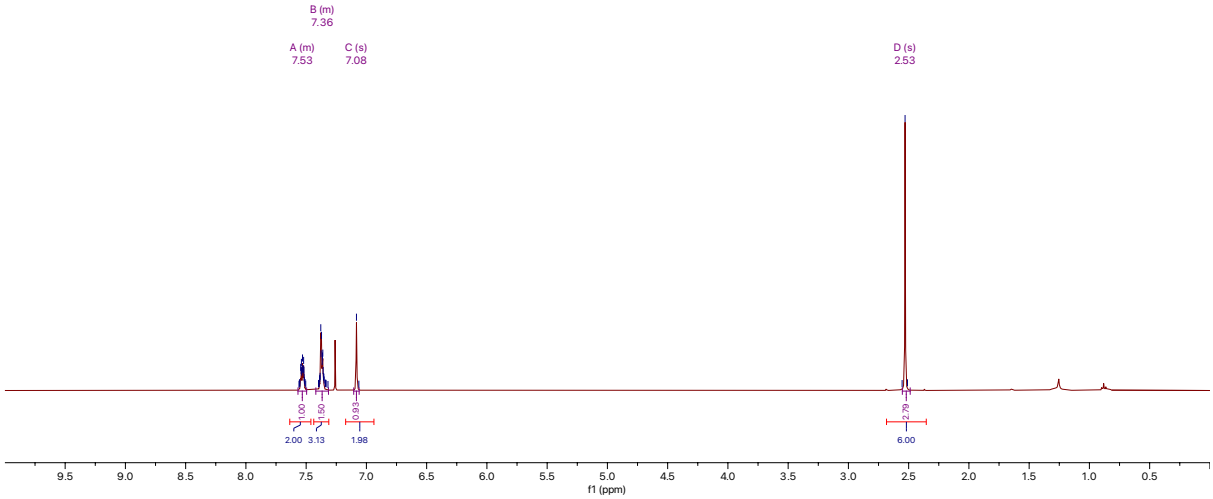

Figure B5. ^{1}H NMR spectrum of **2,6-dimethyl-4-(phenylethynyl)pyridine** in $CDCl_3$ (400 MHz)

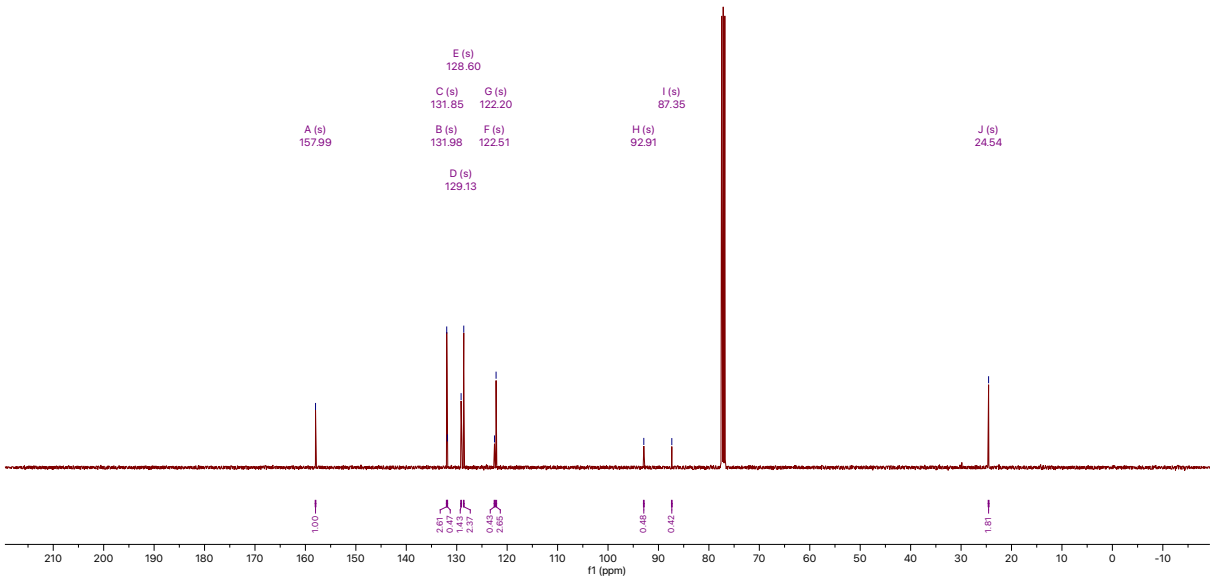

Figure B6. ^{13}C NMR spectrum of **2,6-dimethyl-4-(phenylethynyl)pyridine** in $CDCl_3$ (101 MHz)

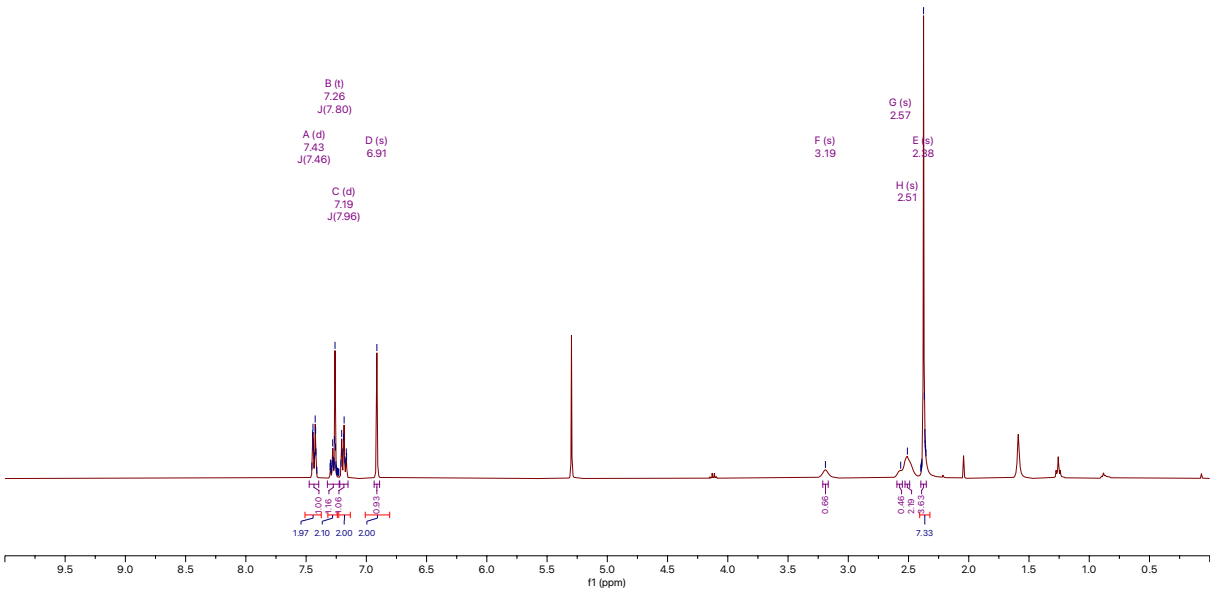

Figure B7. ^{1}H NMR spectrum of **1-(2,6-dimethyl-4-pyridinyl)-2-phenyl-*o*-carborane** in $CDCl_3$ (400 MHz).

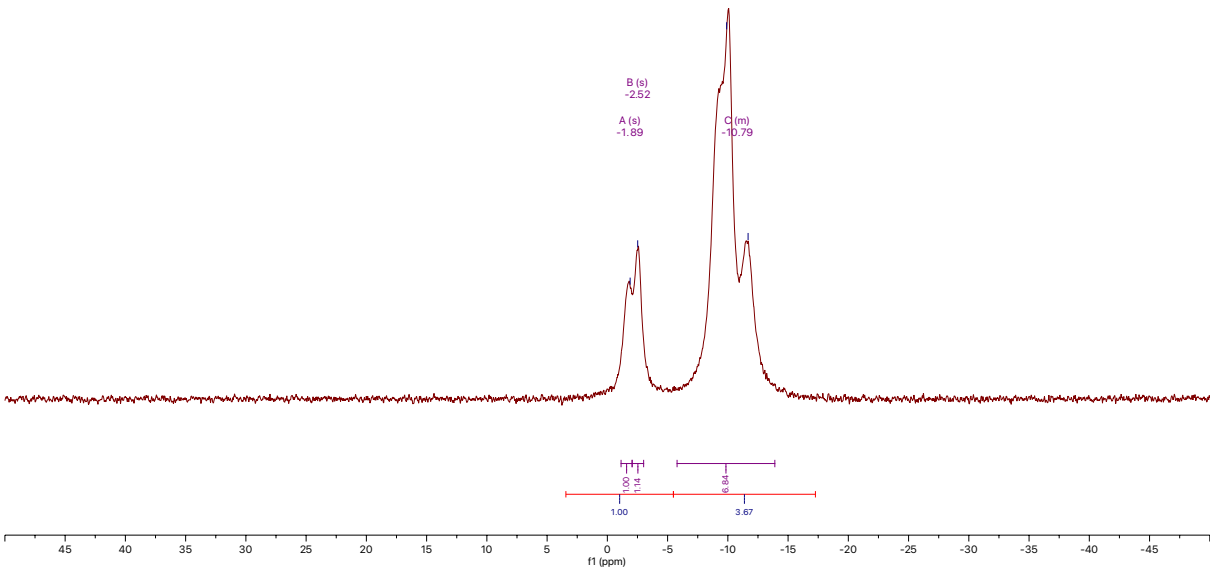

Figure B8. ^{11}B NMR spectrum of **1-(2,6-dimethyl-4-pyridinyl)-2-phenyl-*o*-carborane** in $CDCl_3$ (128 MHz)

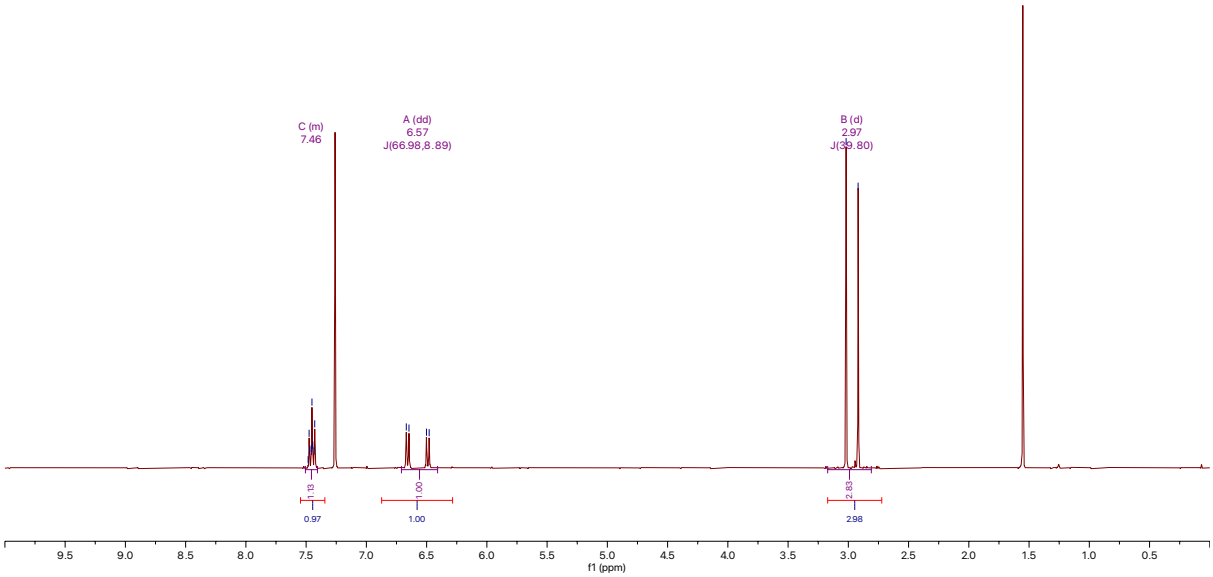

Figure B9. ^{1}H NMR spectrum of ***N*,*N*-dimethyl-4-((pentafluorophenyl)ethynyl)aniline** in $CDCl_3$ (400 MHz)

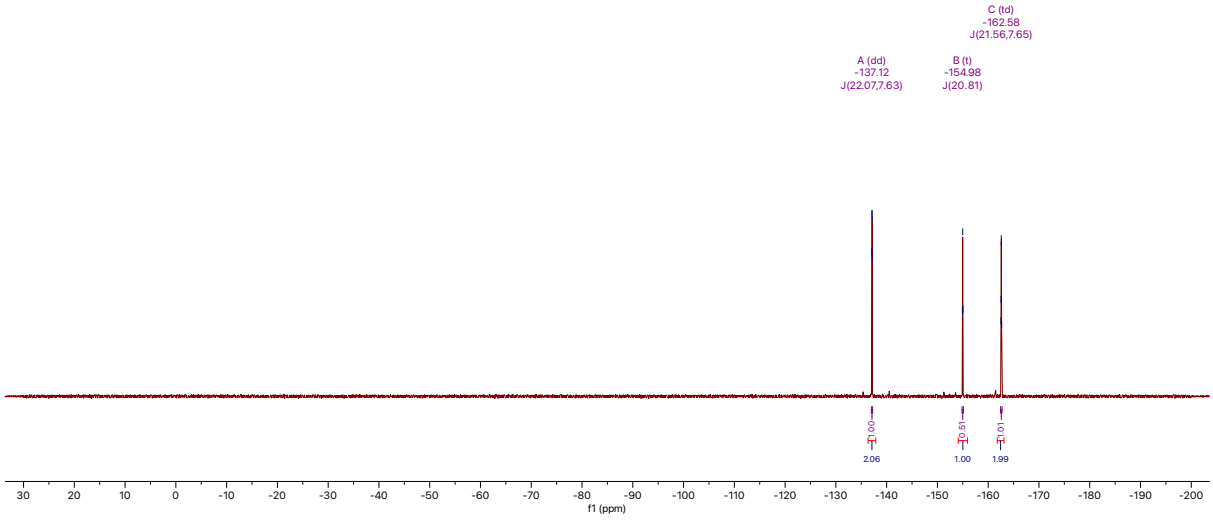

Figure B10. ^{19}F NMR spectrum of ***N*,*N*-dimethyl-4-((pentafluorophenyl)ethynyl)aniline** in $CDCl_3$ (376 MHz)

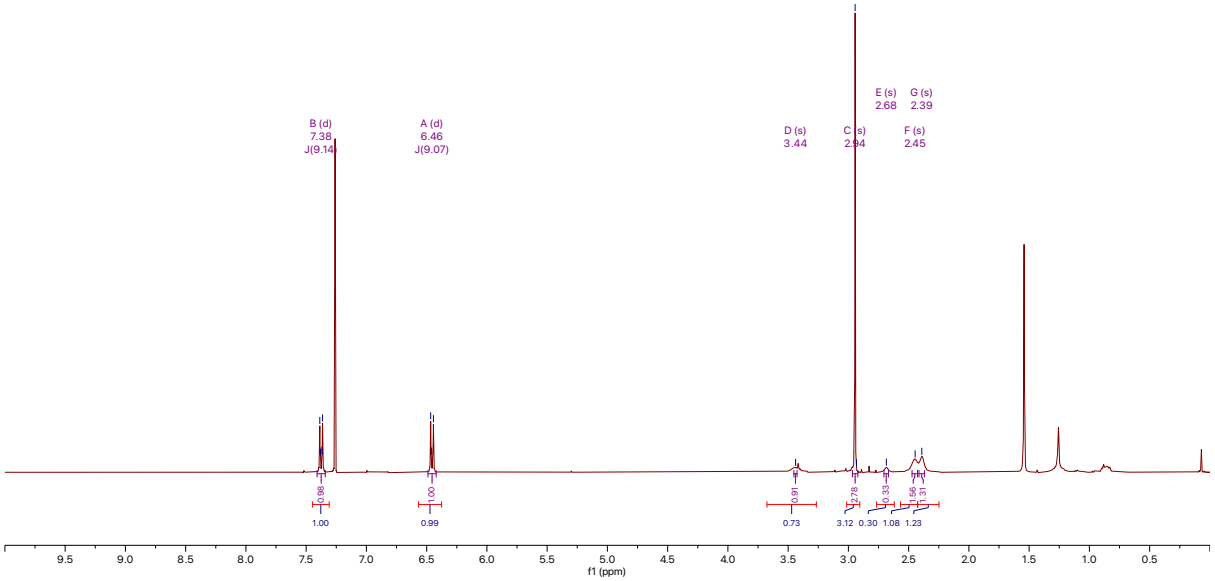

Figure B11. ^{1}H NMR spectrum of **1-*(N,N*-dimethylaniline)-2-(pentafluorophenyl)-*o*-carborane** in $CDCl_3$ (400 MHz)

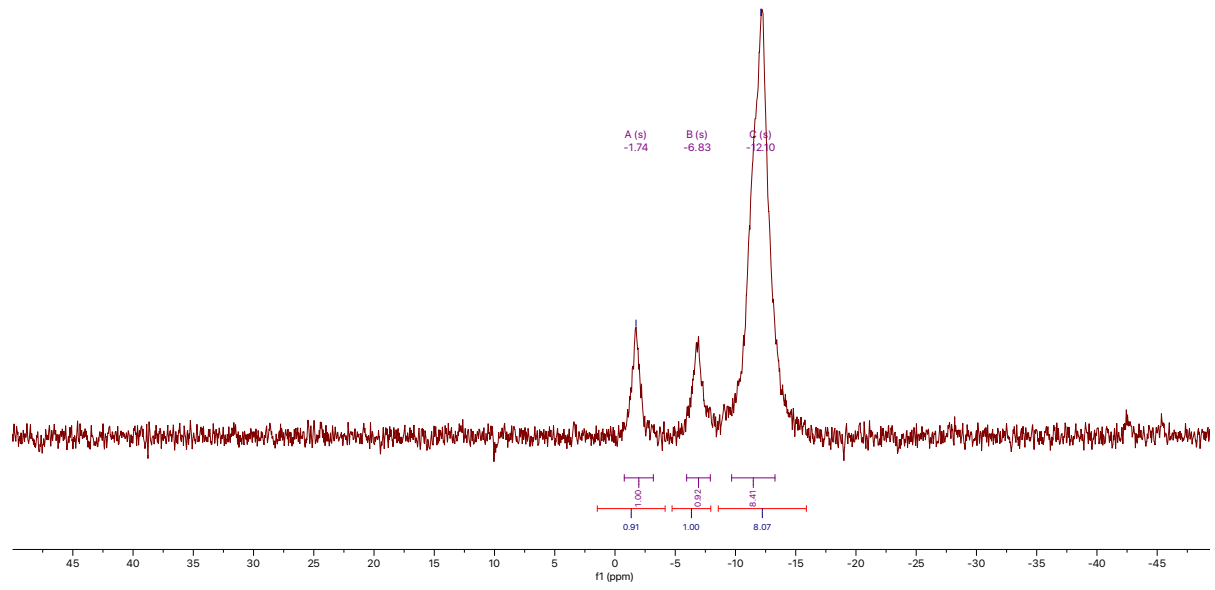

Figure B12. ^{11}B NMR spectrum of **1-*(N,N*-dimethylaniline)-2-(pentafluorophenyl)-*o*-carborane** in $CDCl_3$ (128 MHz)

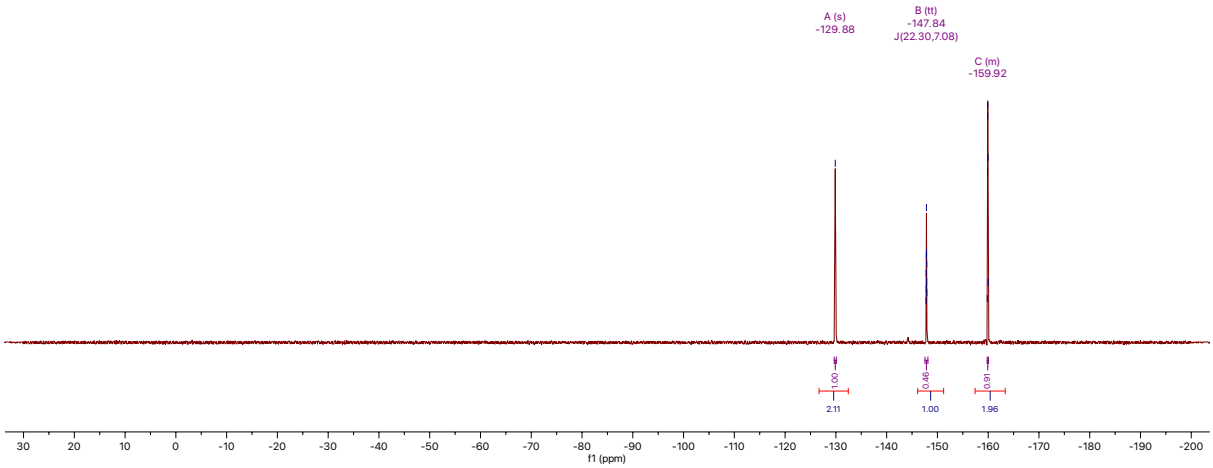

Figure B13. ^{19}F NMR spectrum of **1-*(N,N*-dimethylaniline)-2-(pentafluorophenyl)-*o*-carborane** in $CDCl_3$ (376 MHz)

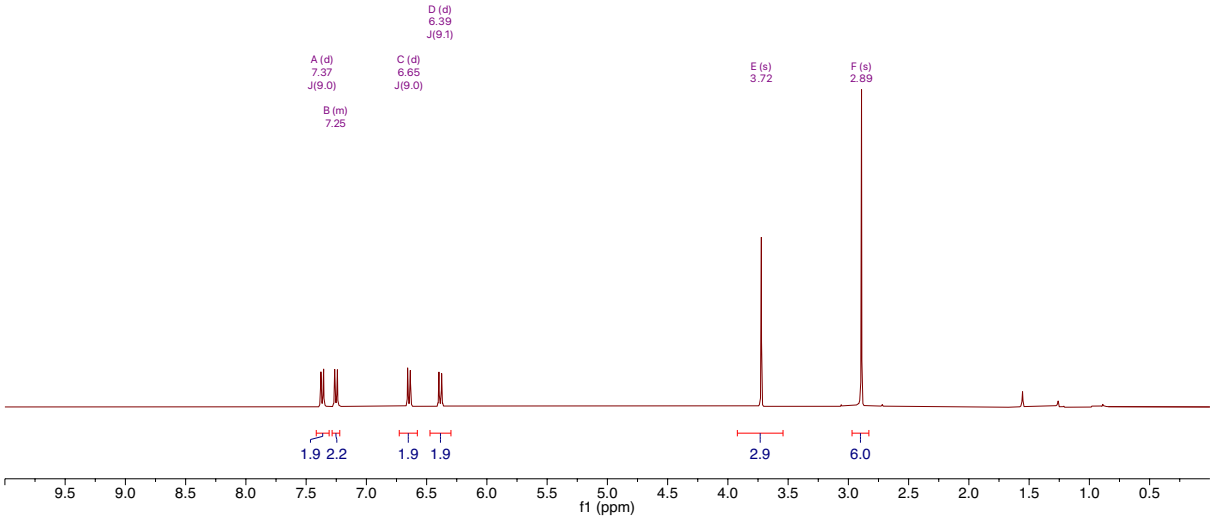

Figure B14. ^{1}H NMR spectrum of **1-*(N,N*-dimethylaniline)-2-(4-methoxyphenyl)-*o*-carborane** in $CDCl_3$ (400 MHz)

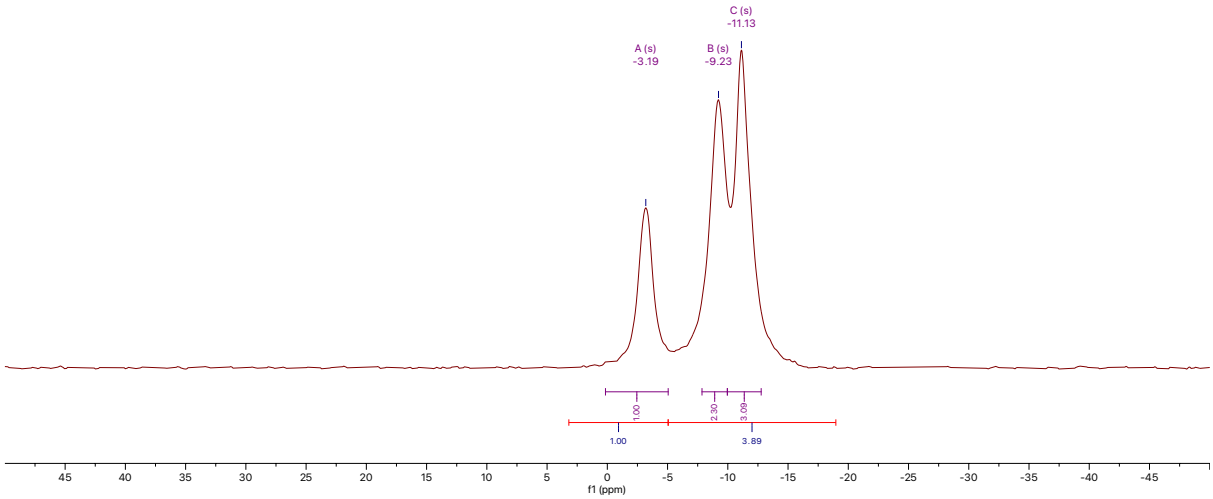

Figure B15. ^{11}B NMR spectrum of **1-*(N,N*-dimethylaniline)-2-(4-methoxyphenyl)-*o*-carborane** in $CDCl_3$ (128 MHz)

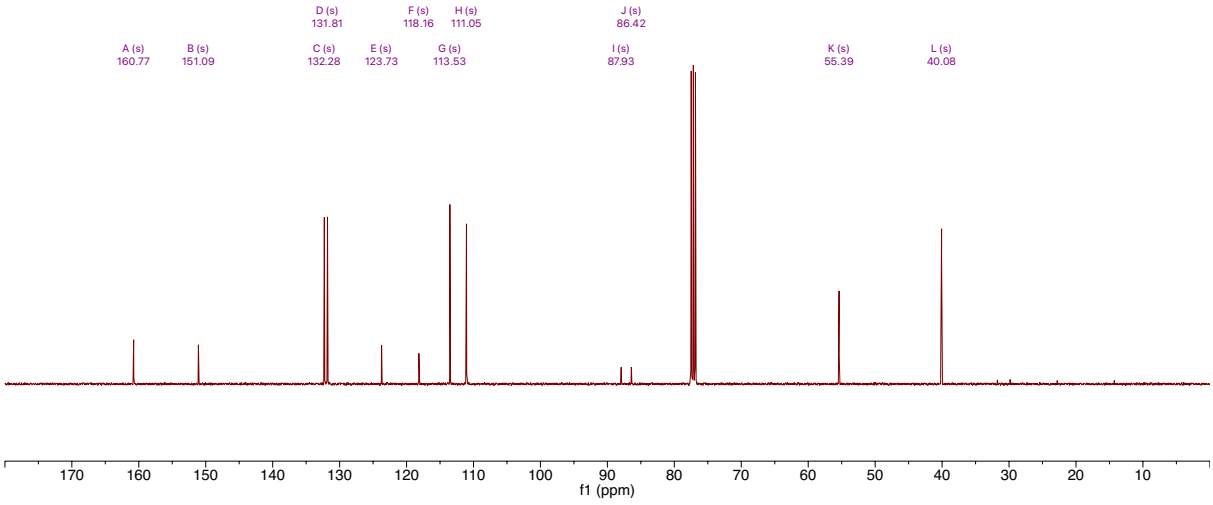

Figure B16. ^{13}C NMR spectrum of **1-*(N,N*-dimethylaniline)-2-(4-methoxyphenyl)-*o*-carborane** in $CDCl_3$ (101 MHz)

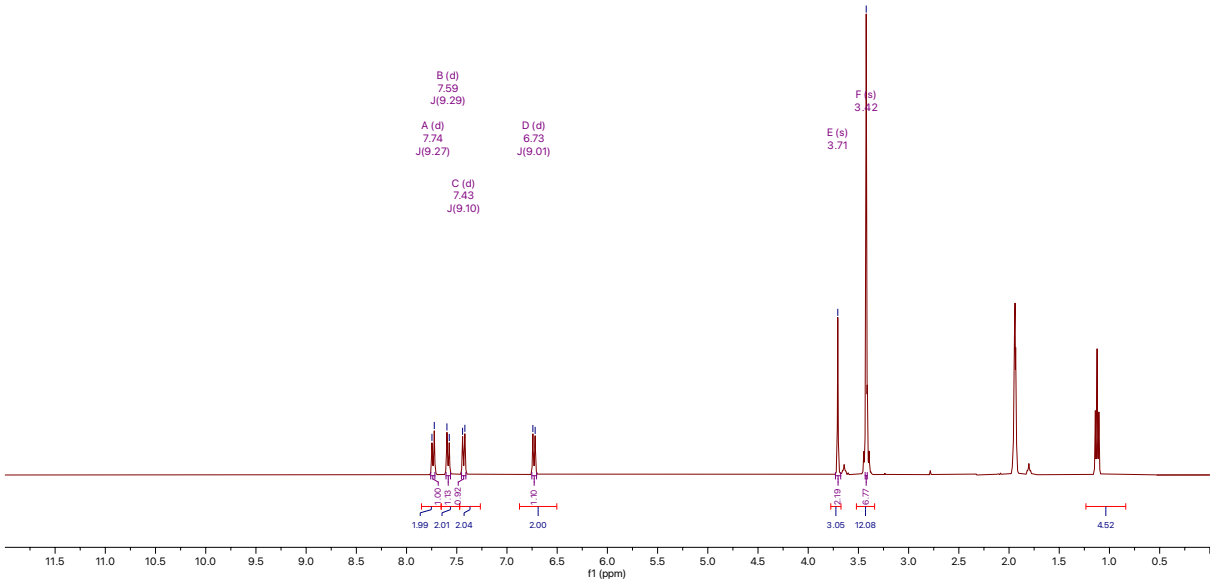

Figure B17. ^{1}H NMR spectrum of **1-*(N,N,N*-trimethylaniline)-2-(4-methoxyphenyl)-*o*-carborane triflate** in CD_3CN (400 MHz)

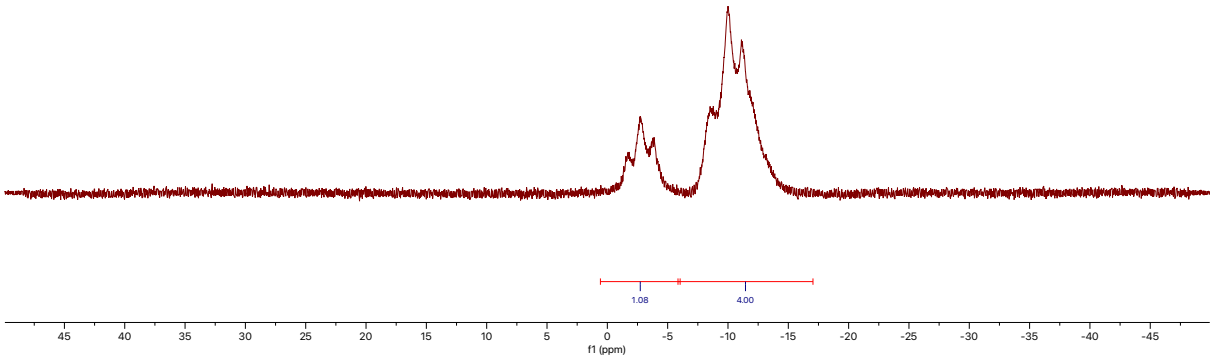

Figure B18. ^{11}B NMR spectrum of **1-*(N,N,N*-trimethylaniline)-2-(4-methoxyphenyl)-*o*-carborane triflate** in CD_3CN (128 MHz)

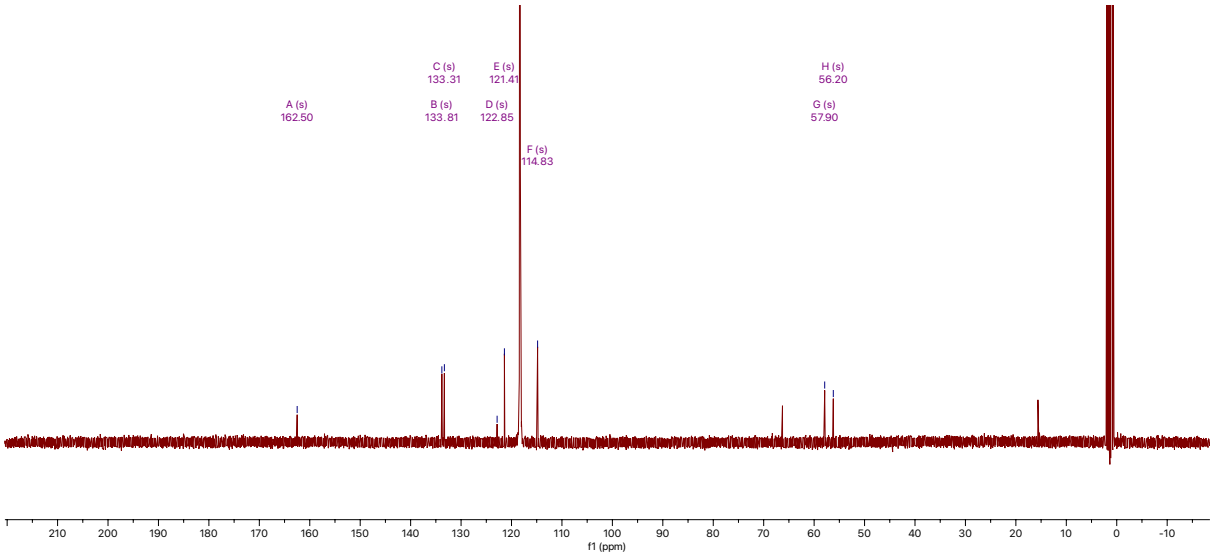

Figure B19. ^{13}C NMR spectrum of **1-*(N,N,N*-trimethylaniline)-2-(4-methoxyphenyl)-*o*-carborane triflate** in CD_3CN (101 MHz)

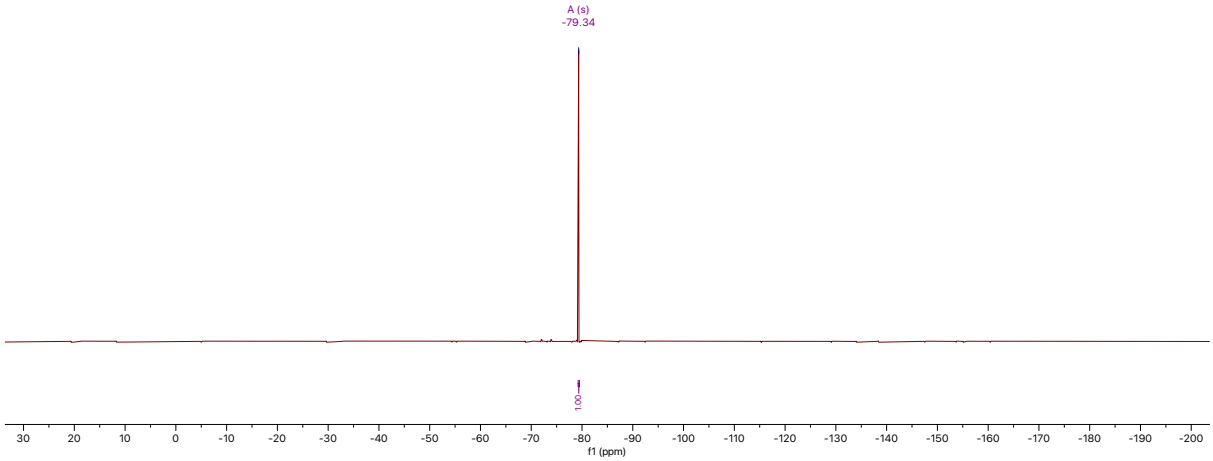

Figure B20. ^{19}F NMR spectrum of **1-*(N,N,N*-trimethylaniline)-2-(4-methoxyphenyl)-*o*-carborane triflate** in CD_3CN (376 MHz)

B4. X-RAY CRYSTALLOGRAPHY

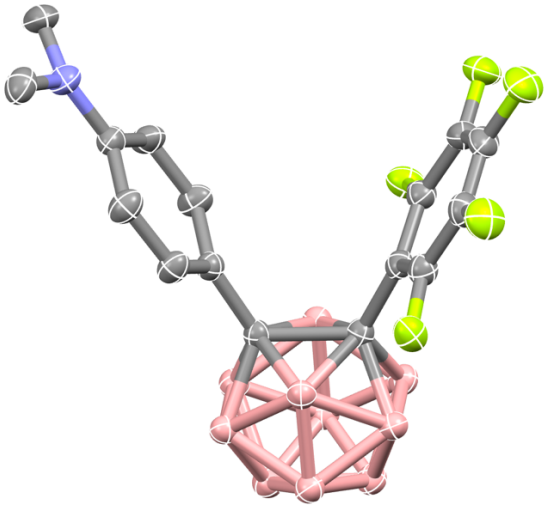

Figure B21. X-ray diffraction structure of **1-*(N,N*-dimethylaniline)-2-(pentafluorophenyl)-*o*-carborane** with thermal ellipsoids set at 50%.

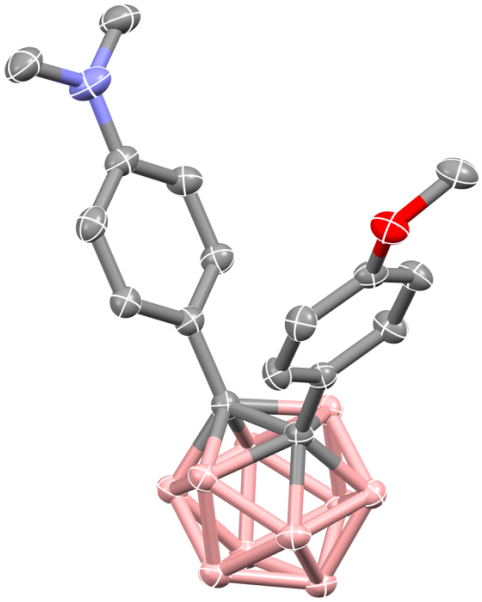

Figure B22. X-ray diffraction structure of **1-*(N,N*-dimethylaniline)-2-(4-methoxyphenyl)-*o*-carborane** with thermal ellipsoids set at 50%.

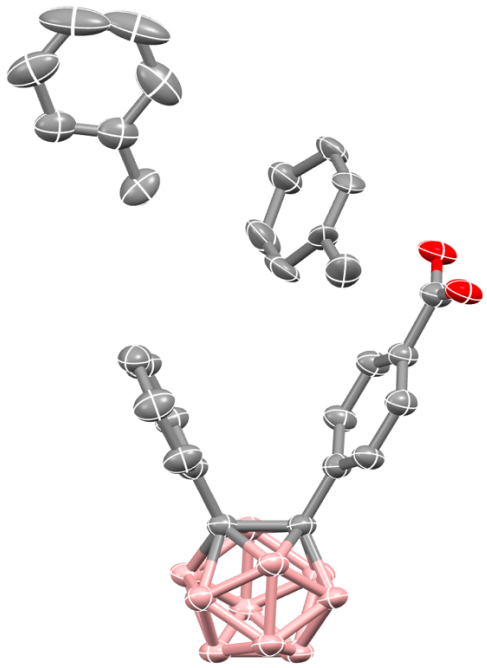

Figure B23. X-ray diffraction structure of **1-*(*4-carboxyphenyl)-2-(phenyl)-*o*-carborane** with thermal ellipsoids set at 50%.

B5. pK_a TITRATIONS

The pK_a values of the acid-appended carboranes were determined using a known method.[7] In brief, ^{1}H NMR spectroscopy is used to measure the proton-transfer equilibrium between an acid of interest and an acid with a known pK_a. The chemical shifts of the unknown acid and reference acid can be used to determine their concentration as well as their conjugate acid concentrations using the following equation:

$$[CbAr^{H+}] = \frac{\delta_{obs} - \delta_{CbAr}}{\delta_{CbAr^{H+}} - \delta_{CbAr}}$$

$$[CbAr] = [Cb]_{tot} - [CbAr^{H+}]$$

Similarly for $^{2\text{-Cl}}PhNH_3^+$ / $^{2\text{-Cl}}PhNH_2$:

$$[^{2-Cl}PhNH_3^+] = \frac{\delta_{obs} - \delta_{^{2-Cl}PhNH_2}}{\delta_{^{2-Cl}PhNH_3^+} - \delta_{^{2-Cl}PhNH_2}}$$

$$[^{2-Cl}PhNH_2] = [^{2-Cl}PhNH_2]_{tot} - [^{2-Cl}PhNH_3^+]$$

From these concentrations, the K_{eq} can be determined:

$$K_{eq} = \frac{[CbAr][^{2-Cl}PhNH_3^+]}{[CbAr^{H+}][^{2-Cl}PhNH_2]}$$

With K_{eq} and the known reference acid pK_a ($K_{a,ref}$), the analyte pK_a can be determined:

$$K_a = \frac{K_{eq}}{K_{a,ref}}$$

$$pK_a = -\log\{K_{eq}/K_{a,ref}\}$$

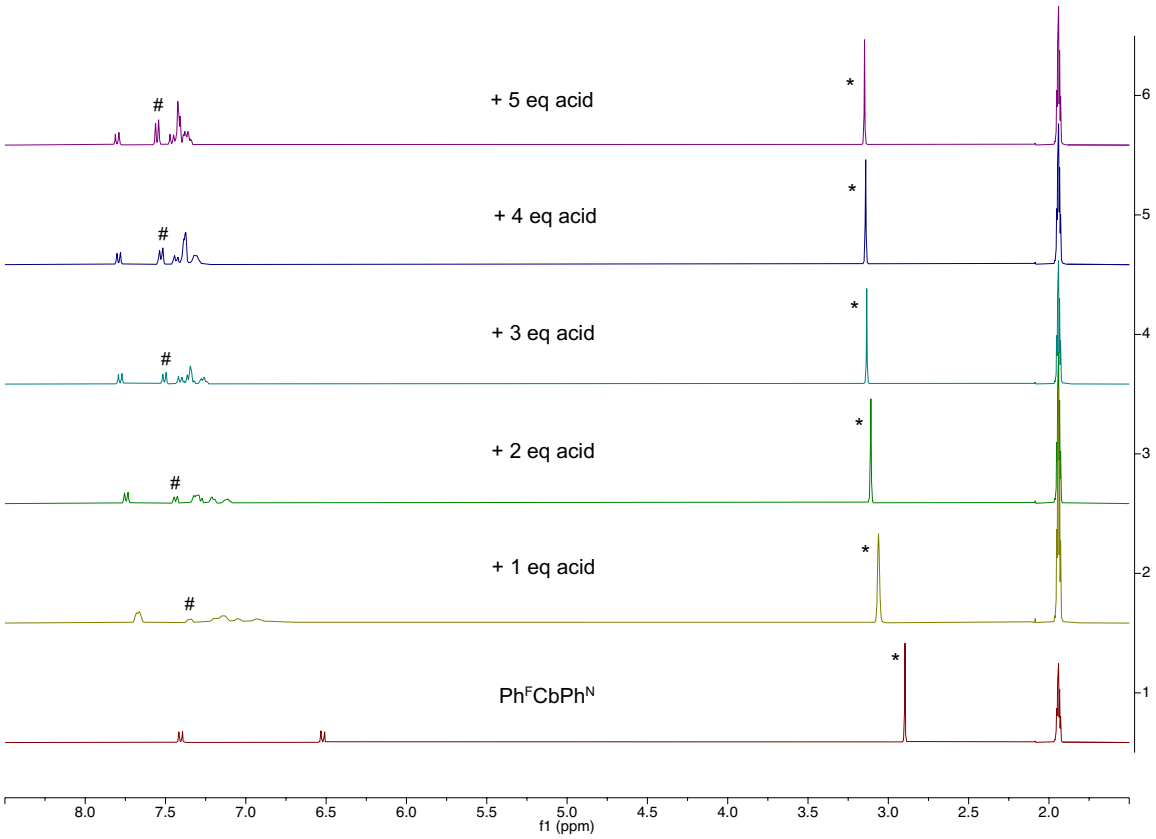

Figure B24. ^{1}H NMR Spectra of $Ph^{F}CbPh^{N}$ with 0-5 equivalents of [$^{2\text{-Cl}}PhNH_3$]OTf added in CD_3CN. The starred (*) and tagged (#) Cb-N*Me*$_2$ peak and $^{2\text{-Cl}}PhNH_2$ *ortho*-H peak shifts, respectively, are used as reporters of the analytes' concentrations.

Table B1. Reporter peak shifts from the ^{1}H NMR spectroscopy acid titration of $Ph^{F}CbPh^{N}$ and the resulting equilibrium constant K_{eq}

equiv. acid	# shift (ppm)	* shift (ppm)	[$Ph^{F}CbPh^{NH+}$]	[$Ph^{F}CbPh^{N}$]	[$^{2\text{-Cl}}PhNH_3^+$]	[$^{2\text{-Cl}}PhNH_2$]	K_{eq}
0	7.206	2.896	0	1	0	0	-
0.7	7.341	3.061	0.616	0.384	0.445	0.225	3.17
1.4	7.426	3.109	0.795	0.205	0.647	0.783	3.20
2.7	7.496	3.134	0.888	0.112	0.757	1.962	3.06
3.3	7.517	3.141	0.914	0.086	0.754	2.576	3.12
4.8	7.543	3.148	0.940	0.060	0.783	4.057	3.04

Determined as the average of rows in **Table B1**, the resulting equilibrium constant K_{eq} is determined to be 3.12. From this K_{eq} value and the known pK_a of $^{2\text{-Cl}}PhNH_3^+$ (7.86) in MeCN, the pK_a of [$Ph^{F}CbPh^{NH}$]$^+$ is determined to be 8.35 ± 0.01.

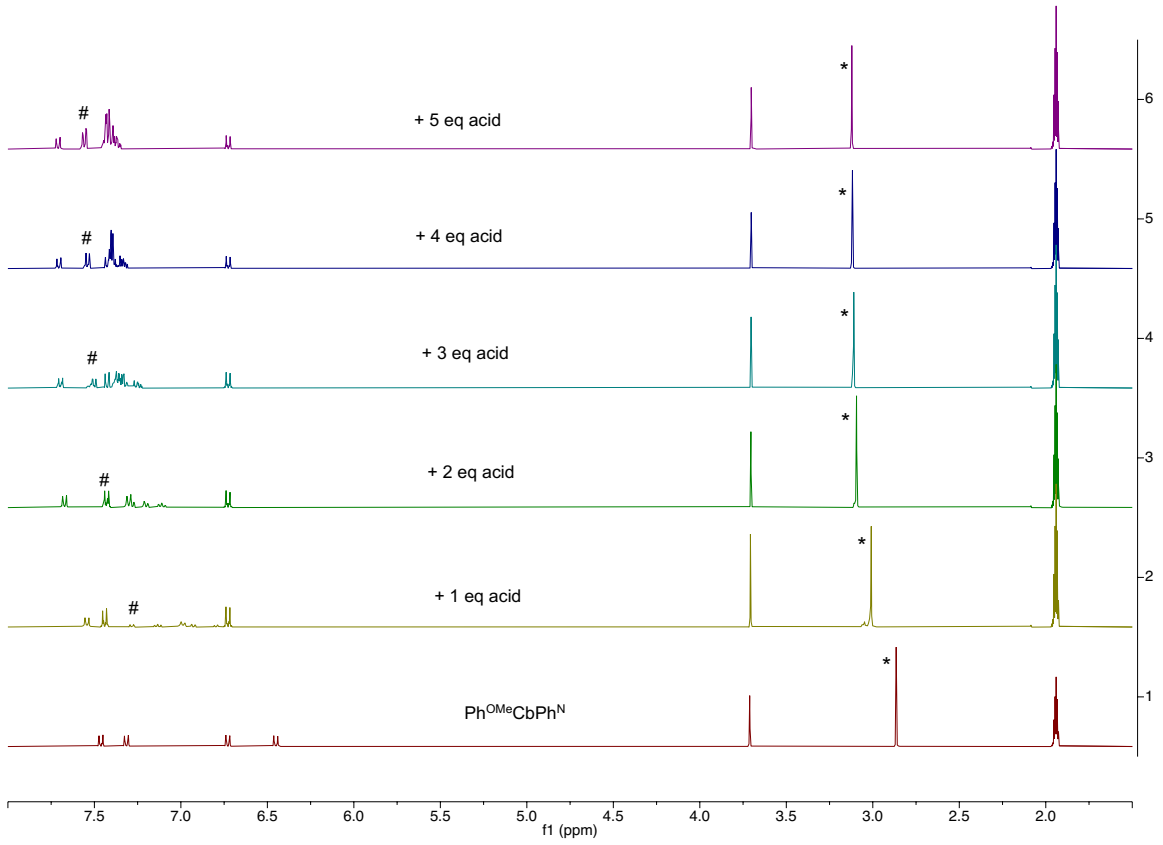

Figure B25. ^{1}H NMR Spectra of $Ph^{OMe}CbPh^{N}$ with 0-5 equivalents of $[^{2\text{-}Cl}PhNH_3]OTf$ added in CD_3CN. The starred (*) and tagged (#) Cb-N*Me*$_2$ peak and $^{2\text{-}Cl}PhNH_2$ *ortho*-H peak shifts, respectively, are used as reporters of the analytes' concentrations.

Table B2. Reporter peak shifts from the ^{1}H NMR spectroscopy acid titration of $Ph^{OMe}CbPh^{N}$ and the resulting equilibrium constant K_{eq}

equiv. acid	# shift (ppm)	* shift (ppm)	$[Ph^{OMe}CbPh^{NH+}]$	$[Ph^{OMe}CbPh^{N}]$	$[^{2\text{-}Cl}PhNH_3^+]$	$[^{2\text{-}Cl}PhNH_2]$	K_{eq}
0	7.27	3.009	0	1	0	0	
1	7.423	3.094	0.545	0.455	0.841	0.159	6.338
2	7.488	3.11	0.867	0.133	0.920	1.080	5.578
3	7.523	3.118	0.928	0.072	0.896	2.104	5.487
4	7.545	3.121	0.958	0.042	0.846	3.154	6.167
5	7.27	3.009	0.970	0.030	0.784	4.216	5.947

Determined as the average of rows in **Table B2**, the resulting equilibrium constant K_{eq} is determined to be 5.90. From this K_{eq} value and the known pK_a of $^{2\text{-}Cl}PhNH_3^+$ (7.86) in MeCN, the pK_a of $[Ph^{OMe}CbPh^{NH}]^+$ is determined to be 8.63 ± 0.03.

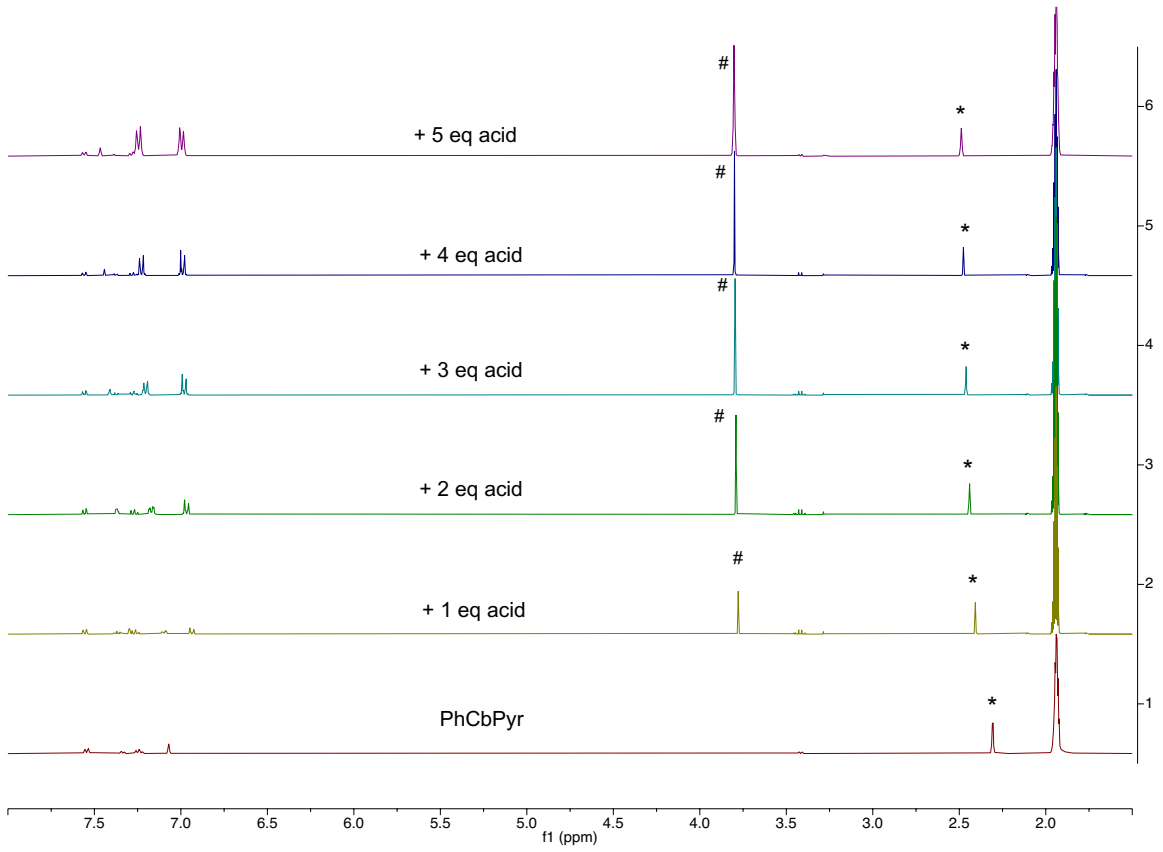

Figure B26. ^{1}H NMR Spectra of PhCbPyr with 0-5 equivalents of [^{MeO}PhNH$_3$]OTf added in CD_3CN. The starred (*) and tagged (#) Cb-pyr*Me*$_2$ peak and ^{MeO}PhNH$_2$ O*Me* peak shifts, respectively, are used as reporters of the analytes' concentrations.

Table B3. Reporter peak shifts from the ^{1}H NMR spectroscopy acid titration of PhCbPyr and the resulting equilibrium constant K_{eq}

equiv. acid	# shift (ppm)	* shift (ppm)	[PhCbPyr^{H+}]	[PhCbPyr]	[^{MeO}PhNH$_3^+$]	[^{MeO}PhNH$_2$]	K_{eq}
0	3.678	2.307	0	1	0	0	-
1	3.778	2.407	0.606	0.394	1.060	0.350	0.214
2	3.79	2.44	0.476	0.524	2.383	0.447	0.206
3	3.796	2.46	0.398	0.602	3.770	0.479	0.193
4	3.8	2.476	0.335	0.665	5.201	0.469	0.179
5	3.802	2.488	0.287	0.713	6.601	0.479	0.180

Determined as the average of rows in **Table B3**, the resulting equilibrium constant K_{eq} is determined to be 0.194. From this K_{eq} value and the known pK_a of ^{MeO}PhNH$_3^+$ (11.87) in MeCN, the pK_a of [PhCbPyr^{H}]$^+$ is determined to be 11.1 ± 0.1.

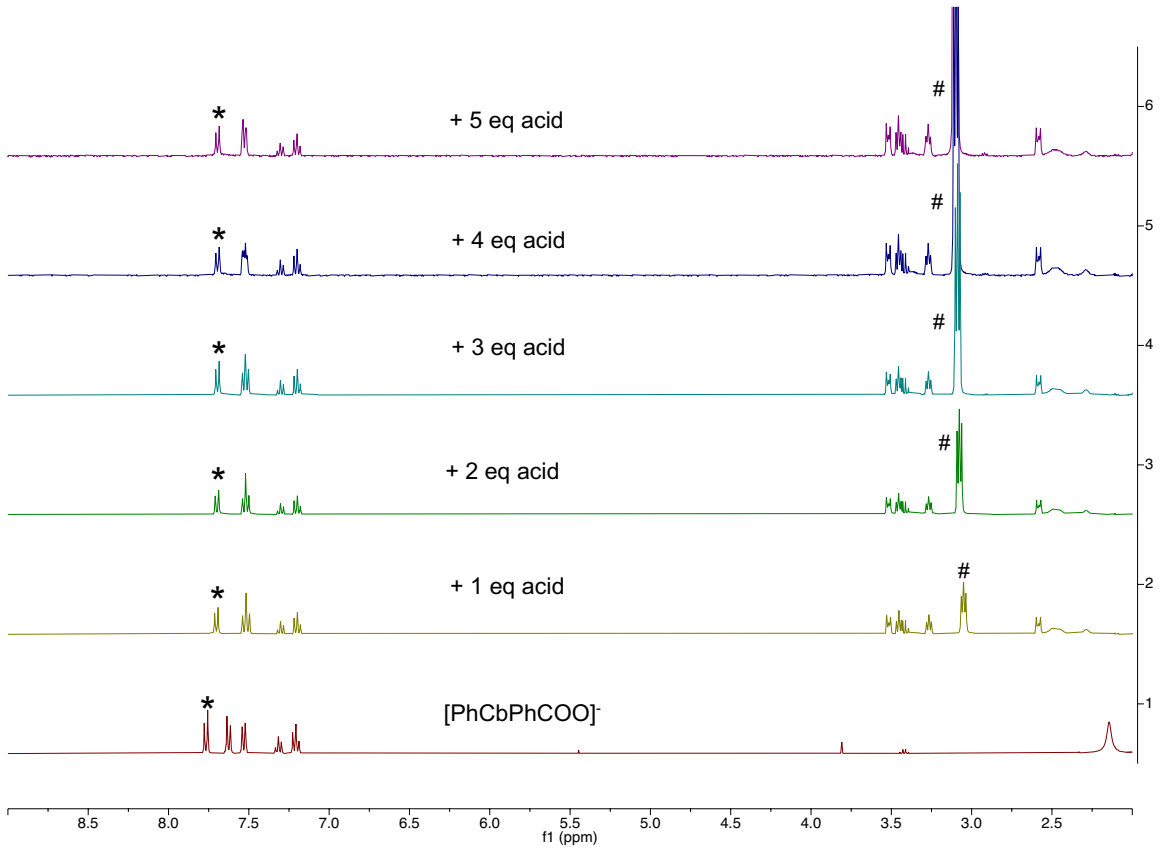

Figure B27. ^{1}H NMR Spectra of ^{n}Bu$_4$N[PhCbPh^{COO}] with 0-5 equivalents of [Et$_3$NH]OTf added in CD$_3$CN. The starred (*) and tagged (#) Cb-Ph*H* peak and Et$_3$NH$^+$ *CH*$_2$ peak shifts, respectively, are used as reporters of the analytes' concentrations.

Table B4. Reporter peak shifts from the ^{1}H NMR spectroscopy acid titration of PhCbPh^{COOH} and the resulting equilibrium constant K_{eq}

equiv. acid	# shift (ppm)	* shift (ppm)	[PhCbPh^{COOH}]	[PhCbPh^{COO}]	[Et$_3$NH$^+$]	[Et$_3$N]	K$_{eq}$
0	-	-	0	1	0	0	-
1.6	3.050	7.701	0.477	0.523	0.197	1.393	0.155
3.3	3.077	7.685	0.327	0.673	0.286	3.054	0.192
5.1	3.087	7.677	0.252	0.748	0.358	4.782	0.221
7.0	3.098	7.676	0.243	0.757	0.382	6.588	0.180
8.9	3.102	7.676	0.243	0.757	0.431	8.509	0.157

Determined as the average of rows in **Table B4**, the resulting equilibrium constant K$_{eq}$ is determined to be 0.182. From this K$_{eq}$ value and the known pK_a of Et$_3$NH$^+$ (18.8) in MeCN, the pK_a of PhCbPh^{COOH} is determined to be 18.1 ± 0.1.

B6. ELECTROCHEMISTRY

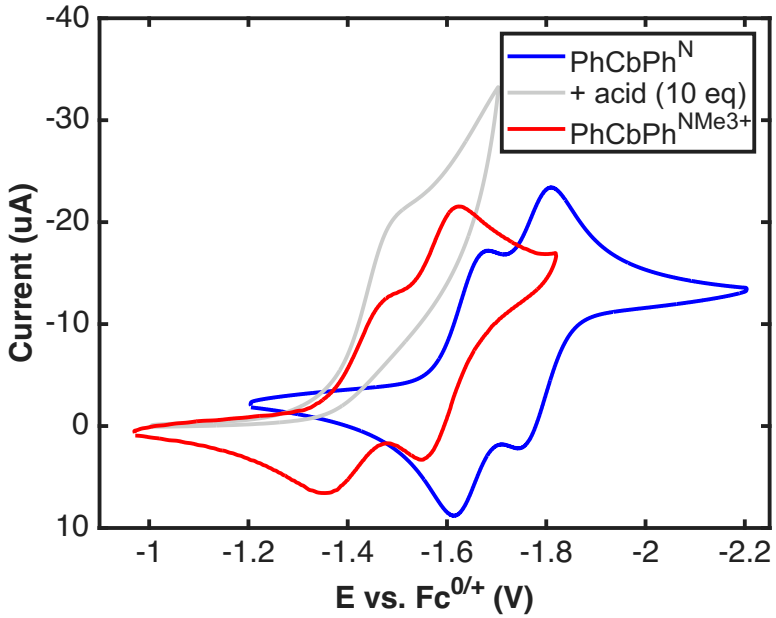

Figure B28. Cyclic voltammogram of **PhCbPh^{N}** (1 mM, *blue*) with 4-cyanoanilinium triflate (10 mM, *grey*) and **[PhCbPh^{NMe3}]OTf** (1mM, *red*) in MeCN with $^{n}Bu_4PF_6$ (200 mM) supporting electrolyte. The scans are swept cathodic, then anodic at 100 mV/s.

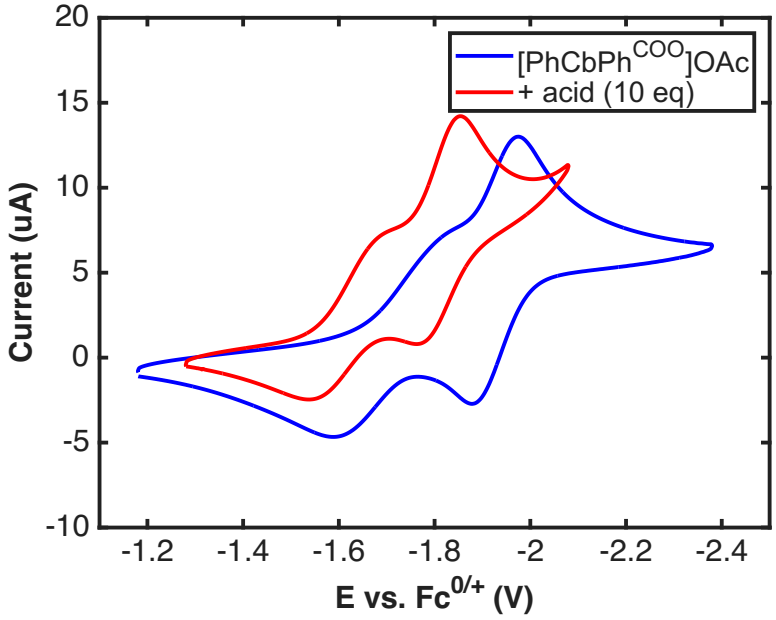

Figure B29. Cyclic voltammogram of **[PhCbPh^{COO}]OAc** (1 mM, *blue*) with acetic acid (10 mM, *red*) in MeCN with $^{n}Bu_4PF_6$ (200 mM) supporting electrolyte. The scans are swept cathodic, then anodic at 100 mV/s.

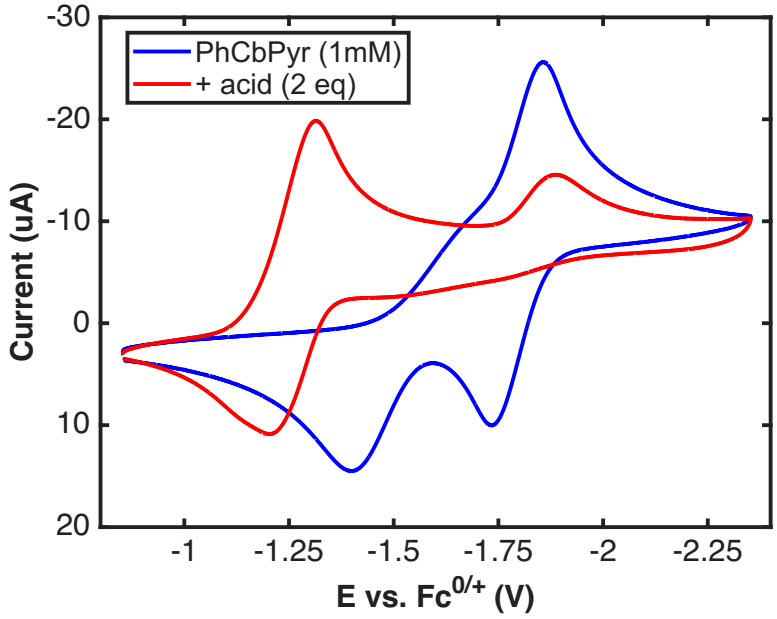

Figure B30. Cyclic voltammogram of **PhCbPyr** (1 mM, *blue*) with anilinium triflate (2 mM, *red*) in MeCN with $^{n}Bu_4PF_6$ (200 mM) supporting electrolyte. The scans are swept cathodic, then anodic at 100 mV/s.

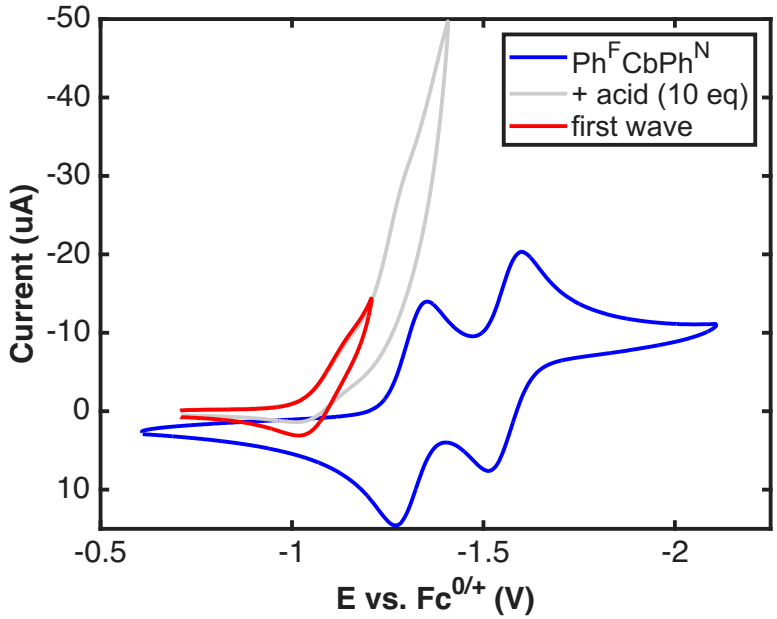

Figure B31. Cyclic voltammogram of **Ph^{F}CbPh^{N}** (1 mM, *blue*) with 4-cyanoanilinium triflate (10 mM, *grey*), and a shortened scan [–0.7 V to –1.2 V] centered around the first feature (*red*) in MeCN with $^{n}Bu_4PF_6$ (200 mM) supporting electrolyte. The scans are swept cathodic, then anodic at 100 mV/s.

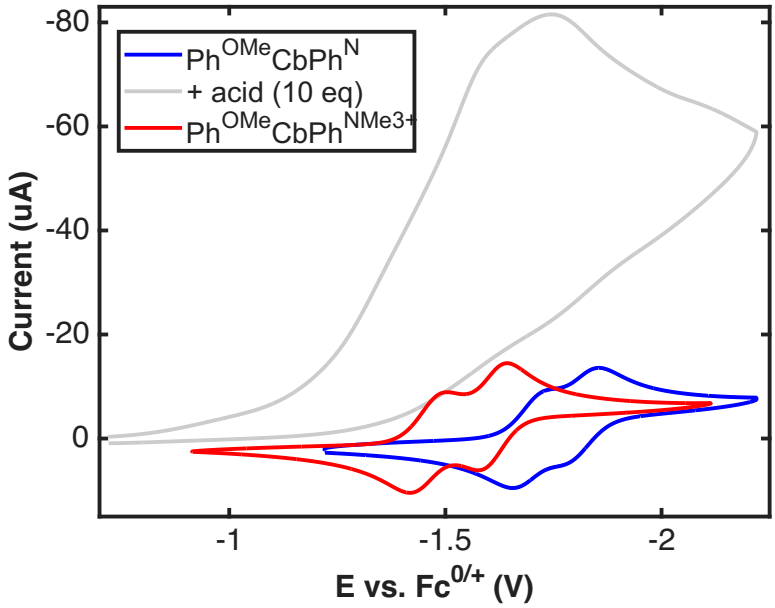

Figure B32. Cyclic voltammogram of **Ph^{OMe}CbPh^{N}** (1 mM, *blue*) with 4-cyanoanilinium triflate (10 mM, *grey*) and **[Ph^{OMe}CbPh^{NMe3}]OTf** (1mM, *red*) in MeCN with $^{n}Bu_4PF_6$ (200 mM) supporting electrolyte. The scans are swept cathodic, then anodic at 100 mV/s.

B7. COMPUTATIONS

Table B5. Computed energies of *o*-carboranes in their neutral free-base, reduced free-base, and reduced protonated states.

Compound	Energy (eH)	BDFE (kcal/mol)
$PhCbPh^{N}$	-926.50393123	-
$PhCbPh^{N}$ anion	-926.62042208	-
$PhCbPh^{NH}$	-927.06125017	**33.4**
$Ph^{F}CbPh^{N}$	-1422.14085248	-
$Ph^{F}CbPh^{N}$ anion	-1422.26854562	-
$Ph^{F}CbPh^{NH}$	-1422.70930199	**40.4**
$Ph^{OMe}CbPh^{N}$	-1040.85556169	-
$Ph^{OMe}CbPh^{N}$ anion	-1040.97040230	-
$Ph^{OMe}CbPh^{NH}$	-1041.41334198	**33.7**
PhCbPyr	-887.28932541	-
PhCbPyr anion	-887.41178398	-
$PhCbPyr^{H}$	-887.87398524	**50.6**
$PhCbPh^{COO}$ anion	-980.65327133	-
$PhCbPh^{COO}$ dianion	-980.77131449	-
$PhCbPh^{COOH}$ anion	-981.25094117	**58.8**

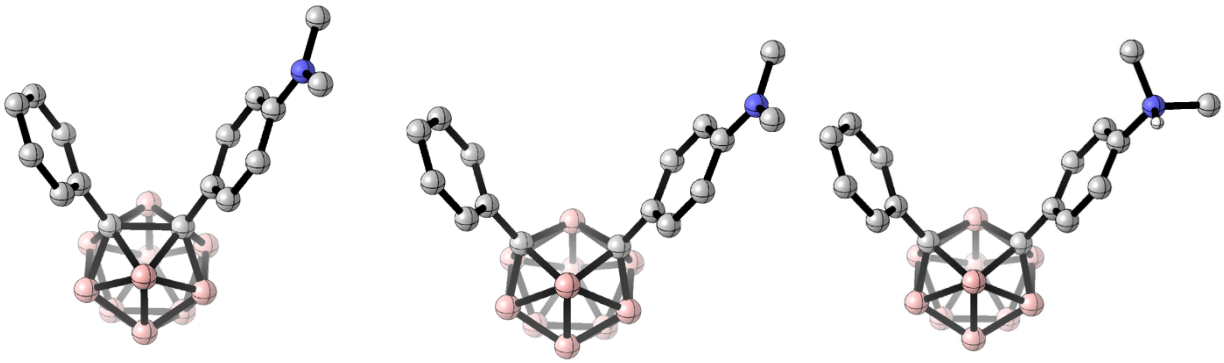

Figure B33. Optimized geometries of $PhCbPh^{N}$, $[PhCbPh^{N}]^{-}$, and $PhCbPh^{NH}$

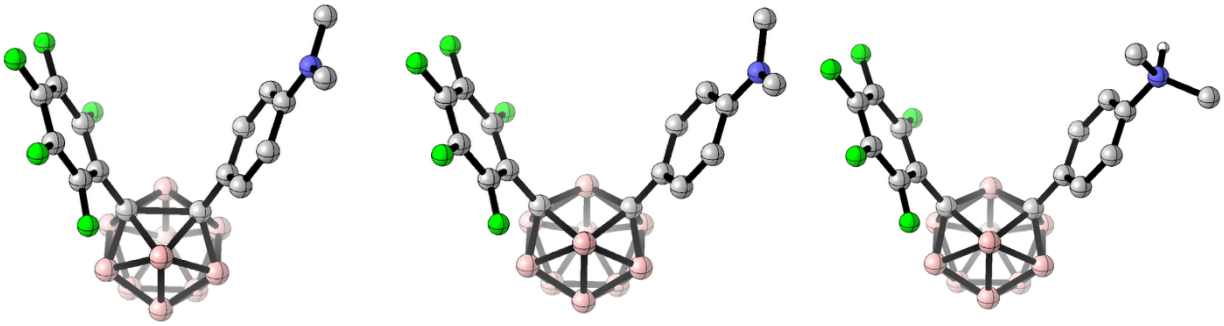

Figure B34. Optimized geometries of $Ph^{F}CbPh^{N}$, $[Ph^{F}CbPh^{N}]^{-}$, and $Ph^{F}CbPh^{NH}$

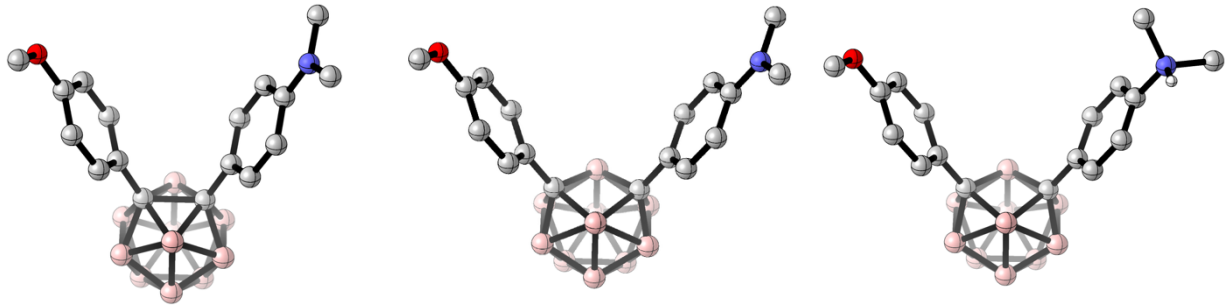

Figure B35. Optimized geometries of $Ph^{OMe}CbPh^{N}$, $[Ph^{OMe}CbPh^{N}]^{-}$, and $Ph^{OMe}CbPh^{NH}$

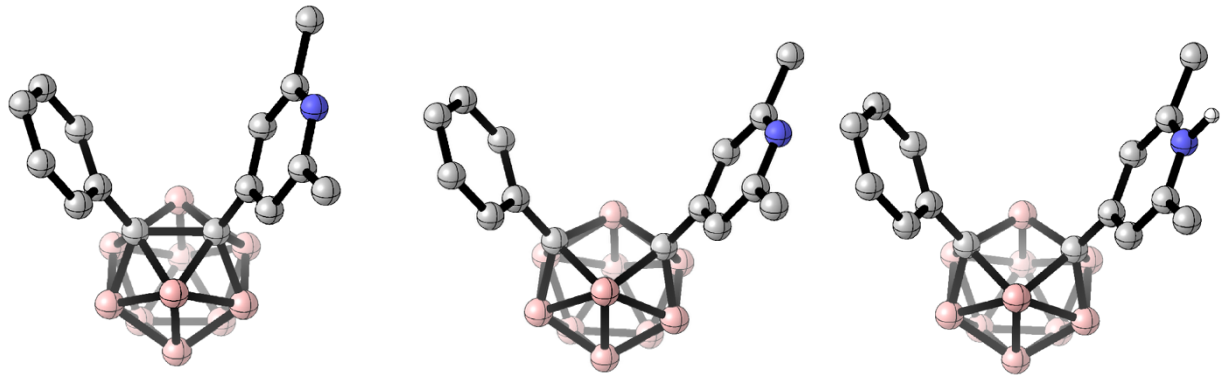

Figure B36. Optimized geometries of PhCbPyr, $[PhCbPyr]^{-}$, and $PhCbPyr^{H}$

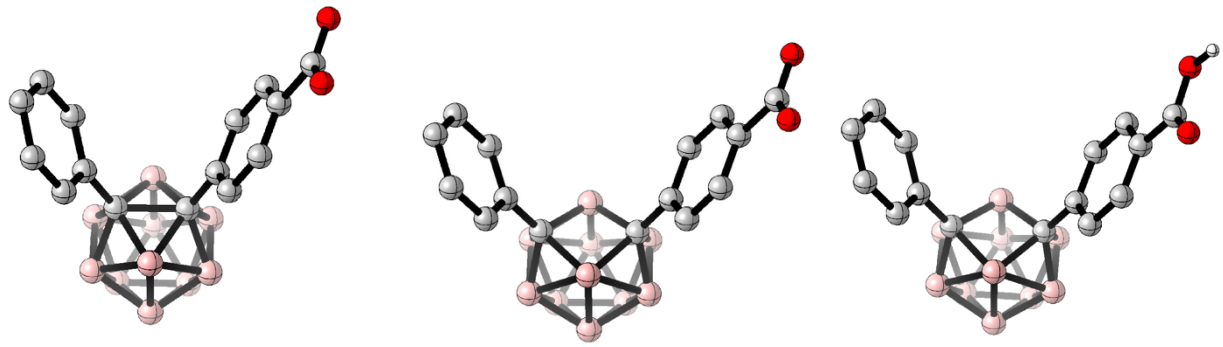

Figure B37. Optimized geometries of $[PhCbPh^{COO}]^{-}$, $[PhCbPh^{COO}]^{2-}$, and $[PhCbPh^{COOH}]^{-}$

Minimum Geometry Coordinates and Sample Input File

The Cartesian coordinates resulting from geometry optimization using ORCA are attached below for the specified species of interest.

The geometry optimization was done with def2-SVP. The output xyz coordinate was used for single-point energy calculation.

A sample input file is included here for reference and convenience:

```
! B3LYP def2-SVP Opt NumFreq SlowConv

!CPCM

%cpcm smd true

    SMDsolvent "ACETONITRILE"

end

%pal

nprocs 8

end

%maxcore 3000

!NormalPrint

!Printbasis

!PrintMOs

%scf

maxiter 1000

end

* xyz Q S

#insert coordinates here#

*
```

Minimum Energy Cartesian Coordinates

CARBORANES # # #

PhCbPhN, Q = 0, S = 1

C	-0.88109807513760	-0.00535815436165	1.36878223903351
C	0.90870765104199	0.01887923758000	1.37831533598866
B	0.02905970370025	-1.39727196855879	0.92706612070838
H	0.04248221097018	-2.34104886781351	1.64652212659567
B	-1.42414154156739	-0.89747759773797	0.02533567101157
H	-2.42691323956827	-1.53422294789814	0.16408285532908
B	-1.44609975938240	0.87689697023979	0.02888572032361
H	-2.46485256487975	1.48747814086722	0.16724765363084
B	-0.00602064493877	1.41238674805366	0.93233406991820
H	-0.02184411564257	2.35249353309947	1.65682400860542
B	1.46677016237442	-0.85839866846717	0.02728898102237
H	2.48580592497334	-1.46962339958406	0.16139394898701
B	0.03014952679441	-1.43268203611233	-0.84712919718776
H	0.04444799278255	-2.48106302423700	-1.43229665328063
B	-0.87904455920201	0.00022786027588	-1.41325458362262
H	-1.53279866355070	-0.00590198770089	-2.42148102823382
B	-0.00672916059000	1.45410373307742	-0.84203372457295
H	-0.02092053664484	2.50444598353815	-1.42367998296881
B	1.44442061137812	0.91555253857954	0.02968492273602
H	2.44749488173318	1.55194371200716	0.16789728525097

B	0.89858660966479	0.02308270105910	-1.41273329275960
H	1.55297980253893	0.03288304262509	-2.42062923097661
C	-1.62579135676362	-0.00970467969090	2.68003964671392
C	-1.93794564486596	-1.21724339382873	3.33108868603754
H	-1.62748913701025	-2.17005278546536	2.90223605617145
C	-2.65749605569977	-1.21511513192114	4.52891897568895
H	-2.88889877484644	-2.16525530225941	5.01748423911369
C	-3.08088438290882	-0.00966866402866	5.09672022896375
H	-3.64363420498956	-0.00976781790396	6.03410444739182
C	-2.78451591639771	1.19561404832456	4.45282998282676
H	-3.11555242132034	2.14514407006618	4.88152345855462
C	-2.06465254957108	1.19712854814037	3.25560577687349
H	-1.85235099042715	2.14838414229272	2.76709559561445
C	1.64294503624707	0.02076149977493	2.68181753512690
C	2.07499622810128	-1.17912610734476	3.28197987238819
H	1.85859272451415	-2.13709444180356	2.80680728174547
C	2.78833357723948	-1.18972067463936	4.47404814764169
H	3.09463905888094	-2.15131268061992	4.88451231070858
C	3.11650140950368	0.01935750432804	5.14977473236699
N	3.80972936335283	0.01849249893515	6.33024141924877
C	2.69183932008754	1.22971430972363	4.53267982639361
H	2.92321228020585	2.19164319559747	4.98890818787283
C	1.98059613753619	1.22073587905152	3.33917641983728

H	1.69020316096195	2.18039337567281	2.90938344754302
C	4.13115049583972	1.27256464528224	6.99145347575445
C	4.24828897779617	-1.23546872754199	6.92076158140671
H	4.93121916355866	-1.79125719500813	6.25289473955887
H	3.39836538608587	-1.89989630343783	7.15979794927995
H	4.78561635874716	-1.02728341646067	7.85438493840189
H	3.22354910525570	1.84933061384537	7.24468759773501
H	4.77587032295220	1.91827031281634	6.36759219897600
H	4.66742796308639	1.06203655057206	7.92508882852469

PhCbPhN, Q = -1, S = 2

N	7.54255865320178	6.90332912054107	11.81923642517229
C	7.74436957756651	4.93038316978508	13.25028357835893
H	7.59408405193889	5.52721414133132	14.14998367077429
C	5.18594731574281	-0.12159994620610	12.33467173679451
C	8.12841652452774	3.32377161334628	11.01147491758394
H	8.27743215122364	2.71458929077606	10.11675768596309
C	7.73230345393817	5.54715619401560	11.96905741978583
C	7.92670942668333	4.69145511894451	10.85008691090336
H	7.92376291769928	5.09883457124946	9.83898783070024
C	8.14926700086424	2.70856227971369	12.28311121144795
C	6.62923478663549	-0.41093862726692	12.47798905888005
C	8.38127173228741	1.26097311114943	12.44613312829199

C	7.94795929152018	3.56090970686604	13.39170223384951
H	7.95229018224469	3.14045212330125	14.40015459428963
C	4.56088623148201	-0.11828339214471	11.06656041619163
H	5.15275568984801	-0.32937281283050	10.17339557948532
C	4.37751905611337	0.15138130065474	13.46198819462729
H	4.82512327074179	0.15234444657487	14.45805592016657
C	3.01296373113246	0.41658348765605	13.32636839956247
H	2.41420421546774	0.62385432416920	14.21823810599144
C	7.45840113686513	7.48477350808199	10.49177509593014
H	8.37779618134695	7.30713041461050	9.90537677160658
H	7.32339834892904	8.57041014970289	10.57956250502910
H	6.60871404681426	7.08203942166160	9.90792920400861
C	3.19584516730250	0.14616730201570	10.93394215814094
H	2.74085163717209	0.13935120297909	9.93903683533342
C	2.41131974123221	0.41808594206086	12.06170951025957
H	1.34315898712204	0.62708875341814	11.95632614711275
C	7.28741118480467	7.73699505645143	12.97960914585756
H	6.34740473626324	7.46599762913652	13.49810241120517
H	7.20779681823026	8.78470600825018	12.66253923506036
H	8.10480889538907	7.67266754980315	13.71978628763161
B	7.78379085681799	0.10597897780965	11.30388819587980
H	7.36324186263216	0.52695063570048	10.26098938018064
B	9.43195259451017	0.59042207666345	13.50365084814961

H	10.08370249411028	1.33941112219859	14.18407577282183
B	9.57542696238131	0.40997437786145	11.72385574403279
H	10.33921073838100	1.01704073682084	11.01841756006090
B	7.59298060249369	0.34596321260699	13.68939527965899
H	7.02183571233515	0.96154103141739	14.54778858522416
B	7.25984600789970	-1.48501650847236	13.53969124886243
H	6.48854257334258	-2.08730875735329	14.24053111290738
B	9.05308714584581	-1.22658893334958	11.30742914556119
H	9.53247068022294	-1.74582625022080	10.32889066380466
B	8.82635522963610	-0.93938451006580	14.15157663725555
H	9.14125217211904	-1.24637391687036	15.27573587031676
B	10.01824420423136	-0.93542447712562	12.80100320613544
H	11.17437302133280	-1.26145541120606	12.92691878575737
B	7.40128573194150	-1.66234138234573	11.76127557643104
H	6.74311507121778	-2.40589880745617	11.08081663112292
B	8.74188226422170	-2.15300514945388	12.82196817980887
H	9.01714793199557	-3.32063522695771	12.96157225003095

PhCbPhNH, Q = 0, S = 2

C	1.98811108370008	-0.19345940114119	2.59701658588970
C	-2.38488871334321	1.42007351109392	3.06817628555875
H	-1.98352282236354	2.33022619292213	2.61761918872057
C	-2.06994071662239	0.16358534233518	2.50318460614487

C	-2.61676572502953	-0.98667160121262	3.11572842646341
H	-2.39879826932218	-1.97346465227897	2.70198971592834
C	-3.43850680796478	-0.88387391415965	4.24010387671325
H	-3.84900261699770	-1.79190974773561	4.69133261378462
C	1.18209028421986	-0.16423027958740	1.36208877059324
C	-1.21207836663180	0.05691778520744	1.30315682962290
C	-3.20729616012307	1.51972984694928	4.19246751464235
H	-3.43527678097025	2.50631671322379	4.60638595159784
C	2.57745528234781	0.98510192695886	3.11159766490366
H	2.42866117609969	1.93502472050426	2.59566896816686
C	2.21219360689046	-1.39682941869589	3.30154447176152
H	1.77645094177799	-2.32894873420180	2.93879241209712
C	-3.73878649967382	0.36937247420144	4.78807161900777
H	-4.38148465983550	0.44853733465959	5.66916094859554
C	3.35872280670526	0.96669150796836	4.26483128706017
H	3.80788989946834	1.89264126323557	4.63046302754857
C	2.98848241954340	-1.42459532115769	4.45966047128355
H	3.15102072223680	-2.36844238907408	4.98786234587629
C	3.55906242890508	-0.24316098567668	4.93425408285063
N	4.39543368972386	-0.29714066557213	6.15315626892062
B	0.09983898976200	1.14677832034167	1.02276516875192
H	0.17545468637358	2.11756005238557	1.72368425767969
B	-1.39640811511496	0.93731532398043	-0.06206088152892

H	-2.31070773945045	1.71831196728650	-0.09615778157035
B	1.43032674187848	-1.12248878802066	0.05912639100150
H	2.34376493327088	-1.90323549788224	0.11750936935356
B	1.58878710074786	0.66612981030739	0.01395007962136
H	2.62702201259946	1.27303827199257	0.03027692235616
B	-1.55552451169104	-0.85159170767691	-0.01041432665267
H	-2.59278827452593	-1.46056305691963	-0.00631876288191
B	0.16314451118117	1.31346308936479	-0.80583815550090
H	0.27316464977873	2.35103760431545	-1.41103906378564
B	0.92600387346396	-0.21161980443548	-1.38492072192421
H	1.56193483506464	-0.29459305038830	-2.40708755125061
B	-0.11402987520625	-1.26843355687044	1.08877453912882
H	-0.22015140024448	-2.20032264255883	1.83605398035272
B	-0.82959597953504	-0.05533727710706	-1.42755117857498
H	-1.41924550209750	-0.03212845124315	-2.48012958219658
B	-0.09441073223132	-1.54297752043566	-0.72827013367118
H	-0.18043826738450	-2.61461845340755	-1.27522678617967
C	3.85931529224762	0.53601657153472	7.28130984754726
C	5.84395248316615	-0.00518988920764	5.88321609322177
H	3.92145227745107	1.59503470874986	7.00427972314901
H	4.47364585808501	0.34041643202866	8.16935598941289
H	2.81803497987785	0.24433875351313	7.46346118861019
H	6.19316348990097	-0.68296018065133	5.09493566994839

H	6.40527174378455	-0.17391442371117	6.81121997760263
H	5.94175031422383	1.03958900560140	5.56474655096172
H	4.35980702888271	-1.27272924765218	6.48040368828566

PhFCbPhN, Q = 0, S = 1

F	7.55296662073754	9.31665915553937	9.99848475703664
N	11.81990448040906	3.26995984995978	8.41126731831397
C	6.11997325290769	6.44879464077065	7.30466643510634
C	6.70672433115402	3.87979883212086	5.91421142739658
C	7.09119002427751	8.41367179111782	9.14505659902820
C	9.20608403489914	4.24206310629130	5.97580491084793
H	9.15217110777839	4.76834761088234	5.02164813073958
C	5.61947010953181	5.41751443387267	6.33482646927102
C	8.03021243376088	3.73104599456601	6.56732938514797
C	6.81078449982939	7.60830475051677	6.88418274343714
F	7.00987392650401	7.87696950420380	5.59485869361911
C	8.17838812826063	3.03791914142339	7.78855635496086
H	7.30509995150324	2.60717029963130	8.28057742485387
C	7.29943798253637	8.56273202983964	7.77649248797399
F	7.95124565044261	9.62779573127673	7.31688478741438
C	9.41535723495344	2.87506897802566	8.39467965623409
H	9.46261657020691	2.32916308682948	9.33615161171125
C	6.37435548276212	7.31110510313345	9.60095192070417

F	6.13133289585484	7.16625202785267	10.90110066859678
C	5.89186071453689	6.36491392107345	8.69650108978335
F	5.16861935092451	5.38420002862123	9.23341820637622
C	10.45134886405473	4.08853838076434	6.56750448392012
H	11.32075191925763	4.50181977395673	6.05743314077993
C	10.60074775062841	3.40781624786361	7.81042980534886
C	13.00968117504399	3.83876846433077	7.79716189008194
H	13.21973457051108	3.39088190675011	6.80917959683123
H	13.87497378156264	3.65129032363191	8.44461959614338
H	12.91865092264657	4.93087297010776	7.65947203401772
C	11.93909285125953	2.55883560155361	9.67492241165729
H	11.35333676270083	3.04239461267142	10.47735011155260
H	12.99125555367774	2.54553684933875	9.98459932373077
H	11.59645376667749	1.51206373022416	9.59228910854045
B	5.28265269067626	3.80964354584524	6.89065007591639
H	5.39522541985517	3.52524187357831	8.03240054511169
B	4.01264046656403	4.92617682208243	6.27601437685344
H	3.26033583367968	5.43522246157871	7.05386768254790
B	5.64442957412184	2.60383283115092	5.62745902510323
H	6.00887977158809	1.51678278285469	5.96851238147215
B	6.45779793887996	5.20563439984567	4.83343315377460
H	7.38339326375759	5.89127932319388	4.56132343059067
B	3.98628318952381	3.20623812289019	5.82795471932018

H	3.12501678892125	2.48587139801128	6.25360355953982
B	5.21672810156679	4.66793306788403	3.67268044047147
H	5.25291590904953	5.01407473090180	2.52344824845529
B	4.68092956327018	3.04423802994635	4.19001993890501
H	4.33019852774742	2.19656544756013	3.41377336535833
B	3.69068600288341	4.45839279103787	4.58517051496565
H	2.60967381409955	4.65122425342501	4.09728862193536
B	4.77161173728790	5.82936472035399	4.94183036290375
H	4.56643022637142	6.99131912712483	4.75136455289244
B	6.40313877454780	3.50494042653110	4.29973648444713
H	7.32290570381618	3.07708496546176	3.66582593827727

PhFCbPhN, Q = -1, S = 2

N	7.14900087072786	6.89880670323953	11.75431531674372
C	7.55990657991985	4.96088179093811	13.19312189503214
H	7.46188926209557	5.56749915285647	14.09314103899611
C	5.12928112369233	-0.23549325884657	12.32804001844675
C	7.81484683919955	3.32503688437028	10.95899102254171
H	7.90965679953520	2.70435030745739	10.06512610673666
C	7.40736928109164	5.55089418517572	11.90838036139126
C	7.53634267120237	4.67846601047025	10.79331383720766
H	7.42376783170244	5.06043784611811	9.77877346896702
C	7.97612746421591	2.73843211246497	12.23347558087422

C	6.57917223180243	-0.44495533306449	12.47848299468892
C	8.27442469277774	1.30343738646758	12.40703807097505
C	7.83680860178705	3.60534558819748	13.34011606811827
H	7.94690656475998	3.20812898081549	14.35195647688006
C	4.47534814402212	-0.28822717363528	11.07530032566796
F	5.15240855528328	-0.59616520858474	9.96154678718352
C	4.27758388709320	0.03025270240600	13.42484855364895
F	4.75586444246693	0.03807614953292	14.67542149304995
C	2.91337689898634	0.28066738847389	13.28722925873313
F	2.17005956762347	0.54043228445738	14.36579189279151
C	6.75327240287064	7.41933360901407	10.45692877157886
H	7.47481038481315	7.14108878074783	9.67284955336804
H	6.72522254329454	8.51635727356065	10.50215507436347
H	5.75279852427509	7.06287310344321	10.13889898731519
C	3.11232690111535	-0.04382839056512	10.91754188028768
F	2.55968664442953	-0.10229645322782	9.70342459825802
C	2.31946839950434	0.24791482451887	12.02654479207496
F	1.01577619573667	0.48572847658085	11.88398793258969
C	6.86933269017971	7.71816605929859	12.92049246245868
H	5.91655138867132	7.44824300323580	13.41888148272951
H	6.80708438831654	8.77108713776256	12.61476427462676
H	7.67349578640821	7.63878324675244	13.66957878952620
B	7.72620631806994	0.11645605783832	11.29094213413891

H	7.29705091173759	0.50397235898880	10.24382910086952
B	9.35571126576282	0.70064033899942	13.47239859126839
H	9.97535038277322	1.48725438790945	14.13898563369128
B	9.50616942876973	0.49168810324816	11.70028507903367
H	10.23776441490551	1.11756409990135	10.97811789734621
B	7.52677487790193	0.38914556265502	13.67116117682208
H	6.94666146014381	1.01451178671834	14.51011134315639
B	7.26576219189366	-1.46481556420019	13.56133387299788
H	6.53458699104315	-2.09859441007471	14.27413816511779
B	9.04157558007147	-1.16969128606989	11.31684184439821
H	9.53137452889228	-1.69024645989818	10.34476192105746
B	8.80737664066733	-0.83732877412518	14.15397886328343
H	9.13220637837117	-1.10782481544614	15.28420423721493
B	9.99903786578913	-0.81629775200534	12.80229332378707
H	11.16600519662525	-1.09655051661105	12.93367062279815
B	7.41117606952007	-1.66949590901953	11.78316245358563
H	6.79521348688146	-2.46395062032174	11.12473616823880
B	8.77235842813584	-2.07965611523626	12.84887055592700
H	9.09273902244365	-3.23264564368317	13.00874784741457

PhFCbPhNH, Q = 0, S = 2

N	7.05367060005278	6.89975464488889	11.67491378759620
C	7.43135571795923	4.93469962700051	13.16785992944244

H	7.27977228782863	5.56661353961663	14.04554483392070
C	5.12097139770282	-0.28636387134920	12.34340199199206
C	7.82609330284068	3.29925791813492	10.93123955288705
H	7.98078392827902	2.67779771250661	10.04792876013181
C	7.34837979568950	5.46372975582492	11.87775380943579
C	7.54418305385474	4.65441820874310	10.75849038710363
H	7.48004542065120	5.07897435294775	9.75265228182464
C	7.91772884893089	2.72939191832131	12.21924885836402
C	6.57571746955050	-0.47362676889817	12.48690228244114
C	8.23286522645254	1.29790637282718	12.40589146474814
C	7.71268194811708	3.57962888390810	13.32968486595966
H	7.77863778542295	3.17606231121236	14.34121543605194
C	4.46346494698862	-0.36122738305981	11.09435877047760
F	5.14127649059772	-0.66275699483785	9.98048886969178
C	4.27247504397970	-0.02870947352583	13.44378852621219
F	4.75791063427053	0.00070599802158	14.69025594682628
C	2.90260393120852	0.19277631889990	13.31209838729809
F	2.16059528060863	0.44659237266285	14.39201084834397
C	8.11728716298633	7.80249819573525	12.23173486989623
H	9.08416065029616	7.50148641202950	11.81073328781798
H	8.12558852255845	7.70842329941873	13.32425575790461
H	7.87574199550772	8.83275918543692	11.94112704583770
C	3.09476954928775	-0.14624148853143	10.94280958499246

F	2.53632892811860	-0.22494811048391	9.73336208370660
C	2.30330176841958	0.13724799145658	12.05487574924202
F	0.99554326849545	0.34759332601393	11.91805475946931
C	5.68424402213375	7.29205658729752	12.15055617291633
H	4.94829104054495	6.63833098158970	11.66725992568420
H	5.51247696006906	8.33882151312530	11.86874337824771
H	5.64223370507699	7.18073714859470	13.24057753740352
B	7.70446650394965	0.09847817917137	11.28754371892159
H	7.26251400654839	0.48518504532885	10.24616296810714
B	9.33340184880527	0.72755921367082	13.46761297713537
H	9.93423953437317	1.53299368093909	14.12750032838991
B	9.47311133302249	0.51469140582031	11.68873169873756
H	10.18226755288590	1.15311875023722	10.95699210730861
B	7.51558114773822	0.38366348254863	13.67892154746475
H	6.92819790928233	0.99989165663047	14.51802361849323
B	7.28465299154916	-1.47070422191853	13.57275608579280
H	6.56668495425633	-2.10598447243952	14.29599147672079
B	9.04533497126507	-1.15889992522867	11.31692843851844
H	9.54307407785016	-1.67149560091661	10.34590160766651
B	8.82173622025420	-0.81941230814153	14.15385345561602
H	9.15728724673412	-1.07978529387201	15.28226667173133
B	10.00311239671172	-0.77813765239719	12.79464150936361
H	11.17647179303180	-1.02972309995369	12.91788561348987

B	7.42570732442353	-1.68443380433045	11.79102420435804
H	6.81878222318717	-2.48712139810049	11.13604066135997
B	8.80142877463214	-2.06356788082186	12.85413584648752
H	9.13851490296694	-3.21025343065110	13.01819893471716
H	7.05686160205076	7.04985718889622	10.65595678575130

PhOMeCbPhN, Q = 0, S = 1

O	7.48994832116306	9.44607455439995	9.82403488333330
N	11.79073715901723	3.25093112482203	8.39964773174100
C	6.14052437770462	6.43573823981230	7.25528080509596
C	6.65919582084362	3.93820281797306	5.92833844339725
C	7.02865939669806	8.44442842835544	9.04950376890367
C	9.16652790043838	4.30173468796676	6.00305441530921
H	9.11390393809126	4.84558660072243	5.05877878654981
C	5.63078619214746	5.39790792706315	6.29920930451453
C	7.99155950063240	3.78629122429770	6.58701871534370
C	6.83485262076313	7.57292974349537	6.78981125640922
H	7.03212222384680	7.69918607699961	5.72464344226865
C	8.13907606242374	3.07370236829877	7.79452811556873
H	7.26571005417431	2.63795797725621	8.28239514595754
C	7.27096174550042	8.55798421246511	7.66635175079891
H	7.80572758636810	9.43608983317467	7.29676471658885
C	9.37901055921203	2.89086227934306	8.39360071589663

H	9.42524234276864	2.32808390074583	9.32534159868085
C	6.33159149197102	7.32174827210232	9.52817999592007
H	6.11827118534300	7.20298357370192	10.59070530669237
C	5.89809072974352	6.33890408824141	8.63579904879883
H	5.35088439419186	5.48565777433303	9.03771862702261
C	10.41480336692095	4.13009982499363	6.58809615834947
H	11.28422618311132	4.54966707838722	6.08292068268396
C	10.56588525958019	3.42054531956963	7.81285784788965
C	7.27871399991216	9.39978563121551	11.22901718606574
H	6.20360713536970	9.39679938413644	11.47789907473427
H	7.73903095026555	10.30818958922299	11.64086233691734
H	7.75887084817695	8.51576776685033	11.68271295451194
C	12.98213185334047	3.81359689801604	7.78482575712725
H	13.17684027978814	3.38374740213154	6.78525433330376
H	13.85110836052865	3.60069281122996	8.41971421062552
H	12.90685237659266	4.90971516817377	7.66997290343621
C	11.91271482903823	2.49569299030400	9.63609061480116
H	11.34382147858071	2.95918306106083	10.46242670920939
H	12.96811852119738	2.45620717804576	9.93288455026861
H	11.55360563917980	1.45685195682118	9.52285666753664
B	5.23693996976840	3.83315387029855	6.89948550690322
H	5.34163018049954	3.60744804339451	8.06053019230010
B	3.99776833736107	4.93787204431769	6.24649253484336

H	3.25438449667026	5.48028169321206	7.01094204857442
B	5.62476461883258	2.61824233630268	5.65323341526468
H	6.01226037582793	1.54197027063728	6.00293928058869
B	6.43352860133715	5.21053015650446	4.78750859189232
H	7.34686932274385	5.92132918045327	4.52055529809778
B	3.95975137411668	3.21034614861754	5.83176113688805
H	3.09738572233717	2.49497819117570	6.26439889379653
B	5.19612769561304	4.63542314335118	3.64811656621571
H	5.23276865261995	4.95783542507826	2.49177096543582
B	4.67050061233835	3.01950634726357	4.20246714652385
H	4.32417864456602	2.15543495103080	3.44200665891260
B	3.67286649291916	4.44175628661898	4.56664406975552
H	2.59215949834867	4.62594594435633	4.07388073029133
B	4.75803047811429	5.81358464302440	4.90408211230397
H	4.55509887957297	6.97716855328890	4.71564808380883
B	6.38500068269255	3.49413990176843	4.31082025645004
H	7.31372667909437	3.04059010357626	3.70839894890016

PhOMeCbPhN, Q = -1, S = 2

O	6.93988904704020	9.95657553794404	9.87155608984299
N	12.06398173021132	2.81590312434953	8.23586573586650
C	5.86643962329716	6.77606208735765	7.34049499086655
C	6.89182130398352	3.75499068309951	5.92894423662376

C	6.56488184724602	8.89985398820427	9.10921860195205
C	9.40575281249860	4.01527199349624	5.93170262594566
H	9.34221325053803	4.59840936695399	5.00988621134745
C	5.49586412737022	5.67968552486328	6.41970319095461
C	8.22258616189793	3.51606379818684	6.52052465961714
C	6.54187045846248	7.93149342783898	6.87900335584213
H	6.80254518153689	8.01866194242361	5.82205261147909
C	8.38670741665389	2.76404304364126	7.70549574622044
H	7.50814485076181	2.34650216843433	8.20319807255843
C	6.88329778436303	8.96930800808485	7.73914277607837
H	7.40346724353168	9.85572786674214	7.36684363675266
C	9.63658689559341	2.52512763276856	8.26919534018424
H	9.68833650167263	1.93305807267933	9.18296094183975
C	5.89228742991903	7.76429976799512	9.59084869464111
H	5.62561626269018	7.67551634902081	10.64477829059744
C	5.55487598636303	6.72766197930834	8.71441058653509
H	5.03068821456312	5.85860036004111	9.11799674777557
C	10.66458230109772	3.78762810207175	6.48099784904032
H	11.53503224254706	4.19953484985493	5.97008429170083
C	10.82410591781152	3.03689420215771	7.67794158781892
C	6.64816270978050	9.94841191780040	11.25854378624482
H	5.56129733333394	9.90320685224013	11.44912568925527
H	7.04086282748414	10.89051967089016	11.66602913788118

H	7.13784668884215	9.10463002331010	11.77614030574921
C	13.25652306778592	3.33464760543794	7.59222608063927
H	13.41466068209593	2.90408875526325	6.58499436830673
H	14.13445563600192	3.09049161524514	8.20382622672719
H	13.22058186318706	4.43348216087561	7.48035894031208
C	12.19185136153174	1.99908550375586	9.42853935335679
H	11.63253361599316	2.42143871932333	10.28343533512231
H	13.24902049972917	1.94063940229981	9.71723835423568
H	11.82667975266564	0.96642010363123	9.27199623479500
B	5.49676474373201	4.02851747511328	6.91750991776354
H	5.60236449382940	3.80293920219109	8.09252881211473
B	4.01180518268689	4.99741017025071	6.32994923937270
H	3.15624127068367	5.42950519669942	7.05879256276650
B	5.74018834687498	2.61328828095739	5.72190222350987
H	6.00927766767302	1.48720079177580	6.05229134127045
B	6.50781385350018	5.22160319470707	5.09963376758614
H	7.41710152648088	5.95383474013411	4.81679136320775
B	4.11635565603426	3.27140290866741	5.96214626858069
H	3.26554699747890	2.53967428091104	6.40809612951596
B	5.32250348473814	4.69861283714822	3.78849506468987
H	5.36279323985630	5.02620014525285	2.62702578650493
B	4.77390356349810	3.05975519072181	4.29733345660191
H	4.39245598341941	2.21026796855067	3.52786742845510

B	3.76000227673589	4.45901692480330	4.65401745734924
H	2.67808718735924	4.57684263695505	4.12977381907488
B	4.76593906382129	5.88966620582527	4.97166251384616
H	4.49683408623301	7.01608746004182	4.64229397752220
B	6.49479998781620	3.50558476275780	4.36251939039693
H	7.35262675746610	3.07571841894453	3.63484979516340

PhOMeCbPhN, Q = -1, S = 2

O	6.94938511377131	9.93167762489018	9.88551339784613
N	12.09303604626859	2.83120524996260	8.24347042134019
C	5.87323967251925	6.76544377292797	7.34403350807848
C	6.88909351904231	3.76721977575385	5.92963446728595
C	6.57381519375572	8.87952936053484	9.11987085936885
C	9.39354008790414	4.02418466695624	5.89921517429605
H	9.31822408217297	4.58882749122504	4.96851016603884
C	5.49691549113703	5.67524614395270	6.41910187365635
C	8.22064194614087	3.53306336186172	6.51823519530024
C	6.55402192529885	7.91906663543504	6.88653909227414
H	6.81687372117036	8.00845428889655	5.83032195699277
C	8.37292389063450	2.80193938967802	7.71765824358377
H	7.49434734571780	2.40008954693752	8.22493481161433
C	6.89645809206243	8.95262900651364	7.75060736205235
H	7.42013043325720	9.83883948507387	7.38274064312537

C	9.63103912492304	2.57580004498505	8.27427040782047
H	9.72670832375868	2.00517725833424	9.20240505009274
C	5.89636192542752	7.74449623396343	9.59691339216039
H	5.62663502749705	7.65390686249722	10.64992420721399
C	5.55809487100948	6.71207621504340	8.71681747782537
H	5.02960117154932	5.84344221538273	9.11568481812506
C	10.65563192458539	3.80345639587007	6.44715158214297
H	11.54098111153965	4.19438894424322	5.94104462171821
C	10.76616523263470	3.08080627644308	7.63809099038490
C	6.65152918941481	9.92306264464821	11.27205474647018
H	5.56369391998241	9.88108208237952	11.45695687175138
H	7.04559501403088	10.86370916106823	11.68141454652620
H	7.13674714436775	9.07714042445676	11.79012601168790
C	12.80520997601784	4.09144223755813	8.64163091059342
H	13.04922819906088	4.66241237375811	7.73814981675432
H	13.72400722323630	3.81028101247060	9.17207586924695
H	12.14429161547605	4.67006188273248	9.29804902416315
C	12.96197148896452	1.94212378086925	7.40230485852085
H	13.87646038809139	1.72370630907544	7.96858006257092
H	13.20816595429142	2.46597300365663	6.47076168810119
H	12.41086296830455	1.01764352877397	7.19177884498330
B	5.49286955183448	4.02060629012936	6.91963610266526
H	5.60029093374234	3.79403058662963	8.09309891065006

B	4.01540035282335	4.98912956008004	6.33023533346701
H	3.16224950719170	5.41705863182433	7.06269823244525
B	5.74801717012107	2.61491985741268	5.72294480691571
H	6.02730168255755	1.49364375141116	6.05805175482443
B	6.50806948894297	5.22845907865711	5.08912490524427
H	7.41678489364905	5.96133509063819	4.81073330765250
B	4.12096285701553	3.26378293539006	5.95700031313399
H	3.27301326930970	2.52954492295962	6.40166116274091
B	5.32435658970631	4.69781984639092	3.78471702168302
H	5.36480546132769	5.02612836952781	2.62444476334256
B	4.78369896073182	3.05689449718492	4.29424864691434
H	4.41016474451471	2.20525523830406	3.52469254031915
B	3.76504220036409	4.45155859577500	4.65110682304091
H	2.68317978388659	4.57003463456623	4.12890237749184
B	4.76897502319518	5.88674392399782	4.97090282841592
H	4.50248702669643	7.01354502574741	4.64419383552394
B	6.50268681152642	3.51339838231649	4.36147439698027
H	7.36822341966286	3.09059348463609	3.64046297029516
H	11.91739191618298	2.31628260761145	9.11731599454573

PhCbPyr, Q = 0, S = 1

C	0.83093507962672	-0.00009697293432	1.36195127356882
C	-0.90384691808529	-0.02412919298145	1.32367104090758

B	-0.04106101947639	1.41544639492325	0.91043865827563
H	-0.07286399820755	2.33960635533018	1.65296685426831
B	1.43027054084328	0.91636022931053	0.04789466443175
H	2.43172846255856	1.54215680441667	0.23342946700732
B	1.45231833736196	-0.85928690319690	0.02091587880539
H	2.47073021151369	-1.46320727982586	0.18240749964369
B	-0.00402798611556	-1.42590270030175	0.86764240320680
H	-0.00001320157094	-2.37082403951406	1.58469092960144
B	-1.45357349716737	0.87643034207425	-0.02253890315232
H	-2.47991607577536	1.47546763313320	0.10472677804919
B	0.00137934359192	1.46642183527775	-0.85821046959301
H	0.00033105739198	2.52373762056898	-1.42608376846002
B	0.92484202620787	0.04224672740540	-1.41934817429938
H	1.60626819452940	0.06593080230550	-2.40818914099436
B	0.03947072553483	-1.42252431846679	-0.90192270895645
H	0.06956106569365	-2.46160865470336	-1.50164251144944
B	-1.43105999379519	-0.89925598732554	-0.04945407307703
H	-2.44111603594687	-1.52868710626630	0.06301494463019
B	-0.85460350900926	0.01885035768225	-1.46328798036185
H	-1.48636486887584	0.02707384118181	-2.48485373153615
C	1.55101513903260	-0.02288319064642	2.69208595309538
C	1.80568869980566	1.15493643076896	3.40603434587456
H	1.47426429665470	2.12437079096734	3.03665801711219

C	2.51288820846070	1.08677415046760	4.61684947108152
N	2.95632222505044	-0.07629311429863	5.11432615012877
C	2.72777405619074	-1.21366110279244	4.44212819664585
C	2.02773738085489	-1.22746345408508	3.22598189093569
H	1.87204304275375	-2.17502486327831	2.71149975095569
C	-1.68959037508668	-0.04640155354200	2.61392260794313
C	-2.15988200337317	1.15194167021145	3.18165672571238
H	-1.93955241743739	2.10914725288240	2.70871617105306
C	-2.92350375353976	1.13364268699965	4.35136517956181
H	-3.27976328411199	2.07646270899224	4.77456838479754
C	-3.23144116245124	-0.07950003727019	4.97456500072536
H	-3.82850767456820	-0.09245624831491	5.89036487545305
C	-2.77528607070508	-1.27623889304368	4.41404911260112
H	-3.01499699392136	-2.23241909849400	4.88647684114268
C	-2.01274423447781	-1.26215795493322	3.24330466980766
H	-1.67842785516514	-2.20874006682305	2.81884049541506
C	2.81103645414905	2.32655853358894	5.41856917027660
H	3.89978801869384	2.44449370563213	5.55029649868377
H	2.37567321131857	2.24322568718805	6.42866276914493
H	2.41449770292192	3.23260796216136	4.93864400640291
C	3.25976456250071	-2.48344532791970	5.05303446551329
H	3.03130910522008	-3.36426765108968	4.43626081205179
H	2.82930887660540	-2.63498036600574	6.05724731398975

H	4.35315690379654	-2.41703444541655	5.18236219337836

PhCbPyr, Q = -1, S = 2

C	-2.08403864316334	0.05711635072995	2.45081656113948
C	2.37570731296200	-1.16331561806161	3.16818141607377
H	2.06438584445423	-2.13846990316152	2.79027467220201
C	1.99353640934924	0.01747504454367	2.50001073133362
C	2.44445799341822	1.23137363939734	3.05716889412623
H	2.18866613324363	2.18368967855127	2.58978801761091
C	3.23148134333014	1.22117232929103	4.21497141880025
C	3.73319183833689	2.50225256856752	4.83300626529669
C	-1.23023919453037	0.01101530275828	1.24341039670314
C	1.17446645775195	-0.01399338921127	1.27406198819649
C	3.16433277280666	-1.09081312209032	4.32280665474921
C	3.59217000910867	-2.33562970754501	5.05921753218072
C	-2.52549379965616	-1.12853996809857	3.08048956006072
H	-2.22367341155897	-2.09772121805089	2.67788768506437
C	-2.50272437637581	1.28859903788915	3.00343256851835
H	-2.18283019064390	2.22437657664712	2.54032404973880
N	3.58055430919600	0.08038877557366	4.83418973447374
C	-3.34834749598419	-1.08331925091899	4.20806117261104
H	-3.67649642207376	-2.01776371111457	4.67264041551324
C	-3.32553901810191	1.33073802404209	4.13111390107889

H	-3.63574701146169	2.29886070831468	4.53513727076347
C	-3.75370089824776	0.14589758093464	4.74244139226373
H	-4.39681796207257	0.18013687523054	5.62617027083704
B	-0.03743078307109	-1.22145946649926	1.01831056668969
H	-0.05550102005968	-2.15738974518684	1.76845040479725
B	1.47833619178590	-0.95593627949340	-0.02647033325722
H	2.44959336036367	-1.66428595764116	0.01707463001515
B	-1.50051995193090	0.87146922763369	-0.12041277319798
H	-2.47252742595944	1.57966238285772	-0.14448487703236
B	-1.51950536907663	-0.92340679285482	-0.06662031794518
H	-2.50619495715646	-1.61124771444752	-0.04864595205329
B	1.49793870742305	0.84122878717049	-0.08066435882081
H	2.48482673773147	1.52879592095822	-0.08052273870648
B	-0.01638751709464	-1.49818509634522	-0.79866048416816
H	-0.01972854405307	-2.57555969327489	-1.34152294783113
B	-0.87385837878755	-0.07469234505763	-1.49270606045656
H	-1.47423470354239	-0.10030265093347	-2.53927408603740
B	-0.01145941819441	1.20216628241923	0.94608024470754
H	-0.00853595315366	2.17963240264062	1.64154896371643
B	0.88985738084639	-0.09291584163025	-1.46877153878754
H	1.51783275963914	-0.13163008231073	-2.49854517976944
B	0.01461057374298	1.36858064923302	-0.88454741024360
H	0.03451874742388	2.41052679691451	-1.49204959165417

H	3.41381896954707	3.38757695796712	4.26426358511826
H	4.83515498433628	2.49830364822841	4.88662837218961
H	3.36635828258134	2.60016016111054	5.86900362650737
H	3.20882387082992	-3.24963220809496	4.58282972998881
H	3.23497397535531	-2.30753726399066	6.10272509949900
H	4.69286840014855	-2.39825750222620	5.10319597802047

PhCbPyrH, Q = 0, S = 2

C	-2.01408401596928	0.06572582157495	2.46085428496159
C	2.34509219373815	-1.18292376229525	3.13851930873839
H	2.05989996827194	-2.15541709334776	2.73852648922175
C	1.96185963350727	0.01280491104875	2.47505282318281
C	2.38208962474970	1.24002799690493	3.05343510039546
H	2.12591524400706	2.19021452620467	2.58581850316056
C	3.12808360785043	1.26135159885823	4.21694418912335
C	3.61186034084516	2.50694182304542	4.89020562373543
C	-1.18896466033984	0.01139517430157	1.23017301481066
C	1.17516474566026	-0.01769740955065	1.25258240986295
C	3.09190743850413	-1.14505158009846	4.30094288066215
C	3.54070841194328	-2.35418104776273	5.05873711769635
C	-2.43026031643734	-1.11506915793884	3.11387233816494
H	-2.13321884086560	-2.08708480538942	2.71532541496419
C	-2.42646675649288	1.30199076441425	3.00481761646634

H	-2.12648827029252	2.23316765118812	2.52019681651819
N	3.45128570907198	0.07174467084944	4.79857116073794
C	-3.22385878929757	-1.06017263960816	4.26180284790544
H	-3.53362416237651	-1.99009354278411	4.74715125771486
C	-3.22024144049575	1.35365865622654	4.15250883162691
H	-3.52726405423508	2.32459789021446	4.55159421872336
C	-3.62246907238496	0.17363719397758	4.78962002876629
H	-4.24266360227609	0.21529579984918	5.68922748923390
B	-0.03446851714977	-1.24964461309954	0.98587649094254
H	-0.04760704001208	-2.18011812926861	1.73963025476449
B	1.47144052478854	-0.96797256606581	-0.04492822134145
H	2.44161924768526	-1.67484254798190	0.00990799015768
B	-1.49118780248651	0.86868095118864	-0.13135579828806
H	-2.46235992746716	1.57604166770860	-0.13565600766695
B	-1.51336454361357	-0.92517608785318	-0.07323979064003
H	-2.50170951660458	-1.60721694824551	-0.03123480151037
B	1.49422548414260	0.83906348823126	-0.10308513103438
H	2.48267788678337	1.52224841039167	-0.09459028170422
B	-0.01964728570867	-1.50614508973498	-0.82284759933010
H	-0.02497405691076	-2.58208469585023	-1.36525044085955
B	-0.87662037008185	-0.08132387118396	-1.50894148454870
H	-1.48663109655478	-0.10713669298745	-2.54838568178830
B	-0.00314066544292	1.22483700732091	0.90621471420752

H	0.00671828021181	2.20065636531688	1.60026733848961
B	0.88587008491710	-0.10253069077199	-1.49009789115641
H	1.51973222708083	-0.14392817878865	-2.51470682714655
B	0.01647654323932	1.36224238465021	-0.91585194259592
H	0.03753067220354	2.40055178936015	-1.52689941737792
H	3.29576524560797	3.39633427739125	4.33003111765699
H	4.71246645830540	2.50593424910518	4.96374245752489
H	3.21228511130860	2.57367694467062	5.91623240137722
H	3.18826600944589	-3.27059224016460	4.56815871278545
H	3.15174972366473	-2.33127229076445	6.09068923768320
H	4.64155530572395	-2.38595515109245	5.12165595564973
H	3.99932547323779	0.09270148063524	5.66058778637573

PhCbPhCOO, Q = -1, S = 1

C	-0.88768738265444	0.00534993018117	1.30277428514453
C	0.86686196364735	-0.01009036426651	1.32127882781888
B	-0.01691853630968	-1.41091339854041	0.84116065137167
H	-0.03606418969552	-2.36076582184935	1.55124318149551
B	-1.44885741894794	-0.85960020428488	-0.05781991467049
H	-2.46828894034460	-1.47159343732598	0.06630635713857
B	-1.43681000712756	0.91497018889505	-0.03552213041316
H	-2.44711102113893	1.53798518879186	0.10873734204077
B	0.00244541952816	1.41813830626858	0.87889377355377

H	0.00728836837621	2.34802722991752	1.61559577548732
B	1.43790149129120	-0.88417606329032	-0.03238101992966
H	2.44508838332284	-1.51196595028942	0.11245871621280
B	-0.00217609647964	-1.41678447954797	-0.93018958666537
H	-0.00660377592767	-2.45792109685449	-1.52784105232444
B	-0.87626690811379	0.04116162297007	-1.48282598664761
H	-1.52268365665533	0.05871094682322	-2.49548558208165
B	0.01938299931129	1.47068510256953	-0.89154578906422
H	0.03397217422273	2.52686996787864	-1.46202775272373
B	1.44990541917401	0.89016684049137	-0.00786202760961
H	2.46631239813929	1.49944856373268	0.14850154244958
B	0.90307215764297	0.02728329715034	-1.46649358057397
H	1.56777775739557	0.03687339949219	-2.46737354634157
C	-1.64669684466349	-0.01568608975504	2.60786509590866
C	-2.09039202156343	-1.23386103087778	3.15444365591222
H	-1.87266739344566	-2.17525942992310	2.64965694866062
C	-2.82166999523882	-1.25630024733634	4.34451468347240
H	-3.15577931246170	-2.21435132662809	4.75123198720325
C	-3.12474723096063	-0.06416461610392	5.00928883322700
H	-3.69603710469501	-0.08287939552377	5.94129228912035
C	-2.69681488518051	1.15239525743380	4.46951840061389
H	-2.93310996441992	2.09260056039674	4.97464107050708
C	-1.96591865736066	1.17871242573077	3.27881263073238

H	-1.65195774354187	2.13998190945191	2.87213339065504
C	1.59781815984433	-0.02251522317968	2.64002312830466
C	1.88555779186051	-1.23109741536260	3.30206734261181
H	1.56655917201167	-2.18180082724827	2.87367301203414
C	2.58918268938260	-1.22938490140832	4.50765297645731
H	2.81388058114041	-2.16454479117158	5.02562621145196
C	3.03201711868192	-0.03393440512029	5.09059957737564
C	3.80930954397395	-0.04079238612583	6.43110912506105
C	2.75468055297945	1.16708567940939	4.42266256378687
H	3.10820487377736	2.09689351973860	4.87413751431750
C	2.05033689823925	1.17927214508141	3.21794441616020
H	1.85844996807709	2.13234776768186	2.72322665282564
O	4.17064782654022	1.08028109487555	6.85661818867306
O	3.99278877636641	-1.16694096694831	6.94732077225928

PhCbPhCOO, Q = -2, S = 2

C	-2.08231767646267	0.00492045079481	2.46162568103430
C	2.42050018130449	-1.13794104028631	3.15577116099068
H	2.11098448102391	-2.10409098819081	2.74978638706647
C	2.01322007625401	0.05143816749674	2.50815681582492
C	2.44303350944176	1.27603354803446	3.07041869215338
H	2.15051960245188	2.21678763311270	2.59760207031912
C	3.24151303948065	1.30292597327008	4.21418261791943

H	3.57716062130750	2.25130889401052	4.64158270690959
C	-1.22586846502921	-0.00464550813225	1.25559573865064
C	1.18784587508241	0.01875055420088	1.28195372431379
C	3.21555951097043	-1.09854783178454	4.30206797645741
H	3.52768949293429	-2.02040927958169	4.79977358942416
C	-2.50109404453236	-1.19937531429941	3.07194377957457
H	-2.17931582793586	-2.15564660880919	2.65409291603479
C	-2.52677951099602	1.21803979560843	3.03507238790169
H	-2.22529449305898	2.16782219960214	2.58824642151745
C	3.64291742281048	0.11946070344177	4.85486070317191
C	4.52688234231201	0.15780556861407	6.12271224423894
C	-3.32537108869353	-1.18958145030015	4.19932851760229
H	-3.63457769647494	-2.13828111764752	4.64793161886409
C	-3.35112489157441	1.22489115836224	4.16249439074068
H	-3.68074850638840	2.17993279823084	4.58215849660071
C	-3.75616554921349	0.02193239179020	4.75407159208183
H	-4.40036303788091	0.02851000037402	5.63767210377045
B	-0.00637918362114	-1.20437025833067	1.01312984181536
H	-0.00611641225345	-2.15219822166403	1.74930724133945
B	1.50145306730938	-0.89710552824304	-0.03532530189749
H	2.48776183016888	-1.58621069995361	-0.00957382310089
B	-1.51749936817338	0.86797719105695	-0.09686722557162
H	-2.50494254111820	1.55575720702751	-0.11120761137881

B	-1.49910949530537	-0.92585692072094	-0.06755912747534
H	-2.47229269333368	-1.63380878847713	-0.05920396350721
B	1.48358236074870	0.89779129637124	-0.06380097625033
H	2.45590682150640	1.60674024669500	-0.06103591136095
B	0.01435352958460	-1.45971675810633	-0.80834091818083
H	0.03116815564982	-2.52987319457612	-1.36630585527059
B	-0.87514576425472	-0.04523156237864	-1.48234073701976
H	-1.47621614572359	-0.06868894869812	-2.52917497815086
B	-0.03107200695207	1.20989056235312	0.97449506841170
H	-0.04735585323039	2.17930223238658	1.68203775089002
B	0.88894866999287	-0.02767549630441	-1.46321051731384
H	1.51313228766502	-0.03814568172149	-2.49658980186129
B	-0.01404280686005	1.40696202450923	-0.85413725522693
H	-0.01710787743893	2.45855290522846	-1.44639779697212
O	4.88431775136197	1.29635489442968	6.50846686810005
O	4.79690573217368	-0.95304065671731	6.63825376700623

PhCbPhCOOH, Q = -1, S = 2

C	-2.05114639051712	0.01072648578984	2.46710941011508
C	2.42547428026921	-1.14885607344221	3.12410699583161
H	2.14485210331903	-2.11290018904978	2.69614811214190
C	2.00365128488819	0.04710320121716	2.49315433493896
C	2.39982299653174	1.27230949046989	3.08144698356272

H	2.09873130309802	2.21438891554889	2.61982638358417
C	3.17081991370519	1.30284689120839	4.23912653468553
H	3.46150294550053	2.26298516964378	4.66898628840351
C	-1.21050235916631	-0.00396230705900	1.24891500795704
C	1.18991055432016	0.01741942502773	1.26807885993985
C	3.19630718280179	-1.11868102078896	4.28020491662672
H	3.51485972493962	-2.04989558874776	4.75380370634356
C	-2.45788182944024	-1.19036142496422	3.09038828949374
H	-2.14438516660510	-2.14870484326286	2.67141586960479
C	-2.48568963200501	1.22722489113323	3.03974323187728
H	-2.19415607793490	2.17405117271611	2.58064117932367
C	3.57892654714172	0.10615001791697	4.85838788809174
C	4.39795289823249	0.08681324656201	6.09629343013568
C	-3.25980591047472	-1.17400954458061	4.23369655708350
H	-3.55966124465258	-2.11982383951723	4.69416369612858
C	-3.28766145183053	1.24068170686324	4.18290235343838
H	-3.60961456635942	2.19786699832656	4.60316287096161
C	-3.67908196367658	0.04082903975006	4.78952067861990
H	-4.30519245542171	0.05244185995836	5.68585766057592
B	-0.00115146221838	-1.21326895465871	0.99917418740519
H	0.00234212918659	-2.15868511179871	1.73712509221673
B	1.50267696781855	-0.90132556798006	-0.04754472405504
H	2.48929391922255	-1.58859436125475	-0.01744613704569

B	-1.51380813243936	0.86621440708510	-0.10257705215237
H	-2.50105237424318	1.55313351288562	-0.10917042496506
B	-1.49474433556910	-0.92833385762782	-0.06988748945485
H	-2.46719068592067	-1.63596503619075	-0.05171372370875
B	1.48390964175912	0.89820568076582	-0.07676588736414
H	2.45599758365509	1.60651696653175	-0.07085123532620
B	0.01518470268334	-1.46360360262001	-0.81902032829951
H	0.03024059880570	-2.53273887850771	-1.37706045376329
B	-0.87570602405467	-0.04923973834041	-1.48966176632127
H	-1.48233082854838	-0.07343136347674	-2.53241396336787
B	-0.02617639289472	1.21703700057105	0.95729148778523
H	-0.03871266106254	2.18670966561225	1.66282466553667
B	0.88817765587729	-0.03148141446392	-1.47479548862950
H	1.51313317038099	-0.04278915312077	-2.50690221110094
B	-0.01340007915528	1.40422767002277	-0.86856750226308
H	-0.01707995651836	2.45358060654457	-1.46318909623698
O	4.69540749613278	1.31748391161895	6.55685406299438
H	5.23130949497058	1.20402092392202	7.36512388481262
O	4.77601180546860	-0.92084952023914	6.66093781883819

B8. REFERENCES

[1] Sheldrick, G. M. A short history of SHELX. *Acta Cryst. A*, **2008**, *64*, 112–122.

[2] Dolomanov, O. V.; Bourhis, L. J.; Gildea, R. J.; Howard, J. A. K.; Puschmann, H. OLEX2: A Complete Structure Solution, Refinement and Analysis Program. *J. Appl. Crystallogr.* **2009**, *42*, 339.

[3] Neese, F.; Wennmohs, F.; Becker, U.; Riplinger, C. The ORCA Quantum Chemistry Program Package. *J. Chem. Phys.* **2020**, *152*, 224108.

[4] Neese, F. Software update: The ORCA program system—Version 5.0. *WIREs Comput. Mol. Sci*. **2022**, 12:e1606.

[5] F. Weigend, R. Ahlrichs, Balanced basis sets of split valence, triple zeta valence and quadruple zeta valence quality for H to Rn: Design and assessment of accuracy, *Phys. Chem. Chem. Phys.* **2005**, *7*, 3297–3305.

[6] A. V. Marenich, C. J. Cramer, D. G. Truhlar, Universal solvation model based on solute electron density and on a continuum model of the solvent defined by the bulk dielectric constant and atomic surface tensions *J. Phys. Chem. B.* **2009**, *113*, 6378–6396

[7] Chalkley, M. J.; Garrido-Barros, P.; Peters, J. C. A Molecular Mediator for Reductive Concerted Proton-Electron Transfers via Electrocatalysis. *Science* **2020**, *369* (6505), 850–854. DOI: 10.1126/science.abc1607.

Appendix C

Supplementary Information for Chapter 4

C1. Experimental Details

General Considerations

All manipulations were carried out using standard Schlenk or glovebox techniques under an N_2 atmosphere unless stated otherwise. Solvents were degassed by thoroughly sparging with N_2 gas and dried by passage through an activated alumina column in the solvent purification system by SG Water, USA LLC. All solvents were stored over activated 3 or 4 Å sieves prior to use. THF, 2-MeTHF, and diethyl ether were dried over NaK alloy and passed over activated alumina prior to use and were checked with a standard solution of sodium benzophenone ketyl in tetrahydrofuran to test for the presence of oxygen and moisture. All reagents were purchased from commercial vendors and used without further purification unless otherwise stated. $[Ph_3C]BAr^F_4$ was prepared by halide abstraction from Ph_3CCl with 0.95 eq. THF-free $NaBAr^F_4$ in fluorobenzene, then the PhF solution filtered over Celite and recrystallized by layering with pentane and chilling to −40°C –the crystals were stored in the glovebox freezer protected from light. BAr^F_4 is used here to denote the 3,5-CF_3-substituted tetraarylborate anion. Commercial $[Cp_2Co]PF_6$ from Strem was repurified by dissolving in acetonitrile and filtration over neutral alumina before crystallization by vapor diffusion with Et_2O on the bench. For large-scale reactions, $[Cp_2Co]PF_6$ prepared from NaCp by the method of Bildstein was used.[1] $^nBu_4NPF_6$ was recrystallized from hot EtOH three times and dried under vacuum at 100 °C overnight. High resolution mass spectra (HRMS) were obtained either by direct injection electrospray ionization (ESI+) at the Caltech Center for Catalysis and Chemical Synthesis using an Agilent 6200 Series TOF with an Agilent G1978A Multimode source, or the Caltech Mass Spectral Facility using an JEOL JMS-T2000GC AccuTOF™ GC-Alpha High Resolution Mass Spectrometer in field desorption (FD+) mode.

NMR Spectroscopy

NMR spectroscopy was performed using Varian and Bruker 400 MHz NMR spectrometers fitted with broadband auto-tune probes. Deuterated solvents were purchased from Cambridge Isotope Laboratories, Inc. Acetonitrile-d_3 and benzene-d_6 were degassed by three freeze-pump-thaw cycles, dried over activated 3 Å sieves, and passed over activated alumina. ^1H and ^{13}C chemical shifts are reported in ppm relative to tetramethylsilane using residual solvent resonances as internal standards. ^{19}F chemical shifts are reported in ppm relative to trichlorofluoromethane using absolute referencing to a ^{13}C NMR spectrum collected concurrently.

UV-vis Spectroscopy

Spectra were collected using a Cary 60 instrument with Cary WinUV software. Time-course spectra were collected with the Scanning Kinetics application of the Cary WinUV software. 1-cm path quartz cells were pre-cooled in a Unisoku cryostat prior to analysis. All spectra were background corrected at the temperature at which spectra were collected.

X-ray Crystallography

X-ray diffraction (XRD) studies were carried out at the Beckman Institute Crystallography Facility on a Bruker Kappa Apex II diffractometer (Mo Kα radiation, λ = 0.71073 Å, or Cu Kα radiation, λ = 1.5406 Å). All crystals were mounted with Mitegen loops under STP oil. Structures were solved using SHELXS or SHELXT and refined against F^2 on all data by full-matrix least squares with SHELXL.[2] All of the solutions were performed in the Olex2 program.[3] Hydrogen atoms were

placed in calculated positions and refined with a riding model. Non-hydrogen atoms were refined anisotropically.

Electrochemistry

Cyclic voltammetry (CV) measurements were carried out in an N_2-filled glovebox in a 20 mL scintillation vial fitted with a septum cap containing punched-out holes for insertion of electrodes. A CH Instruments 600B or Biologic VSP electrochemical analyzer was used for data collection. For cyclic voltammetry experiments, a boron-doped diamond disk electrode was used as the working electrode; a freshly polished glassy carbon disk electrode was used as the counter electrode; a silver wire immersed in a solution of silver triflate (5 mM) and $^{n}Bu_4PF_6$ (200 mM) separated from the working solution by a Coralpor frit was used as a pseudoreference electrode. $E_{1/2}$ values for reversible waves were determined as the half potential between the peak oxidative and reductive potentials. Solution resistance was measured, and a correction of 85% of the uncompensated resistance was applied. All reported potentials are referenced to the ferrocene/ferrocenium couple, measured at the end of each experiment. Solvents were passed over a pipet filter of activated alumina immediately before use.

Controlled potential electrolysis (CPE) was carried out in a gas-tight two-compartment H-cell equipped with a fine glass frit. The cell was washed with acetone, water, and sonicated for 10 minutes with isopropanol and assembled in the glovebox. A boron-doped diamond plate (2x1cm) was used as the working electrode and was pretreated according to literature procedure.[4] Zinc foil was used as the counter electrode and was polished with steel wool and rinsed with acetone and water. A silver pseudoreference electrode was used (*vide infra*). The solution was stirred throughout the CPE experiment. Electrolyte (200 mM $^{n}Bu_4PF_6$) and acid (100 mM TsOH) were added to both compartments which each contained 3 mL of DME solvent. In the cathode compartment, 1 mM [Co(III), N]BAr^{F}_4 (2 mol%) and 50 mM of acetophenone were added. The potential of the pseudoreference electrode was calibrated to ferrocene before CPE in a separate CV solution. CPE was performed inside the glovebox at −1.30 V until 14.4 C passed (1 mol e^{-}/mol substrate). The solution was transferred to a 20 mL scintillation vial, and the solvent was evaporated. The electrode and cell were washed with 10 mL of saturated aq. $NaHCO_3$ solution. The aqueous layer was separated and extracted with Et_2O (4 x 10 mL), and the combined organic layers were filtered through a silica plug, dried over Na_2SO_4, and evaporated to dryness. The crude product was dissolved in $CDCl_3$, was analyzed by ^{1}H NMR spectroscopy with dibromomethane (1.0 eq) as an internal standard.

DFT Calculations

All calculations were performed using density functional theory (DFT) implemented in the ORCA 6.0.1 program.[5,6] The TPSSh (for DFT) and TPSS0 (for TD-DFT) functionals with Grimme's D4 correction were used throughout this study.[7,8] Geometry optimizations were performed with Ahlrich's full electron def2-SVP basis set,[9] where Fe and Co were treated with def2-TZVP, with the SMD solvation model using acetonitrile or THF.[10] The resolution of identity approximation was exploited to accelerate the evaluation of Coulomb integrals using def2/J auxiliary basis set.[11] In cases where crystal structures were available, those coordinates were used as the input. Single-point vibrational frequency calculations were performed to ensure that stationary points were absent of any imaginary frequencies, and thermochemistry correction energy (G-E) was acquired. The energies of the optimized structures were reevaluated with a high-quality triple-ζ basis set

def2-TZVPP with SMD solvation model. Bond dissociation free energies (BDFEs) were calculated by an established method using the calculated free energy of the H atom.[12]

C2. Synthetic Procedures

Cp(η^4-C_5H_5-*o*-$PhNMe_2$)Co

[Cp_2Co]PF_6 [250 mg, 0.75 mmol] was suspended in 5 mL of THF and cooled in the glovebox cold well at −78 °C. A solution of 2-lithido-N,N-dimethylaniline [95 mg, 1.0 eq] in 5 mL of THF was added dropwise, forming a red solution. The reaction was stirred overnight in the cold well, during which time it warmed to room temperature. The solvent was removed under vacuum, and the resulting red solid was extracted with pentane [3 x 5 mL], filtered over Celite, and concentrated in vacuum to yield 163 mg (70 %) of a crystalline red solid. XRD quality crystals were prepared by slow evaporation of pentane.

^{1}H NMR (C_6D_6, 400 MHz, 298 K) δ: 7.10 (d, 7.1 Hz, 1H), 7.00 (dd, J = 7.1, 6.4 Hz, 1H), 6.87 (d, 7.9 Hz, 1H), 5.15 (s, 2H), 4.62 (s, 5H), 2.98 (s, 2H), 2.52 (s, 6H). ^{13}C{^{1}H} (C_6D_6, 128 MHz, 298 K) δ: 150.31, 140.88, 128.01, 126.93, 123.97, 119.36, 79.53, 75.41, 51.17, 46.14, 45.67.

CpCoCp$^{o\text{-}N}$

In the nitrogen glovebox, Cp(η^4-C_5H_5-*o*-$PhNMe_2$)Co [102 mg] was dissolved in benzene [8 mL] and methylcyclohexane [40 mL] in a sealed 250-mL Schlenk tube. The flask was taken out of the glovebox and heated in an oil bath at 110 °C. A wine-red solution formed. The reaction progress was monitored by intermittent sampling and ^{1}H NMR spectroscopy analysis in C_6D_6. After three days, the starting material was consumed, and the flask was brought back into the glovebox. The solvent was evacuated, and the solid was extracted with pentane [3 x 5 mL], filtered over Celite, and concentrated *in vacuo*, yielding a purple solid. The solid was crystallized from a concentrated pentane solution at −35 °C and washed with cold HMDSO [2 x 1 mL], yielding 65 mg (64%) of a purple crystalline powder. Similarly, XRD quality crystals were grown from a concentrated pentane solution at −35 °C. If needed, purification by the following redox sequence was performed: 1) oxidation with stoichiometric silver triflate in THF 2) filtration, drying and washing of the Co(III) salt with copious ether 3) recrystallization from THF/Toluene layering in the freezer, 4) reduction with sodium amalgam to the Co(II) salt, and 5) recrystallization from cold pentane.

^{1}H NMR (C_6D_6, 400 MHz, 298 K) δ: 14.87 (s, 1H), 13.98 (s, 1H), 1.12 (s, 1H), -8.93 (bs, 1H), -10.78 (bs, 1H), -15.68 (bs, 2H), -49.17 (bs, 5H), -53.03 (bs, 2H).

[CpCoCp$^{o\text{-}N}$]BAr^F_4

A scintillation vial containing a solution of Cp(η^4-C_5H_5-*o*-$PhNMe_2$)Co [55 mg, 0.18 mmol, 1 eq.] in 3 mL PhMe was placed in an Al vial block and the whole block pre-cooled in the glovebox freezer to −40°C. After 30 minutes, the block was quickly pulled out and set on a stir plate, then in one portion solid [Ph_3C]BAr^F_4 [187 mg, 0.17 mmol, 0.95 eq.] was dumped into the Co^I solution from a tooled-neck dram vial. This operation was completed in <1 minute. As the vial warmed with active stirring, the cold, heterogeneous mixture was observed to deepen in its red color with formation of a mobile oil of Co^{III} product. After 1 hour, the stir bar was removed and the crude mixture dried in vacuo to a red oil, which was brought out of the glovebox and sonicated with portions of hexane [3x10 mL] to liberate a red powder by removal of starting material and the stoichiometric byproduct Ph_3CH. Orange plate crystals (125.4 mg, *60%*) suitable for X-ray

diffraction were obtained by vapor diffusion of pentane into a supersaturated PhMe solution obtained by boiling and slow cooling to room temperature (~50 mg/mL in PhMe, ca. 3 mL, diffused with 20 mL pentane).

^{1}H NMR (CD_3CN, 400 MHz, 298 K) δ: 7.73-7.65 (m, 13H), 7.38 (t, J = 8.2 Hz, 1H), 7.21 (d, J = 8.2 Hz, 1H), 7.14 (t, J = 7.7 Hz, 1H), 6.25 (t, J = 2.1 Hz, 2H), 5.67 (s, 2H), 5.42 (s, 5H), 2.55 (s, 6H).
^{13}C{^{1}H}(CD_3CN, 101 MHz, 298 K) δ: 162.56 (q), 154.87, 135.60 (m), 132.79, 131.96, 129.87, 126.77, 124.07, 123.82, 121.34, 120.89, 118.64 (m), 87.04, 84.79, 44.67.

The product can also be recrystallized from Et_2O/pentane (1:20 v/v layered and cooled to −20°C). This low-viscosity mixture is often effective for decreasing the oiliness of BAr^F_4 salts and purging $NaBAr^F_4$, likely due to the comparatively poor crystallinity of the $[Na(OEt_2)_x][BAr^F_4]$ solvate. Similarly, sonication or boiling of insoluble $[CpCoCp^R]BAr^F_4$ salts in H_2O can remove $NaBAr^F_4$, which is decanted away as fine white emulsions of the hydrate $[Na(OH_2)_x][BAr^F_4]$. If necessary, the product can be further purified by silica gel chromatography (pack and load column in PhMe, product elutes as red streak with PhMe→$CHCl_3$ gradient at ~20% $CHCl_3$).

Cp(η^4-C_5H_5-*m*-PhNMe$_2$)Co
In the nitrogen glovebox, $[Cp_2Co]PF_6$ [200 mg, 0.60 mmol] was suspended in 5 mL of THF and cooled in the cold well at −78 °C. A solution of 3-lithido-N,N-dimethylaniline was prepared by dropwise addition of ^{n}BuLi [0.23 mL, 2.6 M in hexanes] to a solution of 3-bromo-N,N-dimethylaniline [122 mg, 0.61 mmol] in THF [5 mL] in the cold well at −78 °C and stirring for 10 minutes. The aryl lithium solution was added dropwise to the cobaltocenium suspension in the cold well. The reaction was stirred overnight, during which time it warmed to room temperature. The solvent was removed under vacuum, and the resulting red solid was extracted with pentane [3 x 5 mL], filtered over Celite, and concentrated in vacuum. The remaining solid was washed with HMDSO [2 x 1 mL] and recrystallized by slow evaporation of pentane to yield 213 mg (75 %) of a crystalline red solid.

^{1}H NMR (C_6D_6, 400 MHz, 298 K) δ: 7.16 (t, 7.9 Hz, 1H), 6.51-6.44 (m, 2H), 6.37 (s, 1H), 5.12 (t, J = 1.9 Hz, 2H), 4.62 (s, 5H), 3.99 (t, J = 2.6 Hz, 1H), 2.94 (td, J = 2.6, 1.9 Hz), 2.57 (s, 6H).
^{13}C{^{1}H} (C_6D_6, 128 MHz, 298 K) δ: 151.05, 147.28, 129.10, 114.59, 111.01, 110.25, 79.47, 75.14, 57.30, 45.31, 40.47.

CpCoCp$^{m\text{-}N}$
In the nitrogen glovebox, Cp(η^4-C_5H_5-*m*-PhNMe$_2$)Co [100 mg] was dissolved in benzene [8 mL] and methylcyclohexane [40 mL] in a 250 mL Schlenk tube. The tube was sealed, removed from the box, and heated in an oil bath at 110 °C. The reaction progress was monitored by intermittent sampling and ^{1}H NMR spectroscopy analysis in C_6D_6. After two days of heating, the starting material was consumed, and the desired product was formed. The solution was brought back into the glovebox and pumped down to yield a wine-red solid which was extracted with pentane [3 x 5 mL] and filtered over Celite. The pentane was pumped down to ~1.5 mL. The concentrate was placed in the freezer over the weekend, yielding crystals suitable for XRD. The crystals were washed with cold HMDSO [2 x 1 mL] to yield 85 mg (86%) of purple crystalline product. If needed, purification by the following redox sequence was performed: 1) oxidation with

stoichiometric silver triflate in THF 2) filtration, drying and washing of the Co(III) salt with copious ether 3) recrystallization from THF/Toluene layering in the freezer, 4) reduction with sodium amalgam to the Co(II) salt, and 5) recrystallization from cold pentane.

^{1}H NMR (C_6D_6, 400 MHz, 298 K) δ: 13.06 (bs, 1H), 2.34 (s, 6H), -6.75 (bs, 1H), -8.89 (bs, 1H), -10.74 (bs, 1H), -25.3 (bs, 2H), -50.13 (bs, 5H), -51.06 (bs, 2H).

[CpCoCp$^{m\text{-}N}$]BAr$^F{}_4$

A scintillation vial containing a solution of Cp(η^4-C_5H_5-*m*-PhNMe$_2$)Co [66 mg, 0.21 mmol, 1 eq.] in 3 mL PhMe was placed in an Al vial block and the whole block pre-cooled in the glovebox freezer to −40°C. After 30 minutes, the block was quickly pulled out and set on a stir plate, then in one portion solid [Ph_3C]BAr$^F{}_4$ [225 mg, 0.20 mmol, 0.95 eq.] was dumped into the Co^I solution from a tooled-neck dram vial. This operation was completed in <1 minute. As the vial warmed with active stirring, the cold, heterogeneous mixture was observed to deepen in its red color with formation of a red oily slurry of Co^{III} product. After 3 hours, the crude mixture was removed from the glovebox and the crude product precipitated directly by addition of hexane [15 mL] to liberate a red powder. Sonication and mechanical trituration first with several portions of hexane [3x5 mL] and then with deionized water [5 mL] removed residual Ph_3CH and a white cloudy emulsion. The product was redissolved in DCM and filtered over a pipette of neutral Al_2O_3 to remove a dark impurity. Red plate crystals (174.3 mg, *70%*) were obtained by cooling a supersaturated, opaque red emulsion of the product in DCM/hexane (1:3 v/v, 5:15 mL) in a −20°C freezer overnight.

Red plate crystals suitable for X-ray diffraction were obtained by vapor diffusion of pentane into a supersaturated PhMe solution obtained by boiling and slow cooling to room temperature (~50 mg/mL in PhMe, ca. 3 mL, diffused with 20 mL pentane). The product may also be crystallized from vapor diffusion of pentane into PhF (ca. 1:25 v/v inner/outer solvent). If necessary, the crude product can be purified by silica gel chromatography prior to any crystallization (pack and load column in PhMe, product elutes as red streak with PhMe→$CHCl_3$ gradient at ~20% $CHCl_3$). When the raw product was purified this way, black material remained stuck to the column, while a blue trace impurity was observed to elute at 10% $CHCl_3$.

^{1}H NMR (CD_3CN, 600 MHz, 298 K) δ 7.71 – 7.68 (m, 8H), 7.67 (br s, 4H), 7.29 (dd, *J* = 8.4, 7.5 Hz, 1H), 7.05 (ddd, *J* = 7.5, 1.7, 0.8 Hz, 1H), 7.00 (dd, *J* = 2.6, 1.6 Hz, 1H), 6.87 (ddd, *J* = 8.4, 2.6, 0.8 Hz, 1H), 6.19 – 6.18 (m, 2H), 5.74 – 5.73 (m, 2H), 5.47 (s, 5H), 3.01 (s, 6H).

^{13}C NMR (CD_3CN, 101 MHz, 298 K) δ 162.61 (q), 152.23, 135.66 (m), 131.15, 130.95, 129.92, 129.51 (qq), 126.81, 124.11, 121.41, 118.67, 118.34 (m), 116.47, 115.45, 111.82, 106.97, 86.67, 85.24, 81.82, 40.67.

Cp(η^4-C_5H_5-*p*-PhBr)Co

Method A: Lithiation-Addition

SAFETY NOTE: Unlike the lithioanilines used to synthesize other Co^I complexes in this report, p-bromolithiobenzene is self-reactive and therefore *must not* be isolated as an unstabilized ether-free solid, e.g. by drying a toluene solution in vacuo. Reconstitution in THF of p-bromolithiobenzene dried in this manner led to violent deflagration even under an N_2 glovebox atmosphere.

In a scintillation vial, $[Cp_2Co]PF_6$ [253 mg, 0.76 mmol] was suspended in 5 mL of THF and cooled in the cold well at −78°C with active stirring. In a separate scintillation vial in the cold well, a solution of *p*-dibromobenzene [179 mg, 0.76 mmol] in ca. 15 mL toluene was lithiated by dropwise addition of 1 equivalent of nBuLi [0.475 mL, 1.6 M, in hexanes] and aging for 1 hour at −78°C with stirring. At this point, the cold solution of p-bromolithiobenzene was transferred dropwise via a Pasteur pipette to the cobaltocenium suspension over ~5 minutes, then the vial reclosed and allowed to warm naturally in the coldwell overnight (~16 hrs). A dark red color was observed to develop. The resulting crude THF-toluene solution was filtered over a ~1 cm Pasteur pipette plug of activated neutral Al_2O_3 and dried in vacuo to a sticky red paste. Extraction of the paste by stirring with copious pentane, refiltration over Al_2O_3 and drying of the pentane extracts in vacuo afforded 150 mg (*64%*) of Cp(η^4-C_5H_5-*p*-PhBr)Co as a red powder which was further recrystallized by layering a concentrated toluene solution with HMDSO (1:3 PhMe/HMDSO at −35°C). Yields typically vary from 40-60%.

Notes: If the concentration of the bromoarene is too high, the lithiation becomes a slurry that is difficult to transfer quantitatively with a Pasteur pipette while cold. At ~10 mg/mL, it remains relatively homogeneous and the lithiation is more reliable. Precise control of the stoichiometry with titrated nBuLi is important. With the use of in-situ generated p-bromolithiobenzene, there is no isolation and washing of the aryllithium to remove residual nBuLi from excess addition or incomplete lithium-halogen exchange. The nBuLi leads to several problems:

1. Formation of the oily contaminant Cp(η^4-C_5H_5-nBu)Co by direct addition to $[Cp_2Co]PF_6$. If found, it is essential to purge this impurity at the Co^I stage by washing with cold HMDSO (in which it is moderately soluble) before hydride abstraction with $[Ph_3C]BAr^F{}_4$. ^{1}H NMR of the red oil obtained by drying of the HMDSO extracts in vacuo establishes its identity as the butylated side product. The oxidized form, $[CpCoCp^{nBu}]BAr^F{}_4$, is difficult to separate from desired cobaltocenium $BAr^F{}_4$ salts either by chromatography or crystallization.
2. Any unreacted organolithium leads to slow decomposition and darkening of the crude product, even in the solid state – possibly by further reaction to anionic CpCo metallates that liberate Co^0 black. Exposure of the purified authentic product to 5% Na/NaCl powder or nBuLi in THF both led to similar darkening and decomposition to black material. A batch that is contaminated can be recovered by repeated dissolution in aliphatic hydrocarbons and filtration over Al_2O_3.

Method B: Large-scale Lithium Arylmagnesiate Addition
In the glovebox, $[Cp_2Co]PF_6$ [5 g, 15 mmol mmol] was suspended in 100 mL of dry THF in a 250 mL Schlenk-type round-bottom flask with a stir bar and a septum was fitted with copper wire. In parallel, in a scintillation vial, nBuLi [9.9 mmol, 6.19 mL, 1.6 M in hexanes] and $MgBu_2$ [4.95 mmol, 4.95 mL, 1 M in heptane] were combined and stirred for 15 minutes to generate an active higher-order magnesiate with nominal composition Li_2MgBu_4. The magnesiate was transferred by pipette to a concentrated solution of *p*-dibromobenzene [3.54 g, 15 mmol] in 10 mL PhMe and allowed to stir at room temperature for 1 hour. After this, the solution was transferred to a 50 mL round-bottom flask which was then closed with a septum. The $[Cp_2Co]PF_6$ suspension and arylmagnesiate solution were brought out of the glovebox together, then the flask containing $[Cp_2Co]PF_6$ was connected to N_2 on the Schlenk line and chilled to 0°C in an ice-water bath. The arylmagnesiate was cannulated dropwise into the cold $[Cp_2Co]PF_6$ over 5 minutes, leading to

formation of a red color. After stirring for 4 hours, the reaction was dried in vacuo to a thick red paste. The Schlenk flask was opened to air and with the aid of a spatula the paste was quickly extracted with copious pentane followed by minimal toluene until the red color was fully removed. **(SAFETY NOTE)** Due to the possibility of incomplete consumption of arylmetal reagents, the crude should be handled as a potential pyrophor in a clean hood free of excess flammable material. The red hydrocarbon extracts were directly poured from the reaction vessel onto a short plug of neutral Al_2O_3 (1x3") and pushed through with N_2 from the Schlenk line into a round-bottom flask. Arylmagnesiate residues and O_2-sensitive $CpCo^{I}$ impurities in the crude visibly decomposed on exposure to air, leaving black tars which stuck irreversibly to the top of the alumina plug. The hydrocarbon extracts were concentrated on the rotary evaporator to afford 2.2 g (*42%*) of red solid product which was further recrystallized from cold hexane in the freezer at −20°C.

Notes: The product is moderately soluble in pentane, hexane, Et_2O and MeCN, very soluble in aromatic solvents (especially benzene), and sparingly soluble in HMDSO. ^{1}H and ^{13}C NMR spectra were obtained in CD_3CN, which also allows residual $LiPF_6$ to be dissolved if present and detected via the ^{7}Li, ^{19}F and ^{31}P channels. A sufficiently long ^{1}H relaxation delay of 5-10s is required to obtain precise Cp proton integrations in CpCo compounds.

In contrast to more electron-rich $CpCo^{I}$-diene analogues, Cp(η^4-C_5H_5-*p*-PhBr)Co is moderately stable to oxidation on the bench, both in the solid state and in hydrocarbon solution. Single crystals suitable for X-ray diffraction were grown from a saturated, filtered hexane solution chilled to −20°C in a freezer outside the glovebox. Although isolated by neutral Al_2O_3 filtration, it decomposes on silica or alumina TLC plates in air - streaking is observed during development with hexanes, with conversion from red product to an unidentified blue substance. Exposure to air is not necessary in the *Method B* workup but is expedient for the large-scale purification.

The *Method B* magnesiate route has the advantage that the nucleophile is easy to manipulate at ambient temperature and forms stable stock solutions, akin to many Grignards. The extent of conversion of dibromobenzene to monomagnesiated aryl bromide nucleophile is conveniently assayed by ^{1}H WET-1D solvent-suppressed NMR in PhMe or by dilution into d^8-toluene.

^{1}H NMR (CD_3CN, 400 MHz, 298 K) δ 7.26 (d, J = 8.3 Hz, 2H), 6.70 (d, J = 8.3 Hz, 2H), 5.27 (t, J = 2.0 Hz, 2H), 4.81 (s, 5H), 3.80 (t, J = 2.6 Hz, 1H), 2.91 (q, J = 2.2 Hz, 2H).

$^{13}C\{^{1}H\}$ (CD_3CN, 101 MHz, 298 K) δ 146.15, 131.72, 128.00, 119.70, 80.13, 75.40, 55.47, 44.32.

[$CpCoCp^{Br}$]BAr^{F}•0.5(Et_2O)

A scintillation vial containing a slurry of $[Ph_3C]BAr^{F}_4$ [980 mg, 0.89 mmol, 0.95 eq] in 12 mL of PhMe was placed in an Al vial block and the whole block pre-cooled in the glovebox freezer to −40°C. After 30 minutes, the block was quickly pulled out and set on a stir plate, then in one portion solid Cp(η^4-C_5H_5-*p*-PhBr)Co [322 mg, 0.93 mmol, 1 eq.] was dumped into the $[Ph_3C]BAr^{F}_4$ from a tooled-neck dram vial. This operation was completed in <1 minute. As the vial warmed, the heterogeneous slurry of $[Ph_3C]BAr^{F}_4$ in benzene was observed to turn from a dark red to a lighter orange color with formation of a mobile semi-solid slurry of Co^{III} product. The reaction mixture was allowed to stir for 16 hours overnight. On removal from stirring and settling of the reaction solution, two phases were observed (~1 cm of oily orange product and a red supernatant). The solution was chilled to -40°C for an hour and then the red supernatant quickly removed with a Pasteur pipette while cold. Drying in vacuo of the oily remainder afforded 1.2 g of crude yellow solids which were triturated with 3x5 mL pentane, using a spatula to break up and thoroughly wash the material. The solids were recrystallized by layering a concentrated Et_2O solution with pentane (3 mL Et_2O/5 mL pentane) and cooling to −40°C to yield large clusters of yellow crystals (1.00 g, *86%*) after decantation of solvent and drying in vacuo. ^{1}H NMR analysis in CD_3CN showed that this thoroughly dried crystalline material was a hemisolvate of Et_2O.

^{1}H NMR (CD_3CN, 400 MHz, 298 K) δ 7.72–7.66 (m, 16H, overlapping BArF and Ph^{Br} resonances), 6.16 (t, *J* = 2.1 Hz, 2H), 5.77 (t, *J* = 2.1 Hz, 2H), 5.50 (s, 5H).
$^{13}C\{^{1}H\}$(CD_3CN, 101 MHz, 298 K) δ 162.56 (q), 135.60 (m), 133.04, 130.12, 129.67, 129.51 (qq), 129.10, 126.40, 124.80, 123.70, 121.00, 118.25 (m), 117.90, 103.96, 86.45, 85.37, 81.57, 65.86 (Et_2O), 15.20 (Et_2O).
HRMS: (ESI) calculated for $CoC_{16}H_{13}Br$ [M^+]: 342.9527, found: 342.9533, δ = 0.25 ppm. The $^{79/81}Br$ doublet is observed.

On scales smaller than 1 g of BAr^{F}_4, solid $[Ph_3C]BAr^{F}_4$ was instead typically added to the cold PhMe solution of Co(I).

Well-formed single crystals were not obtained from the preparative-scale crystallization from Et_2O. Instead, vapor diffusion of pentane into a concentrated 1,2-dichloroethane solution on the bench (~100 mg/mL, 1:10 v/v DCE/pentane) yielded diffraction-quality, clear yellow plates of [$CpCoCp^{Br}$]BAr^{F} which were solvent-free. The equivalent diffusion with DCM/pentane led to oiling.

[$CpCoCp^{PhN}$]BAr^{F}_4

A scintillation vial containing a solution of Cp(η^4-C_5H_5-*p*-$PhNMe_2$)Co [158 mg, 0.5 mmol, 1 eq.] in 10 mL PhMe was placed in an Al vial block and the whole block pre-cooled in the glovebox freezer to −40°C. After 30 minutes, the block was quickly pulled out and set on a stir plate, then in one portion solid $[Ph_3C]BAr^{F}_4$ [534.6 mg, 0.475 mmol, 0.95 eq.] was dumped into the Co^{I} solution from a tooled-neck dram vial. This operation was completed in <1 minute. As the vial warmed with active stirring, the cold, heterogeneous mixture was observed to turn to a rich red-violet color with formation of a mobile oil of Co^{III} product. After stirring overnight for 16 hours, the stir bar was removed and the reaction solution layered with 10 mL of pentane at −40°C to

precipitate the crude product. Decanting of the cold supernatant yielded a crude red solid which was further washed and triturated with 2x10 mL portions of pentane to remove residual Ph_3CH. The product was dissolved in dry Et_2O and filtered over ~3 cm of activated neutral Al_2O_3 in a "Monstr-Pette" (large volume Pasteur pipette), eluting completely after ~20 mL. The resulting red solution was brought out of the glovebox, transferred to a 100 mL round-bottom flask, and concentrated by rotary evaporation. ~50 mL of PhMe was added and hot recrystallization was carried out directly in the flask by warming the solvent to reflux with a heat gun. Solvent-free red-violet needles (266 mg, *45%*) suitable for X-ray diffraction were obtained by slow cooling of the boiling PhMe solution (~5 mg/mL) in two stages: first to room temperature, then to −20°C in a freezer. NMR analysis of the pure product in CD_3CN confirms that its ^{1}H and ^{13}C spectra are identical to those previously reported except for new peaks corresponding to the BArF anion.

Notes: The product and the most significant impurity (the unsubstituted metallocenium salt $[Cp_2Co]BAr^F_4$ arising from aryl group abstraction by $[Ph_3C]BAr^F_4$) are poorly resolved by SiO_2 chromatography with typical eluents ($CHCl_3$ or DCM). A compact initial band can be prepared by loading in PhMe, but this is frustrated by the tendency of the product to crystallize from PhMe as cosolubilizing impurities are removed.

$[CpCoCp^{Ph2N}][BAr^F_4]$•1.5(C_6H_6)
In the glovebox, $[CpCoCp^{Br}]BAr^F_4$ [364.4 mg, 0.3 mmol, 1 eq.], $Pd(PPh_3)_4$ [17.5 mg, 5 mol%], anhydrous Na_2CO_3 [96 mg, 0.9 mmol, 3 eq.] and 4-(dimethylamino)phenylboronic acid [59.8 mg, 0.36 mmol, 1.2 eq.] were added sequentially as solids to a wide-necked (~1 cm) 100 mL Schlenk bomb with a Kontes Teflon screw cap, along with a stir bar. The residual powders and sparingly soluble Pd catalyst were rinsed in with 8 mL dry THF in total. The Schlenk bomb was removed from the glovebox and 2 mL of DI H_2O (previously degassed by N_2 sparging for 30 min.) added by syringe through a septum against a positive pressure of dynamic N_2. On addition of water, the slurry became homogeneous. The reaction vessel was sealed and heated to reflux with stirring at 70°C, the light orange mixture becoming dark red within 15 minutes. Reaction monitoring by UHPLC-MS (direct dilution into MeCN, gradient 5→95% MeCN with H_2O/0.1% AcOH as weak solvent) confirmed full consumption of the starting cobaltocenium aryl bromide (**$[M^+]$** m/z = 343/345, $^{79/81}$Br doublet) and formation of product (**$[M^+]$** m/z = 384.1) after 16 hrs. The crude reaction mixture was concentrated to dryness on Schlenk line vacuum (30 micron Hg) with a warm water bath, then pumped into the glovebox, rinsed and triturated mechanically with 2x5 mL pentane to remove organic impurities. The solid was extracted with 2x3 mL Et_2O, taking advantage of the relative insolubility of $Pd(PPh_3)_4$ in Et_2O, and the extracts filtered over a Celite pipette. Outside the box, the dark red Et_2O solution was concentrated to a thick red oil in a scintillation vial under a gentle stream of compressed air, then purified by chromatography over silica gel. The compound was loaded as a slurry in the column packing solvent, PhMe (R_f ~ 0), then purified by gradient elution (PhMe to $CHCl_3$ to DCM in 20% steps per 40 mL using 2 cm x 7.5 cm SiO_2). The product begins to elute as an intense red band with $CHCl_3$ and is removed completely by the final DCM flush. A faint early band of organic side product elutes with 20% $CHCl_3$ in PhMe, while oxidized Pd catalyst material sticks to the top of the column and turns orange. The dark red fractions were concentrated by rotary evaporation, refiltered in minimal DCM over a short pipette of neutral Al_2O_3, and reconcentrated by a stream of compressed air. Finally, the oily product was recrystallized by vapor diffusion (~4 mL benzene/400 mg crude solid diffused at RT with 25 mL

pentane) to afford 370.8 mg (*90%*) of [CpCoCp^{Ph2N}]BAr$^{F}_4$•1.5(C_6H_6) as red needles suitable for X-ray diffraction.

The BAr$^{F}_4$ salt is insoluble in water but freely soluble in CH_3CN, ethereal solvents (THF, Et_2O) and halogenated solvents (DCM, $CHCl_3$, PhF), in which it is dark red. It is moderately soluble in benzene and PhMe (~10s of mg/mL), forming oily purple solutions.

^{1}H NMR (CD_3CN, 400 MHz, 298 K) δ 7.82 – 7.76 (m, 2H), 7.74 – 7.68 (m, 10H, overlapped PhPh and BArF), 7.67 (br s, 4H), 7.64 – 7.59 (m, 2H), 7.37 (s, 9H, 1.5 eq. C_6H_6), 6.88 – 6.80 (m, 2H), 6.22 – 6.17 (m, 2H), 5.79 – 5.73 (m, 2H), 5.48 (s, 5H), 2.98 (s, 6H).
^{13}C{^{1}H} (CD_3CN, 101 MHz, 298 K) δ 162.41 (q), 151.64, 143.83, 135.46, 129.72 (qq), 129.31, 129.10, 129.04, 128.20, 127.52, 127.25, 127.13, 126.61, 123.91, 121.21, 118.49 (p), 118.10, 113.40, 105.92, 86.43, 85.20, 81.07, 40.34.
HRMS: (ESI) calculated for $CoC_{24}H_{23}N$ [M^+]: 384.1157, found: 384.1162, δ = 0.26 ppm.

CpCoCp^{Ph2N}
In the glovebox, 0.5 wt% Na/Hg amalgam [820 mg, 1.0 eq.] freshly prepared with clean Na^0 wire was carefully transferred via Pasteur pipette to a tared 20 mL scintillation vial with a stir bar. The amalgam was covered with 2 mL NaK-dried THF and a solution of [CpCoCp^{Ph2N}]BAr$^{F}_4$ [220 mg, 0.176 mmol, 1.0 eq.] in 2 mL NaK-dried THF added dropwise with stirring. The vial was capped and the reaction mixture allowed to stir vigorously with the vial clamped at an angle to promote dispersion of the amalgam. Within 15 minutes, the crimson red solution was first observed to turn brown and then an inky blue-black after an hour. When complete conversion to Co^{II} was inferred from the color change after 20 hours, the reaction mixture was filtered through a Celite pipette filter to remove residual Hg, concentrated in vacuo and redissolved in benzene to remove colorless crystals of NaBAr$^{F}_4$. The benzene solution was filtered again over Celite (early purple band flows through, residual Co^{III} visible as a later-eluting reddish streak), then lyophilized to a green-black powder in *96%* yield. The product is very sparingly soluble in pentane and slightly more so in methylcyclohexane (<0.5 mM), forming clear purple solutions from which green fluffy microcrystals (pure Co^{II}) precipitate at low temperature. Dark green needles suitable for X-ray diffraction were obtained by chilling a dilute MeCN stock solution (~1 mM) to −40°C in the glovebox freezer. Preparative recrystallization from MeCN is effective for removal of trace Co^{III} or NaBAr$^{F}_4$, which are observable by 1H NMR via the BAr$^{F}_4$ aryl protons (δ 8.33, 7.61 in C_6D_6) and downfield shifts of Co^{II} resonances.

^{1}H NMR (C_6D_6, 400 MHz, 298 K) δ 14.97 (br s, 2H), 7.85 (d, *J* = 8.1 Hz, 2H), 4.27 (d, *J* = 8.3 Hz, 2H), 3.23 (d, *J* = 0.9 Hz, 6H), -10.27 (br s, 2H), -21.25 (br s, 2H), -49.91 (br s, 5H), -50.59 (br s, 2H).

Although reduction to Co^{II} could also be achieved by NaHg in benzene, the dark purple color of the starting material when reslurried in aromatic solvents makes it difficult to monitor the course of the reaction optically in contrast to the red color of the $[Co^{III}][BAr^F_4]$ starting material in ethereal, polar or halogenated solvents.

$[CpCoCp^{Ph2NH}][BAr^F_4]_2$

In the glovebox, $[CpCoCp^{Ph2N}]BAr^F_4 \bullet 1.5(C_6H_6)$ [46.0 mg, 34 μmol, 1.0 eq.] was dissolved in 2 mL of dry Et_2O in a scintillation vial with a stir bar. $[H(Et_2O)_2]BAr^F$ [34.1 mg, 34 μmol, 1.0 eq.] was dissolved in 2 mL of dry Et_2O in a separate vial, then slowly transferred dropwise with stirring using a Pasteur pipette. Immediate lightening of the dark red solution to a pale yellow was observed on protonation of $[CpCoCp^{Ph2N}]BAr^F_4$. After an hour of stirring, the solution was dried in vacuo to a gummy yellow mass which was triturated with 2x3 mL portions of pentane and benzene. The residual crude solids were brought out of the box and reprecipitated twice by dissolution in 1 mL of fluorobenzene and layering with 10 mL of hexane followed by cooling to −20°C in the freezer. This microcrystalline precipitate retained residual PhF by NMR even after extensive drying in vacuo. Finally, the product was further recrystallized by vapor diffusion of pentane into a concentrated *para*-difluorobenzene solution to afford 20 mg (*40%*) of product as long, fragile yellow needles. Contact with bench Celite 545 should be avoided - the protonated cobaltocenium dication turns red due to adventitious deprotonation by the basic sorbent.

^1H NMR (400 MHz, CD_3CN) δ 9.19 (s, 1H), 7.94 – 7.85 (m, 4H), 7.83 – 7.75 (m, 2H), 7.73 – 7.62 (m, 26 H), 6.27 – 6.21 (m, 2H), 5.84 – 5.77 (m, 2H), 5.51 (s, 5H), 3.27 (s, 6H).

$[D(Et_2O)_2]BAr^F_4$

In the nitrogen glovebox, triflic acid-d [324 mg, 2.14 mmol] was dissolved in diethyl ether [5 mL] in the cold well at −78 °C. The acid solution was added to a pre-cooled solution of $NaBAr^F_4$ [1.90 g] in diethyl ether [10 mL]. The reaction was allowed to stir cold for 30 minutes and then was stirred at room temperature for 10 minutes. The reaction was placed in the freezer [−35 °C] for 15 minutes, during which time a fine, translucent white mass (presumably NaOTf) settled to the bottom of the vial. The supernatant was filtered over Celite into a scintillation vial, yielding a clear solution. The solution was concentrated *in vacuo* to approximately 5 mL, and pentane [3 mL] was layered above. The vial was placed in the freezer overnight, during which time large white crystals formed. The supernatant was decanted off, and the crystals were dried *in vacuo*, yielding 1.93 g (89%) of a fine white powder. The powder was analyzed by ^1H, ^{13}C, and ^{19}F NMR spectroscopy in CD_3CN. The NMR spectra are identical to that of $[H(Et_2O)_2]BAr^F$ except for the diminished intensity of the peak in the ^1H NMR spectrum at ~13.8 ppm whose integration revealed the product to be at least 87% deuterated.

C3. NMR SPECTRA

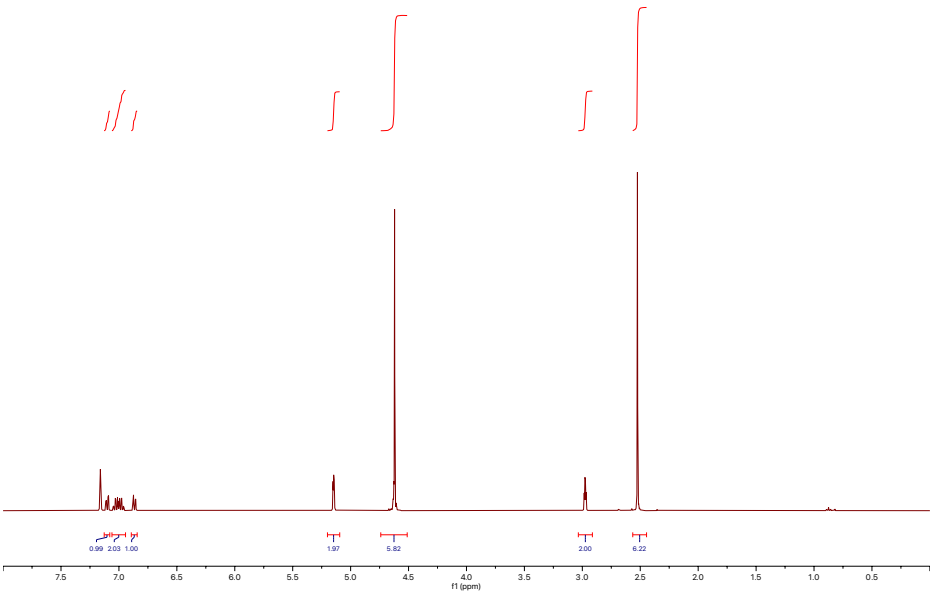

Figure C1. ^{1}H NMR spectrum of **Cp(η^4-C_5H_5-*o*-PhNMe$_2$)Co** in C_6D_6 (400 MHz)

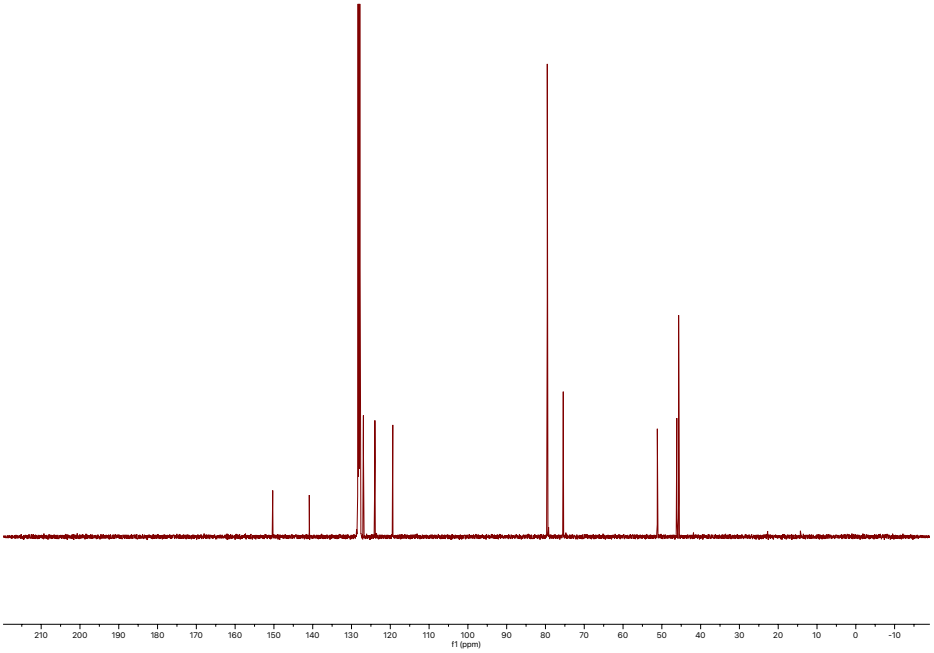

Figure C2. ^{13}C{^{1}H} NMR spectrum of **Cp(η^4-C_5H_5-*o*-PhNMe$_2$)Co** in C_6D_6 (101 MHz).

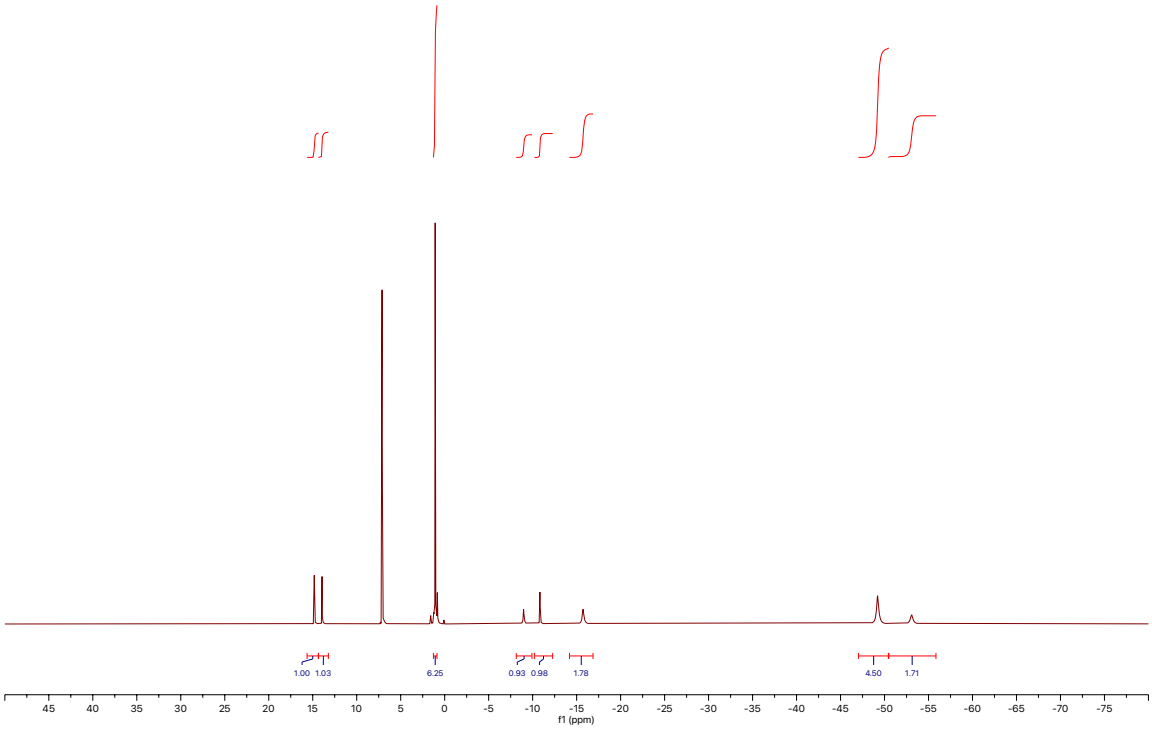

Figure C3. ^{1}H NMR spectrum of **CpCoCp$^{o\text{-}N}$** in C_6D_6 (400 MHz).

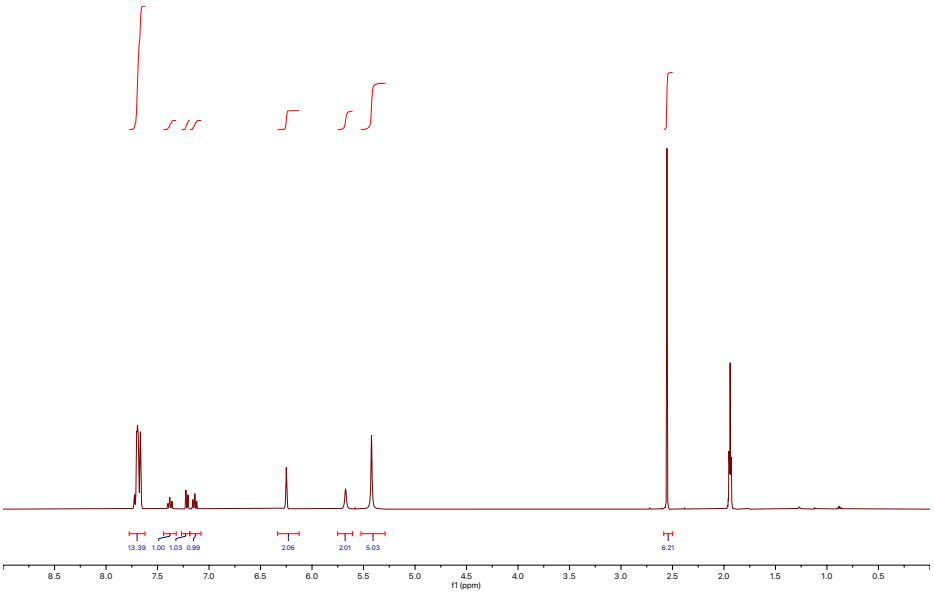

Figure C4. ^{1}H NMR spectrum of **[CpCoCp$^{o\text{-}N}$]BAr$^{F}_{4}$** in CD_3CN (400 MHz).

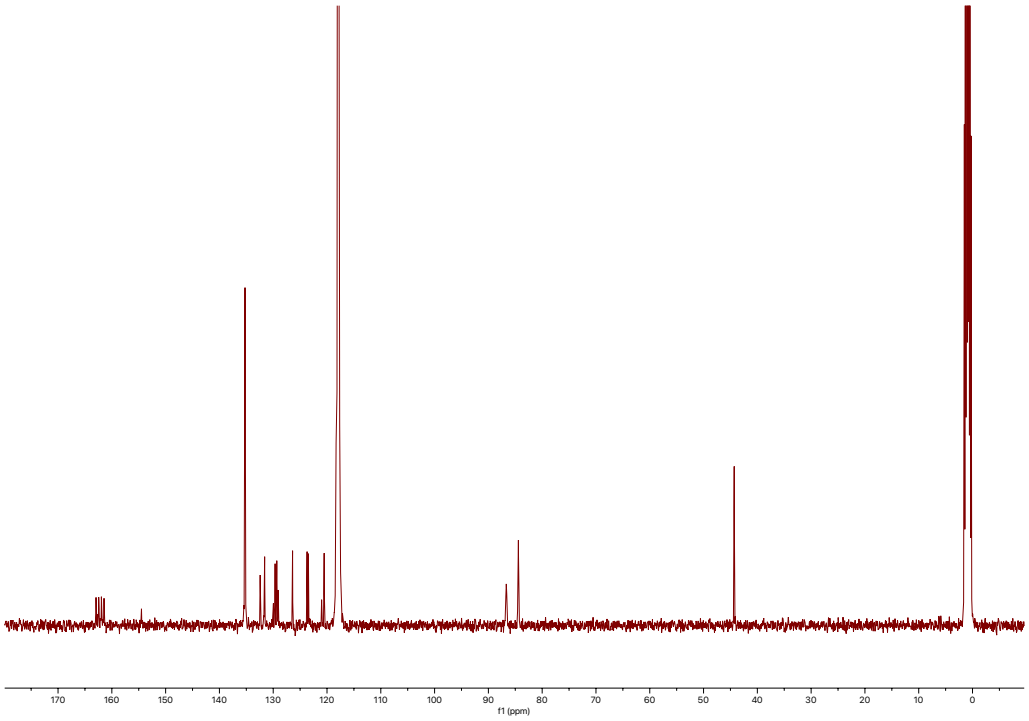

Figure C5. $^{13}C\{^{1}H\}$ NMR spectrum of **[CpCoCp$^{o\text{-}N}$]BAr$^{F}_{4}$** in CD_3CN (101 MHz).

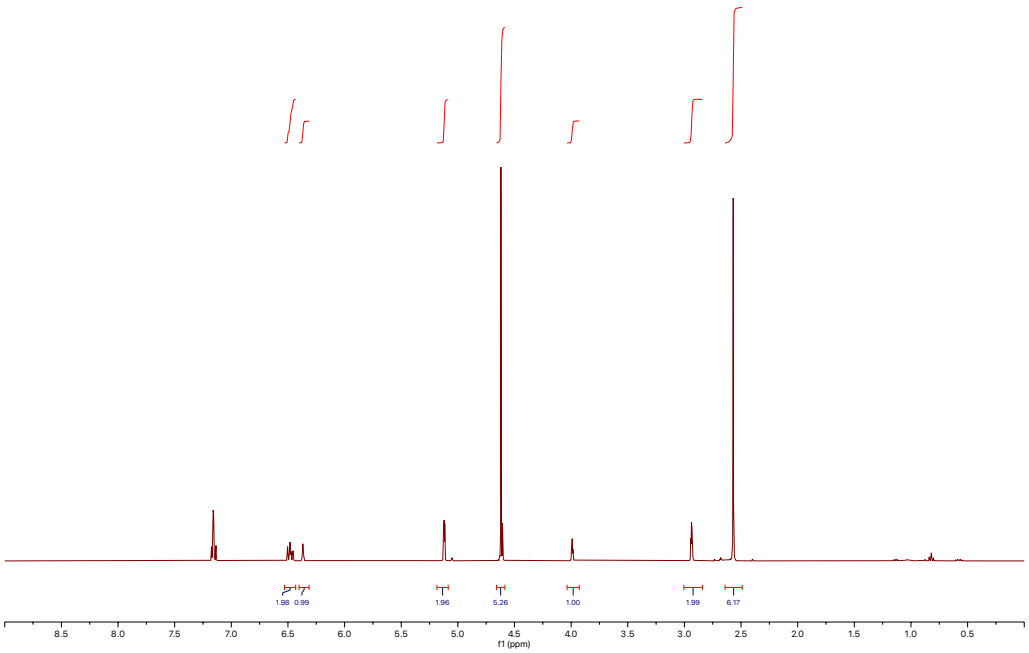

Figure C6. ^{1}H NMR spectrum of **Cp(η^4-C$_5$H$_5$-*m*-PhNMe$_2$)Co** in C_6D_6 (400 MHz).

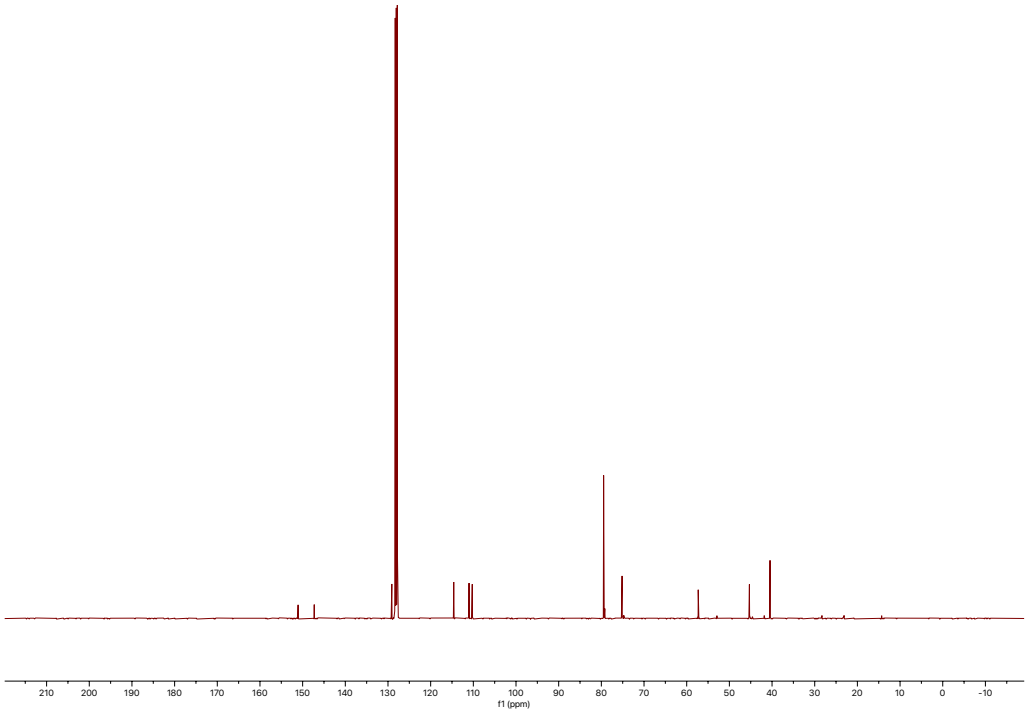

Figure C7. $^{13}C\{^{1}H\}$ NMR spectrum of **Cp(η^4-C_5H_5-*m*-PhNMe$_2$)Co** in C_6D_6 (101 MHz).

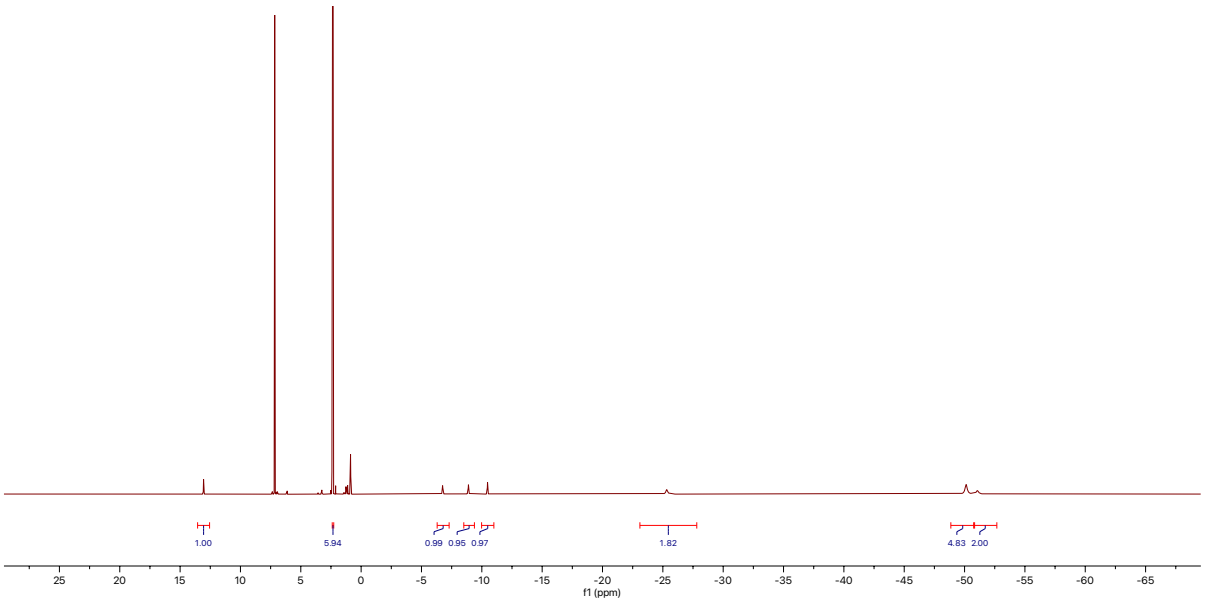

Figure C8. ^{1}H NMR spectrum of **CpCoCp$^{m\text{-}N}$** in C_6D_6 (400 MHz).

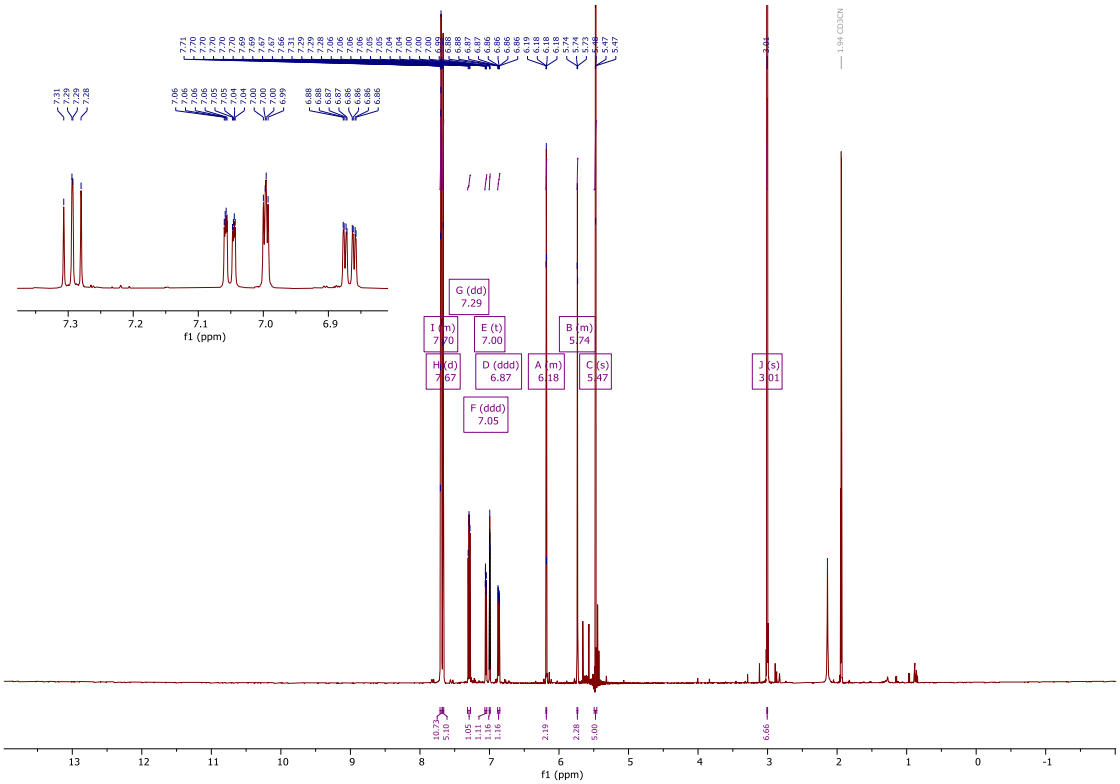

Figure C9. ^{1}H NMR spectrum of **[CpCoCp$^{m\text{-}N}$]BAr$^{F}_{4}$** in CD_3CN (600 MHz).

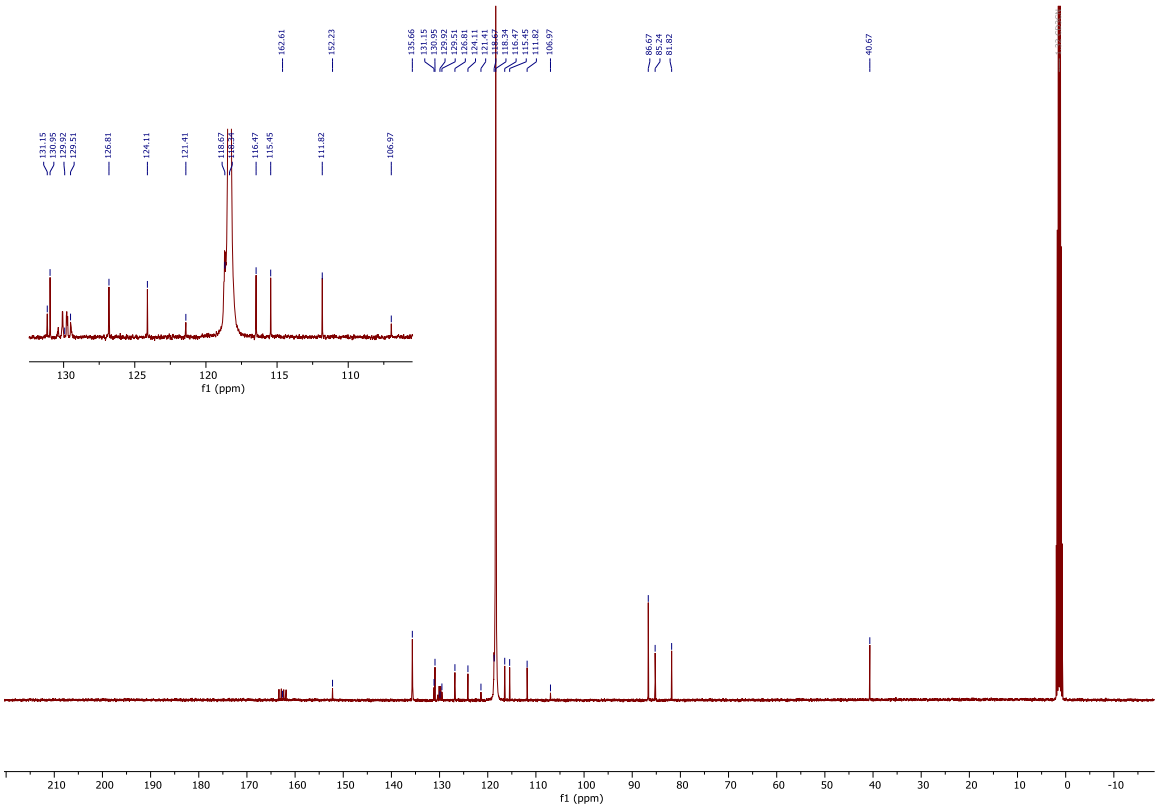

Figure C10. ^{13}C{^{1}H} NMR spectrum of **[CpCoCp$^{m\text{-}N}$]BAr$^{F}_{4}$** in CD_3CN (101 MHz).

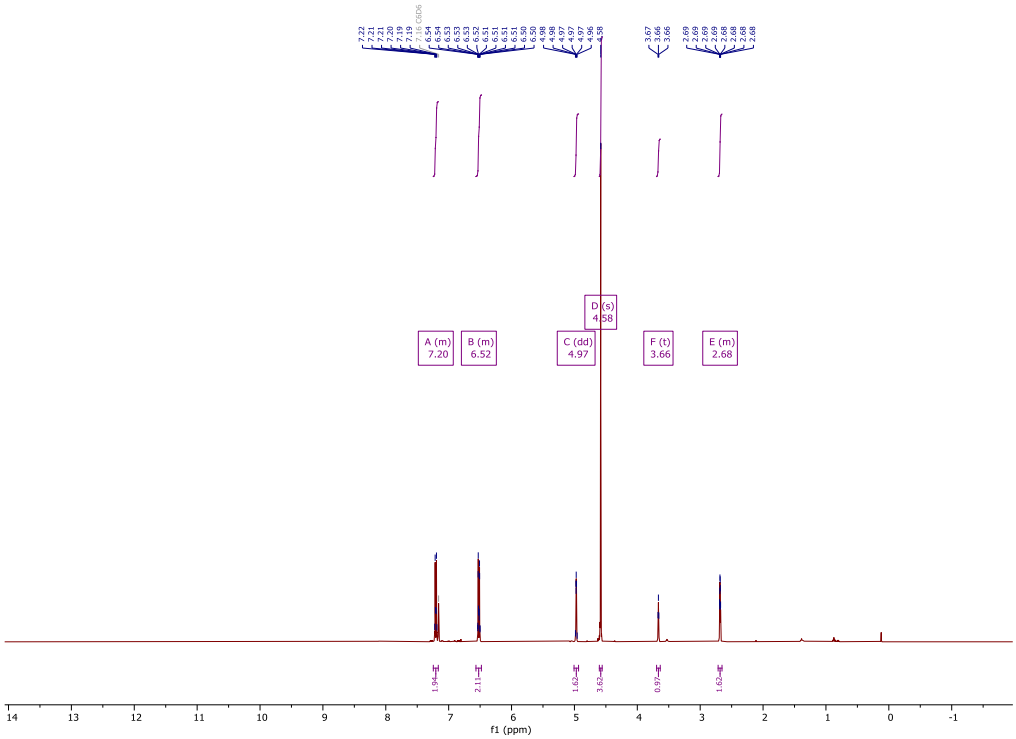

Figure C11. ^{1}H NMR spectrum of **Cp(η^4-C$_5$H$_5$-*p*-PhBr)Co** in C_6D_6 (400 MHz).

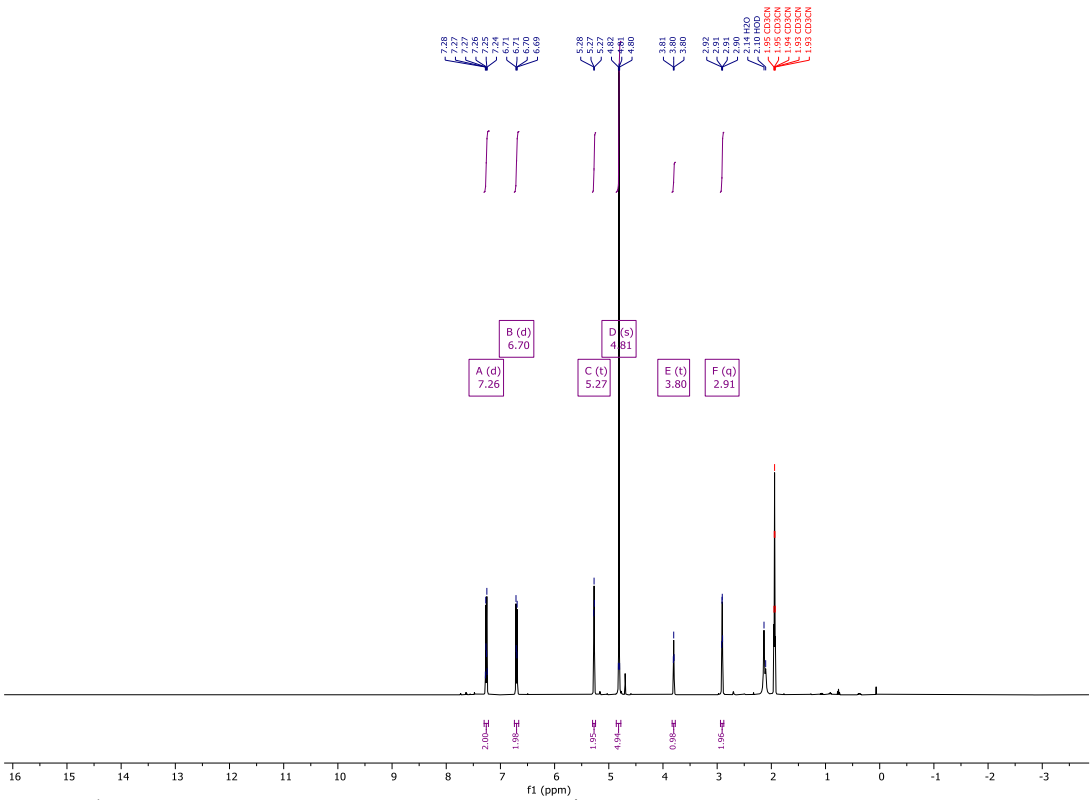

Figure C12. ^{1}H NMR spectrum of saturated **Cp(η^4-C$_5$H$_5$-*p*-PhBr)Co** in CD_3CN (400 MHz).

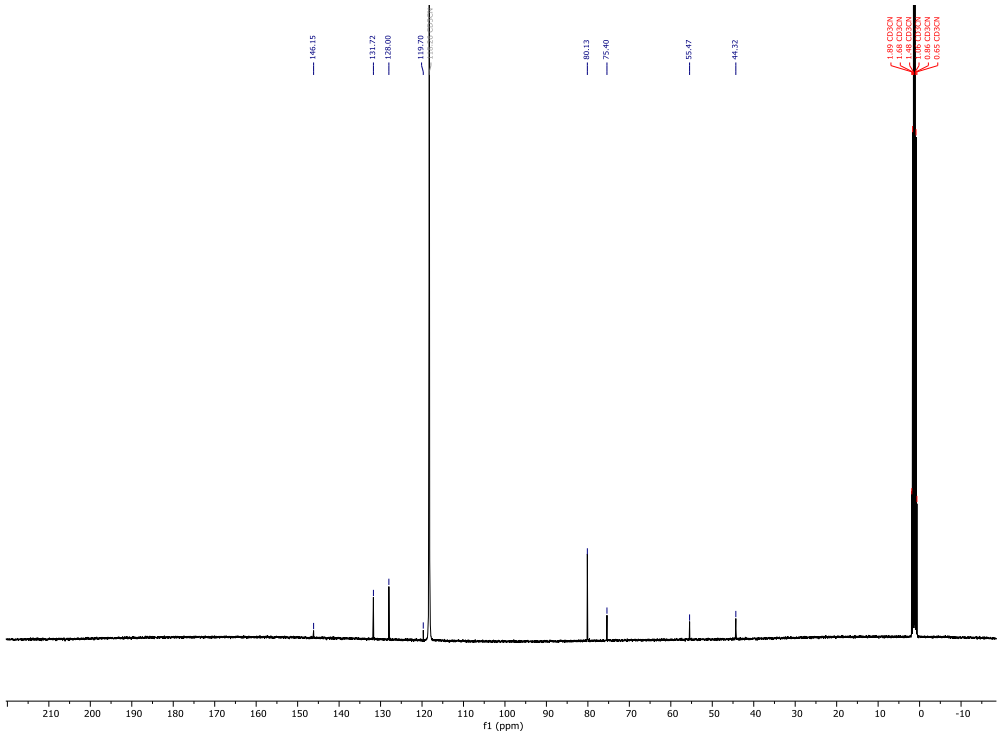

Figure C13. $^{13}C\{^{1}H\}$ NMR spectrum of saturated **Cp(η⁴-C₅H₅-*p*-PhBr)Co** in CD_3CN (101 MHz).

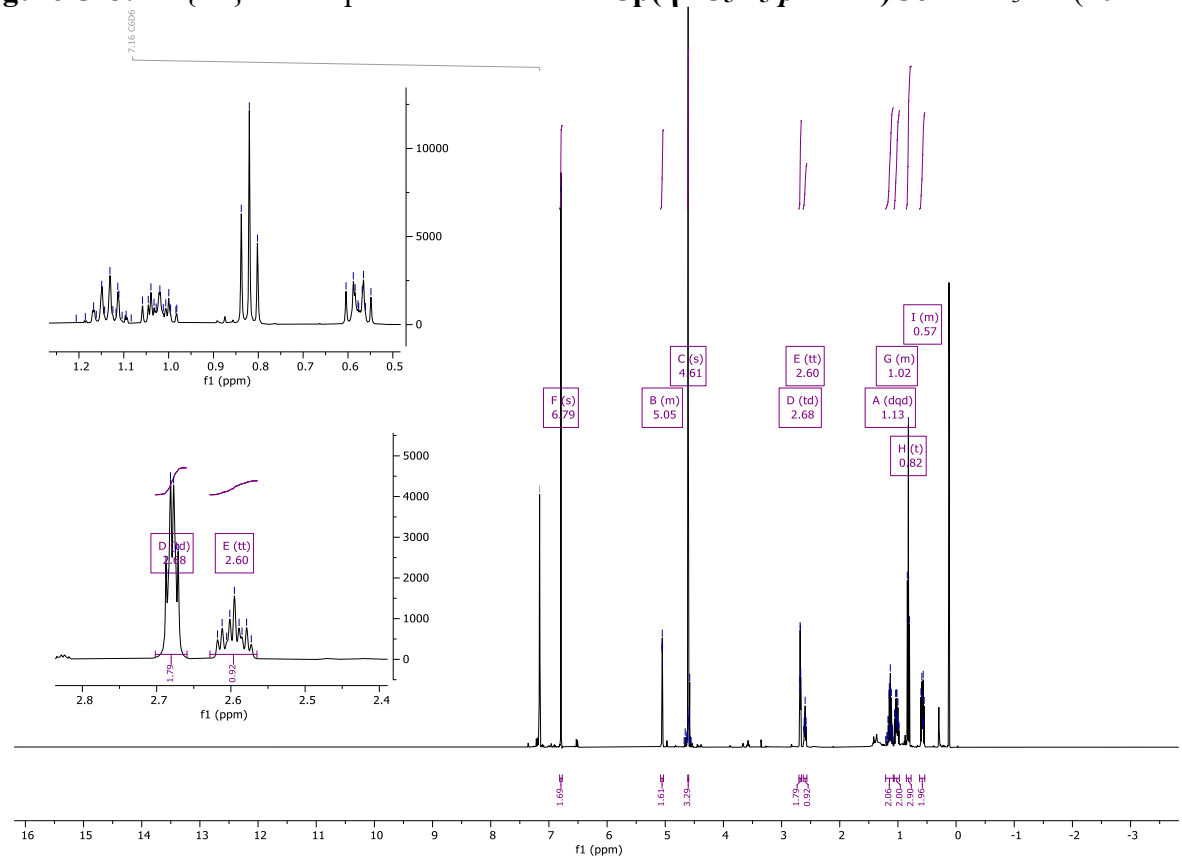

Figure C14. ^{1}H NMR spectrum of isolated **Cp(η⁴-C₅H₅-ⁿBu)Co** in C_6D_6 (400 MHz). Inset: aliphatic region and characteristic triplet-of-triplets CpH resonance.

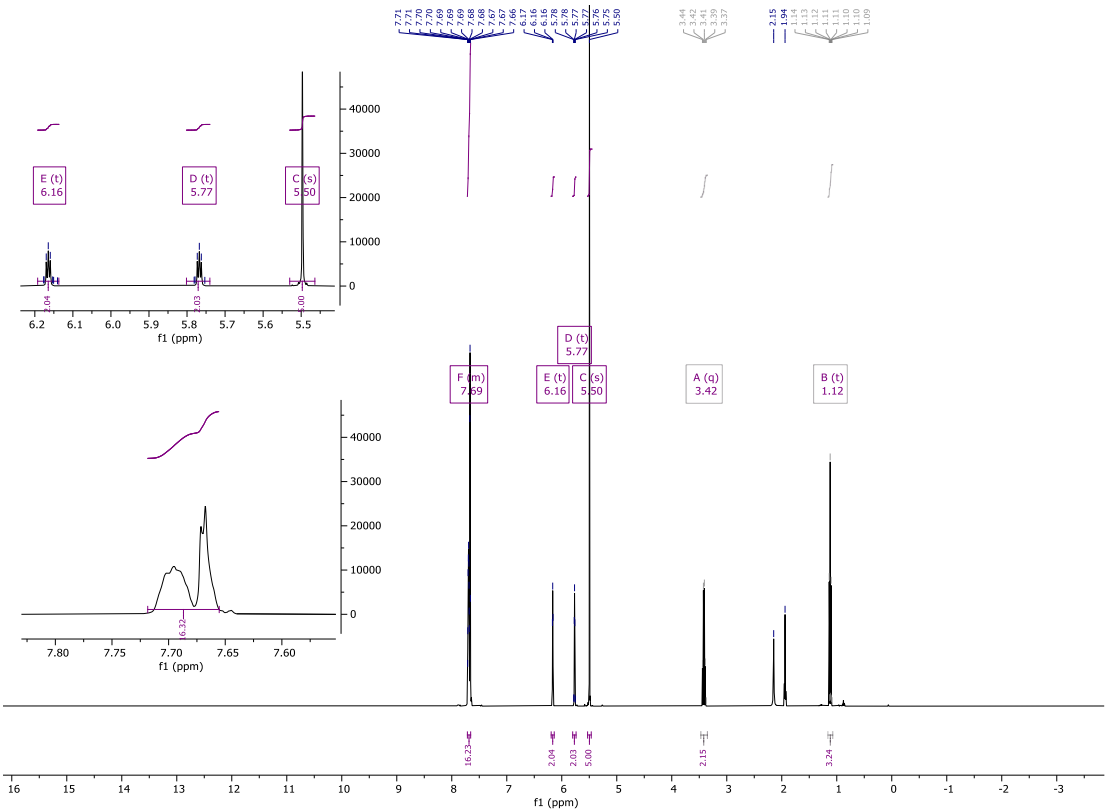

Figure C15. ^{1}H NMR spectrum of **[CpCoCp^{Br}]BAr$^{F}_{4}$•0.5(Et$_2$O)** in CD_3CN (400 MHz).

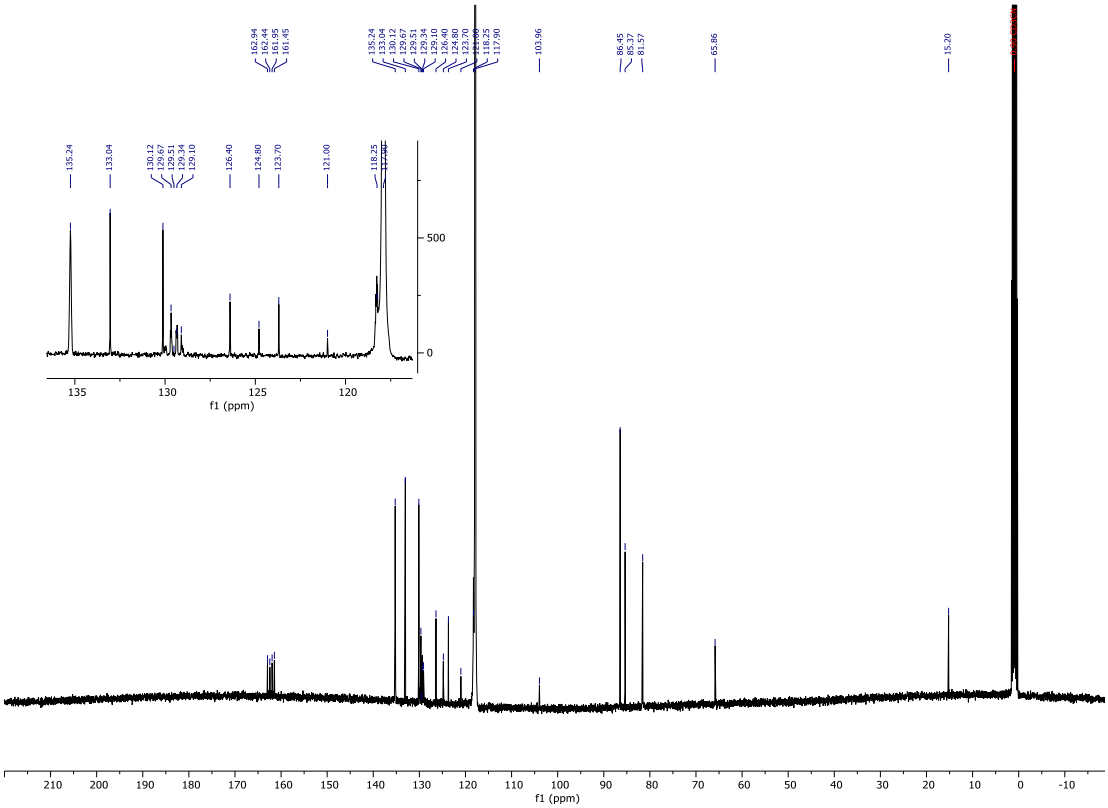

Figure C16. ^{13}C{^{1}H} NMR spectrum of **[CpCoCp^{Br}]BAr$^{F}_{4}$** in CD_3CN (400 MHz).

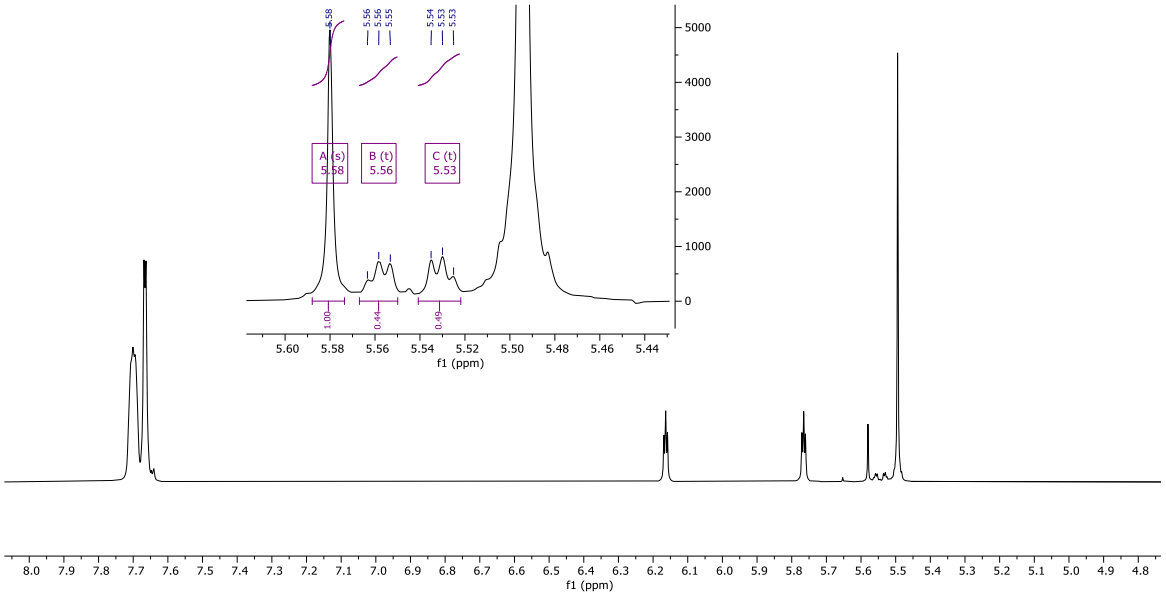

Figure C17. ^{1}H NMR spectrum of impure **[CpCoCp^{Br}]BAr$^F_4$** in CD_3CN (400 MHz). Inset: Characteristic Cp resonances of **[CpCoCp^{nBu}]BAr$^F_4$**.

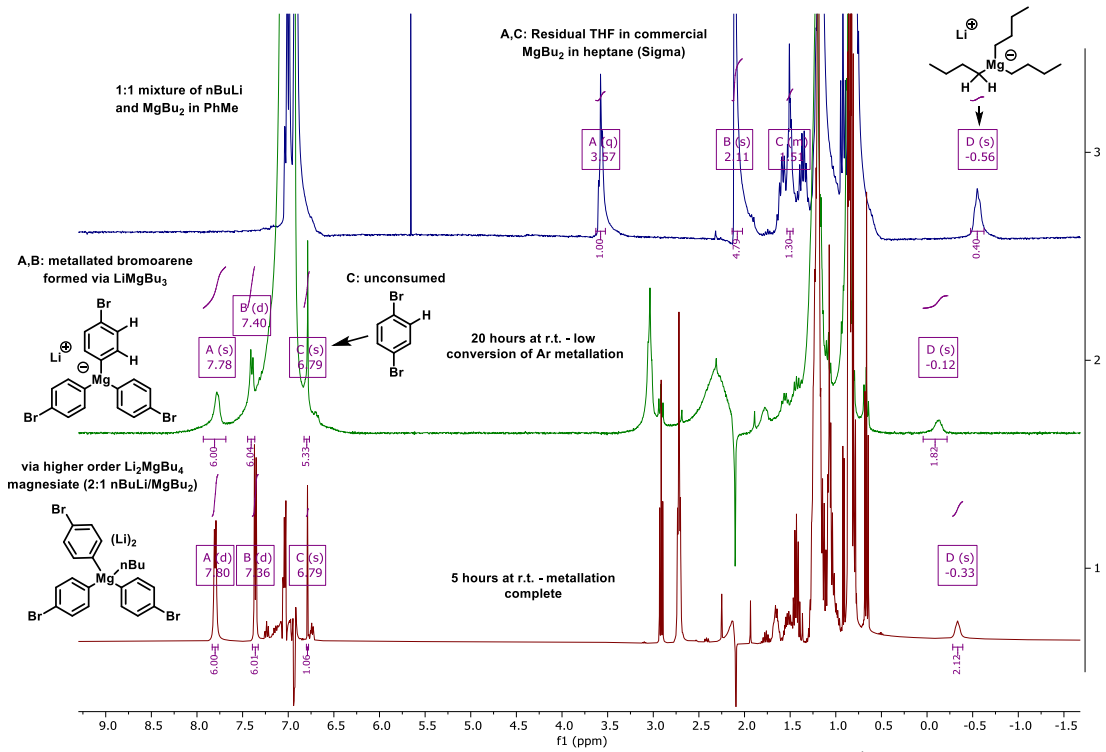

Figure C18. NMR determination of arylmagnesiate reagents. *(Top)* ^{1}H NMR spectrum at zero gain of 1:1 mixture of nBuLi and $MgBu_2$ in protio-toluene to form $LiMgBu_3$ (400 MHz). *(Middle)* ^{1}H WET-1D solvent-suppressed NMR spectrum of crude metalation reaction of 1 eq. p-dibromobenzene mixed with 0.33 eq. $LiMgBu_3$ in toluene. *(Bottom)* ^{1}H WET-1D solvent-

suppressed NMR spectrum of crude metalation reaction of 1 eq. p-dibromobenzene mixed with 0.33 eq. "Li_2MgBu_4" that was formed as a 2:1 mixture of nBuLi and $MgBu_2$ in toluene.

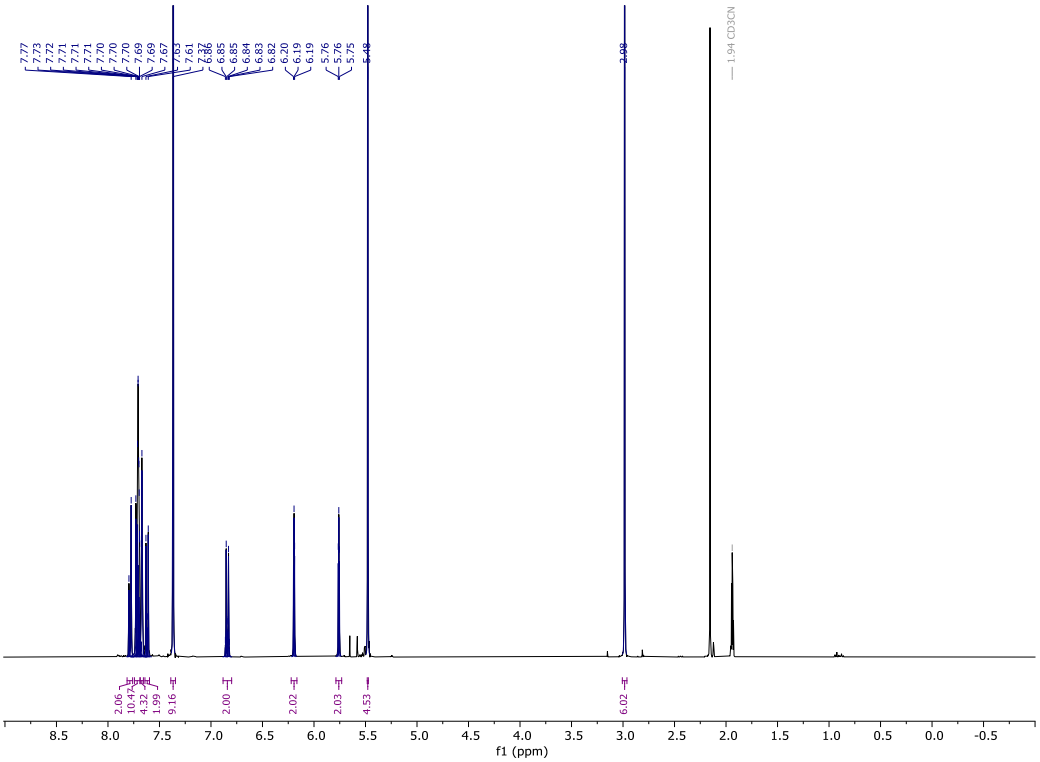

Figure C19. ^{1}H NMR spectrum of [**CpCoCp^{Ph2N}**]**BAr$^F_4$** in CD_3CN (400 MHz).

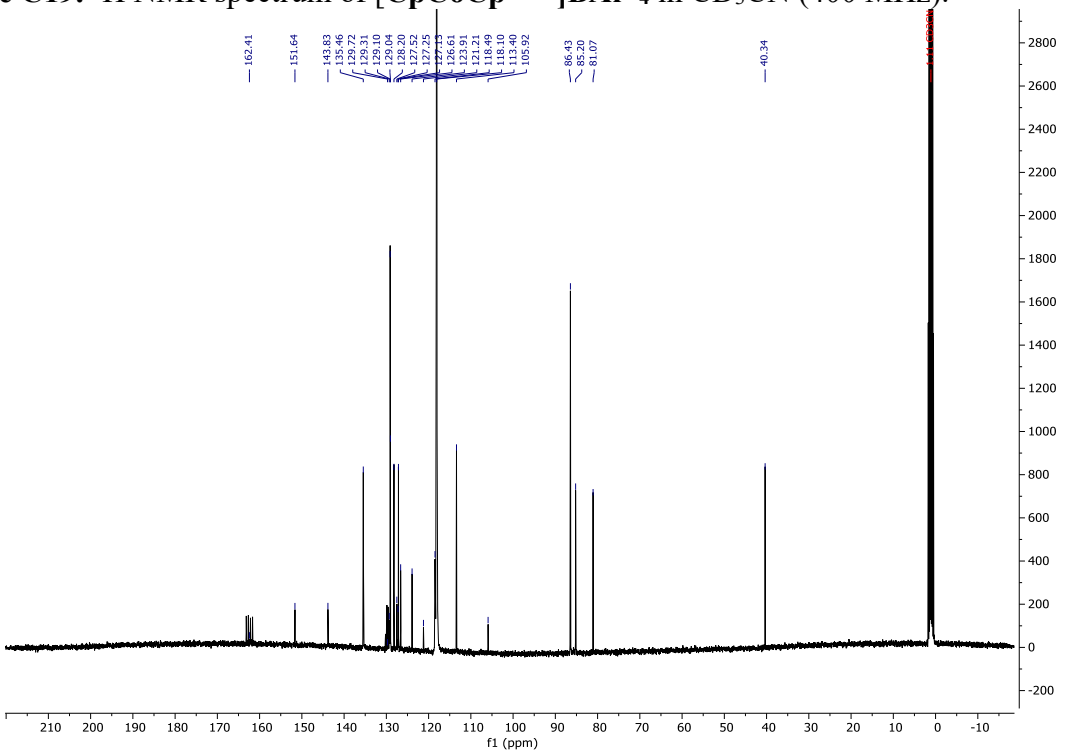

Figure C20. ^{13}C NMR spectrum of [**CpCoCp^{Ph2N}**]**BAr$^F_4$** in CD_3CN (101 MHz).

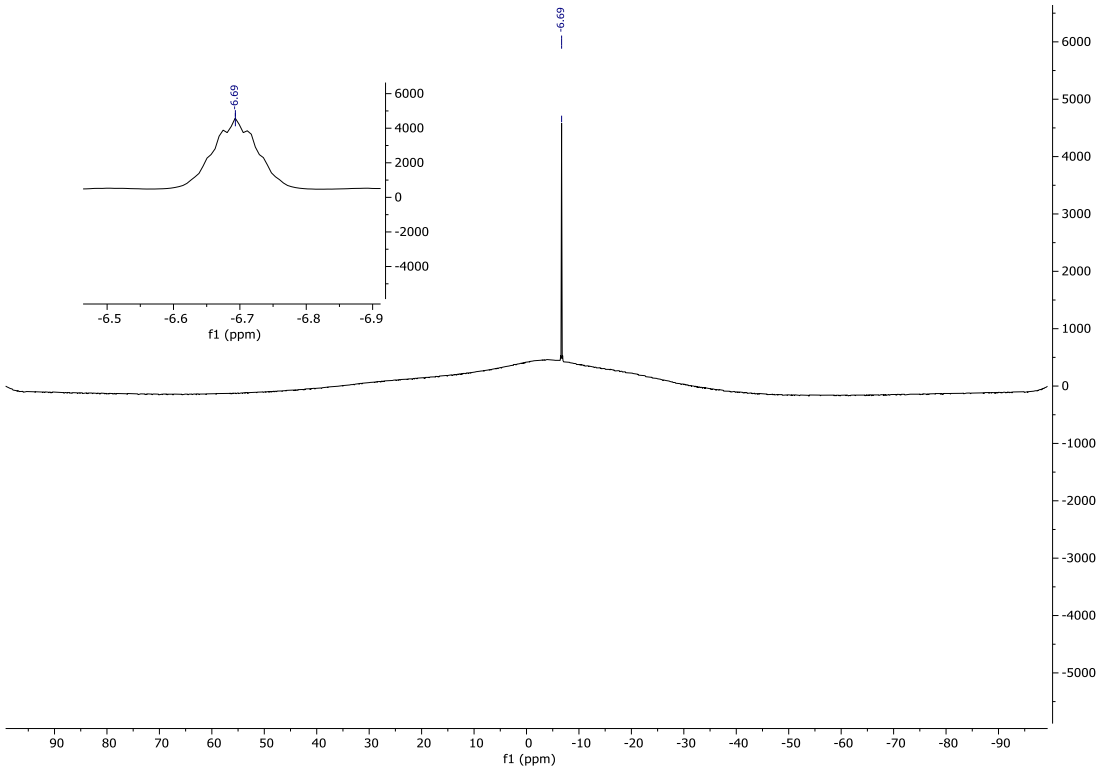

Figure C21. ^{11}B NMR spectrum of [**CpCoCp^{Ph2N}**]**BAr$^{F}_{4}$** in CD_3CN (128.38 MHz) without decoupling. The broad background originates from the borosilicate glass NMR tube.

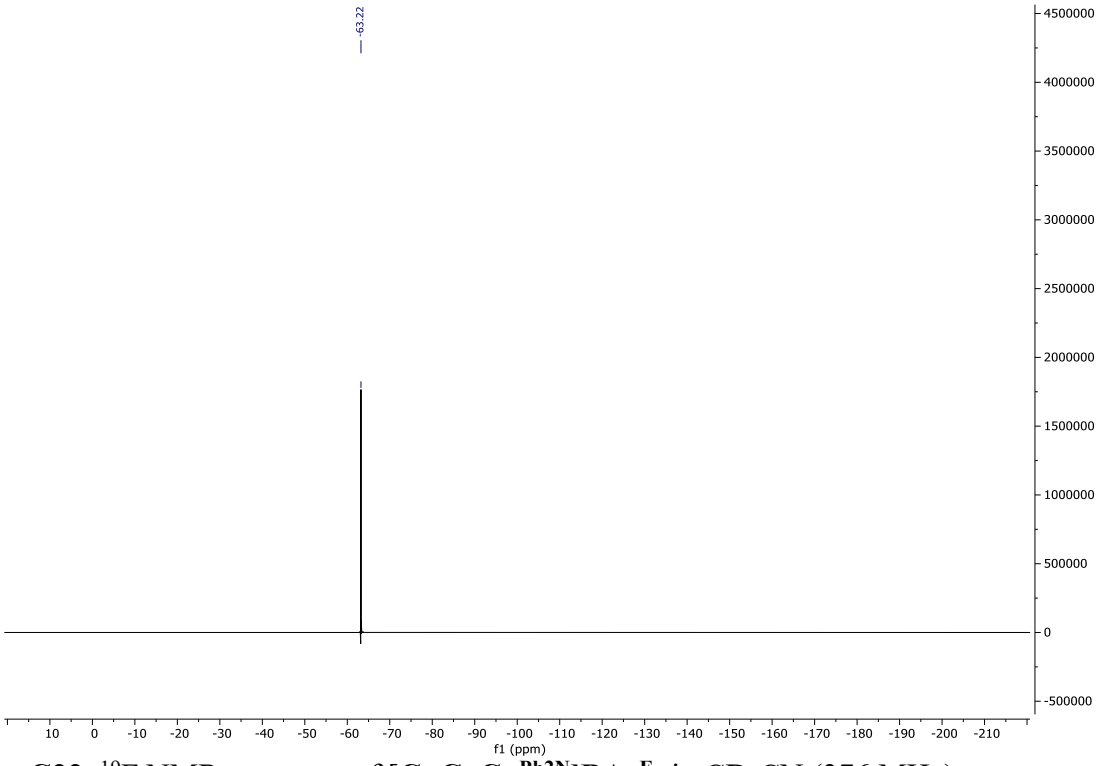

Figure C22. ^{19}F NMR spectrum of [**CpCoCp^{Ph2N}**]**BAr$^{F}_{4}$** in CD_3CN (376 MHz).

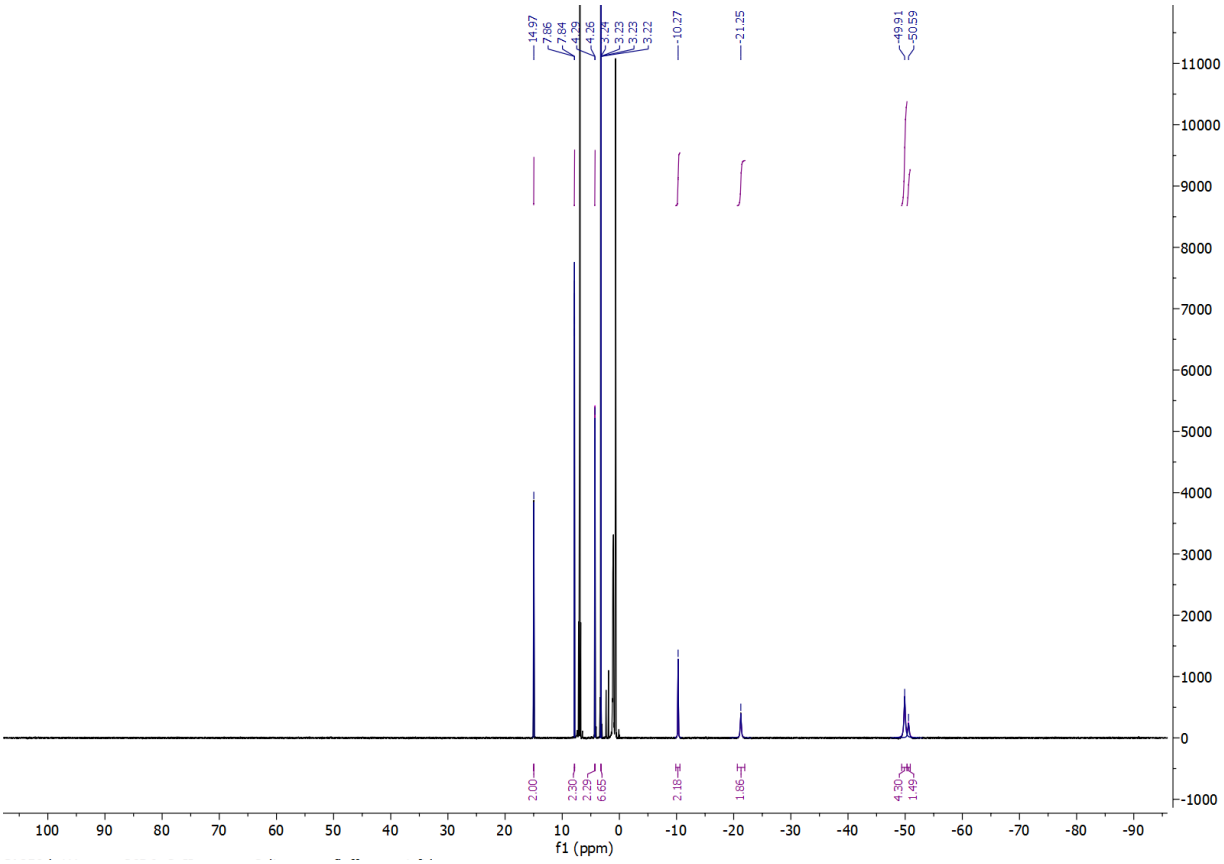

Figure C23. ^{1}H NMR spectrum of **CpCoCp^{Ph2N}** in C_6D_6 (400 MHz).

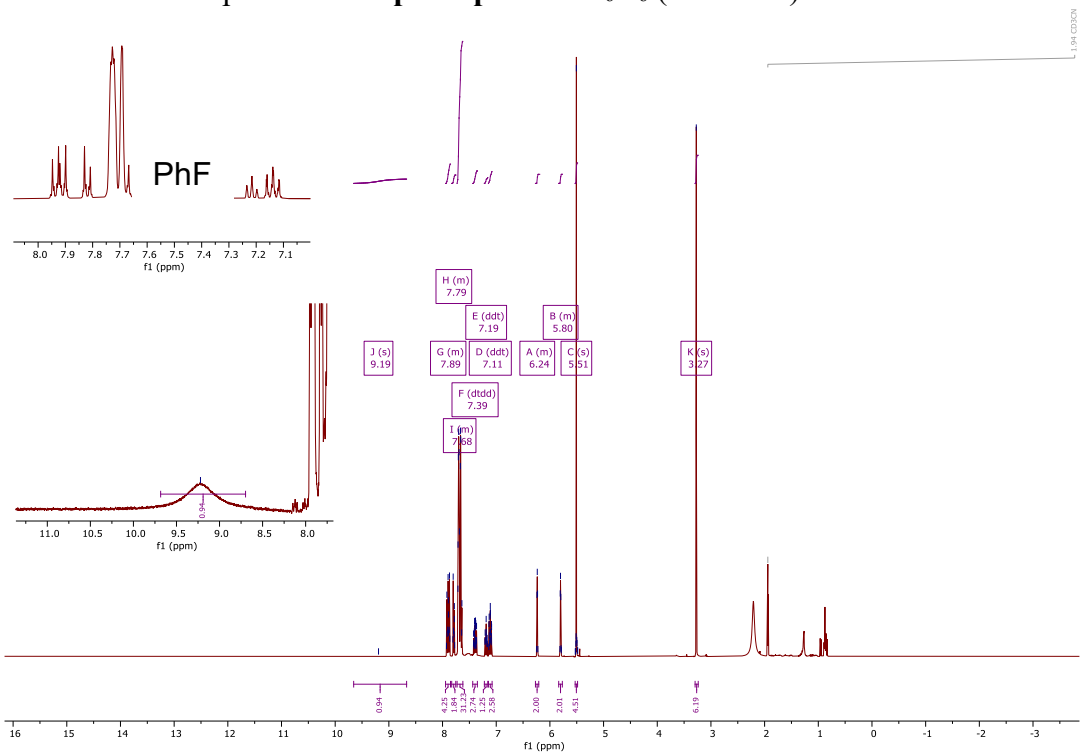

Figure C24. ^{1}H NMR spectrum of **[CpCoCp^{Ph2NH}][BAr$^{F}_{4}$]$_2$** in CD_3CN (400 MHz).

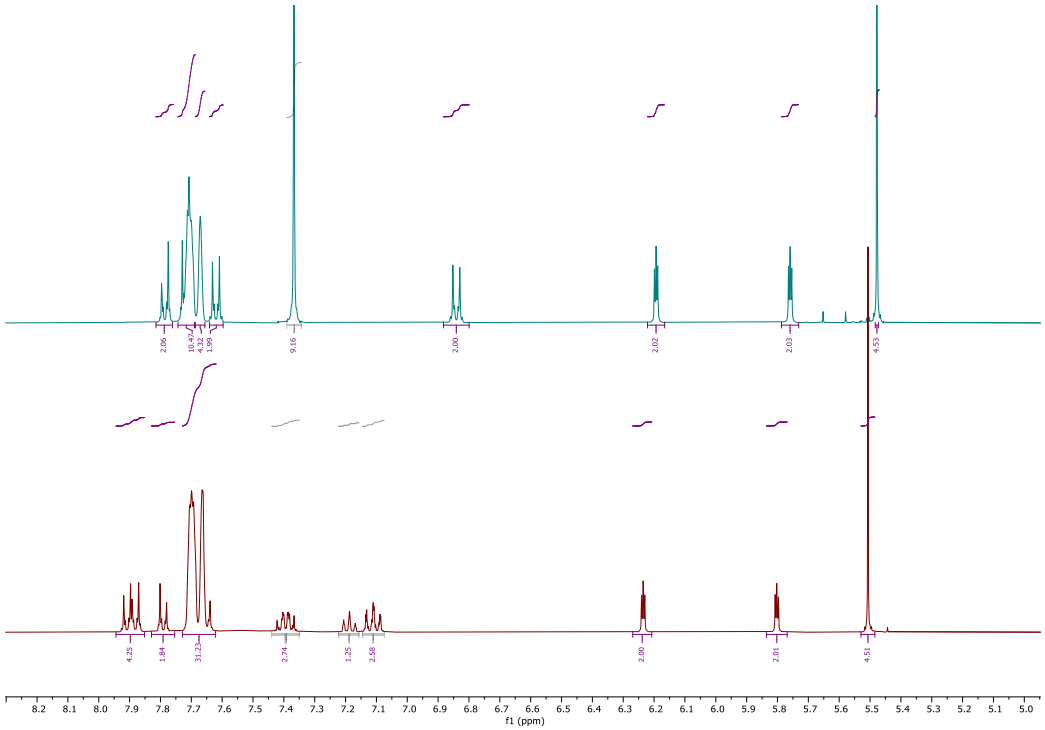

Figure C25. Comparison of aromatic region of ^{1}H NMR spectra of **[CpCoCp^{Ph2N}]BAr$^{F}_{4}$** (top) and **[CpCoCp^{Ph2NH}][BAr^{F}]$_2$** (bottom) in CD_3CN (400 MHz).

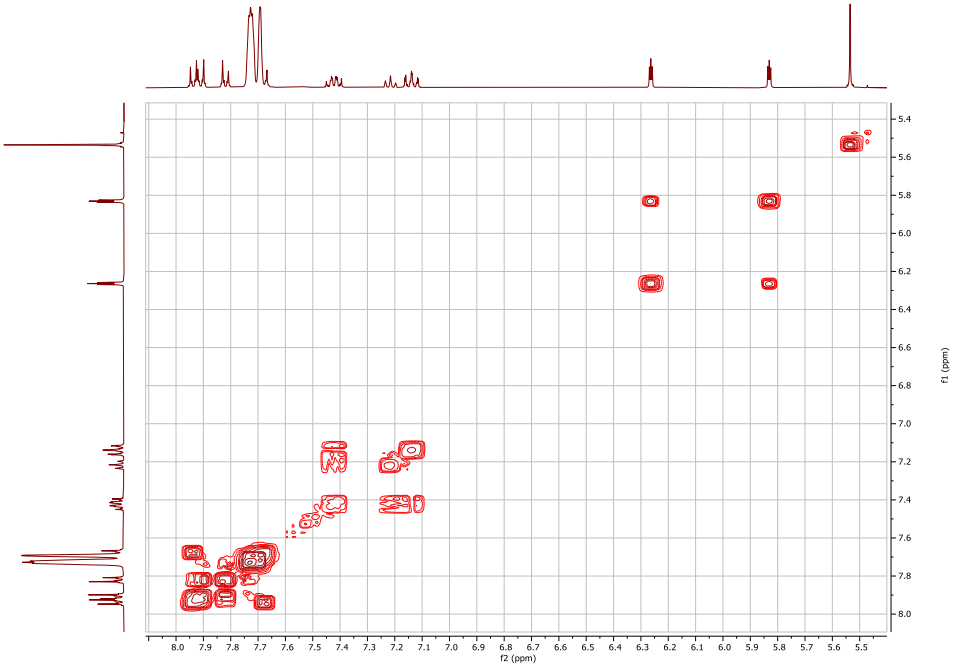

Figure C26. ^{1}H-^{1}H gradient COSY NMR spectrum of **[CpCoCp^{Ph2NH}][BAr$^{F}_{4}$]$_2$** in CD_3CN (400 MHz).

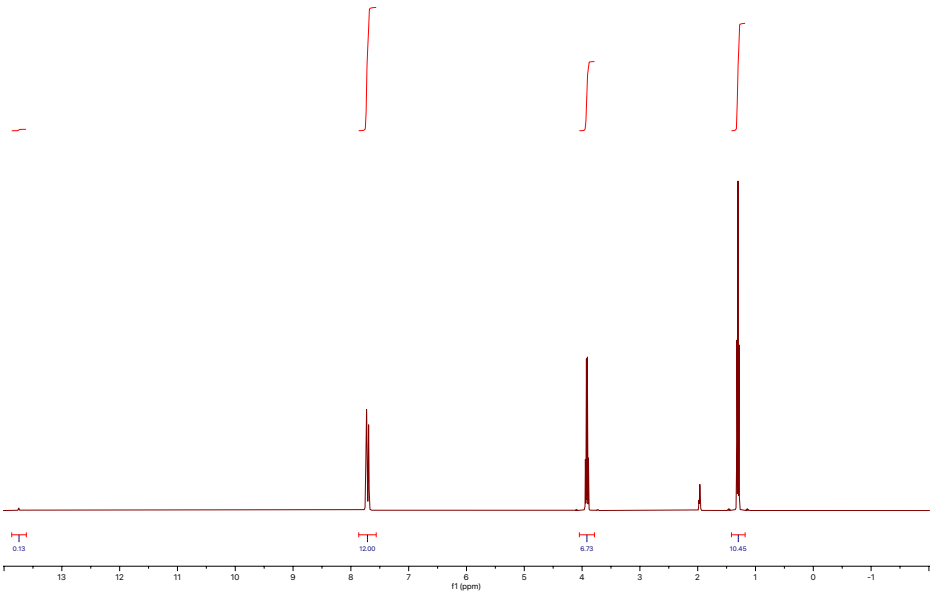

Figure C27. ^{1}H NMR spectrum of **[D(Et$_2$O)$_2$]BAr$^{F}_{4}$** in CD_3CN (400 MHz).

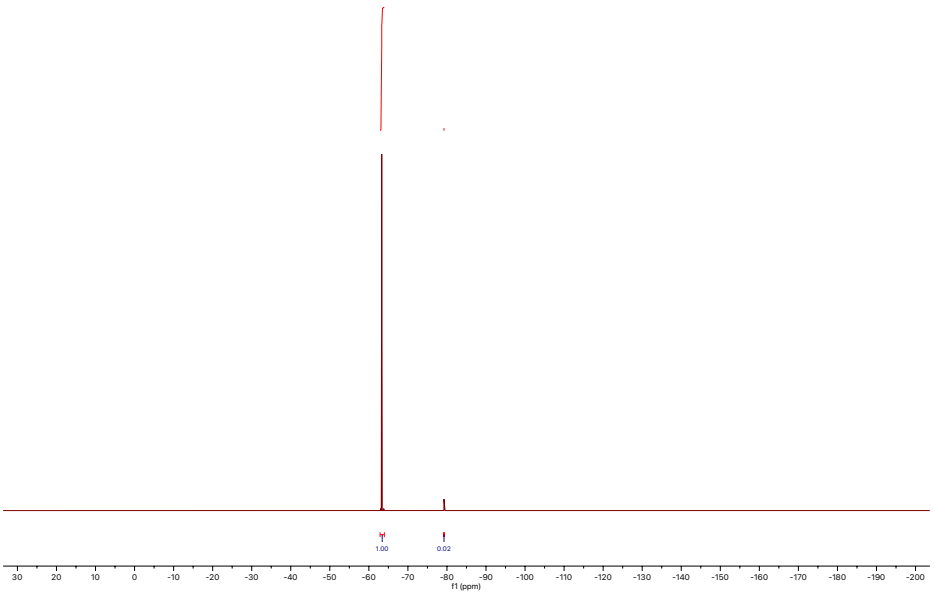

Figure C28. ^{19}F NMR spectrum of **[D(Et$_2$O)$_2$]BAr$^{F}_{4}$** in CD_3CN (400 MHz).

C4. X-Ray Crystallography

CCDC 2528361-2528370 contains the supplementary crystallographic data for this paper. These data can be obtained free of charge from the Cambridge Crystallographic Data Centre via http://www.ccdc.cam.ac.uk/data_request/cif

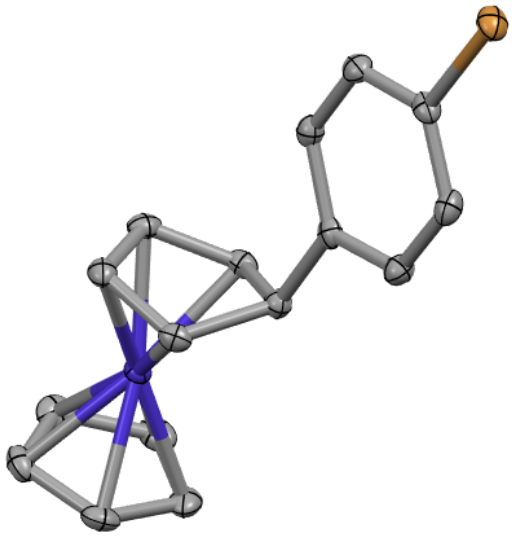

Figure C29. X-Ray Diffraction structure of **CpCo(η^4-C_5H_5-*p*-PhBr)** with thermal ellipsoids set at 50%.

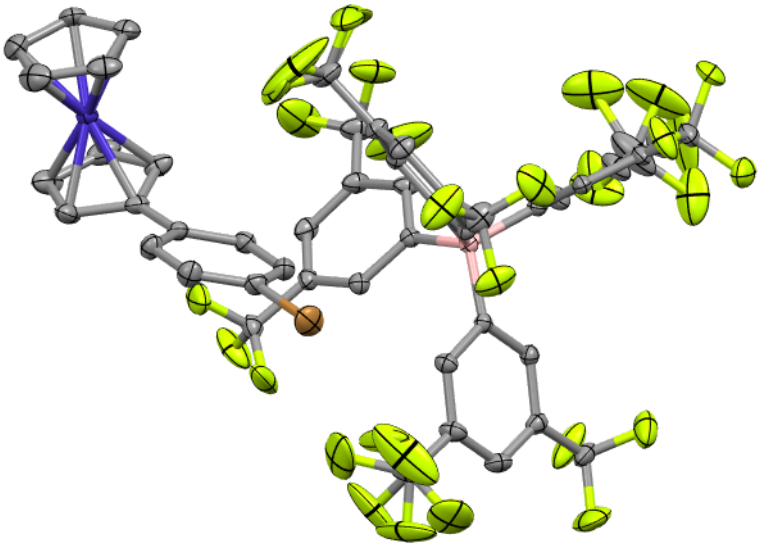

Figure C30. X-Ray Diffraction structure of **[CpCoCp^{PhBr}]BAr$^F_4$** with thermal ellipsoids set at 50%. The structure contains rotational disorder of the trifluoromethyl moiety on [BAr$^F_4$] anion.

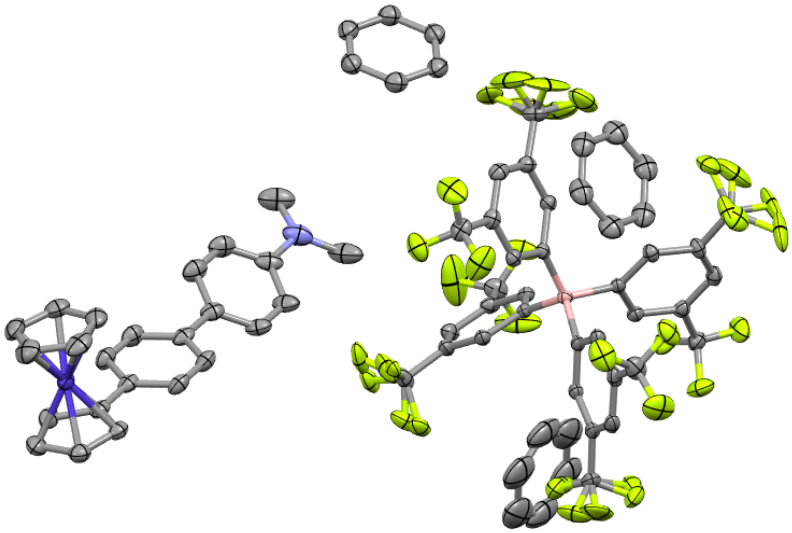

Figure C31. X-Ray Diffraction structure of [**CpCoCp$^{Ph2\text{-}N}$]BAr$^{F}_{4}$** with thermal ellipsoids set at 50%. The structure contains rotational disorder of the trifluoromethyl moiety on [BAr$^{F}_{4}$] anion.

Table C1. Crystallographic data for complexes.

Compound	**CpCo(η^4-C_5H_5-*p*-PhBr)**	**[CpCoCp^{PhBr}]BAr$^{F}_{4}$**	**[CpCoCp$^{Ph2\text{-}N}$]BAr$^{F}_{4}$**
Empirical formula	$C_{16}H_{14}BrCo$	$C_{48}H_{25}BBrCoF_{24}$	$C_{65}H_{44}BNF_{24}Co$
Formula weight	345.11	1207.36	1364.80
Temperature (K)	100.00	100.00	100.00
Crystal system	Triclinic	Triclinic	Triclinic
Space group	P-1	P-1	P-1
a (Å)	7.5440(9)	13.626(2)	9.8679(6)
b (Å)	9.2825(11)	13.739(4)	13.7678(9)
c (Å)	10.3033(13)	13.811(3)	23.3920(16)
α (°)	75.612(4)	65.180(9)	100.595(2)
β (°)	75.387(4)	85.300(10)	93.668(2)
γ (°)	70.649(3)	86.327(8)	108.695(2)
Volume (Å^3)	647.90(14)	2337.4(9)	2933.1(3)
Z	2	2	2
ρ_{calc} [g/cm^3]	1.769	1.715	1.545
μ (mm^{-1})	4.384	1.356	0.412
F (000)	344.0	1193.6	1380.1
Radiation	MoKα (λ = 0.71073)	MoKα (λ = 0.71073)	MoKα (λ = 0.71073)
Reflections collected	10837	67387	89164
Unique reflections	2983	14266	13483
Data/restraints /parameters	2983/0/163	14266/1581/760	13483/1023/943
R(int)	0.0382	0.0405	0.0383
R_1 (I > 2 σ(I))	0.0280	0.0483	0.0475
wR_2	0.0650	0.1321	0.1272
GOOF	1.049	0.986	1.044

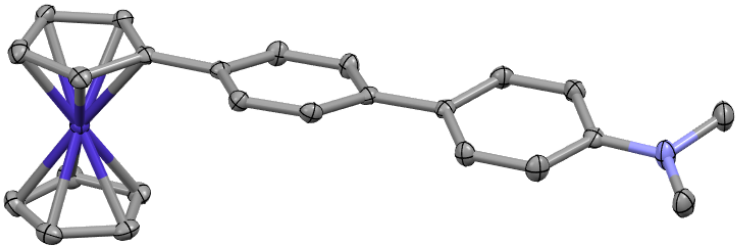

Figure C32. X-Ray Diffraction structure of **CpCoCp$^{Ph2\text{-}N}$** with thermal ellipsoids set at 50%.

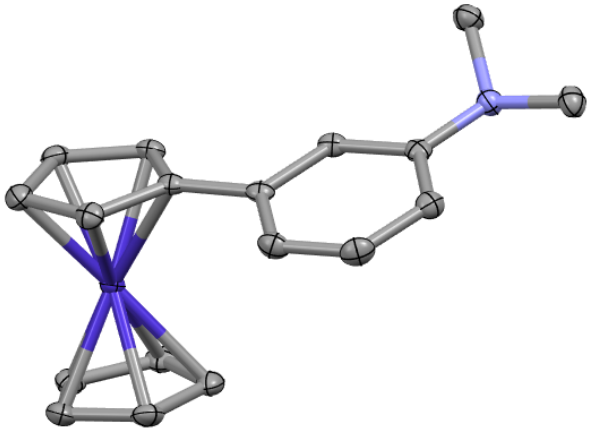

Figure C33. X-Ray Diffraction structure of **CpCoCp$^{m\text{-}N}$** with thermal ellipsoids set at 50%.

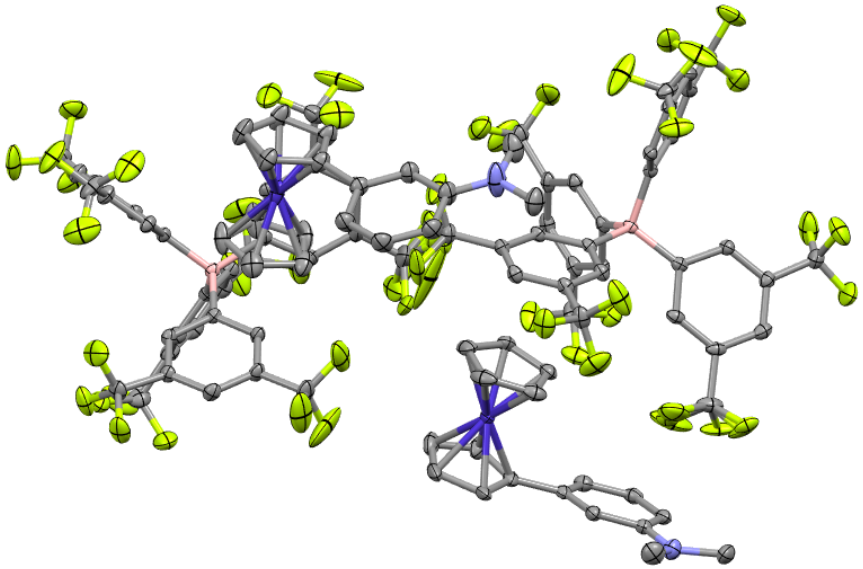

Figure C34. X-Ray Diffraction structure of **[CpCoCp$^{m\text{-}N}$]BAr$^{F}_{4}$** with thermal ellipsoids set at 50%. The structure contains rotational disorder of the trifluoromethyl moiety on [BAr$^{F}_{4}$] anion.

Table C2. Crystallographic data for complexes.

Compound	**CpCoCp^{Ph2-N}**	**CpCoCp^{m-N}**	**[CpCoCp^{m-N}]BAr$^{F}_{4}$**
Empirical formula	$C_{24}H_{23}NCo$	$C_{18}H_{19}NCo$	$C_{50}H_{31}BNF_{24}Co$
Formula weight	384.36	308.27	1171.50
Temperature (K)	100.00	100.00	100.00
Crystal system	Monoclinic	Monoclinic	Triclinic
Space group	$P2_1/c$	$P2_1/c$	P-1
a (Å)	19.127(5)	9.9954(3)	13.309(3)
b (Å)	7.6397(8)	7.4638(2)	13.766(5)
c (Å)	12.390(4)	18.9098(5)	28.359(10)
α (°)	90	90	91.099(16)
β (°)	98.229(19)	90.6790(10)	93.063(14)
γ (°)	90	90	112.622(9)
Volume (Å^3)	1791.8(7)	1410.64(7)	4785(3)
Z	4	4	4
ρ_{calc} [g/cm^3]	1.425	1.452	1.626
μ (mm^{-1})	0.964	1.205	0.490
F (000)	804.0	644.0	2344.0
Radiation	MoKα (λ = 0.71073)	MoKα (λ = 0.71073)	MoKα (λ = 0.71073)
Reflections collected	25208	18783	198569
Unique reflections	5470	3225	46210
Data/restraints /parameters	5470/0/237	3225/0/183	46210/1532/1447
R(int)	0.0520	0.0819	0.0506
R_1 (I > 2 σ(I))	0.0368	0.0316	0.0642
wR_2	0.0802	0.0811	0.1650
GOOF	1.045	1.085	1.004

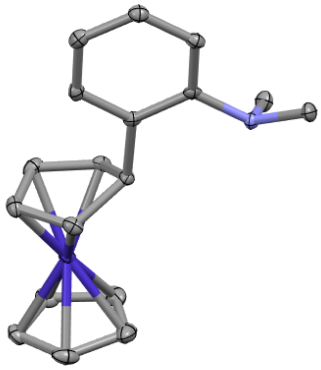

Figure C35. X-Ray Diffraction structure of **Cp(η^4-C_5H_5-*o*-$PhNMe_2$)Co** with thermal ellipsoids set at 50%.

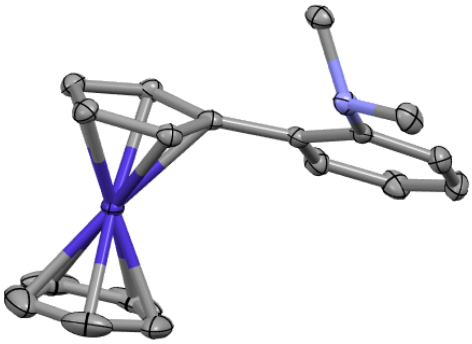

Figure C36. X-Ray Diffraction structure of **$CpCoCp^{o\text{-}N}$** with thermal ellipsoids set at 50

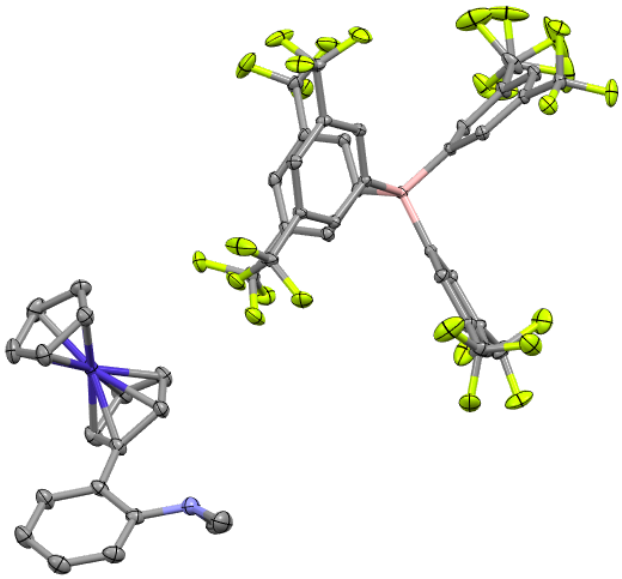

Figure C37. X-Ray Diffraction structure of **[CpCoCp$^{o\text{-}N}$]BAr$^{F}_4$** with thermal ellipsoids set at 50%. The structure contains rotational disorder of the trifluoromethyl moiety on [BAr^{F}] anion.

Table C3. Crystallographic data for complexes.

Compound	**Cp(η^4-C_5H_5-*o*-$PhNMe_2$)Co**	**CpCoCp$^{o\text{-}N}$**	**[CpCoCp$^{o\text{-}N}$]BAr$^{F}_4$**
Empirical formula	$C_{18}H_{20}CoN$	$C_{18}H_{19}NCo$	$C_{50}H_{31}BNF_{24}Co$
Formula weight	309.299	308.27	1171.50
Temperature (K)	100.00	100.00	100.00
Crystal system	Monoclinic	Orthorhombic	Triclinic
Space group	Cc	$P2_12_12_1$	P-1
a (Å)	13.8462(4)	19.7249(11)	12.667(5)
b (Å)	15.0333(5)	5.7895(3)	13.803(4)
c (Å)	7.7313(2)	12.5792(8)	15.192(3)
α (°)	90	90	114.142(7)
β (°)	117.832(1)	90	98.723(9)
γ (°)	90	90	96.012(11)
Volume (Å^3)	1423.14(7)	1436.51(14)	2354.4(12)
Z	4	4	2
ρ_{calc} [g/cm^3]	1.444	1.425	1.653
μ (mm^{-1})	1.194	1.183	0.498
F (000)	649.8	644.0	1172.0
Radiation	MoKα (λ = 0.71073)	MoKα (λ = 0.71073)	MoKα (λ = 0.71073)
Reflections collected	5779	19564	97331
Unique reflections	2623	3294	22836
Data/restraints /parameters	2623/2/183	3294/243/183	22836/748/724
R(int)	0.0195	0.0302	0.0391
R_1 (I > 2 σ(I))	0.0196	0.0234	0.0422
wR_2	0.0461	0.0563	0.1040
GOOF	1.031	1.073	1.013

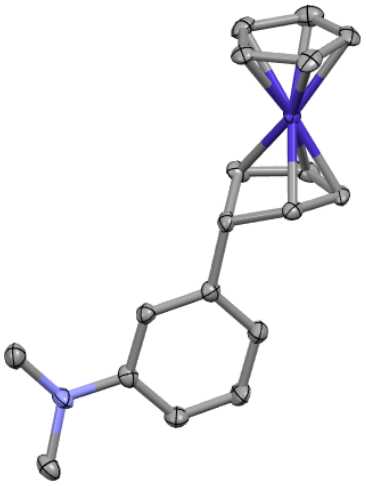

Figure C38. X-Ray Diffraction structure of **Cp(η^4-C_5H_5-*m*-PhNMe$_2$)Co** with thermal ellipsoids set at 50%.

Table C4. Crystallographic data for complexes.

Compound	**Cp(η^4-C_5H_5-*m*-PhNMe$_2$)Co**
Empirical formula	$C_{18}H_{20}NCo$
Formula weight	309.28
Temperature (K)	100.00
Crystal system	Monoclinic
Space group	$P2_1/n$
a (Å)	11.5469(5)
b (Å)	7.5013(3)
c (Å)	16.9060(7)
α (°)	90
β (°)	99.627(2)
γ (°)	90
Volume (Å^3)	1443.72(10)
Z	4
ρ_{calc} [g/cm^3]	1.423
μ (mm^{-1})	1.177
F (000)	648.0
Radiation	MoKα (λ = 0.71073)
Reflections collected	16257
Unique reflections	3303
Data/restraints /parameters	3303/0/183
R(int)	0.0872
R_1 (I > 2 σ(I))	0.0604
wR_2	0.1549
GOOF	1.021

C5. Electrochemistry

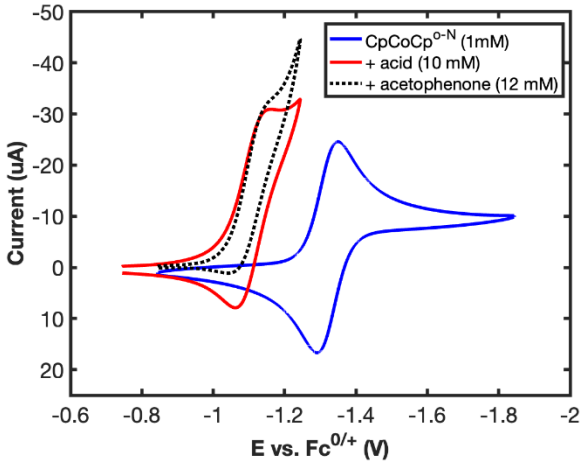

Figure C39. Cyclic voltammogram of **[CpCoCp$^{o\text{-}N}$]BAr$^{F}_4$** (1 mM, *blue*) with 4-cyanoanilinium triflate (10 mM, *red*) and acetophenone (12 mM, *black*) in MeCN with $^{n}Bu_4PF_6$ (200 mM) supporting electrolyte. The scans are swept cathodic, then anodic at 100 mV/s.

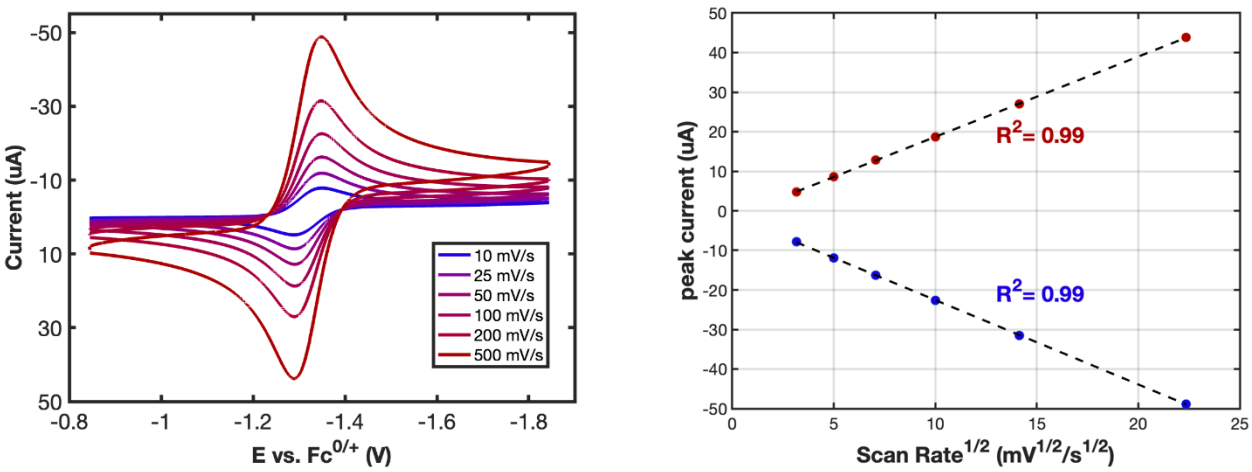

Figure C40. (left) Cyclic voltammograms of **[CpCoCp$^{o\text{-}N}$]BAr$^{F}_4$** (1 mM) at various scan rates in MeCN with $^{n}Bu_4PF_6$ (200 mM) supporting electrolyte. The scans are swept cathodic, then anodic at the scan rate indicated in the legend. (right) Peak cathodic and peak anodic currents plotted as a function of the square of the scan rate.

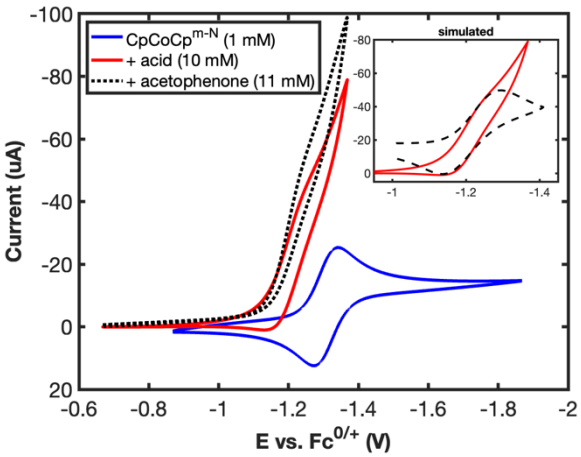

Figure C41. Cyclic voltammogram of **[CpCoCp$^{m\text{-N}}$]BAr$^{F}_4$** (1 mM, *blue*) with 4-cyanoanilinium triflate (10 mM, *red*) and acetophenone (11 mM, *black*) in MeCN with $^{n}Bu_4PF_6$ (200 mM) supporting electrolyte. The scans are swept cathodic, then anodic at 100 mV/s. *Inset*: Cyclic voltammogram of **[CpCoCp$^{m\text{-N}}$]BAr$^{F}_4$** with acid fitted with a simulation[12] of the wave using the following parameters: $E_{1/2}$ = −1.22 V, k_0 (heterogeneous ET rate constant) = 2.2 x 10^{-4} s^{-1}, k_c (chemical rate constant) = 10^{-6} s^{-1}, D = 1.0 x 10^{-5} cm^2/s, v = 100 mV/s, T = 298.15, α = 0.5

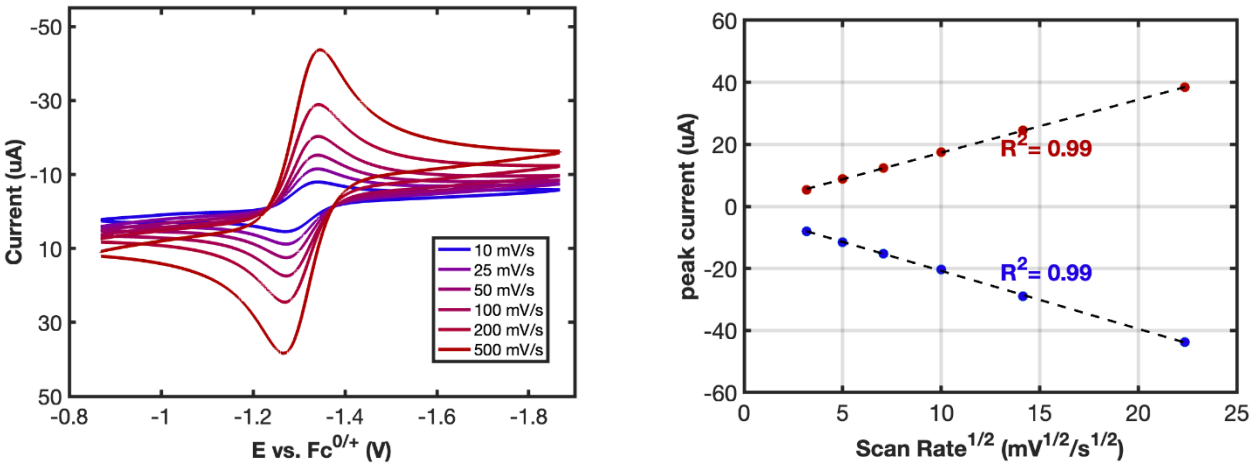

Figure C42. (left) Cyclic voltammograms of **[CpCoCp$^{m\text{-N}}$]BAr$^{F}_4$** (1 mM) at various scan rates in MeCN with $^{n}Bu_4PF_6$ (200 mM) supporting electrolyte. The scans are swept cathodic, then anodic at the scan rate indicated in the legend. (right) Peak cathodic and peak anodic currents plotted as a function of the square of the scan rate.

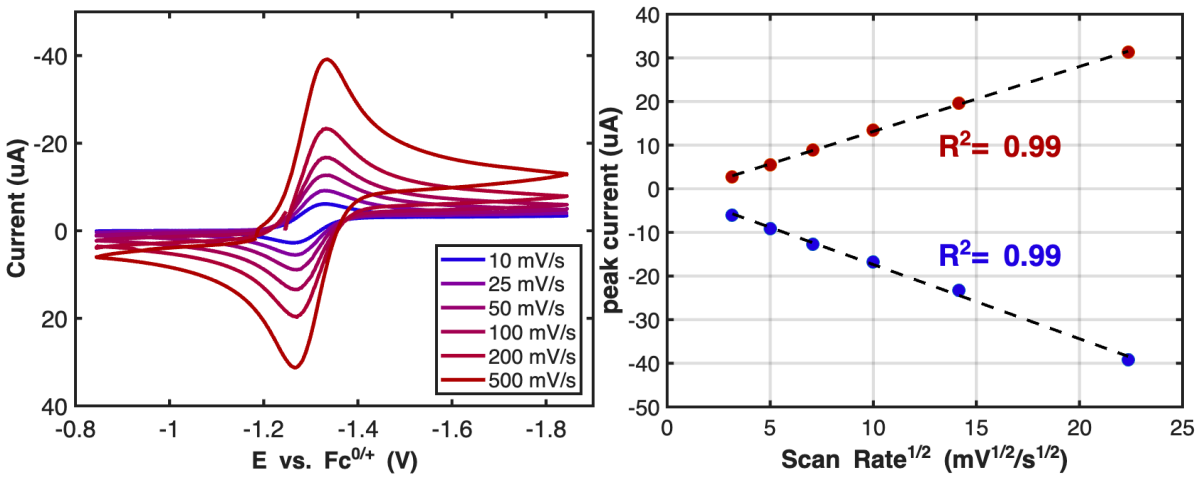

Figure C43. (left) Cyclic voltammograms of **[CpCoCp$^{Ph2\text{-}N}$]BAr$^{F}_{4}$** (1 mM) at various scan rates in MeCN with $^{n}Bu_4PF_6$ (200 mM) supporting electrolyte. The scans are swept cathodic, then anodic at the scan rate indicated in the legend. (right) Peak cathodic and peak anodic currents plotted as a function of the square of the scan rate.

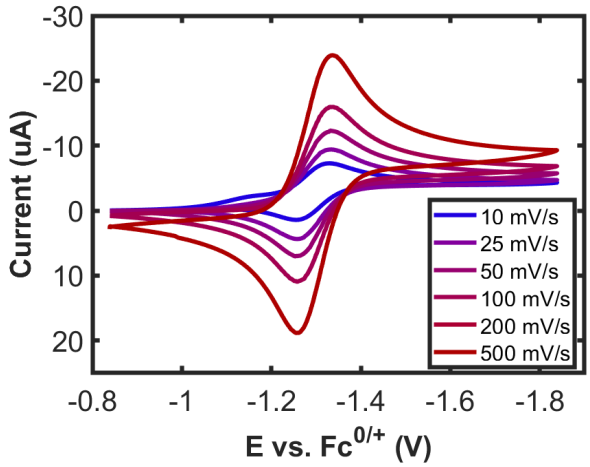

Figure C44. Cyclic voltammograms of **[CpCoCp$^{Ph2\text{-}NH}$][BAr$^{F}_{4}$]$_2$** (1 mM) at various scan rates in MeCN with $^{n}Bu_4PF_6$ (200 mM) supporting electrolyte. The scans are swept cathodic, then anodic at the scan rate indicated in the legend. At very slow scan rate, a reductive pre-wave is observed.

C6. pK_a Determination

The pK_a values of the aniline-appended cobaltocene complexes were determined using a method used in previous studies from our group. In brief, ^{1}H NMR spectroscopy is used to measure the proton-transfer equilibrium between an aniline of interest and an acid with a known pK_a. The chemical shifts of the unknown aniline and reference acid can be used to determine their concentration as well as their conjugate acid concentrations using the following equation:

$$[CpCoCp^{X-NH+}] = \frac{\delta_{obs} - \delta_{CpCoCp^{X-N}}}{\delta_{CpCoCp^{X-NH+}} - \delta_{CpCoCp^{X-N}}}$$

$$[CpCoCp^{X-N}] = [Co]_{tot} - [CpCoCp^{X-NH+}]$$

Similarly for $^{2\text{-Cl}}PhNH_3^+$ / $^{2\text{-Cl}}PhNH_2$:

$$[^{2-Cl}PhNH_3^+] = \frac{\delta_{obs} - \delta_{^{2-Cl}PhNH_2}}{\delta_{^{2-Cl}PhNH_3^+} - \delta_{^{2-Cl}PhNH_2}}$$

$$[^{2-Cl}PhNH_2] = [^{2-Cl}PhNH_2]_{tot} - [^{2-Cl}PhNH_3^+]$$

From these concentrations, the K_{eq} can be determined:

$$K_{eq} = \frac{[CpCoCp^{X-N}][^{2-Cl}PhNH_3^+]}{[CpCoCp^{X-NH+}][^{2-Cl}PhNH_2]}$$

With K_{eq} and the known reference acid pK_a ($K_{a,ref}$), the analyte pK_a can be determined:

$$K_a = \frac{K_{eq}}{K_{a,ref}}$$

$$pK_a = -\log\{K_{eq}/K_{a,ref}\}$$

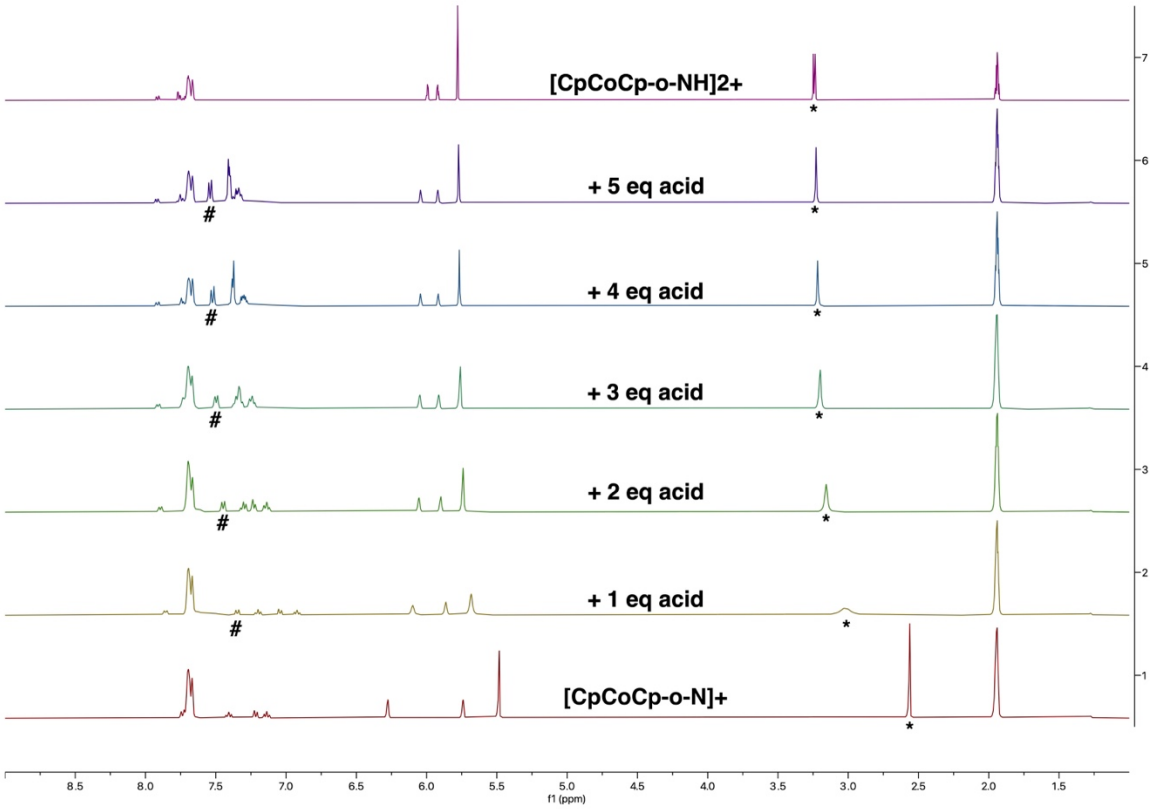

Figure C45. ^{1}H NMR Spectra of [CpCoCp$^{o\text{-}N}$]BAr$^{F}_{4}$ with 0-5 equivalents of [$^{2\text{-}Cl}$PhNH$_3$]OTf added in CD$_3$CN. The starred (*) and tagged (#) Co-N*Me*$_2$ peak and $^{2\text{-}Cl}$PhNH$_2$ *ortho*-H peak shifts, respectively, are used as reporters of the analytes' concentrations.

Table C5. Reporter peak shifts from the ^{1}H NMR spectroscopy acid titration of **[CpCoCp$^{o\text{-}N}$]BAr$^{F}_{4}$** and the resulting equilibrium constant K_{eq}

equiv. acid added	# shift (ppm)	* shift (ppm)	[Co$^{o\text{-}NH+}$]	[Co$^{o\text{-}N}$]	[$^{2\text{-}Cl}$PhNH$_3^+$]	[$^{2\text{-}Cl}$PhNH$_2$]	K$_{eq}$
0	7.229	2.512	0	1	0	0	-
1	7.358	3.021	0.680	0.320	0.323	0.677	0.224
2	7.459	3.158	0.864	0.136	1.153	0.847	0.214
3	7.506	3.198	0.917	0.083	2.083	0.917	0.205
4	7.533	3.218	0.944	0.056	3.048	0.952	0.190
5	7.55	3.229	0.959	0.041	4.023	0.977	0.178

Determined as the average of rows in Table C**5**, the resulting equilibrium constant K$_{eq}$ is determined to be 0.202. From this K$_{eq}$ value and the known pK_a of $^{2\text{-}Cl}$PhNH$_3^+$ (7.86) in MeCN, the pK_a of **[CpCoCp$^{o\text{-}NH}$]$^+$** is determined to be 8.55 ± 0.02.

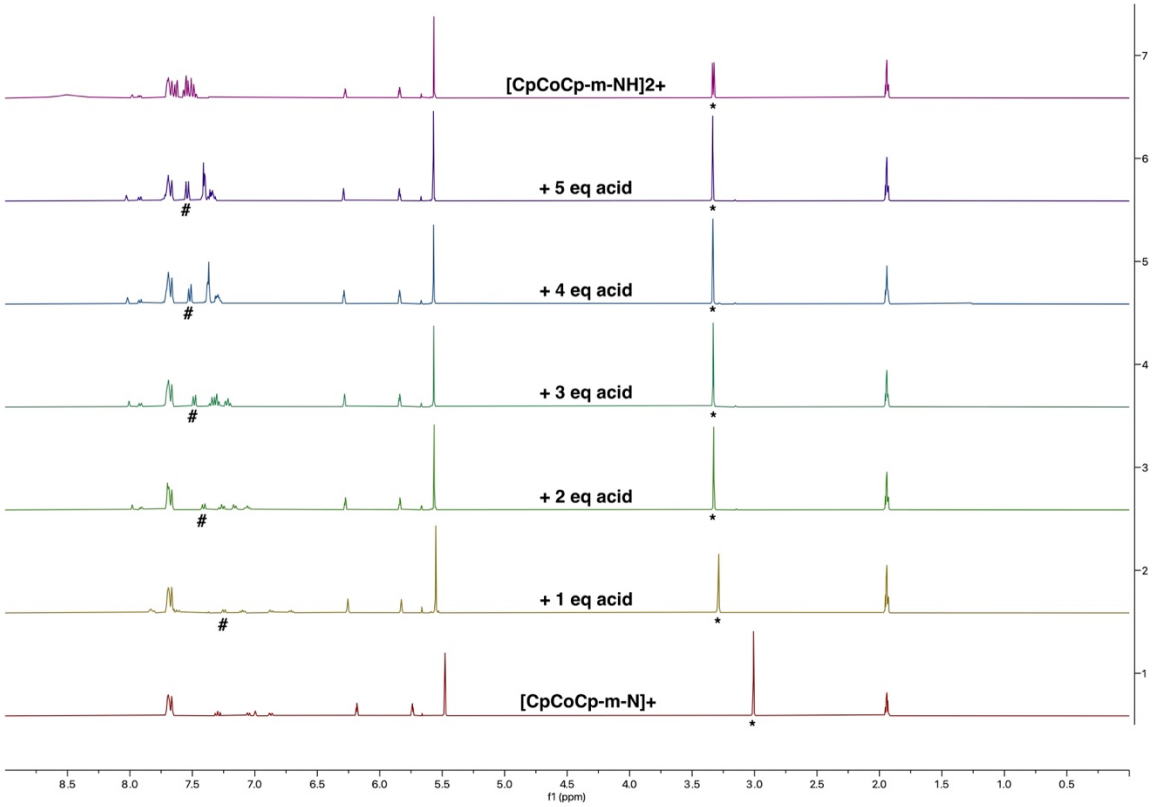

Figure C46. ^{1}H NMR Spectra of [CpCoCp$^{m\text{-}N}$]BAr$^{F}_{4}$ with 0-5 equivalents of [$^{2\text{-}Cl}$PhNH$_3$]OTf added in CD_3CN. The starred (*) and tagged (#) Co-N*Me*$_2$ peak and $^{2\text{-}Cl}$PhNH$_2$ *ortho*-H peak shifts, respectively, are used as reporters of the analytes' concentrations.

Table C6. Reporter peak shifts from the ^{1}H NMR spectroscopy acid titration of **[CpCoCp$^{m\text{-}N}$]BAr$^{F}_{4}$** and the resulting equilibrium constant K_{eq}

equiv. acid added	# shift (ppm)	* shift (ppm)	[Co$^{m\text{-}NH+}$]	[Co$^{m\text{-}N}$]	[$^{2\text{-}Cl}$PhNH$_3^+$]	[$^{2\text{-}Cl}$PhNH$_2$]	K_{eq}
0	-	3.009	0	1	0	0	-
1	7.237	3.287	0.840	0.160	0.020	0.980	0.004
2	7.4	3.327	0.961	0.039	0.857	1.143	0.031
3	7.473	3.331	0.973	0.027	1.835	1.165	0.044
4	7.511	3.333	0.979	0.021	2.827	1.173	0.052
5	7.53	3.334	0.982	0.018	3.772	1.228	0.057

Determined as the average of rows in Table C**6**, the resulting equilibrium constant K_{eq} is determined to be 0.037. From this K_{eq} value and the known pK_a of $^{2\text{-}Cl}$PhNH$_3^+$ (7.86) in MeCN, the pK_a of **[CpCoCp$^{m\text{-}NH}$]$^+$** is determined to be 9.42 ± 0.48.

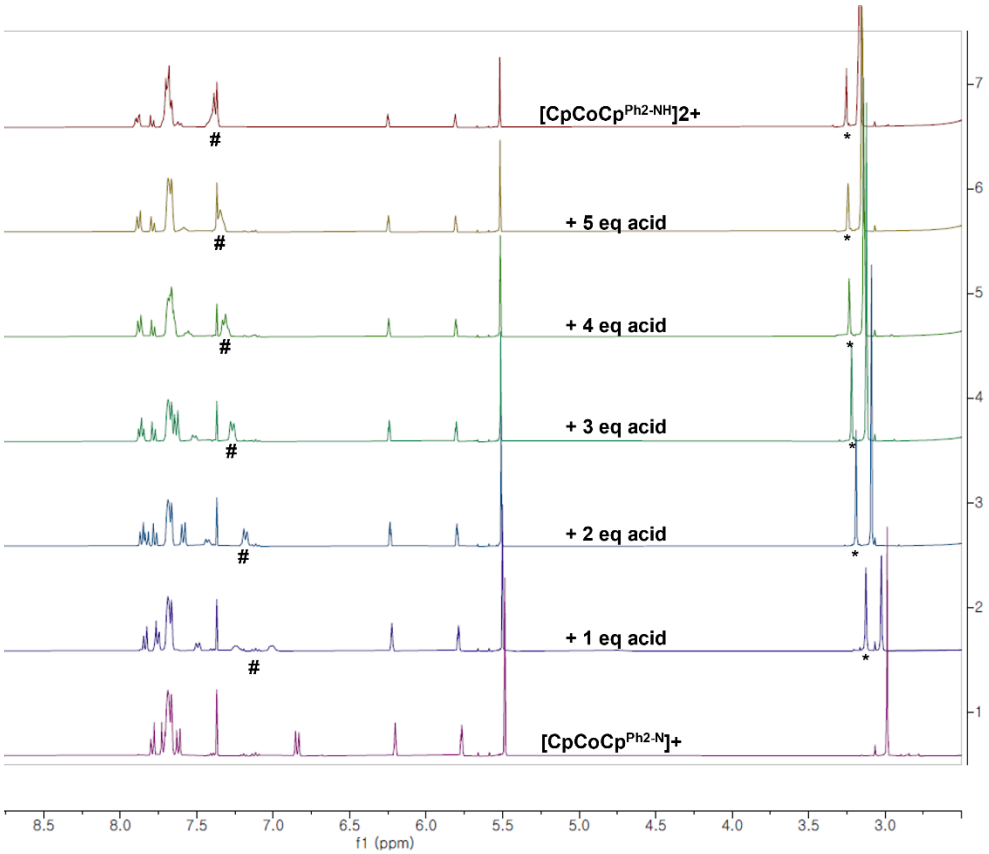

Figure C47. ^{1}H NMR Spectra of **[CpCoCp$^{Ph2\text{-}N}$]BAr$^{F}_{4}$** with 0-4 equivalents of [$^{4\text{-}Br}$PhNMe$_2$H]OTf added in CD$_3$CN. The starred (*) and tagged (#) Co-N*Me*$_2$ peak and $^{4\text{-}Br}$PhNMe$_2$ *meta*-H peak shifts, respectively, are used as reporters of the analytes' concentrations.

Table C7. Reporter peak shifts from the ^{1}H NMR spectroscopy acid titration of **[CpCoCp$^{Ph2\text{-}N}$]BAr$^{F}_{4}$** and the resulting equilibrium constant K_{eq}

equiv. acid added	# shift (ppm)	* shift (ppm)	[Co$^{Ph2\text{-}NH+}$]	[Co$^{Ph2\text{-}N}$]	[$^{4\text{-}Br}$PhNMe$_2$H^{+}]	[$^{4\text{-}Br}$PhNMe$_2$]	K_{eq}
0	-	2.987	0	1	0	0	
1	7.011	3.125	0.478	0.522	0.420	0.580	0.792
2	7.182	3.190	0.702	0.298	1.237	0.763	0.687
3	7.267	3.220	0.806	0.193	2.152	0.848	0.610
4	7.323	3.234	0.855	0.145	3.130	0.870	0.612
5	7.348	3.243	0.886	0.114	4.058	0.942	0.555

Determined as the average of rows in Table C**7**, the resulting equilibrium constant K_{eq} is determined to be 0.651. From this K_{eq} value and the known pK_a of $^{4\text{-}Br}$PhNMe$_2$H^{+} (10.13) in MeCN, the pK_a of **[CpCoCp$^{Ph2\text{-}NH}$]$^{+}$** is determined to be 10.32 ± 0.06.

C7. UV-Visible Spectroscopy

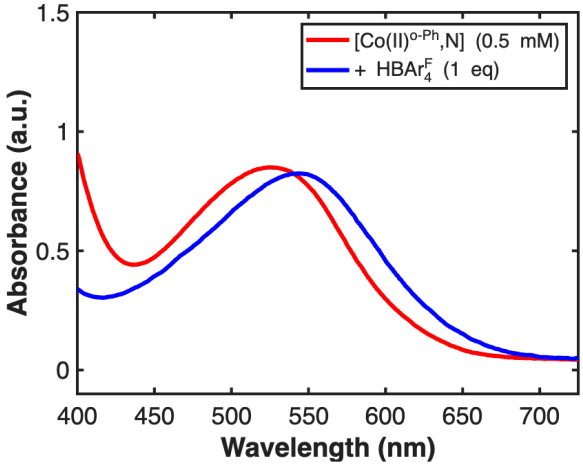

Figure C48 UV-Visible spectrum of [Co(II)$^{o\text{–Ph}}$, N] (red trace, λ_{max} = 524 nm) and [Co(II)$^{o\text{–Ph}}$, NH]BAr$^{F}_{4}$ (blue trace, λ_{max} = 544 nm) in THF at 0 °C.

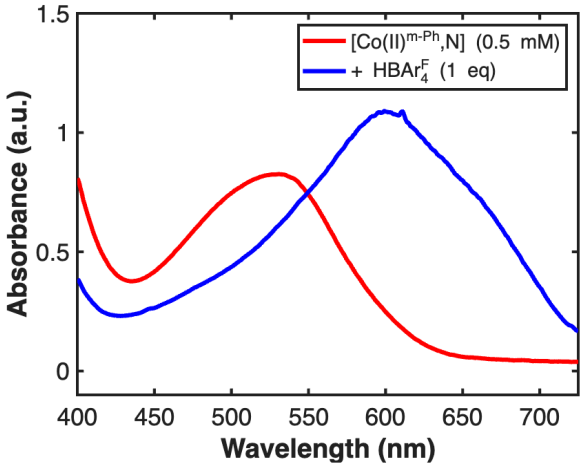

Figure C49 UV-Visible spectrum of [Co(II)$^{m\text{–Ph}}$, N] (red trace, λ_{max} = 531 nm) and [Co(II)$^{m\text{–Ph}}$, NH]BAr$^{F}_{4}$ (blue trace, λ_{max} = 599 nm) in THF at 0 °C.

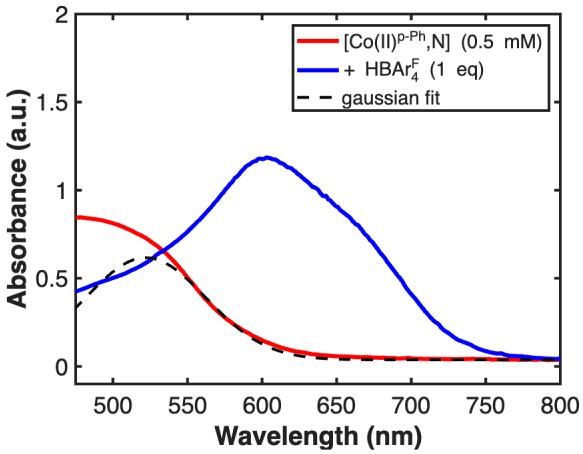

Figure C50 UV-Visible spectrum of [Co(II)$^{p\text{–Ph}}$, N] (red trace) with gaussian peak deconvolution (black trace, λ_{max} = 525 nm) and [Co(II)$^{p\text{–Ph}}$, NH]BAr$^{F}_{4}$ (blue trace, λ_{max} = 602 nm) in THF at 0 °C.

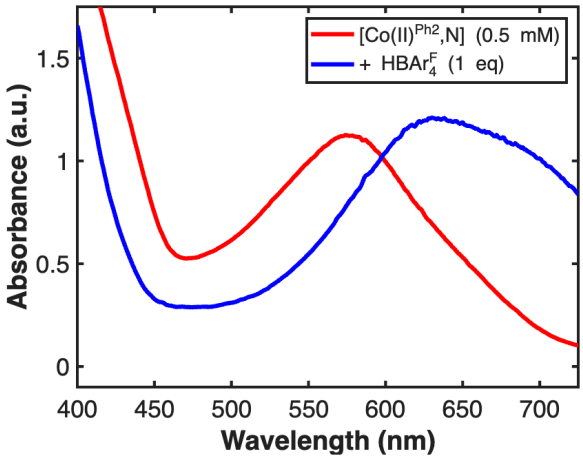

Figure C51 UV-Visible spectrum of [Co(II)$^{p\text{–Ph2}}$, N] (red trace, λ_{max} = 579 nm) and [Co(II)$^{p\text{–Ph2}}$, NH]BAr$^{F}_{4}$ (blue trace, λ_{max} = 626 nm) in THF at 0 °C.

C8. Kinetic Analysis

Kinetics measurements were performed on a Cary 300 UV-vis spectrophotometer with a Unisoku Cryostat sample holder. In the nitrogen glovebox, a solution of cobaltocene in THF [2.0 mL, 500 uM] was prepared in a septum-capped quartz cuvette. Solutions of $HBAr^F$ in Et_2O [200 uL, 1.0 mM] and substrate in THF [200 uL, 50-300 mM] were loaded into 1 mL syringes and pierced into a septum. The cuvette and syringes were removed from the box. The cuvette was placed into the cryostat with a nitrogen inlet needle in the septum, and collection began. After 10 minutes, the acid solution was added into the cuvette, and after another 36 seconds, the substrate solution was added. The decay of the cobalt feature was monitored as a function of time and fitted to an exponential decay function. The observed pseudo-first order rate constant was extracted from the fit and plotted as a function of the substrate concentration. Linear regression of the k_{obs} versus substrate concentration plot provides the desired second-order rate constant for the PCET reaction.

For each k_{PCET} measurement, there is a scheme describing the conditions, a sample set of UV-visible spectra, the kinetics traces for each substrate concentration measured, and a plot of k_{obs} as a function of substrate concentration. The wavelength at which absorbance is monitored is described in the figure caption.

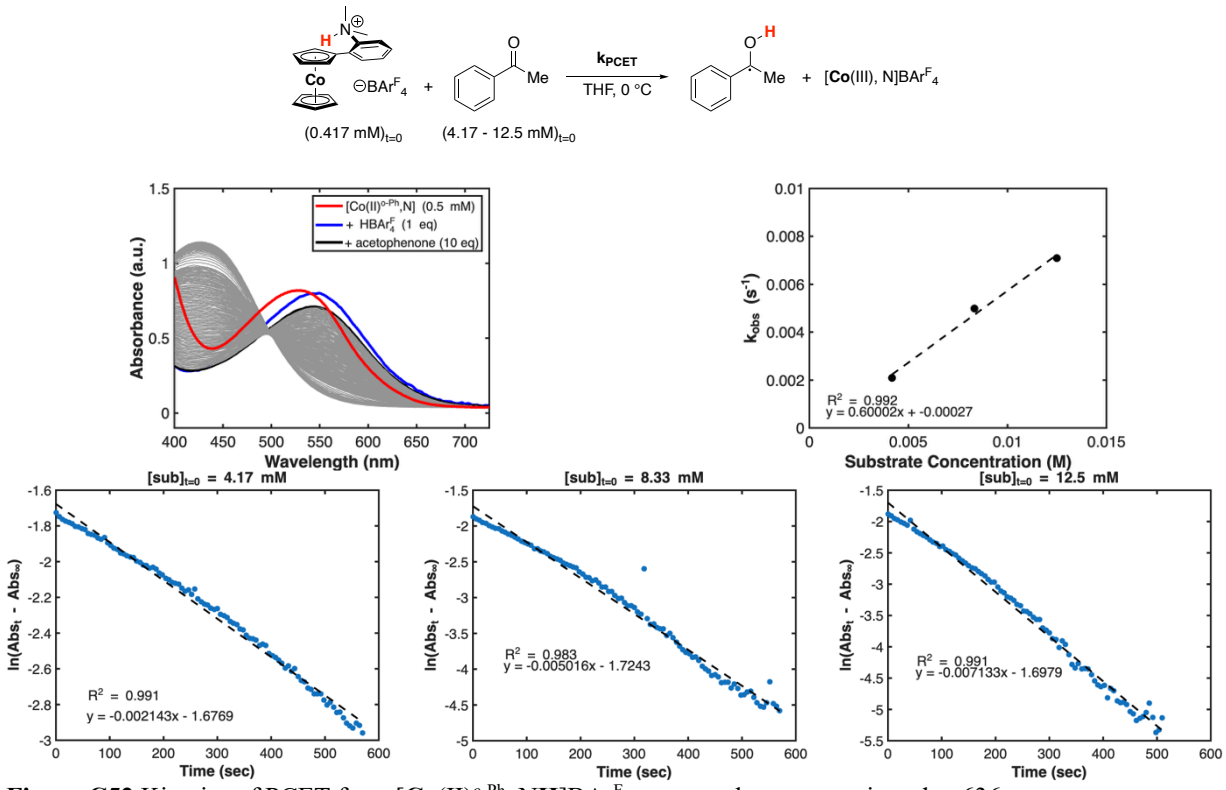

Figure C52 Kinetics of PCET from [**Co**(II)$^{o\text{-Ph}}$, N**H**]BAr^F_4 to acetophenone monitored at 636 nm

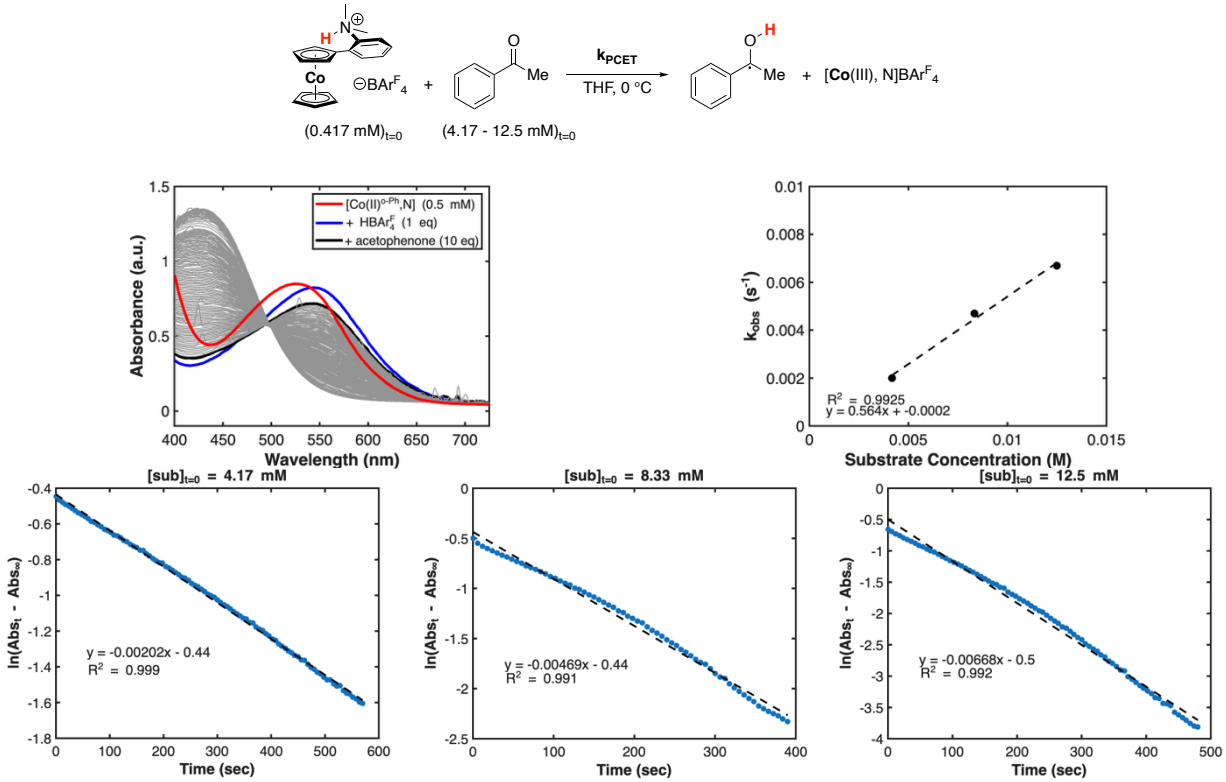

Figure C53 Kinetics of PCET from [**Co**(II)$^{o\text{-Ph}}$, N**H**]BAr$^F_4$ to acetophenone monitored at 636 nm

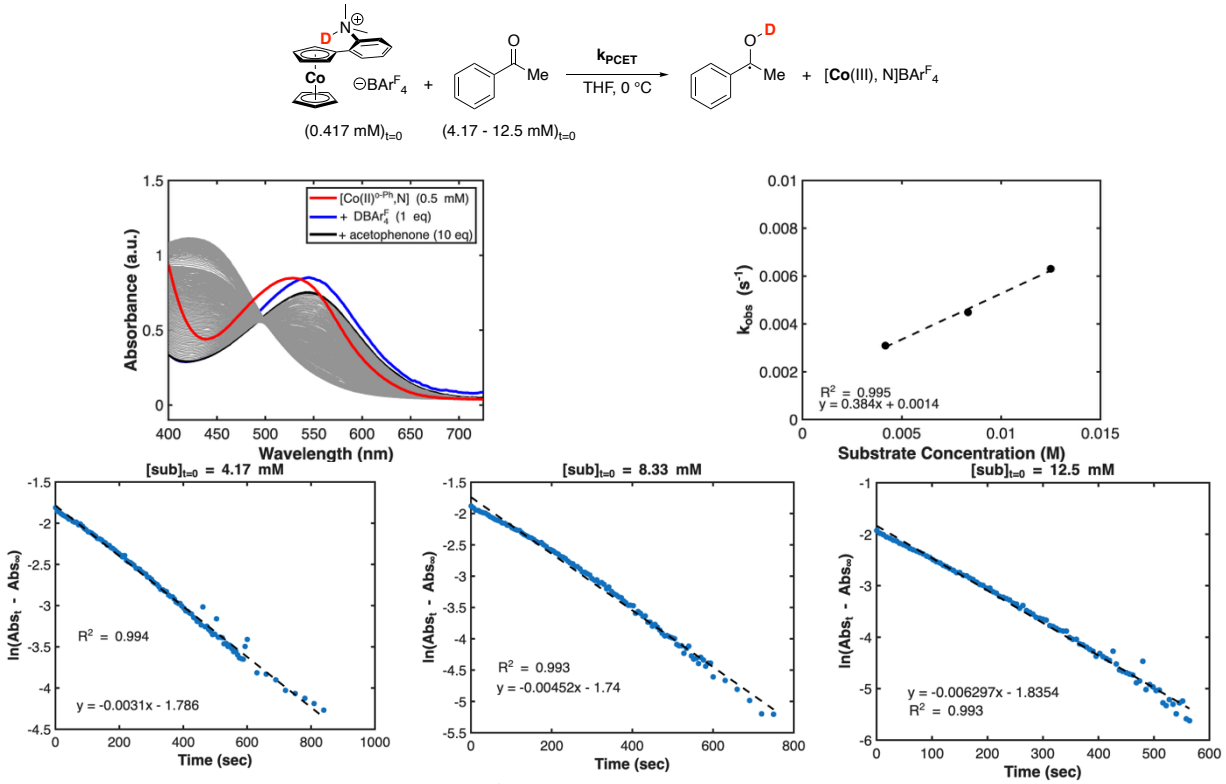

Figure C54 Kinetics of PCET from [**Co**(II)$^{o\text{-Ph}}$, N**D**]BAr$^F_4$ to acetophenone monitored at 636 nm

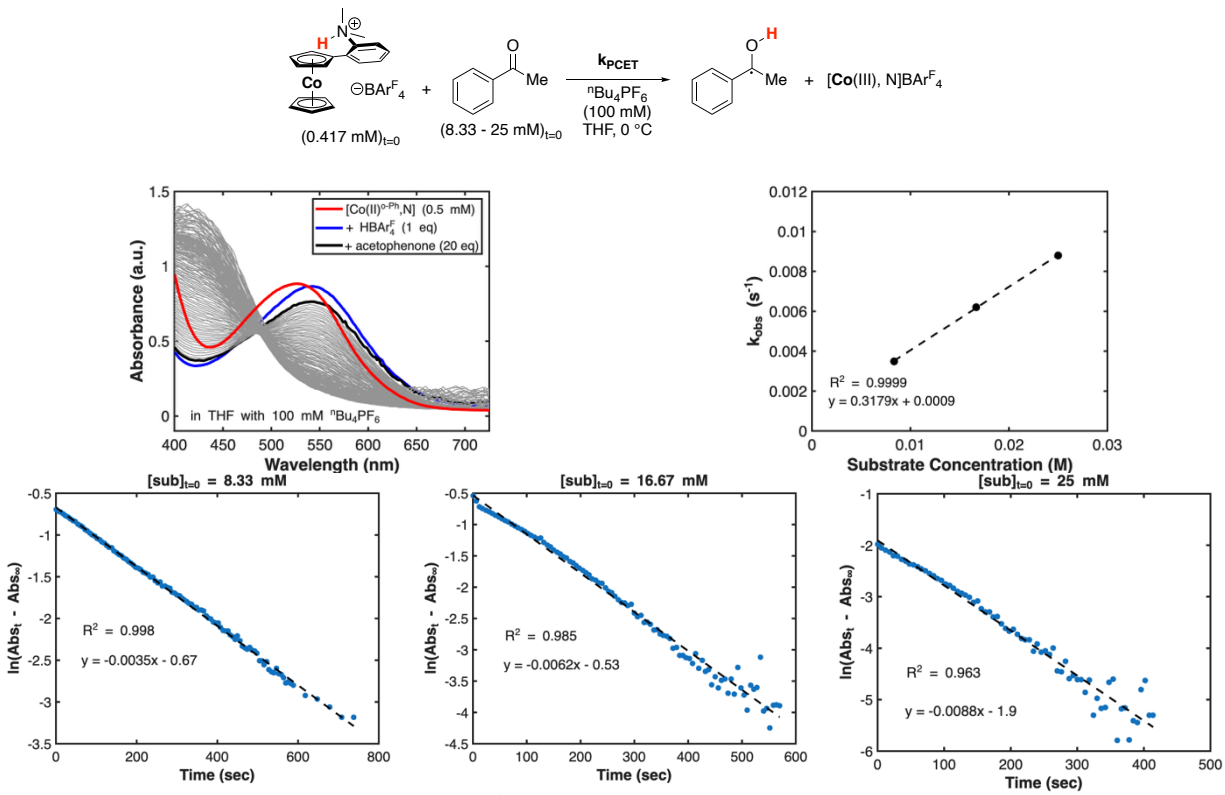

Figure C55 Kinetics of PCET from [**Co**(II)$^{o\text{-Ph}}$, N**H**]BAr$^{F}_{4}$ to acetophenone with electrolyte monitored at 636 nm

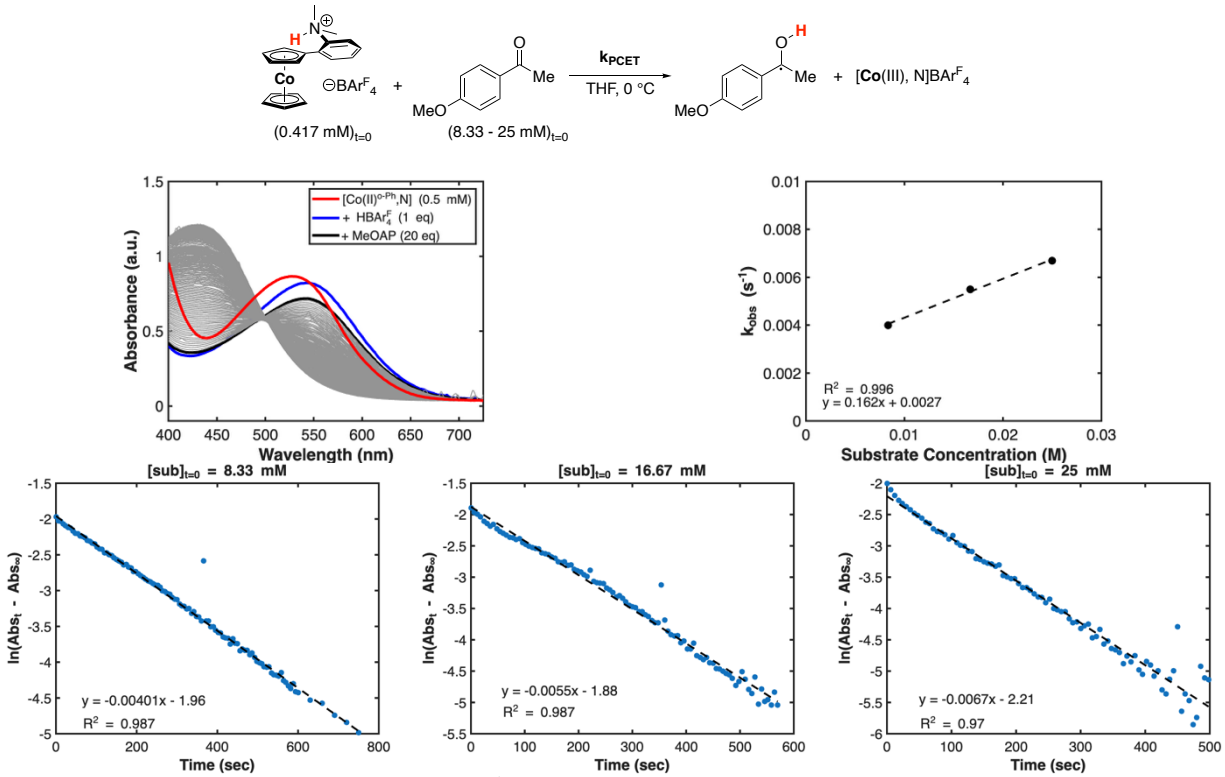

Figure C56 Kinetics of PCET from [**Co**(II)$^{o\text{-Ph}}$, N**H**]BAr$^{F}_{4}$ to acetophenone with electrolyte monitored at 636 nm

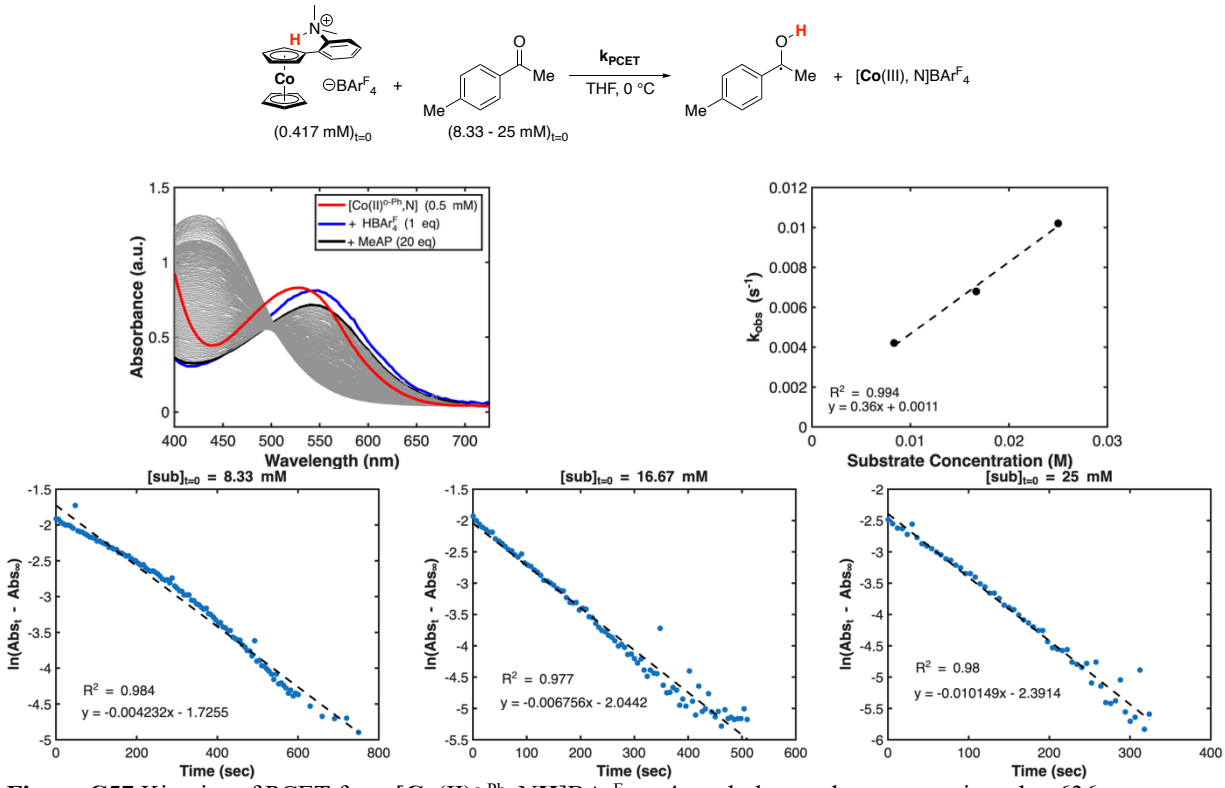

Figure C57 Kinetics of PCET from [**Co**(II)$^{o\text{-Ph}}$, N**H**]BAr$^F_4$ to 4-methylacetophenone monitored at 636 nm

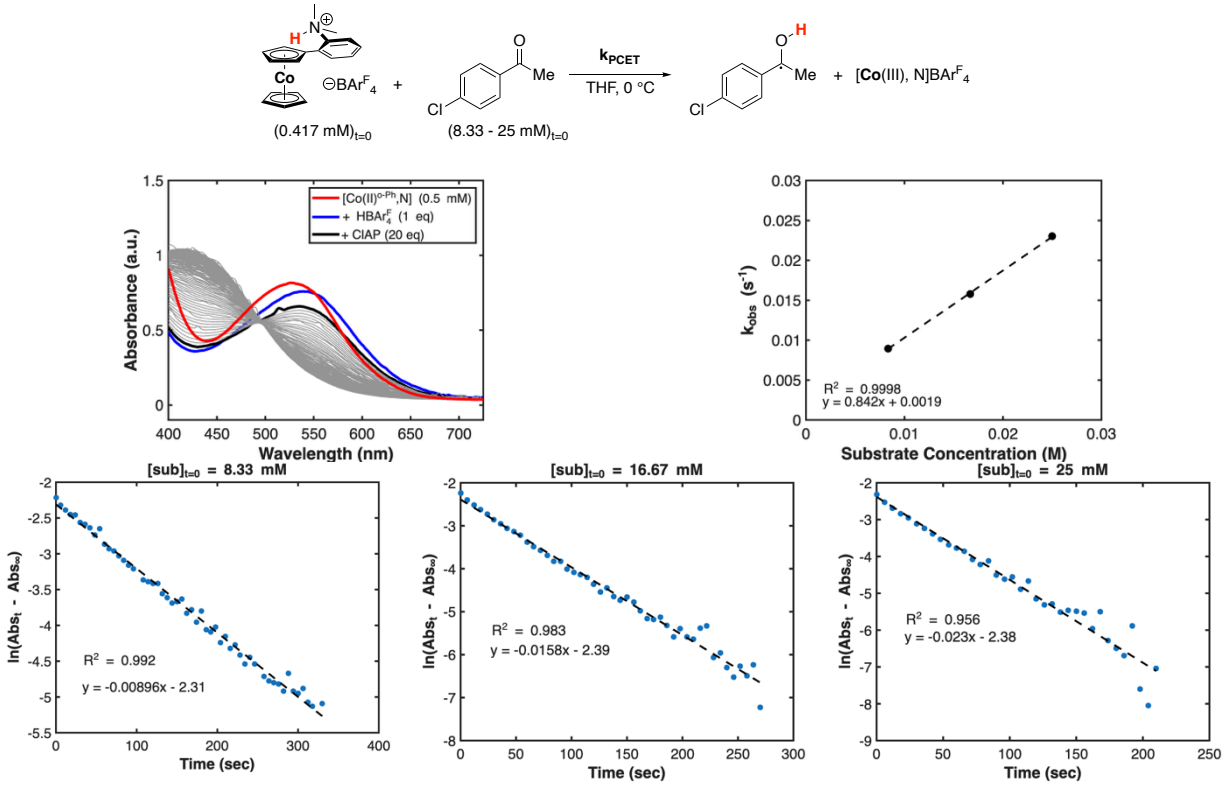

Figure C58 Kinetics of PCET from [**Co**(II)$^{o\text{-Ph}}$, N**H**]BAr$^F_4$ to 4-chloroacetophenone monitored at 636 nm

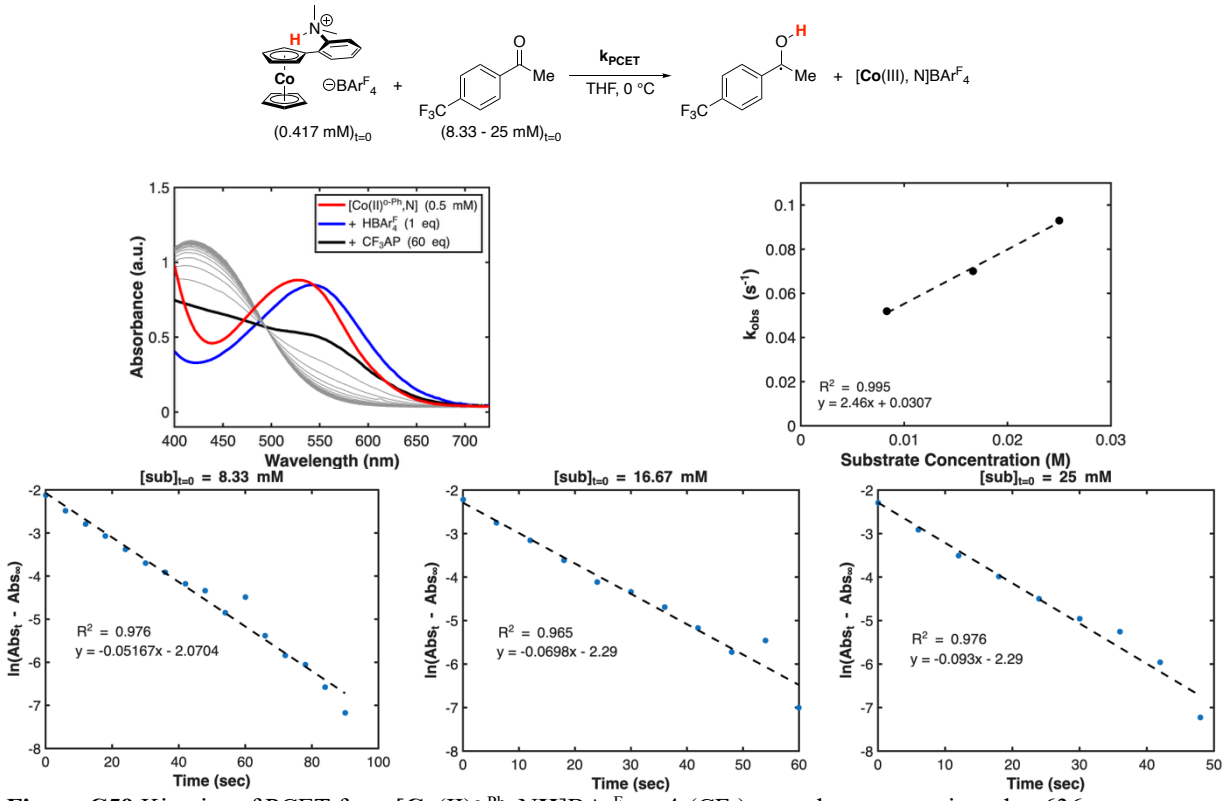

Figure C59 Kinetics of PCET from [**Co**(II)$^{o\text{-Ph}}$, N**H**]BAr$^{F}_{4}$ to 4-(CF$_3$)acetophenone monitored at 636 nm

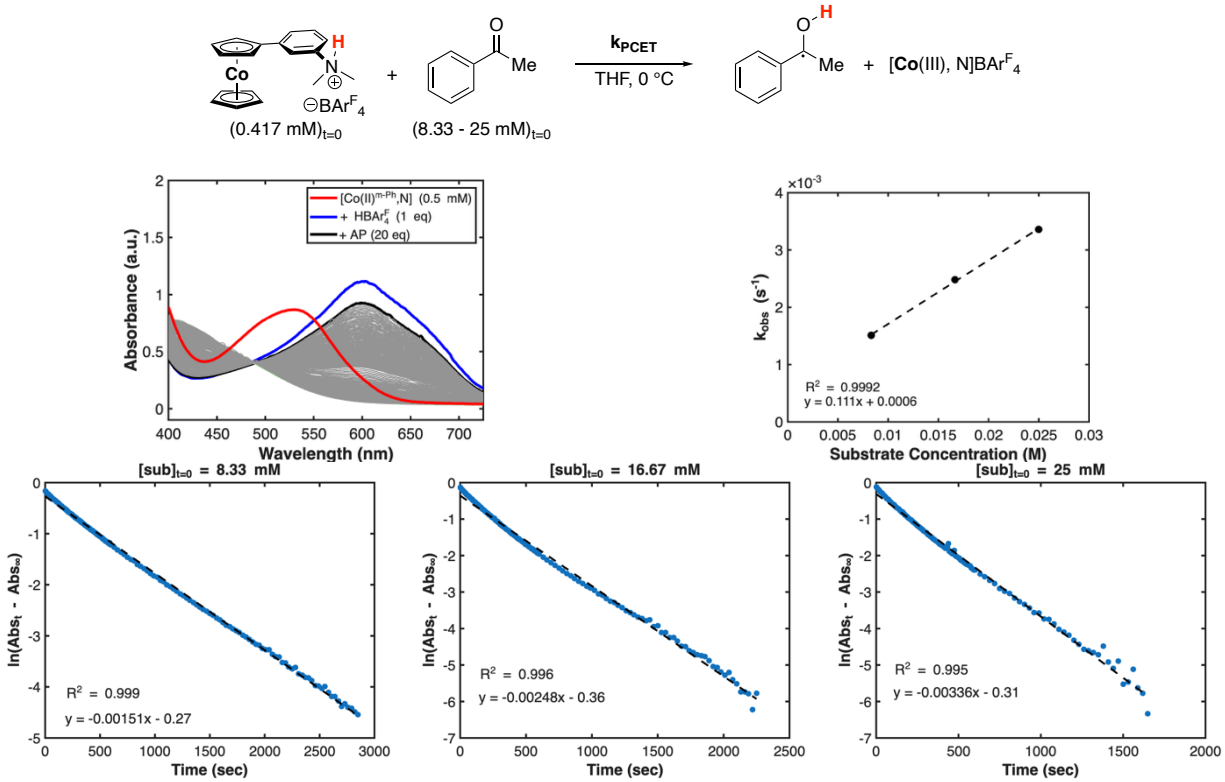

Figure C60 Kinetics of PCET from [**Co**(II)$^{m\text{-Ph}}$, N**H**]BAr$^{F}_{4}$ to acetophenone monitored at 610 nm

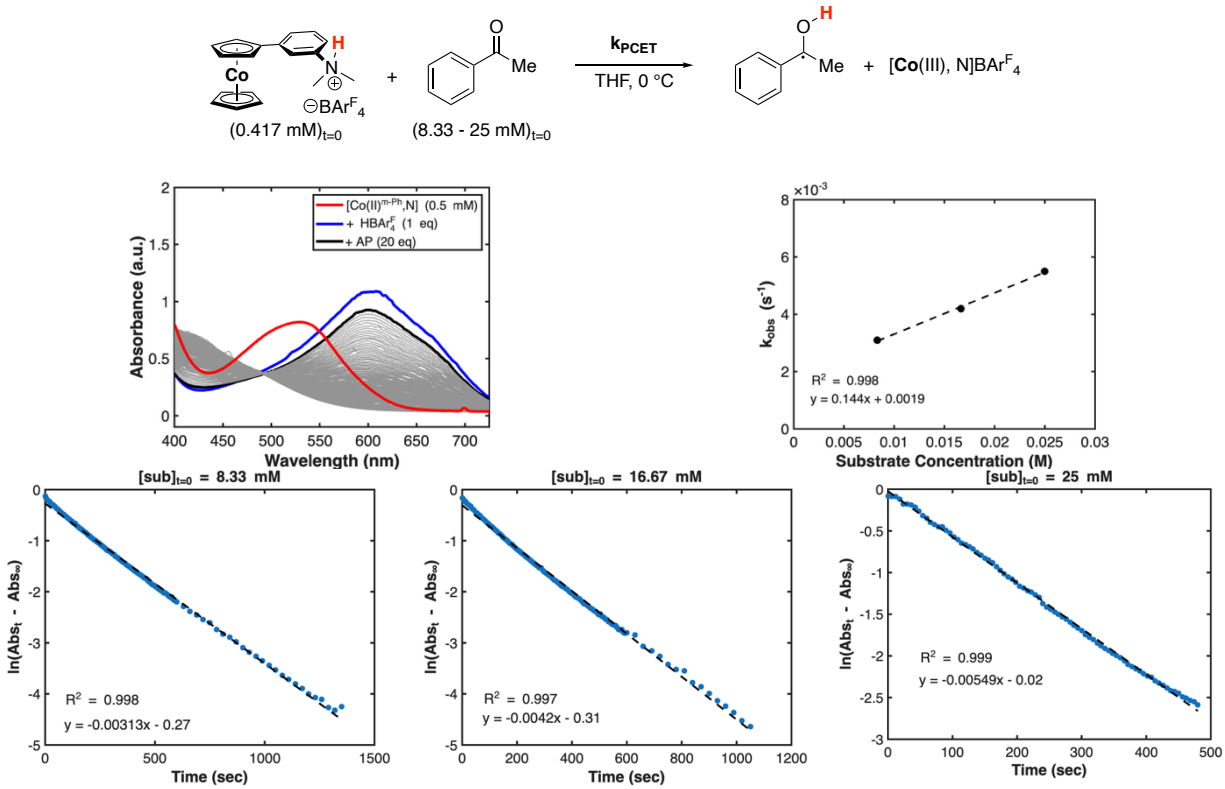

Figure C61 Kinetics of PCET from [**Co**(II)$^{m\text{-Ph}}$, N**H**]BAr$^F_4$ to acetophenone monitored at 610 nm

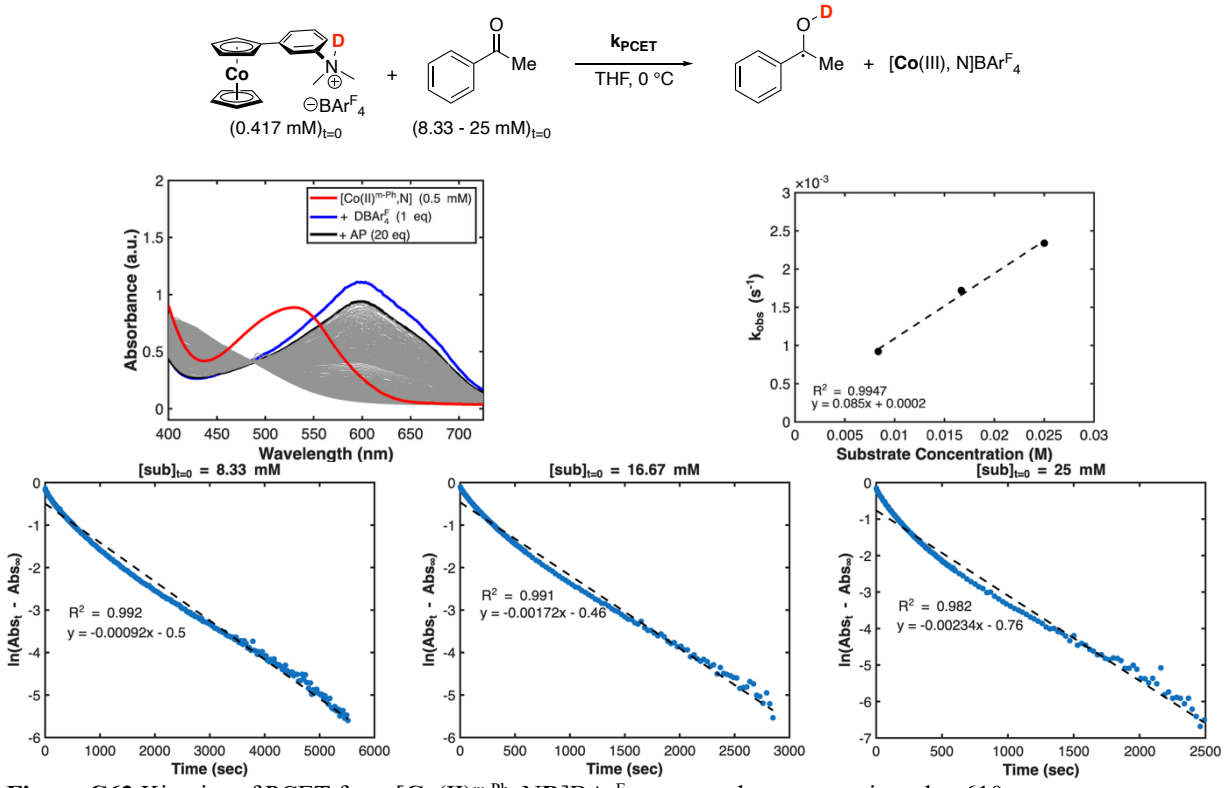

Figure C62 Kinetics of PCET from [**Co**(II)$^{m\text{-Ph}}$, N**D**]BAr$^F_4$ to acetophenone monitored at 610 nm

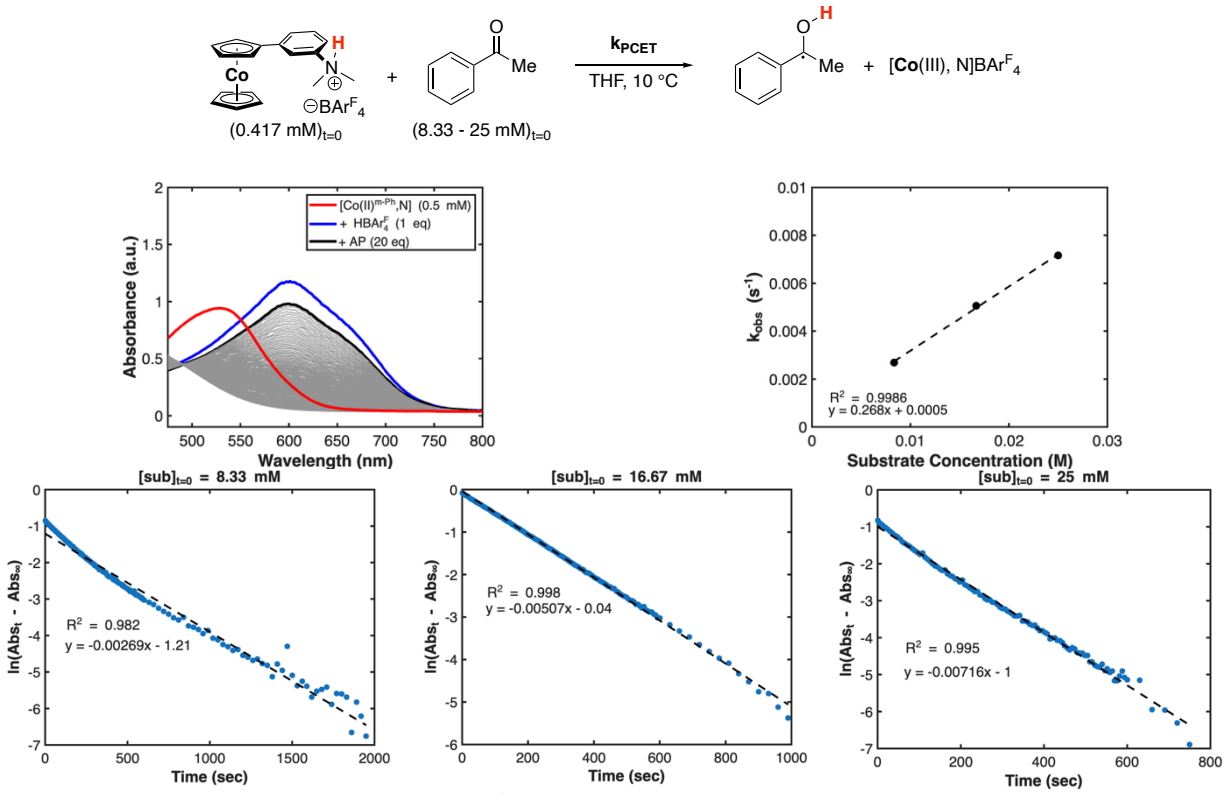

Figure C63 Kinetics of PCET from [**Co**(II)$^{m\text{-Ph}}$, N**H**]BAr$^{F}_{4}$ to acetophenone monitored at 610 nm

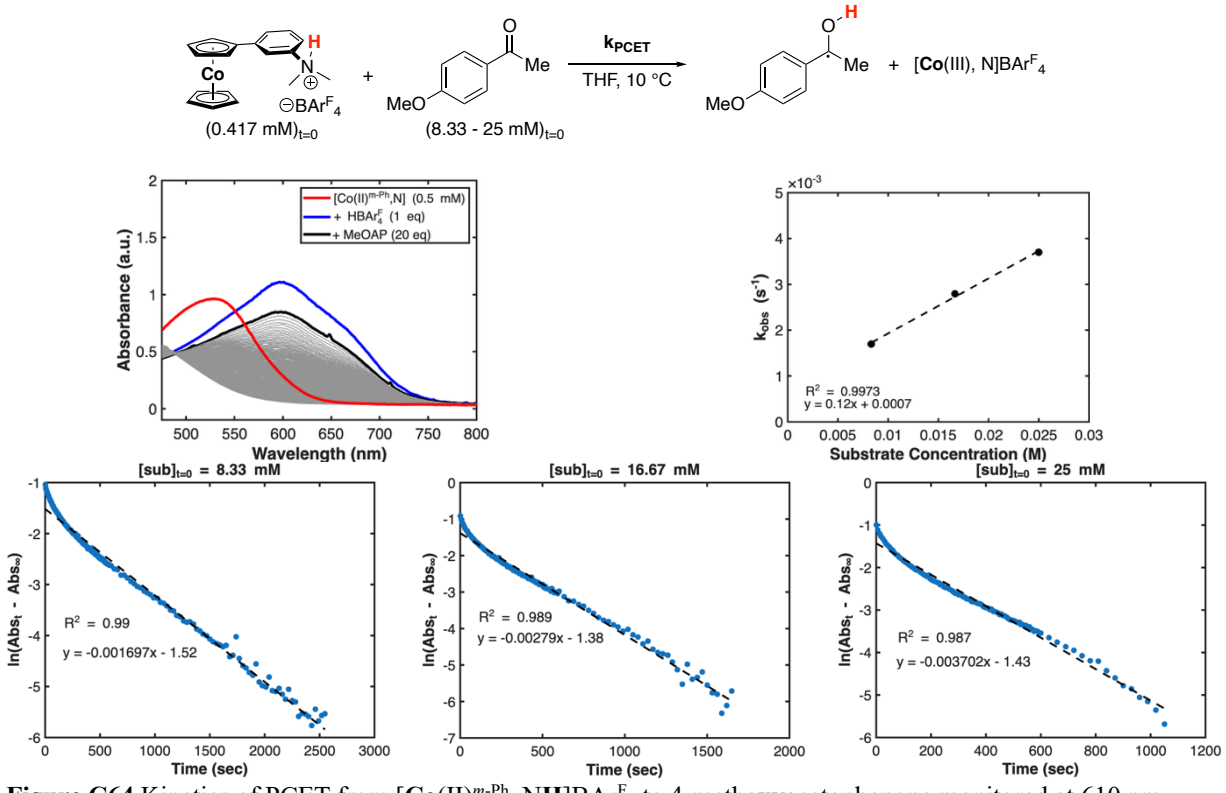

Figure C64 Kinetics of PCET from [**Co**(II)$^{m\text{-Ph}}$, N**H**]BAr$^{F}_{4}$ to 4-methoxyacetophenone monitored at 610 nm

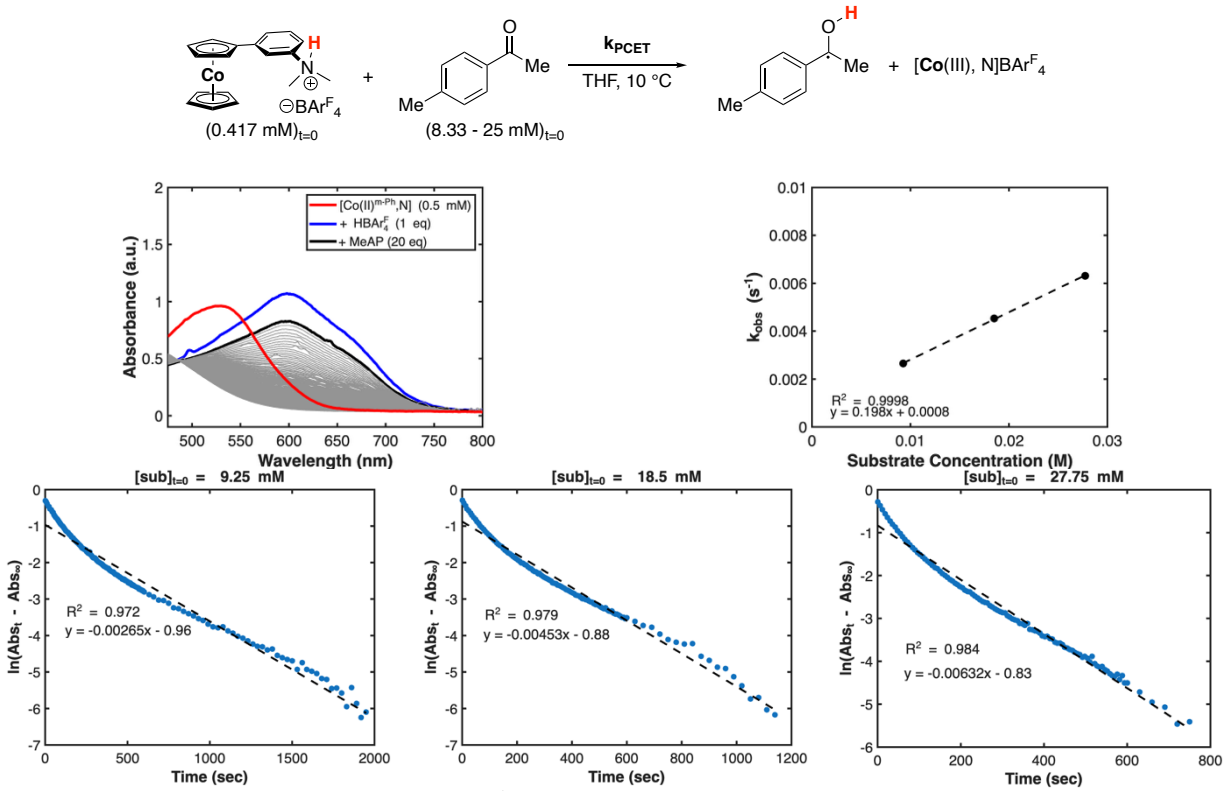

Figure C65 Kinetics of PCET from [**Co**(II)$^{m\text{-Ph}}$, N**H**]BAr$^F_4$ to 4-methylacetophenone monitored at 610 nm

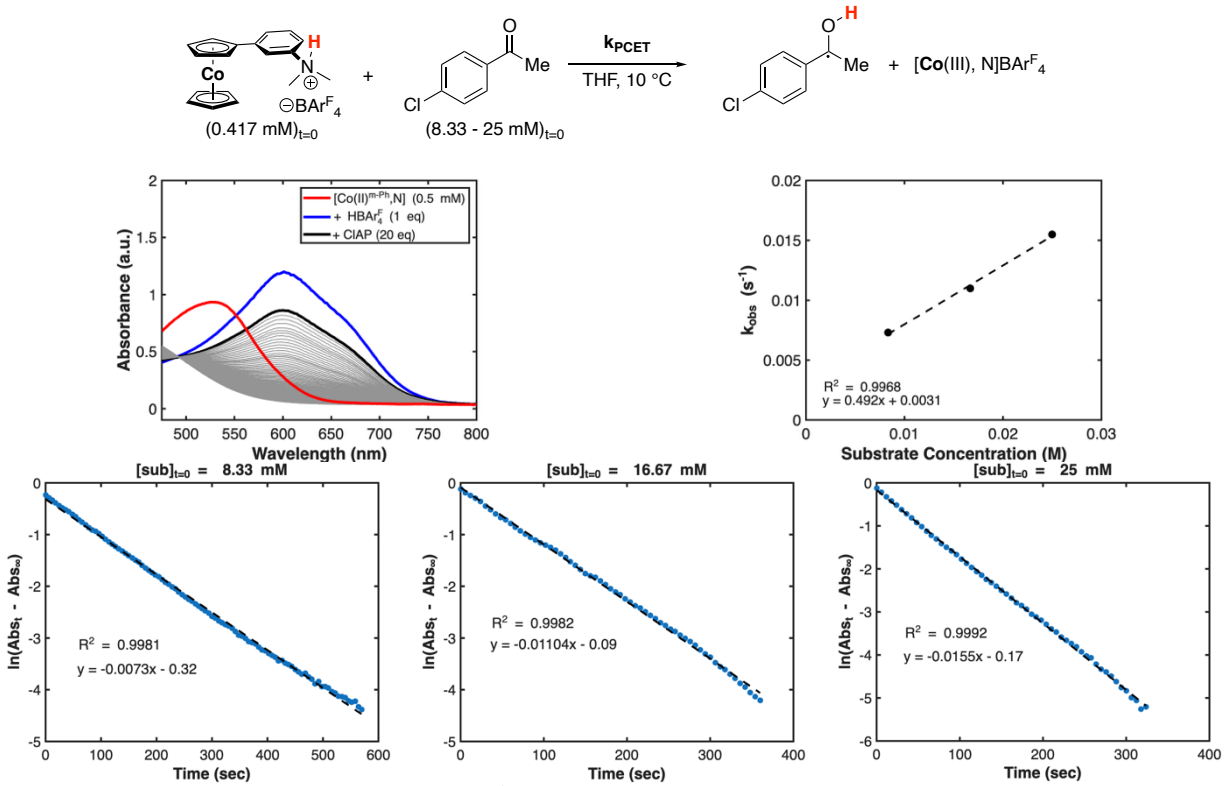

Figure C66 Kinetics of PCET from [**Co**(II)$^{m\text{-Ph}}$, N**H**]BAr$^F_4$ to 4-chloroacetophenone monitored at 610 nm

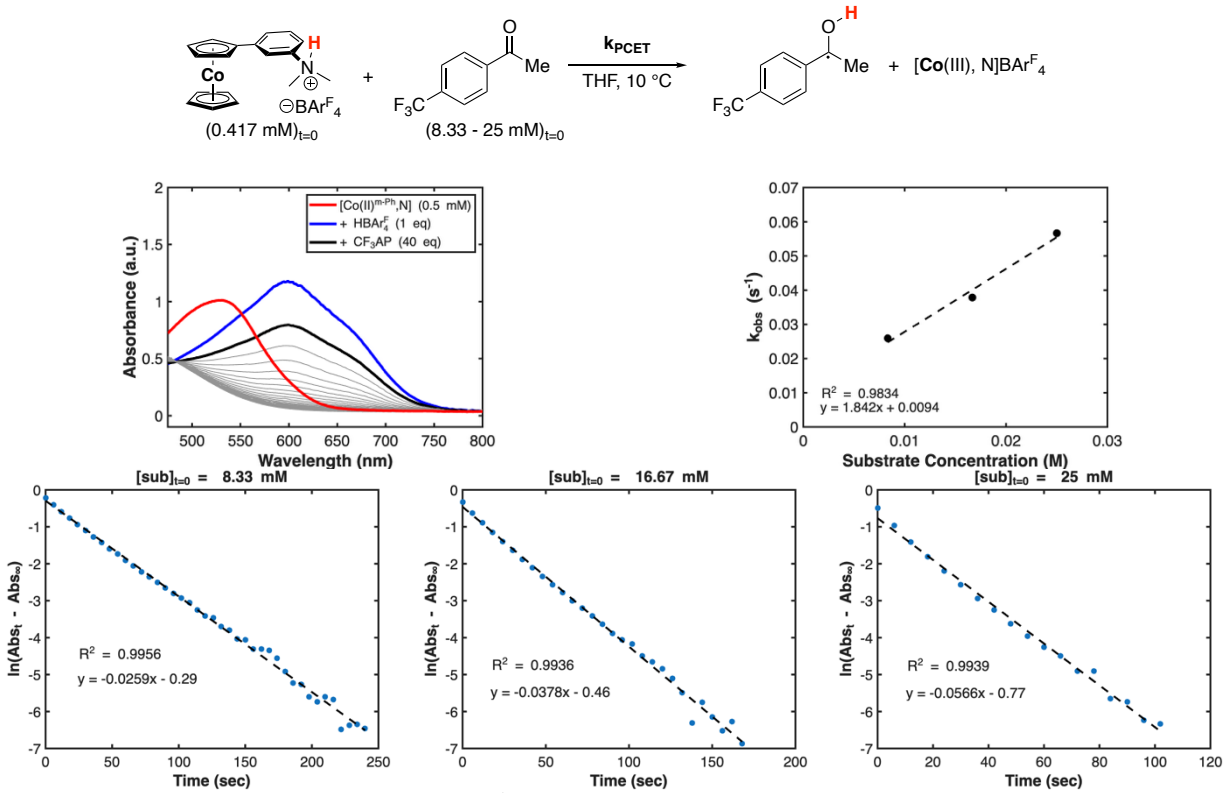

Figure C67 Kinetics of PCET from [**Co**(II)$^{m\text{-Ph}}$, N**H**]BAr$^{F}_{4}$ to 4-(CF$_3$)acetophenone monitored at 610 nm

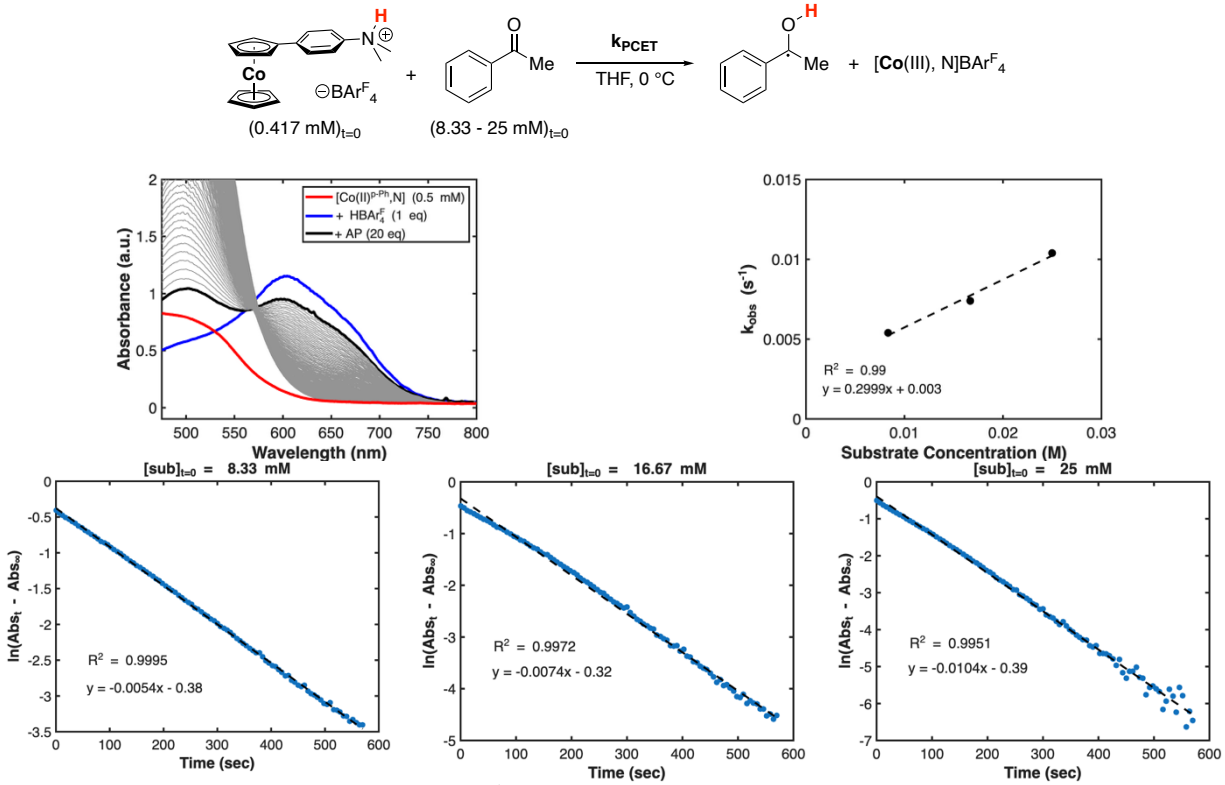

Figure C68 Kinetics of PCET from [**Co**(II)$^{p\text{-Ph}}$, N**H**]BAr$^{F}_{4}$ to acetophenone monitored at 610 nm

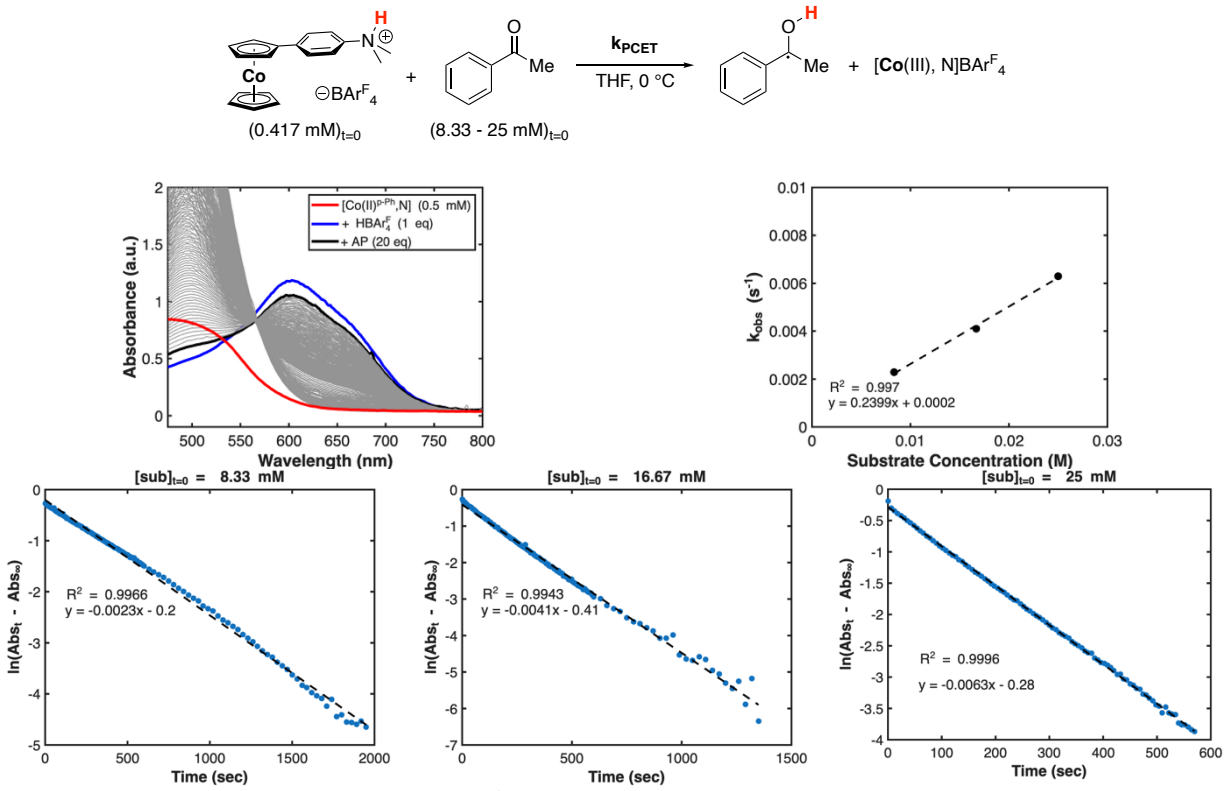

Figure C69 Kinetics of PCET from [**Co**(II)$^{p\text{-Ph}}$, N**H**]BAr$^F_4$ to acetophenone monitored at 610 nm

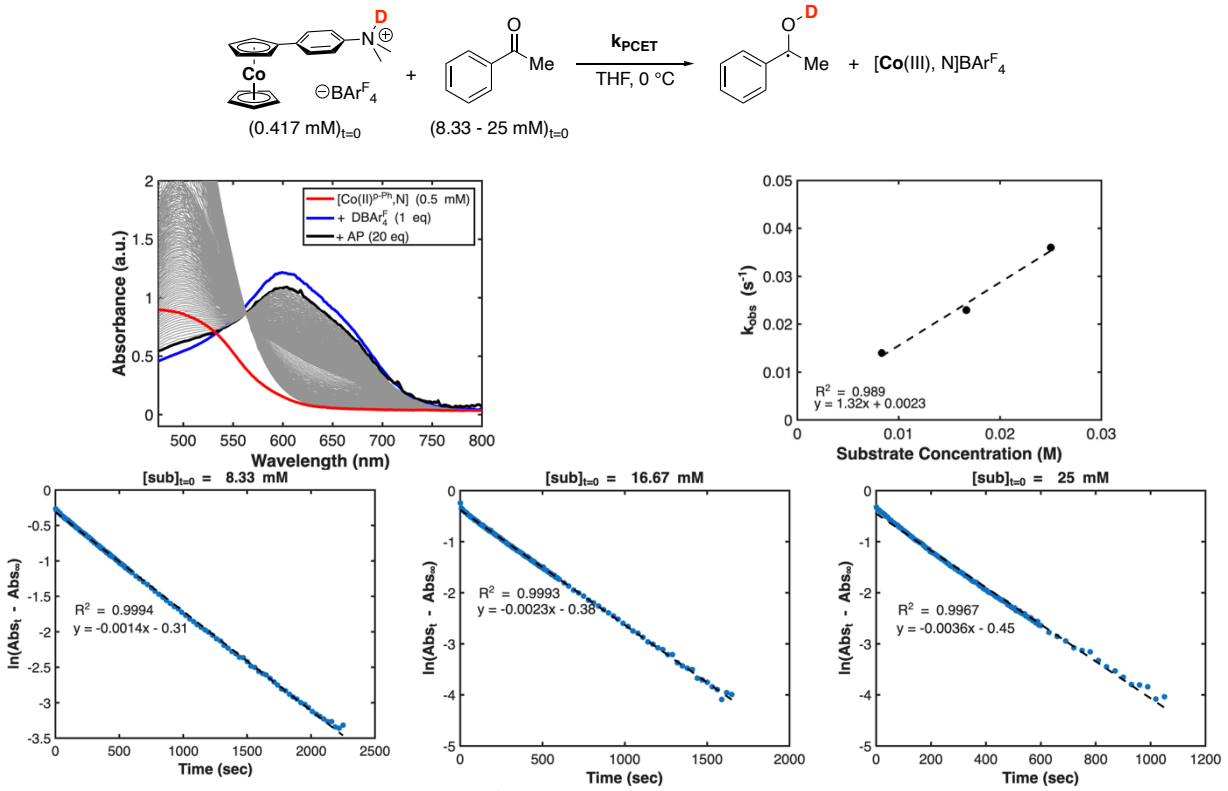

Figure C70 Kinetics of PCET from [**Co**(II)$^{p\text{-Ph}}$, N**D**]BAr$^F_4$ to acetophenone monitored at 610 nm

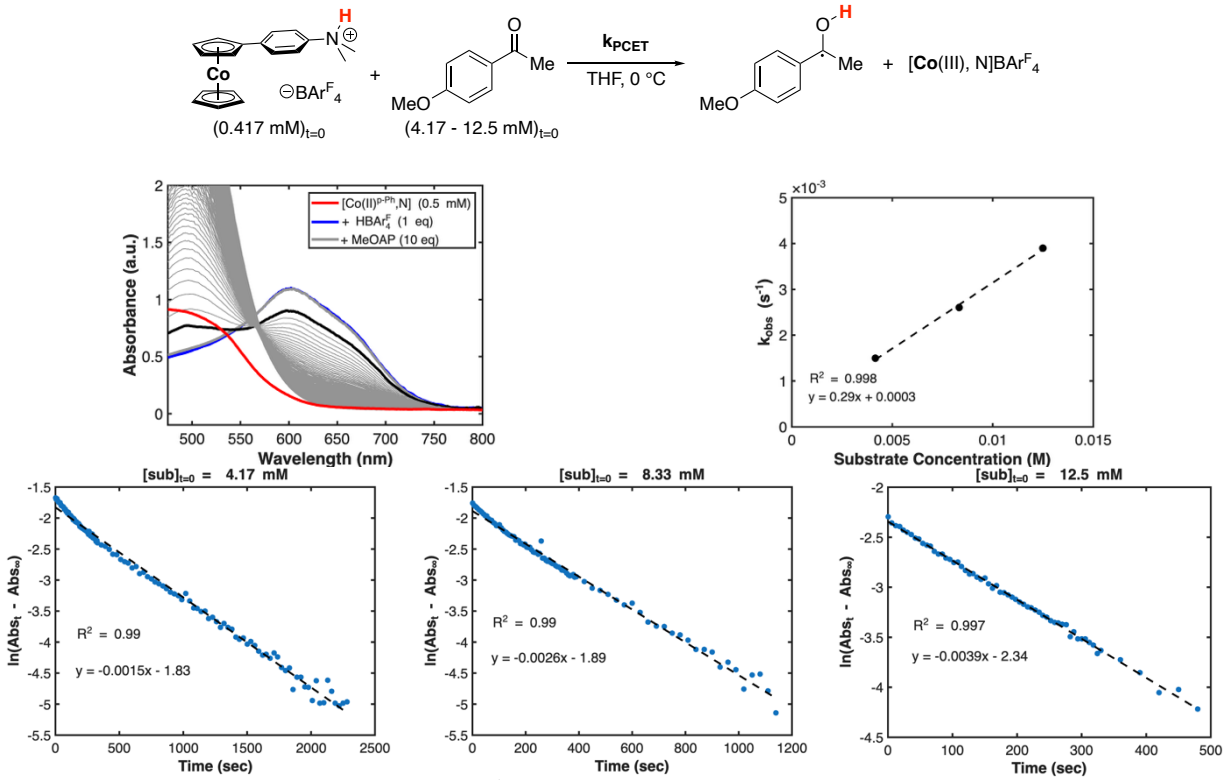

Figure C71 Kinetics of PCET from [**Co**(II)$^{p\text{-Ph}}$, N**H**]BAr$^F_4$ to 4-methoxyacetophenone monitored at 610 nm

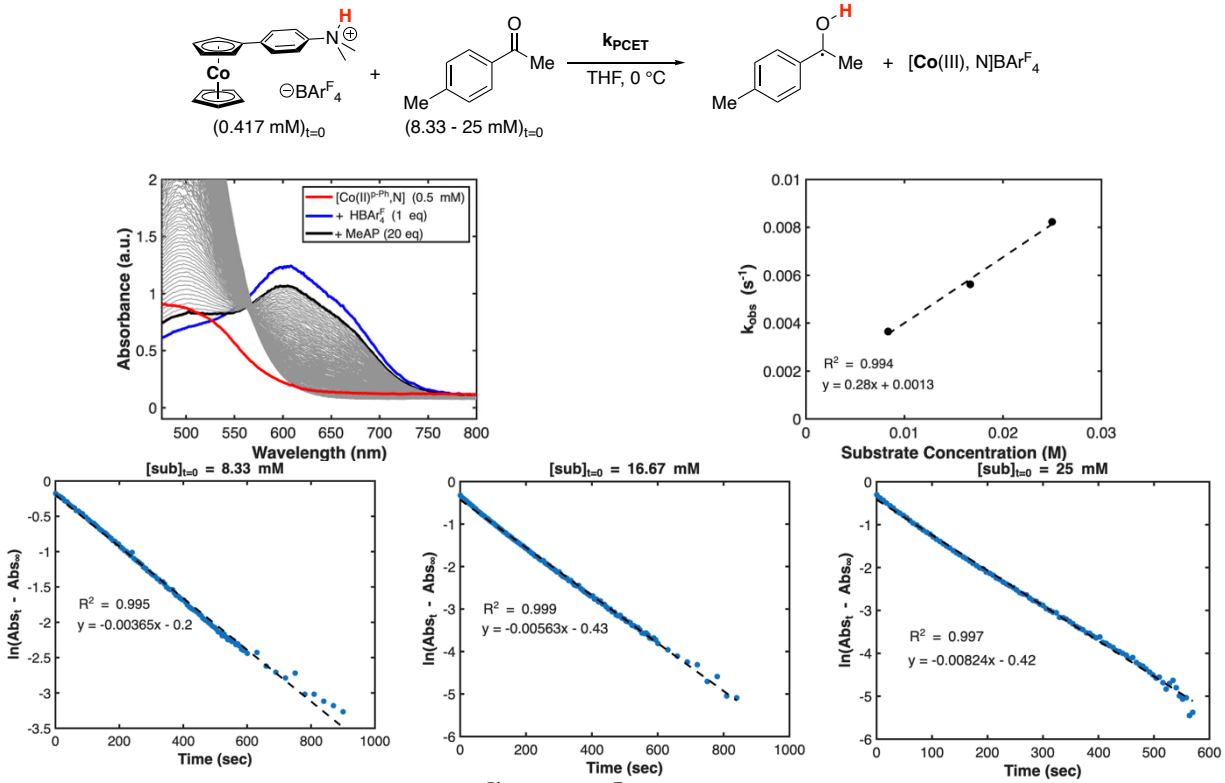

Figure C72 Kinetics of PCET from [**Co**(II)$^{p\text{-Ph}}$, N**H**]BAr$^F_4$ to 4-methylacetophenone monitored at 610 nm

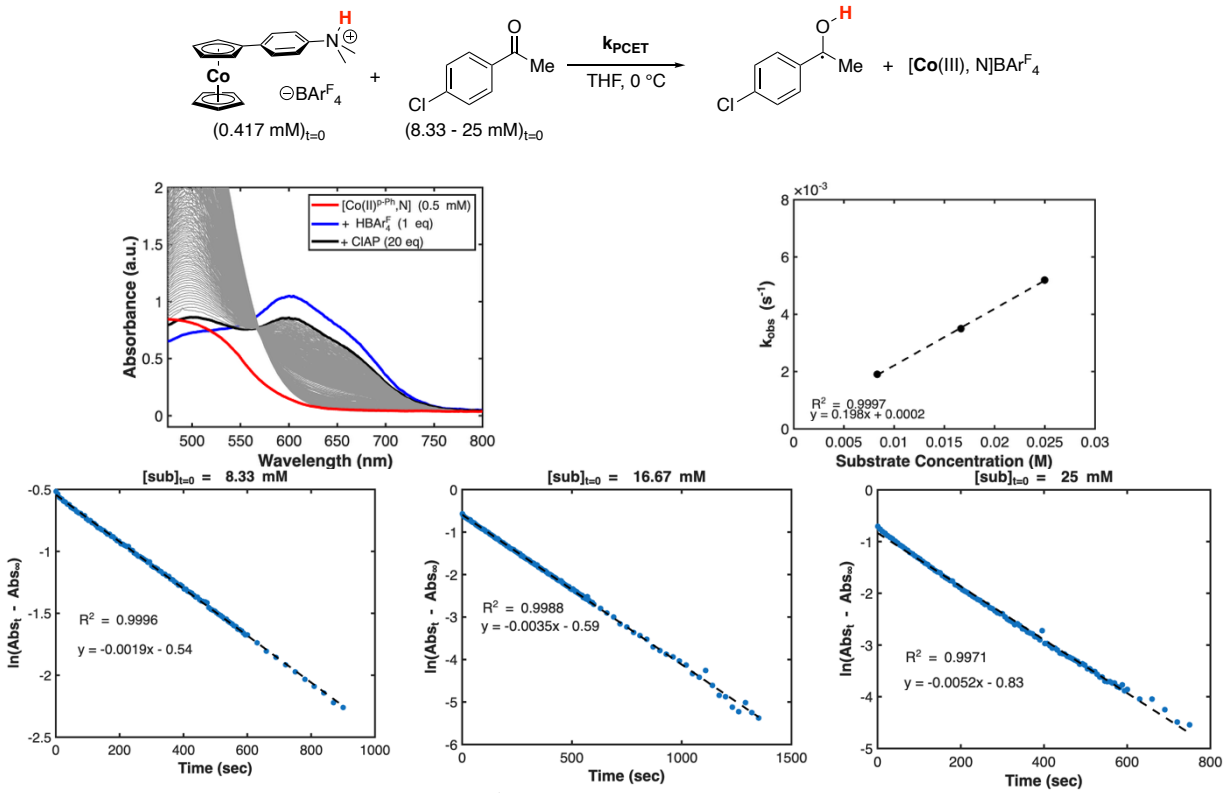

Figure C73 Kinetics of PCET from [**Co**(II)$^{p\text{-Ph}}$, N**H**]BAr$^{F}_{4}$ to 4-chloroacetophenone monitored at 610 nm

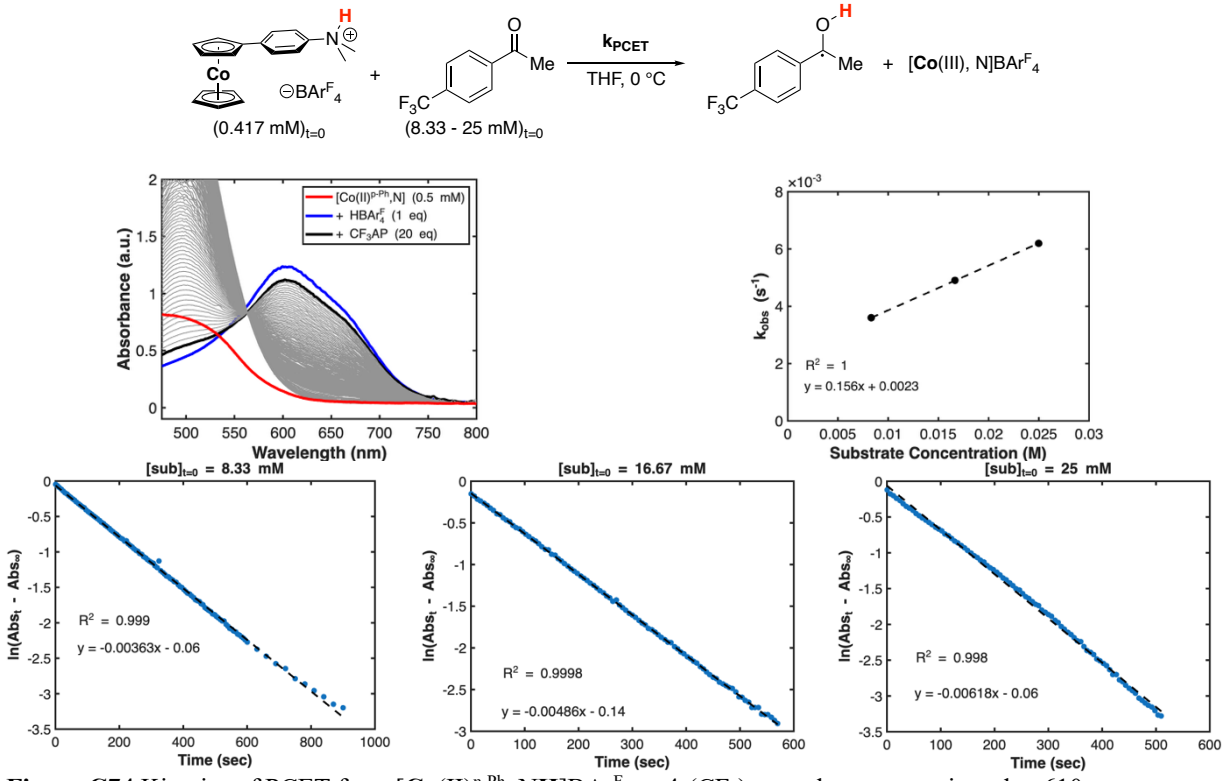

Figure C74 Kinetics of PCET from [**Co**(II)$^{p\text{-Ph}}$, N**H**]BAr$^{F}_{4}$ to 4-(CF_3)acetophenone monitored at 610 nm

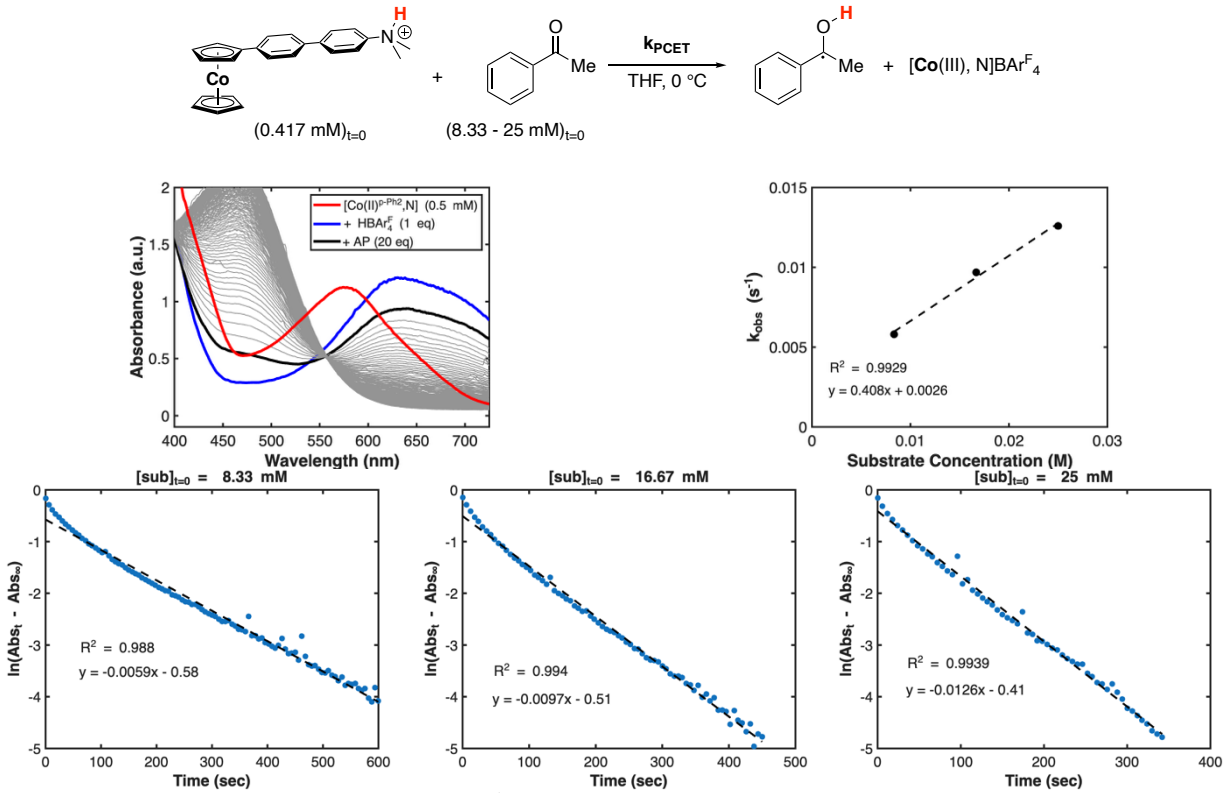

Figure C75 Kinetics of PCET from [**Co**(II)$^{p\text{-}Ph2}$, N**H**]BAr$^F_4$ to acetophenone monitored at 650 nm

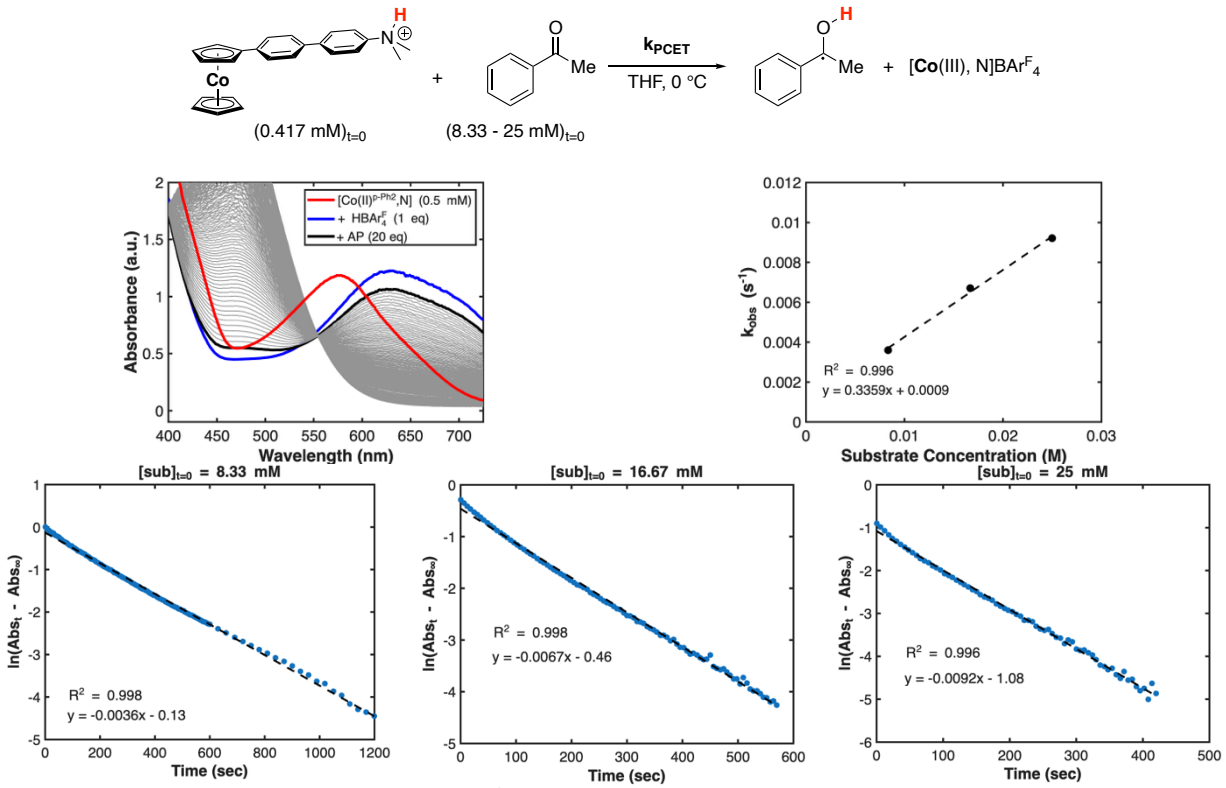

Figure C76 Kinetics of PCET from [**Co**(II)$^{p\text{-}Ph2}$, N**H**]BAr$^F_4$ to acetophenone monitored at 650 nm

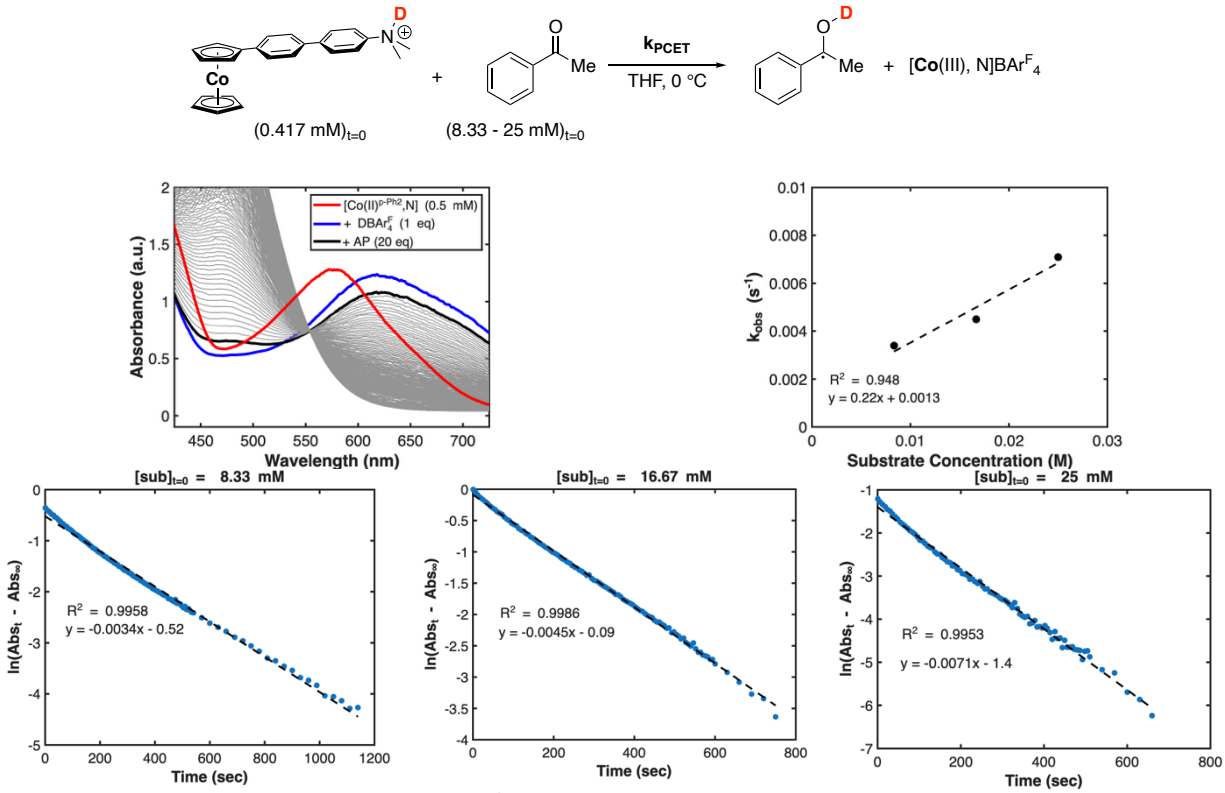

Figure C77 Kinetics of PCET from [**Co**(II)$^{p\text{-Ph2}}$, N**D**]BAr$^{F}_{4}$ to acetophenone monitored at 650 nm

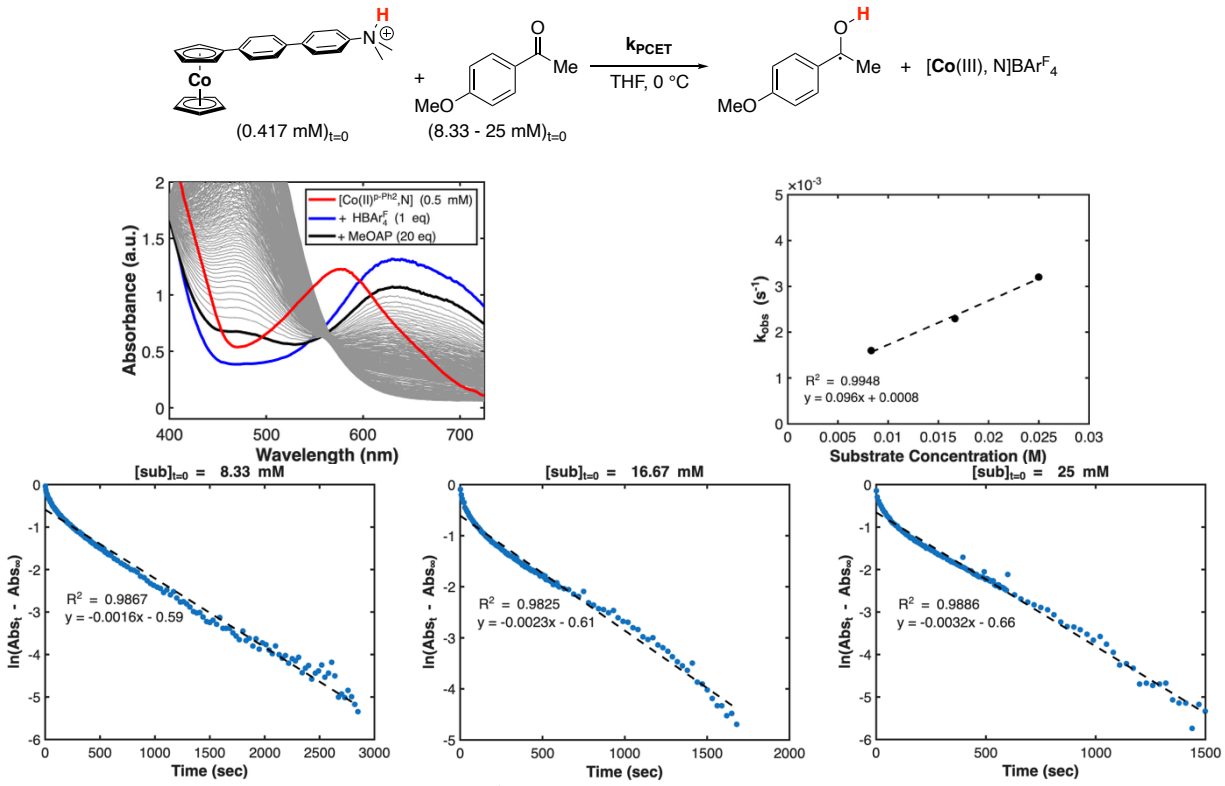

Figure C78 Kinetics of PCET from [**Co**(II)$^{p\text{-Ph2}}$, N**H**]BAr$^{F}_{4}$ to acetophenone monitored at 650 nm

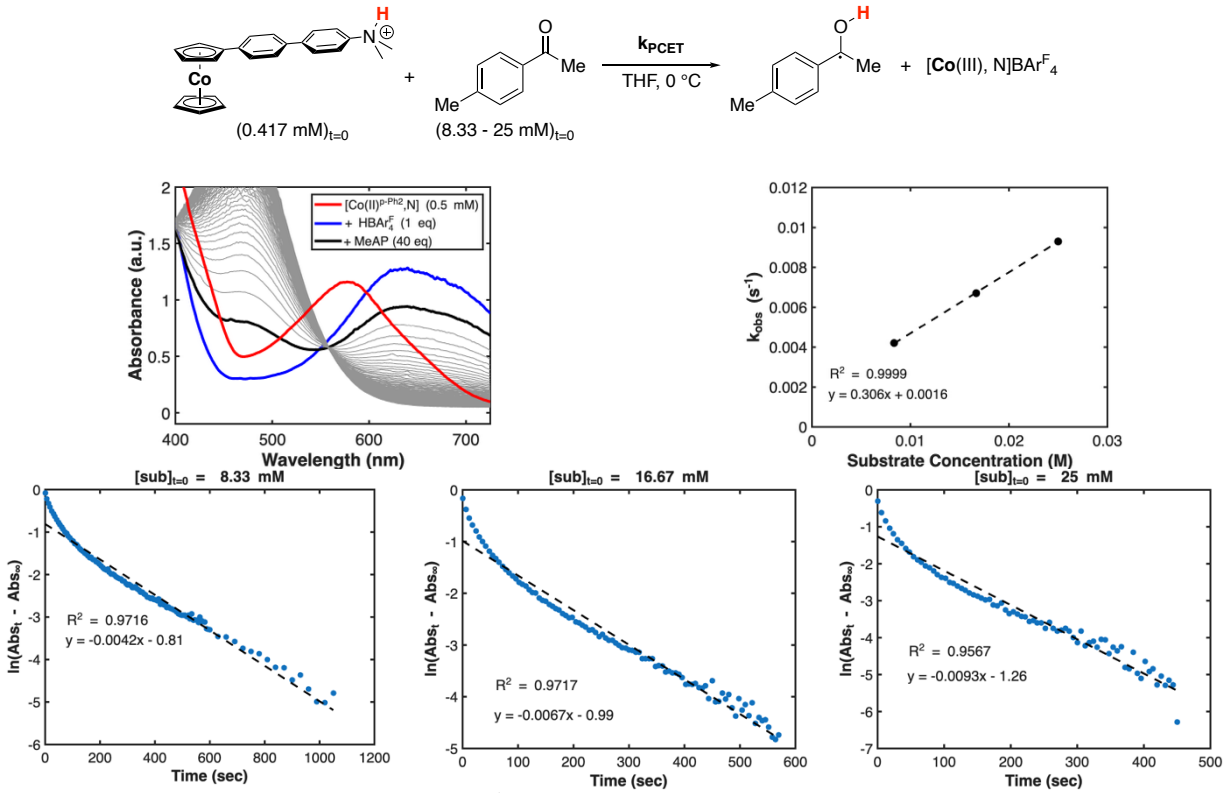

Figure C79 Kinetics of PCET from [**Co**(II)$^{p\text{-}Ph2}$, N**H**]BAr$^{F}_{4}$ to 4-methylacetophenone monitored at 650 nm

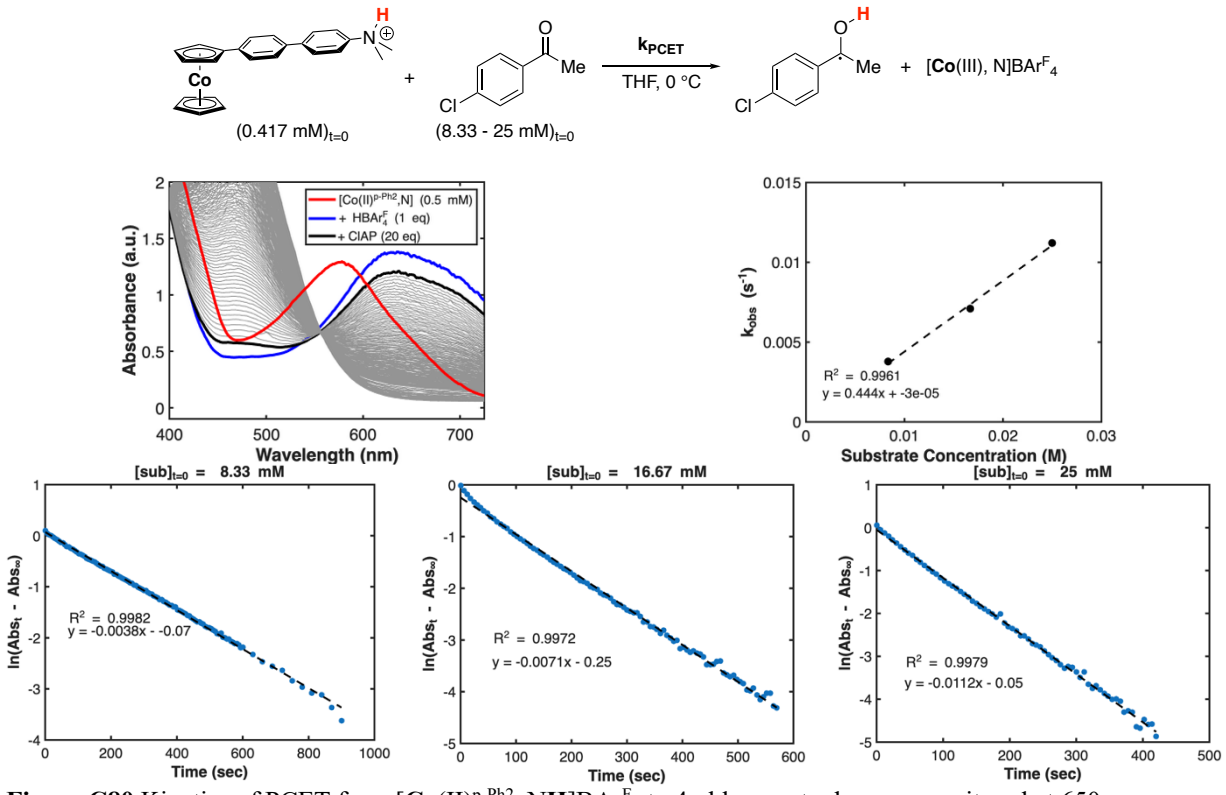

Figure C80 Kinetics of PCET from [**Co**(II)$^{p\text{-}Ph2}$, N**H**]BAr$^{F}_{4}$ to 4-chloroacetophenone monitored at 650 nm

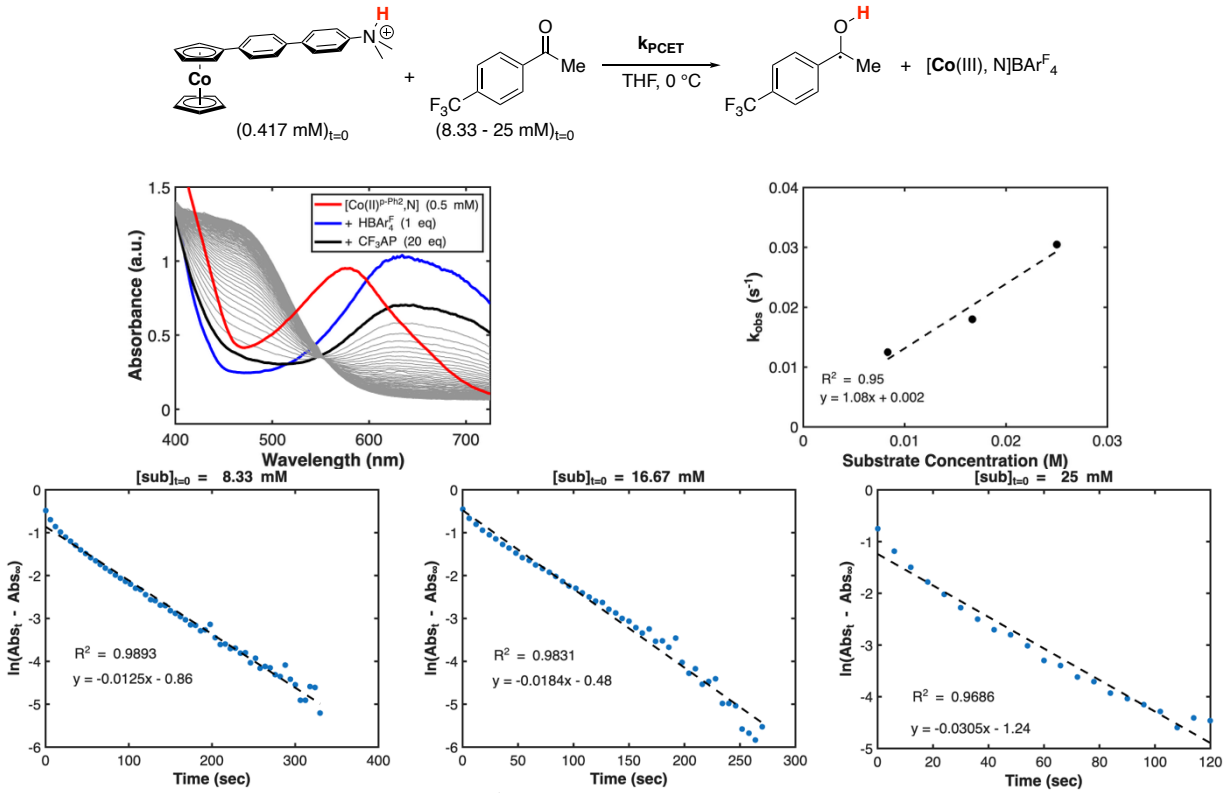

Figure C81 Kinetics of PCET from [**Co**(II)$^{p\text{-}Ph2}$, N**H**]BAr$^{F}_{4}$ to 4-(CF_3)acetophenone monitored at 650 nm

Multivariate Regression

The following code was written to perform the two-variable regression analysis of the kinetic data. Independent variables (x1, x2) were input pairwise to the function below along with the dependent variable (y), returning two slopes (m1, m2), an offset (b), and R^2 to indicate the quality of the fit to the data. For each two-variable combination, the R^2 was calculated and reported in the corresponding box in **Figure 3d**. The code was written and run in the Visual Studio Code environment using Python 3.13.3. The input data were formatted as a Pandas DataFrame.

1) definition of the two-variable multiple regression function

```
def multiple_regression_2var(x1, x2, y):
    """
    Multiple linear regression: y = m1*x1 + m2*x2 + b
    Returns (m1, m2, b, r2)
    """
    import numpy as np
    import pandas as pd
    from numpy.linalg import lstsq

    x1 = pd.to_numeric(x1, errors='coerce').to_numpy(dtype=float)
    x2 = pd.to_numeric(x2, errors='coerce').to_numpy(dtype=float)
    y  = pd.to_numeric(y,  errors='coerce').to_numpy(dtype=float)

    # mask finite values
    mask = np.isfinite(x1) & np.isfinite(x2) & np.isfinite(y)
    if mask.sum() < 3:
        return (np.nan, np.nan, np.nan, np.nan)

    x1s = x1[mask]
    x2s = x2[mask]
    ys  = y[mask]

    # build design matrix [x1, x2, 1] for least-squares fit
    X = np.column_stack([x1s, x2s, np.ones(len(x1s))])
    coeffs, residuals, rank, s = lstsq(X, ys, rcond=None)
    m1, m2, b = coeffs

    # compute R²
    y_pred = m1 * x1s + m2 * x2s + b
    ss_res = ((ys - y_pred) ** 2).sum()
    ss_tot = ((ys - ys.mean()) ** 2).sum()
    r2 = 1.0 - ss_res / ss_tot if ss_tot != 0 else np.nan

    return (float(m1), float(m2), float(b), float(r2))
```

2) example usage: determine the piecewise

Pandas DataFrame =

	linker	o	m	p	ph2
0	rate	0.582000	0.128000	0.270000	0.372000
1	lnrate	-0.541285	-2.055725	-1.309333	-0.988861
2	EN	-1.320000	-1.310000	-1.350000	-1.300000
3	ENH	-1.110000	-1.220000	-1.210000	-1.280000
4	pKa(II)	12.100000	10.800000	11.000000	10.500000
5	pKa(III)	8.600000	9.300000	8.600000	10.200000
6	BDFE	38.800000	37.200000	36.500000	37.100000
7	dlambda	87.000000	261.000000	302.000000	153.000000
8	dE	210.000000	100.000000	140.000000	20.000000
9	KIE	1.500000	1.500000	2.100000	1.700000
10	roe	1.300000	1.400000	-0.300000	1.100000

Input:

```
m1, m2, b, r2 = multiple_regression_2var(df.iloc[7], df.iloc[9], df.iloc[1])
print(f"y = {m1:.6g}*x1 + {m2:.6g}*x2 + {b:.6g}, R² = {r2:.6g}")
```

Output:

```
y = -0.00829238*x1 + -0.639757*x2 + 1.00068, R² = 0.970306
```

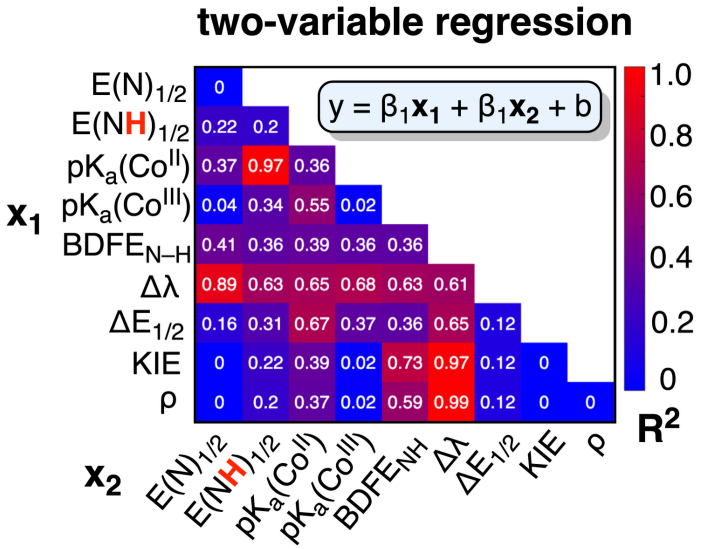

Figure C82. Linear regression with either one variable (along the diagonal) or two-variables (off-diagonal), with the coefficient of determination (R^2) reported in the box colored from blue (low correlation) to red (high correlation)

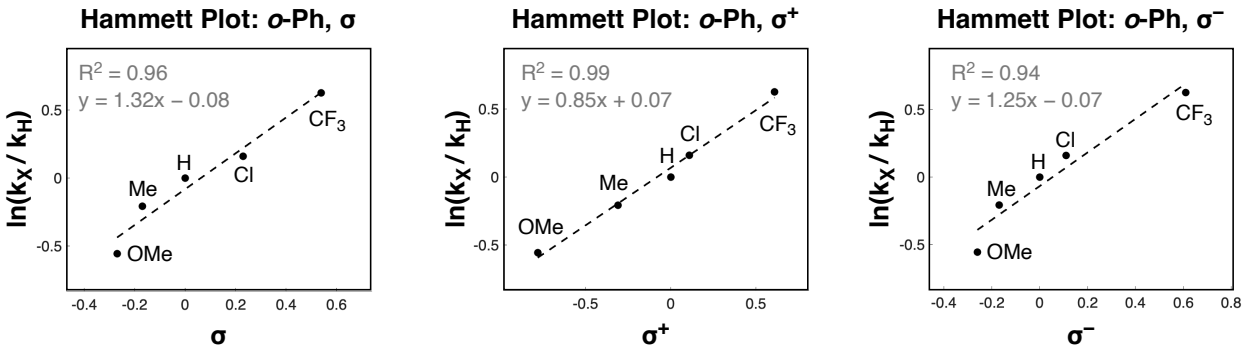

Figure C83. Hammett analysis of PCET from [**Co**(II)$^{o\text{-Ph}}$, N**H**]BAr$^{F}_{4}$ to *p*-X-acetophenone

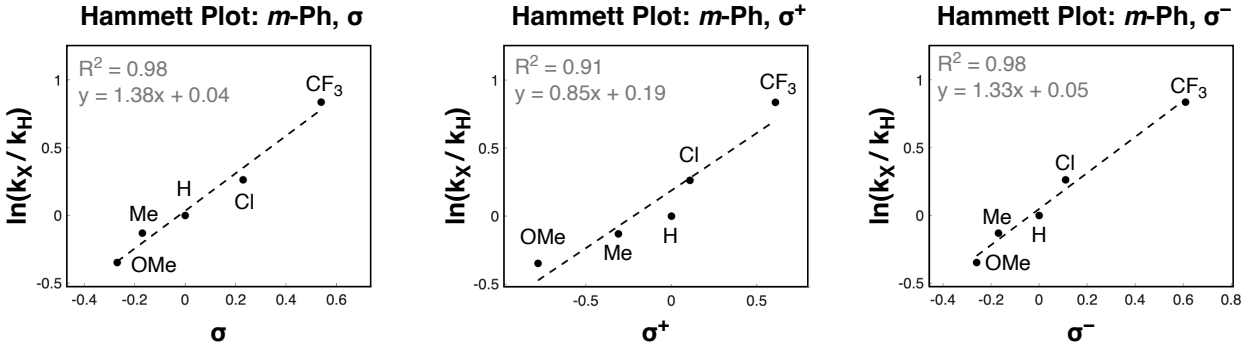

Figure C84. Hammett analysis of PCET from [**Co**(II)$^{m\text{-Ph}}$, N**H**]BAr$^{F}_{4}$ to *p*-X-acetophenone

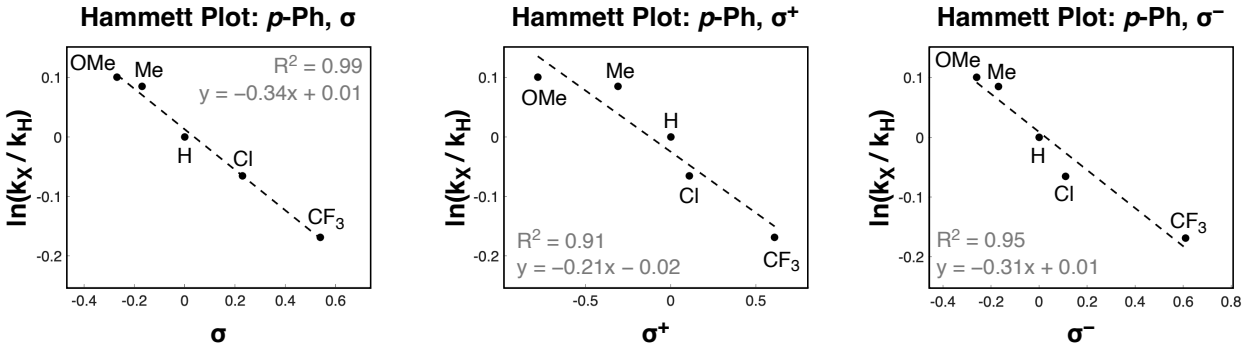

Figure C85. Hammett analysis of PCET from [**Co**(II)$^{p\text{-Ph}}$, N**H**]BAr$^{F}_{4}$ to *p*-X-acetophenone

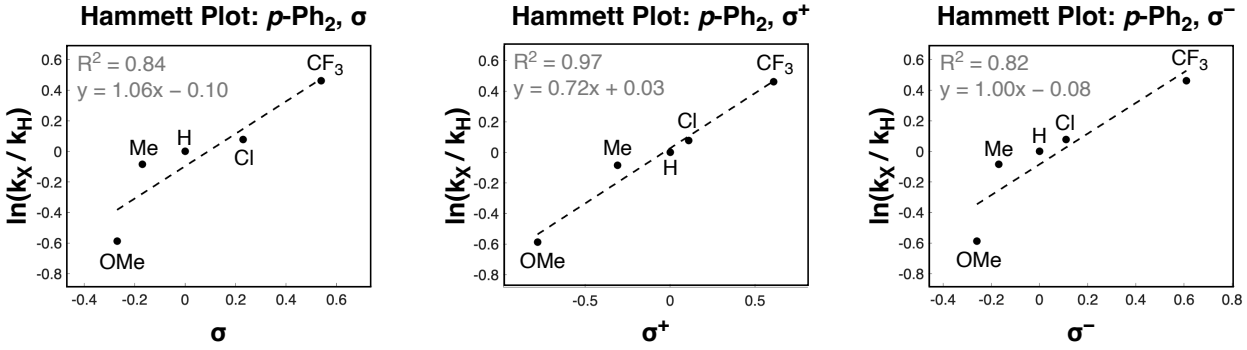

Figure C86. Hammett analysis of PCET from [**Co**(II)$^{p\text{-Ph2}}$, N**H**]BAr$^{F}_{4}$ to *p*-X-acetophenone

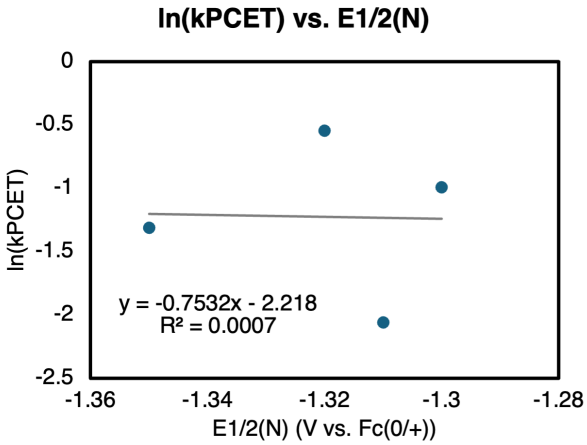

Figure C87. PCET Rate versus $[Co, N]^{0/+}$ potential plot

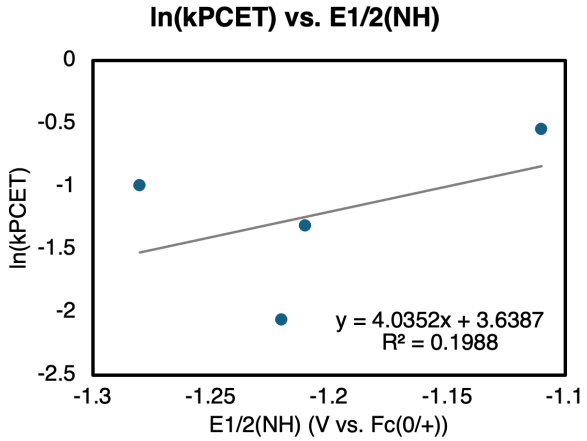

Figure C88. PCET Rate versus $[Co, NH]^{+/2+}$ potential plot

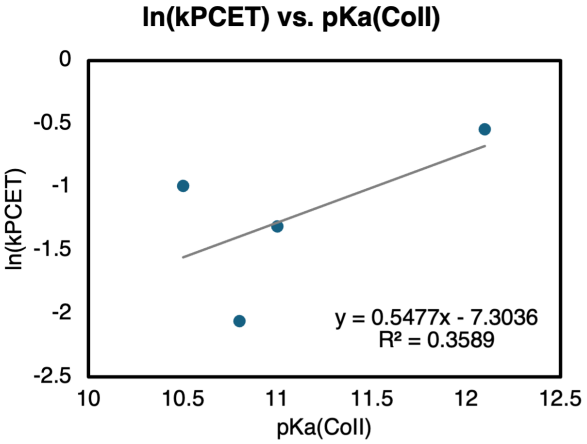

Figure C89. PCET Rate versus $[Co(II), NH]^{+}$ pK_a plot

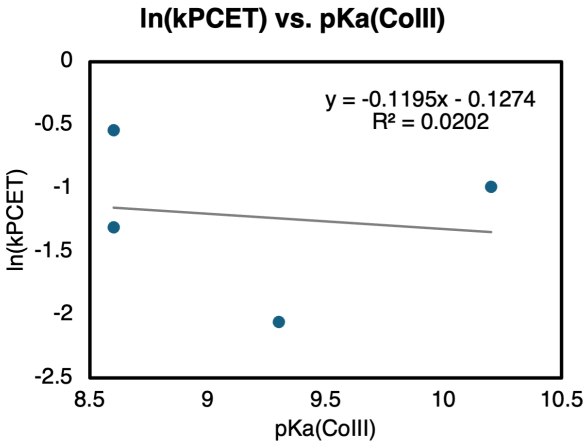

Figure C90. PCET Rate versus [Co(III), NH]$^{2+}$ pK_a plot

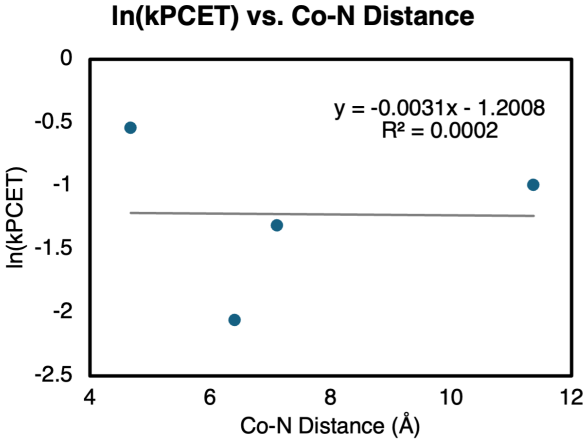

Figure C91. PCET Rate versus Co-N Distance plot. The Co-N distance was determined from the crystal structures of the corresponding [Co(II), N] complexes.

C9. Controlled Potential Electrolysis

Table C8. Cobaltocene-mediated Reduction of Acetophenone to Pinacol

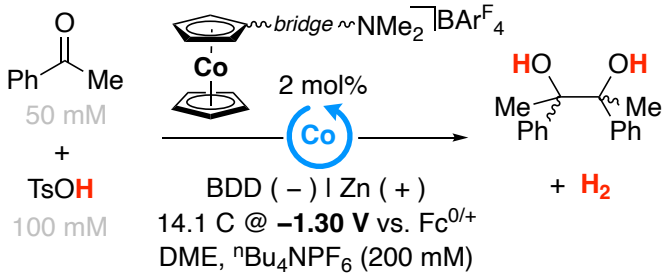

linker	Pinacol turnover number[a]	Pinacol Faradaic Efficiency (%)
o-Ph	8.7 ± 2.0	17 ± 4
m-Ph	17.8 ± 1.2	36± 2
p-Ph	18.9 ± 0.3	38 ± 1
p-Ph$_2$	21.9 ± 1.5	44 ± 3

[a] Electrolyses were performed in triplicate

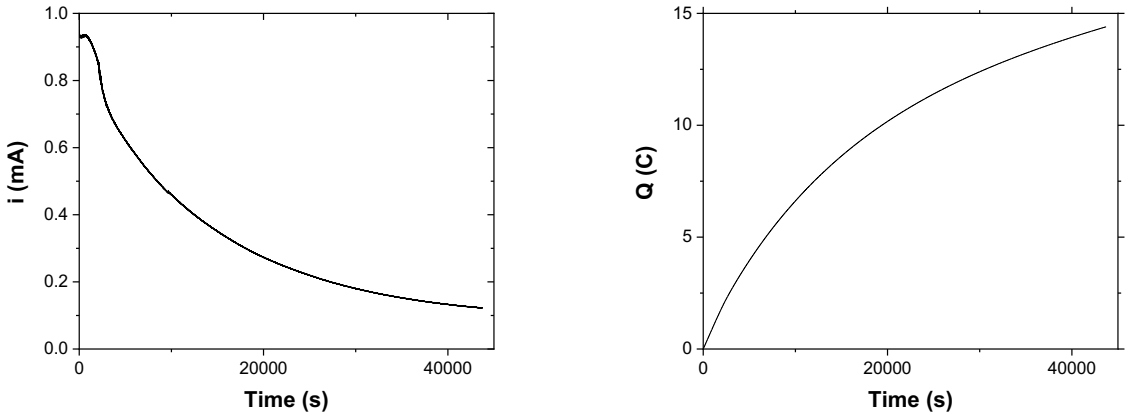

Figure C92. (Left) Representative chronoamperomogram (current vs. time) under standard conditions. (Right) Representative integrated chronoameromogram (charge vs. time) under standard conditions.

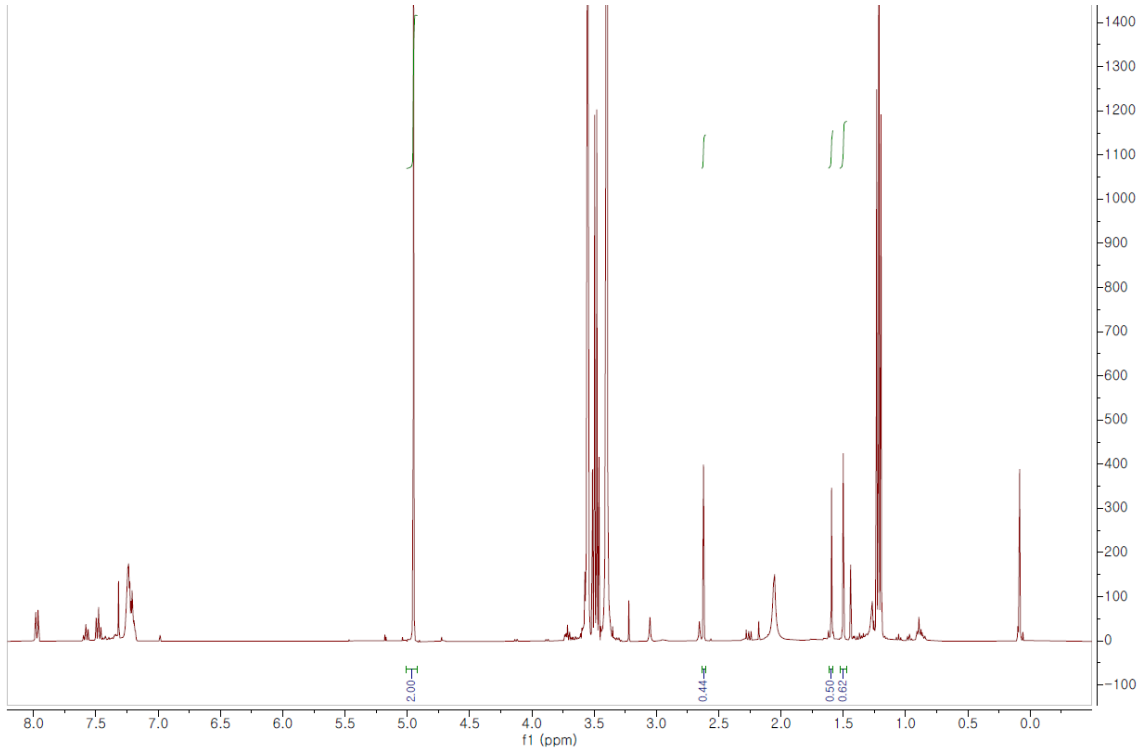

Figure C93. ^{1}H NMR spectrum of the products of CPE with [Co(III)$^{p\text{-Ph}}$, N]BAr$^{F}_{4}$ with CH_2Br_2 internal standard

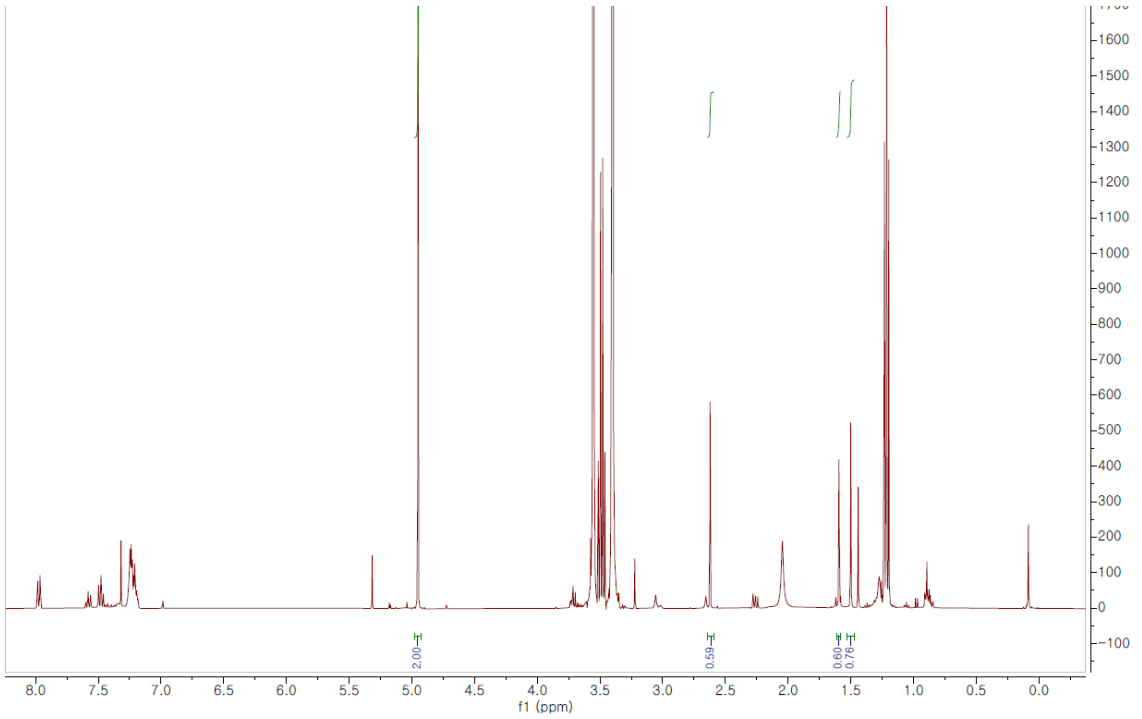

Figure C94. ^{1}H NMR spectrum of the products of CPE with [Co(III)$^{p\text{-Ph2}}$, N]BAr$^{F}_{4}$ with CH_2Br_2 internal standard

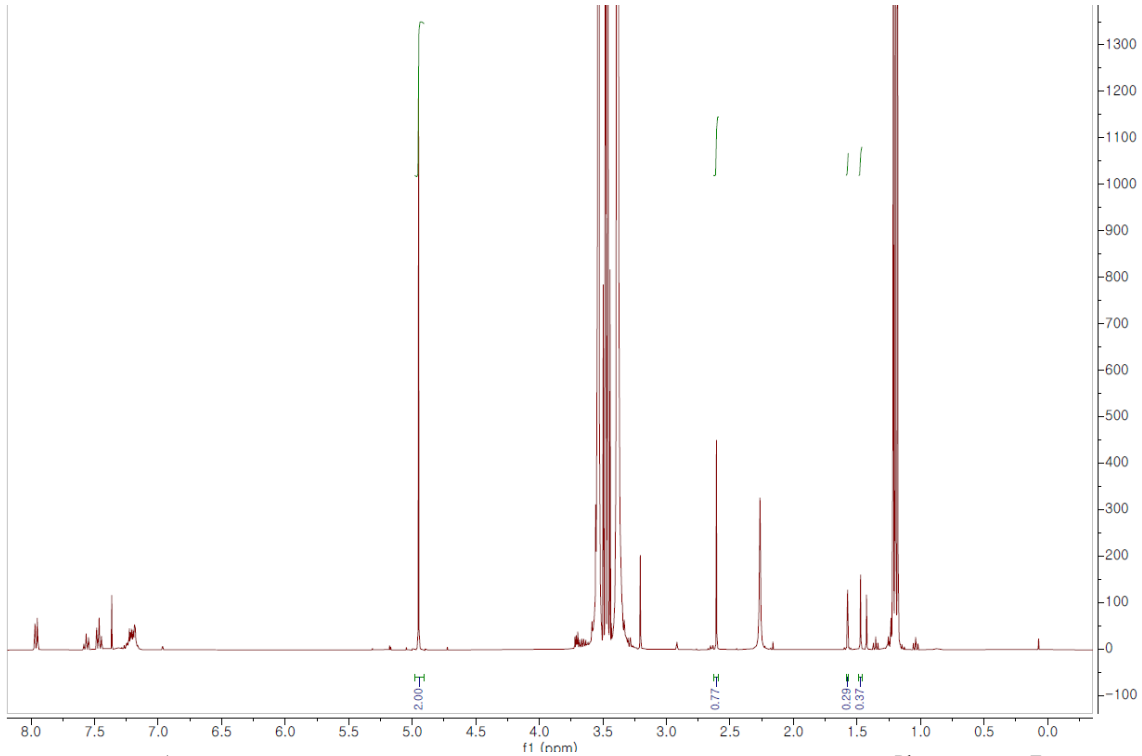

Figure C95. ^{1}H NMR spectrum of the products of CPE with [Co(III)$^{o\text{-Ph}}$, N] BAr^{F}_{4} with CH_2Br_2 internal standard

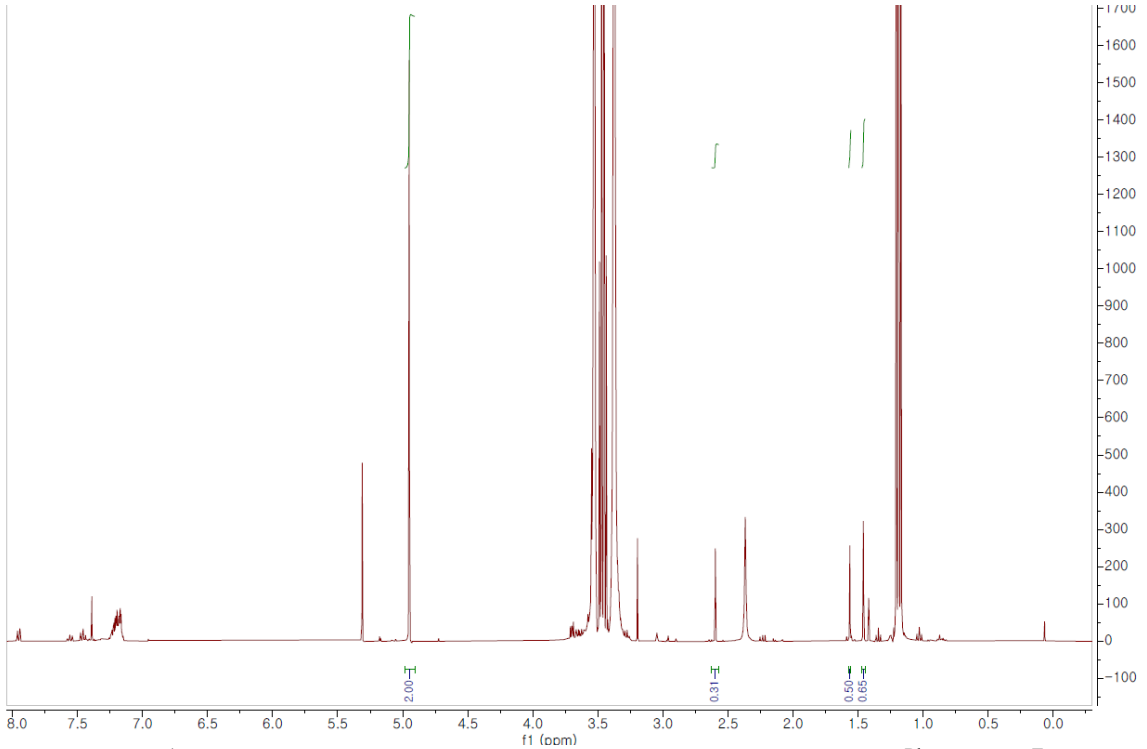

Figure C96. ^{1}H NMR spectrum of the products of CPE with [Co(III)$^{m\text{-Ph}}$, N]BAr^{F}_{4} with CH_2Br_2 internal standard

C10. Computational Details

E(sol) refers to single-point energy calculation, using SMD(THF)-TPSSh-D4/def2-TZVPP. G-E refers to thermochemistry correction energy obtained from frequency calculations using SMD(THF)-TPSSh-D4/def2-SVP|def2-TZVP(Co or Fe). The energies of the optimized structures were recalculated with a triple-ζ basis set def2-TZVPP with SMD(THF). (E(sol) (SCF/TZ)).
The final Gibbs free energies were calculated as follows:

$$G_{sol} = E_{sol} + (G - E) \quad (1)$$

$$\Delta G(sol) = \sum G_{sol}(\text{products}) - \sum G_{sol}(\text{reactants}) \quad (2)$$

Table C9. Calculated energy components of DFT-optimized structures of [Co, N]s.

Compound	E(sol) (SCF/TZ) [eV]	G-E [eV]	G(sol) [eV]
[Co(III)$^{p\text{-}Ph}$, N]	-58081.513	7.607	-58095.320
[Co(II)$^{p\text{-}Ph}$, N]	-58084.773	7.418	-58098.770
[Co(III)$^{p\text{-}Ph}$, NH$^+$]	-58093.145	8.072	-58106.569
[Co(II)$^{p\text{-}Ph}$, NH$^+$]	-58096.979	7.900	-58110.565
[Co(III)$^{p\text{-}Ph2}$, N]	-64365.709	9.680	-64383.933
[Co(II)$^{p\text{-}Ph2}$, N]	-64369.098	9.504	-64387.496
[Co(III)$^{p\text{-}Ph2}$, NH$^+$]	-64377.538	10.083	-64395.442
[Co(II)$^{p\text{-}Ph2}$, NH$^+$]	-64381.23	9.951	-64399.258
[Co(III)$^{o\text{-}Ph}$, N]	-58081.222	7.646	-58094.982
[Co(II)$^{o\text{-}Ph}$, N]	-58084.607	7.474	-58098.545
[Co(III)$^{o\text{-}Ph}$, NH$^+$]	-58092.911	8.068	-58106.340
[Co(II)$^{o\text{-}Ph}$, NH$^+$]	-58096.91	7.904	-58110.489
[Co(III)$^{m\text{-}Ph}$, N]	-58081.405	7.647	-58095.174
[Co(II)$^{m\text{-}Ph}$, N]	-58084.793	7.442	-58098.771
[Co(III)$^{m\text{-}Ph}$, NH$^+$]	-58093.119	8.093	-58106.522
[Co(II)$^{m\text{-}Ph}$, NH$^+$]	-58096.978	7.895	-58110.574

Table C10. Calculated energy components of DFT-optimized structures of substituted acetophenones (^{R}AP).

Compound	E(sol) (SCF/TZ) [eV]	G-E [eV]	G(sol) [eV]	BDFE [kcal/mol]
^{MeO}AP	-13582.131	3.656	-13593.328	
^{Me}AP	-11537.096	3.532	-11545.972	
^{H}AP	-10467.725	2.860	-10476.153	
^{Cl}AP	-22970.626	2.541	-22983.693	
^{CF3}AP	-19632.105	2.847	-19651.562	
^{MeO}AP-H•	-13597.353	3.895	-13608.362	33.3
^{Me}AP-H•	-11552.407	3.763	-11561.103	35.5
^{H}AP-H•	-10483.067	3.098	-10491.315	36.2
^{Cl}AP-H•	-22985.99	2.776	-22998.879	36.8
^{CF3}AP-H•	-19647.557	3.064	-19666.859	39.4
^{MeO}AP-H^{+}	-13593.596	3.994	-13604.470	
^{Me}AP-H^{+}	-11548.412	3.868	-11556.977	
^{H}AP-H^{+}	-10478.95	3.186	-10487.075	
^{Cl}AP-H^{+}	-22981.799	2.863	-22994.568	
^{CF3}AP-H	-19643.163	3.170	-19662.313	

Table C11. Calculated driving forces (−ΔG [kcal/mol]) for proton transfer from [Co(II), NH^{+}] to substituted-acetophenone.

Compounds	p-Ph	p-Ph2	o-Ph	m-Ph
^{MeO}AP	-15.0582	-14.2972	-18.4941	-15.2427
^{Me}AP	-18.2174	-17.4564	-21.6533	-18.4019
^{H}AP	-20.1314	-19.3704	-23.5673	-20.3159
^{Cl}AP	-21.2152	-20.4542	-24.6511	-21.3997
^{CF3}AP	-24.0746	-23.3137	-27.5106	-24.2591

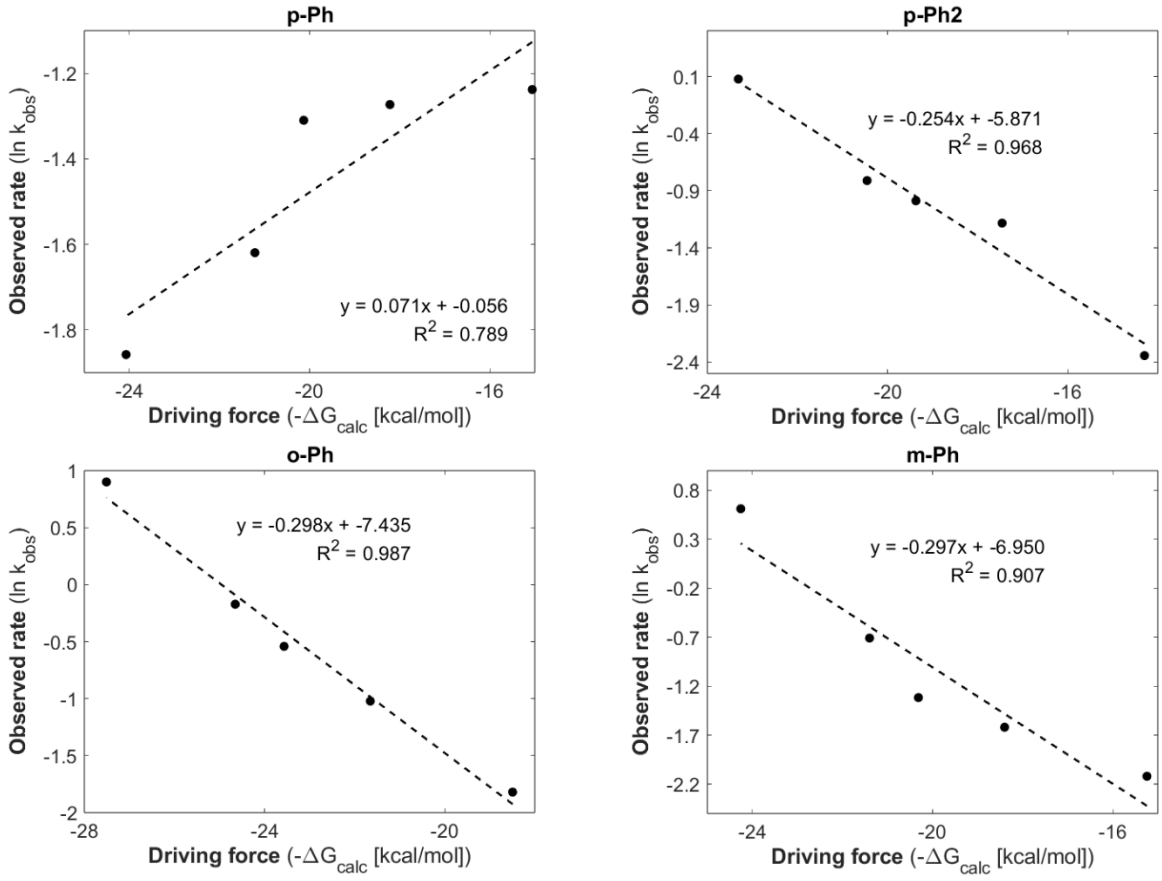

Figure C97. Calculated proton transfer driving force *vs.* PCET rate plot.

10.1 PCET Transition State Barrier Calculation

We evaluated the transition states for the PCET reaction from a given cobaltocene mediator to acetophenone by first identifying a reasonable mediator-acetophenone adducts (IM-X) and then searching for the geometry of the PCET transition state by using a relaxed scan of the proton coordinate. The highest energy scan was entered as the coordinates into a transition state calculation to identify the transition state (TS-X).

Table C12. Calculated energy components of transition state for PCET from $[Co(II)^{o\text{-}Ph}, NH]^+$ to acetophenone.

Compound	E(sol) (SCF/TZ) [eV]	G-E [eV]	G(sol) [eV]	ΔG (kcal/mol)
IM-1	-68565.172	11.377	-68586.400	5.58
TS-1	-68564.644	11.321	-68585.869	17.83
IM-2	-68564.966	11.395	-68586.194	10.33
TS-2	-68564.398	11.279	-68585.701	21.70
IM-3	-68597.901	11.433	-68586.468	5.97
TS-3	-68597.463	11.286	-68586.177	12.68
IM-4	-68597.914	11.378	-68586.536	4.20
TS-4	-68597.398	11.275	-68586.123	13.72
IM-5	-74888.674	13.443	-74875.231	4.15
TS-5	-74888.142	13.321	-74874.821	13.61

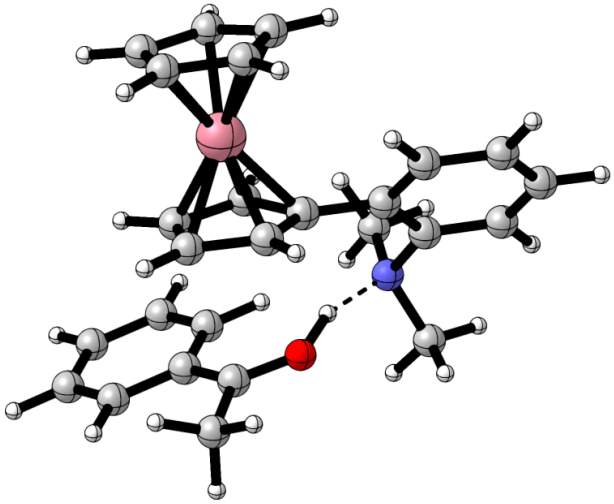

Figure C98. Optimized transition state geometry of $[Co(II)^{o\text{-}Ph}, NH]^+$ (**TS-1**), with the lowest transition state barrier. (Cp ring – carbonyl overlap)

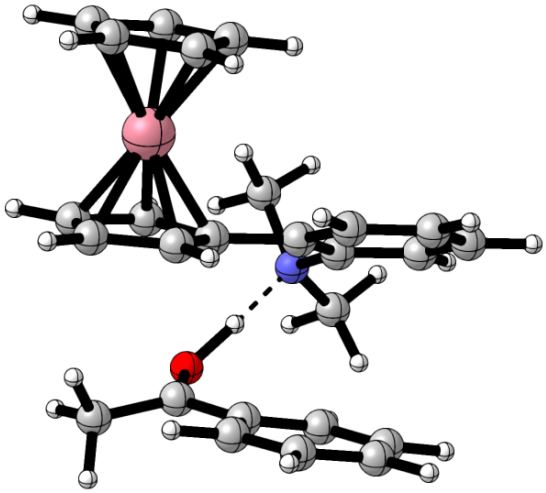

Figure C99. Optimized transition state geometry of $[Co(II)^{o\text{-}Ph}, NH]^+$ (**TS-2**), with Ph-Ph stacking geometry.

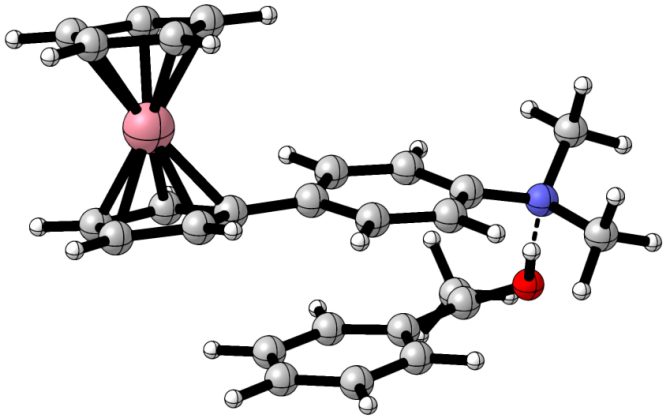

Figure C100. Optimized transition state geometry of $[Co(II)^{p\text{-}Ph}, NH]^+$. (**TS-3**)

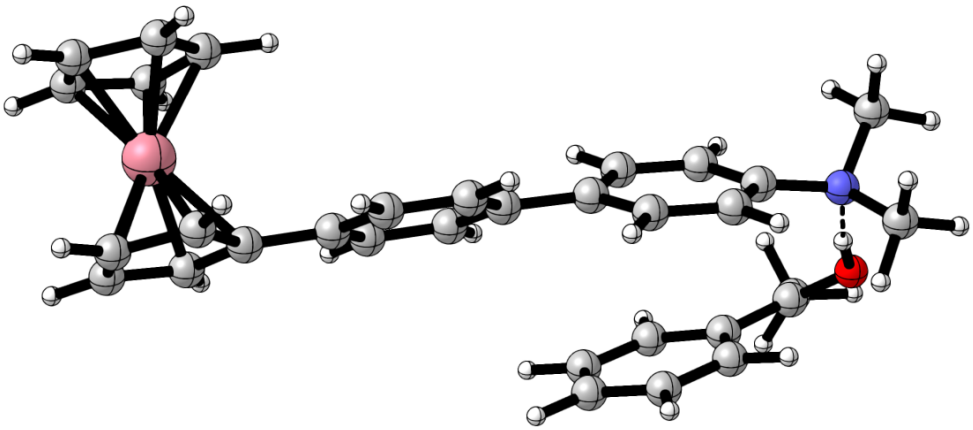

Figure C101. Optimized transition state geometry of $[Co(II)^{p\text{-}Ph2}, NH]^+$. (**TS-4**)

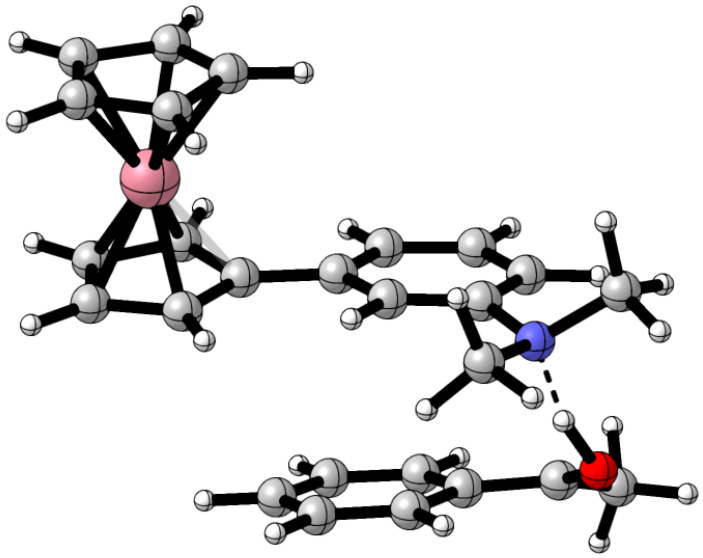

Figure C102. Optimized transition state geometry of $[Co(II)^{m\text{-}Ph}, NH]^+$ (**TS-5**)

10.2 NOCV Analysis

The updated implementation of ETS-NOCV in ORCA 6.11 was used. Cp-stacked and Ph-stacked transition state geometries for the *o*-phenylene mediator were obtained by selecting the highest energy point of a relaxed scan of the proton transfer coordinate as input for the OptTS procedure, with an initial analytical Hessian and a final Hessian calculation confirming 1 imaginary mode. The TPSSh functional with Grimme's D4 correction was used with Ahlrich's full electron def2-TZVP basis set on all atoms and SMD(THF) solvation. The fragment reference states used were those of the reactants: $[Co(II)^{o\text{-}Ph}, NH^+]$ and acetophenone. Annotated sample inputs are provided in .txt format along with the transition state geometries.

NOCVs are grouped as donor-acceptor pairs indexed by a label *k*. In a spin-unrestricted calculation, they are single-electron spin-orbitals divided into separate α and β sets. Each pair is ranked in order of decreasing magnitude of their eigenvalues ν_k, which can be interpreted as the fraction of the electron transferred from the donor to the acceptor orbital as the fragment electron density is allowed to relax.

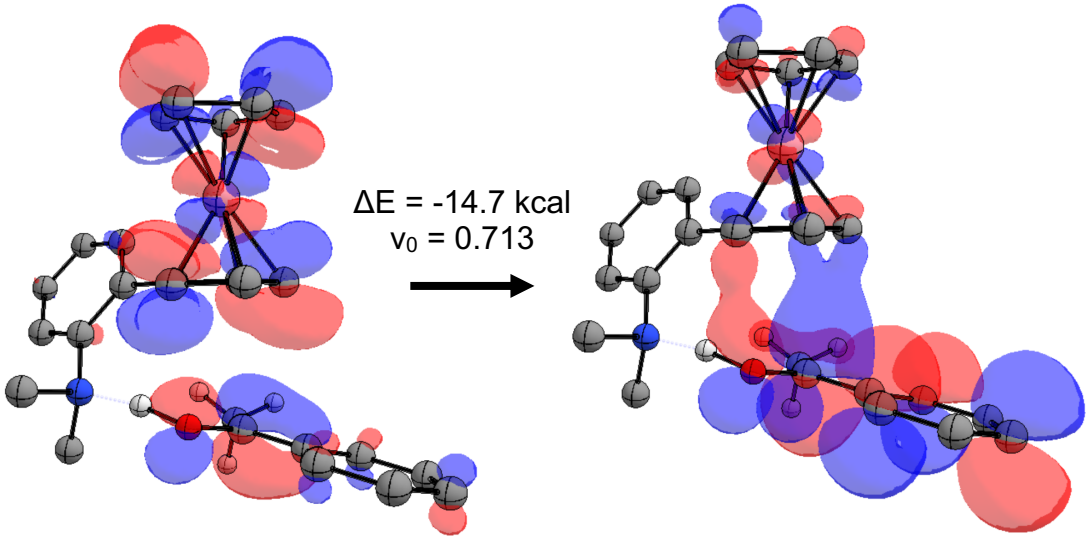

Figure C103. NOCV[0α] donor (left) and acceptor (right) pair in Cp-stack TS (contour value: 0.025 a.u). Hydrogen atoms without a significant orbital weight are removed for clarity.

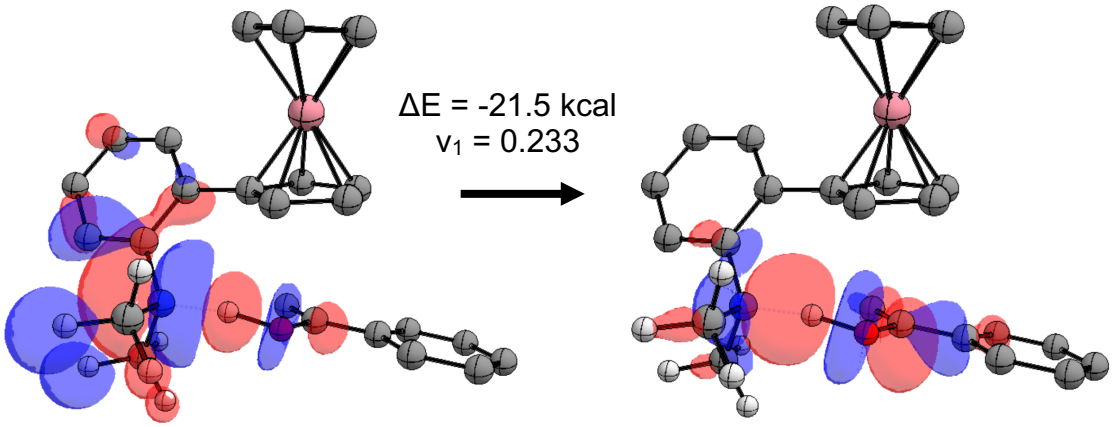

Figure C104. NOCV[1α] donor (left) and acceptor (right) pair in Cp-stack TS (contour: 0.025 a.u.).

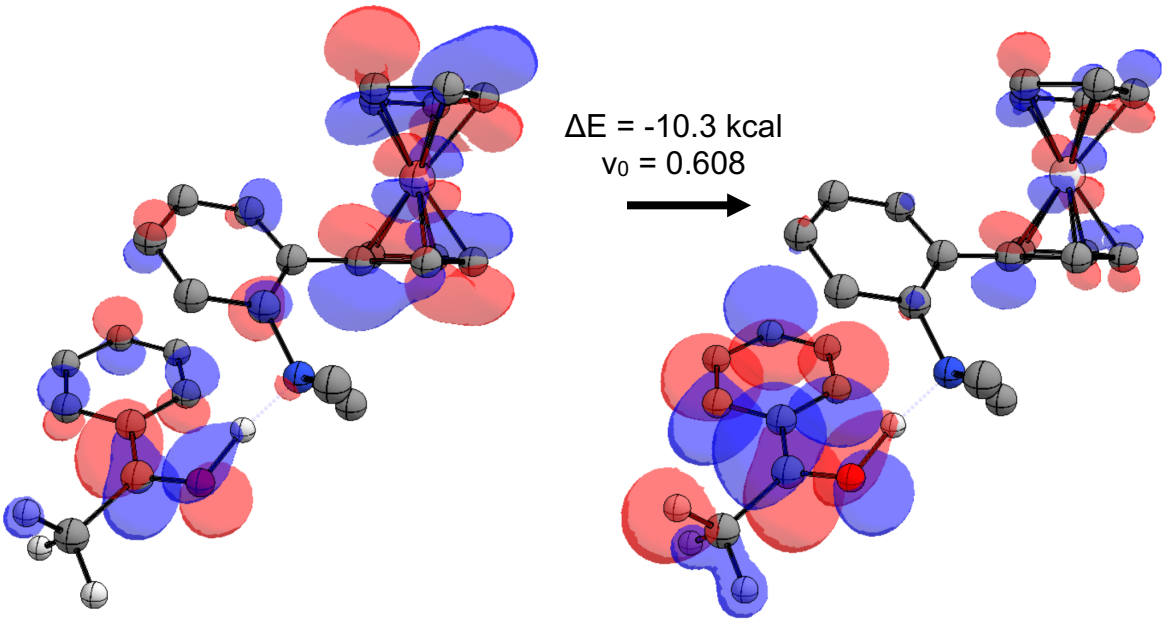

Figure C105. NOCV[0α] donor (left) and acceptor (right) pair in Ph-stack TS (contour: 0.025 a.u).

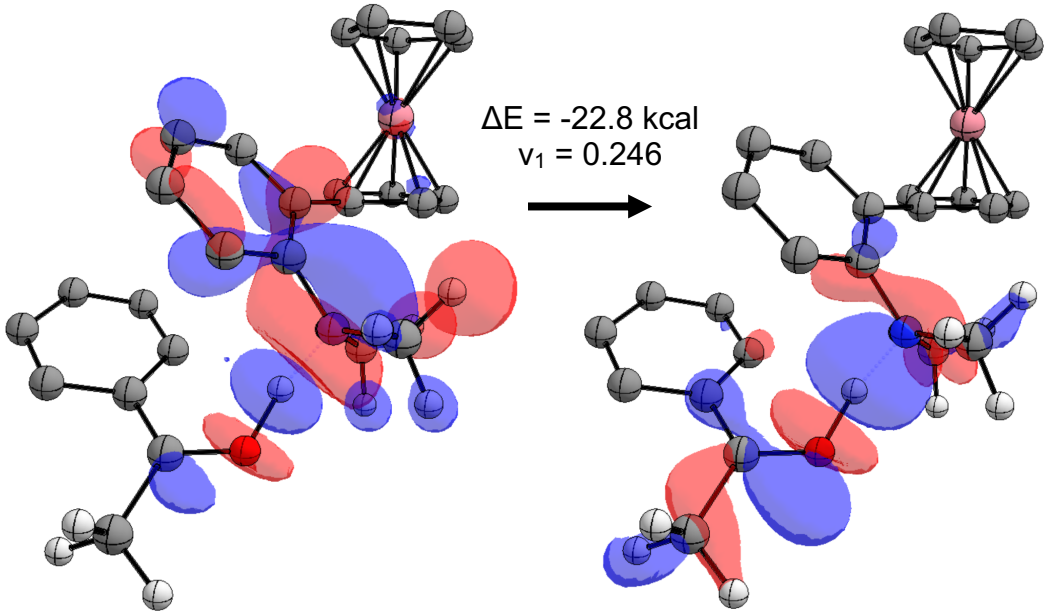

Figure C106. NOCV[1α] donor (left) and acceptor (right) pair in Ph-stack TS (contour: 0.025 a.u).

10.3 TD-DFT

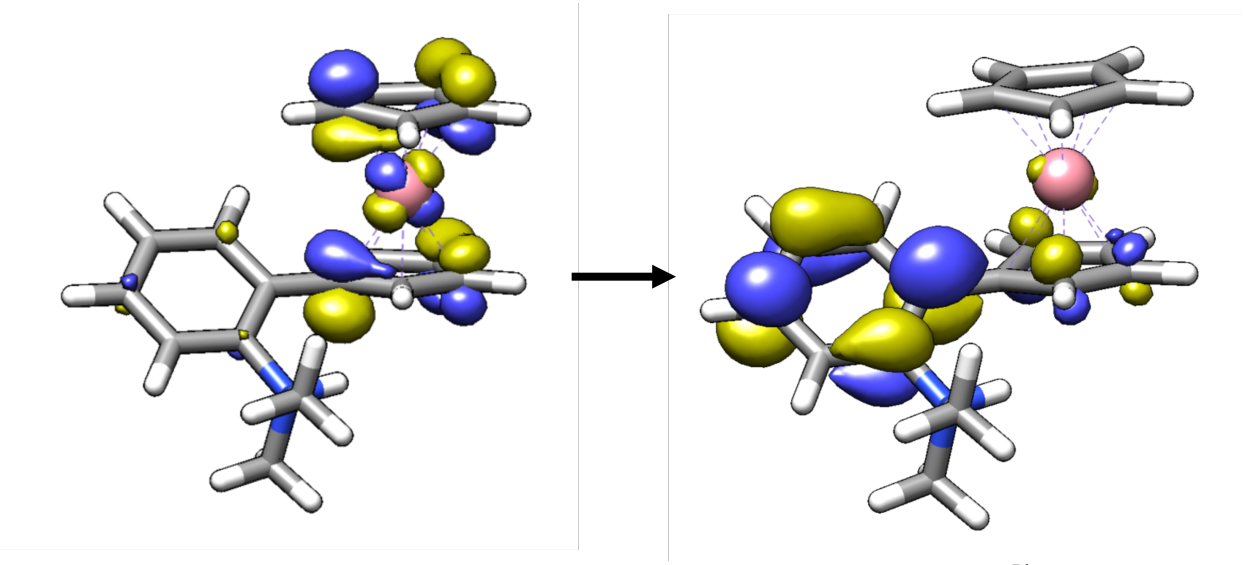

Figure C103. Contour plots (isovalue = 0.05) of molecular orbitals of [Co(II)$^{o\text{-}Ph}$, NH]$^{+}$ involved in the MLCT transition by TD-DFT calculations at SMD(THF)-TPSS0-D3/def2-SVP level of theory (def2-TZVP on Co).

C11. DFT Minimum Geometry Coordinates and Sample Input Files

The Cartesian coordinates resulting from geometry optimization using ORCA are attached below for the specified species of interest.
The geometry optimization was done with def2-SVP, further single point energy optimization was done with def2-TZVPP. The output xyz coordinate was used for single-point energy calculation.

A sample input file is included here for reference and convenience:

###SAMPLE input file for geometry optimization###

```
! UKS TPSSh D4 def2-SVP def2/J
! Opt Freq Defgrid2 RIJCOSX TightSCF TightOpt cpcm

%basis
newgto Co "def2-TZVP" end
end

%cpcm
smd true
SMDsolvent "tetrahydrofuran"
end

%scf MaxIter 300 end
%maxcore 3000

* xyzfile 1 1 P1CH12c.xyz
%pal nprocs 16 end
```

SAMPLE input file for single-point energy

```
! UKS TPSSh D4 def2-TZVPP def2/J
! CPCM Defgrid2 TightSCF

%cpcm
smd true
SMDsolvent "tetrahydrofuran"
end

%scf MaxIter 300 end
%maxcore 3000

* xyzfile 1 1 P1CH12cs.xyz
```

MEDIATORS

p-Ph [Co(III),N]

C	2.76777415532439	2.00303856030440	18.62152248797154
H	2.08731872127091	1.40368375631758	19.22242247878079
C	3.67706883525850	3.00674441928992	19.12144120857530
C	3.84444187577323	3.42055735399742	20.50926882420832
C	3.01588936911444	2.91154612554709	21.53276071069602
H	2.22381917256877	2.20058030129639	21.28949737137409
C	3.17053477030683	3.29274555471309	22.85675209381129
H	2.49893849769459	2.87236957464179	23.60439568754396
C	4.18198792704523	4.21943908164775	23.24029791443034
C	5.01669167039691	4.73373492165800	22.20665250642549
H	5.80394565043923	5.44905076252133	22.44149044258865
C	4.84460777159827	4.34225600988838	20.88812730507415
H	5.51115906521938	4.76524200563515	20.13384839859648
Co	4.65609559443578	1.46472146925607	18.13560790167599
N	4.34332688014738	4.60014790689762	24.54145829999237
C	5.38993627226233	5.54253473757695	24.90546353457793
H	5.25886248290393	6.51212573670281	24.39454578637717
H	5.35003606615484	5.71607041461132	25.98705179278532
H	6.39216972137636	5.15379167684938	24.65413763783363
C	3.47678653561842	4.05853591718971	25.57658779574115
H	2.41722465597904	4.30250857781590	25.38697324224896
H	3.56913615404873	2.96099541710949	25.65164694284029
H	3.76209231122412	4.49440990143155	26.54117839023101
C	4.97534746889959	-0.32275931807044	19.03310374906553
H	4.23762669041414	-0.85628377315671	19.63026839394055
C	5.90011756392178	0.65418067371636	19.51826394272583
H	5.98110873257554	1.00369192914214	20.54640921103804
C	6.63947766552228	1.15269345638770	18.40016626091164
H	7.39099906378003	1.94005360977927	18.43042667206987
C	6.18055361951035	0.47343926993563	17.22430448550289
H	6.52265431919631	0.65530069039968	16.20683634671438
C	5.15191685264976	-0.43805273028343	17.61552122464093
H	4.57096127504724	-1.07327498815135	16.94898295318816
C	4.43239236370590	3.46811929595295	17.98100153405658
H	5.24565589662036	4.19038381083416	18.00475754561546
C	3.95343632768677	2.80797582554566	16.80848805989234
H	4.33993334756948	2.94091626962910	15.79954598735538
C	2.92211204137398	1.90002600824490	17.20532285884068
H	2.38170572836454	1.21620909919510	16.55317567405972

p-Ph [Co(II),NH]

C	5.16925130460136	-0.35834969380821	18.95749938538191

H	4.48160210373495	-0.97042306836100	19.54125534170648
C	6.06765878943896	0.61977592373824	19.48238796743977
H	6.15908447044602	0.92058610003917	20.52505135611529
C	6.71792375042151	1.22117035976155	18.36754387859932
H	7.43264767977836	2.04305035791532	18.41080985311494
C	6.32033251443807	0.52183853659765	17.16547349855364
H	6.67262461885121	0.74032445814803	16.15799479090958
C	5.37266109177956	-0.45999788550976	17.53144134921520
H	4.85014527838307	-1.14052332661678	16.86028744348955
C	4.29434182046198	3.47272899252980	17.98950664868558
H	5.05205951180348	4.25536124172212	17.98744098872100
C	3.78180525469501	2.82298369730273	16.80785410113804
H	4.10323270106433	3.02008312077117	15.78601654583650
C	2.82812205766280	1.86632730560466	17.22437898020784
H	2.27428727983363	1.17843696781708	16.58698060111939
C	2.75760763962263	1.92304184468130	18.66327044087073
H	2.12636805304570	1.28525603195263	19.28094948148182
C	3.58690984409962	2.99332322098603	19.14198861731011
C	3.77976355090996	3.40178113732768	20.53644662073865
C	2.92625276933722	2.95231489410804	21.56469628540420
H	2.08384786768476	2.30035296244505	21.32105286102265
C	3.10771390116493	3.32313475324420	22.89451761753482
H	2.40639358228064	2.94785221681671	23.63991797071127
C	4.17509660490923	4.17525707006328	23.28117973732832
C	5.02758862398052	4.64192978728354	22.24609791765323
H	5.85817495571621	5.30916076006985	22.47682171275266
C	4.83172511134369	4.25847770553922	20.92246118273735
H	5.52555942038200	4.63677178817256	20.16804474982313
Co	4.68458626948960	1.45392689047081	18.10769265510811
N	4.37424073274675	4.53341579648298	24.59842779632468
C	5.38334731671735	5.51984019012534	24.93373566134204
H	5.17393664181469	6.51009688617802	24.48459333096339
H	5.41740113319794	5.63787722234520	26.02415814677628
H	6.38465781435205	5.20140215377705	24.59711372300265
C	3.40925256864620	4.14036880654710	25.60714837774004
H	2.40830867430973	4.58028853648313	25.43160692732123
H	3.29379240390820	3.04380966223307	25.64698414476399
H	3.76444861694542	4.47689488801507	26.58932830305146

p-Ph [Co(III),NH+]

C	4.19070574115281	-0.37425832943184	19.00290013367084
H	3.23582542657243	-0.67806116704148	19.42878955489553
C	5.25175157729311	0.28394802399002	19.70140679223383
H	5.24043055933886	0.57801884933218	20.74983387345228
C	6.29546114534842	0.55984347672300	18.76267733473195

H	7.22211814234528	1.09121521986838	18.97336624466573
C	5.88032564879186	0.06912756338778	17.48317597871302
H	6.43572745654210	0.16331363493282	16.55145700864637
C	4.57999240858226	-0.50830459442843	17.63156385373058
H	3.97239241022208	-0.92981683832287	16.83243713079566
C	4.95564629303223	3.42217717964309	18.08179159059519
H	5.92876248149122	3.86984776471824	18.27234081099692
C	4.50309107761570	2.93142663222418	16.82001242003778
H	5.07043152639795	2.94509219647820	15.89115918453285
C	3.20483035447415	2.36214648404093	17.00614521028788
H	2.60464128701417	1.86912170527612	16.24352314945015
C	2.85452008391652	2.49864288323907	18.38334470188505
H	1.93671737848472	2.13490038265935	18.84060576041164
C	3.93240637266598	3.17044649872589	19.06397019585780
C	3.99362631869299	3.50638963846135	20.49736337401042
C	3.07908405413776	2.94702243771627	21.40787646598954
H	2.32374552150825	2.23782094215377	21.06733577593522
C	3.12874694557003	3.28037227262940	22.76034248569675
H	2.41701063420154	2.84182996476093	23.46342279775043
C	4.09808479975656	4.17888898495913	23.20401558521983
C	5.01963440663050	4.74854025157164	22.32579987751003
H	5.77512472934168	5.45317618503585	22.67724570557084
C	4.96112131715512	4.40939923185713	20.97512318581260
H	5.67345127344929	4.86831558315196	20.28862960310581
Co	4.56481617660563	1.44086988917080	18.19021681146230
N	4.13557207840224	4.52166327723030	24.64112701389213
C	3.87293450184756	5.97987132173429	24.90085959581805
H	2.92963686881521	6.24881502309097	24.41251535608136
H	3.80329909085022	6.11840010824995	25.98618947648992
H	4.70499422281791	6.56429375005192	24.49267915967159
C	5.39375354263859	4.04668987221378	25.31418097925735
H	5.49791503779314	2.97255575280237	25.12457869400949
H	6.24331336509371	4.60017956738619	24.89898487890759
H	5.29492809636900	4.24421090424222	26.38807869448917
H	3.35942964704087	4.00606747551490	25.08073355372677

p-Ph [Co(II),NH+]

C	4.29332651573171	-0.43697373030626	18.99660772373896
H	3.35460801796902	-0.78331695178983	19.42884623261041
C	5.35443242275029	0.20302996663606	19.70552384180874
H	5.35892288259126	0.46662194290138	20.76209742324891
C	6.34758117734303	0.54431793631204	18.74279172330159
H	7.27116470500874	1.08809716040926	18.94045411808341
C	5.95685503076206	-0.00088168159561	17.46191890175585
H	6.52616050096728	0.08118097606853	16.53690055766093

C	4.69393343974121	-0.61278167413416	17.62028226979412
H	4.10069960939126	-1.08871967963022	16.84065815830225
C	4.87968829800482	3.45765666335640	18.07426860332422
H	5.83844544967014	3.94499669194851	18.24494011167839
C	4.41576122752226	2.98714385996144	16.79939992359512
H	4.96437190307612	3.05146533914098	15.86101122201348
C	3.14614482213321	2.38750380703600	16.99674417845479
H	2.52986217243156	1.90646576153460	16.23879791381438
C	2.83177326488156	2.48158295856488	18.39442968370430
H	1.92204693417928	2.09610847114019	18.85243514812248
C	3.85585433450307	3.24282024341029	19.06087679642166
C	3.92194076090287	3.57992241161828	20.47774427067450
C	2.96168460891801	3.09273144677666	21.39461512010278
H	2.14894217632620	2.45388316529881	21.04678426360078
C	3.03380288529546	3.40442735667802	22.74982454394757
H	2.28400593802077	3.01741534371576	23.44462082745997
C	4.07303629388287	4.21148759448811	23.21401440847947
C	5.03992878812247	4.71359507682609	22.33924230483877
H	5.85049365741724	5.34936561685569	22.70073314992291
C	4.95856536179432	4.39804740045877	20.98639115611734
H	5.71321303353490	4.80310820358894	20.31065785562622
Co	4.57603124857916	1.42244986653626	18.16706049371202
N	4.13245702244612	4.53225909700367	24.65603384163520
C	3.92238646277949	5.99337945078166	24.93614650988575
H	2.97882192461353	6.29780336318092	24.46960261138805
H	3.88076261571837	6.12879020342597	26.02362065133514
H	4.76285674352416	6.55410588513207	24.51184312765761
C	5.37367596423125	4.00705546762269	25.31936635104457
H	5.44250708864767	2.93321170424030	25.11290907838067
H	6.24093522663296	4.53683139609221	24.90980769528427
H	5.28727408479624	4.19113405630264	26.39696849364276
H	3.34104540515772	4.03687783241174	25.09082871382802

p-Ph2 [Co(III),N]

Co	-7.55497901278240	-0.90823925779352	16.28492831625231
C	-5.50172601398847	-0.09806493464093	18.54280524528546
N	2.20644777222986	-1.29844717762804	22.10423503291315
C	-2.93907104411331	-0.49019619858197	19.74141281789801
C	-7.12517073827876	0.99105944911427	16.83032006210788
H	-6.41922494514260	1.63791947633499	16.31399392006132
C	-6.81325376118809	0.09737041581988	17.91852815539387
C	-4.42068904954321	0.75446900688707	18.24338289671249
H	-4.55191362790291	1.58017674729842	17.54154668624892
C	-3.17345919387283	0.56230296008317	18.82807742125360
H	-2.35743180204453	1.23339311766608	18.55391581016341

C	-0.68347224808317	0.35585479287608	20.48464717849688
H	-0.95022992948026	1.36052079086874	20.14864298553318
C	-1.61559311209734	-0.69665730394318	20.35509270452278
C	-4.03161944766138	-1.33656880546934	20.04027539755884
H	-3.90768418936989	-2.14786752525607	20.75987997826951
C	-8.50971259628420	0.85772824502400	16.50733783095892
H	-9.03165042122519	1.38432499089305	15.71043159849216
C	-8.03104583070818	-0.61221617048925	18.22573222630662
H	-8.14054674842204	-1.39896570103835	18.96901632508485
C	-9.07055388778778	-0.13375356442432	17.37180888595396
H	-10.09688053061177	-0.49602734974207	17.35363272072721
C	0.56664606431463	0.17221990527272	21.06174585820006
H	1.23347306824241	1.02989213934464	21.14761320511958
C	-5.27930786302143	-1.14689651877773	19.45780964267100
H	-6.09234397783460	-1.82588487595478	19.72171363613588
C	-6.09954633521187	-2.21697858997082	15.76538705882281
H	-5.15341461093719	-2.31451803447977	16.29561897967786
C	-6.37204967820157	-1.31081296394349	14.69289252468190
H	-5.66450308169928	-0.60946019349432	14.25357530641461
C	0.97253044738504	-1.10314942801103	21.54301082563300
C	-1.21119273051028	-1.95861733919469	20.84202248324963
H	-1.88119912059551	-2.81640518908499	20.74887057946764
C	0.03729936153703	-2.16687071290670	21.41399492743294
H	0.29434473244015	-3.16919982965391	21.75581057804841
C	-7.31313778439148	-2.90662770852178	16.07840559382640
H	-7.44752920868581	-3.63160211617026	16.87950756694018
C	-8.33480223937094	-2.43267103738120	15.19289038619991
H	-9.38080159838610	-2.73438571289024	15.20401712389299
C	-7.75330300659191	-1.44625315004606	14.33690688767900
H	-8.27837404903522	-0.86504370968815	13.58073796744205
C	2.58477102817456	-2.61148430622531	22.59743299343778
H	1.91405175367566	-2.95512519527516	23.40500274334315
H	3.60425633675178	-2.56026642782050	22.99785802959676
H	2.56792054167579	-3.36915355083345	21.79414037057160
C	3.14074769964842	-0.19176889449772	22.21918096502310
H	3.38544660285519	0.23870096121236	21.23216785096421
H	4.06984889912408	-0.55686615076966	22.67309622647478
H	2.74102816800752	0.61798736990348	22.85535530485415

p-Ph2 [Co(II),N]

Co	-7.60272529230064	-0.92061208696100	16.26270171335701
C	-5.48752438226432	-0.05260651802624	18.55641537864964
N	2.26364366329236	-1.31201713287017	22.07092272621645
C	-2.90018592814143	-0.47325785720939	19.72616007260022
C	-7.11742678986228	0.99985141776419	16.83328565594803

H	-6.41477805916113	1.64087391993316	16.30260380637321
C	-6.80265412198965	0.15425266904406	17.95069308392004
C	-4.38504904840274	0.76354880768131	18.22200398479263
H	-4.51029660662615	1.57496547392147	17.50166876680411
C	-3.13007206902211	0.55701875601718	18.78884555573660
H	-2.30362057316274	1.20225995804045	18.48196578078407
C	-0.63149169590560	0.35656604226564	20.45969674899211
H	-0.89685456165278	1.36361406649564	20.12859563273068
C	-1.56811334574840	-0.68983615237135	20.32873257825371
C	-4.00511492549169	-1.28582304862452	20.06146267380511
H	-3.88551900489338	-2.08340014500660	20.79845577892645
C	-8.52905925775687	0.92781919584703	16.56142132305423
H	-9.05758955522462	1.49058471142847	15.79336271775948
C	-8.01535238677821	-0.56004857562904	18.24351195879717
H	-8.13220915078046	-1.33083601860216	19.00401437776815
C	-9.08546182066326	-0.03517143855024	17.43728144036740
H	-10.12547689375494	-0.35593135702240	17.47559805456788
C	0.62543374311770	0.16379204340609	21.02497064026637
H	1.29816556201924	1.01781781218147	21.10441970340456
C	-5.26014043120070	-1.08433704852348	19.49370154896796
H	-6.08219856632359	-1.74042862220143	19.78785629758965
C	-6.16490840008301	-2.35294526922296	15.66372143769876
H	-5.20516776285207	-2.50642567183674	16.15490696697418
C	-6.44672810791626	-1.41489886718673	14.62923456469640
H	-5.72562388873397	-0.74731723007198	14.15766071407514
C	1.02717859638048	-1.11188413877631	21.50292440091242
C	-1.16168657735738	-1.95549982218482	20.79998735926413
H	-1.83474408037148	-2.81064784464718	20.70039912480299
C	0.09121699645039	-2.17135710126460	21.36569613114919
H	0.34789352866801	-3.17811133519166	21.69552942932064
C	-7.40785676231570	-2.95481886379994	16.02515726179652
H	-7.55535415082224	-3.68458153269929	16.82124364084736
C	-8.43094731400700	-2.49018456733319	15.11768415151793
H	-9.47779465315521	-2.79089917228710	15.13061055481881
C	-7.83997179167845	-1.53494914738648	14.26122699633101
H	-8.34322470517588	-0.96143242664253	13.48370805667446
C	2.66738036404389	-2.64421263757178	22.47987105836886
H	1.97475962450089	-3.06541640056862	23.22918933556052
H	3.66459125993161	-2.59038639808532	22.93373598329999
H	2.71323507982586	-3.34773240374426	21.62733315757642
C	3.22626277559688	-0.22726795845585	22.11661606180052
H	3.51071219328386	0.12255868770551	21.10639895456085
H	4.13278741356944	-0.57667652635139	22.62624966498887
H	2.83353072689588	0.63934335317509	22.67645840453023

p-Ph2 [Co(III),NH+]

Co	-8.41865154171581	-1.21283338012125	18.06416716074881
C	-5.48024448149370	-0.19488414765272	18.61886721034226
N	2.25690570291080	-1.25483965462348	22.22494380235202
C	-2.92991547739607	-0.58234727148883	19.80903640039682
C	-7.19984540716350	-0.39106934889069	16.67573104561180
H	-6.59665678535064	-0.95483436761522	15.96743665188199
C	-6.79227511586051	0.02877254308411	17.99311552173829
C	-4.42633083408543	-0.78260354508464	17.89423417577374
H	-4.57811570013329	-1.09685326443670	16.86068053559964
C	-3.17656545794965	-0.97130459786047	18.47821797905736
H	-2.38591152747003	-1.44342179972846	17.89209293293284
C	-0.42336194239604	-0.69843706284279	19.64489645595693
H	-0.49231508043704	-0.49330456452654	18.57550072071521
C	-1.59458946773384	-0.76650614631498	20.42576826985738
C	-3.98894432163384	-0.00084705713345	20.53363243953607
H	-3.82802122260782	0.33209176887129	21.56069283755767
C	-8.55134864808500	0.01703473131340	16.46412738816221
H	-9.14551085020432	-0.18434690995486	15.57455269959988
C	-7.93252118799567	0.67676087227059	18.59154764010970
H	-7.98505400794642	1.07468624829297	19.60256564593049
C	-9.00424652326996	0.67769730575141	17.64854540024366
H	-10.00475009037691	1.06959477617337	17.82256717391760
C	0.83851927417238	-0.85799821097768	20.21513155143121
H	1.72978201887825	-0.78983838164800	19.58915381269792
C	-5.23837033551392	0.19130071056865	19.95083924156636
H	-6.02911757838392	0.65590843258337	20.54183263633743
C	-7.86726921942263	-2.78154765816967	19.21903592517973
H	-6.89545800249379	-2.87444142245648	19.70151476799783
C	-8.19332627267420	-3.21751694188033	17.89640964054716
H	-7.51615174070384	-3.70852122496747	17.19946435638611
C	0.93241624038059	-1.09062992056364	21.58778925634800
C	-1.46149383379754	-1.00569499664376	21.80653140300930
H	-2.34844647699156	-1.08594493837453	22.43702418051389
C	-0.20494162724086	-1.16810332236098	22.38970817044174
H	-0.11571409101209	-1.35980258099644	23.46176518039238
C	-9.01780390044027	-2.13068780472832	19.76618758824694
H	-9.07737378302990	-1.64995359588233	20.74126439961714
C	-10.05821465896862	-2.16911500490719	18.78292663673510
H	-11.04575987145572	-1.72084102206748	18.87884070723420
C	-9.54836195164293	-2.84019756363404	17.62734612954288
H	-10.08037667360252	-2.99258708996542	16.68968923431018
C	3.00960152255225	-2.44906302550503	21.70931670782356
H	2.36811237801110	-3.33066597061266	21.81777220051403
H	3.92155731227704	-2.55493795680008	22.30846770889682
H	3.26113599850043	-2.27749585048138	20.65692080633939

C	3.08566440295386	-0.00051697364765	22.17432920957139
H	3.33734345399851	0.21197322058791	21.12916887595381
H	3.99556252977504	-0.17561071114323	22.76048459751465
H	2.49580619244822	0.81563907399061	22.60613845001577
H	2.07608396182197	-1.43717451979862	23.22250340480952

p-Ph2 [Co(II),NH+]

Co	-8.44550592879167	-1.25060582040830	18.04334519919543
C	-5.48348351253915	-0.06724200550044	18.63068024231437
N	2.26626073418192	-1.24786429102813	22.23794200883242
C	-2.91278799005118	-0.47785548836753	19.82370272999562
C	-7.21673151378405	-0.27379182468971	16.71307869718417
H	-6.59387168949430	-0.76535790668933	15.96721697254626
C	-6.79342132904598	0.13723140202980	18.02488915583670
C	-4.43052982485007	-0.68872320732298	17.91998780335735
H	-4.59542033284182	-1.03067137146266	16.89662827656445
C	-3.18188826701524	-0.88472994301580	18.49953453367835
H	-2.40651504767600	-1.38694066955336	17.91679672490696
C	-0.41511107166560	-0.73336615205103	19.64786725658851
H	-0.48353195365941	-0.60248168626360	18.56683960307194
C	-1.58440828389464	-0.68217040872448	20.43769719454815
C	-3.96374749275315	0.13840252273386	20.53604065189803
H	-3.79505887318024	0.49243991187475	21.55548529961986
C	-8.57584431713377	0.13977889915018	16.50017877444341
H	-9.14607815454464	0.00104026446235	15.58290844042972
C	-7.97500728742322	0.65236593494518	18.66430639493195
H	-8.04202569715662	1.00018095089390	19.69406195433089
C	-9.04543721096889	0.71414650922515	17.70871422345962
H	-10.04577322773147	1.10026312515098	17.89860668514855
C	0.84294654075551	-0.91933644523114	20.21699966365621
H	1.72841586749216	-0.94592467956022	19.57939212856830
C	-5.21147662603159	0.34157700298302	19.95685454647619
H	-5.98818056737396	0.83771525012887	20.54185307066016
C	-7.83924386236524	-2.96664099126583	19.11156563161841
H	-6.85907880004256	-3.09438010140037	19.56854133251914
C	-8.19267958847163	-3.27421461210687	17.76538001974554
H	-7.53624472858069	-3.71757387314581	17.01679812770570
C	0.94458941996775	-1.05360400120299	21.60267005229727
C	-1.44010641203358	-0.82841090725783	21.83301648288354
H	-2.32073571861145	-0.81972774216078	22.47711976555156
C	-0.18707819580085	-1.01115549569127	22.41589307849972
H	-0.09557131416575	-1.12862194768915	23.49863255184482
C	-8.97538527432288	-2.34000089569268	19.70487863246774
H	-9.02700159428206	-1.93711324564473	20.71627138103145
C	-10.07239361355692	-2.38329251275270	18.76601359233822

H	-11.07604040952986	-1.99857283675934	18.94222975072140
C	-9.58868759325011	-2.95585583302722	17.56898221475228
H	-10.14890373349733	-3.09901605035288	16.64583428765039
C	2.90840027120271	-2.55170528408043	21.85562805456007
H	2.20110264745900	-3.35865314661099	22.07710524151298
H	3.82466084122489	-2.66318985921350	22.44745345384358
H	3.14366447017635	-2.52391933406257	20.78581917836824
C	3.19287154970241	-0.08372255974569	22.02833630167344
H	3.44095389848201	-0.01949916061292	20.96314316131087
H	4.09758383937546	-0.26232487099367	22.62152962969431
H	2.68103050973888	0.82513186237263	22.36383450442095
H	2.09364174835886	-1.29787659761164	23.25219220874280

o-Ph [Co(III),N]

Co	15.67904508973539	4.42876098537277	6.08822737053061
N	11.63512729109548	2.44439731563321	5.10563452059123
C	11.73148521599101	2.87241208590678	6.43513782838574
C	14.30372229786810	3.70498130846876	4.79933109913688
H	14.15118617955805	2.65169044126505	4.57820588776308
C	15.21030267906861	4.58549341546083	4.13420806809951
H	15.87749099977385	4.31696372548750	3.31704362650761
C	10.94643022994366	2.28919244637505	7.45364310462421
H	10.25330645440433	1.48561696550999	7.20448042084883
C	13.63440292886669	4.43556823966005	5.84715737750197
C	14.18144989295882	5.76821692315508	5.83437362697785
H	13.92038999646600	6.56559785567966	6.52779925345722
C	11.30269692542692	3.43464479697455	4.08244324603058
H	10.20684031286241	3.48665917821603	3.92796243551085
H	11.77393415823702	3.16875371853417	3.12280211722963
H	11.64759789257872	4.43342229177286	4.37436187487060
C	12.64558493325249	3.90446719112869	6.80187034619018
C	11.03453712054854	1.14763767894715	4.84191567837712
H	11.44576049732771	0.39080365709714	5.52476457741893
H	11.28103214971636	0.85228191665545	3.81057257844638
H	9.92990539518207	1.15076506883307	4.93672377176742
C	12.65412841486332	4.38090217313746	8.12558318693242
H	13.35274889674359	5.17674340657867	8.39322665114761
C	11.00741794396385	2.74887781326936	8.76867199124841
H	10.37582443617451	2.28112694148106	9.52814095271059
C	15.13644955051871	5.86204466961796	4.77624994083011
H	15.73293205188667	6.73917240997089	4.53145409829516
C	11.84450349897253	3.81797256568577	9.11013497761433
H	11.88206414546312	4.19302685607074	10.13486365148878
C	16.69735093623382	2.81638895985407	6.77034333796484
H	16.51887319694463	1.79077413263971	6.45157596868113

C	17.58841157963894	3.74844549868426	6.14558321732332
H	18.20414478982850	3.55469665802960	5.26881727685067
C	16.03978023242349	3.48745410300199	7.84741438551348
H	15.26470707663593	3.06572625995698	8.48523339165678
C	17.47928018970267	4.99551328072025	6.83687416560231
H	17.99623976475726	5.91806984729798	6.57815880543291
C	16.51790028594404	4.83537338291506	7.88598813091094
H	16.18062546244022	5.61490706395380	8.56718865352891

o-Ph [Co(II),N]

Co	15.72240631105000	4.44949862045255	6.08919934719957
N	11.64267940810786	2.40506531090536	5.08136760092194
C	11.70768752921923	2.87410877825873	6.41026031971721
C	14.29771803496009	3.78607370657743	4.76818315732253
H	14.13868328362344	2.74422233688091	4.49885811095379
C	15.16569990685114	4.70473331335385	4.08435452879040
H	15.79830684222201	4.46916074587687	3.22972947498245
C	10.90498582917987	2.30753401663983	7.42041882181900
H	10.21998237651342	1.49698919065655	7.16857306060327
C	13.58562026377138	4.48419203044572	5.81012389022145
C	14.16225018493693	5.79184850046096	5.85927606807134
H	13.89464123479446	6.57780556837472	6.56483832210173
C	11.22980316312255	3.37257455394642	4.06881766556495
H	10.12604461300293	3.48568255866515	4.04177019116067
H	11.56699429791806	3.04119099630345	3.07383096375343
H	11.66956250050178	4.35660040928845	4.27188177480903
C	12.61013064782942	3.92504736025948	6.76017768827418
C	11.06691770615960	1.09266399793480	4.85588105936676
H	11.50235339476568	0.36059707508850	5.55167388692925
H	11.30544347820039	0.77699736188738	3.82806128954114
H	9.96193092023241	1.06653892825955	4.96482255552030
C	12.59864778665638	4.40202027387612	8.08529450699523
H	13.29483952471898	5.19919880249878	8.35599798155979
C	10.94041934448287	2.77964978569588	8.73557437143469
H	10.30049049915453	2.31767730756617	9.49191101361761
C	15.10168946812645	5.93935341151643	4.77418424729110
H	15.66087796895175	6.84450955705095	4.54089170727400
C	11.77542850978717	3.84971468878406	9.06877759606999
H	11.80728812252205	4.23662744267795	10.09012784454537
C	16.71902000101922	2.80398783157662	6.81375266781294
H	16.51484480067677	1.77703917530577	6.51054451434087
C	17.69049471055411	3.67735156918204	6.20279456496877
H	18.31915628861159	3.43417330512555	5.34719756968531
C	16.12856912371608	3.47781164150469	7.92897377114528
H	15.36720660131922	3.07656384970388	8.59605426005992

C	17.61526547903358	4.92298411704994	6.86621485847676
H	18.18485448416564	5.82022532360468	6.62642602522403
C	16.62523746167728	4.80979291461481	7.91562280856897
H	16.34143899186167	5.60773687114842	8.60172150730403

o-Ph [Co(III),NH+]

Co	15.82726851856721	4.34090518618829	6.14381282673573
N	11.50142277897553	2.67530210492199	4.94426248208839
C	11.66536294440923	3.03970703018585	6.36951489401385
C	14.52707601793512	3.49576969667565	4.85687969830351
H	14.44599061267142	2.41850297934762	4.71242942669183
C	15.42797220904637	4.36081926139888	4.16033910622012
H	16.13253114606669	4.05595380084568	3.38854211327988
C	10.67984097973959	2.63120387508265	7.26891672322319
H	9.84147904463699	2.02104580759742	6.92840418306326
C	13.81020516869454	4.28103745535557	5.83463212110908
C	14.31153594770410	5.62733304411469	5.74236614322082
H	13.99738012658793	6.45963811955937	6.36990855201966
C	10.28859722395535	3.31891580021694	4.32748753567060
H	9.39106163493106	2.89821443619128	4.79351448769525
H	10.30416011073776	3.09806830222462	3.25368590920149
H	10.35031657340632	4.39858676935551	4.50350523437482
C	12.75889004733769	3.82796020551135	6.77308822680983
C	11.54115248959181	1.19164298313666	4.70542136299100
H	12.45922762988260	0.79603922215349	5.15385416565691
H	11.53420881674923	1.02820139606269	3.62126687806473
H	10.65790399162990	0.73663695442260	5.16653290481270
C	12.80135438295182	4.22859197904911	8.12179336690292
H	13.63085881481497	4.85221795391313	8.45726224938666
C	10.76324869681924	3.01986533813272	8.60564953568707
H	9.99522048980877	2.69657094076802	9.31051546053576
C	15.29558761148388	5.67351378856601	4.70963077902930
H	15.87778017971820	6.54792779424058	4.42376923330446
C	11.82167664215368	3.83027575289361	9.02845456946850
H	11.88761390409056	4.14981462492698	10.07022094612660
C	16.97122849640847	2.83004879689512	6.86397273047102
H	16.90098421000335	1.79211669011143	6.54259435494137
C	17.78751566411544	3.84120077426178	6.26504919404457
H	18.44454501812793	3.70840637653754	5.40702275881086
C	16.21785682604670	3.43683309873128	7.91720056200915
H	15.47141181184366	2.93995664506977	8.53461620190026
C	17.53668154699868	5.07325322025085	6.94816394697258
H	17.96963032306709	6.04101324285398	6.70022553579014
C	16.56580447300042	4.82357474293764	7.96944139051486
H	16.13567620317568	5.56824122524763	8.63712161237846

H	12.30787964811350	3.06743184706365	4.43833242447818

o-Ph [Co(II),NH+]

Co	15.83958878494706	4.35831606891274	6.13767377982798
N	11.49937029595157	2.68019944863504	4.93725952699256
C	11.63810506046792	3.04130344136846	6.36527122201010
C	14.45421607816550	3.58992852623336	4.82234041207015
H	14.36220385311024	2.51949002037277	4.63536160877400
C	15.34534635442074	4.47316052781253	4.11275595923393
H	16.00588978226852	4.18185562018791	3.29757747040756
C	10.67563555049825	2.58909269877183	7.26799882893777
H	9.86694705760987	1.93727315783578	6.93129248737897
C	13.72399765297842	4.35170617425702	5.79959138091782
C	14.29962765018282	5.67195628229996	5.77614612910355
H	13.99994152434920	6.49607112031258	6.42261706907554
C	10.25213418009730	3.24557308296067	4.32169185016853
H	9.38163796858312	2.76494924303334	4.78153093173485
H	10.28223863368559	3.03609600609378	3.24569129425147
H	10.24176347482787	4.32575764002323	4.50549691931252
C	12.70322102023128	3.88150804038504	6.74576801703788
C	11.64069836722367	1.20915483768537	4.67983059119117
H	12.57776104365725	0.86767726313895	5.13350690921268
H	11.65573608304477	1.05552688382368	3.59411537174565
H	10.78560874918426	0.69076096842940	5.12798273327237
C	12.73190615850256	4.28728842496603	8.09778657529634
H	13.54243235473787	4.93905983662868	8.42786089272149
C	10.74676822127138	2.99017763712057	8.60250048672332
H	10.00069519419351	2.63604579666281	9.31626700721296
C	15.23231457793271	5.76045164506806	4.68961407157201
H	15.78666337375497	6.65168561869255	4.39982419749399
C	11.77242953687493	3.85269787298377	9.00949706984203
H	11.83111250867696	4.17937885325803	10.05008367169587
C	16.90150737297003	2.78097758508063	6.93786895241015
H	16.76094104905185	1.73683297498192	6.65879544098656
C	17.82995471968738	3.69586213013080	6.30988788900385
H	18.48427172543877	3.45978112297151	5.47160004579197
C	16.25129837588530	3.45518246632362	8.00917109604461
H	15.50020459411315	3.03668135423291	8.67692884783350
C	17.70027259343056	4.94816568994110	6.94776310856939
H	18.23053715501506	5.86470201510689	6.69300938307068
C	16.67742607217203	4.81752489805912	7.95887674747227
H	16.33405304999905	5.61886697954915	8.61311888091947
H	12.28968115680547	3.14361930866807	4.45744697068196

m-Ph [Co(III),N]

Co	5.66571470032921	1.60473217966829	17.77177181171172
N	8.24112478428866	1.70822366360878	12.29965463826902
C	5.44079820420769	1.11334909370327	14.66635868408714
C	6.97128659502886	1.64820703036447	12.81790199257017
C	6.73740510075847	1.17548427287304	14.13291633519701
H	7.57754557294690	0.86645018059436	14.75233204625378
C	5.23761968754921	0.61007178293012	16.03534717811757
C	5.84059708550340	2.05897170051252	12.05873742838551
H	5.96650474681213	2.43206050472372	11.04273043564860
C	4.33675005882193	1.52311422315543	13.89774797624299
H	3.32373834603755	1.46443769039664	14.29731071853814
C	4.55859032947285	1.99004000447262	12.59914500589282
H	3.71013865187677	2.30741044529298	11.98767589570544
C	6.18984744940614	-0.11027087978206	16.84228116271616
H	7.20077710019501	-0.38160935206569	16.54548880990355
C	6.40903783061585	3.39488362137132	17.18818486629797
H	6.52168726261147	3.69740921571690	16.14810160891201
C	5.24008750145456	3.57145570883621	17.99323067665292
H	4.31162261582058	4.04383465526734	17.67672141504812
C	7.37288427092994	2.67383553892140	17.96118424996190
H	8.35092196391069	2.34313696192576	17.61537084616486
C	5.48333600033581	2.96355966121605	19.26723149658416
H	4.77132152972176	2.89205584864932	20.08781102544719
C	4.06151536340565	0.79124551279350	16.84758856661179
H	3.17005541013052	1.34514065354415	16.56069195659835
C	5.59770591259113	-0.38597927609531	18.11217759554504
H	6.08267185668502	-0.89234701778364	18.94484913746656
C	4.28115245194624	0.17262926304296	18.11612255549048
H	3.58603969242575	0.17149382423893	18.95393506767603
C	6.80152353544807	2.40909322999613	19.24771245857965
H	7.26875973528557	1.84152194057577	20.05073769121305
C	8.45647992557222	2.19649458852953	10.94891574019079
H	7.92095157780952	1.58385553768058	10.20206667215210
H	9.52829053303284	2.15012685523883	10.72144503981628
H	8.12505942583319	3.24397521776101	10.83117465052554
C	9.37394072561587	1.29414337112456	13.10642341501026
H	9.46889405825388	1.90269307583403	14.02434400892494
H	10.29278952466034	1.41539105957593	12.52028018062776
H	9.29715586666596	0.23395806858951	13.40851683225558

m-Ph [Co(II),N]

Co	7.73484803617556	4.12167647301767	6.45919942301630
N	3.04531508353054	7.37273876344943	8.55143188642737
C	6.71646623159150	4.16215459636096	4.66380213797470

H	6.11331442091323	3.33849965962352	4.28353893408570
C	3.27933940179985	6.53264165146236	7.48191458481462
C	7.39075167855348	6.03351819187006	5.79140412526393
H	7.39864681159776	6.92675804508131	6.41488411342650
C	6.22879046640095	5.26564325283585	5.43930540543387
C	2.21372504788818	5.86047455367561	6.82557067827457
H	1.18519098991500	5.98721455358879	7.16238305841441
C	8.12417575326620	4.33896837460181	4.41321163041202
H	8.75372097466565	3.67344080052758	3.82421484035823
C	7.97582479658489	4.21103235039907	8.50242201610850
H	7.94299009906727	5.13145778929700	9.08545282096571
C	4.59358274592724	6.30639825811221	7.00577559137057
H	5.43721383619642	6.77553981672517	7.50984589265516
C	8.77864909940743	2.45958154355468	7.23381591620774
H	9.42753069114951	1.80082641212107	6.65793470435098
C	6.86880183308170	3.35307471103682	8.23416001518077
H	5.83549338868528	3.51763420427607	8.53629240106001
C	3.77393273004846	4.82660460018708	5.26158633419095
H	3.95018135647217	4.18536312958142	4.39604385706780
C	8.53915108792081	5.50101038426404	5.10545714269072
H	9.54915092464617	5.90612641972691	5.14992259730109
C	2.47621277257403	5.02907724324039	5.73579544648702
H	1.63842600881411	4.52856577804889	5.24190406773060
C	9.16663102161915	3.62718549569583	7.92773740074477
H	10.17177925819517	4.04255371614091	7.98863893885530
C	4.85156988236894	5.47110402375748	5.90354439226534
C	1.71055911557382	7.47938941122504	9.10911853206612
H	0.98404946988957	7.82221085997682	8.35269645728495
H	1.72254691889517	8.21674689663749	9.92168423801220
H	1.34419513832650	6.51857297997430	9.51955501684947
C	7.34761877265289	2.31781855608857	7.37875148583472
H	6.74619315988941	1.51956734961518	6.94381848153611
C	4.16212754539143	7.94468817609797	9.27791831139417
H	4.78839142347096	7.17474539379520	9.76954861358763
H	3.77607866090508	8.61872530555437	10.05308083903943
H	4.81496098694770	8.53415084077425	8.61167422025880

m-Ph [Co(III),NH+]

Co	7.70985360724480	4.14419723809671	6.46466293214864
N	3.01220781508930	7.40222580375356	8.61045810123512
C	6.71709272972288	4.13206543809457	4.70101103961528
H	6.11238390734495	3.30307212407207	4.33857868087278
C	3.29751691715611	6.49517898197811	7.47650862421947
C	7.40297654916668	6.03588771345391	5.82523539813943
H	7.41090587592218	6.92489319722733	6.45278750175850

C	6.25457085420205	5.21982700657029	5.52380479826110
C	2.22218956326156	5.87652792783263	6.83946141720614
H	1.19860547572691	6.05616559811072	7.17666870083219
C	8.11966304188333	4.29127681816567	4.48667604329588
H	8.76110519278786	3.60719396703624	3.93405751805448
C	8.00301208759008	4.26747268082964	8.46335326583844
H	7.98592639474590	5.19325413878335	9.03606194701200
C	4.61337221728142	6.29303375548763	7.07253347954137
H	5.43417623606492	6.78476154618095	7.59547645997255
C	8.72665470236798	2.51962035405187	7.12832405799472
H	9.35445639126712	1.88406944487380	6.50599730332481
C	6.87378764339600	3.44017084990185	8.16762206145477
H	5.84491507135103	3.63030226041072	8.46975214180996
C	3.79534867041451	4.80776612427673	5.33894599067864
H	3.97965906123114	4.15428631824042	4.48512982601113
C	8.54264999279730	5.46799048153006	5.18001823858566
H	9.56270343865686	5.84242991252497	5.24531380464837
C	2.48414025172018	5.02670347422993	5.76207230058768
H	1.65597228084336	4.53739131410284	5.24647247187406
C	9.14919153625939	3.69738594846810	7.82180138772807
H	10.15503289420828	4.11418222486295	7.82051287913935
C	4.87309006717271	5.43673509612791	5.98870693720811
C	3.62114524011097	6.93598361548727	9.90319085358165
H	3.29717620159581	5.90433626986967	10.08059141478142
H	3.26348290356964	7.59848563241522	10.70011034333972
H	4.71206887866480	6.99389388605327	9.81890173548690
C	7.31981989890047	2.36102800301735	7.34141089128392
H	6.69168961886516	1.58240412227491	6.91168284876322
C	3.35950859986804	8.83258540367546	8.30283077275128
H	4.44616218716405	8.91080333667389	8.18597413161652
H	3.01756357683982	9.45000467267354	9.14188826315704
H	2.84642083973888	9.11618606101573	7.37706507844367
H	1.99122594880502	7.37572617856774	8.74583559974529

m-Ph [Co(II),NH+]

Co	7.74148152553813	4.09586646252832	6.46115613100951
N	2.99449974651100	7.46174334442637	8.59130050231857
C	6.73381122156135	4.24498502134495	4.66830038359753
H	6.13180750446794	3.44852801286765	4.23319714582944
C	3.28338493547223	6.53278964100849	7.47265467176541
C	7.41277679070624	6.04590372604558	5.91113185958087
H	7.42607800399167	6.89867271885788	6.58851099122757
C	6.24626576105514	5.30851272582219	5.50265471924511
C	2.21420925506769	5.84054177233035	6.90538433736758
H	1.19540196106135	5.98396732145241	7.27222684223441

C	8.14026557520899	4.42875233590815	4.44026568040052
H	8.77036260282832	3.79572478371595	3.81746510475558
C	7.98551204067303	4.05285493126887	8.50301364097962
H	7.96211148467652	4.93253266385009	9.14619785237093
C	4.59391638899123	6.38013208162739	7.03484928567217
H	5.40215481110611	6.93192365481573	7.51566669951989
C	8.77349118283231	2.38115126887584	7.12307025914107
H	9.41670878354201	1.75766314161985	6.50346706418095
C	6.87097240600471	3.22420255747872	8.17790051495556
H	5.83932023327554	3.37385805564283	8.49303723142723
C	3.79659398679421	4.78981469104971	5.39315314715223
H	3.98238863510009	4.10595154646625	4.56341468961865
C	8.55861658843230	5.54708325591711	5.20411566468248
H	9.57100246965367	5.94107010532408	5.27847687957590
C	2.49287835992678	4.95983726324323	5.85273845239567
H	1.67625631607174	4.40571845086673	5.38511307944885
C	9.17107404066386	3.49745383493526	7.89097208445137
H	10.17937050362998	3.90031047810202	7.97671829339017
C	4.87779838607251	5.49433214187462	5.97253478301782
C	3.62238383863566	7.02593047212839	9.88426381204630
H	3.30895654625179	5.99529162500610	10.08493768331968
H	3.27192263133414	7.70013877100491	10.67481391284750
H	4.71167869821875	7.08720835693332	9.78277059163865
C	7.34166297606521	2.24074233754288	7.25899347106748
H	6.73451367168177	1.47760838182578	6.77237086432087
C	3.32049391398260	8.88911403876817	8.25873694123235
H	4.40512531479790	8.98076076690723	8.13442264489113
H	2.97534983636875	9.51776144183762	9.08827344735102
H	2.80018657264805	9.15065824772397	7.33051508892717
H	1.97548497009826	7.42181670105459	8.73476310104467

ACETOPHENONES

MeOAP

C	1.63180795532624	-0.62746307349659	-5.11573522596212
C	0.47252656800730	-1.09367357207519	-4.46889645932370
C	2.66335424070412	-0.03250276035258	-4.35770805623846
H	-0.33719166949675	-1.55627912222857	-5.03344483812041
H	3.55508014930804	0.32335047242569	-4.87795155200983
C	0.35636708938004	-0.96189856029916	-3.08365415159986
C	2.53156448814935	0.08971818289568	-2.98386353154994
H	-0.55178673070203	-1.32987962923013	-2.60239912036084
H	3.32339954639466	0.54808483708527	-2.38776345814203
C	1.37598052225124	-0.37189661393814	-2.31771595739382

C	1.29334630716372	-0.21130612340222	-0.83828863217670
O	2.21110653563236	0.30925883041989	-0.21399431068003
C	0.05297137456222	-0.70399732869376	-0.12392258566635
H	-0.09064702319098	-1.78441919920419	-0.28674193084361
H	0.15730544127299	-0.50800922576049	0.95115888955822
H	-0.84716866411299	-0.19370416130093	-0.50313840696311
O	1.84365887230569	-0.70591582410069	-6.44468018910197
C	0.84354437207353	-1.29788663123846	-7.26762159444161
H	0.66770017090297	-2.35035797754401	-6.98933627031474
H	-0.10472611605444	-0.73785589986418	-7.21100666450800
H	1.23062223912272	-1.25364504309722	-8.29335024016102

MeAP

C	1.25462994998134	-0.30970184464525	-5.16555985714930
C	0.10245350133957	-0.64204873765259	-4.43441551723945
C	2.43099249524038	-0.00589654243867	-4.45078978891202
H	-0.82097215945121	-0.88153816959885	-4.96844473301417
H	3.34010724190802	0.25517924319981	-4.99987805458146
C	0.11707351206391	-0.67236653694747	-3.03762659292145
C	2.45018782657983	-0.03446004188233	-3.06034760640742
H	-0.79736421693497	-0.93555506144597	-2.50251850258174
H	3.36131562137506	0.20042647541845	-2.50601487568221
C	1.29297098303163	-0.36859991235452	-2.33122284294838
C	1.37068724424660	-0.38493268434561	-0.83683233483745
O	2.41856693194831	-0.10891973268080	-0.26683606275929
C	0.13063747039921	-0.74923677418274	-0.05158249010747
H	-0.21868818200202	-1.75971129865789	-0.31871644365716
H	0.36148057294231	-0.71359966303689	1.02093585882347
H	-0.69228439974343	-0.05051122454977	-0.27327189456604
C	1.24346499544519	-0.27435737272773	-6.67033504934003
H	2.00331158198358	-0.95651411543307	-7.08638527020037
H	0.26213012056733	-0.56400764298336	-7.07299466631258
H	1.48370821107933	0.73596698894526	-7.04200661460542

HAP

C	1.25995170054873	-0.31605972004204	-5.13988162496802
C	0.08941578263500	-0.60877754516364	-4.43101945467724
C	2.45113820184946	-0.05390881194454	-4.44918296699274
H	-0.83956139435300	-0.81323784116524	-4.96859328533866
H	3.36543784474040	0.17440843407784	-5.00242021867284
C	0.10571809684796	-0.64053507812312	-3.03362561913223
C	2.46788653039167	-0.08501352763700	-3.05539860099659
H	-0.81412050647006	-0.87051057938969	-2.49286114511316

H	3.38405283133377	0.11596629062837	-2.49627924165187
C	1.29671791639242	-0.37849909812817	-2.33294654281481
H	1.24505847504774	-0.29222462110889	-6.23238534925807
C	1.37378855710863	-0.39850808726527	-0.83496320383511
O	2.43132616980574	-0.16033385599180	-0.26765345642842
C	0.12259578536151	-0.71881862422778	-0.04981616107701
H	-0.26026639155659	-1.71735322666856	-0.31598862648502
H	0.35424499387466	-0.68945453814151	1.02264168129086
H	-0.67602679355806	0.00695107629104	-0.27340482484902

ClAP

C	1.26011249189702	-0.31645582414325	-5.12262109933925
C	0.08077394503385	-0.61035786128459	-4.43183793992962
C	2.45898472794588	-0.05203502996387	-4.44917636672731
H	-0.84106966737890	-0.81289664788628	-4.97862460273359
H	3.36644895549720	0.17471455590622	-5.01067355533417
C	0.10601919129413	-0.63980094456809	-3.03651472167379
C	2.46508622886077	-0.08541432434863	-3.05742699266206
H	-0.81657243262250	-0.87002215287699	-2.50121137389746
H	3.38361616637937	0.11611653365468	-2.50286184183694
C	1.29518520721806	-0.37847127683369	-2.33392787233469
C	1.37369957271864	-0.39833253498833	-0.83658406437921
O	2.43308299777317	-0.15953906634530	-0.27347158465603
C	0.12354684557125	-0.71892572774934	-0.05144891538373
H	-0.25873821530783	-1.71765968377666	-0.31780061222902
H	0.35524029082559	-0.68954363706893	1.02090897434993
H	-0.67519111144864	0.00674313004560	-0.27508053622092
Cl	1.23832335274292	-0.27915579477254	-6.86956628601212

CF3AP

C	1.24172144440359	-0.31754377306094	-5.14158607930060
C	0.07404137174955	-0.61913202130909	-4.43468675104895
C	2.43886540422023	-0.04695955584630	-4.45974380219926
H	-0.85292338220689	-0.82805932298477	-4.96995373070992
H	3.34788555681245	0.18824712201460	-5.01735444291090
C	0.10025761506793	-0.64969336557309	-3.03830550540932
C	2.45744096422224	-0.07918318054838	-3.06974831210099
H	-0.81734609937983	-0.88521999523139	-2.49740277196719
H	3.37511775666732	0.12869707083379	-2.51683383720440
C	1.29025180678729	-0.37977632611114	-2.34440205396559
C	1.37456644806474	-0.39584086388262	-0.84286250598910
O	2.43582351883609	-0.14975051567951	-0.28890062365988
C	0.13007655625114	-0.71987916254238	-0.05262614115756
H	-0.24839630739826	-1.72075414862821	-0.31628482465886

H	0.36501125868395	-0.68692976084232	1.01884007277739
H	-0.67227718719465	0.00181236516209	-0.27620174512970
C	1.24444139534026	-0.28223689030635	-6.64609763407994
F	1.69375811983073	0.90275464547911	-7.11572050747258
F	2.05607584072474	-1.22994533443683	-7.16671891701191
F	0.02159074051737	-0.47833067450629	-7.17310383180071

MeOAP-H•

C	1.72163312492269	-0.66704587892488	-5.06095643976826
C	0.53207841748488	-1.09253334831803	-4.43804221179646
C	2.75315296989679	-0.12835458551006	-4.26332548067233
H	-0.28517302607854	-1.51418367566979	-5.02485898241748
H	3.67792332292108	0.18978275957691	-4.75009918811525
C	0.37921484244333	-0.97424137281315	-3.05935209639990
C	2.60332199078425	-0.01293652269575	-2.89108653809387
H	-0.56050283790373	-1.30250305737613	-2.61097096269948
H	3.44846962891001	0.38983295388533	-2.32367750939078
C	1.40295895259689	-0.42684052062163	-2.22711313240926
C	1.22842494147866	-0.30095033870544	-0.82300964633178
O	2.14427880587821	0.33897152558042	-0.04269286090611
C	0.03853999519702	-0.77398942734957	-0.05715808496592
H	-0.33476891093781	-1.73921127655504	-0.43161242427010
H	0.30957324917372	-0.89360717001359	1.00261524663689
H	-0.80178714186003	-0.05436816114653	-0.10518233579081
H	2.82561963292629	0.74809717305945	-0.60401840132900
O	1.96451762268244	-0.73622004487930	-6.39668105740433
C	0.95579642954869	-1.27324380716355	-7.23751371085926
H	0.72564582048277	-2.32119902049021	-6.97741223076552
H	0.02822556757668	-0.67621913581730	-7.19166016128348
H	1.35611968587567	-1.23632978505213	-8.25915977896744

MeAP-H•

C	1.34659734020673	-0.33038403575652	-5.11901395349010
C	0.15528585086144	-0.59634907822545	-4.40521434620942
C	2.51200166868807	-0.10261158119300	-4.36172865481677
H	-0.77000199049023	-0.77766766924010	-4.96072856903437
H	3.45492443156820	0.09671601021940	-4.87956836755191
C	0.12205704087946	-0.62858382385407	-3.01931750839672
C	2.50103760789658	-0.13199913416473	-2.97096048024800
H	-0.82589285593187	-0.82622091605711	-2.51485405778288
H	3.45079944509957	0.02873706430196	-2.45028219905214
C	1.29963179189019	-0.39193686394613	-2.24050864127632
C	1.26679839957248	-0.40993286281729	-0.82086541812847
O	2.35202490976241	-0.05813447732141	-0.08151762331481

C	0.08090649241852	-0.74677584732612	0.01857395877469
H	-0.57021993278754	-1.48635917281613	-0.46804909617403
H	0.41875294543938	-1.15874039309488	0.98206208017227
H	-0.53378895278371	0.14662229550430	0.24109763294607
H	3.05641261078785	0.27081014561019	-0.66717985579023
C	1.35863174571507	-0.29568499854499	-6.62422591719660
H	2.36553200787809	-0.07860712229044	-7.01128152122497
H	1.03095007057149	-1.25858683703104	-7.05325676754134
H	0.67207014775777	0.47518026804359	-7.01553087666385

HAP-H•

C	1.33906687137610	-0.33167433831598	-5.09245351238413
C	0.14985666166172	-0.61462093379664	-4.39669632016331
C	2.51162860071568	-0.08241856106477	-4.35970094660626
H	-0.77139613874919	-0.81039928848284	-4.95222958590178
H	3.44700903456994	0.13095824852872	-4.88401723748387
C	0.12384683411830	-0.64510855009394	-3.00787485803826
C	2.50347780392459	-0.11025304711829	-2.96949011642869
H	-0.81612527855453	-0.85723659509552	-2.49470267134249
H	3.44918990454063	0.06839985354496	-2.44733976520945
C	1.30420877452703	-0.38933555469771	-2.23954815833477
H	1.35187747837256	-0.30790527445100	-6.18439508552436
C	1.27215770310453	-0.40952931051184	-0.81925405184819
O	2.35249867736133	-0.05565753714805	-0.07698096810802
C	0.08167913046714	-0.75660957169409	0.01054432843652
H	-0.49675504128653	-1.58284524593695	-0.42848332264060
H	0.41142269417130	-1.05557203492539	1.01652140169826
H	-0.60471263600218	0.10369734665629	0.12637047302730
H	3.06445675068153	0.26280561560307	-0.65953797314776

ClAP-H•

C	1.33745462146612	-0.33190545807051	-5.07245692024887
C	0.14057144911339	-0.61733798844785	-4.39482874884508
C	2.51939107675212	-0.07878133672580	-4.36031903644259
H	-0.77292814285912	-0.81197085362771	-4.95947629541543
H	3.44622699837929	0.13349161592167	-4.89600139184320
C	0.12559396774017	-0.64518691916908	-3.00817851670541
C	2.50369953998711	-0.10797278046041	-2.97231631658796
H	-0.81555560782481	-0.85893396454353	-2.49888014095339
H	3.45168005262200	0.07344846259166	-2.45666061004953
C	1.30596115467833	-0.38815113535963	-2.23975350252387
C	1.27349141845352	-0.40904613726633	-0.82147241849306
O	2.35240149341321	-0.06127075655504	-0.07696131543830
C	0.08069295280028	-0.75558073611898	0.00525061240593

H	-0.49531317538203	-1.58370032110882	-0.43323034033259
H	0.40795170298853	-1.05095820578252	1.01288950069832
H	-0.60585181364462	0.10499555959397	0.11548253873186
H	3.07014785705503	0.25551615716204	-0.65336288043814
Cl	1.35456694726147	-0.29362801203311	-6.82369683951864

CF3AP-H•

C	1.31632069004311	-0.32429199459817	-5.09109475549762
C	0.13208760935816	-0.62324004553832	-4.39214682226533
C	2.49840458459783	-0.06217648774412	-4.36816074935555
H	-0.78711233491971	-0.82750714149340	-4.94359921552018
H	3.42486841609106	0.16443191317146	-4.90083171146703
C	0.12150898598687	-0.65547753155395	-3.00656496811868
C	2.49679529183144	-0.09327947827867	-2.98457512057519
H	-0.81238507921327	-0.88169072229151	-2.48994383755333
H	3.44346398488443	0.10331159025540	-2.47234172959712
C	1.30447148786525	-0.38791130309270	-2.24691485571085
C	1.27854006526527	-0.41169652039484	-0.82914644913603
O	2.36115127622455	-0.08455961081451	-0.08831375553135
C	0.08250389656021	-0.74981939717716	-0.00316994661771
H	-0.45578660663665	-1.62287040436527	-0.40183279966879
H	0.39981122246617	-0.97130987955812	1.02560286124041
H	-0.63441041486945	0.09082124082255	0.03709937645221
H	3.09410581050488	0.19699053315112	-0.66459954079772
C	1.35243086090464	-0.28896208795556	-6.58415908552030
F	1.81516095404492	0.89515126745360	-7.05907335908782
F	2.17583995681306	-1.23516485361902	-7.10435582733515
F	0.13962619519720	-0.48432441437883	-7.14071346433685

MeOAP-H+

C	1.69830180410418	-0.64496946507981	-5.03538975351823
C	0.50751802196493	-1.08723932244993	-4.40916358719347
C	2.74446464983929	-0.08093694475537	-4.25725480296074
H	-0.30416071374496	-1.52005181818601	-4.99245616066754
H	3.64959716701939	0.25579424451884	-4.76403126527811
C	0.37648236017785	-0.96734598536773	-3.04008898259268
C	2.60450765836007	0.03260028586705	-2.89537366112379
H	-0.54537991037635	-1.31232457313994	-2.57118156380976
H	3.43603149044782	0.47713396620182	-2.34093254524974
C	1.41440311789934	-0.40972575727166	-2.24227029187209
C	1.24519821616830	-0.31004596900804	-0.83420113055649
O	2.17217615980824	0.17555988696421	-0.05422185081392
C	0.02596486727959	-0.73977396370526	-0.10356677339562

H	-0.12972315788152	-1.82168276425210	-0.24154212456503
H	0.13155261443440	-0.51840512716117	0.96486542379274
H	-0.85959390027962	-0.22437668451549	-0.50553052932719
H	2.97629963838255	0.45060752884210	-0.54555131340642
O	1.92551020318758	-0.71605100775162	-6.33763924799675
C	0.93430323527174	-1.27357514832138	-7.21668473035624
H	0.72940612639785	-2.32131084651173	-6.95060343624483
H	0.00908545479280	-0.67928848513763	-7.18007684602183
H	1.37131798074646	-1.22188476677908	-8.22007281484215

MeAP-H+

C	1.31554839676255	-0.27843532466830	-5.08534786081178
C	0.15597151509380	-0.65763621687027	-4.37973147411911
C	2.47202549207642	0.07473390644832	-4.35089725860083
H	-0.74512637411507	-0.92742750159603	-4.93378211298385
H	3.37462354620178	0.37972937444578	-4.88413858902493
C	0.14368877500846	-0.69380483353526	-2.99417481854067
C	2.47435379087331	0.03985669990994	-2.96913170077367
H	-0.76603194233226	-0.99370922286466	-2.47340721365736
H	3.39382944171394	0.33248388441392	-2.45229923366296
C	1.30717074660454	-0.35212492476002	-2.25891377164472
C	1.28545886888365	-0.41954016731572	-0.82838194048882
O	2.34282887522606	-0.17650210975958	-0.11475108848084
C	0.09208748186309	-0.77584398417927	-0.02663956598784
H	-0.20795814969856	-1.81081346962565	-0.25984969210789
H	0.31511096285350	-0.69081233623879	1.04317240233329
H	-0.75322908244692	-0.12274242905097	-0.29151085801684
H	3.13083181276507	0.04159023632855	-0.66082282752428
C	1.33891451208829	-0.25338244154020	-6.58159131882980
H	2.04753507402628	-1.01047297112133	-6.95933577507987
H	0.34802312652971	-0.45807775246544	-7.00835406643699
H	1.69605263402237	0.72275147504499	-6.94801654556021

HAP-H+

C	1.31944430478392	-0.30197024901552	-5.04976536456273
C	0.13923136520384	-0.62993050945210	-4.36878410533924
C	2.49635976316627	-0.00568382566862	-4.34425828156834
H	-0.77093216733141	-0.85700723865335	-4.92617895159024
H	3.40783887527764	0.25815338993034	-4.88273153018443
C	0.12792714456121	-0.66562539761218	-2.98009396738688
C	2.49801952931970	-0.04467798415901	-2.95737274248394
H	-0.79080911712812	-0.92381117790200	-2.45305184874050
H	3.42681129290500	0.20922579209171	-2.43687240306280
C	1.31205345745515	-0.38068748854484	-2.25425574657836

H	1.32408738179984	-0.27278865214576	-6.14158243333183
C	1.29046577305196	-0.44234030078292	-0.81671304987236
O	2.36912650366222	-0.29965019462571	-0.11389306799116
C	0.07340769114664	-0.67648926122967	-0.00979449090144
H	-0.31050996861933	-1.68894737975724	-0.22092831556134
H	0.30252065943086	-0.58754515618739	1.05826201647608
H	-0.71504825988300	0.03620618629553	-0.29536292912427
H	3.17339359619755	-0.16973533158126	-0.66589115819608

ClAP-H+

C	1.31911204820795	-0.30585226566538	-5.03942392733672
C	0.12865148420056	-0.62253867969832	-4.36761543852006
C	2.50721201598192	-0.01576507977323	-4.34684356986762
H	-0.77929088614486	-0.84107648663483	-4.92981424823489
H	3.41600938150416	0.23541499649059	-4.89365041193700
C	0.12901813384180	-0.65291363982098	-2.98242141822515
C	2.50028348293369	-0.05266585001729	-2.96331904434453
H	-0.79465005197793	-0.90135812014069	-2.45965471778120
H	3.43601987454539	0.19017658717107	-2.45103474730914
C	1.31413269689980	-0.37624148850897	-2.25447759401582
C	1.29048376441950	-0.43519910721976	-0.81894560031652
O	2.36312572210285	-0.27002793105814	-0.11025245619121
C	0.07440098391946	-0.69241592571881	-0.01679632821024
H	-0.30238724411955	-1.70430324756687	-0.24164995261583
H	0.30196250473672	-0.61440142368501	1.05243126884922
H	-0.71912749208921	0.01928965170988	-0.29180123936790
H	3.16910814639092	-0.11936140627897	-0.65352253176619
Cl	1.32611792764681	-0.26773339358426	-6.76518066480912

CF3AP-H

C	1.31206864986847	-0.32243015336230	-5.05879434111772
C	0.11507270842523	-0.56829522529979	-4.37815477946288
C	2.51327520699722	-0.10973829788636	-4.36254443809807
H	-0.80959884444260	-0.73356267508287	-4.93071040885594
H	3.44329311266430	0.06891961420778	-4.90414083704100
C	0.11138800204932	-0.60097179561232	-2.98820995514387
C	2.51187921487731	-0.13317914312945	-2.97696685030102
H	-0.82423701509534	-0.78845270790563	-2.46175484257083
H	3.46782069609869	0.01344590394528	-2.46648333562970
C	1.30765300507609	-0.37322994431870	-2.27035237734701
C	1.27947194575076	-0.38838829167026	-0.82508262906642
O	2.30304233278451	-0.02237888115224	-0.12649091639927
C	0.11094790640245	-0.80244322389219	-0.02362760206552
H	-0.25329436378166	-1.78482325180791	-0.36001067638257

H	0.36771353778265	-0.82726284288709	1.04152793306238
H	-0.70718854101225	-0.07926704347985	-0.18657041204572
H	3.06135695572268	0.28349799416027	-0.67550278482755
C	1.34264284944988	-0.28288310547662	-6.57120439317780
F	1.80167800773353	0.90413063283023	-7.01044712824507
F	2.16221428582366	-1.23164622489501	-7.06171175672069
F	0.13019719982507	-0.47461666528500	-7.11160322456366

2,3-diphenylbutane-2,3-diol

C	0.35635932993625	0.99554952421664	-5.09330400684070
C	-0.66077887106302	0.49630921645192	-4.26598721424814
C	1.68842516760609	0.94401784903464	-4.65325964809413
H	-1.70589862114533	0.53713925464005	-4.59303274068282
H	2.49212598876686	1.33459203431340	-5.28790439297970
C	-0.34854077209522	-0.05419004104398	-3.01276615788956
C	1.99940617854137	0.38890480126075	-3.40413833929028
H	-1.16048926887294	-0.43297470318537	-2.38431000816456
H	3.03599385260073	0.33770583208913	-3.06163762577318
C	0.98719583280376	-0.12484837042015	-2.56826081149394
H	0.11211899305574	1.42617918635622	-6.07086562561866
C	1.36408402340556	-0.77979945567433	-1.23877548171748
O	2.66679604858264	-0.31097966568111	-0.87754453583217
C	0.38857694215702	-0.40914341921363	-0.10418179107700
H	-0.65835813871602	-0.67015329327982	-0.32666937361917
H	0.68714301746394	-0.92951721269291	0.82112227188699
H	0.44992726906041	0.67872150285073	0.06607401246875
H	2.98803618541366	-0.99385223896723	-0.24930042663655
C	2.64889429303777	-3.15951126416047	-4.98638636637170
C	4.04384517481896	-3.19834913459516	-4.83544990371265
C	4.60441281627838	-2.99723019414294	-3.56539003983161
H	4.68876591681175	-3.38529812113671	-5.70126340639252
H	2.19735287315990	-3.31322900003088	-5.97284812484986
C	1.82467159909758	-2.91691113427773	-3.87843516238500
H	5.69187665922398	-3.02638078793173	-3.43311135736681
C	3.77786819294813	-2.75522767471441	-2.45735382359559
H	0.74157569873016	-2.86827763453820	-4.02281526649992
C	2.37602393559412	-2.70826760270241	-2.59700332617488
H	4.22864316183726	-2.59601275593457	-1.47366543533632
O	2.15178653930405	-2.73703584866854	-0.16111466066678
C	1.48706276042600	-2.36921197445155	-1.39532671115364
C	0.13212067013605	-3.08655541256871	-1.45111205890425
H	-0.50580116303230	-2.72025675496065	-2.27116527937434
H	0.29111802112541	-4.16898891959022	-1.60150208273155
H	-0.40419338863577	-2.94452489809773	-0.50017092071922
H	2.47442651063689	-3.65416612555219	-0.25720292233077

TRANSITION STATE CALCULATIONS

All optimized structures were re-evaluated with def2-TZVPP for single-point energy(vide supra).

SAMPLE INPUT FILE FOR INTERMEDIATE CALCULATION

```
! UKS TPSSh D4 def2-SVP def2/J
! Opt Freq Defgrid2 RIJCOSX TightSCF TightOpt cpcm

%basis
newgto Co "def2-TZVP" end
end

%cpcm
smd true
SMDsolvent "tetrahydrofuran"
end

%scf MaxIter 300 end
%maxcore 3000

* xyzfile 1 2 P1CH147S1.xyz
%pal nprocs 16 end
```

SAMPLE INPUT FILE FOR TRANSITION-STATE SCAN

```
! UKS TPSSh D4 def2-SVP def2/J
! Defgrid2 LooseOpt cpcm

%basis
newgto Co "def2-TZVP" end
end

%cpcm
smd true
SMDsolvent "tetrahydrofuran"
end

%scf MaxIter 300 end
%maxcore 3000

%geom Scan
B 39 52 = 1.82, 1.00, 20 end
end

* xyzfile 1 2 P1CH147S1sc.xyz
```

```
%pal nprocs 16 end

### SAMPLE INPUT FILE FOR TRANSITION-STATE BARRIER ###

! UKS TPSSh D4 def2-SVP def2/J
! OptTS Freq Defgrid2 RIJCOSX TightSCF TightOpt cpcm

%basis
newgto Co "def2-TZVP" end
end

%cpcm
smd true
SMDsolvent "tetrahydrofuran"
end

%scf MaxIter 300 end
%maxcore 3000

%geom
calc_hess true
end

* xyzfile 1 2 P1CH147S1sc.017.xyz
%pal nprocs 16 end


### COORDINATES FOR INTERMEDIATES AND TRANSITION-STATE ##

IM-1
  Co       9.17369446498967     2.75291694422315    10.81190703056011
  N       12.54545497445493     5.18905384358065    13.36748442371694
  C       13.03540992052556     4.05468932646435    12.55426802486638
  C        9.76870607825207     4.19337445152486    12.15863093055811
  H        9.79101922406759     4.02965270681238    13.23439666012957
  C        8.62030264368011     4.66050068255740    11.42668380478737
  H        7.65456904251538     4.91169957809280    11.86091874391324
  C       14.31234542322354     3.55267959823472    12.81531785031295
  H       14.90819138289756     3.96179829372727    13.63269488898266
  C       10.85756088358030     4.00713546249446    11.24586373686349
  C       10.31025675322072     4.22222763812299     9.93110007836603
  H       10.86691110395238     4.12639002050306     8.99953185249058
  C       13.50956579371443     6.33827104608114    13.41012023274611
  H       14.39892608243434     6.04932889883759    13.98034274906767
  H       13.00262900700505     7.17589874179112    13.90289051697521
  H       13.77207464119128     6.60419653009179    12.38133686058908
```

C	12.22331745718295	3.53913042764644	11.52376730676018
C	12.14077253633761	4.77181914824961	14.74820387165389
H	11.44412710969040	3.93046589907071	14.67325686893142
H	11.66333591329627	5.62690313721583	15.24174909083198
H	13.03992595569438	4.46715196122258	15.29682191969271
C	12.79366997414544	2.53011552038087	10.71636198306966
H	12.19200774349333	2.11830505924977	9.90471743213977
C	14.83411607260982	2.53441955736523	12.01748263215566
H	15.83142632926284	2.14116066341927	12.22342693689686
C	8.96644558276010	4.70613793216609	10.05439673959966
H	8.31560829337231	4.99413427443012	9.23066008628927
C	14.07434637188018	2.03721697141566	10.95199058362171
H	14.47676467417404	1.24950663528268	10.31123840004435
C	8.60176482431407	1.08777901607119	11.88187805568977
H	8.55755137005600	1.03833184551716	12.96974190600902
C	7.51074266860519	1.48111065150366	11.01873403189369
H	6.52163698907922	1.79575386390074	11.34932796409550
C	9.71538849333674	0.72268621648575	11.07220378520721
H	10.68648740834409	0.37907543945349	11.42475261815229
C	7.97478861408206	1.42965909477011	9.68620116240399
H	7.41403270350890	1.69981943196792	8.79245326860048
C	9.35793607043827	1.01573197135391	9.72174666248682
H	10.00077700642561	0.89494510809715	8.84983281227405
H	11.71128104399888	5.58904906905118	12.87618153180616
C	8.94471226620367	7.74284319178342	12.28601853472825
C	9.02993890894392	7.34671952354695	13.63433127936597
C	7.75066017650228	8.32039839686194	11.81589862775462
H	9.96007608795535	6.90866811133039	13.99882330949899
H	7.66316480128075	8.63724208738758	10.77548972019807
C	7.94279510533022	7.50930376229766	14.49045521385809
C	6.66010163949881	8.47962154753808	12.67389539743784
H	8.01808713279170	7.19886891009448	15.53525035050123
H	5.73452271534854	8.92237607271504	12.29902713172895
C	6.75244185203815	8.07259846733248	14.00980151161964
H	5.89794174930182	8.19793187080929	14.67919490123088
C	10.12001846362340	7.52793525187264	11.39667366623987
O	11.11999764218561	6.93733287192426	11.81034385676322
C	10.10035450941781	8.07702325328280	9.99401860585353
H	10.04108658010577	9.17788111742019	10.02366056547276
H	11.01851480044354	7.77537258676805	9.47479864365567
H	9.22397398423296	7.71916709360693	9.43420114085839

TS-1

Co	9.14767476545473	2.71778757892349	10.73895128170786
N	12.37745995085140	5.34893439940164	13.32097742695193

C	12.93489018480943	4.21795200667453	12.57928849252225
C	9.64811726441303	4.14635731878174	12.10271199219691
H	9.61292161250330	3.99281925366513	13.17784122193107
C	8.55334581858248	4.61311973646842	11.30207043126106
H	7.55966591849897	4.86223229639065	11.66869919343953
C	14.25093579072595	3.80907161394202	12.83303894340254
H	14.83955460611143	4.32269210715687	13.59413791229735
C	10.78506675940839	3.94253942284761	11.25238768985442
C	10.32902202044204	4.15581509104836	9.90645043143144
H	10.94215630660718	4.04950200615643	9.01308088721867
C	13.34191303362879	6.46689036830414	13.48966079038103
H	14.14675648225775	6.21539759530319	14.19680685025506
H	12.79001810456444	7.33182031959575	13.88431201822298
H	13.77310416611996	6.72528051369387	12.51446151241346
C	12.16191572372768	3.54489933594929	11.60589088729246
C	11.90334773568352	4.90309431947364	14.65463195302793
H	11.14218910463898	4.12234226476537	14.54530278980964
H	11.48119461164590	5.75941027768524	15.19774935065974
H	12.74661481449506	4.49795346701478	15.23743296868593
C	12.77067822010626	2.49795106027911	10.88502114086763
H	12.18456183575254	1.98526498916617	10.12049385069112
C	14.82648007142651	2.75641309607905	12.12075541646814
H	15.85402649932694	2.45458120716981	12.33506580330006
C	8.97723611658197	4.62350142166011	9.94573833173264
H	8.36875206725792	4.88834518268068	9.08293493623866
C	14.08359729461197	2.10299641809838	11.13310333935145
H	14.52310206391278	1.28387295732308	10.55966977754556
C	8.49126383230030	1.09825547454781	11.79375020780250
H	8.37788258138656	1.07180057507032	12.87690187165278
C	7.47593625107252	1.49804012820854	10.85577155596206
H	6.47202405060807	1.83614986159596	11.10811059833413
C	9.66250861066582	0.72580612241600	11.06523916733551
H	10.60378516832098	0.38528435973518	11.49295610253299
C	8.04060461406020	1.43287814257348	9.55496808239980
H	7.54906634945522	1.70928104235095	8.62335376915311
C	9.40244952347675	0.98139704674847	9.68653240773062
H	10.10555533947897	0.84670880991532	8.86537167667387
H	11.47606493561619	6.03682476018894	12.44136802626034
C	9.09761504687662	7.54284062027244	12.28906826789046
C	9.25956962382662	7.07775828339375	13.61682728899643
C	7.93741823845330	8.30009062614479	11.98320296876383
H	10.14426137752468	6.50515826650788	13.88280764726857
H	7.78311966106167	8.68346890869977	10.97391524580393
C	8.29825602607289	7.33445761874139	14.58847558723522
C	6.98065884885037	8.55652026321607	12.96152939872442
H	8.44399760963332	6.96083248093456	15.60482264013996

H	6.09260206170411	9.13946004787953	12.70624500567289
C	7.14982403354418	8.07307916479386	14.26757938818477
H	6.39506517910948	8.27578692883093	15.03078127297814
C	10.09730432140310	7.26816324785867	11.27471962260504
O	11.18456483647105	6.61908776656789	11.51289245465382
C	10.00295132029019	7.84467027927700	9.89480626032623
H	10.24644596842927	8.92246516809868	9.92527985798096
H	10.73038250520677	7.34620510095896	9.24175333955366
H	8.99678018194596	7.75019805377085	9.46480115821701

IM-2

Co	7.75512923533135	1.27802534075900	11.36861972652817
N	12.58353201543575	2.27085091321157	12.70231617776733
C	12.03490094819121	2.55920213665595	11.35093004251581
C	9.30742244543072	-0.06312220902061	11.13793447750914
H	9.56535152688724	-0.58880699293767	10.21890105064330
C	8.41642560963403	-0.55008712435087	12.15742975903412
H	7.86175679677152	-1.48645943107467	12.12010417798849
C	12.83541710023592	3.41331662668161	10.58265240086317
H	13.71269068768157	3.87808152714955	11.03614528589566
C	9.89475485668768	1.16915229760725	11.57856310148765
C	9.21195706097746	1.51726890978093	12.79239642519577
H	9.35138238848907	2.43711363403060	13.35853572389474
C	12.33062035433465	0.90914265096118	13.27947675680697
H	11.36421755669042	0.88360763950314	13.78841359410789
H	13.13754510538379	0.71828964941719	13.99783952928344
H	12.35688203098692	0.16870533749570	12.47355498520052
C	10.86752137046106	1.97226722558961	10.82116043203073
C	12.30773539225071	3.35315826783199	13.70195065844558
H	12.64191883494521	4.30844016322348	13.28188417548611
H	12.86916517469775	3.12230520246882	14.61579333447702
H	11.23277153340414	3.38274817766855	13.90856891611025
C	10.63017670536818	2.18939088015438	9.44370762790587
H	9.74734201009374	1.72443660715227	9.00265753553562
C	12.54285738627261	3.65031420830242	9.24246933848414
H	13.17923153332479	4.31413309031468	8.65495729590837
C	8.35582797444896	0.42587731760001	13.18048031008821
H	7.73692630536185	0.39117383250068	14.07580496300105
C	11.44838902136912	2.99954876815674	8.66242410891409
H	11.21731358308149	3.14301636312760	7.60468546872121
C	5.91017970628617	0.99421055907529	10.40461582576161
H	5.43950900449946	0.02749264683500	10.22933525171231
C	5.71411631265222	1.83286581966490	11.52374379014493
H	5.07478782020682	1.63172293644052	12.38225832628309
C	6.87178941471163	1.63214442834513	9.53053573010478

H	7.22436407675531	1.22688509382319	8.58226987099570
C	6.58693151615594	2.96932145848904	11.36814843267829
H	6.68859012799374	3.78866868083628	12.07994055170255
C	7.23199759004487	2.88614905426669	10.09322938174294
H	7.93713814892654	3.60509990187445	9.67957257894135
H	13.62885632889434	2.27231047449186	12.54735729344887
C	15.54736484894337	1.68464804848389	10.16146256843069
C	16.00416656779159	2.19142538908925	8.93141392256071
C	14.54461084507507	0.69656514135525	10.17260378401393
H	16.78271561744485	2.95606541239450	8.90541511542463
H	14.22507250905474	0.26838708256582	11.12337845312491
C	15.43148267770926	1.74763206477492	7.73723554348813
C	13.99049905223790	0.23984359327249	8.97852545497519
H	15.77190126573574	2.16181767411090	6.78561806797653
H	13.21895147676770	-0.53305556262429	8.99523554048129
C	14.42373593835383	0.77662129919672	7.75914553667760
H	13.98020636713220	0.43040082373240	6.82259514691266
C	16.04880847388030	2.21877123497482	11.45510182616929
O	15.32115601394397	2.22200039026600	12.45535815012819
C	17.44001449684017	2.77727518165046	11.53638581116226
H	17.49370369879523	3.71078396737109	10.95096333412788
H	17.68905487322473	2.99836720766744	12.58183033040499
H	18.17267711671014	2.07995769961443	11.10241198659133

TS-2

Co	7.82642632439968	1.25507802127081	11.34934197408384
N	12.59032358745844	2.28515897129164	12.64726272679185
C	12.03788178904498	2.59364791302293	11.34025110086296
C	9.35160884581170	-0.08079893787142	11.07120565824429
H	9.58972407472766	-0.58956325475971	10.13795378397557
C	8.46238912959964	-0.56708910769804	12.08670913509989
H	7.89087475007927	-1.49271743135661	12.04175541485181
C	12.78030877793692	3.51552629477671	10.57976384484638
H	13.63555782281571	4.01232290010359	11.04225309065737
C	9.93601572060947	1.15422007189581	11.51475345933644
C	9.28729455471986	1.48378016898078	12.75164941056211
H	9.44291307549935	2.39788564711937	13.32208283075326
C	12.31325197153000	0.96734487743016	13.25205745434205
H	11.39230541079903	0.96048551918604	13.85120435748355
H	13.15769742594941	0.71912547549328	13.91350579649527
H	12.23665111447719	0.20069694870871	12.47175570184242
C	10.89796775923214	1.98307659385339	10.76694050570176
C	12.43726027169825	3.37479191758679	13.63753691013906
H	12.76663024873873	4.32493113953323	13.19815379361235
H	13.06393519772452	3.14883759605020	14.51173847222314

H	11.38793018407553	3.46903833310579	13.96136052873701
C	10.65253697410414	2.20922931983448	9.39333423919640
H	9.79615648900174	1.71054662665073	8.93643878627926
C	12.48027301345020	3.77201773507507	9.24604315423280
H	13.08673253605596	4.48163194524284	8.67959280499817
C	8.41690346245950	0.40284888458523	13.12455254068244
H	7.79976324180539	0.36222921583993	14.02060273548747
C	11.42805401161402	3.07938016204644	8.63463822735237
H	11.19835542488627	3.23584280197818	7.57844439330142
C	5.99728775768171	0.96971948186703	10.41833674165301
H	5.52955776081472	0.00137819026557	10.24667863333370
C	5.82917015206212	1.79329527727611	11.56184412554243
H	5.21394764712050	1.57143890657922	12.43254613127617
C	6.93587786205313	1.61870097488636	9.53905346348157
H	7.28309354660739	1.22582967575021	8.58424956564983
C	6.67808610190003	2.94273276351527	11.40068974045581
H	6.79752884248829	3.74886020564426	12.12371337039682
C	7.31571779268782	2.86205414672912	10.12385737516267
H	8.02382515204987	3.57926134989428	9.71282235233287
H	14.05450690106588	2.20200478627370	12.44500340088653
C	15.40004960347519	1.65565464217734	10.22469773647478
C	15.99788917541706	2.02400806320532	8.99077763384305
C	14.29516515506534	0.76486742186693	10.20492095228429
H	16.85317248065956	2.70161408008838	8.98059810494530
H	13.87313297219370	0.40654574789204	11.14302779803350
C	15.46462494149396	1.56906499118760	7.78972562308173
C	13.78544596970472	0.29624964783978	8.99942506049167
H	15.91413658694685	1.88347205647074	6.84507593679937
H	12.94421900836412	-0.40021368392000	9.00093636634346
C	14.35240717026047	0.71208671876306	7.78584764329499
H	13.94057991051611	0.35562967179449	6.83898214437520
C	15.88399727595299	2.20944338226934	11.46431300209061
O	15.14671967882168	2.27290556026743	12.52917769331116
C	17.25244583413613	2.78550412948540	11.60867642201286
H	17.23958847271617	3.84914472610595	11.30596525375184
H	17.55234387756323	2.74896595990029	12.66528314142750
H	17.99330361086653	2.26574348894701	10.98693674108570

IM-3

Co	7.99080808465788	3.90148213480318	6.65118172256206
N	2.98053731598179	7.34007070156948	8.31633882517773
C	7.00282769113878	3.90206015115624	4.84285948334300
H	6.45142021562768	3.05306960728327	4.44146918863883
C	3.37220756741357	6.26492731216623	7.36631586195894
C	7.56021957441727	5.80082840048027	5.99780441343680

H	7.51672274373238	6.68616185926937	6.63021066672170
C	6.44416170093157	4.97750373458087	5.61571101634600
C	2.34938714242731	5.49984963505924	6.79252919494176
H	1.30289545615004	5.65449751371348	7.05481821228476
C	8.39920272352402	4.15370180893628	4.62077286215767
H	9.07330106064964	3.52646349139774	4.03955989460197
C	8.22524643600799	3.97899401817265	8.69374922408637
H	8.15009704001789	4.88871666524170	9.28933009152782
C	4.70200232475712	6.08872208795541	7.00679906619892
H	5.48475585579402	6.68996162178633	7.46204979882133
C	9.11230776156938	2.28229152943855	7.40637607863608
H	9.79264767153247	1.66322132095089	6.82309995195233
C	7.15986009303344	3.07531678394347	8.40809918319423
H	6.11977813297718	3.18427250073835	8.71194233906736
C	4.02571239970228	4.34702506010656	5.46596605050773
H	4.26552887939790	3.60314143987382	4.70474663830389
C	8.74317169186089	5.33018257005739	5.33302603383652
H	9.73122938151536	5.78285208845766	5.40048210292332
C	2.69856698264052	4.53072013105607	5.84748941802248
H	1.91364008317802	3.92493121122564	5.38965707899939
C	9.44269538334808	3.45837346162511	8.11441019837180
H	10.42675265820643	3.92038406149350	8.18185671993017
C	5.05550067148845	5.12772058260518	6.03270052480603
C	2.13380783365532	6.83487181174991	9.44724628310984
H	1.25490813899075	6.32161958756019	9.04639525608360
H	1.82015824731544	7.69924431792259	10.04418680073085
H	2.73770578931268	6.14630604150257	10.05035835892780
C	7.68943618386099	2.07207065801187	7.54367894815359
H	7.12768587700846	1.25169032921737	7.09724954048256
C	4.10569635948897	8.16013006275874	8.85660999916143
H	4.74655502116626	7.52490634611089	9.47912928825087
H	3.66309596909029	8.95997885304415	9.46093929969256
H	4.67417686019149	8.59179100721431	8.02772595739244
H	2.37968616570699	7.98777995271172	7.73212254826749
C	2.94993063994044	8.26972450028095	4.81973804500190
C	3.90253451844098	9.11042705334869	5.42545429699599
C	3.34445252547032	7.42788791978121	3.76358252836227
H	3.58416186970113	9.78760522543070	6.22100389838674
H	2.61787053431761	6.77294280824833	3.28021135026855
C	5.22999919240184	9.09370230411266	4.99997400998895
C	4.67939641589762	7.39710470435269	3.35533624185790
H	5.96164341807593	9.75696801446917	5.46709545042940
H	4.98613332823774	6.72064643934054	2.55469059502995
C	5.62335753773921	8.22512557640289	3.97314344957464
H	6.66602596777131	8.19987365457243	3.64830901253715
C	1.56040964223578	8.26604502767114	5.34874110163816

O	1.33977196008293	8.59251268804703	6.52215904490817
C	0.42784103750128	7.85652702501185	4.45161305121053
H	0.51941310784620	6.78434031931845	4.21018467293269
H	-0.52780146943894	8.02687864334053	4.96304596136440
H	0.45830571031080	8.40711203432164	3.49873997590159

TS-3

Co	8.00932396760152	4.00082634214433	6.61955829714869
N	2.94072207829301	7.35805126540064	8.33798467494969
C	7.04022778928928	4.09628338903390	4.82340882264628
H	6.50508117060375	3.26630522819317	4.36591810334648
C	3.35213848509493	6.27855636264112	7.46148219037741
C	7.56078436569902	5.92446529388303	6.11431465860267
H	7.49858339255129	6.75603435352971	6.81340219149950
C	6.46124294150196	5.10511029642390	5.67435200794530
C	2.36466634904271	5.49319624728983	6.84035368476551
H	1.31115947066239	5.60491672370460	7.09395484342823
C	8.43255586995912	4.37381927054434	4.64429133323432
H	9.12426467704552	3.79364708978491	4.03587866288098
C	8.21224792126893	3.96270847134459	8.65096399793202
H	8.11785338713785	4.83446667558999	9.29738678202117
C	4.69160243197655	6.11414870688606	7.10538292089024
H	5.46219733591259	6.71105146956721	7.58601373083630
C	9.12129567658566	2.36157633719576	7.25402292394767
H	9.81487766975037	1.79551458347415	6.63415907111665
C	7.15554748455210	3.08184465808015	8.27278781889620
H	6.10826920916951	3.17269158590230	8.55666544347062
C	4.06865815874462	4.41431291265018	5.48913439079600
H	4.33054662976846	3.70426423993704	4.70353951977713
C	8.75584196627785	5.50570164322245	5.44582501291324
H	9.74013414969956	5.95642495785529	5.56105420828787
C	2.73856445676990	4.55393968714070	5.87444324158561
H	1.96795662708466	3.94423375999220	5.39761044860323
C	9.43336954293028	3.49852733042124	8.04293303152024
H	10.41172241033031	3.96626267298946	8.14243251726761
C	5.06925128464490	5.19978984878401	6.09796423973933
C	1.88406778180044	6.99132791900350	9.31344865068229
H	1.00514670787281	6.58877281228428	8.79943848604337
H	1.58561136088046	7.90147310600628	9.84950114265830
H	2.26363999388128	6.24809139953629	10.03219185927660
C	7.70568668478686	2.12561331392843	7.36485466048112
H	7.15215360098437	1.33984792581513	6.85213473686225
C	4.02819171109698	8.08242261077125	9.02455233349319
H	4.56868171599746	7.41721800504438	9.71707941174046
H	3.57670833691153	8.90611565590613	9.59171615931016

H	4.73030705483069	8.50317639519805	8.29639937485054
H	2.30280448017215	8.19217110980950	7.41951879617442
C	3.05114221656616	8.10095964541512	4.86492929351388
C	4.15126638355857	8.76895649582887	5.46161040409786
C	3.28192849521190	7.32423430083541	3.69969855429284
H	3.97800185386284	9.41971469799982	6.32068791877284
H	2.45140671421260	6.80538835332687	3.21835332114891
C	5.43011807972972	8.64161233932217	4.93197532815746
C	4.56859911254976	7.18682860961723	3.18897681256477
H	6.26441526066273	9.17383040873565	5.39470928430444
H	4.73630921477844	6.56501860933600	2.30664108249769
C	5.65135808934424	7.83012897358281	3.80845144828380
H	6.65863193241697	7.72109641066471	3.40080581030215
C	1.73161782531415	8.20835748195436	5.44558018934835
O	1.56104699443946	8.61670383914685	6.66079867837158
C	0.49523086074630	7.91538876901796	4.65637890719340
H	0.39203502831852	6.82746584358307	4.49972916701988
H	-0.38424722080336	8.26753891084434	5.21095519662466
H	0.52699593592348	8.38513104487486	3.66168102950189

IM-4

C	2.39941191104909	0.52887742832891	20.31395801852988
H	1.46675220782373	1.04800481057054	20.53435707099948
C	3.50835496255688	0.38886677252415	21.19907808879076
H	3.59509312408031	0.81061152059440	22.19933466823022
C	4.52992805872460	-0.29551670952885	20.47650896772207
H	5.52963195458590	-0.52497248157389	20.84519934070146
C	4.00125450043729	-0.69583021341676	19.19257490654885
H	4.54188755463802	-1.25268905340078	18.42837479309732
C	2.68820408813272	-0.18677161349132	19.09191013816921
H	2.02144663605268	-0.27610239506138	18.23523410466832
C	5.72540326957175	2.56636184225145	19.26909436085982
H	6.70507057233461	2.28866611549636	19.65541430646422
C	5.24475491670171	2.25262947896945	17.95237882163191
H	5.78937192289018	1.69248766387761	17.19386945897291
C	3.92496077810315	2.75880614429349	17.84397100364582
H	3.26187171083658	2.66442824622209	16.98541047200520
C	3.59256662306290	3.38262763408164	19.09409561138406
H	2.63628377430889	3.85267005319894	19.31812426682898
C	4.74435438904599	3.36324789243334	19.95520610972722
C	4.84400400168469	3.92064234728989	21.29842887666324
C	3.73702402389333	4.55118730017653	21.91300949352472
H	2.77984854011936	4.60552396845675	21.39329642954944
C	3.84485325041673	5.13064182801154	23.17048964537097
H	2.97762728923541	5.62790722767165	23.60923645540302

C	5.06598188039372	5.09433036633444	23.85346839186733
C	6.16792058639228	4.44979466145495	23.29170883845676
H	7.12627467198199	4.40424305275264	23.80793584621016
C	6.05103676212700	3.87027747887246	22.02837274649794
H	6.92900575077896	3.38860109964727	21.59564282722431
Co	4.03612939000093	1.40120970157603	19.42297725797733
N	5.14825252815426	5.82118968263984	25.14026290628804
C	6.53202045669202	6.08802762459448	25.63072003635878
H	7.10512946398593	6.57694057002678	24.83506145004613
H	6.44933539725556	6.75256595505210	26.49871996056745
H	7.00546072844810	5.14451444851016	25.92577270112952
C	4.31860221369968	5.17901550643382	26.21174420266236
H	3.28986160426260	5.07745214693198	25.84948548499678
H	4.74355547906791	4.19340685324915	26.43641744148906
H	4.34445145179128	5.82405296403925	27.09871249088759
H	4.72547017714830	6.77286337245074	24.94605797955232
C	4.02663955928427	8.26552450734805	22.32651576850354
C	5.37379931280253	7.86434883576643	22.24758299268314
C	3.22141580152204	8.21278580460809	21.17406017140031
H	6.00772082304367	7.93407868543168	23.13362598562082
H	2.17532713154095	8.52072215499081	21.21977930665620
C	5.90307475622616	7.40805372556778	21.04182633627592
C	3.74661113467016	7.72640517572330	19.97476536356835
H	6.95214200985086	7.11049035425998	20.98442756544844
H	3.11017833955595	7.66121298088046	19.08952270803337
C	5.08535031836927	7.32434577290812	19.90717394018516
H	5.49456926340579	6.94755422091442	18.96690234201762
C	3.47002518966597	8.68159136257106	23.64076228685921
O	3.95427916538645	8.25249627282595	24.69500271210693
C	2.29881314460684	9.62123934375170	23.68112133691989
H	1.40248870127428	9.10570382715871	23.29652970496199
H	2.11201460245222	9.93373291927891	24.71619275650558
H	2.47078027187483	10.49715809147184	23.03734361454874

TS-4

C	2.33574238884395	0.74479840628034	20.19360176469791
H	1.41882620037855	1.28900643960511	20.41617954887543
C	3.42943104792759	0.54367493678186	21.08822562666360
H	3.50768059307088	0.92446520823222	22.10529803564236
C	4.44611290528656	-0.15569335798224	20.36730788767458
H	5.43022961751215	-0.42413863021937	20.74943014523547
C	3.94801294552699	-0.45592909505656	19.05190073039343
H	4.49398142952644	-0.97698579664923	18.26701640274474
C	2.64742817629211	0.10465865130573	18.94254253234784
H	2.01196182317484	0.09137799883165	18.05835560418076

C	5.73451031003301	2.67866647669805	19.35667996106879
H	6.68983347536183	2.34229292499038	19.75550987824258
C	5.26879476772317	2.44470600457693	18.02346965887417
H	5.80548494981872	1.90213789468373	17.24709492521729
C	3.95967300664878	2.99650232803952	17.91744648456280
H	3.31223587366530	2.95920027003691	17.04304711190360
C	3.62255103110641	3.57327031024546	19.18421695728099
H	2.67651826457116	4.05621050471161	19.42086275782933
C	4.74675049598661	3.44426488018282	20.07313465326779
C	4.82958357913098	3.91999544108156	21.45115589146315
C	3.69190349894026	4.42168223643096	22.11971058647254
H	2.71413956722621	4.38859350747844	21.63708807038972
C	3.79630755768396	4.99811768494333	23.37874338203009
H	2.90276419272003	5.42235601064098	23.83917608279872
C	5.04360767909376	5.09526484262433	24.01864129166275
C	6.16598449646651	4.52345895243117	23.40468807017560
H	7.14498618422310	4.55633366685500	23.88083586521807
C	6.05566727277923	3.94630235519947	22.14033122063804
H	6.95539371279780	3.54796668047903	21.66803167836154
Co	4.01496822456916	1.58497554332343	19.39935658253001
N	5.15146907359705	5.91689131783875	25.20306576333917
C	6.51688184421490	6.10575203988434	25.72885799050432
H	7.16486335906641	6.51218054899413	24.94190741368523
H	6.46231871609900	6.82739799115820	26.55432603316883
H	6.93857354659079	5.16016564652190	26.10509215426006
C	4.21749682123956	5.54168898944001	26.29307867513483
H	3.18941696923942	5.50338279450946	25.91540253252391
H	4.49164242469086	4.56015564270986	26.71067134411317
H	4.27831239756192	6.30561045932695	27.07909621235216
H	4.75219217447707	7.17295397359150	24.78597647431690
C	4.13708616702845	7.96419336880412	22.22644772845583
C	5.49216743307000	7.56669790799376	22.07195873043830
C	3.27825548188671	7.86950329736446	21.09864905231061
H	6.17750411850531	7.66195122538326	22.91626403718776
H	2.23109938954387	8.16441423941050	21.18634498769810
C	5.95693416298557	7.08654265391417	20.85456456930526
C	3.74881340181498	7.36593926575057	19.88874279653428
H	7.00549214578502	6.79804545009901	20.75278338851543
H	3.06788963103280	7.28092739894942	19.03836063125172
C	5.08750497848528	6.96746600403387	19.75632586613593
H	5.45671604548595	6.58564195502407	18.80208088274746
C	3.64096092477545	8.42349597677845	23.50221651817163
O	4.27324115853137	8.19956115871953	24.61175724540280
C	2.35832175206287	9.18414600181077	23.62676968184734
H	1.51032693373106	8.47835452082464	23.70832901961913
H	2.37965140405039	9.77856797703455	24.55106059393197

H	2.16748040435945	9.83907424534422	22.76554115259174

IM-5

Co	-8.74998800501227	-1.38859217021113	17.99542068354184
C	-5.73998909167060	-0.31657391278359	18.52473790596816
N	1.95752344030910	-1.33673609142308	22.28202871392612
C	-3.20595354676829	-0.77245245210397	19.77392716389546
C	-7.47447104603223	-0.56709430555730	16.61068935698555
H	-6.87256856096496	-1.13285250504820	15.90103845554397
C	-7.03461186651533	-0.08726293949359	17.89361671907445
C	-4.78369999939805	-1.18906340964568	17.95539011817225
H	-5.01578906822359	-1.71783946017429	17.02888928300806
C	-3.55146406654560	-1.40687030933713	18.56202936317093
H	-2.85327085852350	-2.10624190083177	18.09664434851919
C	-0.75190896293741	-1.30902711560733	19.64758053738785
H	-0.83358800280406	-1.40824339988054	18.56403179915704
C	-1.89076387520239	-0.98797770356426	20.41130734808508
C	-4.16137076535432	0.09393799250239	20.34649226362271
H	-3.92711613081039	0.62718890834288	21.27018758898496
C	-8.80942997554614	-0.09891433382484	16.36054525416136
H	-9.38248576287969	-0.27028528493069	15.45054568124485
C	-8.18804640716541	0.53186857716065	18.48777420070054
H	-8.23925636750303	0.94773108568362	19.49305039397358
C	-9.25348629863596	0.57799074087998	17.52445004611158
H	-10.23505226288938	1.02204263894084	17.68283717038176
C	0.50572024166343	-1.46054261659474	20.23452703993335
H	1.36349440175619	-1.68352592206929	19.60126935436763
C	-5.39214815619005	0.31894122196710	19.73824857297913
H	-6.09195300613412	1.01536623997219	20.20444357957133
C	-8.24284311591088	-3.04736472825428	19.19880336236904
H	-7.28070378799604	-3.18282912765091	19.69059362217703
C	-8.57521136104266	-3.43500076938960	17.86817038825622
H	-7.91910760786961	-3.95568171390332	17.17084939161763
C	0.63935320534881	-1.28918029503912	21.61072996257190
C	-1.72484917754220	-0.85364658841021	21.80614247437515
H	-2.58479440937763	-0.63464867890110	22.44048804030542
C	-0.47687370774234	-1.00019578861048	22.40196924811580
H	-0.37843785739707	-0.87938261287031	23.48225612012664
C	-9.36615952066383	-2.33501088930967	19.71538239829672
H	-9.42609945088154	-1.86015183749810	20.69458231187203
C	-10.44041248361241	-2.40144942415831	18.75211792670404
H	-11.43142293375207	-1.96606330292890	18.87350174746927
C	-9.95163672463876	-3.07586719372440	17.61144832441150
H	-10.49463900217369	-3.26161364971635	16.68563287080792
C	2.08088944250195	-2.50909567382761	23.20954709318765

H	1.24374307324706	-2.49036193818495	23.91558095226162
H	3.03214163493808	-2.41916167198574	23.74816806692539
H	2.05818308133636	-3.42897529299842	22.61317131466112
C	3.13596563377157	-1.25337432997615	21.37087198304136
H	3.20077459258635	-2.16721129805966	20.76947381879993
H	4.02902677241677	-1.15557303386063	21.99894700024818
H	3.02899982607306	-0.37277745718405	20.72764771054551
H	1.99500791847974	-0.46148763200643	22.87990051368627
C	-1.40218786958651	2.66245489715639	20.80749277335641
C	-1.84451235190750	2.85639039694975	22.12131555834734
C	-0.09893695126568	2.20984619678922	20.56440138936526
H	-2.85967603508549	3.21258901688389	22.30948124826200
H	0.25273080391318	2.07678852436826	19.53921528343271
C	-0.98932551124647	2.59739796732977	23.19449836043946
C	0.74734442631169	1.92280469487661	21.63392677829311
H	-1.34456056045027	2.74662699857738	24.21571536129300
H	1.76599001423579	1.57609531979456	21.45014431360981
C	0.30807299231136	2.10711458387924	22.95872665499263
H	-2.07273950635755	2.86949280065714	19.97045218167257
C	1.20756433031156	1.72442353222356	24.07825575550201
O	2.06277291674197	0.84345228187172	23.92525065768857
C	1.06362525452885	2.40526549859867	25.40890650059642
H	0.11534374359456	2.09313533005278	25.87841201218092
H	1.89526048098365	2.11522333448332	26.06322108866067
H	1.02443462684736	3.49902676458837	25.29376481099403

TS-5

Co	-8.72407368384179	-1.28181780646437	18.05183247593932
C	-5.64445679878536	-0.42998409383468	18.43723716104931
N	2.00721843107257	-1.22464122682243	22.27394520172929
C	-3.12762063491056	-0.86853468778358	19.71445880865593
C	-7.40196128551331	-0.82042246216551	16.56793360380436
H	-6.86084668768436	-1.55254347517059	15.97138650244625
C	-6.92718522751342	-0.19960587152204	17.77661939689617
C	-4.63267351274560	-1.19546994695768	17.81836593279882
H	-4.80636433067663	-1.63129541187016	16.83277634107167
C	-3.40707004583357	-1.40707688843091	18.44077679521064
H	-2.65736874258827	-2.01753376598353	17.93323187178889
C	-0.64492389736830	-1.24944147750498	19.60943740393690
H	-0.69855442817878	-1.26330288005806	18.51919219512051
C	-1.81664370384618	-1.06976381946631	20.36633475312331
C	-4.14342855473059	-0.11059718958884	20.33582261932655
H	-3.96189931800693	0.34064215868269	21.31318749266939
C	-8.69929252596519	-0.30114416445160	16.25156404661253
H	-9.30127842165245	-0.57672239905893	15.38732277250569

C	-8.01378589712916	0.61685219409460	18.25382856795434
H	-8.02164110218760	1.19026924485103	19.17883677105741
C	-9.07662044419282	0.59146073161234	17.29430251912410
H	-10.01988154370542	1.12905676345380	17.37533584118234
C	0.60853830931449	-1.35945410309441	20.21431645559952
H	1.48843026145069	-1.46342012745640	19.58064983165834
C	-5.36903673160093	0.10534695380097	19.71434169490542
H	-6.12209837282778	0.70580391968224	20.22799819763296
C	-8.33213984585326	-2.75439343020200	19.45918695181434
H	-7.36836714962593	-2.90592992675816	19.94271957195674
C	-8.75078888664207	-3.31636846652631	18.21586691750160
H	-8.16936384905006	-3.99488308150051	17.59293020182535
C	0.72561448965202	-1.29114489324747	21.60725800145933
C	-1.68402318642346	-1.05137843254006	21.77074791808239
H	-2.56864096245249	-0.94586423493214	22.40108784897306
C	-0.44013835387377	-1.16429642929726	22.38068086011706
H	-0.37666025862392	-1.11684989135304	23.46919657699166
C	-9.36607941615472	-1.87094692176859	19.89591660469531
H	-9.33769158096079	-1.24667359567219	20.78815984146125
C	-10.45961382450306	-1.95146316840896	18.96418316478423
H	-11.39128864753913	-1.39104448799028	19.02437474854937
C	-10.07822138859742	-2.84164159764509	17.92507040911423
H	-10.66463120053984	-3.09105217748021	17.04206289947677
C	2.19134686238724	-2.27168650577477	23.30864252897372
H	1.34911826593175	-2.25999554309489	24.00986957640842
H	3.11692651995783	-2.05923260677535	23.86023380853261
H	2.26299951280538	-3.26660763384446	22.84055266829314
C	3.18297930340509	-1.15892247487514	21.38793647098953
H	3.31235596460897	-2.09160530140085	20.81533097383285
H	4.07043133314038	-1.00097325308430	22.01485838838666
H	3.08070060051172	-0.31411534333431	20.69444151779784
H	2.01395013348063	-0.00201964107854	22.99572842133186
C	-1.60252416324727	2.58282591840832	20.77795442860076
C	-2.01592213843058	2.71496523484048	22.11190681123685
C	-0.29491282705029	2.15680998244343	20.49410613837844
H	-3.03121899395885	3.04927723161317	22.33791167762460
H	0.03880024156837	2.07306323452328	19.45758585638206
C	-1.13976162166760	2.42345995759346	23.15402734435360
C	0.57996423024483	1.84102068842515	21.52652390130152
H	-1.47874011384032	2.52211126335196	24.18677715285986
H	1.59938024690443	1.52635380909919	21.29721146309765
C	0.17329538843119	1.95898535196815	22.88131270126301
H	-2.29128618020402	2.81788153853431	19.96373237413610
C	1.06677576960112	1.59199952921172	23.95546859778045
O	2.08685270184627	0.81511836711749	23.76753378322540
C	0.87149008624111	2.07477111823406	25.35596285561586

```
  H         0.18739531905773     1.39197667341208     25.89398959061631
  H         1.83565705946009     2.05445595744501     25.88324455612073
  H         0.44092029365330     3.08434779687126     25.39753895623556
```

NOCV METHOD INPUTS AND GEOMETRY

###Cp-stacked o-phenylene TS input###

```
!TPSSh def2-TZVP EDA
!SMD(THF) D4
!printbasis printmos
!UCO UNO

%EDA              #EDA block
  FRAG1 "TPSSh def2-TZVP SMD(THF) D4"  #Method for [Co(II),NH]+, fragment 1
  FRAG2 "TPSSh def2-TZVP SMD(THF) D4"  #Method for acetophenone, fragment 2
  FRAG1_C 0         #Charge of fragment 1
  FRAG1_M 2          #Multiplicity of fragment 1
  FRAG2_C 1         #Charge of fragment 2
  FRAG2_M 1          #Multiplicity of fragment 2
END

%pal nprocs 16
end

%maxcore 1000

*xyz 1 2
  Co       16.24091469673258     3.14217791353975     5.99384523448370
  N        11.50436821811190     2.07615449026034     5.18568593045534
  C        11.78001950429151     3.20742743981416     6.07171182098303
  C        14.75324002283709     1.82378140521028     5.43894748829855
  H        14.41630714161235     1.00185614794495     6.05279888024751
  C        15.85591599476218     1.78112180512700     4.53363717269201
  H        16.47544605858701     0.91775262138233     4.33399160231424
  C        10.72788441418375     3.80161025271560     6.77274244313596
  H         9.72509801757426     3.39828145103824     6.68183461316820
  C        14.24207504990142     3.16134964889699     5.45921729823543
  C        15.03202834205358     3.92924653910235     4.52243050989727
  H        14.89570011361569     4.98239524005658     4.31780895647973
  C        11.50004999731179     0.78800537484449     5.94091905253183
  H        11.44094577953209    -0.03578715917842     5.22553853984843
  H        10.63565307499160     0.75448612558875     6.61328604654657
  H        12.41389832816716     0.70353103238031     6.52725207929614
  C        13.08853012765669     3.71473069840952     6.19978472828942
  C        10.21349788407214     2.20885718089166     4.45007421259226
```

```
 H      10.19461258458910   1.43813994143185   3.67542265937717
 H      10.16175370239613   3.19512693718770   3.98750577846877
 H       9.35536669868852   2.06118248507935   5.11174218296069
 C      13.27819809780529   4.85288744607876   7.00028324071702
 H      14.27846215967660   5.26494014029841   7.07903346106549
 C      10.94451562599714   4.91337270247031   7.58174707905845
 H      10.11267707801555   5.35867424229486   8.11949228314161
 C      15.99536687818416   3.07251213880021   3.93157703402263
 H      16.74808545786473   3.36043145710532   3.21050120426466
 C      12.22689627371741   5.45029089098303   7.68569841007739
 H      12.41020941545620   6.32632115884416   8.30093950894520
 C      17.10196983163564   2.41903481877999   7.73387428436319
 H      16.87087311149062   1.46127376508691   8.18016822338966
 C      18.08759587935541   2.65958716536236   6.71834763339789
 H      18.73588788556434   1.91383383482676   6.27752680473341
 C      16.43113513775401   3.64722514468734   7.98227293288340
 H      15.60110863611492   3.79301236984740   8.66024381456291
 C      18.06502046937761   4.05235657946538   6.38545875466441
 H      18.68321707952957   4.53938807734166   5.64354996326236
 C      17.02149805673629   4.65732311999479   7.14266177927003
 H      16.71766868395809   5.69442002969989   7.09155877833728
 C      12.70249219297204   3.77971650760022   2.28003211064740
 C      13.37637117331770   2.44131354648065   2.32612926714361
 C      14.30137942680513   2.00091667310745   1.31072878718987
 C      14.67346206812008   2.83076499789776   0.22469697031653
 C      14.85506498849647   0.69643463120884   1.37584289408712
 O      13.02985388057921   1.57454111850781   3.23428623067826
 H      12.38778110786487   1.92948516738190   4.13445642327059
 H      11.80397963419057   3.71626555525941   1.64760284280813
 H      13.34639803010204   4.55302361334156   1.85707407283044
 H      12.38562806588120   4.09534469302732   3.27615911754909
 C      15.57025999692103   2.38043925520228  -0.73540181997548
 C      15.75235500370589   0.25899091661222   0.41312084233048
 C      16.12112945078074   1.09605812439907  -0.64842681872036
 H      14.56927368859616   0.04628472314924   2.19551120628732
 H      16.16985197917032  -0.74224523320596   0.48265892997336
 H      15.84346338321459   3.03289475613305  -1.56048131613338
 H      16.82316106055180   0.74956443275706  -1.40142482611398
 H      14.25886335882637   3.82974386744847   0.13620266537126
*

%Frag
  Definition
    1 {0:38} end
    2 {39:56} end
  end
```

```
end

###Ph-stacked o-phenylene TS input###

!TPSSh def2-TZVP EDA
!SMD(THF) D4
!printbasis printmos
!UCO UNO

%EDA              #EDA block
  FRAG1 "TPSSh def2-TZVP SMD(THF) D4"  #Method for fragment 1
  FRAG2 "TPSSh def2-TZVP SMD(THF) D4"  #Method for fragment 2
  FRAG1_C 0         #Charge of fragment 1
  FRAG1_M 2          #Multiplicity of fragment 1
  FRAG2_C 1         #Charge of fragment 2
  FRAG2_M 1          #Multiplicity of fragment 2
END

%pal nprocs 16
end

%maxcore 1000

*xyz 1 2
Co     16.327045000     4.272901000     5.864818000
N      11.501437000     2.933075000     5.184285000
C      12.032513000     3.458477000     6.440205000
C      14.877723000     3.332512000     4.782618000
H      14.659917000     2.276030000     4.859080000
C      15.844910000     3.927627000     3.903008000
H      16.479921000     3.394941000     3.208056000
C      11.208140000     3.241380000     7.551845000
H      10.319592000     2.629271000     7.432463000
C      14.243953000     4.369059000     5.545559000
C      14.915051000     5.592991000     5.201377000
H      14.706947000     6.561785000     5.636323000
C      11.607898000     1.449830000     5.078862000
H      12.655561000     1.149351000     4.978227000
H      11.047733000     1.126587000     4.198402000
H      11.177980000     0.993235000     5.971357000
C      13.211797000     4.215618000     6.582028000
C      11.914944000     3.579917000     3.912131000
H      12.820458000     3.130752000     3.500261000
H      12.077133000     4.646197000     4.069865000
H      11.098028000     3.441594000     3.197700000
C      13.426541000     4.856209000     7.819620000
```

```
H      14.315131000     5.469958000     7.926271000
C      11.477167000     3.829356000     8.779254000
H      10.812945000     3.654404000     9.620039000
C      15.860972000     5.327167000     4.157889000
H      16.507392000     6.057000000     3.689161000
C      12.577625000     4.680293000     8.901658000
H      12.785241000     5.183569000     9.841380000
C      17.349118000     2.830466000     6.889207000
H      17.189022000     1.767166000     6.768566000
C      18.277490000     3.629076000     6.136744000
H      18.922346000     3.272975000     5.344550000
C      16.677431000     3.678451000     7.823373000
H      15.905857000     3.375901000     8.517956000
C      18.140169000     4.975765000     6.568238000
H      18.665167000     5.832740000     6.167932000
C      17.135085000     5.010552000     7.597845000
H      16.786326000     5.898976000     8.107309000
H      10.148282000     3.182216000     5.219196000
C      10.428880000     6.868770000     6.656909000
C       9.780953000     7.407717000     7.774898000
C       9.913622000     5.749578000     6.022128000
C       8.728114000     5.128206000     6.489130000
C       8.058984000     5.714384000     7.594619000
C       8.588730000     6.827855000     8.229946000
C       8.236542000     3.920874000     5.886675000
C       6.837911000     3.434724000     6.098315000
H       6.788946000     2.803102000     6.998109000
H       6.536774000     2.815972000     5.248455000
H       6.127381000     4.255009000     6.225567000
O       8.981967000     3.157137000     5.135825000
H      11.334076000     7.334021000     6.276666000
H      10.396437000     5.372882000     5.129034000
H       8.075427000     7.248802000     9.090185000
H      10.190366000     8.279264000     8.277325000
H       7.145473000     5.265252000     7.971277000
*

%Frag
  Definition
    1 {0:38} end
    2 {39:56} end
  end
end


###SAMPLE input file for TD-DFT calculations###
```

```
# P1CH129n

! UKS TPSS0 D3ZERO def2-SVP def2/J
! Defgrid2 cpcm

%basis
newgto Co "def2-TZVP" end
end

%cpcm
smd true
SMDsolvent "tetrahydrofuran"
end

%tddft
nroots 50
maxdim 5
DoNTO true
NTOStates 1,2,3,4,5,6
end

%output
  Print[ P_Loewdin ] 1  # default = on
  Print[ P_AtPopMO_L    ] 1     # Print atomic charges in each MO
end

%scf MaxIter 300 end
%maxcore 3000

* xyzfile 1 2 P1CH129n.xyz
%pal nprocs 16 end
```

C11. REFERENCES

[1] S. Vanicek, H. Kopacka, K. Wurst, T. Müller, H. Schottenberger, B. Bildstein, "Chemoselective, Practical Synthesis of Cobaltocenium Carboxylic Acid Hexafluorophosphate" *Organometallics* **2014**, *33*, 1152–1156.
[2] Sheldrick, G. M. A short history of SHELX. *Acta Cryst. A*, **2008**, *64*, 112–122.
[3] Dolomanov, O. V.; Bourhis, L. J.; Gildea, R. J.; Howard, J. A. K.; Puschmann, H. OLEX2: A Complete Structure Solution, Refinement and Analysis Program. *J. Appl. Crystallogr.* **2009**, *42*, 339.
[4] Macpherson, J. V. A Practical Guide to Using Boron Doped Diamond in Electrochemical Research. *Phys. Chem. Chem. Phys.* **2015**, 17 (5), 2935–2949.
[5] Neese, F.; Wennmohs, F.; Becker, U.; Riplinger, C. The ORCA Quantum Chemistry Program Package. *J. Chem. Phys.* **2020**, *152*, 224108.
[6] Neese, F. Software update: The ORCA program system—Version 5.0. *WIREs Comput. Mol. Sci*. **2022**, 12:e1606.
[7] J. Tao, J. P. Perdew, V. N. Staroverov, G. E. Scuseria, Climbing the density functional ladder: nonempirical meta-generalized gradient approximation designed for molecules and solids. *Phys. Rev. Lett.* **2003**, *91*, 146401.
[8] V. N. Staroverov, G. E. Scuseria, J. Tao, J. P. Perdew, Comparative assessment of a new nonempirical density functional: Molecules and hydrogen-bonded complexes. *J. Chem. Phys.* **2003**, *119*, 12129–12137.
[9] F. Weigend, R. Ahlrichs, Balanced basis sets of split valence, triple zeta valence and quadruple zeta valence quality for H to Rn: Design and assessment of accuracy, *Phys. Chem. Chem. Phys.* **2005**, *7*, 3297–3305.
[10] A. V. Marenich, C. J. Cramer, D. G. Truhlar, Universal solvation model based on solute electron density and on a continuum model of the solvent defined by the bulk dielectric constant and atomic surface tensions *J. Phys. Chem. B.* **2009**, *113*, 6378–6396
[11] F. Weigend, Accurate Coulomb-fitting basis sets for H to Rn, *Phys. Chem. Chem. Phys.* **2006**, *8*, 1057–1065.
[12] Brown, J. H. Development and Use of a Cyclic Voltammetry Simulator To Introduce Undergraduate Students to Electrochemical Simulations. *J. Chem. Educ.* **2015**, *92*, 1490–1496.

Appendix D

Supplementary Information for Chapter 5

D1. Experimental Details

General Considerations

All manipulations were carried out using standard Schlenk or glovebox techniques under an N_2 atmosphere unless stated otherwise. Solvents were degassed by thoroughly sparging with N_2 gas and dried by passage through an activated alumina column in the solvent purification system by SG Water, USA LLC. All solvents were stored over activated 3 or 4 Å sieves prior to use. THF and diethyl ether were dried over NaK alloy and passed over activated alumina prior to use and were checked with a standard solution of sodium benzophenone ketyl in tetrahydrofuran to test for the presence of oxygen and moisture. All reagents were purchased from commercial vendors and used without further purification unless otherwise stated. Commercial $[Cp_2Co]PF_6$ from Strem was purified by recrystallization from acetonitrile/ether. $^nBu_4NPF_6$ was recrystallized from hot EtOH three times and dried under vacuum at 100 °C overnight. (4-bromophenyl)dichlorophosphine was prepared by a reported procedure.[1]

NMR Spectroscopy

NMR spectroscopy was performed using Varian and Bruker 400 MHz NMR spectrometers fitted with broadband auto-tune probes. Deuterated solvents were purchased from Cambridge Isotope Laboratories, Inc. Acetonitrile-d_3 and benzene-d_6 were degassed by three freeze-pump-thaw cycles, dried over activated 3 Å sieves, and passed over activated alumina. ^1H and ^{13}C chemical shifts are reported in ppm relative to tetramethylsilane using residual solvent resonances as internal standards. ^{31}P chemical shifts are reported using absolute referencing to an ^1H NMR spectrum collected concurrently.

UV-vis Spectroscopy

Spectra were collected using a Cary 60 spectrometer. 1-cm path quartz cells were pre-cooled in a Unisoku cryostat prior to analysis. All spectra were background corrected at the temperature at which spectra were collected.

X-ray Crystallography

X-ray diffraction (XRD) studies were carried out at the Beckman Institute Crystallography Facility on a Bruker Kappa Apex II diffractometer (Mo Kα radiation, λ = 0.71073 Å, or Cu Kα radiation, λ = 1.5406 Å). All crystals were mounted with Mitegen loops under STP oil. Structures were solved using SHELXS or SHELXT and refined against F^2 on all data by full-matrix least squares with SHELXL.[2] All structure solutions were performed in the Olex2 program.[3] Hydrogen atoms were placed in calculated positions and refined with a riding model. Non-hydrogen atoms were refined anisotropically.

Electrochemistry

Cyclic voltammetry (CV) measurements were carried out in an N_2-filled glovebox in a 20 mL scintillation vial with a Biologic potentiostat. For cyclic voltammetry experiments, a boron-doped diamond disk electrode was used as the working electrode; a freshly polished glassy carbon disk electrode was used as the counter electrode; a silver wire immersed in a solution of silver triflate (5 mM) and $^nBu_4PF_6$ (200 mM) separated from the working solution by a Coralpor frit was used as a pseudoreference electrode. Solution resistance was measured, and a correction of 85% of the

uncompensated resistance was applied. All reported potentials are referenced to the ferrocene/ferrocenium couple, measured at the end of each experiment.

DFT Calculations

All calculations were performed using density functional theory (DFT) implemented in the ORCA 6.0.1 program.[4,5] The TPSS functional with Grimme's D4 correction was used throughout this study.[6,7] Geometry optimizations were performed with the def2-TZVP basis set[8] with the SMD solvation model using THF.[9] In cases where crystal structures were available, those coordinates were used as the input. Single-point vibrational frequency calculations were performed to ensure that stationary points were absent of any imaginary frequencies and thus were local minima on the potential energy surface. Bond dissociation free energies (BDFEs) were calculated by an established method using the calculated free energy of the H atom.

D2. Synthetic Procedures

(4-bromophenyl)dimethylphosphine

Adapted from a literature procedure.[10] In the N_2 glovebox, (4-bromophenyl)dichlorophosphine [2.00 g] was added to a 250 mL round bottom flask containing a stir bar and dissolved in diethyl ether [50 mL]. The flask was cooled in the cold well with an ice-water bath. Methyl magnesium chloride [5.4 mL, 3.0 M] was added dropwise to the flask, forming a white precipitate. The reaction was stirred in the cold well for one hour and then at room temperature for one hour. The reaction was filtered over Celite and washed with ether [2 x 5 mL]. The solution was pumped down, yielding a crude, pale brown oil. The oil was purified by vacuum distillation [50 mTorr, 110 °C], yielding 775 mg (46%) of a colorless oil that was analyzed by ^{1}H and ^{31}P NMR spectroscopy.

^{1}H NMR (400 MHz, C_6D_6) δ 7.24 (d, *J* = 8.0 Hz, 2H), 6.96 (dd, *J* = 8.2, 6.2 Hz, 2H), 0.93 (d, *J* = 3.3 Hz, 6H).
^{13}C NMR (101 MHz, C_6D_6) δ 142.44 (d, J = 17.1 Hz), 132.51 (d, J = 18.0 Hz), 131.68 (d, J = 5.7 Hz), 122.60, 14.36 (d, J = 14.5 Hz).
^{31}P NMR (162 MHz, C_6D_6) δ −46.41.

Cp(η^4-C_5H_5-PhPMe_2)Co

In the N_2 glovebox, (4-bromophenyl)dimethylphosphine [300 mg] was dissolved in THF [12 mL] and cooled in the cold well with a dry ice-acetone bath. n-butyllithium [0.48 mL, 2.6 M] was added dropwise, forming a pale-yellow solution, and the reaction was stirred in the cold well for 45 minutes. Solid cobaltocenium hexafluorophosphate [414 mg, 1.24 mmol] was added, forming a red solution. The reaction was allowed to stir overnight, during which time it warmed up to room temperature. The volatiles were removed *in vacuo*, yielding a red solid which was extracted with pentane [4 x 5 mL], filtered over alumina, and concentrated via slow evaporation to yield 318 mg (71 %) of diffraction-quality red crystals.

^{1}H NMR (C_6D_6, 400 MHz, 298 K) δ: 7.33 (t, J = 7.2 Hz, 2H), 6.87 (d, J = 7.8 Hz, 2H), 5.06 – 5.04 (m, 2H), 4.60 (s, 5H), 3.88 (t, J = 2.6 HZ, 1H), 2.83 – 2.81 (m, 2H), 1.06 (d, J = 2.3 Hz, 6H).
^{13}C{^{1}H} NMR (C_6D_6, 101 MHz, 298 K) δ: 146.25, 130.95, 125.68, 79.53, 75.08, 56.34, 44.65, 14.80
^{31}P{^{1}H} NMR (C_6D_6, 162 MHz, 298 K) δ: −47.81.

Cp(η^4-C_5H_5-PhP(BH_3)Me_2)Co

In the N_2 glovebox, Cp(η^4-C_5H_5-PhPMe_2)Co [200 mg] was dissolved in benzene [~5 mL] in a scintillation vial fitted with a septum. The vial was removed from the glovebox, connected to an N_2 inlet needle, and borane dimethylsulfide [116 μL] was added to the vial. The reaction was stirred for 30 minutes. The solvent was removed, yielding a red powder that was recrystallized from hot hexanes to yield 194 mg (93%) of red needles.

^{1}H NMR (C_6D_6, 400 MHz, 298 K) δ: 7.43 (dd, J = 10.6, 8.2 Hz, 1H), 6.79 (dd, J = 8.0, 2.0 Hz, 1H), 5.05 – 4.99 (m, 1H), 3.80 (t, J = 2.6 Hz, 1H), 2.74 (td, J = 2.5, 1.5 Hz, 1H), 0.95 (d, J = 10.2 Hz, 4H).
^{11}B NMR (C_6D_6, 128 MHz, 298 K) δ: −37.40 (dq, J = 97.0, 57.8 Hz).
^{31}P{^{1}H} NMR (C_6D_6, 162 MHz, 298 K) δ: 1.78 (q, J = 56.5 Hz).

$CpCoCp^{PBH3}$

In the N_2 glovebox, $Cp(\eta^4\text{-}C_5H_5\text{-}PhP(BH_3)Me_2)Co$ [100 mg, 0.29 mmol] was dissolved in benzene [8 mL] and methylcyclohexane [40 mL] in a 200 mL Schlenk flask. The flask was sealed, removed from the box, and heated in an oil bath to 120 °C for three days, during which time the reaction became dark blue. The solvent was evacuated, leaving behind a blue solid which was extracted into pentane [~50 mL]. The pentane solution was placed in the freezer overnight [−35 °C], during which time crystals formed. The supernatant was removed, leaving behind 39 mg (40%) of a crystalline blue solid.

^{1}H NMR (C_6D_6, 400 MHz, 298 K) δ: 16.09 (bs, 2H), 2.24 (bq, J = 96.7 Hz, 3H), 2.19 (d, J = 8.7 Hz, 6H), −3.52 (bs, 2H), −17.66 (bs, 2H), −49.76 (bs, 5H), −50.86 (bs, 2H).
^{11}B{^{1}H} NMR (C_6D_6, 128 MHz, 298 K) δ: −31.79 (dq, J = 96.9, 56.9 Hz).
^{31}P{^{1}H} NMR (C_6D_6, 162 MHz, 298 K) δ: −115.57 (bd, J = 56.3 Hz).

$[CpCoCp^{PBH3}]OTf$

In the N_2 glovebox, $CpCoCp^{PBH3}$ [13 mg, 0.038 mmol] was dissolved in THF [1 mL] in a 20 mL scintillation vial and cooled in the freezer [−35 °C]. A pre-cooled solution of ferrocenium triflate [12 mg, 0.036 mmol] in THF [~1 mL] was added dropwise. The reaction was allowed to stir at room temperature for 30 minutes, during which time the mixture warmed to room temperature and changed color from blue to yellow. The solvent was removed *in vacuo*, and the resulting yellow film was washed with pentane [3 x 2 mL] and dried, yielding 16 mg (94%) of a yellow solid.

^{1}H NMR (C_6D_6, 300 MHz, 298 K) δ: 7.92 – 7.77 (m, 4H), 6.24 (t, J = 2.2 Hz, 2H), 5.82 (t, J = 2.3 Hz, 2H), 5.53 (s, 5H), 1.59 (d, J = 10.6 Hz, 6H).
^{31}P{^{1}H} NMR (C_6D_6, 121 MHz, 298 K) δ: 3.21 (q, J = 57.7 Hz).

$[CpCoCp^{P}](OTf)_2$

In the N_2 glovebox, $[CpCoCp^{PBH3}]OTf$ [16 mg, 0.038 mmol] and 1,4-diazobicyclo[2.2.2]octane [11 mg] were dissolved in THF [~1.5 mL] in a J. Young tube. The tube was removed from the box and heated in an oil bath [70 °C] overnight. The tube was brought back into the glovebox, and diphenylammonium triflate [0.9 eq] was added, resulting in the formation of a precipitate. The mixture was placed in the freezer [−35 °C] for one hour. Then, the solution was decanted off, and the solid was washed with cold THF [2 x 1 mL], yielding 16 mg (73%) of a microcrystalline yellow solid.

^{1}H NMR (CD_3CN, 400 MHz, 298 K) δ 8.04 (d, *J* = 6.9 Hz, 2H), 7.96 (t, *J* = 11.1 Hz, 2H), 6.32 (t, J = 1.7 Hz, 2H), 5.87 (t, J = 2.1 Hz, 2H), 5.56 (s, 5H), 2.17 (d, J = 15.6 Hz, 6H).
^{19}F NMR (CD_3CN, 376 MHz, 298 K) δ: 3.21 (s).
^{31}P{^{1}H} NMR (CD_3CN, 162 MHz, 298 K) δ: −0.06 (s)

D3. NMR Spectra

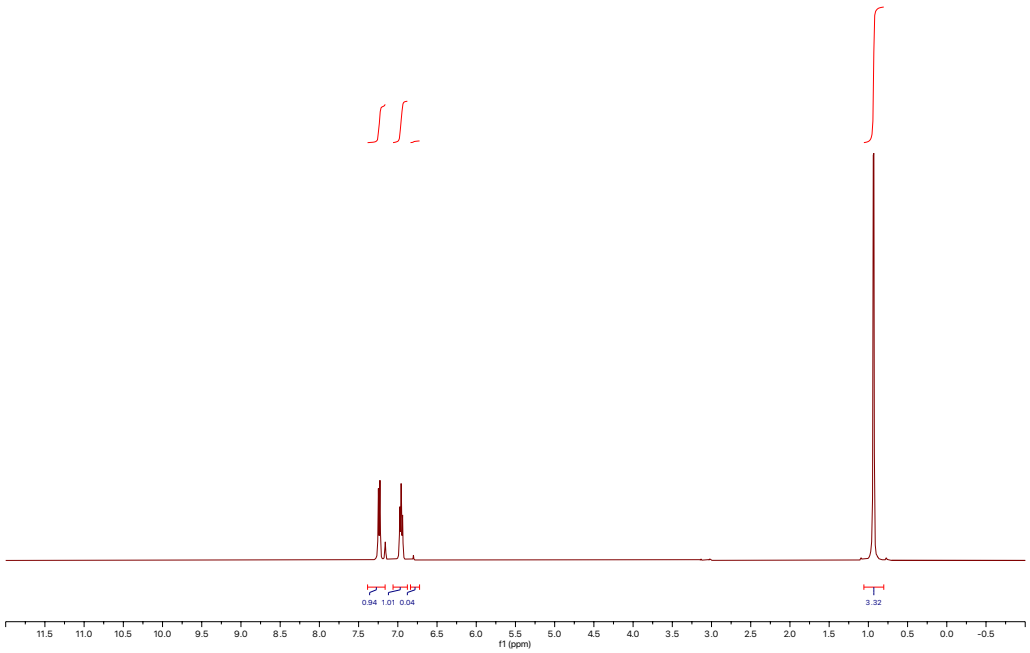

Figure D1. ^{1}H NMR spectrum of **(4-bromophenyl)dimethylphosphine** in C_6D_6 (400 MHz)

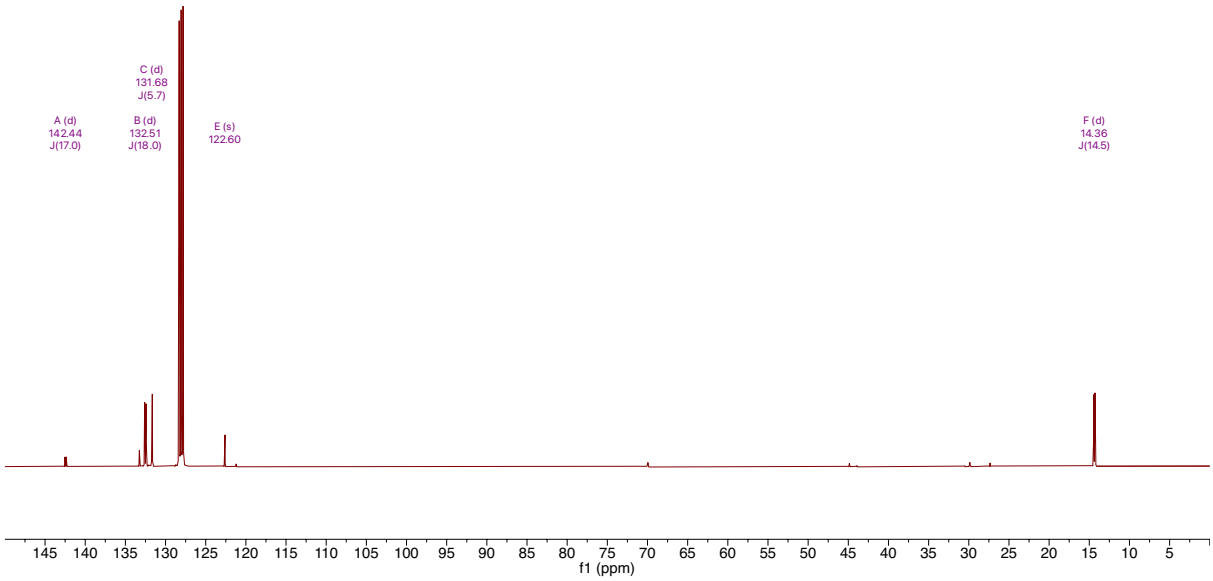

Figure D2. ^{13}C NMR spectrum of **(4-bromophenyl)dimethylphosphine** in C_6D_6 (101 MHz)

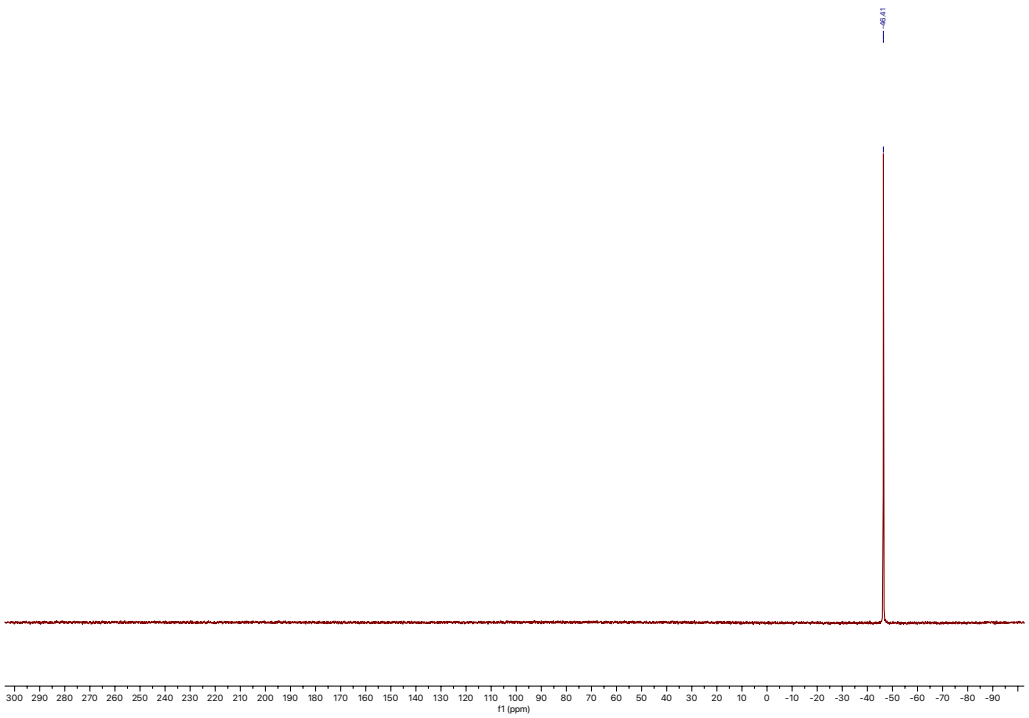

Figure D3. ^{31}P NMR spectrum of **(4-bromophenyl)dimethylphosphine** in C_6D_6 (162 MHz)

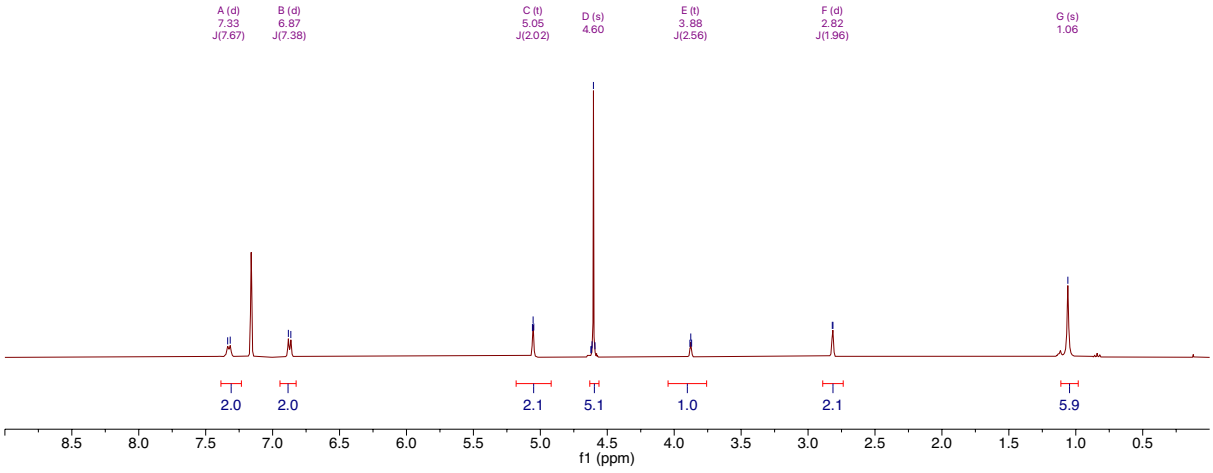

Figure D4. ^{1}H NMR spectrum of **Cp(η^4-C_5H_5-PhPMe$_2$)Co** in C_6D_6 (400 MHz)

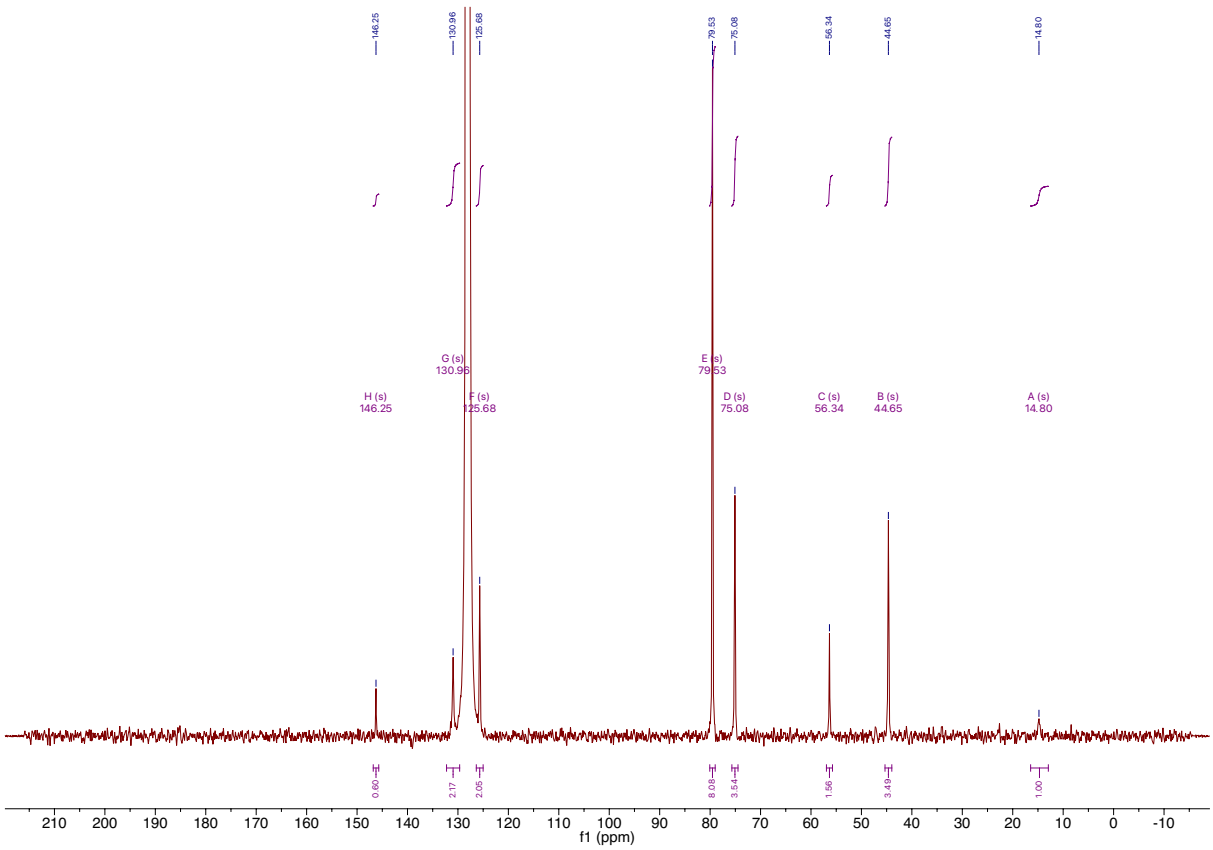

Figure D5. $^{13}C\{^{1}H\}$ NMR spectrum of **Cp(η^4-C_5H_5-PhPMe$_2$)Co** in C_6D_6 (101 MHz).

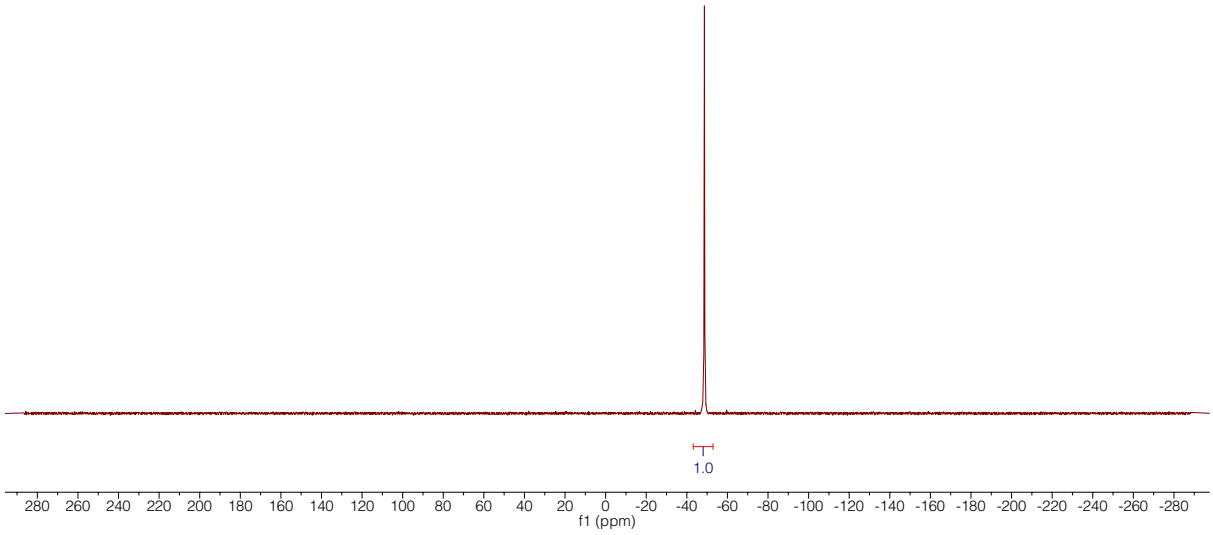

Figure D6. $^{31}P\{^{1}H\}$ NMR spectrum of **Cp(η^4-C_5H_5-PhPMe$_2$)Co** in C_6D_6 (162 MHz).

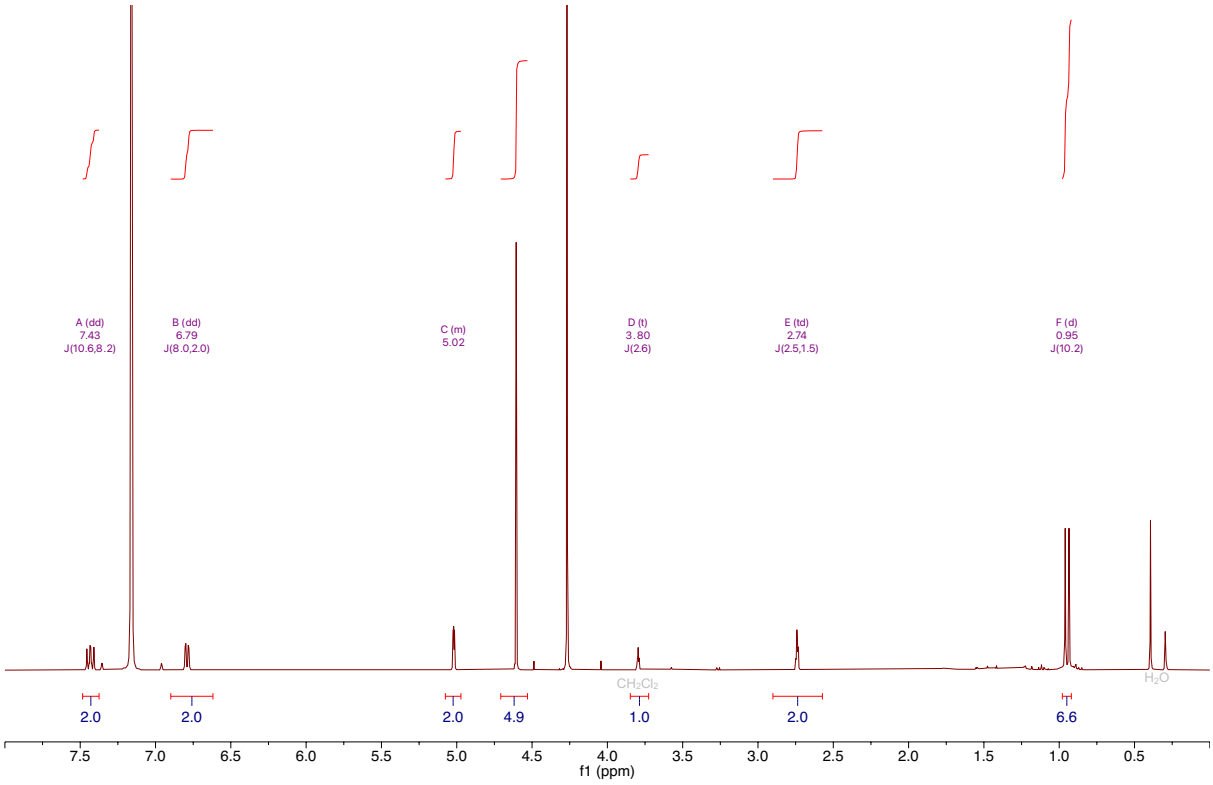

Figure D7. ^{1}H NMR spectrum of **Cp(η^4-C_5H_5-PhP(BH_3)Me_2)Co** in C_6D_6 (400 MHz)

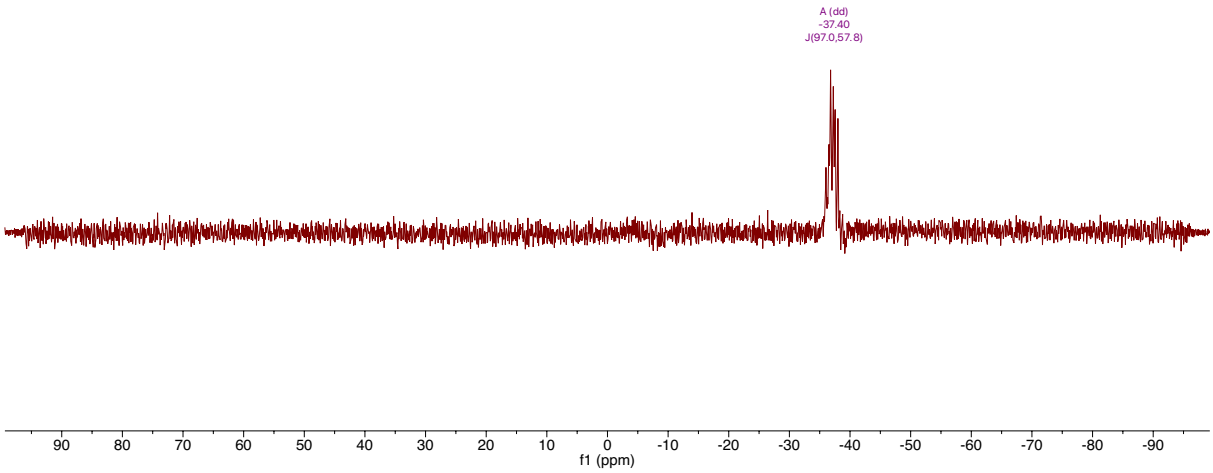

Figure D8. ^{11}B NMR spectrum of **Cp(η^4-C_5H_5-PhP(BH_3)Me_2)Co** in CD_3CN (128 MHz).

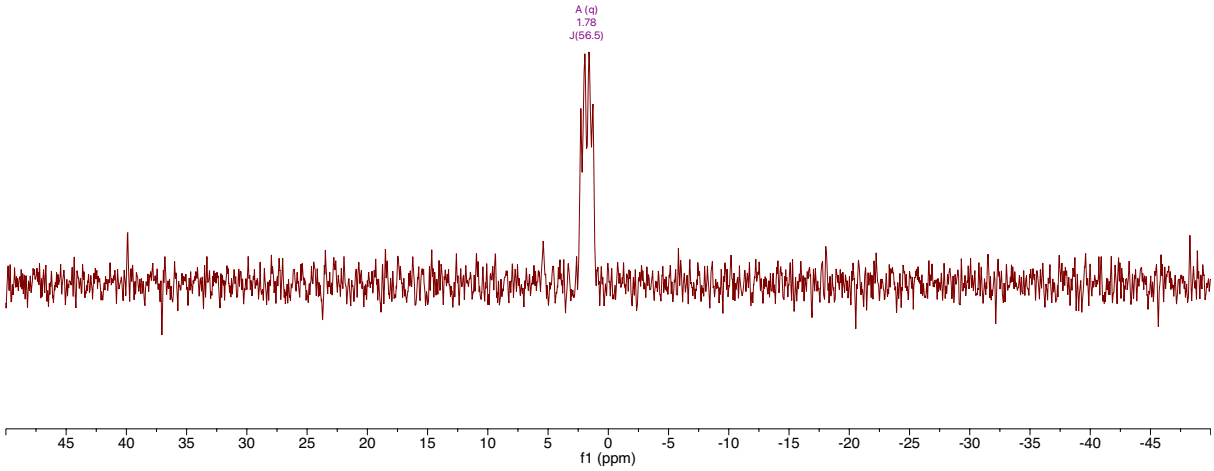

Figure D9. $^{31}P\{^{1}H\}$ NMR spectrum of **Cp(η⁴-C₅H₅-PhP(BH₃)Me₂)Co** in C_6D_6 (162 MHz).

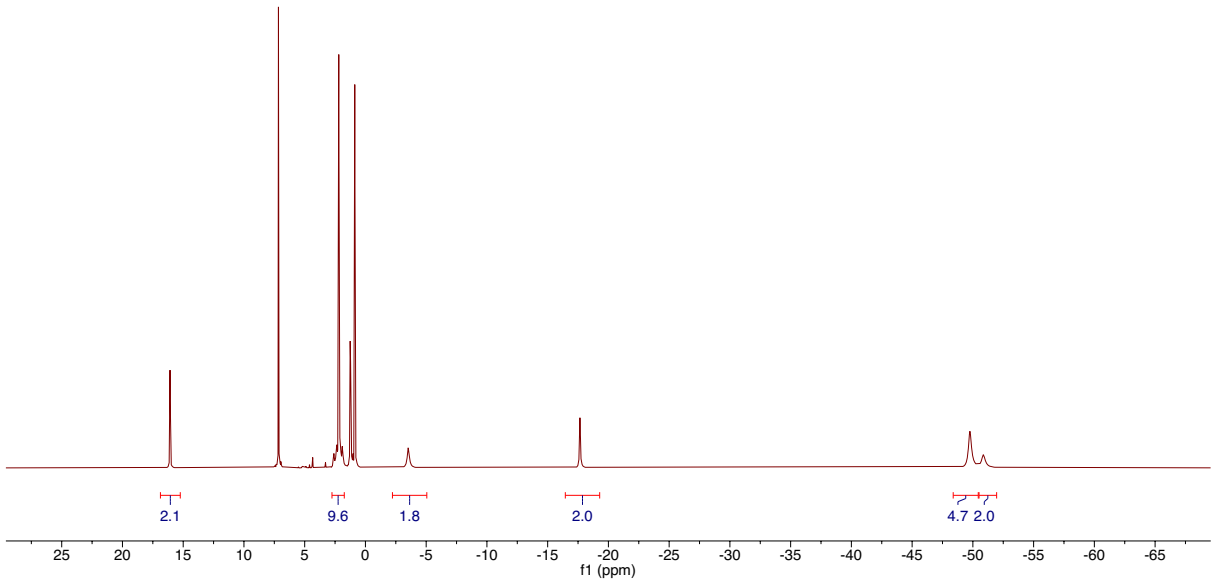

Figure D10. ^{1}H NMR spectrum of **CpCoCp^{PBH3}** in C_6D_6 (400 MHz)

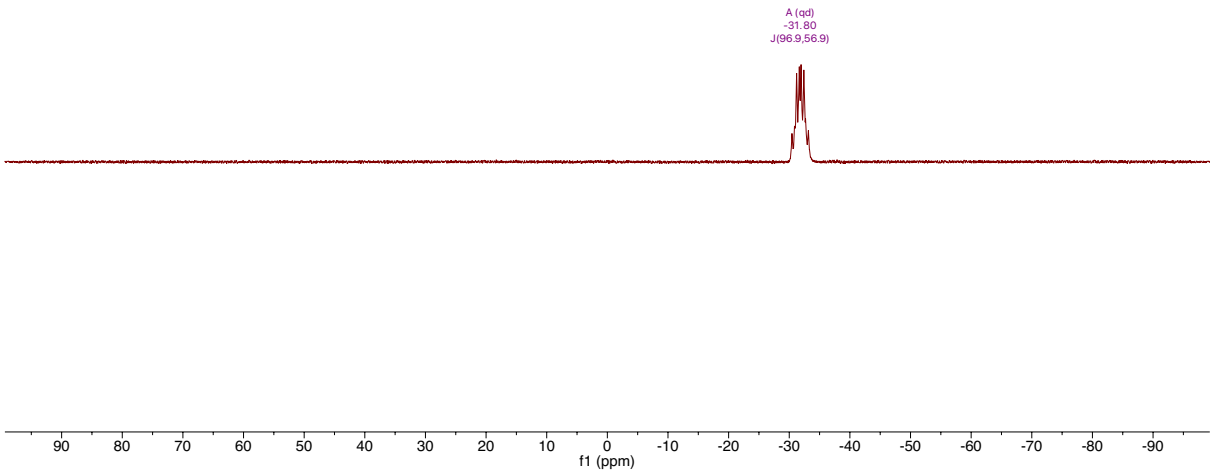

Figure D11. ^{11}B NMR spectrum of **CpCoCp^{PBH3}** in C_6D_6 (128 MHz).

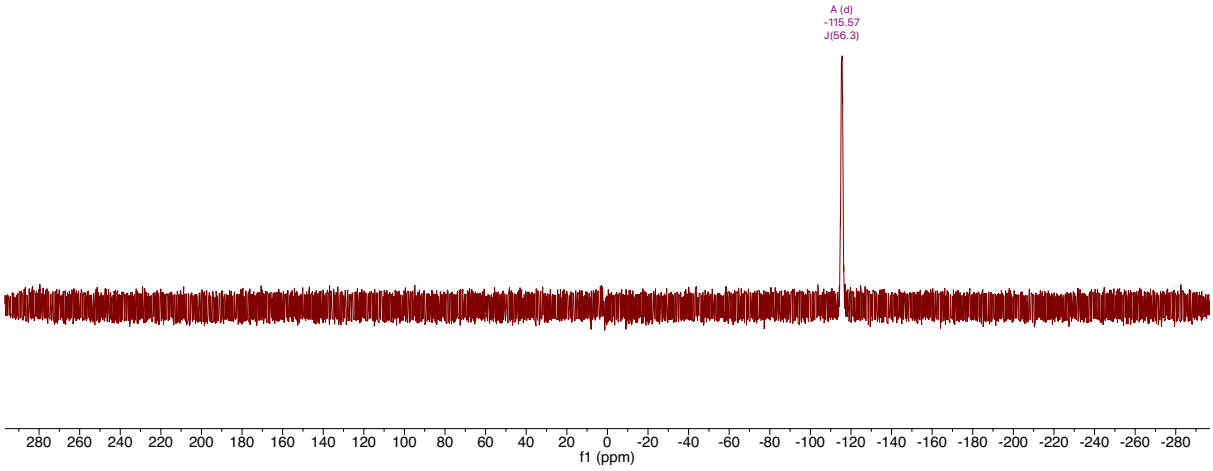

Figure D12. ^{31}P{^{1}H} NMR spectrum of **CpCoCp^{PBH3}** in C_6D_6 (162 MHz).

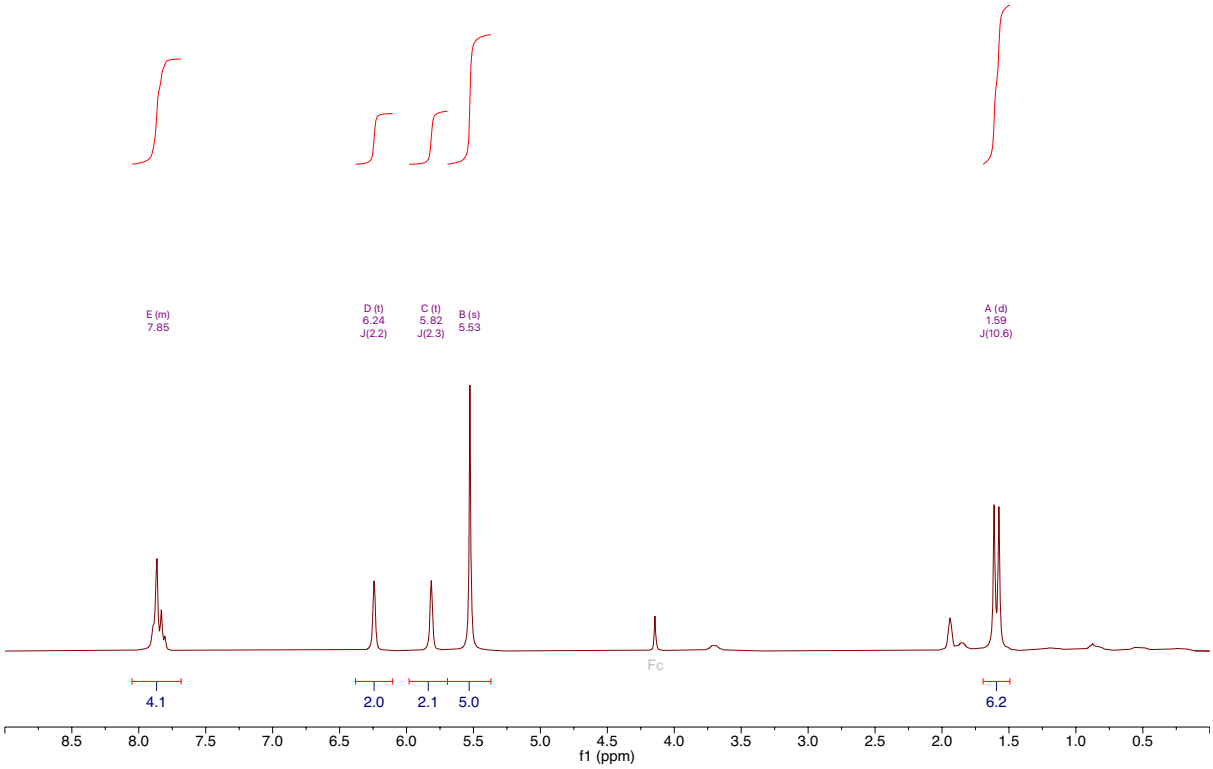

Figure D13. ^{1}H NMR spectrum of **[CpCoCp^{PBH3}]OTf** in CD_3CN (400 MHz).

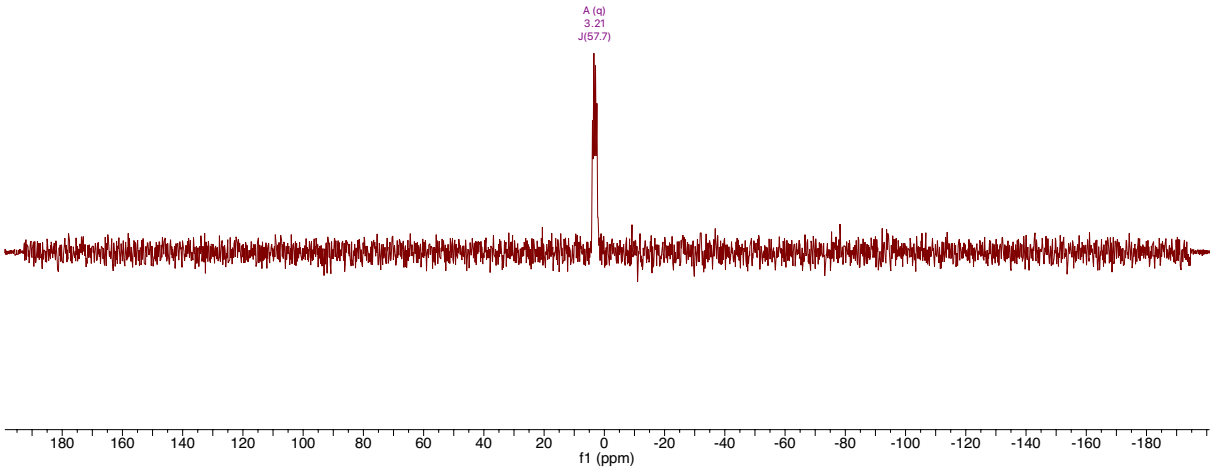

Figure D14. ^{31}P{^{1}H} NMR spectrum of **[CpCoCp^{PBH3}]OTf** in CD_3CN (162 MHz).

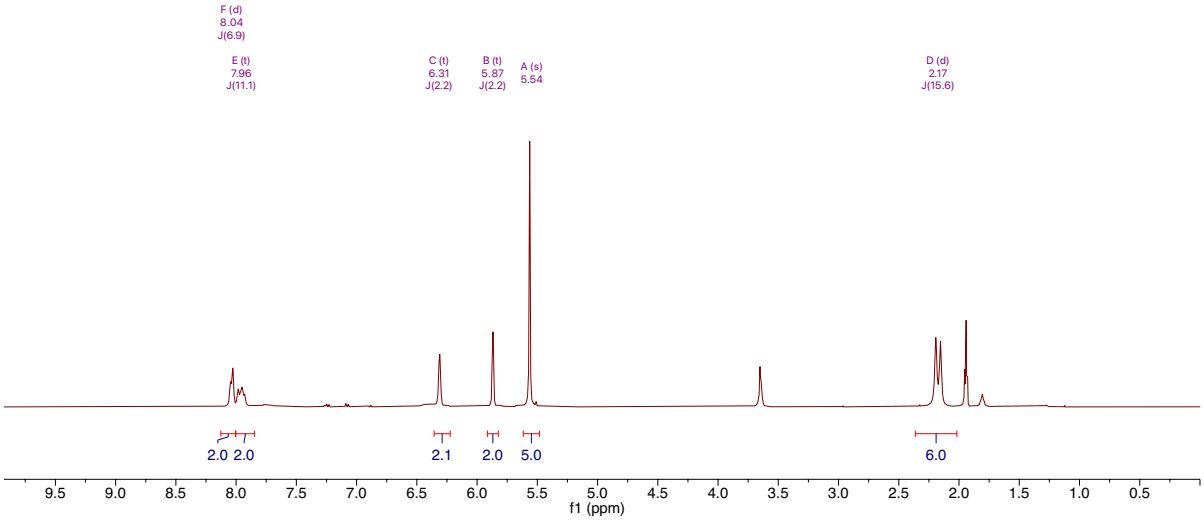

Figure D15. ^{1}H NMR spectrum of **[CpCoCp^{P}]OTf** in CD_3CN (400 MHz).

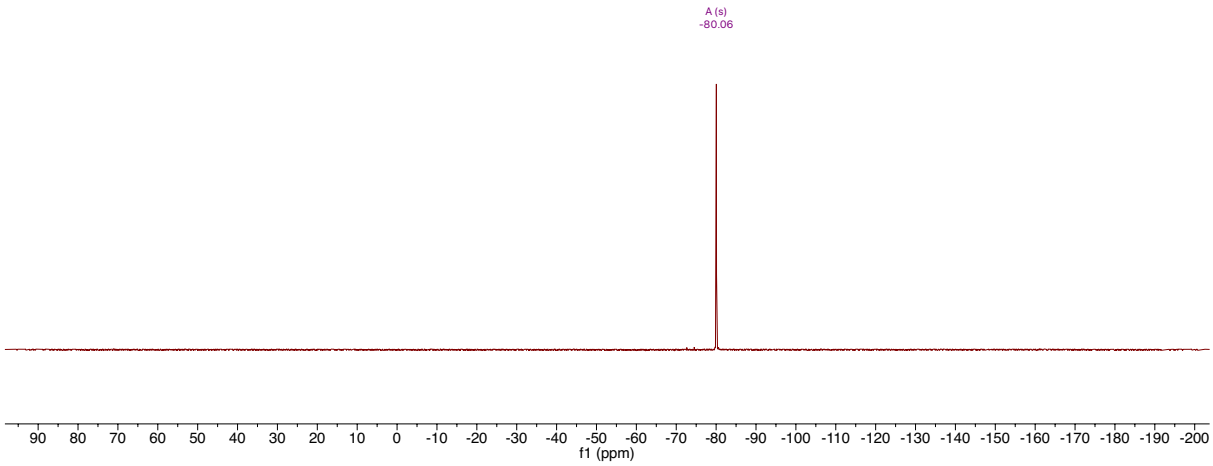

Figure D16. ^{19}F NMR spectrum of **[CpCoCp^{P}]OTf** in CD_3CN (376 MHz).

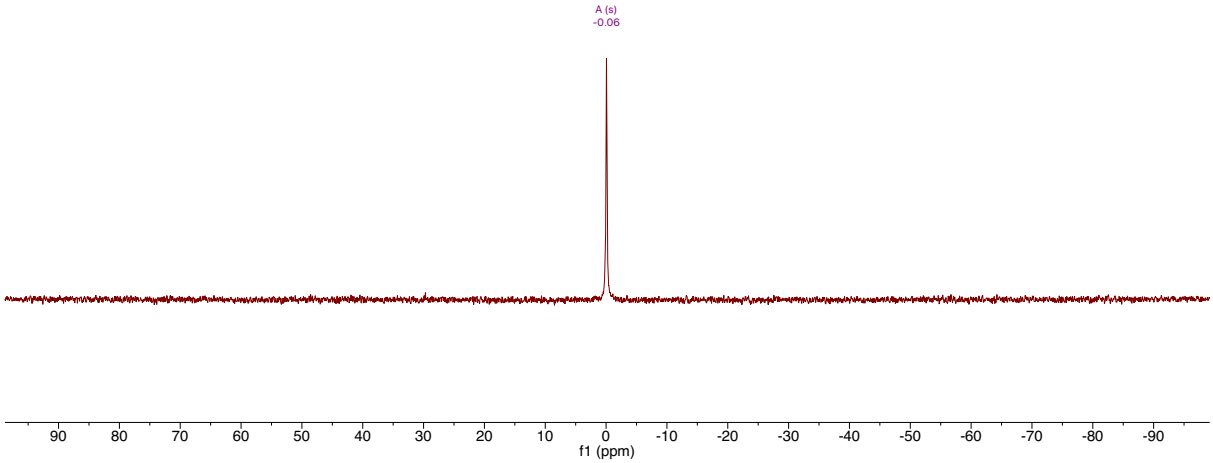

Figure D17. $^{31}P\{^{1}H\}$ NMR spectrum of **[CpCoCp^{P}]OTf** in CD_3CN (162 MHz).

D4. X-Ray Crystallography

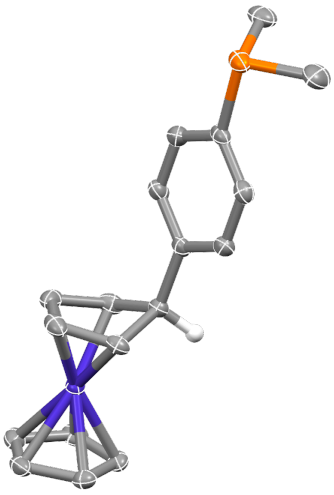

Figure D18. X-Ray Diffraction structure of **CpCo(η^4-C_5H_5-$PhPMe_2$)** with thermal ellipsoids set at 50%.

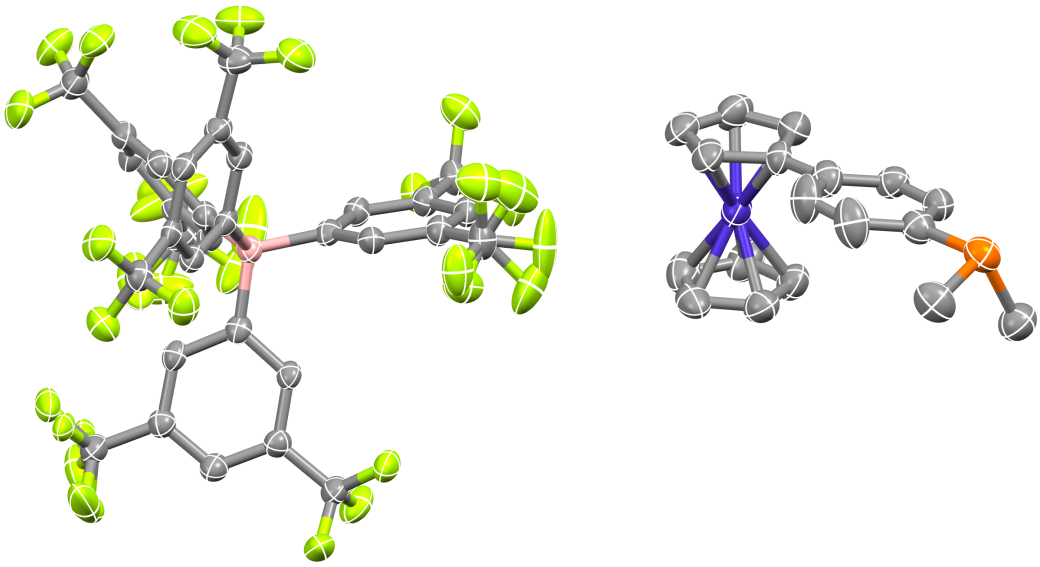

Figure D19. X-Ray Diffraction structure of **[CpCoCp^P]BAr$^F{}_4$** with thermal ellipsoids set at 50%. The structure contains rotational disorder of the trifluoromethyl moiety on [BAr$^F{}_4$] anion.

Table D1. Crystallographic data for complexes.

Compound	**CpCo(η^4-C_5H_5-*p*-PhPMe$_2$)**	**[CpCoCp^P]BAr^F**
Empirical formula	$C_{18}H_{20}PCo$	$C_{50}H_{31}BF_{24}PCo$
Formula weight	326.24	1188.46
Temperature (K)	100.00	100.00
Crystal system	Triclinic	Monoclinic
Space group	P-1	$P2_1/n$
a (Å)	5.7807(5)	9.1283(10
b (Å)	9.2577(12)	32.289(4)
c (Å)	14.4821(12)	16.9753(19)
α (°)	89.788(3)	90
β (°)	83.348(4)	104.674(3)
γ (°)	80.693(4)	90
Volume (Å^3)	759.58(13)	4840.2(9)
Z	2	4
ρ_{calc} [g/cm^3]	1.426	1.631
μ (mm^{-1})	1.222	0.517
F (000)	340.0	2376.0
Radiation	MoKα (λ = 0.71073)	MoKα (λ = 0.71073)
Reflections collected	18388	69485
Unique reflections	3485	11122
Data/restraints /parameters	3485/0/183	11122/794/780
R(int)	0.0423	0.1719
R_1 (I > 2 σ(I))	0.0366	0.0767
wR_2	0.09165	0.2797
GOOF	1.155	1.021

D5. Electrochemistry

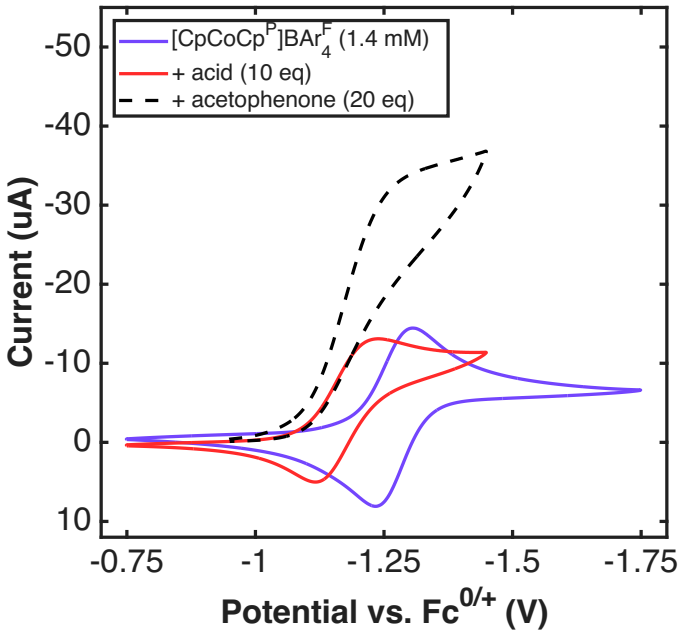

Figure D20. Cyclic voltammogram of **[CpCoCp^{P}]BAr^{F}** (1.4 mM, *blue*) with 4-cyanoanilinium triflate (14 mM, *red*) and acetophenone (24 mM, *black*) in MeCN with $^{n}Bu_4PF_6$ (200 mM) supporting electrolyte. The scans are swept cathodic, then anodic at 100 mV/s.

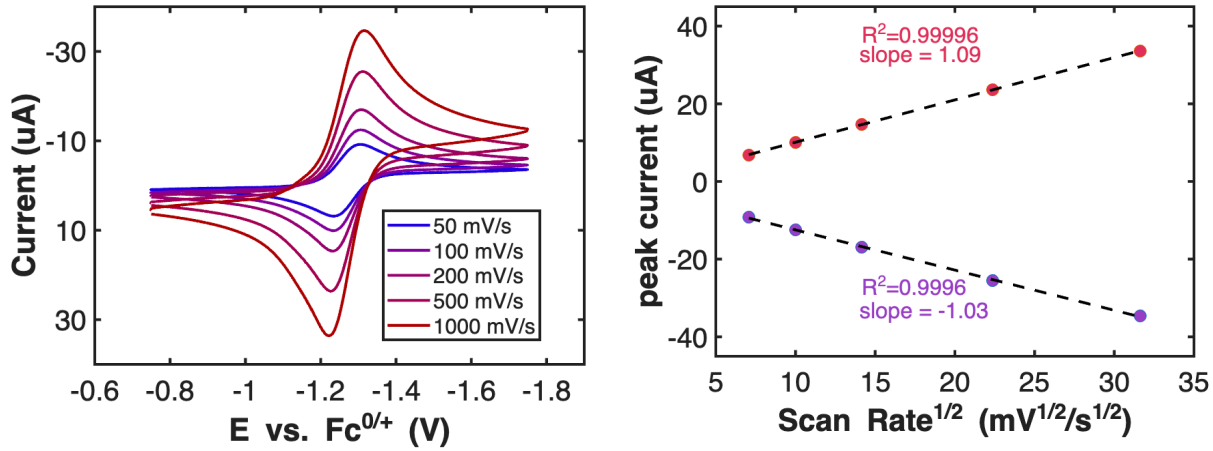

Figure D21. (left) Cyclic voltammograms of **[CpCoCp^{P}]BAr^{F}** (1.4 mM) at various scan rates in MeCN with $^{n}Bu_4PF_6$ (200 mM) supporting electrolyte. The scans are swept cathodic, then anodic at the scan rate indicated in the legend. (right) Peak cathodic and peak anodic currents plotted as a function of the square of the scan rate.

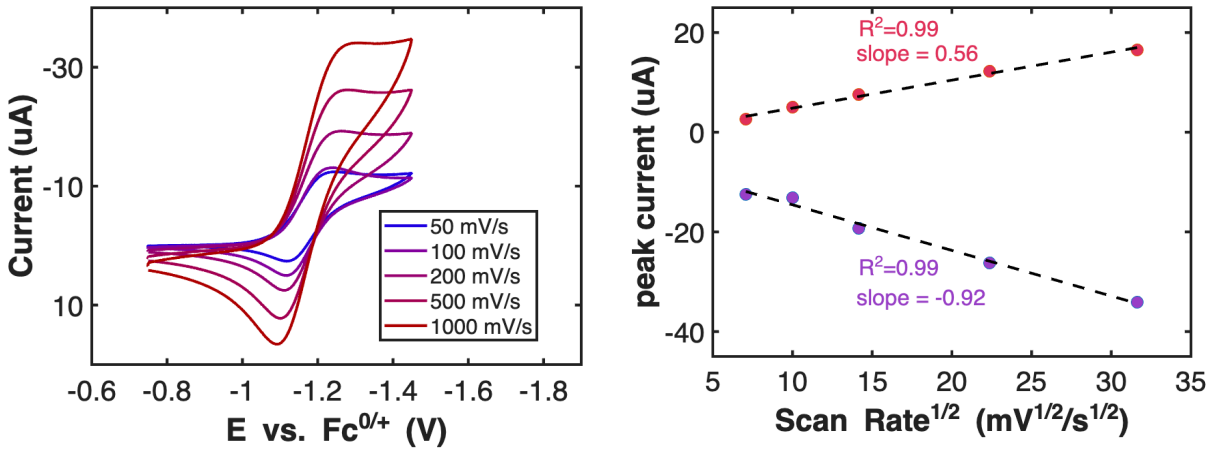

Figure D22. (left) Cyclic voltammograms of **[CpCoCp^{P}]BAr^{F}** (1.4 mM) with 4-cyanoanilinium triflate (14 mM) at various scan rates in MeCN with $^{n}Bu_4PF_6$ (200 mM) supporting electrolyte. The scans are swept cathodic, then anodic at the scan rate indicated in the legend. (right) Peak cathodic and peak anodic currents plotted as a function of the square of the scan rate.

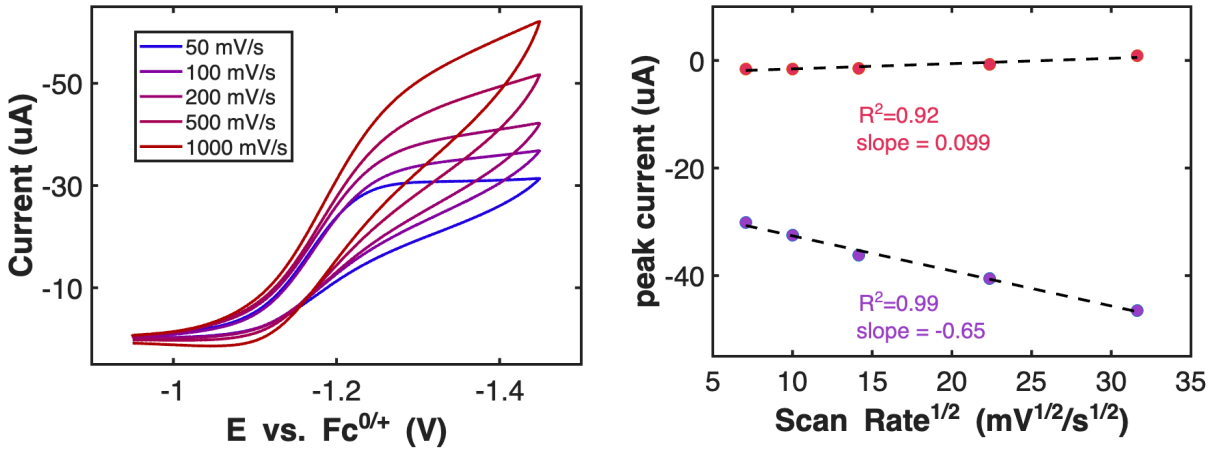

Figure D23. (left) Cyclic voltammograms of **[CpCoCp^{P}]BAr^{F}** (1.4 mM) with 4-cyanoanilinium triflate (14 mM) and acetophenone (24 mM) at various scan rates in MeCN with $^{n}Bu_4PF_6$ (200 mM) supporting electrolyte. The scans are swept cathodic, then anodic at the scan rate indicated in the legend. (right) Peak cathodic and peak anodic currents plotted as a function of the square of the scan rate.

D6. pK_a Determination

The acid dissociation constant of the phosphonium-appended cobaltocene complex was determined using a method used in previous studies from our group.[11] ^{1}H NMR spectroscopy is used to measure the proton transfer equilibrium between a phosphine of interest and an acid with a known pK_a. The chemical shifts of the phosphine and reference acid can be used to determine their concentration as well as their conjugate acid concentrations using the following equation:

$$[CpCoCp^{PH+}] = \frac{\delta_{obs} - \delta_{CpCoCp^P}}{\delta_{CpCoCp^{PH+}} - \delta_{CpCoCp^P}}$$

$$[CpCoCp^P] = [Co]_{tot} - [CpCoCp^{PH+}]$$

Similarly for $^{3\text{-Cl}}$PyrH$^+$ / $^{3\text{-Cl}}$Pyr:

$$[^{3-Cl}PyrH^+] = \frac{\delta_{obs} - \delta_{^{3-Cl}Pyr}}{\delta_{^{3-Cl}PyrH^+]} - \delta_{^{3-Cl}Pyr}}$$

$$[^{3-Cl}Pyr] = [^{3-Cl}Pyr]_{tot} - [^{3-Cl}PyrH^+]$$

From these concentrations, the K_{eq} can be determined:

$$K_{eq} = \frac{[CpCoCp^P][^{3-Cl}PyrH^+]}{[CpCoCp^{PH+}][^{3-Cl}Pyr]}$$

With K_{eq} and the known reference acid pK_a ($K_{a,ref}$), the analyte pK_a can be determined:

$$K_a = \frac{K_{eq}}{K_{a,ref}}$$

$$pK_a = -\log\{K_{eq}/K_{a,ref}\}$$

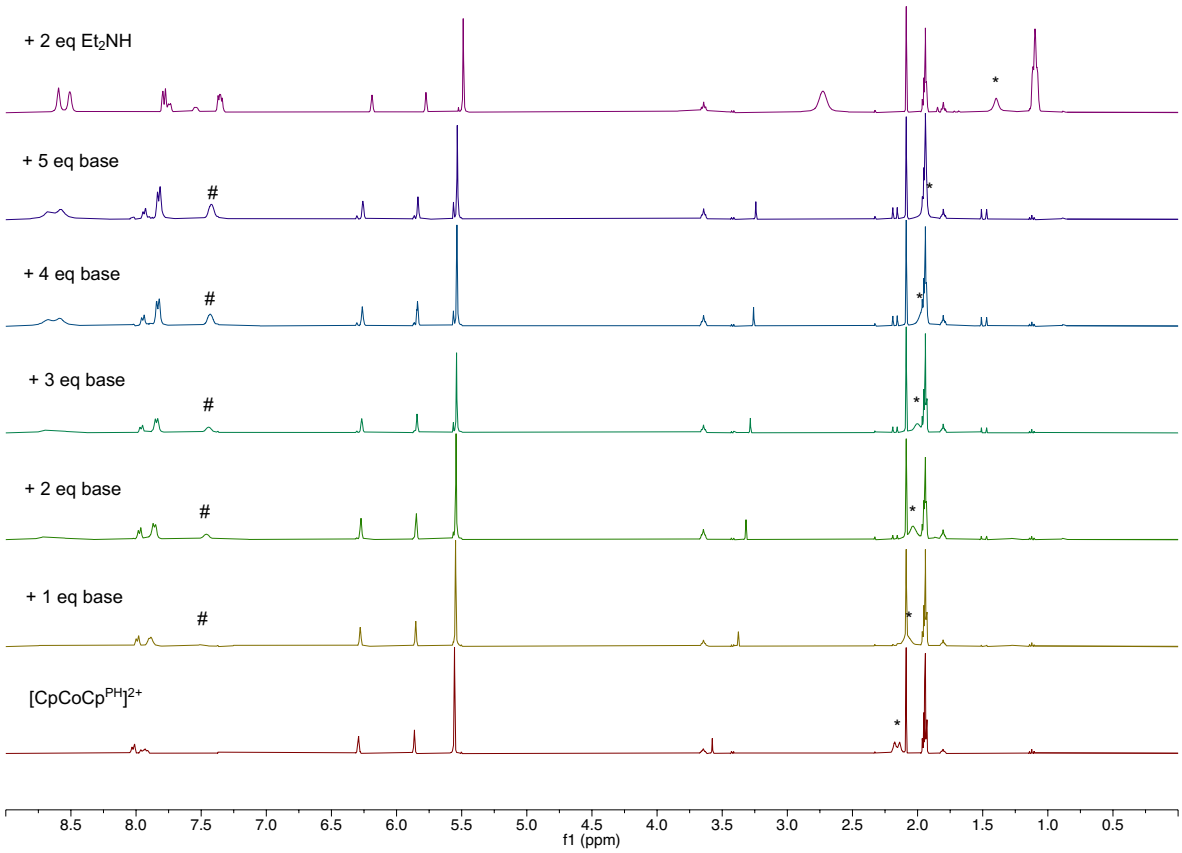

Figure D24. ^{1}H NMR Spectra of [CpCoCp^{PH}](OTf)$_2$ with 0-5 equivalents of 3-chloropyridine added in CD_3CN. The starred (*) and tagged (#) Co-P*Me*$_2$ peak and 3-chloropyridine peak shifts, respectively, are used as reporters of the analytes' concentrations.

Table D2. Reporter peak shifts from the ^{1}H NMR spectroscopy base titration of [CpCoCp^{PH}](OTf)$_2$ and the resulting equilibrium constant K_{eq}.

equiv. base added	# shift (ppm)	* shift (ppm)	[Co^{PH+}]	[Co^{P}]	[$^{3\text{-Cl}}$Pyr]	[$^{3\text{-Cl}}$PyrH^{+}]	K_{eq}
0	-	2.157	0	1	0	0	-
1	7.496	2.080	0.899	0.101	0.777	0.223	30.881
2	7.459	2.036	0.841	0.159	1.656	0.344	25.391
3	7.441	2.002	0.796	0.204	2.558	0.442	22.580
4	7.431	1.963	0.745	0.255	3.466	0.534	18.919
5	7.422	1.940	0.714	0.286	4.394	0.606	18.142

Determined as the average of rows in **Table D2**, the resulting equilibrium constant K_{eq} is determined to be 23.18. From this K_{eq} value and the known pK_a of $^{3\text{-Cl}}$PyrH^{+} (9.56) in MeCN, the pK_a of **[CpCoCp^{PH}]$^{+}$** is determined to be 10.9 ± 0.1.

D7. Kinetic Analysis

Determination of the second order PCET rate constant (k_{PCET}) was performed using cyclic voltammetry according to reported methods.[12] The reaction is modeled as with the catalytic E_rC_i' mechanism, in which a reactive species is generated by electron transfer and undergoes a subsequent rate-limiting chemical step. Here, the Co(III/II) reduction is the electrochemical step, and PCET to acetophenone is the rate-limiting chemical step.

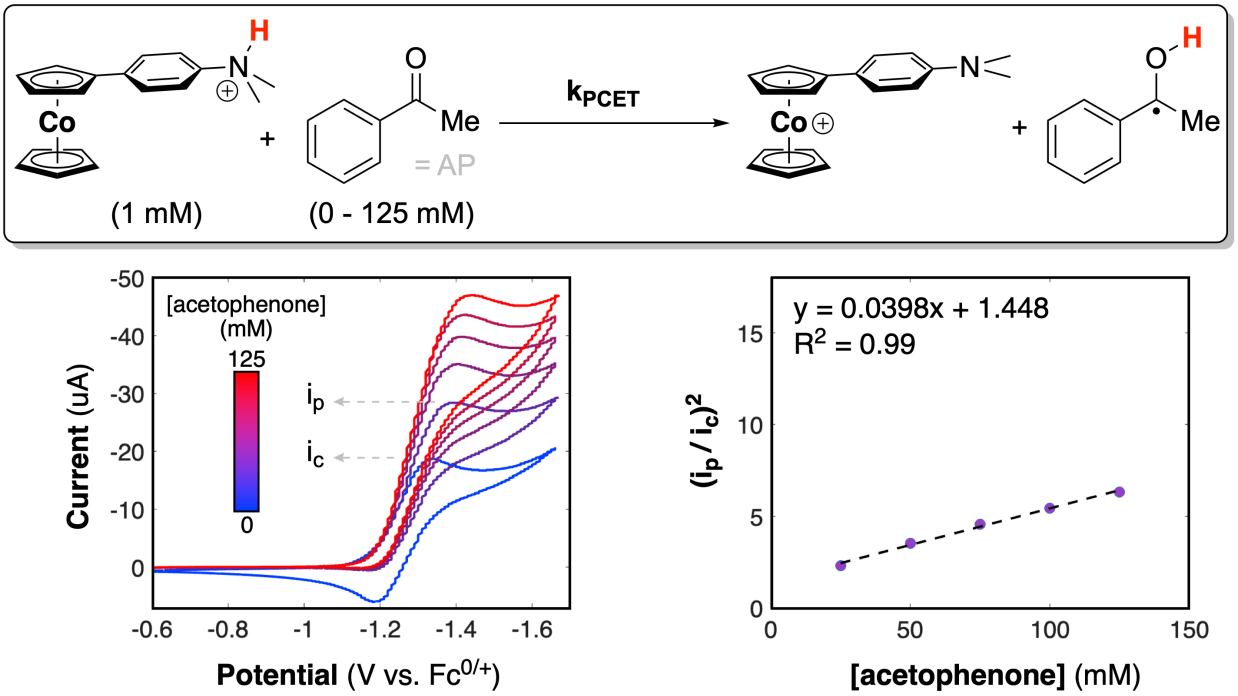

Figure D25. (top) Scheme for the determination of k_{PCET} for Cp**Co**Cp^{NH+} to acetophenone. (bottom left) Cyclic voltammograms of [CpCoCp^N]OTf (1 mM) in acetonitrile with tosic acid (20 mM) and ^{n}Bu$_4$PF$_6$ (100 mM) supporting electrolyte. The scans are swept cathodic, then anodic at a scan rate of 100 mV/s. (bottom right) Plots of the square of the ratio of the catalytic plateau current and the peak current in the absence of substrate as a function of acetophenone concentration.

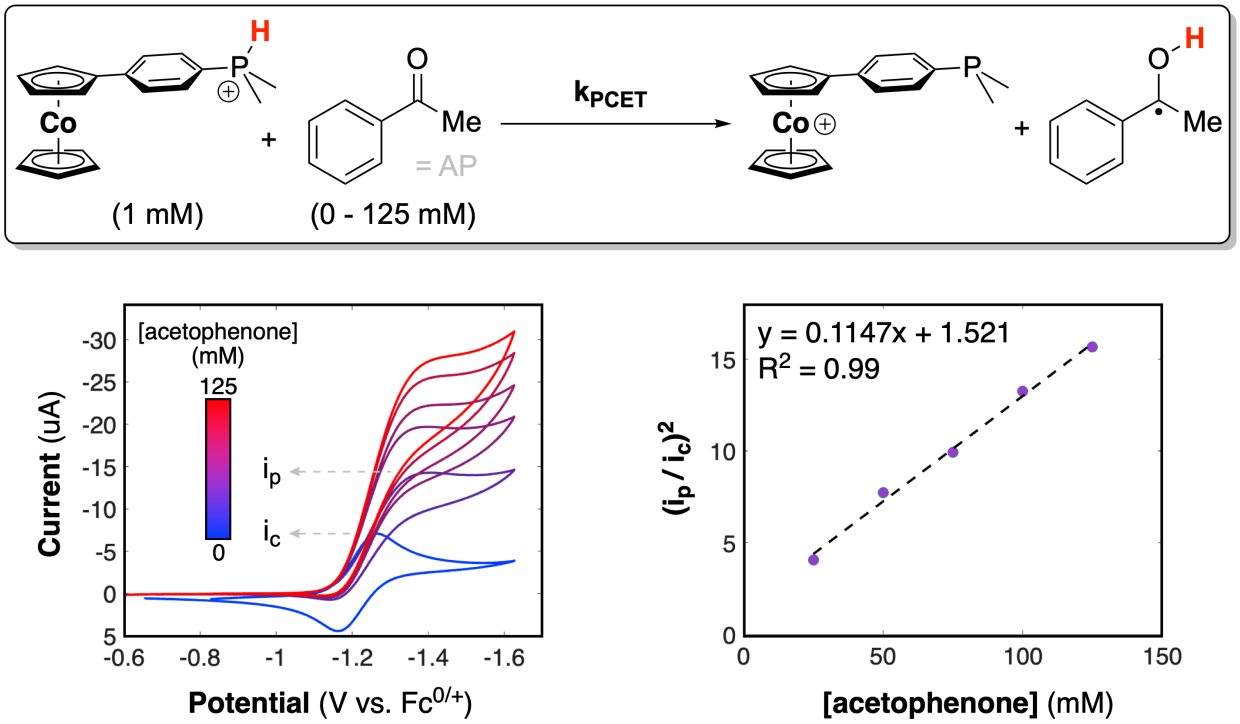

Figure D26. (top) Scheme for the determination of k_{PCET} for Cp**Co**Cp^{PH+} to acetophenone. (bottom left) Cyclic voltammograms of [CpCoCp^{PH}](OTf)$_2$ (1 mM) in acetonitrile with tosic acid (20 mM) and $^{n}Bu_4PF_6$ (100 mM) supporting electrolyte. The scans are swept cathodic, then anodic at a scan rate of 100 mV/s. (bottom right) Plots of the square of the ratio of the catalytic plateau current and the peak current in the absence of substrate as a function of acetophenone concentration.

D8. Computational Details

Electrostatic Potential Maps

Using ORCA 6.1, geometry optimization was performed using the TPSS functional and the def2-TZVP basis set with a CPCM solvation model with THF and D4 dispersion correction. The resulting .gbw file was fed into orca_plot to generate an electron density (scf) plot as a gaussian cube file (resolution = 120), and the mep.py script from Marius Retegan was used to generate a mep.cube file. The cube files were visualized using the Chimera program with the following charge-color coding: red = +0.05, yellow = +0.075, green = +0.1, cyan = +0.125, blue = +0.15.

Computed Structures of the Protonated, Reduced Forms of $[Cp\mathbf{Co}Cp^{\mathbf{XH}}]^+$ (X = N, P)

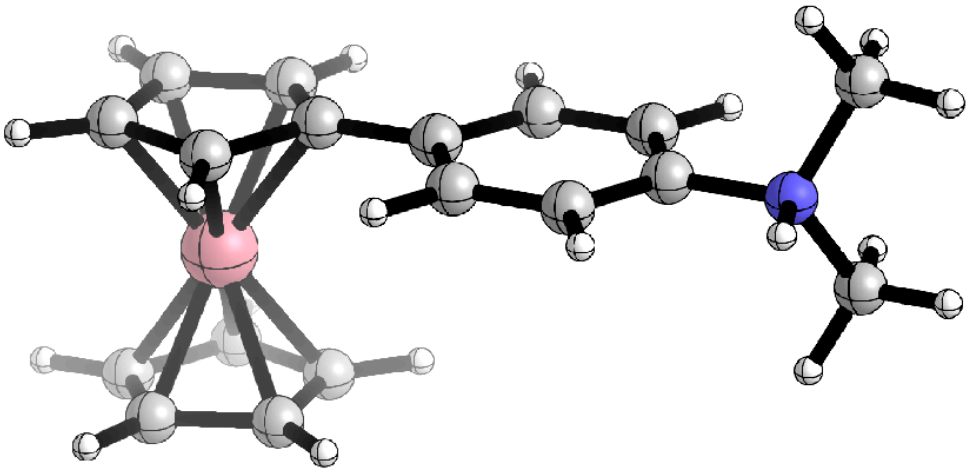

Figure D27. Optimized geometry of $[Cp\mathbf{Co}Cp^{\mathbf{NH}}]^+$

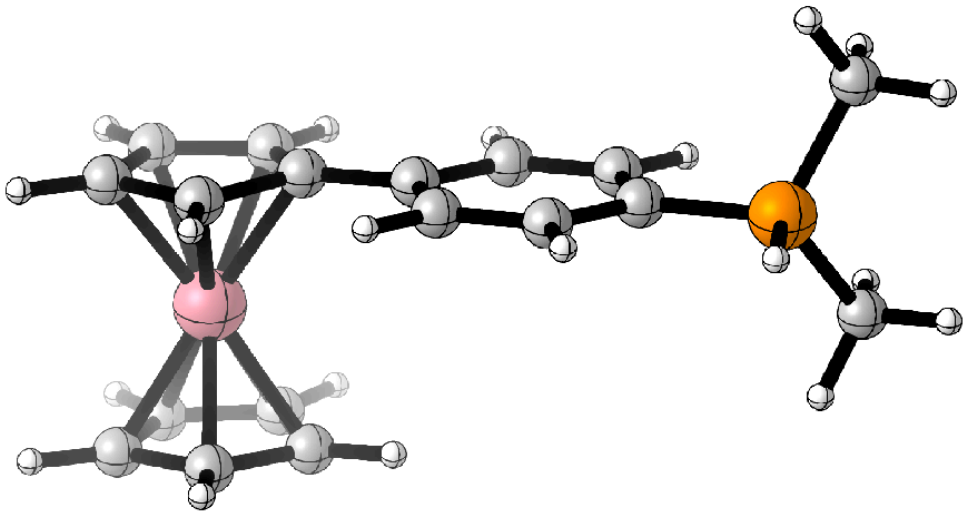

Figure D28. Optimized geometry of $[Cp\mathbf{Co}Cp^{\mathbf{PH}}]^+$

Computed Thermochemistry

Table D3. Calculated energy components of DFT-optimized structures

compound	**S**	**free energy** (eH)	**BDFE** (kcal/mol)
$CpCoCp^{P}$	½	-2421.71995699	-
$[CpCoCp^{PH}]^{+}$	½	-2422.17472436	47.5
$[CpCoCp^{PH}]^{2+}$	0	-2422.04233483	-
$[CpCoCp^{P}]^{+}$	0	-2421.59504869	-

Minimum Energy Geometries and Sample Input File

The Cartesian coordinates resulting from geometry optimization using ORCA are attached below for the specified species of interest. The geometry optimization was done with def2-TZVP. The output xyz coordinate was used for single-point energy calculation.

A sample input file is included here for reference and convenience:

###sample input file for geometry optimization###

! TPSS def2-TZVP Opt Freq SMD(THF) D4

%pal
nprocs 8
end

%maxcore 800

%scf
maxiter 1000
end

* xyz Q S
#insert coordinates here#
*

PHOSPHORUS # # #

CpCoCpP, Q = 0, S = 2

Co	11.28483458755371	2.95082308756864	7.57893212943131
P	10.17958313864198	-3.93355874393364	4.67152075629661
C	11.76867240486655	-0.12098696151586	4.99350318669399
H	12.73846027471981	0.34556598555442	4.86363235055717
C	10.80624202024069	2.07998946487235	5.66744247536265
C	9.31722386221411	-1.36398355161778	5.31574736321518
H	8.35004448960407	-1.83676252926122	5.45889861978074

C	10.67085412490881	0.65417447071382	5.39791308261100
C	11.64231891078376	-1.48243042366159	4.74890556559456
H	12.51904689978766	-2.03584977647130	4.43341417042923
C	10.41354100840576	-2.13526709947482	4.89952125292783
C	9.43717604199155	-0.00409273597285	5.54917273169244
H	8.56304525762121	0.55523345437055	5.86212091765516
C	9.79319964924202	2.96588889894971	6.15428345474728
H	8.76381150915681	2.70539639075342	6.35049757428593
C	11.74483352685653	-4.44601060664504	3.85567772854730
H	11.98624075814399	-3.83492094465461	2.98122586041327
H	11.62834231743358	-5.48542917243915	3.53724902168536
H	12.57418024990374	-4.40707935814897	4.56550600145056
C	12.01454110159404	2.84911382215370	5.65381904439424
H	12.99661089114490	2.48104567637736	5.39653298673598
C	12.66430259655468	2.08123939992392	8.84892776563360
H	13.59374663634352	1.63801550531932	8.52182040517618
C	10.33759237947555	4.28756534336507	6.27819397594708
H	9.79346498367860	5.16444033319943	6.59616986687861
C	11.13360688034907	3.64223675987784	9.57241787933994
H	10.66264348358136	4.56859002059888	9.86627323986399
C	11.71105020791957	4.21558084257298	5.96568026639273
H	12.42353088213139	5.02629497760943	6.00019207206062
C	11.43060734704052	1.40169984928573	9.01988385389232
H	11.23772938073240	0.36029806972987	8.81015775977525
C	12.48689519957946	3.46038843074392	9.23265013871737
H	13.25475066475819	4.21987787224622	9.22141533286731
C	10.46434808839190	2.38166535506677	9.38375660624280
H	9.41024584089140	2.20344122524805	9.54075679498266
C	9.03538442064141	-3.94631540563209	3.22208676174192
H	8.07258029496225	-3.52028382892983	3.51268397086553
H	8.86727200546746	-4.98195739601954	2.91403970246725
H	9.43979568268573	-3.38023670172309	2.37834733264690

CpCoCpP, Q = 1, S = 1

Co	11.27128304226508	2.93475988642975	7.55742887794025
P	10.32125359262358	-3.93476725159563	4.70001268337237
C	11.87267144844071	-0.12112041832850	5.03374206989182
H	12.83559357897582	0.35331145668910	4.88795548857636
C	10.91059829717146	2.06441319062477	5.73562151131965
C	9.42511550922281	-1.37609396073576	5.38155146566790
H	8.46215816075214	-1.85189020470276	5.53251247037769
C	10.77641612894810	0.63148844983729	5.46755437084166
C	11.74594086304623	-1.47885312806303	4.77288246085623
H	12.61626338324709	-2.02604994190531	4.43204512844282
C	10.51939965970647	-2.13283992847932	4.93574462003326
C	9.54690624044889	-0.02022696893446	5.63499393109172

H	8.67912467216445	0.53222235720764	5.97421210133004
C	9.86011875788040	2.97175257451573	6.10707231422681
H	8.82322839099367	2.71604698489718	6.25699722138651
C	11.72510363199129	-4.34789118705542	3.58774141684293
H	11.78859136547888	-3.67948113230848	2.72477239115801
H	11.57427013661745	-5.37133285497708	3.23419019781312
H	12.66808399158347	-4.32372807016181	4.13782084829133
C	12.12787225312858	2.82752524016358	5.72690868145159
H	13.11770021357076	2.44054986511306	5.54318643570152
C	12.57480643576969	2.07499038232683	8.85028618000479
H	13.51071909681880	1.62543078230464	8.55620076330883
C	10.42003929711477	4.26645768580178	6.29310954311436
H	9.88263336095976	5.14645153972398	6.61145318016665
C	10.98393010170224	3.63890710354854	9.44217810535708
H	10.50485599205022	4.57801354386172	9.67274181078852
C	11.82298970888871	4.17720824983278	6.05815184268780
H	12.53828885081710	4.97789149882525	6.16705591841417
C	11.31082959220930	1.41770640152616	8.90311870449919
H	11.12160397063346	0.38654057071308	8.64673673035496
C	12.37284416071617	3.44813824451727	9.18528201945607
H	13.12958234590841	4.21757782679311	9.18757335783893
C	10.32663729325373	2.38419834023528	9.26466504198169
H	9.26427936699440	2.20953596147605	9.33857469933785
C	8.91960102988530	-3.97429379564689	3.50180318880426
H	8.00305996028075	-3.63711545443943	3.98969858453566
H	8.76946128505579	-5.00961083311989	3.18462683252443
H	9.11333483268380	-3.35233300651080	2.62405681021107

CpCoCpPH, Q = 2, S = 1

Co	6.81843519794236	8.24225518810674	8.42287331562711
P	10.74896620040361	8.09046703459178	2.10615415335818
C	9.51122434999906	8.17939126979593	3.38985710912009
C	7.55545220673135	8.33667064979259	5.37618194386244
C	8.00317745422362	9.49374037119944	4.73097093968068
H	7.58693856947724	10.45880717134731	4.99044991508803
C	8.97524491144274	9.41892111218466	3.74445633721501
H	9.31231337207629	10.32321592908296	3.25159696122684
C	6.52161306196873	8.42373001534490	6.41335446988919
C	4.88422867695309	7.85123580202230	7.95298005897718
H	4.21354819027916	7.26912673967371	8.56590897822192
C	5.75893215492613	7.33503927858338	6.95711266271856
H	5.85195256327482	6.29621428586172	6.68171096566274
C	12.23700865413708	7.27712924618963	2.68263277873961
H	12.62633047067914	7.81348955294730	3.54908035313795
H	12.97314014543188	7.28166506677343	1.87626355284461

H	11.99706740369082	6.24845373857736	2.95706163293721
C	8.40365995186893	9.10316806214556	9.34988210855417
H	8.75948764522272	10.10063023682162	9.14261406518776
C	7.39872365545311	8.75217173310621	10.30081701314328
H	6.86089394999280	9.43859590148982	10.93644752430273
C	7.17692313756869	7.34674407313238	10.20941219451820
H	6.44138919911399	6.78383192897285	10.76309687098410
C	8.09922054582358	7.09745079503977	5.01162611202537
H	7.77360634667056	6.19293383239219	5.50928662689710
C	9.06888726479411	7.01517664889200	4.02784427640345
H	9.48229235857238	6.04950015547295	3.76208297946962
C	5.10227500650098	9.25668167975665	8.04766204909639
H	4.62929119998123	9.92763882849212	8.74803545671806
C	6.11013378627998	9.61045735023737	7.10813927010928
H	6.52914711391384	10.59633688049943	6.98151690091070
C	10.11592995173926	7.28553013278200	0.63616132434832
H	10.89183812361284	7.29432233963622	-0.13218039785109
H	9.84882695510063	6.25623026102561	0.88170631198082
H	9.23524525149051	7.82568149420063	0.28540929778683
C	8.80277251739213	7.91363329781092	8.67240414127545
H	9.50514538293117	7.85463651545784	7.85500388620323
C	8.04377859414389	6.82835748172574	9.20110574243433
H	8.07864587045091	5.80523537722540	8.85988756516391
H	11.05575260774413	9.41343254160902	1.78739255203026

CpCoCpPH, Q = 1, S = 2

Co	6.81080626126781	8.26674560861721	8.47114218758861
P	10.78279238345113	8.07733303517463	2.11979817001270
C	9.51684207031984	8.13867401164413	3.35794424861648
C	7.49762558173540	8.26622117729148	5.32007350960868
C	8.08665965760991	9.43786948167160	4.80561583737092
H	7.76317078266156	10.40673498121649	5.16532029607713
C	9.07793099008322	9.37806064235632	3.84398605851309
H	9.51596920448640	10.29554803395819	3.46722452607550
C	6.47342618099248	8.33087551969716	6.34130991811489
C	4.87551598261272	7.72472422124939	7.93320170978222
H	4.22058962683132	7.12205999382561	8.54444973983161
C	5.82852787627672	7.22645569865500	6.99071095904507
H	5.99008664531965	6.18146157969492	6.77292882055457
C	12.18144177812688	7.07996986364967	2.63303285078065
H	12.58587994477358	7.47958118693318	3.56381158464684
H	12.94288515031538	7.10699551809484	1.85091165045481
H	11.84791857683236	6.05176376263918	2.78480572579643
C	8.34778469228145	9.26927402859469	9.40742639822424
H	8.64071305248811	10.28275266679117	9.17443985449945
C	7.38017037469662	8.88950268602727	10.40480879546791

H	6.81224643039933	9.56970632277102	11.02198829413265
C	7.26549116562248	7.48731137319251	10.37811835132869
H	6.59288734529626	6.88574520137630	10.97128716643877
C	7.94789348375271	7.02778870052285	4.81637953773183
H	7.51612893630892	6.10686080041061	5.18857130075208
C	8.93740259988080	6.96109329848511	3.85535482619373
H	9.26365200690145	5.99337211865063	3.49088265404924
C	4.98947945505809	9.13434421038079	7.95683130214494
H	4.43873565621520	9.81374544139405	8.58993413323655
C	6.01319510026435	9.50314461250176	7.02906984846957
H	6.34327119151590	10.51482857573215	6.84656182233286
C	10.17082982020407	7.49022225941136	0.53900582273120
H	10.98244554564812	7.51701081088710	-0.19093142422268
H	9.81316568338863	6.46540795809476	0.65478940719493
H	9.35160207153169	8.13215733454207	0.21218814617735
C	8.88546284405735	8.08976236709532	8.82391158840558
H	9.63078700810857	8.04330860198158	8.04418802670039
C	8.16292502368455	6.99230620974744	9.36544377441246
H	8.28836606290669	5.95413610188859	9.09416807839402
H	11.21673575609201	9.39307400315155	1.95331450233385

NITROGEN FOR ESP # # #

CpCoCpNH, Q = 1, S = 2

Co	6.83564071562713	8.18384122861510	8.41519120080025
N	10.67569840208291	8.14572325156305	2.29067104858108
C	9.60319200493852	8.16045310359264	3.31388333503818
C	7.57530971582866	8.15487702986450	5.25039841947297
C	8.09428052320524	9.36476602374650	4.73495517904159
H	7.70492102321870	10.31339224380325	5.09031585124435
C	9.09775394237689	9.37384889415021	3.77646143292100
H	9.47754993110473	10.31761514531832	3.39748067492898
C	6.53785032331389	8.15341058559570	6.26413901082270
C	4.98095776117894	7.44011157625116	7.86861557002521
H	4.37577772037140	6.79327877096402	8.49020094707562
C	5.99501348110027	7.00892231024554	6.94759461450959
H	6.26160536983804	5.97607711633623	6.76452504542921
C	11.94644470522776	8.79796809659784	2.77705989315622
H	12.24840041765306	8.30001911192716	3.69782464126955
H	11.74046808572735	9.85296118196653	2.95318977850016
H	12.70218967094872	8.67648487602312	2.00055463791469
C	8.72210824753136	8.92913149476486	8.92157093742312
H	9.31050611828915	9.57711177050752	8.28491977609383
C	7.71761867591933	9.36046482249485	9.86737041848082
H	7.44629272374907	10.38933849713095	10.06782125055883
C	7.18060432824499	8.21138631744885	10.51736682099078

H	6.40529608681990	8.20533147826846	11.27207845831857
C	8.11401299495704	6.94758408337958	4.75371486595174
H	7.74179335597564	5.99655137595824	5.12064154092094
C	9.11852141834902	6.94789826207368	3.79494106547220
H	9.52173938521894	6.00921406993512	3.42324290639488
C	4.96039242570205	8.85859490277070	7.85151389742477
H	4.33610835177888	9.50224939576901	8.45732453503120
C	5.96130281223597	9.29734265832990	6.91950571621952
H	6.19648224279011	10.33302829983068	6.71121939138145
C	10.22828791442663	8.73524834614020	0.97579413495179
H	10.01114805319633	9.79107379227281	1.13270601415916
H	11.04193531597392	8.61096216993370	0.26062268378323
H	9.33777523689602	8.19765164726900	0.65172511523026
C	8.74675225530300	7.51590917756496	8.93579189267577
H	9.35778598017769	6.87609336472219	8.31232553074308
C	7.75770850018202	7.06899666404115	9.89046546528351
H	7.52264609937570	6.03543640172401	10.11163375091727
H	10.89963768316439	7.15893046110814	2.11192255086146

D9. References

[1] Kirst, C.; Tietze, J.; Ebeling, M.; Horndasch, L.; Karaghiosoff, K. The Formation of P–C Bonds Utilizing Organozinc Reagents for the Synthesis of Aryl- and Heteroaryl-Dichlorophosphines. *J. Org. Chem.* **2021**, *86* (23), 17337–17343.
[2] Sheldrick, G. M. A short history of SHELX. *Acta Cryst. A*, **2008**, *64*, 112–122.
[3] Dolomanov, O. V.; Bourhis, L. J.; Gildea, R. J.; Howard, J. A. K.; Puschmann, H. OLEX2: A Complete Structure Solution, Refinement and Analysis Program. *J. Appl. Crystallogr.* **2009**, *42*, 339.
[4] Neese, F.; Wennmohs, F.; Becker, U.; Riplinger, C. The ORCA Quantum Chemistry Program Package. *J. Chem. Phys.* **2020**, *152*, 224108.
[5] Neese, F. Software update: The ORCA program system—Version 5.0. *WIREs Comput. Mol. Sci*. **2022**, 12:e1606.
[6] J. Tao, J. P. Perdew, V. N. Staroverov, G. E. Scuseria, Climbing the density functional ladder: nonempirical meta-generalized gradient approximation designed for molecules and solids. *Phys. Rev. Lett.* **2003**, *91*, 146401.
[7] V. N. Staroverov, G. E. Scuseria, J. Tao, J. P. Perdew, Comparative assessment of a new nonempirical density functional: Molecules and hydrogen-bonded complexes. *J. Chem. Phys.* **2003**, *119*, 12129–12137.
[8] F. Weigend, R. Ahlrichs, Balanced basis sets of split valence, triple zeta valence and quadruple zeta valence quality for H to Rn: Design and assessment of accuracy, *Phys. Chem. Chem. Phys.* **2005**, *7*, 3297–3305.
[9] A. V. Marenich, C. J. Cramer, D. G. Truhlar, Universal solvation model based on solute electron density and on a continuum model of the solvent defined by the bulk dielectric constant and atomic surface tensions *J. Phys. Chem. B.* **2009**, *113*, 6378–6396
[10] Davies, W. C.; Walters, W. P. The Constitution of Some Additive Compounds of Tertiary Phosphines. *J. Chem. Soc.* **1935**, 1786–1792.
[11] Chalkley, M. J.; Garrido-Barros, P.; Peters, J. C. A Molecular Mediator for Reductive Concerted Proton-electron Transfers via Electrocatalysis. *Science* **2020**, *369*, 850–854.
[12] Rountree, E. S.; McCarthy, B. D.; Eisenhart, T. T.; Dempsey, J. L. Evaluation of Homogeneous Electrocatalysts by Cyclic Voltammetry. *Inorg. Chem.* **2014**, *53* (19), 9983–10002. DOI: 10.1021/ic500658x.

A p p e n d i x E

Miscellaneous X-ray Diffraction Structures

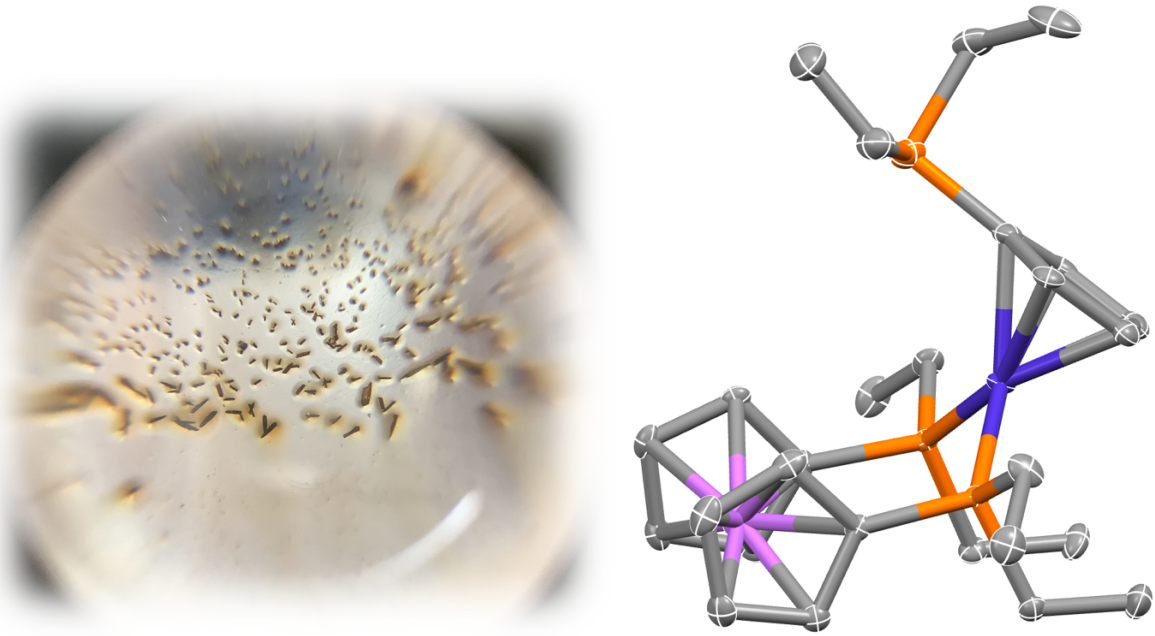

Figure E1. (left) photograph of crystals and (right) X-ray diffraction structure of (1,1'-bis(diethylphosphino)lithanocene) ((diethylphosphino)cyclopentadienyl)cobalt

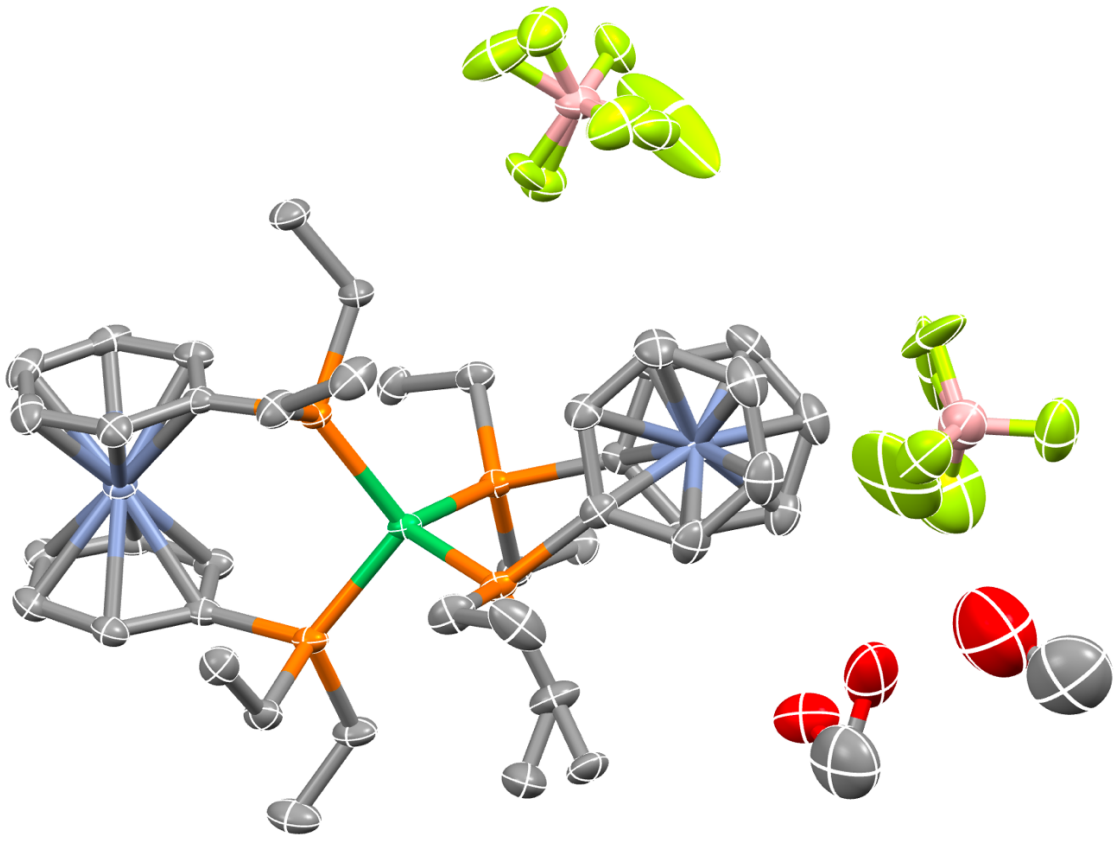

Figure E2. X-Ray Diffraction structure of [bis(1,1'-(bis(diethylphosphino)benzene)Cr)Ni]$(BF_4)_2$

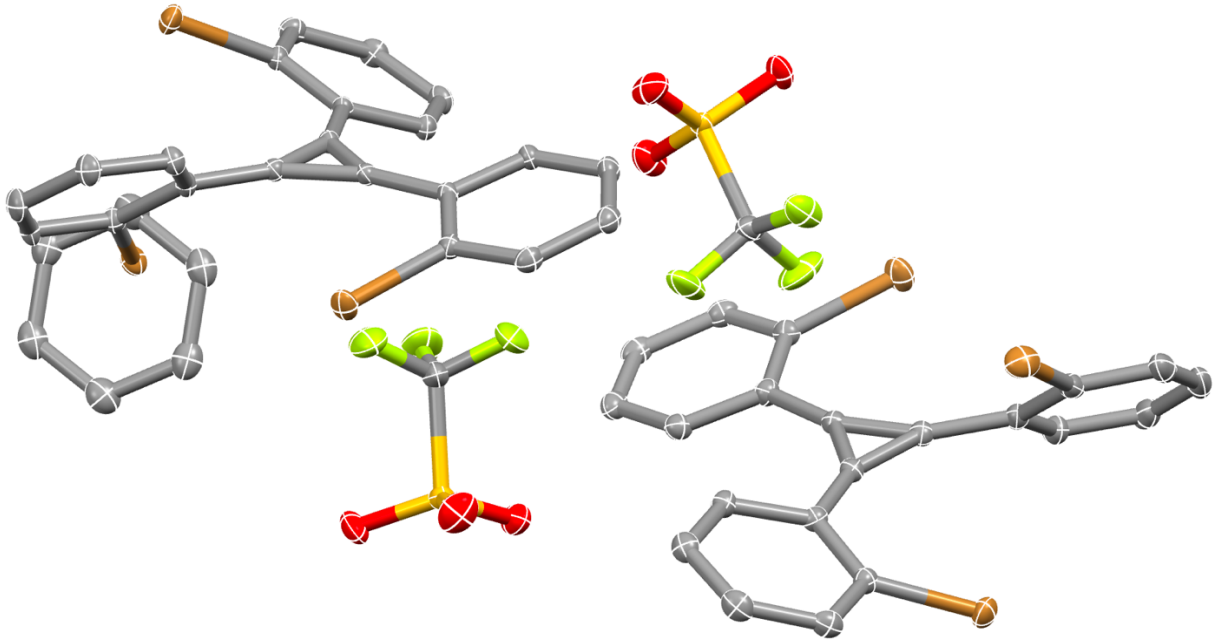

Figure E3. X-Ray Diffraction structure of tris(2-bromophenyl)cyclopropenium triflate

Figure E4. X-Ray Diffraction structure of tris(2-bromophenyl)cyclopropene

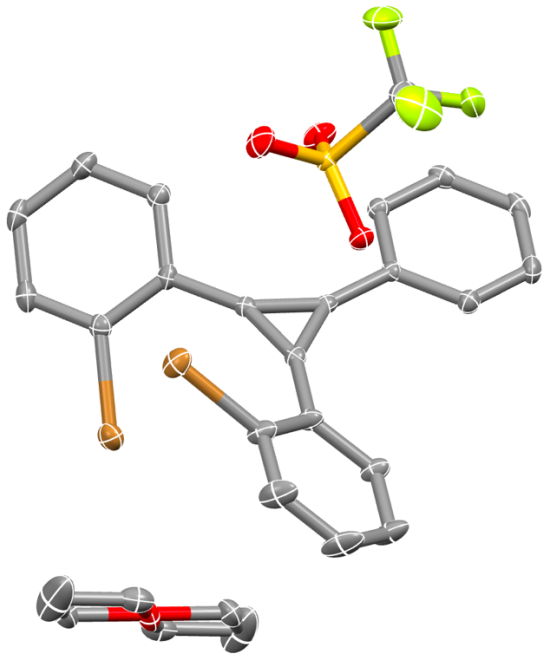

Figure E5. X-Ray Diffraction structure of bis(2-bromophenyl)(phenyl)cyclopropenium triflate

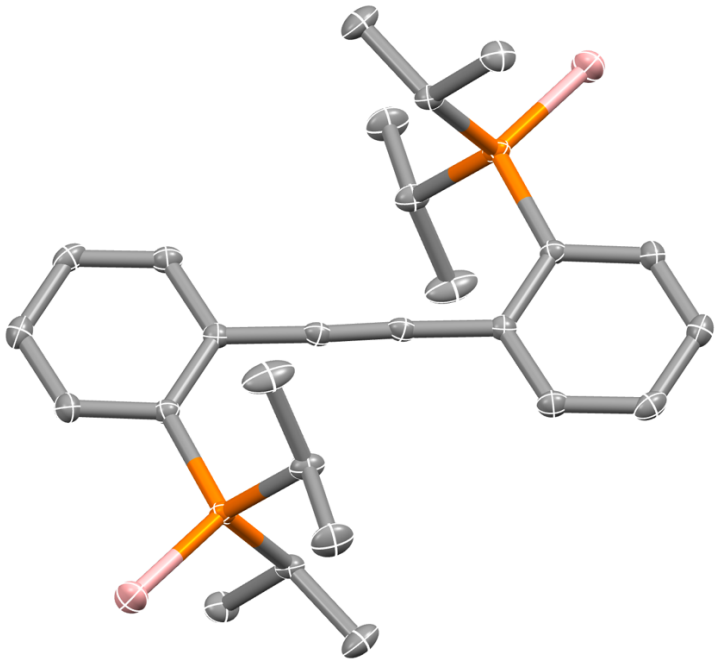

Figure E6. X-Ray Diffraction structure of (1,2-bis(2-diisopropylphosphinophenyl)tolane)$(BH_3)_2$

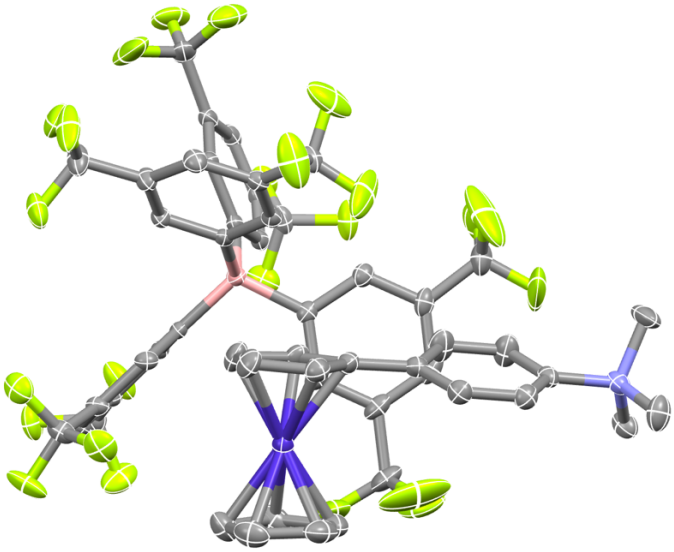

Figure E7. X-Ray Diffraction structure of $[Co(II)^{p\text{-}Ph},NMe_3]BAr^F{}_4$

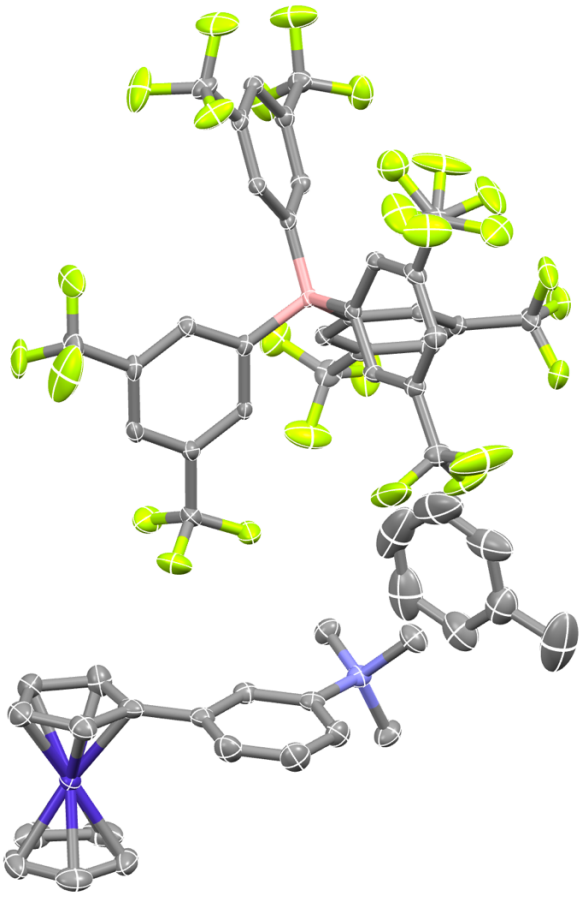

Figure E8. X-Ray Diffraction structure of $[Co(II)^{m\text{-}Ph},NMe_3]BAr^F{}_4$

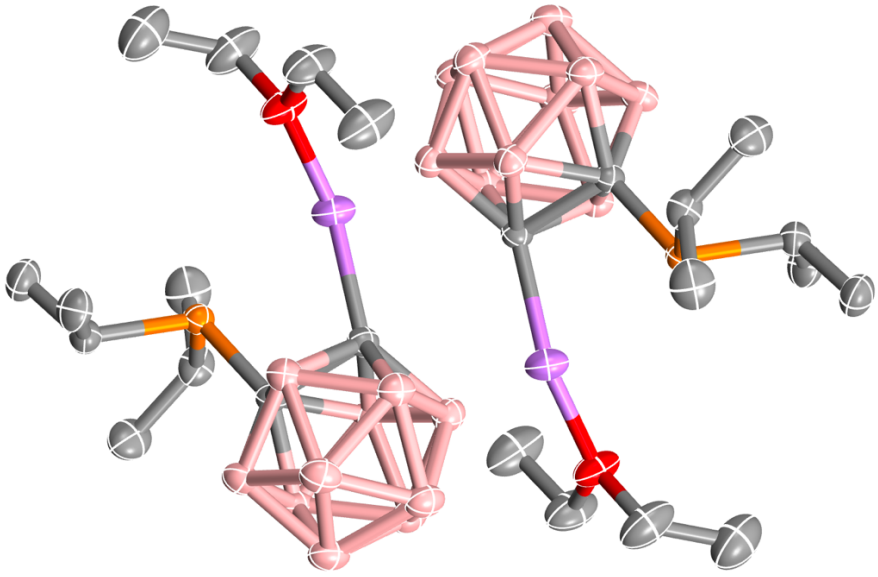

Figure E9. X-Ray Diffraction structure of 1-lithio-2-(diisopropylphosphinyl)-*o*-carborane etherate

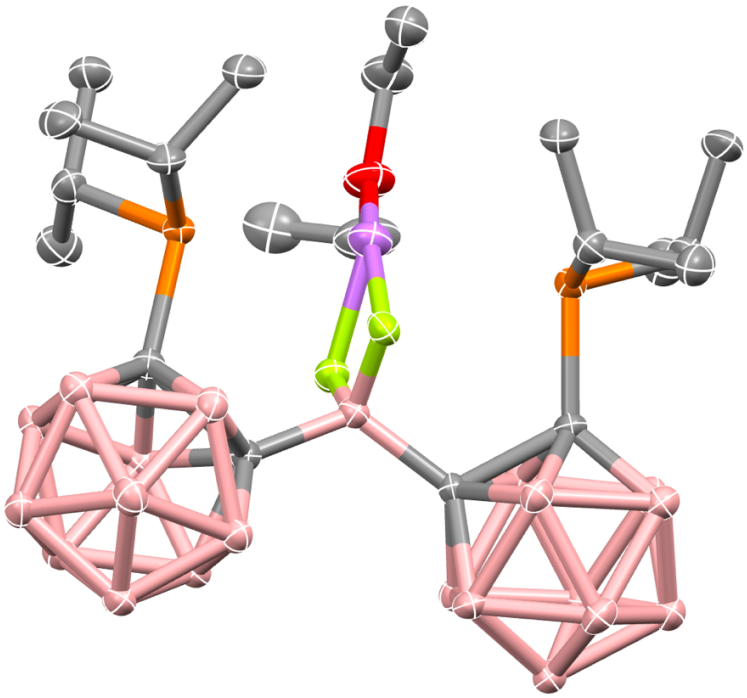

Figure E10. X-Ray Diffraction structure of lithium(etherate) di(diisopropylphosphinyl-*o*-carboranyl)difluoro borate